



Publicly Accessible Penn Dissertations

1-1-2014

Palladium-Catalyzed C-C Bond Forming Reactions With Weakly Acidic C(sp³)-H Bonds

Jiadi Zhang

University of Pennsylvania, jiadizh@sas.upenn.edu

Follow this and additional works at: <http://repository.upenn.edu/edissertations>

 Part of the [Chemistry Commons](#)

Recommended Citation

Zhang, Jiadi, "Palladium-Catalyzed C-C Bond Forming Reactions With Weakly Acidic C(sp³)-H Bonds" (2014). *Publicly Accessible Penn Dissertations*. 1519.

<http://repository.upenn.edu/edissertations/1519>

This paper is posted at Scholarly Commons. <http://repository.upenn.edu/edissertations/1519>

For more information, please contact libraryrepository@pobox.upenn.edu.

Palladium-Catalyzed C-C Bond Forming Reactions With Weakly Acidic C(sp³)-H Bonds

Abstract

Metal-catalyzed cross-coupling reactions to form C-C bonds are a mainstay in the preparation of small molecules, which have applications ranging from biological studies to treatment of human disease. Traditional cross-coupling methods (such as Negishi, Suzuki, etc.) require prefunctionalized coupling partners, consisting of an organometallic reagent and an aryl halide or pseudohalide. Because prefunctionalization requires substantial time and effort, chemists are turning to direct functionalization of C-H bonds as a more efficient and atom-economical synthetic approach. Catalytic C-H bond functionalization has therefore emerged as a promising synthetic tool in organic chemistry, with the vast majority concentrated on the functionalization of sp² hybridized C-H bonds of arenes and heteroarenes. Recently the functionalization of more challenging sp³ hybridized C-H bonds has received attention and has become the focus of increasing effort.

This dissertation describes two strategies for directing group free C(sp³)-H bond functionalizations. These involve the direct metallation and subsequent cross-coupling of benzylic C-H bonds with high pK_a values (> 30).

The first strategy is directed toward functionalization of challenging toluene derivatives (pK_a = 44 ± 1). It relies on η⁶-coordination of arenes to tricarbonylchromium, which increases the acidity of the benzylic C-H bonds to the point that they can be reversibly deprotonated under relatively mild conditions. The resulting benzylic nucleophiles undergo palladium-catalyzed allylic substitution processes, including enantioselective variants. Furthermore, a tandem C(sp³)-H bond functionalization/demetallation procedure is developed that affords the corresponding metal-free products, rendering arene-metal π-complexation as a traceless activation strategy for C(sp³)-H bond functionalization.

The second strategy does not employ η⁶-arene activation, but is based on the direct, reversible deprotonation of weakly acidic C(sp³)-H bonds (pK_a > 30). This approach to C-C bond formation, which will be abbreviated as DCCP (Deprotonative-Cross-Coupling Process), enables rapid access to polyarylmethane and heteroaryl-containing derivatives frameworks. Current catalysts are not available for such DCCPs. We have discovered a unique catalyst system (Pd-NiXantphos) capable of conducting room temperature DCCPs under mild conditions with the C(sp³)-H bonds of diarylmethanes (pK_a up to > 32) and 2-substituted furans (pK_a up to > 30).

Mechanistic studies reveal the origin of the unique reactivity of this Pd-NiXantphos catalyst system. Under the basic DCCP conditions, the heterobimetallic Pd(M-NiXantphos)-based catalyst system (M = main group metal) readily activates aryl chlorides at room temperature and successfully promotes the arylation of diarylmethane derivatives with a broad scope of aryl chlorides.

Degree Type

Dissertation

Degree Name

Doctor of Philosophy (PhD)

Graduate Group
Chemistry

First Advisor
Patrick J. Walsh

Subject Categories
Chemistry

PALLADIUM-CATALYZED C–C BOND FORMING REACTIONS WITH WEAKLY
ACIDIC C(SP³)–H BONDS

Jiadi Zhang

A DISSERTATION

in

Chemistry

Presented to the Faculties of the University of Pennsylvania

in

Partial Fulfillment of the Requirements for the
Degree of Doctor of Philosophy

2014

Supervisor of Dissertation

Professor Patrick J. Walsh, Alan G. MacDiarmid Professor of Chemistry

Graduate Group Chairperson

Professor Gary A. Molander, Hirschmann-Makineni Professor of Chemistry

Dissertation Committee:

Professor Eric J. Schelter, Assistant Professor of Chemistry

Professor Gary A. Molander, Hirschmann-Makineni Professor of Chemistry

Professor Marisa C. Kozlowski, Professor of Chemistry

PALLADIUM-CATALYZED C–C BOND FORMING REACTIONS WITH WEAKLY
ACIDIC C(SP³)–H BONDS

COPYRIGHT

2014

Jiadi Zhang

Dedicated to my family

Acknowledgements

Firstly, I would like to thank my advisor, Prof. Pat Walsh for taking me into his group in Jan 2010. He has been extremely supportive over the past four years, always giving me helpful advice and suggestions when I need him. I feel grateful for the opportunity he has given me to grow both professionally and personally. He is a great mentor and I especially appreciate that he has offered me a lot of creative freedom to pursue projects that interest me most, and that he has helped me become a better chemist.

I would also like to thank my committee members, Professors Eric Schelter, Gary Molander and Marisa Kozlowski for their help, critical comments and constructive advice throughout my graduate career. The advice and criticism they have provided during our annual committee meetings have made my chemistry better.

A special thanks to the Kozlowski group for having joint group meetings every week, sharing ideas and chemicals. Many thanks to the Schelter group members for being nice neighbors and sharing music and happiness.

None of my research projects would have been possible without the support of the wonderful people at Penn Chemistry. Among them, I would like to thank Dr. Pat Carroll, Dr. George Furst, Dr. Jun Gu, Dr. Rakesh Kohli and Judith Currano for all of their help with instrumentation, spectroscopy and references.

Without the collaboration with Dr. Spencer Dreher (Merck & Co.), the high-throughput experimentation (HTE) contained in this dissertation would not have been possible. In particular, Dr. Ana Bellomo, Dr. Cornell Stanciu, Dr. Matthew Tudge and Dr. Simon Berritt are acknowledged for their experimental support, invaluable training, and helpful discussion.

I have worked with an amazing group of people over the past four years in the Walsh group. Dr. Genette McGrew deserves special mention for being a good teacher starting from my first day in the Walsh group. I am indebted to her and Byeong-Seon Kim for their continued help and friendship, and especially their company in lab at late hours of the night. Dr. Jerome Robinson, Nusrah Hussain, and myself started in the Walsh group together, and have been helping and supporting each other throughout the journey. I would also like to thank Tiezheng Jia and Sheng-Chun Sha for being not only great co-workers in lab but also close friends in life. Many thanks to the past and present Walsh group members who have shared memories with me, including Dr. Mahmud Hussain, Dr. Petr Valenta, Dr. Gretchen Stanton, Dr. Kevin Cheng, Dr. Ismael Nieto, Minyan Li and Mengnan Zhang. The Walsh group members are always international, friendly, and welcoming and it has always been my pleasure to work with them.

Many thanks to the undergraduate students Beibei Wang, Andrea Creamer and Nisalak Trongsirawat who worked with me in our projects, along with the visiting scholar Dr. Chao-Shan Da. I am fortunate to have had the opportunity to work with all of them, and I could not have completed these projects without their hard work and dedication.

I would also like to thank my chemistry and non-chemistry friends since I started graduate school. Yanran Ai has been a nice roommate, a great friend, and an organic chemistry mentor for me over the past five years. Chen Zheng and Haolin Yin are acknowledged for their friendship, especially for having coffee breaks with me in the afternoons rain or shine, and for going to the gym together. I also acknowledge Dr. O. Andreea Argintaru and DaWeon Ryu for sharing chemicals, knowledge and ideas. I would like to thank my friends who started the journey with me together, including Na Zhang, Rong Shen, Lu Gao, Tingting Wu, Shi Liu, Zhaoxia Qian. They have been a

great group of friends over the years, and I cannot thank them enough for all they have done for me.

Prof. Xuefeng Fu (Peking University) is gratefully acknowledged for encouraging me to become a chemist and carry out research back in 2008. I am indebted to her for her guidance, supervision, encouragement, patience and support. I could not have even joined Penn Chemistry without her.

Special thanks are given to my wonderful wife, Mengyi Yang, for her love, devotion, understanding, support, encouragement, and sharing the ups and downs in my life over the past seven years. Finally, I am most thankful to my parents and my grandfather for giving me their endless love and support.

ABSTRACT

PALLADIUM-CATALYZED C–C BOND FORMING REACTIONS

WITH WEAKLY ACIDIC C(SP³)–H BONDS

Jiadi Zhang

Professor Patrick J. Walsh

Metal-catalyzed cross-coupling reactions to form C–C bonds are a mainstay in the preparation of small molecules, which have applications ranging from biological studies to treatment of human disease. Traditional cross-coupling methods (such as Negishi, Suzuki, etc.) require prefunctionalized coupling partners, consisting of an organometallic reagent and an aryl halide or pseudohalide. Because prefunctionalization requires substantial time and effort, chemists are turning to direct functionalization of C–H bonds as a more efficient and atom-economical synthetic approach. Catalytic C–H bond functionalization has therefore emerged as a promising synthetic tool in organic chemistry, with the vast majority concentrated on the functionalization of sp² hybridized C–H bonds of arenes and heteroarenes. Recently the functionalization of more challenging sp³ hybridized C–H bonds has received attention and has become the focus of increasing effort.

This dissertation describes two strategies for directing group free C(sp³)–H bond

functionalizations. These involve the direct metallation and subsequent cross-coupling of benzylic C–H bonds with high pK_a values (> 30).

The first strategy is directed toward functionalization of challenging toluene derivatives ($pK_a = 44 \pm 1$). It relies on η^6 -coordination of arenes to tricarbonylchromium, which increases the acidity of the benzylic C–H bonds to the point that they can be reversibly deprotonated under relatively mild conditions. The resulting benzylic nucleophiles undergo palladium-catalyzed allylic substitution processes, including enantioselective variants. Furthermore, a tandem C(sp³)–H bond functionalization/demetallation procedure is developed that affords the corresponding metal-free products, rendering arene–metal π -complexation as a traceless activation strategy for C(sp³)–H bond functionalization.

The second strategy does not employ η^6 -arene activation, but is based on the direct, reversible deprotonation of weakly acidic C(sp³)–H bonds ($pK_a > 30$). This approach to C–C bond formation, which will be abbreviated as DCCP (Deprotonative-Cross-Coupling Process), enables rapid access to polyarylmethane and heteroaryl-containing derivatives frameworks. Current catalysts are not available for such DCCPs. We have discovered a unique catalyst system (Pd–NiXantphos) capable of conducting room temperature DCCPs under mild conditions with the C(sp³)–H bonds of diarylmethanes (pK_a up to > 32) and 2-substituted furans (pK_a up to > 30).

Mechanistic studies reveal the origin of the unique reactivity of this Pd–NiXantphos catalyst system. Under the basic DCCP conditions, the heterobimetallic Pd(M–NiXantphos)-based catalyst system (M = main group metal) readily activates aryl chlorides at room temperature and successfully promotes the arylation of diarylmethane

derivatives with a broad scope of aryl chlorides.

TABLE OF CONTENTS

Title Page.....	i
Copyright.....	ii
Dedication.....	iii
Acknowledgements.....	iv
Abstract.....	vii
Table of Contents.....	x
List of Tables.....	xv
List of Figures.....	xvii
List of Schemes.....	xxvi
Chapter 1. Palladium-Catalyzed Allylic Substitution with (η^6-Arene- CH₂Z)Cr(CO)₃-based Nucleophiles	
1.1 Introduction.....	1
1.2 Results and Discussion.....	4
1.2.1 Development and Optimization of Palladium-Catalyzed Allylic Substitution with (η^6 -C ₆ H ₅ -CH ₃)Cr(CO) ₃	5
1.2.2 Scope of Nucleophiles in Palladium-Catalyzed Allylic Substitution Reactions.....	7
1.2.3 Scope of Electrophiles in Palladium-Catalyzed Allylic Substitution Reactions.....	10
1.2.4 Tandem Allylic Substitution/Demetallation with Diphenylmethane	

Derivatives.....	14
1.2.5 Allylic Substitution with Benzyl Amine and Ether Derivatives.....	17
1.2.6 Allylic Substitution at Multiple Benzylic Sites.....	18
1.2.7 Internal vs External Attack of (η^6 -Ar-CH ₂ Li)Cr(CO) ₃ on π -Allyl Palladium Intermediate.....	19
1.2.8 Asymmetric Allylic Substitution with (η^6 -C ₆ H ₅ -CH ₃)Cr(CO) ₃	20
1.3 Conclusions.....	21
1.4 Experimental Section.....	22
1.5 References.....	57
Chapter 2. Palladium-Catalyzed C(sp³)-H Arylation of Diarylmethanes at Room Temperature: Synthesis of Triarylmethanes via Deprotonative-Cross- Coupling Processes (DCCP)	
2.1 Introduction.....	66
2.2 Results and Discussion.....	69
2.2.1 Development of Room-Temperature Deprotonation/Benylation of Diphenylmethane.....	70
2.2.2 Development and Optimization of Palladium-Catalyzed DCCP of C(sp ³)-H of Diarylmethanes.....	72
2.2.3 Scope of Diarylmethanes in Palladium-Catalyzed DCCP.....	75
2.2.4 Scope of Aryl Bromides in Palladium-Catalyzed DCCP.....	78
2.3 Conclusions.....	81

2.4 Experimental Section.....	82
2.5 References.....	109

Chapter 3. NiXantphos: A Deprotonatable Ligand for Room Temperature Palladium-Catalyzed Cross-Couplings of Aryl Chlorides

3.1 Introduction.....	118
3.2 Results and Discussion.....	119
3.2.1 Initial Studies with NiXantphos.....	119
3.2.2 Deprotonation of NiXantphos.....	121
3.2.2.1 Solution Studies.....	121
3.2.2.2 DFT Calculations with NiXantphos and Relevant Bidentate Phosphines.....	123
3.2.2.3 Structures of Deprotonated NiXantphos.....	125
3.2.2.4 Probing NiXantphos N-Arylation.....	127
3.2.3 Oxidative Addition with Aryl Chlorides.....	129
3.2.4 Development of DCCP with Aryl Chlorides.....	133
3.2.5 Optimization of DCCP with Diphenylmethane and Aryl Chloride	
3.2a	135
3.2.6 Scope of Aryl Chlorides in DCCP with Diphenylmethane.....	137
3.2.7 Scope of Diarylmethanes in DCCP.....	141
3.2.8 Identification of the Catalyst Resting State and Counteraction Effects.....	143

3.3 Conclusions.....	147
3.4 Experimental Section.....	148
3.5 References.....	204

Chapter 4. Site-Selective sp^2 and sp^3 C–H Functionalization: Divergent Palladium-Catalyzed C3 and Benzylic Direct Arylation of 2-Substituted Furans

4.1 Introduction.....	214
4.2 Results and Discussion.....	219
4.2.1 Initial Studies with 2-Benzylfuran.....	219
4.2.2 Development and Optimization of Palladium-Catalyzed C3 and Benzylic Arylations.....	221
4.2.3 Scope of Aryl Bromides in Pd–NiXantphos-Catalyzed C3 and Benzylic Arylations of 4.1a	226
4.2.4 Scope of Furans in Pd–NiXantphos-Catalyzed C3 and Benzylic Arylations.....	230
4.2.5 Pd–NiXantphos-Catalyzed Homo-Diarylations.....	234
4.3 Conclusions.....	237
4.4 Experimental Section.....	238
4.5 References.....	273

Appendices

Appendix A1 NMR Spectra Relevant to Chapter 1.....	278
Appendix A2 NMR Spectra Relevant to Chapter 2.....	318
Appendix A3 NMR Spectra Relevant to Chapter 3.....	354
Appendix A4 NMR Spectra Relevant to Chapter 4.....	395
Appendix B X-ray Structure Reports.....	444

List of Tables

Table 1.1 Optimization of allylic substitution with 1.1a	6
Table 1.2 Scope of nucleophiles in allylic substitution reactions.....	8
Table 1.3 Scope of electrophiles in allylic substitution reactions.....	12
Table 1.4 Tandem synthesis of diphenylmethane derivatives.....	14
Table 2.1 Optimization of Pd-catalyzed DCCP of 2.1a	73
Table 2.2 Scope of diarylmethanes in Pd-catalyzed DCCP.....	76
Table 2.3 Scope of aryl bromides in Pd-catalyzed DCCP.....	79
Table 2.4 HTE using ligands 1–96	102
Table 2.5 HTE using ligands 97–112 and PdCl ₂ (PPh ₃) ₂	106
Table 2.6 HTE using ligands 1, 14, 28, 50, 75, 76, 85, 87, 97–112 and 3 Pd sources.....	107
Table 2.7 HTE using 6 Pd sources.....	108
Table 3.1 ¹ H and ³¹ P{ ¹ H} NMR studies of NiXantphos deprotonated by base...122	
Table 3.2 Calculated natural charges for members of the Xantphos ligand family and relevant bidentate phosphines.....	124
Table 3.3 Optimization of Pd–NiXantphos-catalyzed DCCP of 3.1a with 3.2a ..	135
Table 3.4 Scope of aryl chlorides in Pd–NiXantphos-catalyzed DCCP with 3.1a	137
Table 3.5 Scope of diarylmethanes in Pd–NiXantphos-catalyzed DCCP.....	142
Table 3.6 Collected diffusion data from ¹ H DOSY NMR experiments for NiXantphos and Pd[K(THF) ₂ (NiXantphos)] ₂	158

Table 3.7 Acquisition parameters for 2D- ¹ H DOSY.....	158
Table 3.8 HTE with 1-bromo-4- <i>tert</i> -butylbenzene using 7 ligands and 2 3.1a loadings.....	191
Table 3.9 HTE with 1-bromo-4- <i>tert</i> -butylbenzene using 8 ligands and 3 3.1a loadings.....	192
Table 4.1 Optimization of Pd-catalyzed C3 arylation of 4.1a	223
Table 4.2 Main group counteraction-controlled site-selective arylation of 4.1a	225
Table 4.3 Scope of aryl bromides in Pd-NiXantphos-catalyzed C3 arylation of 4.1a	227
Table 4.4 Scope of aryl bromides in Pd-NiXantphos-catalyzed benzylic arylation of 4.1a	229
Table 4.5 Scope of furans in Pd-NiXantphos-catalyzed C3 and benzylic arylations with 4.2a	232
Table 4.6 Pd-NiXantphos-catalyzed homo-diarylations.....	235
Table 4.7 HTE using 4 solvents and 6 Pd sources.....	272

List of Figures

Figure 1.1 Selected bioactive compounds and natural products containing the “ α -2-propenyl benzyl” motif.....	3
Figure 1.2 ORTEP drawing of 1.3a with 30% probability thermal ellipsoids.....	7
Figure 3.1 (a) ORTEP diagram of $[\text{K}(\text{THF})_3\text{-NiXantphos}]_2$ with 50% probability thermal ellipsoids displayed, and (b) ORTEP diagram of $\text{K}(\text{THF})(18\text{-crown-6})\text{-NiXantphos}$ with 50% probability thermal ellipsoids displayed.....	127
Figure 3.2 ORTEP diagram of $(\text{NiXantphos})\text{Pd}(\text{Ph})(\text{Cl})$ with 50% probability thermal ellipsoids displayed.....	132
Figure 3.3 Proposed “turn on” form of palladium(0) bearing a deprotonated NiXantphos and the “turn off” form of palladium(0) bearing a neutral <i>N</i> -Bn-NiXantphos or Xantphos for the DCCP with aryl chlorides.....	135
Figure 3.4 Drawing of the solid state structure of polymeric $\text{Pd}(\text{K-NiXantphos})_2$ illustrating the connectivity.....	145
Figure 3.5 Structure of polymeric $[\text{PdK}_2(\text{THF})_4(\text{NiXantphos})_2]_\infty$	145
Figure 3.6 (a) Points used for determination of $r_{\text{H}(\text{theo})}$ (2.376(6) Å) from the crystal structure of TMS (CSD ref = TIVWOL), (b) Points used for determination of $r_{\text{H}(\text{theo})}$ (2.790(2) Å) from the crystal structure of Fc (CSD ref = FEROCF), (c) Points used for determination of $r_{\text{H}(\text{theo})}$ (7.3295(4) Å) taken from the crystal structure of NiXantphos (CSD ref = KIXFAZ), and (d) Points used for determination of $r_{\text{H}(\text{theo})}$ (8.5945(2) Å) from the crystal structure of $\text{Pd}[\text{K}(\text{THF})_2(\text{NiXantphos})]_2$	160
Figure 3.7 (a) 2D- ^1H DOSY NMR spectrum of NiXantphos and internal	

references at 300 K in THF-d ₈ , and (b) 2D- ¹ H DOSY NMR spectrum of Pd[K(THF) ₂ (NiXantphos)] ₂ and internal references at 300 K in THF-d ₈	161
Figure A1.1 500 MHz ¹ H and 125 MHz ¹³ C{ ¹ H} NMR of 1.3a in CDCl ₃	279
Figure A1.2 500 MHz ¹ H and 125 MHz ¹³ C{ ¹ H} NMR of 1.3b in CDCl ₃	280
Figure A1.3 500 MHz ¹ H and 125 MHz ¹³ C{ ¹ H} NMR of 1.3e in CDCl ₃	281
Figure A1.4 500 MHz ¹ H and 125 MHz ¹³ C{ ¹ H} NMR of 1.3f in CDCl ₃	282
Figure A1.5 500 MHz ¹ H and 125 MHz ¹³ C{ ¹ H} NMR of 1.3d in CDCl ₃	283
Figure A1.6 500 MHz ¹ H and 125 MHz ¹³ C{ ¹ H} NMR of 1.3g in CDCl ₃	284
Figure A1.7 500 MHz ¹ H and 125 MHz ¹³ C{ ¹ H} NMR of 1.3h in CDCl ₃	285
Figure A1.8 500 MHz ¹ H and 125 MHz ¹³ C{ ¹ H} NMR of 1.3i in CDCl ₃	286
Figure A1.9 500 MHz ¹ H and 125 MHz ¹³ C{ ¹ H} NMR of 1.3c in CDCl ₃	287
Figure A1.10 500 MHz ¹ H and 125 MHz ¹³ C{ ¹ H} NMR of 1.4ad in CDCl ₃	288
Figure A1.11 500 MHz ¹ H and 125 MHz ¹³ C{ ¹ H} NMR of 1.4kd in CDCl ₃	289
Figure A1.12 500 MHz ¹ H and 125 MHz ¹³ C{ ¹ H} NMR of 1.4ld in CDCl ₃	290
Figure A1.13 500 MHz ¹ H and 125 MHz ¹³ C{ ¹ H} NMR of 1.4ke in CDCl ₃	291
Figure A1.14 500 MHz ¹ H and 125 MHz ¹³ C{ ¹ H} NMR of 1.4od in CDCl ₃	292
Figure A1.15 500 MHz ¹ H and 125 MHz ¹³ C{ ¹ H} NMR of 1.4pd in CDCl ₃	293
Figure A1.16 500 MHz ¹ H and 125 MHz ¹³ C{ ¹ H} NMR of 1.4qd in CDCl ₃	294
Figure A1.17 500 MHz ¹ H and 125 MHz ¹³ C{ ¹ H} NMR of 1.11 in CDCl ₃	295
Figure A1.18 500 MHz ¹ H and 125 MHz ¹³ C{ ¹ H} NMR of 1.7 in CDCl ₃	296
Figure A1.19 500 MHz ¹ H and 125 MHz ¹³ C{ ¹ H} NMR of 1.8 in CDCl ₃	297
Figure A1.20 500 MHz ¹ H and 125 MHz ¹³ C{ ¹ H} NMR of 1.9 in CDCl ₃	298

Figure A1.21 500 MHz ^1H and 125 MHz $^{13}\text{C}\{^1\text{H}\}$ NMR of 1.2j in CDCl_3	299
Figure A1.22 500 MHz ^1H and 125 MHz $^{13}\text{C}\{^1\text{H}\}$ NMR of 1.1b in CDCl_3	300
Figure A1.23 500 MHz ^1H and 125 MHz $^{13}\text{C}\{^1\text{H}\}$ NMR of 1.1e in CDCl_3	301
Figure A1.24 500 MHz ^1H and 125 MHz $^{13}\text{C}\{^1\text{H}\}$ NMR of 1.1f in CDCl_3	302
Figure A1.25 500 MHz ^1H and 125 MHz $^{13}\text{C}\{^1\text{H}\}$ NMR of 1.1g in CDCl_3	303
Figure A1.26 500 MHz ^1H and 125 MHz $^{13}\text{C}\{^1\text{H}\}$ NMR of 1.1i in CDCl_3	304
Figure A1.27 500 MHz ^1H and 125 MHz $^{13}\text{C}\{^1\text{H}\}$ NMR of 1.1q in CDCl_3	305
Figure A1.28 500 MHz ^1H and 125 MHz $^{13}\text{C}\{^1\text{H}\}$ NMR of 1.3'a in CDCl_3	306
Figure A1.29 500 MHz ^1H and 125 MHz $^{13}\text{C}\{^1\text{H}\}$ NMR of 1.3'c in CDCl_3	307
Figure A1.30 500 MHz ^1H and 125 MHz $^{13}\text{C}\{^1\text{H}\}$ NMR of 1.5lb in CDCl_3	308
Figure A1.31 500 MHz ^1H and 125 MHz $^{13}\text{C}\{^1\text{H}\}$ NMR of 1.5lg in CDCl_3	309
Figure A1.32 500 MHz ^1H and 125 MHz $^{13}\text{C}\{^1\text{H}\}$ NMR of 1.5ld in CDCl_3	310
Figure A1.33 500 MHz ^1H and 125 MHz $^{13}\text{C}\{^1\text{H}\}$ NMR of 1.5lf in CDCl_3	311
Figure A1.34 500 MHz ^1H and 125 MHz $^{13}\text{C}\{^1\text{H}\}$ NMR of 1.5lh in CDCl_3	312
Figure A1.35 500 MHz ^1H and 125 MHz $^{13}\text{C}\{^1\text{H}\}$ NMR of 1.5li in CDCl_3	313
Figure A1.36 500 MHz ^1H and 125 MHz $^{13}\text{C}\{^1\text{H}\}$ NMR of 1.4'qd in CDCl_3	314
Figure A1.37 500 MHz ^1H and 125 MHz $^{13}\text{C}\{^1\text{H}\}$ NMR of 1.6 in CDCl_3	315
Figure A1.38 Determination of the relative stereochemistry of 1.6	316
Figure A1.39 500 MHz ^1H and 125 MHz $^{13}\text{C}\{^1\text{H}\}$ NMR of 1.10 in CDCl_3	317
Figure A2.1 500 MHz ^1H and 125 MHz $^{13}\text{C}\{^1\text{H}\}$ NMR of 2.1l in CDCl_3	319
Figure A2.2 500 MHz ^1H and 125 MHz $^{13}\text{C}\{^1\text{H}\}$ NMR of 2.4 in CDCl_3	320
Figure A2.3 500 MHz ^1H and 125 MHz $^{13}\text{C}\{^1\text{H}\}$ NMR of 2.3aa in CDCl_3	321

Figure A2.4 500 MHz ^1H and 125 MHz $^{13}\text{C}\{^1\text{H}\}$ NMR of 2.3ba in CDCl_3	322
Figure A2.5 500 MHz ^1H and 125 MHz $^{13}\text{C}\{^1\text{H}\}$ NMR of 2.3ca in CDCl_3	323
Figure A2.6 500 MHz ^1H and 125 MHz $^{13}\text{C}\{^1\text{H}\}$ NMR of 2.3da in CDCl_3	324
Figure A2.7 500 MHz ^1H and 125 MHz $^{13}\text{C}\{^1\text{H}\}$ NMR of 2.3ea in CDCl_3	325
Figure A2.8 500 MHz ^1H and 125 MHz $^{13}\text{C}\{^1\text{H}\}$ NMR of 2.3fa in CDCl_3	326
Figure A2.9 500 MHz ^1H and 125 MHz $^{13}\text{C}\{^1\text{H}\}$ NMR of 2.3ga in CDCl_3	327
Figure A2.10 500 MHz ^1H and 125 MHz $^{13}\text{C}\{^1\text{H}\}$ NMR of 2.3ha in CDCl_3	328
Figure A2.11 500 MHz ^1H and 125 MHz $^{13}\text{C}\{^1\text{H}\}$ NMR of 2.3ij in CDCl_3	329
Figure A2.12 500 MHz ^1H and 125 MHz $^{13}\text{C}\{^1\text{H}\}$ NMR of 2.3ja in CDCl_3	330
Figure A2.13 500 MHz ^1H and 125 MHz $^{13}\text{C}\{^1\text{H}\}$ NMR of 2.3ka in CDCl_3	331
Figure A2.14 500 MHz ^1H and 125 MHz $^{13}\text{C}\{^1\text{H}\}$ NMR of 2.3la in CDCl_3	332
Figure A2.15 500 MHz ^1H and 125 MHz $^{13}\text{C}\{^1\text{H}\}$ NMR of 2.3ma in CDCl_3	333
Figure A2.16 500 MHz ^1H and 125 MHz $^{13}\text{C}\{^1\text{H}\}$ NMR of 2.3na in CDCl_3	334
Figure A2.17 500 MHz ^1H and 125 MHz $^{13}\text{C}\{^1\text{H}\}$ NMR of 2.3oa in CDCl_3	335
Figure A2.18 500 MHz ^1H and 125 MHz $^{13}\text{C}\{^1\text{H}\}$ NMR of 2.3pa in CDCl_3	336
Figure A2.19 500 MHz ^1H and 125 MHz $^{13}\text{C}\{^1\text{H}\}$ NMR of 2.3qa in CDCl_3	337
Figure A2.20 500 MHz ^1H and 125 MHz $^{13}\text{C}\{^1\text{H}\}$ NMR of 2.3ra in CDCl_3	338
Figure A2.21 500 MHz ^1H and 125 MHz $^{13}\text{C}\{^1\text{H}\}$ NMR of 2.3ab in CDCl_3	339
Figure A2.22 500 MHz ^1H and 125 MHz $^{13}\text{C}\{^1\text{H}\}$ NMR of 2.3ac in CDCl_3	340
Figure A2.23 500 MHz ^1H and 125 MHz $^{13}\text{C}\{^1\text{H}\}$ NMR of 2.3ad in CDCl_3	341
Figure A2.24 500 MHz ^1H and 125 MHz $^{13}\text{C}\{^1\text{H}\}$ NMR of 2.3ae in CDCl_3	342
Figure A2.25 500 MHz ^1H and 125 MHz $^{13}\text{C}\{^1\text{H}\}$ NMR of 2.3af in CDCl_3	343

Figure A2.26 500 MHz ^1H and 125 MHz $^{13}\text{C}\{^1\text{H}\}$ NMR of 2.3ag in CDCl_3	344
Figure A2.27 500 MHz ^1H and 125 MHz $^{13}\text{C}\{^1\text{H}\}$ NMR of 2.3ah in CDCl_3	345
Figure A2.28 500 MHz ^1H and 125 MHz $^{13}\text{C}\{^1\text{H}\}$ NMR of 2.3ai in CDCl_3	346
Figure A2.29 500 MHz ^1H and 125 MHz $^{13}\text{C}\{^1\text{H}\}$ NMR of 2.3aj in acetone- d_6	347
Figure A2.30 500 MHz ^1H and 125 MHz $^{13}\text{C}\{^1\text{H}\}$ NMR of 2.3ak in CDCl_3	348
Figure A2.31 500 MHz ^1H and 125 MHz $^{13}\text{C}\{^1\text{H}\}$ NMR of 2.3al in CDCl_3	349
Figure A2.32 500 MHz ^1H and 125 MHz $^{13}\text{C}\{^1\text{H}\}$ NMR of 2.3am in CDCl_3	350
Figure A2.33 500 MHz ^1H and 125 MHz $^{13}\text{C}\{^1\text{H}\}$ NMR of 2.3an in CDCl_3	351
Figure A2.34 500 MHz ^1H and 125 MHz $^{13}\text{C}\{^1\text{H}\}$ NMR of 2.3ao in C_6D_6	352
Figure A2.35 500 MHz ^1H and 125 MHz $^{13}\text{C}\{^1\text{H}\}$ NMR of 2.3ap in CDCl_3	353
Figure A3.1 500 MHz ^1H and 145.8 MHz $^{31}\text{P}\{^1\text{H}\}$ NMR of NiXantphos in THF- d_8	355
Figure A3.2 500 MHz ^1H and 145.8 MHz $^{31}\text{P}\{^1\text{H}\}$ NMR of NiXantphos with 1.5 equiv $\text{LiN}(\text{SiMe}_3)_2$ in THF- d_8	356
Figure A3.3 500 MHz ^1H and 145.8 MHz $^{31}\text{P}\{^1\text{H}\}$ NMR of NiXantphos with 1.5 equiv $\text{KN}(\text{SiMe}_3)_2$ in THF- d_8	357
Figure A3.4 500 MHz ^1H and 125 MHz $^{13}\text{C}\{^1\text{H}\}$ NMR of K-NiXantphos in THF- d_8	358
Figure A3.5 145.8 MHz $^{31}\text{P}\{^1\text{H}\}$ NMR of K-NiXantphos in THF- d_8	359
Figure A3.6 145.8 MHz $^{31}\text{P}\{^1\text{H}\}$ NMR of oxidative addition of chlorobenzene to $(\text{Li-NiXantphos})\text{Pd}(0)$ in THF.....	360

Figure A3.7 500 MHz ^1H and 145.8 MHz $^{31}\text{P}\{^1\text{H}\}$ NMR of $\text{Pd}(\text{K-NiXantphos})_2$ in THF- d_8	361
Figure A3.8 145.8 MHz $^{31}\text{P}\{^1\text{H}\}$ NMR of the catalyst resting state in THF after 10 min and 12 h.....	362
Figure A3.9 500 MHz ^1H and 125 MHz $^{13}\text{C}\{^1\text{H}\}$ NMR of 3.3aa in CDCl_3	363
Figure A3.10 500 MHz ^1H and 125 MHz $^{13}\text{C}\{^1\text{H}\}$ NMR of 3.3ab in CDCl_3	364
Figure A3.11 500 MHz ^1H and 125 MHz $^{13}\text{C}\{^1\text{H}\}$ NMR of 3.3ac in CDCl_3	365
Figure A3.12 500 MHz ^1H and 125 MHz $^{13}\text{C}\{^1\text{H}\}$ NMR of 3.3ad in CDCl_3	366
Figure A3.13 500 MHz ^1H and 125 MHz $^{13}\text{C}\{^1\text{H}\}$ NMR of 3.3ae in CDCl_3	367
Figure A3.14 500 MHz ^1H and 125 MHz $^{13}\text{C}\{^1\text{H}\}$ NMR of 3.3af in CDCl_3	368
Figure A3.15 500 MHz ^1H and 125 MHz $^{13}\text{C}\{^1\text{H}\}$ NMR of 3.3ag in CDCl_3	369
Figure A3.16 500 MHz ^1H and 125 MHz $^{13}\text{C}\{^1\text{H}\}$ NMR of 3.3ah in CDCl_3	370
Figure A3.17 500 MHz ^1H and 125 MHz $^{13}\text{C}\{^1\text{H}\}$ NMR of 3.3ai in CDCl_3	371
Figure A3.18 500 MHz ^1H and 125 MHz $^{13}\text{C}\{^1\text{H}\}$ NMR of 3.3aj in CDCl_3	372
Figure A3.19 500 MHz ^1H and 125 MHz $^{13}\text{C}\{^1\text{H}\}$ NMR of 3.3ak in CDCl_3	373
Figure A3.20 500 MHz ^1H and 125 MHz $^{13}\text{C}\{^1\text{H}\}$ NMR of 3.3al in CDCl_3	374
Figure A3.21 500 MHz ^1H and 125 MHz $^{13}\text{C}\{^1\text{H}\}$ NMR of 3.3am in CDCl_3	375
Figure A3.22 500 MHz ^1H and 125 MHz $^{13}\text{C}\{^1\text{H}\}$ NMR of 3.3an in CDCl_3	376
Figure A3.23 500 MHz ^1H and 125 MHz $^{13}\text{C}\{^1\text{H}\}$ NMR of 3.3ao in CDCl_3	377
Figure A3.24 500 MHz ^1H and 125 MHz $^{13}\text{C}\{^1\text{H}\}$ NMR of 3.3ap in CDCl_3	378
Figure A3.25 500 MHz ^1H and 125 MHz $^{13}\text{C}\{^1\text{H}\}$ NMR of 3.3aq in CDCl_3	379
Figure A3.26 500 MHz ^1H and 125 MHz $^{13}\text{C}\{^1\text{H}\}$ NMR of 3.3ar in CDCl_3	380

Figure A3.27 500 MHz ^1H and 125 MHz $^{13}\text{C}\{^1\text{H}\}$ NMR of 3.3as in CDCl_3	381
Figure A3.28 500 MHz ^1H and 125 MHz $^{13}\text{C}\{^1\text{H}\}$ NMR of 3.3at in CDCl_3	382
Figure A3.29 500 MHz ^1H and 125 MHz $^{13}\text{C}\{^1\text{H}\}$ NMR of 3.3au in CDCl_3	383
Figure A3.30 500 MHz ^1H and 125 MHz $^{13}\text{C}\{^1\text{H}\}$ NMR of 3.3bb in CDCl_3	384
Figure A3.31 500 MHz ^1H and 125 MHz $^{13}\text{C}\{^1\text{H}\}$ NMR of 3.3cb in CDCl_3	385
Figure A3.32 500 MHz ^1H and 125 MHz $^{13}\text{C}\{^1\text{H}\}$ NMR of 3.3db in CDCl_3	386
Figure A3.33 500 MHz ^1H and 125 MHz $^{13}\text{C}\{^1\text{H}\}$ NMR of 3.3eb in CDCl_3	387
Figure A3.34 500 MHz ^1H and 125 MHz $^{13}\text{C}\{^1\text{H}\}$ NMR of 3.3fb in CDCl_3	388
Figure A3.35 500 MHz ^1H and 125 MHz $^{13}\text{C}\{^1\text{H}\}$ NMR of 3.3ga in CDCl_3	389
Figure A3.36 500 MHz ^1H and 125 MHz $^{13}\text{C}\{^1\text{H}\}$ NMR of 3.3ha in CDCl_3	390
Figure A3.37 500 MHz ^1H and 125 MHz $^{13}\text{C}\{^1\text{H}\}$ NMR of 3.5 in CD_2Cl_2	391
Figure A3.38 145.8 MHz $^{31}\text{P}\{^1\text{H}\}$ NMR of 3.5 in CD_2Cl_2	392
Figure A3.39 400 MHz ^1H NMR of 3.4 in CD_2Cl_2	393
Figure A3.40 162.0 MHz $^{31}\text{P}\{^1\text{H}\}$ NMR of 3.4 in CDCl_3	394
Figure A4.1 500 MHz ^1H and 125 MHz $^{13}\text{C}\{^1\text{H}\}$ NMR of 4.1b in CDCl_3	396
Figure A4.2 500 MHz ^1H and 125 MHz $^{13}\text{C}\{^1\text{H}\}$ NMR of 4.1c in CDCl_3	397
Figure A4.3 500 MHz ^1H and 125 MHz $^{13}\text{C}\{^1\text{H}\}$ NMR of 4.6 in CDCl_3	398
Figure A4.4 500 MHz ^1H and 125 MHz $^{13}\text{C}\{^1\text{H}\}$ NMR of 4.3aa in CDCl_3	399
Figure A4.5 500 MHz ^1H and 125 MHz $^{13}\text{C}\{^1\text{H}\}$ NMR of 4.3ab in CDCl_3	400
Figure A4.6 500 MHz ^1H and 125 MHz $^{13}\text{C}\{^1\text{H}\}$ NMR of 4.3ac in CDCl_3	401
Figure A4.7 500 MHz ^1H and 125 MHz $^{13}\text{C}\{^1\text{H}\}$ NMR of 4.3ad in CDCl_3	402
Figure A4.8 500 MHz ^1H and 125 MHz $^{13}\text{C}\{^1\text{H}\}$ NMR of 4.3ae in CDCl_3	403

Figure A4.9	500 MHz ^1H and 125 MHz $^{13}\text{C}\{^1\text{H}\}$ NMR of 4.3af in CDCl_3	404
Figure A4.10	500 MHz ^1H and 125 MHz $^{13}\text{C}\{^1\text{H}\}$ NMR of 4.3ag in CDCl_3	405
Figure A4.11	500 MHz ^1H and 125 MHz $^{13}\text{C}\{^1\text{H}\}$ NMR of 4.3ah in CDCl_3	406
Figure A4.12	500 MHz ^1H and 125 MHz $^{13}\text{C}\{^1\text{H}\}$ NMR of 4.3ai in CDCl_3	407
Figure A4.13	500 MHz ^1H and 125 MHz $^{13}\text{C}\{^1\text{H}\}$ NMR of 4.3aj in CDCl_3	408
Figure A4.14	500 MHz ^1H and 125 MHz $^{13}\text{C}\{^1\text{H}\}$ NMR of 4.3ak in CDCl_3	409
Figure A4.15	500 MHz ^1H and 125 MHz $^{13}\text{C}\{^1\text{H}\}$ NMR of 4.3al in CDCl_3	410
Figure A4.16	500 MHz ^1H and 125 MHz $^{13}\text{C}\{^1\text{H}\}$ NMR of 4.3am in CDCl_3	411
Figure A4.17	500 MHz ^1H and 125 MHz $^{13}\text{C}\{^1\text{H}\}$ NMR of 4.3an in CDCl_3	412
Figure A4.18	500 MHz ^1H and 125 MHz $^{13}\text{C}\{^1\text{H}\}$ NMR of 4.3ao in CDCl_3	413
Figure A4.19	500 MHz ^1H and 125 MHz $^{13}\text{C}\{^1\text{H}\}$ NMR of 4.5ab in CDCl_3	414
Figure A4.20	500 MHz ^1H and 125 MHz $^{13}\text{C}\{^1\text{H}\}$ NMR of 4.5ac in CDCl_3	415
Figure A4.21	500 MHz ^1H and 125 MHz $^{13}\text{C}\{^1\text{H}\}$ NMR of 4.5ad in CDCl_3	416
Figure A4.22	500 MHz ^1H and 125 MHz $^{13}\text{C}\{^1\text{H}\}$ NMR of 4.5ae in CDCl_3	417
Figure A4.23	500 MHz ^1H and 125 MHz $^{13}\text{C}\{^1\text{H}\}$ NMR of 4.5ai in CDCl_3	418
Figure A4.24	500 MHz ^1H and 125 MHz $^{13}\text{C}\{^1\text{H}\}$ NMR of 4.5aj in CDCl_3	419
Figure A4.25	500 MHz ^1H and 125 MHz $^{13}\text{C}\{^1\text{H}\}$ NMR of 4.5al in CDCl_3	420
Figure A4.26	500 MHz ^1H and 125 MHz $^{13}\text{C}\{^1\text{H}\}$ NMR of 4.5am in CDCl_3	421
Figure A4.27	500 MHz ^1H and 125 MHz $^{13}\text{C}\{^1\text{H}\}$ NMR of 4.5an in CDCl_3	422
Figure A4.28	500 MHz ^1H and 125 MHz $^{13}\text{C}\{^1\text{H}\}$ NMR of 4.5ao in CDCl_3	423
Figure A4.29	500 MHz ^1H and 125 MHz $^{13}\text{C}\{^1\text{H}\}$ NMR of 4.3bb in CDCl_3	424
Figure A4.30	500 MHz ^1H and 125 MHz $^{13}\text{C}\{^1\text{H}\}$ NMR of 4.3db in CDCl_3	425

Figure A4.31 500 MHz ^1H and 125 MHz $^{13}\text{C}\{^1\text{H}\}$ NMR of 4.3eb in CDCl_3	426
Figure A4.32 500 MHz ^1H and 125 MHz $^{13}\text{C}\{^1\text{H}\}$ NMR of 4.3fb in CDCl_3	427
Figure A4.33 500 MHz ^1H and 125 MHz $^{13}\text{C}\{^1\text{H}\}$ NMR of 4.3'fb in CDCl_3	428
Figure A4.34 500 MHz ^1H and 125 MHz $^{13}\text{C}\{^1\text{H}\}$ NMR of 4.5bb in CDCl_3	429
Figure A4.35 500 MHz ^1H and 125 MHz $^{13}\text{C}\{^1\text{H}\}$ NMR of 4.5cb in CDCl_3	430
Figure A4.36 500 MHz ^1H and 125 MHz $^{13}\text{C}\{^1\text{H}\}$ NMR of 4.5db in CDCl_3	431
Figure A4.37 500 MHz ^1H and 125 MHz $^{13}\text{C}\{^1\text{H}\}$ NMR of 4.4aa in CDCl_3	432
Figure A4.38 500 MHz ^1H and 125 MHz $^{13}\text{C}\{^1\text{H}\}$ NMR of 4.4ab in CDCl_3	433
Figure A4.39 500 MHz ^1H and 125 MHz $^{13}\text{C}\{^1\text{H}\}$ NMR of 4.4ac in CDCl_3	434
Figure A4.40 500 MHz ^1H and 125 MHz $^{13}\text{C}\{^1\text{H}\}$ NMR of 4.4ad in CDCl_3	435
Figure A4.41 500 MHz ^1H and 125 MHz $^{13}\text{C}\{^1\text{H}\}$ NMR of 4.4ae in CDCl_3	436
Figure A4.42 500 MHz ^1H and 125 MHz $^{13}\text{C}\{^1\text{H}\}$ NMR of 4.4af in CDCl_3	437
Figure A4.43 500 MHz ^1H and 125 MHz $^{13}\text{C}\{^1\text{H}\}$ NMR of 4.4ag in CDCl_3	438
Figure A4.44 500 MHz ^1H and 125 MHz $^{13}\text{C}\{^1\text{H}\}$ NMR of 4.4ah in CDCl_3	439
Figure A4.45 500 MHz ^1H and 125 MHz $^{13}\text{C}\{^1\text{H}\}$ NMR of 4.4am in CDCl_3	440
Figure A4.46 500 MHz ^1H and 125 MHz $^{13}\text{C}\{^1\text{H}\}$ NMR of 4.4bb in CDCl_3	441
Figure A4.47 500 MHz ^1H and 125 MHz $^{13}\text{C}\{^1\text{H}\}$ NMR of 4.4cb in CDCl_3	442
Figure A4.48 500 MHz ^1H and 125 MHz $^{13}\text{C}\{^1\text{H}\}$ NMR of 4.4db in CDCl_3	443

List of Schemes

Scheme 1.1 Palladium-catalyzed benzylic allylations.....	2
Scheme 1.2 Cross-coupling of (η^6 -C ₆ H ₅ -CH ₂ Z)Cr(CO) ₃ complexes with aryl bromides.....	4
Scheme 1.3 Tandem allylic substitution/demetallation with 1.1a and 1.1c	10
Scheme 1.4 Nucleophilic addition of 1.1a to 1.2c	11
Scheme 1.5 Allylic substitution with dimethyl malonate and 1.2e	12
Scheme 1.6 Allylic substitution with benzyl amine and ether derivatives.....	17
Scheme 1.7 Gram-scale tandem allylic substitution/demetallation reaction of 1.1q	18
Scheme 1.8 Allylic substitution at multiple benzylic sites.....	19
Scheme 1.9 Allylic substitution with retention of configuration.....	20
Scheme 1.10 Asymmetric allylic substitution.....	21
Scheme 2.1 Synthetic approaches to triarylmethanes: (A) Friedel–Crafts reaction, (B) cross-coupling, and (C) non-directed C(sp ³)–H arylation (EDG=electron donating group, LG=leaving group)	67
Scheme 2.2 Cross-coupling of (η^6 -C ₆ H ₅ -CH ₂ Z)Cr(CO) ₃ complexes with aryl bromides.....	67
Scheme 2.3 Catalytic C(sp ³)–H arylations.....	69
Scheme 2.4 DCCP with activated benzylic C–H bonds.....	70
Scheme 2.5 Benzylation used as surrogate for the transmetallation step in DCCP.....	72

Scheme 2.6 Deprotonation/benzylation of diphenylmethane by KN(SiMe ₃) ₂	72
Scheme 2.7 HTE variables in Pd-catalyzed DCCP of diarylmethanes.....	73
Scheme 2.8 Gram-scale DCCP of 2.1a with 2.2a	81
Scheme 2.9 Variation of the catalyst loading in DCCP.....	81
Scheme 3.1 DCCP of diarylmethanes with aryl bromides.....	120
Scheme 3.2 Selected HTE results of the cross-coupling of 3.1a with 1-bromo-4- <i>tert</i> -butylbenzene.....	121
Scheme 3.3 Ligand exchange and recovery of NiXantphos.....	128
Scheme 3.4 Oxidative addition of chlorobenzene (3.2b) using 3.4	131
Scheme 3.5 Selected results of the cross-coupling of 3.1a with 3.2a	134
Scheme 3.6 DCCP of 3.1a with alkenyl chloride 3.2u	141
Scheme 3.7 Synthesis of Pd(K-NiXantphos) ₂	145
Scheme 3.8 Impact of the countercation on the catalytic reaction.....	146
Scheme 3.9 DCCP catalyzed by 3.5	147
Scheme 4.1 Site-selective sp ² and benzylic sp ³ C–H arylations of <i>N</i> -oxide...215	
Scheme 4.2 Countercation-controlled site-selective sp ² C3–H and sp ³ benzylic C–H arylation of furans.....	217
Scheme 4.3 C3–H arylation of furan-2-carboxamides.....	218
Scheme 4.4 Example of sp ³ benzylic C–H arylation of furan derivatives.....	218
Scheme 4.5 DCCP of diarylmethanes with aryl bromides.....	219
Scheme 4.6 Reaction of 4.1a with 4.2b under standard DCCP conditions.....	220
Scheme 4.7 Reaction pathways of benzylic and C3 arylations.....	221

Scheme 4.8 Reaction of 4.1a with 4.2b using 2 equiv of $\text{KN}(\text{SiMe}_3)_2$	222
Scheme 4.9 Deprotonation/benzylation of 4.1a using $\text{KN}(\text{SiMe}_3)_2$	226
Scheme 4.10 Isomerization of palladium intermediates.....	234
Scheme 4.11 Regioselective α -arylation of allylarenes.....	234

Chapter 1

Palladium-Catalyzed Allylic Substitution with (η^6 -Arene- CH_2Z)Cr(CO) $_3$ -based Nucleophiles

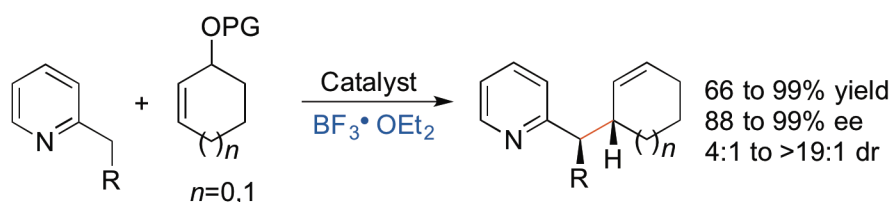
1.1 Introduction

The formation of carbon-carbon bonds represents one of the most fundamental and well-studied processes in organic synthesis. Nonetheless, the efficient catalytic generation of C–C bonds between sp^3 hybridized carbons remains challenging.¹ Although palladium-catalyzed cross-coupling reactions have received significant recent attention, an alternative approach to such C–C bond-formations is the palladium-catalyzed Tsuji–Trost allylic substitution reaction. This reaction has been intensively studied, because it provides a variety of efficient and atom-economical methods for synthesis of natural products and bioactive targets.²

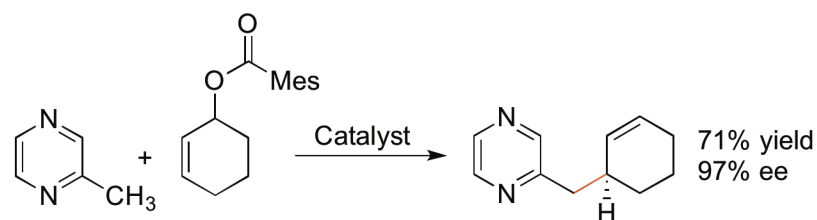
Although a broad array of stabilized or “soft” nucleophiles (those derived from conjugate acids with $\text{p}K_{\text{a}} < 25$) has been explored, palladium-catalyzed allylic substitutions with “hard” nucleophiles (derived from conjugate acids with $\text{p}K_{\text{a}} > 25$) have received considerably less attention. “Hard” nucleophiles used in palladium-catalyzed allylic substitutions are largely organometallic compounds such as alkyllithium and Grignard reagents.³ Their high reactivity and limited functional group tolerance, however, render the use of these hard nucleophiles in allylic substitution less attractive. One strategy to develop allylic substitution reactions with nucleophiles that are traditionally considered hard is to “soften” them by addition of an activating agent to acidify the conjugate acid. Recent advances based on this strategy were reported by Trost and co-workers with nucleophiles derived from 2-methylpyridines (Scheme 1.1A).⁴ The sp^3

hybridized C–H bonds of 2-methylpyridine have a pK_a of 34,⁵ and therefore its conjugate base is classified as hard. To moderate the reactivity of the conjugate base, the pyridine nitrogen was coordinated to BF_3 . The resulting BF_3 -bound complex was deprotonated and employed in palladium-catalyzed asymmetric allylic substitution with excellent enantio- and diastereoselectivity. Interestingly, no such activation was necessary with more activated benzylic C–H bonds, such as those of methylated pyrazine (Scheme 1.1B), pyrimidine, pyridazine, quinoxaline, and benzoimidazole pronucleophiles.^{4c}

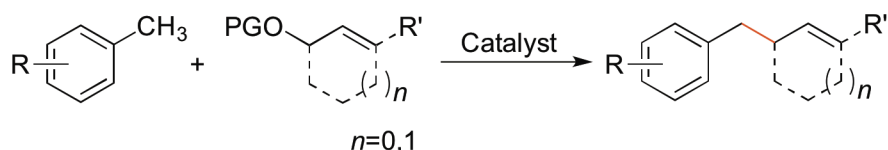
A. 2-Substituted pyridines



B. Polynitrogen-containing heterocycles



C. Our work



Scheme 1.1 Palladium-catalyzed benzylic allylations

Despite the elegance and medicinal relevance of Trost's synthesis of enantioenriched pyridine derivatives, an approach to activation of weakly acidic benzylic C–H bonds for use in allylic substitution reactions is needed. Toluene, for example, with a pK_a of 44 ± 1 ,⁶ is very weakly acidic, and the conjugate base of toluene has not been used in palladium catalyzed allylic substitution reactions (Scheme 1.1C).^{7–9} Yet

hundreds of bioactive compounds and natural products contain the “ α -2-propenyl benzyl” motif (Figure 1.1), with applications ranging from medicinal agents for hyperkalemia,¹⁰ Alzheimer's,¹¹ and urinary tract diseases,¹² to cosmetics,¹³ antibiotics¹⁴ and phytoncides¹⁵.

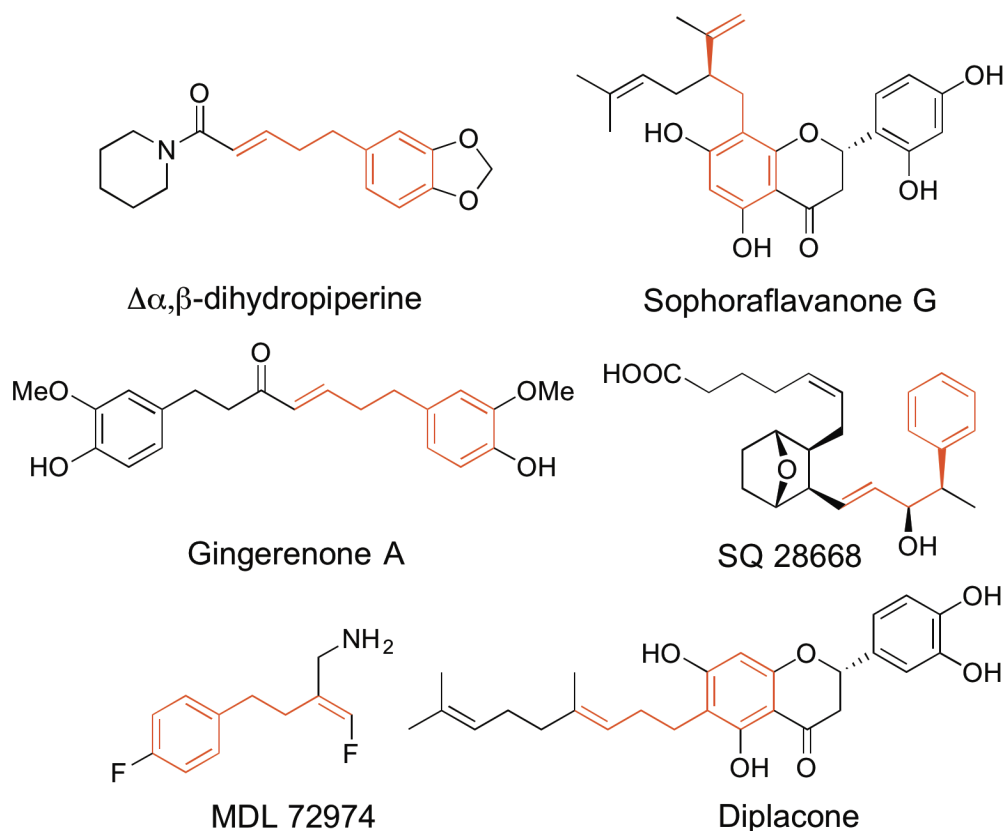


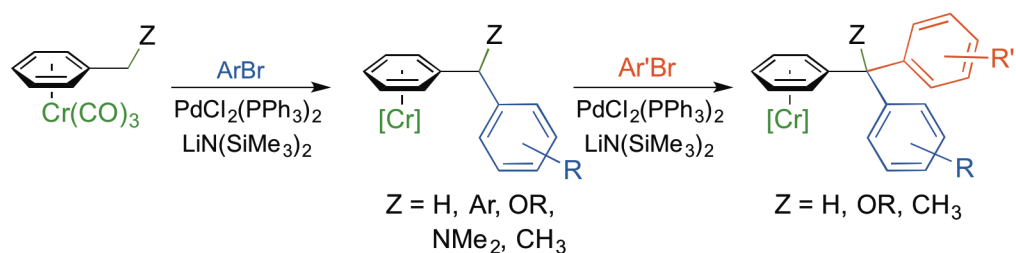
Figure 1.1 Selected bioactive compounds and natural products containing the “ α -2-propenyl benzyl” motif

To broaden the scope of useful nucleophiles for the palladium-catalyzed Tsuji–Trost reaction, we set out to develop the application of toluene derivatives as precursors to benzylic nucleophiles. To achieve this goal, conditions to deprotonate toluene derivatives that are compatible with the catalyst, reagents, and products in the allylic substitution reaction would be necessary. It is known that η^6 -coordination of arenes to

metals activates the benzylic C–H bonds toward deprotonation.^{16,17} We hypothesized that η^6 -arene complexes could be reversibly deprotonated¹⁸ under palladium catalyzed allylic substitution reaction conditions and would serve as surrogates for hard benzylic organometallic reagents. Herein we report the successful application of $(\eta^6\text{-C}_6\text{H}_5\text{-CH}_2\text{Z})\text{Cr}(\text{CO})_3$ complexes as nucleophile precursors in allylic substitution reactions (Scheme 1.1C). This method enables the synthesis of a variety of valuable aryl-containing compounds that would be otherwise difficult to access.

1.2 Results and Discussion

We recently disclosed the palladium–triphenylphosphine-catalyzed cross-coupling of $(\eta^6\text{-C}_6\text{H}_5\text{-CH}_2\text{Z})\text{Cr}(\text{CO})_3$ complexes with aryl bromides in the presence of $\text{LiN}(\text{SiMe}_3)_2$ to afford a broad range of di- and triarylmethanes (Scheme 1.2).¹⁸ The $\text{Cr}(\text{CO})_3$ fragment is easily installed simply by refluxing the arene with $\text{Cr}(\text{CO})_6$. After the coupling reaction, decomplexation of the chromium moiety is performed by exposure of the solution of the chromium-arene complex to room light and air. On the basis of this study, we hypothesized that $(\eta^6\text{-C}_6\text{H}_5\text{-CH}_2\text{Z})\text{Cr}(\text{CO})_3$ complexes might be suitable substrates in palladium-catalyzed allylic substitution reactions.



Scheme 1.2 Cross-coupling of $(\eta^6\text{-C}_6\text{H}_5\text{-CH}_2\text{Z})\text{Cr}(\text{CO})_3$ complexes with aryl bromides

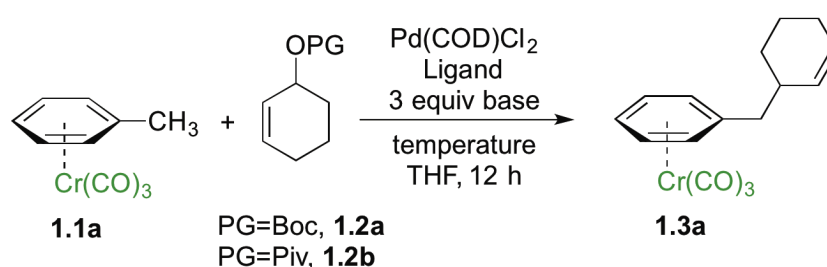
1.2.1 Development and Optimization of Palladium-Catalyzed Allylic Substitution with $(\eta^6\text{-C}_6\text{H}_5\text{-CH}_3)\text{Cr}(\text{CO})_3$ ⁱ

Given that the cross-coupling of $(\eta^6\text{-C}_6\text{H}_5\text{-CH}_3)\text{Cr}(\text{CO})_3$ with aryl bromides was successfully catalyzed by palladium–triphenylphosphine complexes, which also catalyze allylic substitutions,¹⁹ we initially examined the allylic substitution reaction with the same catalyst and base. Combination of the toluene complex $(\eta^6\text{-C}_6\text{H}_5\text{-CH}_3)\text{Cr}(\text{CO})_3$ (**1.1a**) with *tert*-butyl cyclohex-2-enyl carbonate (**1.2a**) as the electrophilic partner, LiN(SiMe₃)₂ to reversibly deprotonate the toluene complex **1.1a** and THF solvent was performed. Heating the reaction mixture to 60 °C in THF resulted in only trace amounts of product **1.3a** after 12 h (Table 1.1, entry 1). We then turned to microscale high-throughput experimentation (HTE) techniques²⁰ to identify an initial catalyst lead. Using 12 diverse phosphine ligands, 4 palladium precursors and 4 bases (see Section 1.4 Experimental Section for details) revealed that the combination of 10 mol % Pd(COD)Cl₂ and Xantphos with 3 equiv LiN(SiMe₃)₂ in THF at 60 °C was the most promising combination of those examined for conversion of **1.1a** to the corresponding allylic substitution product **1.3a**. Translation of this lead to laboratory scale (0.1 mmol) under the same conditions afforded **1.3a** in 39% yield (entry 2). Decreasing the reaction temperature from 60 °C to ambient temperature and further to 0 °C indicated that conducting the reaction above or below ambient temperature (24 °C) proved deleterious to the yield (entries 2–4) and ambient temperature was optimal (entry 3). Combination of 1 equiv of the stronger bases LDA or *n*-BuLi with 3 equiv of LiN(SiMe₃)₂ to favor deprotonation of **1.1a** resulted in poor yields (entries 5–6).

ⁱ HTE screens in this section were run in collaboration with Dr. Corneliu Stanciu at Penn/Merck Laboratory for High-Throughput Experimentation.

A key variable in optimizing organolithium reactions is the degree of aggregation.²¹ To reduce the degree of aggregation, a single equiv of NEt₃ was added in combination with 3 equiv of LiN(SiMe₃)₂. With this mixture, **1.3a** was formed in >95% yield (entry 7). Under these conditions, catalyst loading could be reduced to 5 mol % (entry 8). Switching the allylic partner from the carbonate **1.2a** to the pivalate **1.2b** also resulted in excellent isolated yield (96%, entry 9). The structure of **1.3a** was determined by X-ray diffraction (Figure 1.2) and is consistent with allylic substitution outlined in Table 1. Using these optimized conditions, we then examined various ($\eta^6\text{-C}_6\text{H}_5\text{-CH}_2\text{Z}$)Cr(CO)₃ complexes as nucleophile precursors.

Table 1.1 Optimization of allylic substitution with **1.1a**^a



Entry	PG	mol %	ligand	base	temp (°C)	yield ^b (%)
1	Boc (1.2a)	10	PPh ₃	LiN(SiMe ₃) ₂	60	Trace
2	Boc	10	Xantphos	LiN(SiMe ₃) ₂	60	39
3	Boc	10	Xantphos	LiN(SiMe ₃) ₂	24	72
4	Boc	10	Xantphos	LiN(SiMe ₃) ₂	0	39
5	Boc	10	Xantphos	LiN(SiMe ₃) ₂ /LDA ^d	24	29
6	Boc	10	Xantphos	LiN(SiMe ₃) ₂ / ⁿ BuLi ^d	24	<10
7	Boc	10	Xantphos	LiN(SiMe ₃) ₂ /NEt ₃ ^e	24	>95

8	Boc	5	Xantphos	LiN(SiMe ₃) ₂ /NEt ₃ ^e	24	88 ^c
9	Piv (1.2b)	5	Xantphos	LiN(SiMe ₃) ₂ /NEt ₃ ^e	24	96 ^c

^aReactions conducted on a 0.1 mmol scale using 1 equiv of **1.1a** and 2 equiv of **1.2** at 0.1 M. ^bYield determined by ¹H NMR spectroscopy of the crude reaction mixture. ^cIsolated yield after chromatographic purification. ^dMixed bases of 3 equiv of LiN(SiMe₃)₂ and 1 equiv of LDA (or ⁿBuLi). ^eAmine additive (1 equiv) treated with 3 equiv of LiN(SiMe₃)₂.

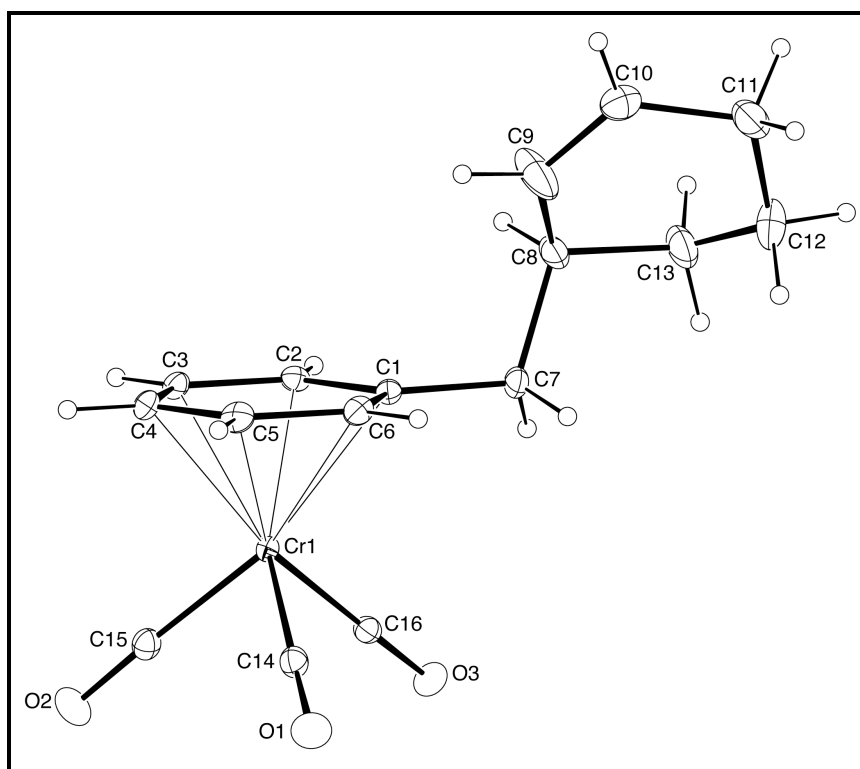


Figure 1.2 ORTEP drawing of **1.3a** with 30% probability thermal ellipsoids

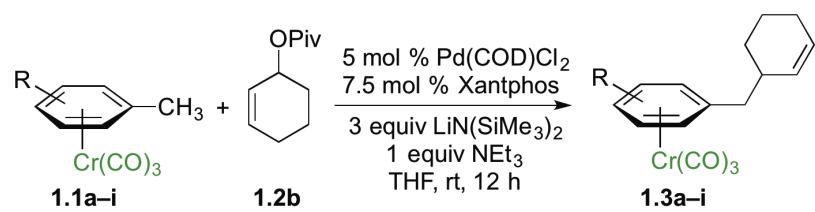
1.2.2 Scope of Nucleophiles in Palladium-Catalyzed Allylic Substitution Reactions

Employing the optimized conditions with the pivalate ester **1.2b** (Table 1.1, entry 9) the scope of the (η^6 -Ar-CH₃)Cr(CO)₃ pronucleophiles in the allylic substitution

reaction was evaluated (Table 1.2). In addition to the toluene complex **1.1a** (Table 1.2, entry 1), use of $(\eta^6\text{-Ar-CH}_3)\text{Cr}(\text{CO})_3$ complexes bearing various substituents on the η^6 -arene were well tolerated. Although the *p*-isopropyl-substituted arene was a good substrate (entry 2, 89% yield), *p*-methylanisole gave only trace product. In contrast, the *meta* isomer underwent allylic substitution in 80% yield (entry 3). The difference between these isomeric substrates is likely due to the decreased acidity of the benzylic C–H bonds *para* to the methoxy group. Aryl substituents on the η^6 -arene were good substrates. To highlight the increase in reactivity of $(\eta^6\text{-tolyl})\text{Cr}(\text{CO})_3$ compared with an unactivated tolyl group, the 4,4'-dimethylbiphenyl complex was employed. This substrate underwent allylic substitution exclusively at the chromium-activated position (entry 4, 90% yield). Although the $\text{Cr}(\text{CO})_3$ moiety is known to “walk” between neighboring arenes at high temperature,²² only the monoallylation product was observed under our conditions, indicating that walking did not occur. Heteroaryl substrates containing 2-pyridyl, 2-thiophenyl, and *N*-pyrrolyl groups attached to the η^6 -tolyl group proved to be good substrates (entries 5–7, 74–80% yield). Heteroaromatic compounds are well known for their utility in medicinal chemistry.

Notably, $(\eta^6\text{-}p\text{-chlorotoluene})\text{Cr}(\text{CO})_3$ complex participated in the allylic substitution to furnish the product in 45% yield (entry 8). Surprisingly, no products derived from oxidative addition of $(\eta^6\text{-}p\text{-chlorotoluene})\text{Cr}(\text{CO})_3$ (Ar-Cl) to palladium were observed, although η^6 -coordination is known to facilitate oxidative addition of chloroarene complexes.²³ The chloro-substituted biphenyl derivative underwent allylic substitution to give the chloro-containing product in 71% yield (entry 9).

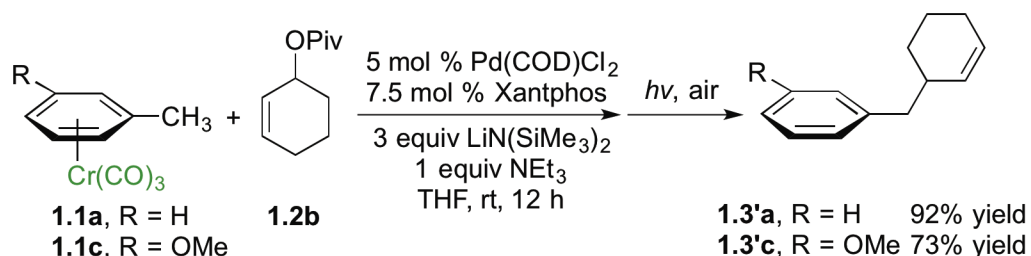
Table 1.2 Scope of nucleophiles in allylic substitution reactions^a



Entry	Product	Compound	Yield (%)
1		1.3a	96 ^b
2		1.3b	89 ^b
3		1.3c	80 ^b
4		1.3d	90 ^b
5		1.3e	77 ^b
6		1.3f	80 ^b
7		1.3g	74 ^b
8		1.3h	45 ^{b,c}
9		1.3i	71 ^b

^aReactions conducted on a 0.1 mmol scale using 1 equiv of **1.1a–i** and 2 equiv of **1.2b** at 0.1 M. ^bIsolated yield after chromatographic purification. ^cReaction time was 1.5 h.

The (η^6 -arene)Cr(CO)₃ allylic substitution product in Table 1.2 could be used in a variety of subsequent transformations facilitated by the chromium.¹⁷ However, the chromium-free complexes are often the desired products. Arene complexes of the type (η^6 -arene)Cr(CO)₃ can be decomplexed simply by exposure to light and air to afford the corresponding arenes. To demonstrate the synthetic utility of this chemistry, a tandem allylic substitution/demetallation procedure was examined. With the (η^6 -toluene)Cr(CO)₃ and 3-methoxy analogue, the allylic substitution was performed to generate the new arene complex, as outlined in Scheme 1.3. The reaction mixture was then exposed to light and air by removing the septum and placing the reaction vessel on a stir plate on the windowsill. After stirring for 3–6 h under light and air, the demetallated products were isolated in 92% (**1.3'a**) and 73% (**1.3'c**) yield.

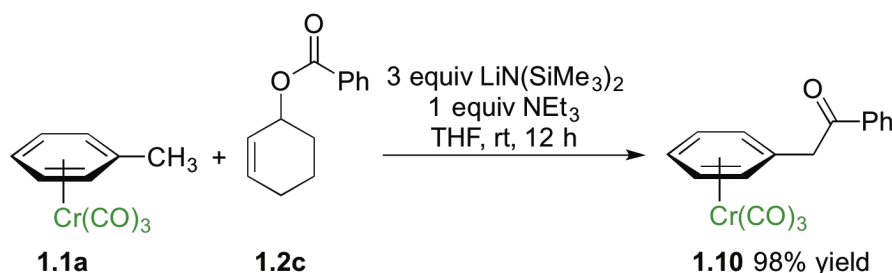


Scheme 1.3 Tandem allylic substitution/demetallation with **1.1a** and **1.1c**

1.2.3 Scope of Electrophiles in Palladium-Catalyzed Allylic Substitution Reactions

We next studied the impact of the leaving group on the allylic substitution (Table 1.3). Varying the leaving group on 2-cyclohexen-1-ol from Boc (**1.2a**) to pivalate (**1.2b**) and benzoate esters (**1.2c**) resulted in 87–96% isolated yields of the allylic substitution product **1.3a** (Table 1.3, entries 1–3). Although the pivalate ester resulted in the highest

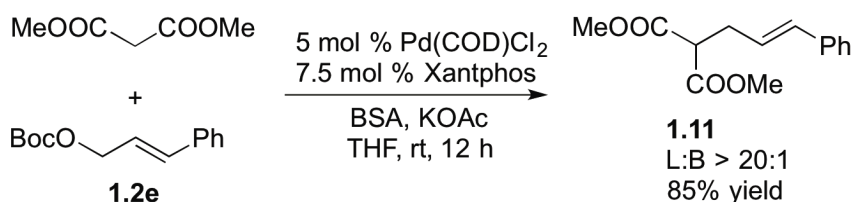
yield, these results indicate that the reaction with this substrate class is tolerant of the nature of the leaving group. The reaction of **1.1a** with **1.2c** *in the absence of* Pd(COD)Cl₂/Xantphos was performed as a control experiment (Scheme 1.4). Instead of formation of the allylic substitution product **1.3a**, PhC(O)CH₂-(η^6 -C₆H₅)Cr(CO)₃ (**1.10**) was isolated in 98% yield as the exclusive product, which was formed from nucleophilic addition to the carbonyl group of **1.2c**. This result indicates that palladium–Xantphos-based catalyst changes the chemoselectivity of the reaction from carbonyl addition to allylic substitution.



Scheme 1.4 Nucleophilic addition of **1.1a** to **1.2c**

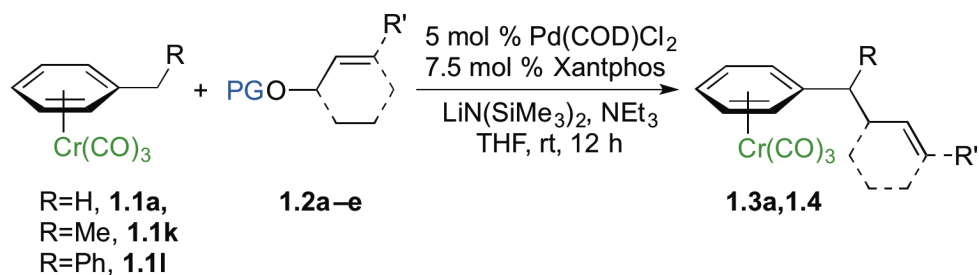
We next examined acyclic electrophiles as partners in the allylic substitution. The Boc derivative of allyl alcohol, **1.2d**, reacted with various (η^6 -arene)Cr(CO)₃ complexes to yield substitution products (Table 1.3, entries 4–6). Reaction of the (η^6 -toluene)Cr(CO)₃ complex with **1.2d** resulted in formation of the diallylation product **1.4ad** (81% yield) when 1 equiv of **1.1a** was treated with 6 equiv of LiN(SiMe₃)₂, 4 equiv of **1.2d**, and 2 equiv of *N,N,N',N'',N'''*-pentamethyldiethylenetriamine (PMDTA) as additive in place of NEt₃. When (η^6 -arene)Cr(CO)₃ complexes derived from ethylbenzene (**1.1k**) and diphenylmethane (**1.1l**) were reacted with **1.2d**, the monoallylation products were obtained in 86% (**1.4kd**) and 91% (**1.4ld**) yields (entries 5 and 6, respectively).

With unsymmetrical linear electrophiles derived from Boc-protected cinnamyl alcohol (**1.2e**), full consumption of (η^6 -ethylbenzene)Cr(CO)₃ (**1.1k**) was observed. It is well known that π -allylpalladium complexes formed from cinnamyl alcohol derivatives tend to react with carbon-based nucleophiles at the unsubstituted terminus of the π -allyl group for both steric and electronic reasons.^{16b} Surprisingly, however, the allylic substitution product was obtained as a mixture of regioisomers at ambient temperature with a linear:branched ratio (L:B) of 77:23 (as determined by ¹H NMR of the crude reaction mixture, entry 7). Regioselectivity in palladium-catalyzed allylic substitution reactions can be influenced by the nature of the ligands,²⁴ solvent, and counterion.²⁵ For the purpose of comparison, we employed the stabilized nucleophile derived from dimethyl malonate under the same reaction conditions with the Xantphos-based palladium catalyst (Scheme 1.5). In this case, the linear product **1.11** was obtained with excellent regioselectivity (linear:branched > 20:1, 85% yield).²⁶ We hypothesize that the reduced regioselectivity with the nucleophile generated from (η^6 -ethylbenzene)Cr(CO)₃ (**1.1k**) is a result of the high reactivity of the Cr(CO)₃-stabilized organolithium, which led to lower selectivity. We therefore conducted the reaction at 0 °C and observed an increase in the linear:branched ratio to 85:15 (entry 8). The linear product was separated from the branched by column chromatography and isolated in 75% yield.



Scheme 1.5 Allylic substitution with dimethyl malonate and **1.2e**

Table 1.3 Scope of electrophiles in allylic substitution reactions^a



Entry	Electrophile	R	Product	Yield
1	PG = Boc (1.2a)	H		88% ^b
2	PG = Piv (1.2b)	H		1.3a 96% ^b
3	PG = Bz (1.2c)	H		87% ^b
4	 1.2d	H		1.4ad 81% ^{b,c}
5		Me		1.4kd 86% ^{b,c}
6		Ph		1.4ld 91% ^{b,c}
7	 1.2e	Me		1.4ke L:B = 77:23 ^{c,d} L: 71% yield ^{b,e}
8		Me		L:B = 85:15 ^{c,d} L: 75% yield ^{b,e}

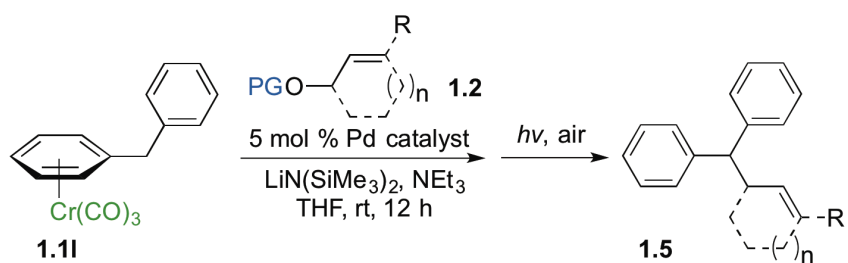
^aReactions conducted on a 0.1 mmol scale using 1 equiv of **1.1**, an excess of LiN(SiMe₃)₂ and **1.2** at 0.1 M. ^bIsolated yield after chromatographic purification. ^cPMDTA was added as an amine additive in place of NEt₃. ^dRatio of linear:branched (L:B) was determined by ¹H NMR of the crude reaction mixture. ^eThe regioisomers were separable by silica gel chromatography.

1.2.4 Tandem Allylic Substitution/Demetallation with Diphenylmethane Derivatives

Diarylmethane derivatives are attracting considerable attention due to their growing importance in developing pharmaceuticals,²⁷ dye precursors,²⁸ and applications in materials science.²⁹ Given the utility of these compounds, we investigated palladium-catalyzed allylic substitutions with (η^6 -C₆H₅CH₂Ph)Cr(CO)₃ (**1.1I**) with a variety of cyclic and acyclic allylic partners. The reaction mixtures were then exposed to light and air to afford metal-free diphenylmethane derivatives in a one-pot tandem fashion (Table 1.4).

We initiated our study employing the cyclohex-2-enyl pivalate **1.2b**. The allylic substitution was performed in THF with 1 equiv of (η^6 -C₆H₅CH₂Ph)Cr(CO)₃ (**1.1I**), 2 equiv of pivalate **1.2b** and 3 equiv of LiN(SiMe₃)₂ (entry 1). When the allylic substitution was complete, as judged by TLC, the flask was opened to air and placed on a stir plate on the windowsill to expose the reaction mixture to sunlight. A green precipitate formed during the demetallation as the chromium was oxidized. The reaction mixture was then filtered through a pad of MgSO₄ and silica, concentrated in vacuo and loaded directly onto a silica gel column. The metal-free product **1.5Ib** was isolated as clear oil in 96% yield after column chromatography. The reaction of *tert*-butyl cyclopent-2-enyl carbonate (**1.2g**) was performed under similar conditions and provided the substitution product in 89% yield (**1.5Ig**, entry 2).

Table 1.4 Tandem synthesis of diphenylmethane derivatives^a



Entry	Electrophile	Product	Yield (%)
1	1.2b		1.5b 96 ^b
2	1.2g		1.5lg 89 ^b
3	1.2d		1.5ld 91 ^b
4	1.2f		1.5lf 96 ^{b,d}
5	1.2h		1.5lh 77 ^{b,d} <i>cis:trans</i> = 2:1
6	1.2i	 	1.5li 73% ^b <i>linear product</i> 1.5li' <i>Crude product</i> 1.5li:1.5li' = 78:22 ^c

^aReactions conducted on a 0.1 mmol scale using 1 equiv of **1.1i**, an excess of LiN(SiMe₃)₂ and **1.2** at 0.1 M. ^bIsolated yield after chromatographic purification. ^c Ratio of linear:branched (L:B) was determined by ¹H NMR of the crude reaction mixture. The regioisomers were separable by silica gel chromatography. ^d[Pd(allyl)Cl]₂/1,3-bis(diphenylphosphino)propane (DPPP) was used as catalyst in place of Pd(COD)Cl₂/Xantphos.

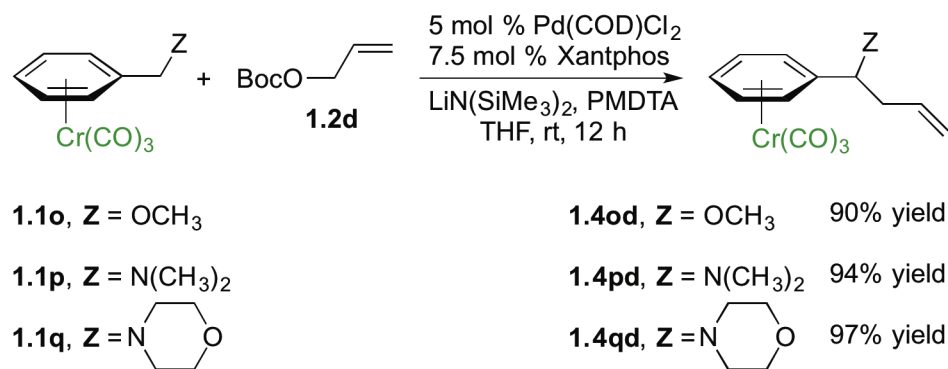
Acyclic allylic alcohol derivatives were also good substrates in the allylic substitution/demetallation tandem reaction. Use of **1.2d** resulted in isolation of the substitution product in 91% yield (**1.5id**, entry 3). Note that the reaction of diphenylmethane [Cr(CO)₃-free] with allylic partners did not give substitution products, underscoring the necessity of the activating Cr(CO)₃ agent. *trans*-1,3-Diphenylallyl acetate (**1.2f**) underwent the allylic substitution/demetallation to give **1.5if** in 96% isolated yield (entry 4). Reaction of **1.1i** with a bifunctional substrate, *cis*-1,4-diacetoxy-2-butene (**1.2h**), gave 77% isolated yield (88% per C–C bond formation) of the diallylation product **1.5ih** as an *E/Z* ratio of 1:2 (entry 5).³⁰

Evaluation of π -geranyl palladium complex was motivated by the recent isolation of several α -geranylated toluene derivatives.³¹ Furthermore, α -geranylated toluene derivatives have shown interesting bioactive properties³² and are key intermediates in total synthesis of antibiotics.³³ Addition of the organolithium derived from (η^6 -C₆H₅CH₂Ph)Cr(CO)₃ (**1.1i**) to *tert*-butyl geranyl carbonate complex **1.2i** exhibited good regioselectivity (L:B = 78:22) and good isolated yield of the linear product **1.5li** (73% yield, entry 6). The carbon–carbon double bond of the products in Table 1.4 will facilitate subsequent functionalizations to afford a variety of diphenylmethane derivatives.

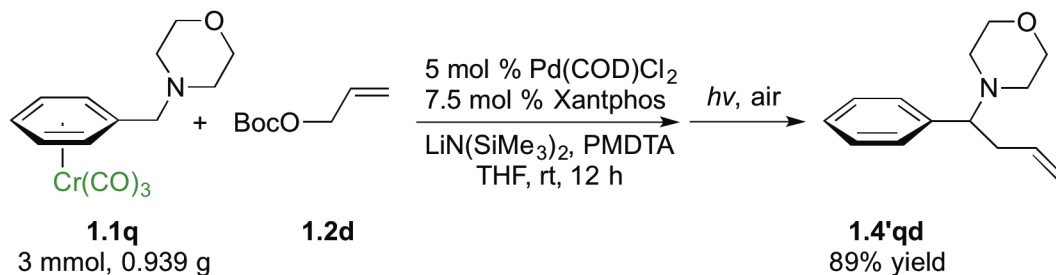
1.2.5 Allylic Substitution with Benzyl Amine and Ether Derivatives

Stereogenic centers α to heteroatoms are important in the synthesis of bioactive compounds. We therefore examined reactions of benzyl ether and amine substrates (η^6 -C₆H₅-CH₂Z)Cr(CO)₃ (Z = OR, NR₂). Benzylamines often direct metallation to the *ortho* position³⁴ as do activated (η^6 -C₆H₅-CH₂Z)Cr(CO)₃ complexes in the presence of strong organolithium bases (Z = NR₂). Interestingly, under the reversible deprotonation conditions employed herein, (η^6 -C₆H₅-CH₂Z)Cr(CO)₃ complexes exhibit orthogonal chemoselectivity with metallation taking place at the benzylic C–H bonds. As illustrated in Scheme 1.6, the (η^6 -C₆H₅-CH₂Z)Cr(CO)₃ benzyl ether (**1.1o**) and amines (**1.1p**, **1.1q**) are excellent substrates for the allylic substitution reaction with allyl *tert*-butyl carbonate **1.2d**, giving products in excellent yields (90–97%).

The scalability of this method was demonstrated by a tandem allylic substitution/demetallation reaction of 4-benzylmorpholine (**1.1q**) on a 3 mmol scale, which afforded the metal-free organic product in 89% yield (Scheme 1.7).



Scheme 1.6 Allylic substitution with benzyl amine and ether derivatives

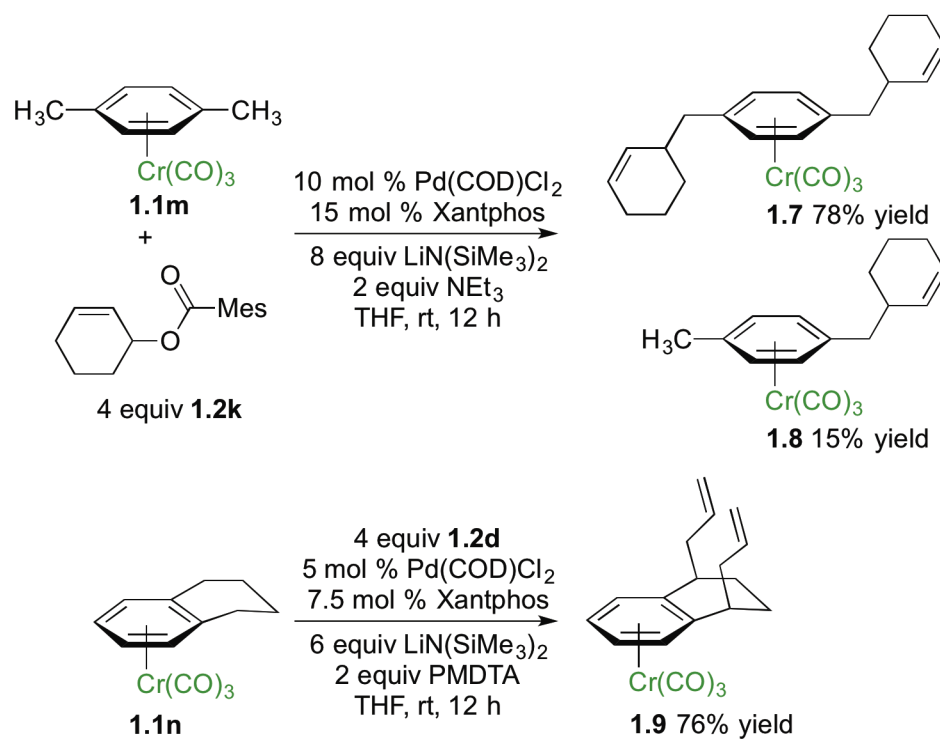


Scheme 1.7 Gram-scale tandem allylic substitution/demetallation reaction of **1.1q**

1.2.6 Allylic Substitution at Multiple Benzylic Sites

Having demonstrated that diallylation could occur on a single benzylic methyl group (Table 1.3, entry 4), we explored the possibility of activation of multiple benzylic positions in (η^6 -arene)Cr(CO)₃ complexes of *p*-xylene and tetralin (Scheme 1.8). Subjecting (η^6 -*p*-xylene)Cr(CO)₃ (**1.1m**) to allylic substitution conditions with a sterically hindered allylic partner, cyclohex-2-enyl mesitoate (**1.2k**), furnished the diallylation product **1.7** in 78% isolated yield, along with 15% yield of the monoallylation product **1.8**.

In the case of (η^6 -tetralin)Cr(CO)₃ (**1.1n**) we were somewhat concerned that after the first allylic substitution, the newly formed 2-propenyl moiety would hinder deprotonation of the second benzylic center by the bulky base, LiN(SiMe₃)₂. As shown in Scheme 1.8, however, the diallylation proceeded smoothly at ambient temperature and the *cis*-diallylation product **1.9** was isolated in 76% yield.^{17,18} Presumably this approach could be coupled with ring closing metathesis to afford bicyclic scaffolds.



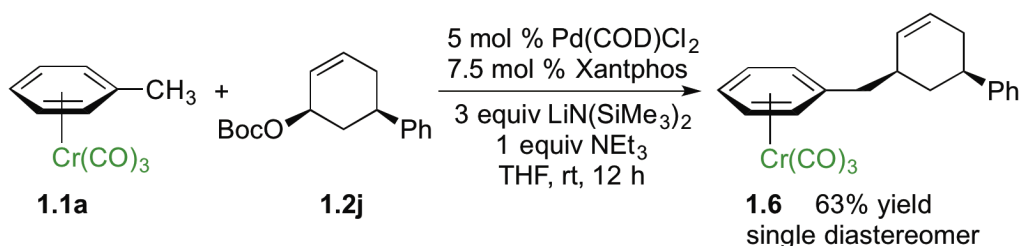
Scheme 1.8 Allylic substitution at multiple benzylic sites

1.2.7 Internal vs External Attack of ($\eta^6\text{-Ar-CH}_2\text{Li}$)Cr(CO)₃ on π -Allyl Palladium Intermediate

One significant difference between “hard” and “soft” nucleophiles in allylic substitution reactions is their distinct mechanistic pathways. Nucleophiles classified as “soft” undergo external attack on the π -allyl ligand,³⁵ and the net process of the allylic substitution is stereoretentive (via double inversion). In contrast, “hard” nucleophiles undergo addition to the metal center of the π -allyl complex (i.e., transmetalation) followed by reductive elimination to form the new C–C bond.³⁶ This latter mechanism results in an overall inversion of configuration in the allylic substitution.

To determine whether the conjugate bases of the ($\eta^6\text{-arene}$)Cr(CO)₃ complexes behave as “soft” or “hard” nucleophiles in the palladium catalyzed allylic substitution, ($\eta^6\text{-$

toluene) $\text{Cr}(\text{CO})_3$ complex **1.1a** was reacted with the *cis*-disubstituted stereochemical probe **1.2j** (Scheme 1.9). In the allylic substitution with **1.2j** the product *cis*-**1.6** was obtained in 63% isolated yield as a single diastereomer, as determined by comparison of the splitting patterns and coupling constants with related products by ^1H NMR spectroscopy. Formation of *cis*-**1.6** indicates that the reaction occurs predominantly via external attack of the “soft” conjugate base derived from $(\eta^6\text{-toluene})\text{Cr}(\text{CO})_3$ on the palladium-bound π -allyl ligand. The observed double inversion is consistent with the ability of the $\text{Cr}(\text{CO})_3$ moiety to stabilize benzyl anions by delocalization of the negative charge onto the chromium to “soften” the organolithium.^{16,17}



Scheme 1.9 Allylic substitution with retention of configuration

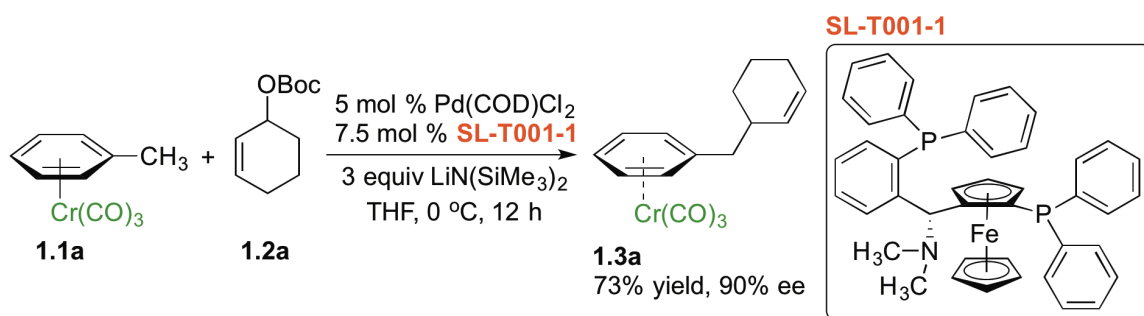
1.2.8 Asymmetric Allylic Substitution with $(\eta^6\text{-C}_6\text{H}_5\text{-CH}_3)\text{Cr}(\text{CO})_3$ ⁱⁱ

Trost ligands have proved successful in a range of asymmetric allylic substitution reactions of cycloalkenyl substrates.² We employed (*R,R*)-DACH-phenyl Trost ligand in place of Xantphos as ligand for the reaction of **1.1a** with the benzoate ester **1.2c**. However, no desired allylic substitution product was observed. $\text{PhCOCH}_2\text{-}(\eta^6\text{-C}_6\text{H}_5)\text{Cr}(\text{CO})_3$ was isolated in 96% yield as the exclusive product. We then switched the

ⁱⁱ HTE screens in this section were run in collaboration with Dr. Ana Bellomo at Penn/Merck Laboratory for High-Throughput Experimentation.

allylic partner from **1.2c** to carbonate **1.2a**, but we did not observe any desired allylic substitution product from either (*R,R*)-DACH-phenyl Trost ligand or (*R,R*)-DACH-naphthyl Trost ligand under the reaction conditions.

The reaction of **1.1a** with **1.2a** was employed in the HTE approach with a large library of enantioenriched mono- and bidentate phosphine ligands to identify catalysts for asymmetric allylic substitution reactions with (η^6 -C₆H₅-CH₂Z)Cr(CO)₃ complexes (see Section 1.4 Experimental Section for a full list of 192 chiral ligands screened). SL-T001-1, from the Taniaphos ligand family, showed the excellent enantioselectivity (90% ee, Scheme 1.10).



Scheme 1.10 Asymmetric allylic substitution

1.3 Conclusions

We have developed the first general method for palladium-catalyzed allylic substitution with the conjugate bases of toluene derivatives. Key to the success of our method is the activation of the arene's benzylic C–H bonds by η^6 -coordination to tricarbonylchromium. Also very important was the HTE approach to identify the Xantphos/Pd(COD)Cl₂ combination as an excellent catalyst for this allylic substitution reaction. Mechanistic studies indicate that (η^6 -toluene)Cr(CO)₃ derivatives behave as “soft” or stabilized nucleophiles. They attack the palladium π -allyl complex externally, leading to a net double inversion in the allylic substitution. The (η^6 -arene)Cr(CO)₃

derivatives are reversibly deprotonated by $\text{LiN}(\text{SiMe}_3)_2$ under mild conditions, allowing the in situ generation of the nucleophilic organolithium intermediates.

The synthetic significance of this method is that it enables the application of a variety of benzylic nucleophiles in palladium catalyzed allylic substitution reactions and provides access to allylic substitution products that are otherwise difficult to prepare. The method is general in that a range of nucleophiles, derived from $(\eta^6\text{-arene})\text{Cr}(\text{CO})_3$ complexes, can be readily employed with structurally diverse allylic alcohol derivatives bearing OAc, OBz, OBoc, or OPiv leaving groups. A tandem allylic substitution/demetallation procedure has been developed for the one-pot synthesis of diarylmethane derivatives, which are increasing in their importance. An HTE survey of a large library of enantioenriched mono- and bidentate phosphine ligands has revealed that the SL-T001-1/ $\text{Pd}(\text{COD})\text{Cl}_2$ combination was as an excellent catalyst for asymmetric allylic substitution reactions. We believe this method will be a valuable complement to the existing arsenal of nucleophiles with applications in allylic substitution reactions.

1.4 Experimental Section

General Methods. All reactions were performed under nitrogen using oven-dried glassware and standard Schlenk or vacuum line techniques. Air- and moisture sensitive solutions were handled under nitrogen and transferred via syringe. THF was freshly distilled from Na/benzophenone ketyl under nitrogen. Unless otherwise stated, reagents were commercially available and used as purchased without further purification. Chemicals were obtained from Sigma-Aldrich or Acros, and solvents were purchased from Fisher Scientific. The progress of all reactions was monitored by thin-layer chromatography using Whatman Partisil K6F 250 μm precoated 60 Å silica gel plates and visualized by short-wave ultra-violet light as well as by treatment with ceric

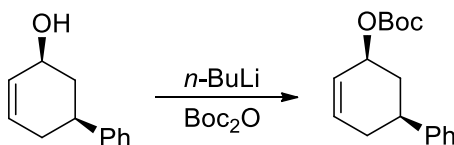
ammonium molybdate (CAM) stain. Silica gel (230–400 mesh, Silicycle) was used for flash chromatography. The ^1H NMR and $^{13}\text{C}\{^1\text{H}\}$ NMR spectra were obtained using a Brüker AM-500 Fourier-transform NMR spectrometer at 500 and 125 MHz, respectively. Chemical shifts are reported in units of parts per million (ppm) downfield from tetramethylsilane (TMS) and all coupling constants are reported in hertz. The infrared spectra were obtained on KBr using a Perkin-Elmer Spectrum 100 Series FTIR spectrometer. The masses of chromium-complexes were recorded with electrospray + (ES+) HRMS methods, and $[\text{M}]^+$ or $[\text{M} - (\text{CO})_3]^+$ (unless otherwise stated) was confirmed by the presence of the characteristic chromium isotope pattern. Chromium-decomplexed masses were recorded with chemical ionization + (CI+) HRMS methods.

Cautionary Note. Care should be taken to avoid direct bright light exposure of reactions, as arene tricarbonylchromium complexes can decompose in solution under bright light and air.

Preparation of Allylic Electrophiles.

Compounds **1.2a**³⁷, **1.2b**³⁸, **1.2c**³⁹, **1.2d**⁴⁰, **1.2e**⁴¹, **1.2f**⁴², **1.2g**³⁷, **1.2i**⁴³, and **1.2k**⁴⁴ were prepared according to literature procedures.

1.2j – (*rac*)-*cis*-*tert*-butyl (5-phenyl-2-cyclohexenyl) carbonate



n-BuLi (2.2 mL of a 2.5 M solution in hexanes) was added to a solution of (*rac*)-*cis*-5-phenyl-2-cyclohexen-1-ol⁴⁵ (0.906 g, 5.20 mmol) in THF (4 mL) at $-78\text{ }^\circ\text{C}$. The mixture was warmed and stirred for 15 min at $0\text{ }^\circ\text{C}$ before di-*tert*-butyl dicarbonate (1.135 g, 5.20

mmol) in THF (1.5 mL) was added. The resulting solution was stirred for 12 h at rt, quenched with saturated aqueous NaHCO₃, and then diluted with 75 mL of EtOAc. The layers were separated and the organic layer was extracted with H₂O (3 x 15 mL), washed with brine, dried over MgSO₄, filtered, and concentrated in vacuo. Silica gel chromatography using 5% to 10% CH₂Cl₂/hexanes afforded 1.166 g (82% yield) of the desired compound as a colorless oil. TLC R_f = 0.45 (CH₂Cl₂/hexanes = 1:4); ¹H NMR (500 MHz, CDCl₃): δ 7.35 – 7.18 (m, 5H), 5.92 (m, 1H), 5.75 (m, 1H), 5.36 (m, 1H), 2.96 (m, 1H), 2.40 – 2.26 (m, 2H), 2.22 – 2.12 (m, 1H), 1.94 – 1.84 (td, J = 13.0 Hz, 10.5 Hz, 1H) 1.49 (s, 9H) ppm; ¹³C{¹H} NMR (125 MHz, CDCl₃): δ 153.5, 145.3, 130.6, 128.8, 127.1, 126.9, 126.7, 82.2, 74.0, 39.3, 35.3, 33.7, 28.0 ppm; IR (thin film): λ_{max} 3031, 2980, 2931, 1737, 1455, 1369, 1276, 1255, 1164, 1091, 983.1, 867.2, 700.0 cm⁻¹; HRMS (ES⁺) calc'd for C₁₇H₂₂O₃Na⁺ 297.1467, observed 297.1479 [MNa]⁺.

Preparation of (η⁶-toluene)Cr(CO)₃ Derivatives.

Compounds **1.1a**⁴⁶, **1.1c**⁴⁷, **1.1d**⁴⁷, **1.1h**⁴⁸, **1.1k**⁴⁹, **1.1l**⁵⁰, **1.1m**⁴⁶, **1.1n**⁵¹, **1.1o**⁵² and **1.1p**⁵³ were prepared according to general literature procedures for the synthesis of arene tricarbonylchromium complexes from Cr(CO)₆ and the parent arene. The complexes were crystallized from diethyl ether and hexanes to afford yellow crystalline solids.

General Procedure A. Synthesis of (η⁶-toluene)Cr(CO)₃ derivatives (**1.1b**, **1.1e**, **1.1f**, **1.1g**, **1.1i**, and **1.1q**): A solution of Cr(CO)₆ (1.10 g, 5.0 mmol), arene (1.2–5 equiv), and THF (3 mL) in 1,4-dioxane (8 mL) was heated under reflux (oil bath temp = 120 °C) under a nitrogen atmosphere for 3–5 days. The yellow-orange solution was allowed to cool, and completion of the reaction was verified by the absence of solid Cr(CO)₆ on the sides of the flask (from sublimation) after refluxing subsided. After cooling to rt, the solution was filtered through Celite, and then evaporated under reduced pressure. The

yellow product was either recrystallized from diethyl ether and hexanes or purified by column chromatography eluting with EtOAc/hexanes.

1.1b – (η^6 -4-isopropyltoluene)Cr(CO)₃: General Procedure A was applied to 4-isopropyltoluene (3.9 mL, 25 mmol) and Cr(CO)₆ (1.10 g, 5.0 mmol). The desired compound was recrystallized from hexanes at –78 °C and isolated as a yellow solid (1.16 g, 86% yield). ¹H NMR (500 MHz, CDCl₃): δ 5.36 (d, *J* = 6.8 Hz, 2H), 5.15 (d, *J* = 6.8 Hz, 2H), 2.57 (septet, *J* = 7.0 Hz, 1H), 2.16 (s, 3H), 1.21 (d, *J* = 7.0 Hz, 6H) ppm; ¹³C{¹H} NMR (125 MHz, CDCl₃): δ 234.0, 117.4, 108.8, 93.7, 92.9, 32.6, 23.7, 20.5 ppm; IR (thin film): λ_{max} 2973, 2932, 2876, 1941, 1867, 1828 (strong CO stretch), 1479, 1382, 1036, 845.2, 667.4, 632.9 cm⁻¹; HRMS (ES⁺) calc'd for C₁₃H₁₅O₃Cr⁺ 271.0426, observed 271.0422 [MH]⁺.

1.1e – (2-(η^6 -*p*-tolyl)pyridine)Cr(CO)₃: General Procedure A was applied to 2-(*p*-tolyl)pyridine (4.2 mL, 25 mmol) and Cr(CO)₆ (1.10 g, 5.0 mmol). The desired compound was recrystallized from diethyl ether and hexanes at –16 °C and isolated as a yellow solid (1.22 g, 80% yield). ¹H NMR (500 MHz, CDCl₃): δ 8.59 (d, *J* = 5.0 Hz, 1H), 7.72 (t, *J* = 7.8 Hz, 1H), 7.53 (d, *J* = 8.0 Hz, 1H), 7.23 (m, 1H), 6.27 (d, *J* = 6.5 Hz, 2H), 5.32 (d, *J* = 6.5 Hz, 2H), 2.25 (s, 3H) ppm; ¹³C{¹H} NMR (125 MHz, CDCl₃): δ 233.0, 153.8, 149.7, 137.1, 123.4, 119.9, 109.6, 103.1, 93.5, 92.4, 20.8 ppm; IR (thin film): λ_{max} 3082, 2925, 1965, 1873 (strong CO stretch), 1587, 1466, 1427, 779.1, 664.9, 630.1 cm⁻¹; HRMS (ES⁺) calc'd for C₁₅H₁₁NO₃Cr⁺ 305.0144, observed 305.0141 [M]⁺.

1.1f – (2-(η^6 -*p*-tolyl)thiophene)Cr(CO)₃: General Procedure A was applied to 2-(*p*-tolyl)thiophene (784 mg, 4.5 mmol) and Cr(CO)₆ (0.99 g, 4.5 mmol). Silica gel

chromatography using 5% to 20% EtOAc/hexanes afforded 1.066 g (77% yield) of the desired compound as a yellow solid. ^1H NMR (500 MHz, CDCl_3): δ 7.28 (d, J = 6.5 Hz, 1H), 7.22 (d, J = 3.5 Hz, 1H), 7.01 (m, 1H), 5.78 (d, J = 6.5 Hz, 2H), 5.28 (d, J = 6.5 Hz, 2H), 2.20 (s, 3H) ppm; $^{13}\text{C}\{^1\text{H}\}$ NMR (125 MHz, CDCl_3): δ 233.1, 139.9, 128.0, 126.2, 124.9, 108.1, 101.2, 92.6, 92.3, 20.6 ppm; IR (thin film): λ_{max} 3079, 1946, 1879, 1855 (strong CO stretch), 714.1, 665.6, 627.0 cm^{-1} ; HRMS (ES^+) calc'd for $\text{C}_{14}\text{H}_{11}\text{O}_3\text{SCr}^+$ 310.9834, observed 310.9825 $[\text{MH}]^+$.

1.1g – (1-(η^6 -*p*-tolyl)-1*H*-pyrrole)Cr(CO)₃: General Procedure A was applied to 1-(*p*-tolyl)-1*H*-pyrrole (2.2 g, 14 mmol) and $\text{Cr}(\text{CO})_6$ (1.10 g, 5.0 mmol). Silica gel chromatography using 5% to 20% EtOAc/hexanes afforded 0.760 g (52% yield) of the desired compound as a yellow solid. ^1H NMR (500 MHz, CDCl_3): δ 6.95 (s, 2H), 6.28 (s, 2H), 5.63 (d, J = 6.0 Hz, 2H), 5.40 (d, J = 6.0 Hz, 2H), 2.17 (s, 3H) ppm; $^{13}\text{C}\{^1\text{H}\}$ NMR (125 MHz, CDCl_3): δ 232.8, 119.9, 115.7, 111.7, 105.7, 93.4, 85.5, 20.3 ppm; IR (thin film): λ_{max} 3132, 3082, 2922, 1949, 1883, 1852 (strong CO stretch), 1549, 1511, 1494, 1326, 733.3, 678.3, 665.6, 629.7 cm^{-1} ; HRMS (ES^+) calc'd for $\text{C}_{14}\text{H}_{11}\text{NO}_3\text{Cr}^+$ 293.0144, observed 293.0142 $[\text{M}]^+$.

1.1i – (4-chloro-4'- η^6 -methylbiphenyl)Cr(CO)₃: General Procedure A was applied to 4-chloro-4'-methylbiphenyl (1.01 g, 5.0 mmol) and $\text{Cr}(\text{CO})_6$ (1.10 g, 5.0 mmol). Silica gel chromatography using 5% to 10% EtOAc/hexanes afforded 0.889 g (53% yield) of the desired compound as a yellow solid. ^1H NMR (500 MHz, CDCl_3): δ 7.46 – 7.32 (m, 4H), 5.73 (d, J = 6.5 Hz, 2H), 5.30 (d, J = 6.5 Hz, 2H), 2.22 (s, 3H) ppm; $^{13}\text{C}\{^1\text{H}\}$ NMR (125 MHz, CDCl_3): δ 233.0, 135.3, 135.0, 129.2, 128.5, 108.8, 106.4, 93.7, 92.7, 20.6 ppm; IR (thin film): λ_{max} 3088, 2925, 1950, 1893, 1874 (strong CO stretch), 1470, 1099, 827.0,

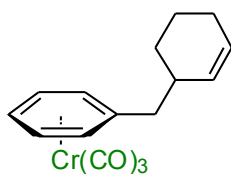
665.7, 631.0 cm^{-1} ; HRMS (ES^+) calc'd for $\text{C}_{16}\text{H}_{11}\text{O}_3\text{ClCr}^+$ 337.9802, observed 337.9789 $[\text{M}]^+$.

1.1q – ($\eta^6\text{-C}_6\text{H}_5\text{CH}_2\text{-morpholine}$) $\text{Cr}(\text{CO})_3$: General Procedure A was applied to 4-benzylmorpholine (1.54 g, 8.7 mmol) and $\text{Cr}(\text{CO})_6$ (1.60 g, 7.25 mmol). The desired compound was recrystallized from diethyl ether and hexanes at $-16\text{ }^\circ\text{C}$ and isolated as a yellow solid (1.66 g, 73% yield). ^1H NMR (500 MHz, CDCl_3): δ 5.40 – 5.30 (m, 4H), 5.28 – 5.22 (m, 1H), 3.76 – 3.63 (m, 4H), 3.24 (s, 2H), 2.57 – 2.44 (m, 4H) ppm; $^{13}\text{C}\{^1\text{H}\}$ NMR (125 MHz, CDCl_3): δ 232.9, 107.7, 94.0, 93.2, 91.6, 67.0, 62.1, 53.7 ppm; IR (thin film): λ_{max} 3066, 2971, 2867, 2817, 1961, 1877 (strong CO stretch), 1458, 1285, 1115, 1007, 865, 662, 630 cm^{-1} ; HRMS (ES^+) calc'd for $\text{C}_{14}\text{H}_{16}\text{NO}_4\text{Cr}^+$ 314.0484, observed 314.0497 $[\text{MH}]^+$.

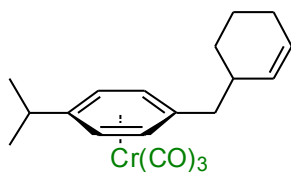
Procedure and Characterization for the Pd-catalyzed Allylic Substitution with ($\eta^6\text{-arene-CH}_2\text{Z}$) $\text{Cr}(\text{CO})_3$ -based Nucleophiles.

General Procedure B. An oven-dried reaction vial equipped with a stir bar was charged with ($\eta^6\text{-arene-CH}_2\text{Z}$) $\text{Cr}(\text{CO})_3$ (0.10 mmol). To the reaction vial was added $\text{LiN}(\text{SiMe}_3)_2$ (50.2 mg, 0.30 mmol, 3 equiv) under a nitrogen atmosphere followed by 0.5 mL of dry THF and the reaction mixture was stirred for 5 min. A solution of $\text{Pd}(\text{COD})\text{Cl}_2$ (1.43 mg, 0.0050 mmol) and Xantphos (4.34 mg, 0.0075 mmol) in 0.5 mL THF was taken up by syringe and added to the reaction vial. After stirring for 5 min, the allylic electrophile (0.2 mmol, 2 equiv) was added to the reaction followed by NEt_3 (14 μL , 0.1 mmol, 1 equiv). The reaction mixture was stirred for 12 h. The reaction mixture was then quenched with two drops of H_2O , diluted with 3 mL of ethyl acetate, and filtered over a pad of MgSO_4 and silica. The pad was rinsed with additional ethyl acetate and the solution was

concentrated in vacuo. The crude material was loaded onto a silica gel column and purified by flash chromatography.

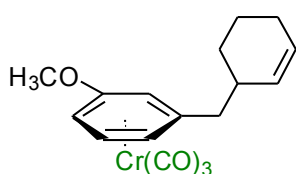


1.3a – (η^6 -(2-cyclohexen-1-ylmethyl)-benzene)Cr(CO)₃: The reaction was performed following General Procedure B with **1.1a** (22.8 mg, 0.1 mmol), LiN(SiMe₃)₂ (50.2 mg, 0.30 mmol) and **1.2b** (39 μ L, 0.2 mmol) in the presence of 5 mol % Pd catalyst and NEt₃ (14 μ L, 0.1 mmol). The crude material was purified by flash chromatography on silica gel (eluted with EtOAc:hexanes = 2:98) to give the product (29.7 mg, 96% yield) as a yellow solid. R_f = 0.45 (EtOAc:hexanes = 1:9); ¹H NMR (500 MHz, CDCl₃): δ 5.74 (m, 1H), 5.55 (m, 1H), 5.39 (t, *J* = 6.0 Hz, 2H), 5.21 – 5.12 (m, 3H), 2.41 – 2.24 (m, 3H), 1.99 (m, 2H), 1.82 – 1.67 (m, 2H), 1.57 – 1.47 (m, 1H), 1.35 – 1.25 (m, 1H) ppm; ¹³C{¹H} NMR (125 MHz, CDCl₃): δ 233.2, 129.6, 128.5, 112.0, 94.00, 93.97, 93.3, 93.2, 90.4, 42.0, 37.4, 28.6, 25.1, 22.3 ppm; IR (thin film): λ_{max} 3019, 2930, 2860, 1966, 1877 (strong CO stretch), 1459, 662.5, 630.2 cm⁻¹; HRMS (ES⁺) calc'd for C₁₆H₁₆O₃Cr⁺ 308.0505, observed 308.0492 [M]⁺.



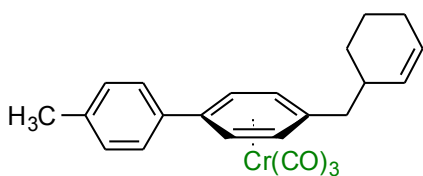
1.3b – (η^6 -(2-cyclohexen-1-ylmethyl)-4-isopropylbenzene)Cr(CO)₃: The reaction was performed following General Procedure B with **1.1b** (27.0 mg, 0.1 mmol), LiN(SiMe₃)₂ (50.2 mg, 0.30 mmol) and **1.2b** (39 μ L, 0.2 mmol) in the presence of 5 mol % Pd catalyst and NEt₃ (14 μ L, 0.1 mmol). The crude material was purified by flash chromatography on silica gel (eluted with EtOAc:hexanes = 2:98) to give the product (31.0 mg, 89% yield) as a yellow solid. R_f = 0.60 (EtOAc:hexanes = 1:9); ¹H NMR (500 MHz, CDCl₃): δ 5.73 (m, 1H), 5.56 (m, 1H), 5.34 (d, *J* = 6.0 Hz, 2H), 5.16 (d, *J* = 6.0 Hz,

2H), 2.59 (septet, $J = 7.0$ Hz, 1H), 2.40 – 2.23 (m, 3H), 1.99 (m, 2H), 1.83 – 1.68 (m, 2H), 1.59 – 1.47 (m, 1H), 1.37 – 1.19 (m, 7H) ppm; $^{13}\text{C}\{^1\text{H}\}$ NMR (125 MHz, CDCl_3): δ 233.9, 130.0, 128.6, 117.9, 111.1, 93.42, 93.37, 93.32, 93.28, 41.9, 37.7, 32.6, 29.0, 25.4, 23.7, 21.2 ppm; IR (thin film): λ_{max} 3021, 2929, 2861, 1960, 1877 (strong CO stretch), 1448, 722.3, 666.0, 627.4 cm^{-1} ; HRMS (ES^+) calc'd for $\text{C}_{19}\text{H}_{22}\text{O}_3\text{Cr}^+$ 350.0974, observed 350.0973 $[\text{M}]^+$.



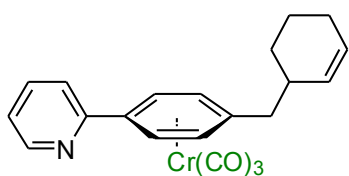
1.3c – **(η^6 -(2-cyclohexen-1-ylmethyl)-3-methoxybenzene) $\text{Cr}(\text{CO})_3$** : The reaction was performed following General Procedure B with **1.1c** (25.8 mg, 0.1 mmol),

$\text{LiN}(\text{SiMe}_3)_2$ (50.2 mg, 0.30 mmol) and **1.2b** (39 μL , 0.2 mmol) in the presence of 5 mol % Pd catalyst and NEt_3 (14 μL , 0.1 mmol). The crude material was purified by flash chromatography on silica gel (eluted with $\text{EtOAc}:\text{hexanes} = 2:98$) to give the product (26.9 mg, dr = 1:1, 80% yield) as a yellow solid. $R_f = 0.45$ ($\text{EtOAc}:\text{hexanes} = 1:9$); ^1H NMR (500 MHz, CDCl_3): δ 5.74 (m, 1H), 5.61 – 5.49 (m, 2H), 5.07 – 4.98 (m, 2H), 4.75 (d, $J = 6.0$ Hz, 1H), 3.72 (s, 3H), 2.49 – 2.26 (m, 3H), 1.99 (m, 2H), 1.84 – 1.67 (m, 2H), 1.58 – 1.48 (m, 1H), 1.38 – 1.27 (m, 1H) ppm; $^{13}\text{C}\{^1\text{H}\}$ NMR (125 MHz, CDCl_3): δ 233.6, 143.79, 143.76, 129.9, 129.8, 128.8, 113.5, 95.0, 87.18, 87.16, 80.7, 80.5, 76.3, 76.2, 55.7, 42.5, 37.79, 37.76, 29.1, 28.9, 25.4, 21.23, 21.17 ppm; IR (thin film): λ_{max} 2931, 1959, 1869 (strong CO stretch), 1537, 1460, 1267, 1150, 1030, 669.9, 629.7 cm^{-1} ; HRMS (ES^+) calc'd for $\text{C}_{17}\text{H}_{19}\text{O}_4\text{Cr}^+$ 339.0688, observed 339.0722 $[\text{MH}]^+$.



1.3d – **(η^6 -(2-cyclohexen-1-ylmethyl)-4-(*p*-tolyl)benzene) $\text{Cr}(\text{CO})_3$** : The reaction was performed following General Procedure B with **1.1d** (31.8 mg,

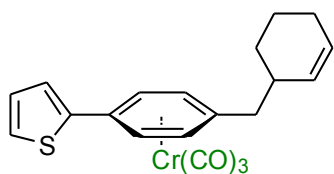
0.1 mmol), LiN(SiMe₃)₂ (50.2 mg, 0.30 mmol) and **1.2b** (39 μL, 0.2 mmol) in the presence of 5 mol % Pd catalyst and NEt₃ (14 μL, 0.1 mmol). The crude material was purified by flash chromatography on silica gel (eluted with EtOAc:hexanes = 2:98) to give the product (38.0 mg, 90% yield) as a yellow solid. R_f = 0.45 (EtOAc:hexanes = 1:19); ¹H NMR (500 MHz, CDCl₃): δ 7.38 (d, *J* = 8.0 Hz, 2H), 7.20 (d, *J* = 8.0 Hz, 2H), 5.79 – 5.68 (m, 3H), 5.58 (m, 1H), 5.32 (d, *J* = 6.5 Hz, 2H), 2.44 – 2.28 (m, 6H), 1.99 (m, 2H), 1.86 – 1.68 (m, 2H), 1.60 – 1.48 (m, 1H), 1.38 – 1.28 (m, 1H) ppm; ¹³C{¹H} NMR (125 MHz, CDCl₃): δ 233.4, 139.1, 133.7, 129.9, 129.7, 128.8, 127.1, 110.7, 108.9, 93.53, 93.49, 93.30, 93.28, 41.9, 37.8, 28.9, 25.4, 21.4, 21.2 ppm; IR (thin film): λ_{max} 3021, 2926, 2859, 1961, 1880 (strong CO stretch), 1471, 1448, 817.2, 721.0, 661.4, 625.5 cm⁻¹; HRMS (ES⁺) calc'd for C₂₃H₂₂O₃Cr⁺ 398.0974, observed 398.0966 [M]⁺.



1.3e – (*η*⁶-(2-cyclohexen-1-ylmethyl)-4-(2-pyridyl)-benzene)Cr(CO)₃: The reaction was performed following

General Procedure B with **1.1e** (30.5 mg, 0.1 mmol), LiN(SiMe₃)₂ (50.2 mg, 0.30 mmol) and **1.2b** (39 μL, 0.2 mmol) in the presence of 5 mol % Pd catalyst and NEt₃ (14 μL, 0.1 mmol). The crude material was purified by flash chromatography on silica gel (eluted with EtOAc:hexanes = 2:98) to give the product (29.4 mg, 77% yield) as a yellow solid. R_f = 0.20 (EtOAc:hexanes = 1:9); ¹H NMR (500 MHz, CDCl₃): δ 8.60 (d, *J* = 6.0 Hz, 1H), 7.73 (td, *J* = 8.0 Hz, 1.5 Hz, 1H), 7.54 (d, *J* = 8.0 Hz, 1H), 7.24 (dd, *J* = 7.5 Hz, 5.0 Hz, 1H), 6.24 (d, *J* = 6.5 Hz, 2H), 5.75 (m, 1H), 5.58 (m, 1H), 5.34 (d, *J* = 6.5 Hz, 2H), 2.48 – 2.31 (m, 3H), 1.99 (m, 2H), 1.86 – 1.69 (m, 2H), 1.58 – 1.49 (m, 1H), 1.40 – 1.30 (m, 1H) ppm; ¹³C{¹H} NMR (125 MHz, CDCl₃): δ 233.0, 153.8, 149.7, 137.1, 129.9, 128.8, 123.5, 120.1, 112.0, 103.8, 93.2, 93.1, 92.9, 92.8, 42.0, 37.7, 28.9, 25.4, 21.2 ppm; IR (thin film): λ_{max} 2927, 2858, 1963, 1885 (strong

CO stretch), 1587, 1462, 1432, 785.1, 661.9, 623.3 cm^{-1} ; HRMS (ES^+) calc'd for $\text{C}_{21}\text{H}_{20}\text{NO}_3\text{Cr}^+$ 386.0848, observed 386.0837 $[\text{MH}]^+$.

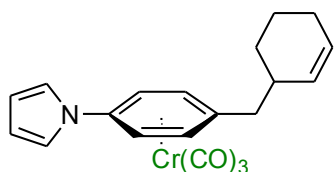


1.3f – (η^6 -(2-cyclohexen-1-ylmethyl)-4-(2-thiophenyl)-

benzene) $\text{Cr}(\text{CO})_3$: The reaction was performed following

General Procedure B with **1.1f** (31.0 mg, 0.1 mmol),

$\text{LiN}(\text{SiMe}_3)_2$ (50.2 mg, 0.30 mmol) and **1.2b** (39 μL , 0.2 mmol) in the presence of 5 mol % Pd catalyst and NEt_3 (14 μL , 0.1 mmol). The crude material was purified by flash chromatography on silica gel (eluted with EtOAc:hexanes = 2:98) to give the product (31.3 mg, 80% yield) as a yellow solid. R_f = 0.33 (EtOAc:hexanes = 1:19); ^1H NMR (500 MHz, CDCl_3): δ 7.28 (dd, J = 5.0 Hz, 1.0 Hz, 1H), 7.23 (dd, J = 3.5 Hz, 1.0 Hz, 1H), 7.02 (dd, J = 5.0 Hz, 3.5 Hz, 1H), 5.79 – 5.72 (m, 3H), 5.58 (m, 1H), 5.30 (d, J = 6.5 Hz, 2H), 2.42 – 2.27 (m, 3H), 1.99 (m, 2H), 1.84 – 1.69 (m, 2H), 1.59 – 1.48 (m, 1H), 1.37 – 1.27 (m, 1H) ppm; $^{13}\text{C}\{^1\text{H}\}$ NMR (125 MHz, CDCl_3): δ 233.1, 139.9, 129.8, 128.8, 128.1, 126.3, 124.9, 110.4, 101.9, 93.12, 93.09, 91.83, 91.80, 41.9, 37.8, 28.9, 25.4, 21.2 ppm; IR (thin film): λ_{max} 3018, 2928, 2858, 1962, 1881 (strong CO stretch), 1471, 1259, 852.1, 703.1, 660.2, 623.9 cm^{-1} ; HRMS (ES^+) calc'd for $\text{C}_{20}\text{H}_{18}\text{O}_3\text{SCr}^+$ 390.0382, observed 390.0384 $[\text{M}]^+$.



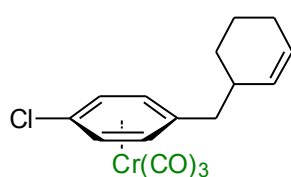
1.3g – (η^6 -(2-cyclohexen-1-ylmethyl)-4-(N-pyrrolyl)-

benzene) $\text{Cr}(\text{CO})_3$: The reaction was performed following

General Procedure B with **1.1g** (29.3 mg, 0.1 mmol),

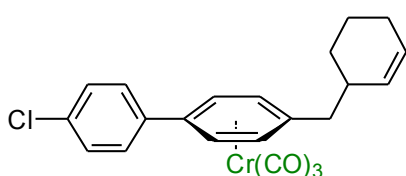
$\text{LiN}(\text{SiMe}_3)_2$ (50.2 mg, 0.30 mmol) and **1.2b** (39 μL , 0.2 mmol) in the presence of 5 mol % Pd catalyst and NEt_3 (14 μL , 0.1 mmol). The crude material was purified by flash chromatography on silica gel (eluted with EtOAc:hexanes = 2:98) to give the product

(27.5 mg, 74% yield) as a yellow solid. $R_f = 0.50$ (EtOAc:hexanes = 1:9); $^1\text{H NMR}$ (500 MHz, CDCl_3): δ 6.96 (t, $J = 7.0$ Hz, 2H), 6.29 (t, $J = 7.0$ Hz, 2H), 5.75 (m, 1H), 5.61 (d, $J = 6.5$ Hz, 2H), 5.56 (m, 1H), 5.41 (d, $J = 6.5$ Hz, 2H), 2.40 – 2.23 (m, 3H), 1.99 (m, 2H), 1.84 – 1.68 (m, 2H), 1.60 – 1.48 (m, 1H), 1.37 – 1.26 (m, 1H) ppm; $^{13}\text{C}\{^1\text{H}\}$ NMR (125 MHz, CDCl_3): δ 232.7, 129.7, 129.0, 119.9, 116.4, 111.8, 107.9, 93.8, 84.88, 84.86, 41.5, 37.8, 28.9, 25.4, 21.2 ppm; IR (thin film): λ_{max} 3018, 2929, 2859, 1965, 1885 (strong CO stretch), 1543, 1492, 1326, 1065, 725.5, 665.7, 624.3 cm^{-1} ; HRMS (ES^+) calc'd for $\text{C}_{20}\text{H}_{19}\text{NO}_3\text{Cr}^+$ 373.0770, observed 373.0771 $[\text{M}]^+$.



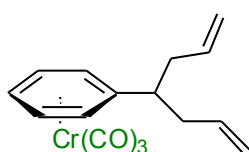
1.3h – **(η^6 -(2-cyclohexen-1-ylmethyl)-4-chlorobenzene) $\text{Cr}(\text{CO})_3$** : The reaction was performed following

General Procedure B with **1.1h** (26.3 mg, 0.1 mmol), $\text{LiN}(\text{SiMe}_3)_2$ (50.2 mg, 0.30 mmol) and **1.2b** (39 μL , 0.2 mmol) in the presence of 5 mol % Pd catalyst and NEt_3 (14 μL , 0.1 mmol). The crude material was purified by flash chromatography on silica gel (eluted with EtOAc:hexanes = 2:98) to give the product (15.3 mg, 45% yield) as a yellow solid. $R_f = 0.67$ (EtOAc:hexanes = 1:9); $^1\text{H NMR}$ (500 MHz, CDCl_3): δ 5.74 (m, 1H), 5.51 (m, 1H), 5.48 (d, $J = 6.5$ Hz, 2H), 5.27 (d, $J = 6.5$ Hz, 2H), 2.31 – 2.19 (m, 3H), 1.98 (m, 2H), 1.80 – 1.67 (m, 2H), 1.59 – 1.47 (m, 1H), 1.32 – 1.24 (m, 1H) ppm; $^{13}\text{C}\{^1\text{H}\}$ NMR (125 MHz, CDCl_3): δ 232.1, 129.5, 129.0, 110.5, 107.9, 93.7, 92.29, 92.27, 41.5, 37.7, 28.8, 25.3, 21.1 ppm; IR (thin film): λ_{max} 3084, 3019, 2929, 2859, 1971, 1889 (strong CO stretch), 1452, 1087, 725.7, 659.1, 620.0 cm^{-1} ; HRMS (ES^+) calc'd for $\text{C}_{16}\text{H}_{15}\text{O}_4\text{Cr}^+$ 323.0375, observed 323.0281 $[\text{M}-\text{Cl}+\text{O}]^+$.



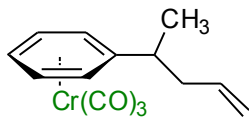
1.3i – **(η^6 -(2-cyclohexen-1-ylmethyl)-4-(p-chlorophenyl)-benzene) $\text{Cr}(\text{CO})_3$** : The reaction was

performed following General Procedure B with **1.1i** (33.9 mg, 0.1 mmol), LiN(SiMe₃)₂ (50.2 mg, 0.30 mmol) and **1.2b** (39 μL, 0.2 mmol) in the presence of 5 mol % Pd catalyst and NEt₃ (14 μL, 0.1 mmol). The crude material was purified by flash chromatography on silica gel (eluted with EtOAc:hexanes = 2:98) to give the product (29.7 mg, 71% yield) as a yellow solid. R_f = 0.45 (EtOAc:hexanes = 1:19); ¹H NMR (500 MHz, CDCl₃): δ 7.47 – 7.33 (m, 4H), 5.76 (m, 1H), 5.70 (d, *J* = 6.5 Hz, 2H), 5.58 (m, 1H), 5.31 (d, *J* = 6.5 Hz, 2H), 2.47 – 2.28 (m, 3H), 2.00 (m, 2H), 1.86 – 1.69 (m, 2H), 1.61 – 1.49 (m, 1H), 1.38 – 1.28 (m, 1H) ppm; ¹³C{¹H} NMR (125 MHz, CDCl₃): δ 233.0, 135.3, 135.1, 129.8, 129.3, 128.9, 128.5, 111.1, 107.0, 93.3, 93.2, 93.13, 93.12, 41.9, 37.7, 28.9, 25.4, 21.2 ppm; IR (thin film): λ_{max} 3019, 2928, 2859, 1964, 1886 (strong CO stretch), 1467, 1094, 1005, 830.0, 720.8, 664.8, 623.1 cm⁻¹; HRMS (ES⁺) calc'd for C₂₂H₁₉O₃ClCr⁺ 418.0428, observed 418.0447 [M]⁺.

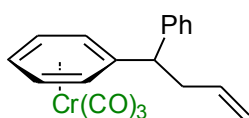


1.4ad – (η⁶-(1-(2-propen-1-yl)-3-buten-1-yl)-benzene)Cr(CO)₃:

The reaction was performed following General Procedure B with **1.1a** (23.7 mg, 0.104 mmol), LiN(SiMe₃)₂ (100.4 mg, 0.60 mmol) and allyl *tert*-butyl carbonate (**1.2d**, 68 μL, 0.4 mmol) in the presence of 5 mol % Pd catalyst and PMDTA (42 μL, 0.2 mmol). The crude material was purified by flash chromatography on silica gel (eluted with EtOAc:hexanes = 1:99) to give the product (25.9 mg, 81% yield) as a yellow solid. R_f = 0.60 (EtOAc:hexanes = 1:9); ¹H NMR (500 MHz, CDCl₃): δ 5.75 (m, 2H), 5.31 – 5.16 (m, 5H), 5.11 – 4.99 (m, 4H), 2.46 (quint, *J* = 6.5 Hz, 1H), 2.40 – 2.29 (m, 4H) ppm; ¹³C{¹H} NMR (125 MHz, CDCl₃): δ 233.4, 135.2, 118.1, 116.9, 93.4, 92.30, 92.26, 42.8, 38.8 ppm; IR (thin film): λ_{max} 3079, 2980, 2922, 1965, 1867 (strong CO stretch), 1641, 1458, 1442, 1419, 997.0, 919.0, 814.6, 663.0, 631.1 cm⁻¹; HRMS (ES⁺) calc'd for C₁₃H₁₆Cr⁺ 224.0657, observed 224.0658 [M-(CO)₃]⁺.



1.4kd – (η^6 -(1-methyl-3-buten-1-yl)-benzene)Cr(CO)₃: The reaction was performed following General Procedure B with **1.1k** (23.0 mg, 0.095 mmol), LiN(SiMe₃)₂ (50.2 mg, 0.30 mmol) and allyl *tert*-butyl carbonate (**1.2d**, 34 μ L, 0.2 mmol) in the presence of 5 mol % Pd catalyst and PMDTA (21 μ L, 0.1 mmol). The crude material was purified by flash chromatography on silica gel (eluted with EtOAc:hexanes = 1:99) to give the product (23.0 mg, 86% yield) as a yellow solid. R_f = 0.50 (EtOAc:hexanes = 1:9); ¹H NMR (500 MHz, CDCl₃): δ 5.75 (m, 1H), 5.35 – 5.21 (m, 5H), 5.08 – 4.98 (m, 2H), 2.58 – 2.49 (m, 1H), 2.39 – 2.30 (m, 1H), 2.25 – 2.16 (m, 1H), 1.23 (d, J = 7.0 Hz, 3H) ppm; ¹³C{¹H} NMR (125 MHz, CDCl₃): δ 233.4, 135.5, 118.5, 117.7, 93.8, 92.7, 92.6, 92.1, 91.6, 43.1, 38.1, 19.7 ppm; IR (thin film): λ_{\max} 2959, 2924, 2853, 1974, 1902 (strong CO stretch), 1462, 917.2, 812.9, 659.7, 628.1 cm⁻¹; HRMS (ES⁺) calc'd for C₁₁H₁₃Cr⁺ 197.0422, observed 197.0424 [M-H-(CO)₃]⁺.

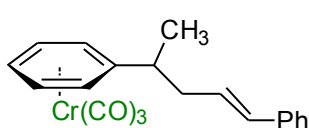
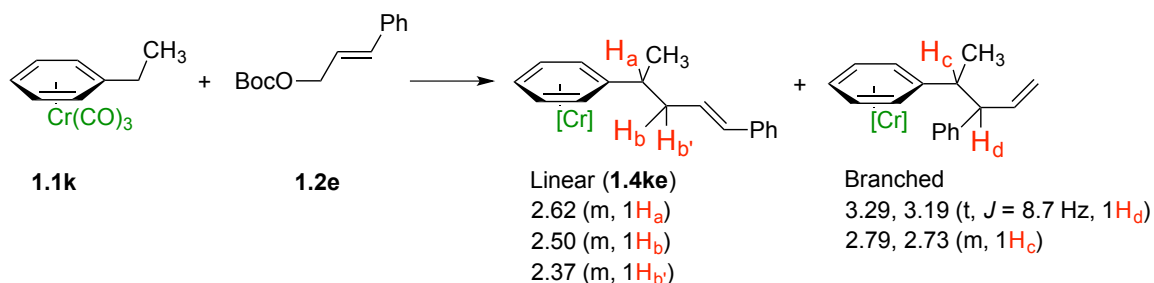


1.4ld – (η^6 -4,4-diphenyl-1-butene)Cr(CO)₃: The reaction was performed following General Procedure B with **1.1l** (29.6 mg, 0.097 mmol), LiN(SiMe₃)₂ (25.1 mg, 0.15 mmol) and allyl *tert*-butyl carbonate (**1.2d**, 25 μ L, 0.15 mmol) in the presence of 5 mol % Pd catalyst and NEt₃ (14 μ L, 0.1 mmol). The crude material was purified by flash chromatography on silica gel (eluted with EtOAc:hexanes = 3:97) to give the product (30.5 mg, 91% yield) as a yellow solid. R_f = 0.40 (EtOAc:hexanes = 1:19); ¹H NMR (500 MHz, CDCl₃): δ 7.40 – 7.15 (m, 5H), 5.67 (m, 1H), 5.51 – 4.95 (m, 7H), 3.68 (dd, J = 10.5 Hz, 5.0 Hz, 1H), 2.80 – 2.62 (m, 2H) ppm; ¹³C{¹H} NMR (125 MHz, CDCl₃): δ 233.2, 142.0, 135.5, 128.9, 128.4, 127.4, 117.6, 116.4, 94.4, 92.5, 92.3, 92.2, 92.0, 49.9, 39.6 ppm; IR (thin film): λ_{\max} 3083, 3030, 2927,

1965, 1888 (strong CO stretch), 1494, 1454, 1417, 996.2, 919.4, 748.4, 703.0, 661.9, 630.1 cm^{-1} ; HRMS (ES^+) calc'd for $\text{C}_{16}\text{H}_{16}\text{Cr}^+$ 260.0657, observed 260.0670 $[\text{M}(\text{CO})_3]^+$.

Determination of Regioselectivity of 1.4ke.

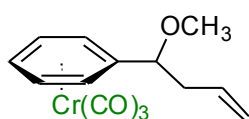
Ratio of linear:branched (L:B) was determined to be 77:23 at room temperature (or 85:15 at 0 °C) by ^1H NMR of the crude reaction mixture based on chemical shifts of indicated protons. The resonances for alkene C–H bonds and (η^6 -arene) C–H bonds of the linear product overlap with those for the branched product.



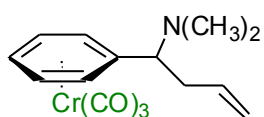
1.4ke - (η^6 - α -(*E*)-cinnamyl-ethylbenzene) $\text{Cr}(\text{CO})_3$: The

reaction was performed following General Procedure B with **1.1k** (24.2 mg, 0.10 mmol), $\text{LiN}(\text{SiMe}_3)_2$ (50.2 mg, 0.30 mmol) and *tert*-butyl (*E*)-cinnamyl carbonate (**1.2e**, 46 μL , 0.20 mmol) in the presence of 5 mol % Pd catalyst and PMDTA (21 μL , 0.1 mmol) at rt. The crude material was purified by flash chromatography on silica gel (eluted with CH_2Cl_2 :hexanes = 5:95) to give the linear product (25.4 mg, 71% yield) as a yellow solid. $R_f = 0.30$ (CH_2Cl_2 :hexanes = 1:9); ^1H NMR (500 MHz, CDCl_3): δ 7.42 – 7.18 (m, 5H), 6.37 (d, $J = 16.0$ Hz, 1H), 6.15 (dt, $J = 16.0$ Hz, 7.5 Hz, 1H), 5.40 – 5.20 (m, 5H), 2.68 – 2.57 (m, 1H), 2.55 – 2.45 (m, 1H), 2.42 – 2.32 (m, 1H), 1.28 (d, $J = 7.0$ Hz, 3H) ppm; $^{13}\text{C}\{^1\text{H}\}$ NMR (125 MHz, CDCl_3): δ 233.4, 137.4, 132.9, 128.8, 127.5, 127.2, 126.3, 118.3, 93.7, 92.7, 92.6, 92.1, 91.5, 42.3, 38.6, 19.9 ppm; IR (thin film): λ_{max} 3082, 3026, 2969, 2930, 1962, 1875 (strong CO stretch), 1529, 1495, 1460, 1420, 1379,

1157, 967.8, 815.0, 741.5, 693.8, 662.6, 631.7 cm^{-1} ; HRMS (ES^+) calc'd for $\text{C}_{17}\text{H}_{18}\text{Cr}^+$ 274.0814, observed 274.0830 $[\text{M}-(\text{CO})_3]^+$.

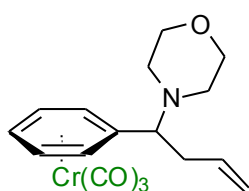


1.4od – (η^6 -1-methoxy-1-phenyl-3-butene) $\text{Cr}(\text{CO})_3$: The reaction was performed following General Procedure B with **1.1o** (24.2 mg, 0.094 mmol), $\text{LiN}(\text{SiMe}_3)_2$ (50.2 mg, 0.30 mmol) and allyl *tert*-butyl carbonate (**1.2d**, 34 μL , 0.20 mmol) in the presence of 5 mol % Pd catalyst and PMDTA (21 μL , 0.1 mmol). The crude material was purified by flash chromatography on silica gel (eluted with EtOAc:hexanes = 5:95 to 10:90) to give the product (25.2 mg, 90% yield) as a yellow solid. R_f = 0.33 (EtOAc:hexanes = 1:9); ^1H NMR (500 MHz, CDCl_3): δ 5.80 (m, 1H), 5.55 (m, 1H), 5.35 – 5.21 (m, 4H), 5.12 – 5.03 (m, 2H), 3.94 (t, J = 6.0 Hz, 1H), 3.52 (s, 3H), 2.48 (m, 2H) ppm; $^{13}\text{C}\{^1\text{H}\}$ NMR (125 MHz, CDCl_3): δ 233.1, 133.4, 118.5, 112.0, 93.1, 91.62, 91.58, 91.54, 91.42, 80.9, 58.5, 42.3 ppm; IR (thin film): λ_{max} 3082, 2984, 2935, 2831, 1965, 1888, 1867 (strong CO stretch), 1642, 1456, 1418, 1099, 997.4, 921.4, 818.0, 665.9, 631.8 cm^{-1} ; HRMS (ES^+) calc'd for $\text{C}_{11}\text{H}_{15}\text{OCr}^+$ 215.0528, observed 215.0523 $[\text{MH}-(\text{CO})_3]^+$.

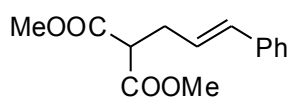


1.4pd – (η^6 - α -allyl-*N,N*-dimethylbenzylamine) $\text{Cr}(\text{CO})_3$: The reaction was performed following General Procedure B with **1.1p** (26.6 mg, 0.098 mmol), $\text{LiN}(\text{SiMe}_3)_2$ (50.2 mg, 0.30 mmol) and allyl *tert*-butyl carbonate (**1.2d**, 34 μL , 0.20 mmol) in the presence of 5 mol % Pd catalyst and PMDTA (21 μL , 0.1 mmol). The crude material was purified by flash chromatography on silica gel (eluted with EtOAc:hexanes = 40:60) to give the product (28.6 mg, 94% yield) as a yellow solid. R_f = 0.25 (EtOAc:hexanes = 4:6); ^1H NMR (500 MHz, CDCl_3): δ 5.92 (m, 1H), 5.40 – 5.24 (m, 5H), 5.21 – 5.09 (m, 2H), 3.41 (dd, J = 9.0 Hz, 5.5 Hz, 1H), 2.60 – 2.50 (m, 1H), 2.49

– 2.40 (m, 1H), 2.24 (s, 6H) ppm; $^{13}\text{C}\{^1\text{H}\}$ NMR (125 MHz, CDCl_3): δ 233.0, 136.0, 117.0, 108.7, 95.9, 93.3, 92.3, 91.46, 91.36, 66.5, 40.8, 33.8 ppm; IR (thin film): λ_{max} 3078, 2938, 2827, 2783, 1965, 1888, 1867 (strong CO stretch), 1641, 1456, 998.7, 915.2, 662.5, 631.5 cm^{-1} ; HRMS (ES^+) calc'd for $\text{C}_{15}\text{H}_{18}\text{NO}_3\text{Cr}^+$ 312.0692, observed 312.0695 $[\text{MH}]^+$.

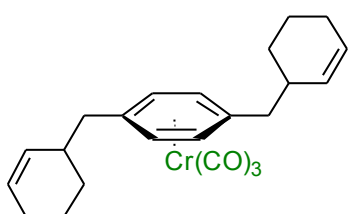


1.4qd – (η^6 -4-(1-phenyl-3-butenyl)morpholine) $\text{Cr}(\text{CO})_3$: The reaction was performed following General Procedure B with **1.1q** (31.0 mg, 0.10 mmol), $\text{LiN}(\text{SiMe}_3)_2$ (50.2 mg, 0.30 mmol) and allyl *tert*-butyl carbonate (**1.2d**, 34 μL , 0.20 mmol) in the presence of 5 mol % Pd catalyst and PMDTA (21 μL , 0.1 mmol). The crude material was purified by flash chromatography on silica gel (eluted with EtOAc:hexanes = 30:70) to give the product (34.4 mg, 97% yield) as a yellow solid. R_f = 0.55 (EtOAc:hexanes = 4:6); ^1H NMR (500 MHz, CDCl_3): δ 5.93 (m, 1H), 5.40 – 5.24 (m, 5H), 5.20 – 5.07 (m, 2H), 3.67 (m, 4H), 3.39 (dd, J = 9.0 Hz, 5.0 Hz, 1H), 2.66 – 2.54 (m, 3H), 2.49 – 2.38 (m, 3H) ppm; $^{13}\text{C}\{^1\text{H}\}$ NMR (125 MHz, CDCl_3): δ 233.0, 135.7, 117.1, 109.1, 95.5, 93.2, 92.2, 91.5, 91.4, 67.4, 66.8, 49.4, 33.7 ppm; IR (thin film): λ_{max} 3079, 2958, 2856, 2818, 1965, 1888, 1867 (strong CO stretch), 1641, 1454, 1292, 1116, 997.3, 916.6, 665.7, 630.9 cm^{-1} ; HRMS (ES^+) calc'd for $\text{C}_{17}\text{H}_{20}\text{NO}_4\text{Cr}^+$ 354.0797, observed 354.0794 $[\text{MH}]^+$.



1.11 – α -(*E*)-cinnamyl dimethyl malonate: The reaction was performed following General Procedure B with dimethyl malonate (23 μL , 0.20 mmol), BSA (49 μL , 0.20 mmol) and *tert*-butyl (*E*)-cinnamyl carbonate (**1.2e**, 23 μL , 0.10 mmol) in the presence of 5 mol % $\text{Pd}(\text{COD})\text{Cl}_2/\text{Xantphos}$ catalyst and KOAc (1.0 mg, 10 mol %) in THF (1 mL) at rt for 12 h. The crude material

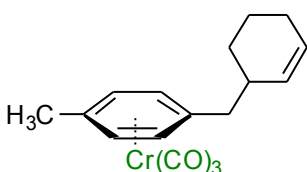
was purified by flash chromatography on silica gel (eluted with EtOAc:hexanes = 5:95) to give the product (L:B > 20:1, 21.0 mg, 85% yield) as a colorless oil. R_f = 0.25 (EtOAc:hexanes = 1:9). The NMR spectral data match the previously published data.⁵⁴



1.7 – **(η^6 -1,4-di(2-cyclohexen-1-ylmethyl)-benzene)Cr(CO)₃**: The reaction was performed following

General Procedure B with **1.1m** (24.2 mg, 0.10 mmol), LiN(SiMe₃)₂ (100.4 mg, 0.60 mmol) and 2-cyclohexenyl

mesitoate (**1.2k**, 94 μ L, 0.40 mmol) in the presence of 10 mol % Pd catalyst and NEt₃ (28 μ L, 0.2 mmol). The crude material was purified by flash chromatography on silica gel (eluted with EtOAc:hexanes = 2:98) to give the product (31.3 mg, 78% yield) as a yellow solid. R_f = 0.50 (EtOAc:hexanes = 1:19); ¹H NMR (500 MHz, CDCl₃): δ 5.74 (m, 2H), 5.55 (m, 2H), 5.23 (s, 4H), 2.38 – 2.20 (m, 6H), 2.05 – 1.91 (m, 4H), 1.83 – 1.66 (m, 4H), 1.58 – 1.47 (m, 2H), 1.35 – 1.23 (m, 2H) ppm; ¹³C{¹H} NMR (125 MHz, CDCl₃): δ 233.7, 130.0, 128.7, 109.9, 94.5, 41.9, 37.7, 29.0, 25.4, 21.2 ppm; IR (thin film): λ_{max} 2957, 2925, 2854, 1968, 1894 (strong CO stretch), 1728, 1463, 1378, 1287, 722.2, 665.4, 626.3 cm⁻¹; HRMS (ES⁺) calc'd for C₂₀H₂₆Cr⁺ 318.1440, observed 318.1450 [M-(CO)₃]⁺.

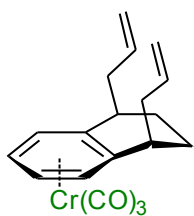


1.8 – **(η^6 -(2-cyclohexen-1-ylmethyl)-4-methylbenzene)Cr(CO)₃**: The product was a byproduct from

the preceding reaction. The crude material was purified by

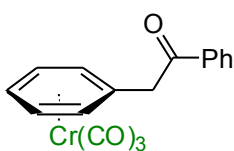
flash chromatography on silica gel (eluted with EtOAc:hexanes = 2:98) to give the product (4.8 mg, 15% yield) as a yellow solid. R_f = 0.40 (EtOAc:hexanes = 1:19); ¹H NMR (500 MHz, CDCl₃): δ 5.73 (m, 1H), 5.54 (m, 1H), 5.30 – 5.15 (m, 4H), 2.36 – 2.20 (m, 3H), 2.15 (s, 3H), 2.02 – 1.92 (m, 2H), 1.82 – 1.65 (m, 2H), 1.57 – 1.46 (m, 1H), 1.35

– 1.22 (m, 1H) ppm; $^{13}\text{C}\{^1\text{H}\}$ NMR (125 MHz, CDCl_3): δ 233.8, 129.9, 128.7, 109.2, 107.6, 95.02, 95.00, 94.07, 94.04, 41.8, 37.7, 28.9, 25.4, 21.2, 20.5 ppm; IR (thin film): λ_{max} 2926, 2859, 1959, 1867 (strong CO stretch), 1448, 1381, 668.4, 631.7, 535.3 cm^{-1} ; HRMS (ES^+) calc'd for $\text{C}_{14}\text{H}_{18}\text{Cr}^+$ 238.0814, observed 238.0867 $[\text{M}-(\text{CO})_3]^+$.



1.9 – (η^6 -(R,S)-1,2,3,4-tetrahydro-1,4-di-2-propen-1-yl-naphthalene) $\text{Cr}(\text{CO})_3$:

The reaction was performed following General Procedure B with **1.1n** (26.8 mg, 0.10 mmol), $\text{LiN}(\text{SiMe}_3)_2$ (100.4 mg, 0.60 mmol) and allyl *tert*-butyl carbonate (**1.2d**, 68 μL , 0.40 mmol) in the presence of 5 mol % Pd catalyst and PMDTA (42 μL , 0.2 mmol). The crude material was purified by flash chromatography on silica gel (eluted with Et_2O :hexanes = 5:95) to give the product (26.2 mg, 76% yield) as a yellow solid. R_f = 0.50 (EtOAc :hexanes = 1:19); ^1H NMR (500 MHz, CDCl_3): δ 5.76 (m, 2H), 5.38 – 5.24 (m, 4H), 5.12 – 5.03 (m, 4H), 2.73 (m, 2H), 2.45 – 2.37 (m, 2H), 2.37 – 2.28 (m, 2H), 1.86 – 1.76 (m, 2H), 1.70 – 1.59 (m, 2H) ppm; $^{13}\text{C}\{^1\text{H}\}$ NMR (125 MHz, CDCl_3): δ 233.7, 135.6, 117.8, 113.6, 93.2, 92.2, 41.3, 36.6, 23.9 ppm; IR (thin film): λ_{max} 2934, 1959, 1870 (strong CO stretch), 1458, 995.3, 917.6, 667.1, 630.7 cm^{-1} ; HRMS (ES^+) calc'd for $\text{C}_{16}\text{H}_{20}\text{Cr}^+$ 264.0970, observed 264.0958 $[\text{M}-(\text{CO})_3]^+$.



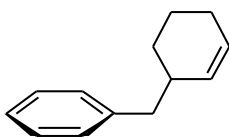
1.10 – (η^6 -benzyl phenyl ketone) $\text{Cr}(\text{CO})_3$:

The reaction was performed following General Procedure B with **1.1a** (23.2 mg, 0.102 mmol), $\text{LiN}(\text{SiMe}_3)_2$ (50.2 mg, 0.30 mmol) and 1-cyclohex-2-enyl benzoate (**1.2c**, 37 μL , 0.2 mmol) and NEt_3 (14 μL , 0.1 mmol) *in the absence of Pd catalyst*. The crude material was purified by flash chromatography on silica gel (eluted with EtOAc :hexanes = 5:95 to 40:60) to give the product (33.2 mg, 98% yield) as a

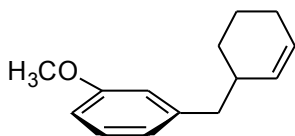
yellow solid. $R_f = 0.33$ (EtOAc:hexanes = 1:9). The NMR spectral data match the previously published data.⁶¹

Procedure and Characterization for the Tandem Allylic Substitution/Demetallation.

General Procedure C. The reaction was conducted according to General Procedure B described above. After 12 h, the reaction was quenched with two drops of H₂O, diluted with 10–20 mL of diethyl ether, and the solution was exposed to sunlight by placing it on the windowsill and stirring for 3–6 h. The demetallation step was monitored until TLC showed complete consumption of the (η^6 -arene)Cr(CO)₃ product. During this time, a green precipitate formed as the chromium was oxidized. The reaction mixture was then filtered through a pad of MgSO₄ and silica, concentrated in vacuo and loaded directly onto a silica gel column.

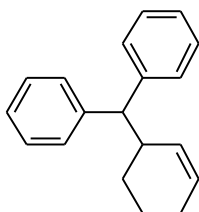


1.3'a – (2-cyclohexen-1-ylmethyl)-benzene: The reaction was performed following General Procedure C with **1.1a** (22.8 mg, 0.1 mmol), LiN(SiMe₃)₂ (50.2 mg, 0.30 mmol) and **1.2b** (39 μ L, 0.2 mmol) in the presence of 5 mol % Pd catalyst and NEt₃ (14 μ L, 0.1 mmol). After demetallation, the crude material was purified by flash chromatography on silica gel (eluted with hexanes to EtOAc:hexanes = 5:95) to give the organic product (15.9 mg, 92% yield) as a colorless oil. $R_f = 0.60$ (EtOAc:hexanes = 1:19). The NMR spectral data match the previously published data.⁵⁵



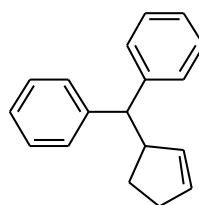
1.3'c – (2-cyclohexen-1-ylmethyl)-3-methoxybenzene: The reaction was performed following General Procedure C with **1.1c** (24.9 mg, 0.0965 mmol), LiN(SiMe₃)₂ (50.2 mg, 0.30 mmol)

and **1.2b** (39 μL , 0.2 mmol) in the presence of 5 mol % Pd catalyst and NEt_3 (14 μL , 0.1 mmol). After demetallation, the crude material was purified by flash chromatography on silica gel (eluted with hexanes to EtOAc:hexanes = 5:95) to give the organic product (14.2 mg, 73% yield) as a colorless oil. $R_f = 0.67$ (EtOAc:hexanes = 1:19); ^1H NMR (500 MHz, CDCl_3): δ 7.19 (t, $J = 7.5$ Hz, 1H), 6.80 – 6.66 (m, 3H), 5.69 (m, 1H), 5.57 (m, 1H), 3.80 (s, 3H), 2.61 (dd, $J = 13.2$ Hz, 7.2 Hz, 1H), 2.51 (dd, $J = 13.2$ Hz, 8.4 Hz, 1H), 2.37 (m, 1H), 1.98 (m, 2H), 1.76 – 1.66 (m, 2H), 1.53 – 1.46 (m, 1H), 1.31 – 1.19 (m, 1H) ppm; $^{13}\text{C}\{^1\text{H}\}$ NMR (125 MHz, CDCl_3): δ 159.7, 142.8, 131.5, 129.3, 127.6, 121.8, 115.1, 111.2, 55.3, 43.0, 37.3, 29.1, 25.6, 21.5 ppm; IR (thin film): λ_{max} 3017, 2925, 2854, 1601, 1585, 1488, 1454, 1260, 1153, 1044, 773.1, 697.0 cm^{-1} ; HRMS (Cl^+) calc'd for $\text{C}_{14}\text{H}_{18}\text{O}^+$ 202.1358, observed 202.1360 $[\text{M}]^+$.



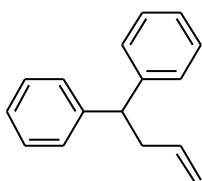
1.5lb – **3-(diphenylmethyl)-1-cyclohexene**: The reaction was performed following General Procedure C with **1.1l** (30.4 mg, 0.10 mmol), $\text{LiN}(\text{SiMe}_3)_2$ (50.2 mg, 0.30 mmol) and **1.2b** (39 μL , 0.2 mmol) in the presence of 5 mol % Pd catalyst and NEt_3 (14 μL , 0.1 mmol).

After demetallation, the crude material was purified by flash chromatography on silica gel (eluted with hexanes to EtOAc:hexanes = 5:95) to give the organic product (24.0 mg, 96% yield) as a colorless oil. $R_f = 0.60$ (EtOAc:hexanes = 3:97). The ^1H NMR spectrum matches the previously published report.⁵⁶ The ^{13}C NMR spectrum of the title compound was not reported before. $^{13}\text{C}\{^1\text{H}\}$ NMR (125 MHz, CDCl_3): δ 144.4, 144.1, 130.2, 128.70, 128.65, 128.5, 128.4, 128.2, 126.32, 126.28, 58.4, 39.1, 28.5, 25.6, 21.7 ppm.

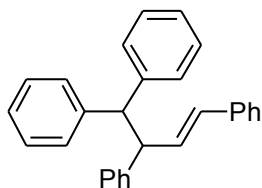


1.5lg – **3-(diphenylmethyl)-1-cyclopentene**: The reaction was performed following General Procedure C with **1.1l** (30.4 mg, 0.10

mmol), $\text{LiN}(\text{SiMe}_3)_2$ (50.2 mg, 0.30 mmol) and *tert*-butyl 2-cyclopentenyl carbonate (**1.2g**, 40 μL , 0.2 mmol) in the presence of 5 mol % Pd catalyst and NEt_3 (14 μL , 0.1 mmol). After demetallation, the crude material was purified by flash chromatography on silica gel (eluted with hexanes to EtOAc:hexanes = 5:95) to give the organic product (20.8 mg, 89% yield) as a colorless oil. $R_f = 0.60$ (EtOAc:hexanes = 3:97). The ^1H NMR spectrum matches the previously published report.⁵⁶ The ^{13}C NMR spectrum of the title compound was not reported before. $^{13}\text{C}\{^1\text{H}\}$ NMR (125 MHz, CDCl_3): δ 145.0, 144.7, 134.1, 131.6, 128.59, 128.56, 128.4, 128.3, 126.3, 58.4, 50.4, 32.2, 29.6 ppm.

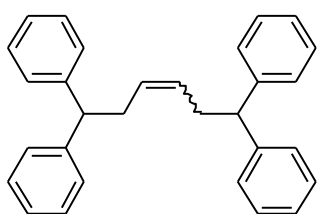


1.5Id – 4,4-diphenyl-1-butene: The reaction was performed following General Procedure C with **1.1I** (30.4 mg, 0.10 mmol), $\text{LiN}(\text{SiMe}_3)_2$ (25.1 mg, 0.15 mmol) and allyl *tert*-butyl carbonate (**1.2d**, 25 μL , 0.15 mmol) in the presence of 5 mol % Pd catalyst and NEt_3 (14 μL , 0.1 mmol). After demetallation, the crude material was purified by flash chromatography on silica gel (eluted with hexanes to EtOAc:hexanes = 5:95) to give the organic product (18.9 mg, 91% yield) as a colorless oil. $R_f = 0.75$ (EtOAc:hexanes = 5:95). The NMR spectral data match the previously published data.⁵⁷



1.5If – (E)-1,1,2,4-tetraphenylbut-3-ene: The reaction was performed following General Procedure C with **1.1I** (30.4 mg, 0.10 mmol), $\text{LiN}(\text{SiMe}_3)_2$ (25.1 mg, 0.15 mmol) and (*E*)-1,3-diphenyl allyl acetate (**1.2f**, 30.3 mg, 0.12 mmol) in the presence of 5 mol % $[\text{Pd}(\text{allyl})\text{Cl}]_2$ and 10 mol % DPPP. After demetallation, the crude material was purified by flash chromatography on silica gel (eluted with hexanes to EtOAc:hexanes = 1:9) to give the organic product (34.3 mg, 91% yield) as a white solid. $R_f = 0.50$ (EtOAc:hexanes = 5:95);

m.p. = 119–120 °C; ^1H NMR (500 MHz, CDCl_3): δ 7.40 – 6.96 (m, 20H), 6.27 (dd, J = 15.5 Hz, 7.5 Hz, 1H), 6.17 (d, J = 15.5 Hz, 1H), 4.39 (d, J = 11.0 Hz, 1H), 4.31 (dd, J = 11.0 Hz, 7.5 Hz, 1H) ppm; $^{13}\text{C}\{^1\text{H}\}$ NMR (125 MHz, CDCl_3): δ 143.5, 143.4, 143.1, 137.8, 133.2, 131.3, 128.9, 128.7, 128.6, 128.52, 128.47, 128.3, 127.2, 126.5, 126.3, 126.1, 57.6, 53.8 ppm; IR (thin film): λ_{max} 3060, 3026, 2907, 1599, 1494, 1450, 961.2, 742.3, 697.5 cm^{-1} ; HRMS (Cl^+) calc'd for $\text{C}_{28}\text{H}_{25}^+$ 361.1956, observed 361.1942 $[\text{MH}]^+$.



cis:trans = 2:1

1.5lh – 1,1,6,6-tetraphenylhex-3-ene (*cis:trans* = 2:1): The

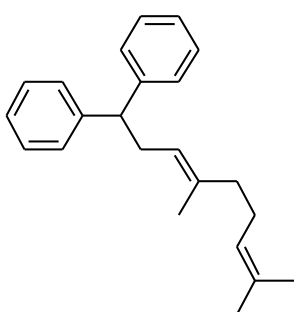
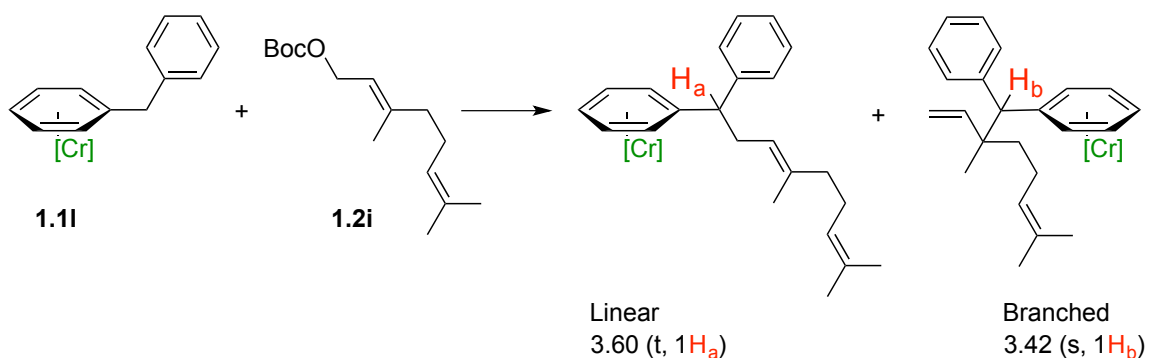
reaction was performed following General Procedure C with

1.1i (68.4 mg, 0.225 mmol), $\text{LiN}(\text{SiMe}_3)_2$ (56.4 mg, 0.337 mmol) and *cis*-1,4-diacetoxy-2-butene (**1.2h**, 12 μL , 0.075

mmol) in the presence of 5 mol % $[\text{Pd}(\text{allyl})\text{Cl}]_2$ and 10 mol % DPPP. After demetallation, the crude material was purified by flash chromatography on silica gel (eluted with hexanes to EtOAc:hexanes = 3:97) to give the organic product (22.3 mg, 77% yield) as a white solid. R_f = 0.50 (EtOAc:hexanes = 5:95); m.p. data for the title compound have been reported⁵⁸; ^1H NMR (500 MHz, CDCl_3): δ 7.29 – 7.09 (m, 10H), 5.35 – 5.24 (m, 2H), 3.86 – 3.76 (m, 2H), 2.76 – 2.60 (m, 4H) ppm; $^{13}\text{C}\{^1\text{H}\}$ NMR (125 MHz, CDCl_3): δ 144.9, 130.3, 129.1, 128.6, 128.5, 128.2, 126.4, 126.3, 51.8, 51.3, 39.0, 33.8 ppm; IR (thin film): λ_{max} 3060, 3025, 2923, 2852, 1599, 1493, 1450, 742.8, 698.5 cm^{-1} ; HRMS (Cl^+) calc'd for $\text{C}_{30}\text{H}_{29}^+$ 389.2269, observed 389.2287 $[\text{MH}]^+$.

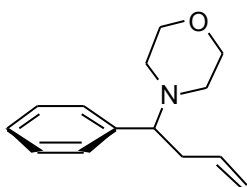
Determination of Regioselectivity of 1.5li.

Ratio of linear:branched (L:B) was determined to be 78:22 by ^1H NMR of the crude reaction mixture based on chemical shifts of indicated protons.



1.5li – **α -geranyldiphenylmethane**: The reaction was performed following General Procedure C with **1.1l** (31.3 mg, 0.103 mmol), LiN(SiMe₃)₂ (50.2 mg, 0.30 mmol) and *tert*-butyl geranyl carbonate (**1.2i**, 56 μ L, 0.20 mmol) in the presence of 5 mol % Pd catalyst and NEt₃ (14 μ L, 0.1 mmol). After demetallation, the crude material was purified by flash chromatography on silica gel

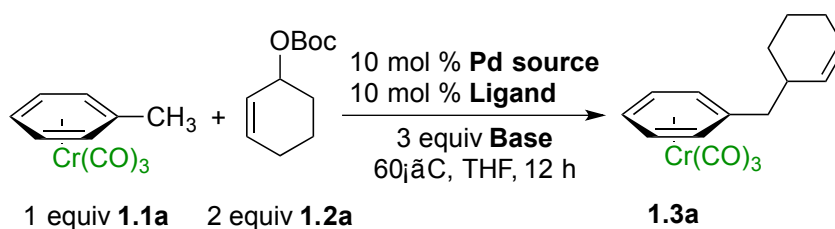
(eluted with hexanes to EtOAc:hexanes = 5:95) to give the organic product (22.9 mg, 73% yield) as a colorless oil. R_f = 0.75 (EtOAc:hexanes = 5:95); ¹H NMR (500 MHz, CDCl₃): δ 7.30 – 7.13 (m, 10H), 5.07 (t, J = 6.5 Hz, 1H), 4.99 (t, J = 6.5 Hz, 1H), 3.94 (t, J = 7.5 Hz, 1H), 2.73 (t, J = 7.5 Hz, 2H), 2.01 – 1.94 (m, 2H), 1.94 – 1.87 (m, 2H), 1.64 (s, 3H), 1.54 (s, 6H) ppm; ¹³C{¹H} NMR (125 MHz, CDCl₃): δ 145.2, 136.5, 131.5, 128.5, 128.3, 126.2, 124.5, 122.8, 51.7, 39.9, 34.5, 26.8, 25.9, 17.9, 16.3 ppm; IR (thin film): λ_{max} 3026, 2965, 2923, 2854, 1494, 1450, 1376, 748.6, 698.6 cm⁻¹; HRMS (CI⁺) calc'd for C₂₃H₂₉⁺ 305.2269, observed 305.2277 [MH]⁺.



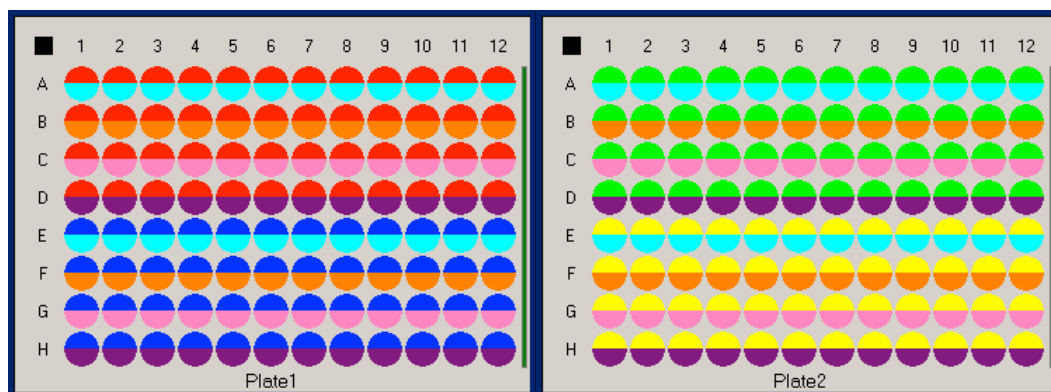
1.4'qd – **4-(1-phenyl-3-butenyl)morpholine**: The reaction was performed following General Procedure C with **1.1q** (0.939 g, 3.0 mmol), LiN(SiMe₃)₂ (1.506 g, 9.0 mmol) and allyl *tert*-butyl carbonate (**1.2d**, 1.0 mL, 6.0 mmol) in the presence of 5 mol % Pd catalyst and PMDTA

(0.63 mL, 3.0 mmol). After demetallation, the crude material was purified by flash chromatography on silica gel (eluted with EtOAc:hexanes = 2:8 to EtOAc:hexanes = 3:7) to give the organic product (0.580 g, 89% yield) as a light yellow oil. $R_f = 0.60$ (EtOAc:hexanes = 3:7). The NMR spectral data match the previously published data.⁵⁹

Microscale High-throughput Experimentation (HTE) for Catalyst Identification.



Ligand was used in a 2:1 ratio relative to Pd for monodentate ligands and 1:1 ratio for bidentate ligands.



12 **Ligands** x 4 **Pd sources** x 4 **Bases** at 60 °C in THF (25 μL) at [**1.1a**] = 0.1 M on a 2.5 μmol scale.

12 **Ligands** were:

1,1'-BIS(DIPHENYLPHOSPHINO)FERROCENE;

1,1'-BIS(DIISOPROPYLPHOSPHINO)FERROCENE;

1,3-BIS(DIPHENYLPHOSPHINO)PROPANE;

1,4-BIS(DIPHENYLPHOSPHINO)BUTANE;
BIS(2-DIPHENYLPHOSPHINOPHENYL)ETHER;
9,9-DIMETHYL-4,5-BIS(DIPHENYLPHOSPHINO)XANTHENE ;
(R)-(+)-2,2'-BIS(DIPHENYLPHOSPHINO)-1,1'-BINAPHTHYL;
(R)-(S)-Cy2PF-PtBu2;
N-PHENYL-2-(DI-T-BUTYLPHOSPHINO)PYRROLE;
2-DI-TERT-BUTYLPHOSPHINO-2',4',6'-TRIIISOPROPYLBIPHENYL;
TRICYCLOHEXYLPHOSPHONIUM TETRAFLUOROBORATE;
TRI-O-TOLYLPHOSPHINE.

The 12 ligands were predosed in each column from 1 to 12 for both plates.

4 Pd sources were: $[\text{Pd}(\text{allyl})\text{Cl}]_2$, $\text{Pd}_2(\text{dba})_3$, $\text{Pd}(\text{COD})\text{Cl}_2$ and $\text{Pd}(\text{OAc})_2$.

Plate 1: A1-D12 = $[\text{Pd}(\text{allyl})\text{Cl}]_2$ and E1-H12 = $\text{Pd}_2(\text{dba})_3$.

Plate 2: A1-D12 = $\text{Pd}(\text{COD})\text{Cl}_2$ and E1-H12 = $\text{Pd}(\text{OAc})_2$.

4 Bases were: $\text{LiN}(\text{SiMe}_3)_2$, LDA, *t*-BuOK and $\text{KN}(\text{SiMe}_3)_2$.

Rows A & E = $\text{LiN}(\text{SiMe}_3)_2$; B & F = LDA; C & G = *t*-BuOK; D & H = $\text{KN}(\text{SiMe}_3)_2$ for both plates.

Experimental.

Set up:

The screening was set up inside a glovebox under a nitrogen atmosphere. Two 96-well aluminum blocks containing 100 μL glass vials were predosed in each column from 1 to 12 for both plates. The solution or slurry of the Pd sources in 25 μL of THF (10 mol %) was dosed in each vial, and the solvent THF was removed using a Genevac vacuum

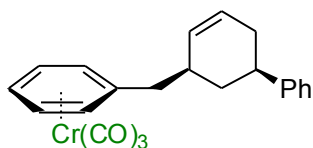
centrifuge. Small parylene magnetic stir bars were added to the reaction vials. A stock solution containing **1.1a**, **1.2a**, and base in THF was prepared at [**1.1a**] = 0.1 M, and 25 μL of the stock solution were dosed in each vial using an Eppendorf multi-channel pipet. The 96-well plates were sealed and agitated at ~ 960 rpm for overnight at 60 $^{\circ}\text{C}$ (control with thermocouple) by using a tumble stirrer provided with heating element.

Work up:

The plates were cooled to room temperature, and then opened to air and 125 μL of acetonitrile (containing 0.25 μmol of biphenyl as internal standard) was syringed into each vial by means of an Eppendorf multi-channel pipet (to ensure complete solubilization of the reaction mixture). The plates were then covered again and the vials stirred for 15-20 minutes to extract the product and to ensure good homogenization. Portions of each reaction mixture (20 μL) were then transferred with the multi-channel pipet into 96-well HPLC blocks pre-filled with 750 μL of acetonitrile. The blocks were then mounted on HPLC instruments for analysis (no filtration necessary for the corresponding volumes and concentrations). Agilent 1200 Series HPLC instruments with reverse phase C-18 columns and acetonitrile/water as mobile phase were used. Data processing was done by using Agilent's ChemStation software and biphenyl as an internal standard.

The lead hit from the screening was the combination of $\text{Pd}(\text{COD})\text{Cl}_2$, $\text{LiN}(\text{SiMe}_3)_2$, and Xantphos, giving 36% yield of the desired product **1.3a**. A scale-up reaction on a 0.1 mmol scale using the General Procedure B for the Pd-catalyzed allylic substitution reaction proved successful with isolation of **1.3a** in 39% yield.

Determination of the Relative Stereochemistry of Compound 1.6.



1.6 – *cis-(η⁶-(5-phenyl-2-cyclohexen-1-ylmethyl)-*

benzene)Cr(CO)₃: The reaction was performed following General Procedure B with **1.1a** (22.8 mg, 0.1 mmol), LiN(SiMe₃)₂ (50.2 mg, 0.30 mmol) and *cis-tert*-butyl (5-phenyl-2-cyclohexenyl) carbonate (**1.2j**, 53 μL, 0.2 mmol) in the presence of 5 mol % Pd catalyst and NEt₃ (14 μL, 0.1 mmol). The crude material was purified by flash chromatography on silica gel (eluted with EtOAc:hexanes = 2:98) to give the product (24.2 mg, 63% yield) as a yellow solid. *R_f* = 0.45 (EtOAc:hexanes = 1:19); ¹H NMR (500 MHz, CDCl₃): δ 7.34 – 7.15 (m, 5H), 5.83 (m, 1H), 5.63 (m, 1H), 5.38 (m, 2H), 5.16 (m, 3H), 2.81 (m, 1H), 2.54 (m, 1H), 2.47 (dd, *J* = 13.5 Hz, 6.5 Hz, 1H), 2.32 (dd, *J* = 13.5 Hz, 8.0 Hz, 1H), 2.27 (m, 1H), 2.13 (m, 1H), 1.96(dm, *J* = 13 Hz, 1H), 1.45 (dt, *J* = 13 Hz, 12 Hz, 12 Hz, 1H) ppm; ¹³C{¹H} NMR (125 MHz, CDCl₃): δ 233.3, 146.7, 129.8, 128.7, 128.3, 127.0, 126.5, 111.6, 94.14, 94.09, 93.4, 93.2, 90.5, 42.5, 40.6, 39.7, 36.9, 34.0 ppm; IR (thin film): λ_{max} 3083, 3025, 2919, 2852, 1965, 1878 (strong CO stretch), 1604, 1493, 1453, 1419, 1154, 758.8, 700.8, 662.6, 630.9 cm⁻¹; HRMS (ES⁺) calc'd for C₁₉H₂₀Cr⁺ 300.0970, observed 300.0966 [M-(CO)₃]⁺.

The relative chemistry of the single diastereomer was established by ¹H NMR splitting patterns and coupling constants.⁶⁰ ¹H NMR spectrum of compound **1.6** is consistent with those of the starting alcohol (*cis*-5-phenyl-2-cyclohexen-1-ol) and carbonate (**1.2j**).

List of Predosed 192 Chiral Ligands Screened in HTE.

SDD Plate 1

A 1 (R)-Solphos A001-1

A 2 (S)-xylyl-binap

A 3 (S)-Cl,MeO-Biphep

A 4 (R,R)-Me-DuPhos
A 5 EtBPE
A 6 SL-J002-1 : (R,S)-Ph₂P-Fc-P(tBu)₂
A 7 SL-J007-1
A 8 SL-J009-1
A 9 SL-J012-1
A 10 (R)-CTH-JAFAPHOS
A 11 (R,R)-Et-FerroTANE
A 12 (R,R,S,S)-Tangphos
B 1 (R)-(S)-Me-BoPhoz
B 2 SL-W001-1
B 3 SL-W006-1
B 4 SL-W005-1
B 5 CTH-(R)-3,5-xylyl-PHANEPHOS
B 6 (S,S)-SL-M002-1
B 7 (S,S)-SL-M001-1
B 8 (S,S)-SL-T001-1
B 9 (S)-(+)-(2,6-Dimethyl-3,5-dioxa-4-phospha-cyclohepta[2,1-a;3,4-a']dinaphthalen-4-yl)dimethylamine
B 10 (R)-MONOPHOS
B 11 catASium D(R)
B 12 catASium I
C 1 (2S,4S)-tBu-(-)-4-(Diphenylphosphino)-2-(diphenylphosphinomethyl)pyrrolidine carboxylate
C 2 (3S,4S)-(-)-1-Benzyl-3,4-bis(diphenylphosphino)pyrrolidine

C 3 (1R,1R',2R,2R')-(-)-2,2'-DIPHENYLPHOSPHINO-1,1'-BICYCLOPENTYL
 C 4 SL-T021-2: Ph₂P-Fc-CH(OH)Ph-PPh₂
 C 5 (R,R)-SL-M004-1
 C 6 Walphos 9-1
 C 7 (R,R) SL-W018-1
 C 8 (R,R)-SL-W019-1
 C 9 (R,R) SL-W020-1
 C 10 (R,R)-SL-W021-1
 C 11 SL-T025-2: xyl₂P-Fc-CH(OH)Ph-Pxyl₂
 C 12 (4S,5S)-(+)-4,5-Bis(diphenylphosphinomethyl)-2,2-dimethyl-1,3-dioxolane
 D 1 (S,S)-SL-M001-1
 D 2 (S,S)-SL-M002-1
 D 3 (S,S)-SL-M003-1
 D 4 (3S,3'S,4S,4'S,11bS,11'bS)-(+)-4,4'-Di-t-butyl-4,4',5,5'-tetrahydro-3,3'-bi-3H-
 dinaphtho[2,1-c:1',2'-e]phosphepin
 D 5 (S,S)-SL-T001-1
 D 6 (R,S)-SL-T002-1
 D 7 SL-T026-2: Ph₂P-Fc-CH(OH)Ph-P(3,5-Me-4-MeO)₂
 D 8 (S)-(-)-2,2'-Bis(N-diphenylphosphinoamino)-5,5',6,6',7,7',8,8'-octahydro-1,1'-
 binaphthyl
 D 9 R,S-(o-tolyl)₂P-F-C-P(o-tolyl)₂
 D 10 (R)-(S)-Et₂P-F-C-PtBu₂
 D 11 s-f-binaphane
 D 12 SL-T027-2: xyl₂P-Fc-CH(OH)Ph-P(3,5-CF₃-Ph)₂
 E 1 (S)-CTH-JAFAPHOS

E 2 (R,R)-Me-DuPhos
E 3 (+)-1,2-Bis((2R,5R)-2,5-di-i-propylphospholano)benzene
E 4 (R,R) Et-DuPhos
E 5 (R)-(+)-BIS-(1,2-DIPHENYLPHOSPHINO)PROPANE
E 6 SL-W023-1: (3,5-Me-4-MeO)₂PPh-Fc-CHMe-P(Nor)₂
E 7 SL-W-A1: Ph₂PPh-Fc-CHMe-PtBu₂
E 8 SL-J215-2: (S)-(R)-Fur₂P-Fc-Pcy₂
E 9 SL-J302-1: (R)-(S)-Et₂P-Fc-PCy₂
E 10 SL-J011-1: (R)-(S)-(4-CF₃-Ph)₂-PFc-PtBu₂
E 11 SL-J304-1: (R)-(S)-Ph,Me-PFc-PCy₂
E 12 SL-J408-1: (R)-(S)-xyl₂P-Fc-Pxyl₂
F 1 SL-J411-2: (S)-(R)-Fur₂P-Fc-P(3,5-Me₂-4-OMe-Ph)₂
F 2 SL-J412-1: (R)-(S)-xyl₂P-Fc-P(3,5-(CF₃)₂-Ph)₂
F 3 SL-W022-1
F 4 SL-F011-2 (Twinphos, analog of Me-BoPhoz)
F 5 SL-F013-2 (Twinphos, analog of P(cyco)-BoPhoz)
F 6 SL-J851-2
F 7 SL-J852-2
F 8 SL-J853-2
F 9 (S,S)-Ph-BPE
F 10 SL-W016-1
F 11 [(1R,2R,3S)-(+)-1,2-Dimethyl-2,3-bis(diphenylphosphinomethyl)cyclopentyl]methanol
F 12 SL-W017-1

G 1 (R)-(-)-1-[(S)-2-(DIPHENYLPHOSPHINO)FERROCENYL]ETHYLDICYLCOHEXYLPHOSPHINE

G 2 (R)-(-)-1-[(S)-2-(DIPHENYLPHOSPHINO)FERROCENYL]ETHYLDI-T-BUTYLPHOSPHINE

G 3 (R)-(-)-1-[(S)-2-(DICYCLOHEXYLPHOSPHINO)FERROCENYL]ETHYLDIPHENYLPHOSPHINE

G 4 (R)-(S)-(3,5-(CF₃)₂Ph)₂PF-Pcy₂

G 5 (R)-(S)-(3,5-(CF₃)₂Ph)₂PF-Pxyl₂

G 6 (R)-(S)-(4-CF₃-Ph)₂-PFc-PCy₂

G 7 (R)-(S)-(3,5-Me₂-4-MeOPh)₂PF-PtBu₂

G 8 (R)-(S)-Fur₂PF-PtBu₂

G 9 (R)-(S)-oTol₂PF-Pxyl₂

G 10 (R)-(S)-(3,5-Me₂-4-MeOPh)₂PF-PoTol₂

G 11 (2-Furyl)₂P-Fc-P(o-Tolyl)₂

G 12 SL-J503-1: (R)-(S)-Et₂P-Fc-P(o-Tolyl)₂

H 1 (R)-(S)-xyl₂P-Fc-PtBu₂

H 2 (R)-(-)-1-[(S)-2-(DICYCLOHEXYLPHOSPHINO)FERROCENYL]ETHYLDICYCLOHEXYLPHOSPHINE

H 3 (R)-(S)-Ph₂P-Fc-P(4-CF₃-Ph)₂

H 4 (R)-(S)-(4-MeO-3,5-Me₂Ph)₂PF-Pcy₂

H 5 (R)-(S)-cy₂PF-PtBu₂

H 6 (R)-(S)-(p-Tol)₂PF-PtBu₂

H 7 (S)-(R)-Fur₂P-Fc-Pxyl₂

H 8 (R)-(S)-(3,5-Me₂-4-MeOPh)₂PF-Pxyl₂

H 9 (R)-(S)-cy₂PF-Po-Tol₂

H 10 (R)-(R)-(S)-PhMePF-Pcy₂

H 11 SL-J507-1: (R)-(S)-Et₂P-Fc-P(xylyl)₂

H 12 SL-J034-1: (R)-(R)-Ph₂P-(2-TMS-Fc)-P(cHex)₂

SDD Plate 2

A 1 Catasium MN An(R)

A 2 Catasium MNN (R)

A 3 Catasium MN MesF (R)

A 4 Catasium MN Mes (R)

A 5 (S,S)-Me-UCAP-DTBM

A 6 (R,R)-QuinoxP*

A 7 SL-P051-1: (R,R,R)-Me-KEPHOS

A 8 SL-P053-2: (S,S,R)-Me-KEPHOS

A 9 SL-J005-1: Ph₂P-Fc-Pxyl₂

A 10 SL-J014-1: (R)-(S)-(4-F-Ph)₂P-Fc-PtBu₂

A 11 SL-J031-1: PPh₂-Fc-P(cyclopentyl)₂

A 12 SL-J211-1: (o-Tol)₂P-Fc-PtBu₂

B 1 SL-J213-1: (3,5-CF₃-Ph)₂P-Fc-P(cyclopentyl)₂

B 2 SL-J216-1: (1-naphthyl)₂P-Fc-PtBu₂

B 3 SL-J219-1: (2-MeO-Ph)₂P-Fc-PtBu₂

B 4 SL-J220-1: (3,5-Me-4-MeO-Ph)₂P-Fc-P(cyclopentyl)₂

B 5 SL-J221-1: (3,5-Me-4-MeO-Ph)₂P-Fc-P(2,4,4-Me-pentyl)₂

B 6 SL-J222-1: (3,5-Me-4-MeO-Ph)₂P-Fc-P(neopentyl)₂

B 7 SL-J305-1: Cy₂P-Fc-P(norbornyl)₂

B 8 SL-J404-1: (R)-(S)-(1-naphthyl)₂P-Fc-Pxyl₂

B 9 SL-J409-1: (R)-(S)-(1-Naphthyl)2PF-PPh₂

B 10 SL-J502-1: tBu₂P-Fc-PPh₂

B 11 SL-J505-1: tBu₂P-Fc-P(o-Tol)₂

B 12 SL-J506-1: tBu₂P-Fc-P(4-CF₃-Ph)₂

C 1 (-)-TMBTP

C 2 (R)-(+)-2,2'-BIS(DI-P-TOLYLPHOSPHINO)-1,1'-BINAPHTHYL

C 3 (R)-Hexaphemp

C 4 (S)-(-)-6,6'-Bis(diphenylphosphino)-1,1'-biphenyl-2,2'-diylbis(acetate),

C 5 (R)-(+)-5,5'-DICHLORO-6,6'-DIMETHOXY-2,2'-BIS(DIPHENYLPHOSPHINO)-1,1'-
BIPHENYL

C 6 (R)-segphos

C 7 SL-A109-2

C 8 (R)-(+)-2,2',6,6'-Tetramethoxy-4,4'-bis(diphenylphosphino)-3,3'-bipyridine

C 9 (R)-DTBM-SEGPPOS

C 10 s-c1-tunaphos

C 11 s-c3-tunaphos

C 12 s-c5-tunaphos

D 1 (S)-(+)-2,2'-BIS(DIPHENYLPHOSPHINO)-1,1'-BINAPHTHYL

D 2 (R)-(+)-2,2'-BIS[DI(3,5-XYLYL)PHOSPHINO]-1,1'-BINAPHTHYL

D 3 (1R)-(+)-[Di(3,5-dimethylphenyl)phosphino]-2-(4-diphenylphosphino-2,5-
dimethylthien-3-yl)-1,7,7-trimethylbicyclo[2.2.1]hept-2-ene [catASium T2]

D 4 (R)-DM-SEGPPOS

D 5 (R)-(-)-5,5'-Bis(diphenylphosphino)-2,2,2',2'-tetrafluoro-4,4'-bi-1,3-benzodioxole

D 6 SL-A120-2

D 7 (R)-H8-BINAP

D 8 (S)-(-)-2,2',6,6'-Tetramethoxy-4,4'-bis(di(3,5-xylyl)phosphino)-3,3'-bipyridine

D 9 (S)-(-)-6,6'-Bis(diphenylphosphino)-1,1'-biphenyl-2,2'-diylbis(cyclohexylcarboxylate),

D 10 c2-tunaphos

D 11 s-C4-tunaphos

D 12 s-c6-tunaphos

E 1 (R)-MP2-SEGPHOS

E 2 (R)-P3-SEGPHOS

E 3 (+)-Cy-SEGPHOS

E 4 SL-A102-1

E 5 SL-A107-1

E 6 SL-A104-1

E 7 SL-A121-1

E 8 SL-A108-1

E 9 SL-A116-1

E 10 SL-A118-1

E 11 (1R,2R)-(+)-1,2-Diaminocyclohexane-N,N'-bis(2'-diphenylphosphinobenzoyl)

E 12 (1R,2R)-(+)-1,2-Diaminocyclohexane-N,N'-bis(2-diphenylphosphino-1-naphthoyl)

F 1 (4R)-(+)-4,5-DIHYDRO-2-[2'-(DIPHENYLPHOSPHINO)PHENYL]-4-ISOPROPYLOXAZOLE

F 2 (R)-(-)-2-[2-(Diphenylphosphino)phenyl]-4-phenyl-2-oxazoline

F 3 SL-N003-2 ((S)-4-Isopropyl-2-[(S)-2-(diphenylphosphino)ferrocen-1-yl]oxazoline)

F 4 SL-N008-2 ((S)-4-Isopropyl-2-[(S)-2-(bis(3,5-dimethyl-4-methoxyphenyl)phosphino)ferrocen-1-yl]oxazoline)

F 5 SL-N011-2 ((S)-4-Isopropyl-2-[(S)-2-(bis(1-naphthyl)phosphino)ferrocen-1-yl]oxazoline)

F 6 SL-N012-2 ((S)-4-Isopropyl-2-[(S)-2-(bis(2-methoxyphenyl)phosphino)ferrocen-1-yl]oxazoline)

F 7 SL-N004-2

F 8 SL-N007-2

F 9 SL-N013-1

F 10 (S)-Xyl-SDP

F 11 (S)-Tol-SDP

F 12 (S)-SDP

G 1 (R)-MonoPhos

G 2 (S)-N-Me-N-Bn-MonoPhos

G 3 (S)-PipPhos

G 4 (S)-2,6-Me-MonoPhos

G 5 (S,R)-(a-MeBn)-MonoPhos

G 6 (S,R,R)-(a-MeBn)₂-MonoPhos

G 7 (S,S,S)-(a-MeBn)₂-MonoPhos

G 8 (S)-H8-MonoPhos

G 9 (S)-H8-PipPhos

G 10 (R)-BINOL-P-OiPr

G 11 (R)-BINOL-P-OiBu

G 12 (R,R)-TADDOL-P-NMe₂

H 1 (R)-SIPHOS

H 2 (R)-SIPHOS-PE

H 3 (R)-ShiP

H 4 (S,S)-Mikami Ligand

H 5 (S,S)-tBu-Mikami Ligand

H 6 (R)-Quinap
H 7 (R)-N-PINAP
H 8 (R)-MOP
H 9 (R,R)-Me-DuPhos Monoxide
H 10 (S,S)-Me-RajPhos
H 11 (S,S)-Et-RajPhos
H 12 (S,S,S)-DiazaPhos-PPE

1.5 References

- (1) (a) Cardenas, D. J. *Angew. Chem., Int. Ed.* **2003**, *42*, 384. (b) Netherton, M. R.; Fu, G. C. *Adv. Synth. Catal.* **2004**, *346*, 1525. (c) Frisch, A. C.; Beller, M. *Angew. Chem., Int. Ed.* **2005**, *44*, 674. (d) Rudolph, A.; Lautens, M. *Angew. Chem., Int. Ed.* **2009**, *48*, 2656. (e) Jana, R.; Pathak, T. P.; Sigman, M. S. *Chem. Rev.* **2011**, *111*, 1417.
- (2) (a) Trost, B. M.; Van Vranken, D. L. *Chem. Rev.* **1996**, *96*, 395. (b) Trost, B. M.; Crawley, M. L. *Chem. Rev.* **2003**, *103*, 2921. (c) Trost, B. M. *J. Org. Chem.* **2004**, *69*, 5813. (d) Trost, B. M.; Machacek, M. R.; Aponick, A. *Acc. Chem. Res.* **2006**, *39*, 747. (e) Trost, B. M.; Fandrick, D. R. *Aldrichim. Acta* **2007**, *40*, 59. (f) Lu, Z.; Ma, S. *Angew. Chem., Int. Ed.* **2008**, *47*, 258.
- (3) (a) Castanet, Y.; Petit, F. *Tetrahedron Lett.* **1979**, *34*, 3221. (b) Keinan, E.; Roth, Z. *J. Org. Chem.* **1983**, *48*, 1769, and references therein. (c) Shukla, K. H.; DeShong, P. J. *Org. Chem.* **2008**, *73*, 6283, and references therein.
- (4) (a) Trost, B. M.; Thaisrivongs, D. A. *J. Am. Chem. Soc.* **2008**, *130*, 14092. (b) Trost, B. M.; Thaisrivongs, D. A. *J. Am. Chem. Soc.* **2009**, *131*, 12056. (c) Trost, B. M.; Thaisrivongs, D. A.; Hartwig, J. *J. Am. Chem. Soc.* **2011**, *133*, 12439.

(5) Dewick, P. M. *Essentials of Organic Chemistry: For Students of Pharmacy, Medicinal Chemistry and Biological Chemistry*; John Wiley & Sons, Ltd: Chichester, West Sussex, UK, 2006.

(6) Bordwell, F. G.; Bares, J. E.; Bartmess, J. E.; Drucker, G. E.; Gerhold, J.; McCollum, G. J.; Van Der Puy, M.; Vanier, N. R.; Matthews, W. S. *J. Org. Chem.* **1977**, *42*, 326.

(7) Although metal-catalyzed benzylic allylation reaction of toluene has never been reported, a few toluene analogues bearing electron-withdrawing groups (cyano, carbonyl, nitro, etc.) on benzylic or *para* position have been reported to undergo metal-catalyzed allylic substitution reactions. Benzyl cyanides (nucleophile stabilized by cyano group): (a) Tsuji, J.; Shimizu, I.; Minami, I.; Ohashi, Y. *Tetrahedron Lett.* **1982**, *23*, 4809. (b) Tsuji, J.; Shimizu, I.; Minami, I.; Ohashi, Y.; Sugiura, T.; Takahashi, K. *J. Org. Chem.* **1985**, *50*, 1523. (c) Minami, I.; Ohashi, Y.; Shimizu, I.; Tsuji, J. *Tetrahedron Lett.* **1985**, *26*, 2449. (d) Ikeda, I.; Gu, X.-P.; Okuhara, T.; Okahara, M. *Synthesis* **1990**, 32. (e) Nowicki, A.; Mortreux, A.; Agbossou-Niedercorn, F. *Tetrahedron Lett.* **2005**, *46*, 1617. Benzyl carbonyls (nucleophile stabilized by carbonyl group): (f) Suzuki, O.; Hashiguchi, Y.; Inoue, S.; Sato, K. *Chem. Lett.* **1988**, 291. (g) Suzuki, O.; Inoue, S.; Sato, K. *Bull. Chem. Soc. Jpn.* **1989**, *62*, 239. (h) Gravel, D.; Benoit, S.; Kumanovic, S.; Sivaramakrishnan, H. *Tetrahedron Lett.* **1992**, *33*, 1407. (i) Gravel, D.; Benoit, S.; Kumanovic, S.; Sivaramakrishnan, H. *Tetrahedron Lett.* **1992**, *33*, 1403. (j) Trost, B. M.; Schroeder, G. M.; Kristensen, J. *Angew. Chem., Int. Ed.* **2002**, *41*, 3492. (k) Yan, X.-X.; Liang, C.-G.; Zhang, Y.; Hong, W.; Cao, B.-X.; Dai, L.-X.; Hou, X.-L. *Angew. Chem., Int. Ed.* **2005**, *44*, 6544. (l) Lebeuf, R.; Hirano, K.; Glorius, F. *Org. Lett.* **2008**, *10*, 4243. (m) Trost, B. M.; Xu, J.; Schmidt, T. *J. Am. Chem. Soc.* **2009**, *131*, 18343. (n) Zhao, Y.; Zhou, Y.; Liang, L.; Yang, X.; Du, F.; Li, A.; Zhang, H. *Org. Lett.* **2009**, *11*, 555. *p*-Nitrotoluenes: (a) Waetzig,

S. R.; Tunge, J. A. *J. Am. Chem. Soc.* **2007**, *129*, 14860. (b) Kim, I. S.; Ngai, M.-Y.; Krische, M. J. *J. Am. Chem. Soc.* **2008**, *130*, 6340.

(8) Non-metal-catalyzed allylation of toluene derivatives (3 examples) with several allyl bromides via radical process (yield average: 61%): (a) Tanko, J. M.; Sadeghipour, M. *Angew. Chem., Int. Ed.* **1999**, *38*, 159. (b) Struss, J. A.; Sadeghipour, M.; Tanko, J. M. *Tetrahedron Lett.* **2009**, *50*, 2119.

(9) Non-metal-catalyzed allylation of toluene derivatives with allyl bromide via arene η^6 -coordination to organometallic fragment. Fe: (a) Moulines, F.; Astruc, D. *J. Chem. Soc., Chem. Commun.* **1989**, 614. (b) Martinez, V.; Blais, J.-C.; Astruc, D. *Org. Lett.* **2002**, *4*, 651. (c) Martinez, V.; Blais, J.-C.; Astruc, D. *Angew. Chem., Int. Ed.* **2003**, *42*, 4366. Cr: (d) Hata, T.; Koide, H.; Taniguchi, N.; Uemura, M. *Org. Lett.* **2000**, *2*, 1907. Ru: (e) Pigge, F. C.; Fang, S.; Rath, N. P. *Tetrahedron Lett.* **1999**, *40*, 2251.

(10) Ono Pharmaceutical Co., Ltd. Preventive and/or Remedy for Hyperkalemia Containing EP4 Agonist. Eur. Patent 1782829 (A1), 2007.

(11) Merrell Pharmaceuticals, Inc. Use of (*E*)-2-(*p*-Fluorophenethyl)-3-Fluoroallylamine in the Treatment of Alzheimer's Disease. Eur. Patent 0642338 (B1), 1997.

(12) Ono Pharmaceutical Co., Ltd. Preventive and/or Remedy for Lower Urinary Tract Diseases Containing EP4 Agonist. Eur. Patent 1782830 (A1), 2007.

(13) (a) Unilever Home and Personal Care USA, Division of Conopco, Inc. Cosmetic Compositions Containing Sophora Alopecuroides L. Extracts. US Patent 2006/110341 (A1), 2006. (b) Gupta, S. K. New Ubiquitin-Proteasome Regulating Compounds and Their Application in Cosmetic and Pharmaceutical Formulations. US Patent 2006/269494 (A1), 2006.

(14) (a) Kouznetsov, V.; Urbina, J.; Palma, A.; Lopez, S.; Devia, C.; Enriz, R.; Zacchino, S. *Molecules* **2000**, *5*, 428. (b) Vargas, L. Y.; Castelli, M. V.; Kouznetsov, V. V.; Urbina, J.

M.; Lopez, S. N.; Sortino, M.; Enriz, R. D.; Ribas, J. C.; Zacchino, S. *Bioorg. Med. Chem.* **2003**, *11*, 1531. (c) Gomez-Barrio, A.; Montero-Pereira, D.; Nogal-Ruiz, J. J.; Escario, J. A.; Muelas-Serrano, S.; Kouznetsov, V. V.; Mendez, L. Y. V.; Gonzalez, J. M. U.; Ochoa, C. *Acta Parasitol.* **2006**, *51*, 73.

(15) (a) Kang, T. H.; Jeong, S. J.; Ko, W. G.; Kim, N. Y.; Lee, B. H.; Inagaki, M.; Miyamoto, T.; Higuchi, R.; Kim, Y. C. *J. Nat. Prod.* **2000**, *63*, 680. (b) Chi, Y. S.; Jong, H. G.; Son, K. H.; Chang, H. W.; Kang, S. S.; Kim, H. P. *Biochem. Pharmacol.* **2001**, *62*, 1185. (c) Sohn, H. Y.; Son, K. H.; Kwon, C. S.; Kwon, G. S.; Kang, S. S. *Phytomedicine* **2004**, *11*, 666.

(16) For books: (a) Kündig, E. P. Transition Metal Arene π -Complexes in Organic Synthesis and Catalysis. *Topics in Organometallic Chemistry*, *7*; Springer-Verlag: Berlin, Heidelberg, New York. 2004. (b) Hartwig, J. F. *Organotransition Metal Chemistry: From Bonding to Catalysis*; University Science Books: Sausalito, CA. 2010. For reviews: (c) Kalinin, V. N. *Usp. Khim.* **1987**, *56*, 1190. *Russ. Chem. Rev.* **1987**, *56*, 682. (d) Rosillo, M.; Dominguez, G.; Perez-Castells, J. *Chem. Soc. Rev.* **2007**, *36*, 1589. For recent reports on asymmetric benzylic deprotonation of $(\eta^6\text{-arene})\text{Cr}(\text{CO})_3$: (e) Koide, H.; Hata, T.; Uemura, M. *J. Org. Chem.* **2002**, *67*, 1929, and references therein. (f) Castaldi, M. P.; Gibson, S. E.; Rudd, M.; White, A. J. P. *Chem.–Eur. J.* **2006**, *12*, 138, and references therein. For early reports on benzylic deprotonation of $(\eta^6\text{-arene})\text{Cr}(\text{CO})_3$ under mild conditions: (g) Kalinin, V. N.; Cherepanov, I. A.; Moiseev, S. K. *Metalloorg. Khim.* **1991**, *4*, 177. *Organomet. Chem. USSR* **1991**, *4*, 94. (h) Kalinin, V. N.; Cherepanov, I. A.; Moiseev, S. K. *J. Organomet. Chem.* **1997**, *536-537*, 437. Density functional theory calculations: (i) Merlic, C. A.; Walsh, J. C.; Tantillo, D. J.; Houk, K. N. *J. Am. Chem. Soc.* **1999**, *121*, 3596. (j) Merlic, C. A.; Miller, M. M.; Hietbrink, B. N.; Houk, K. N. *J. Am.*

Chem. Soc. **2001**, 123, 4904. (k) Merlic, C. A.; Hietbrink, B. N.; Houk, K. N. *J. Org. Chem.* **2001**, 66, 6738.

(17) Uemura, M. *Organic Reactions*: Wiley: New York, 2006; Vol. 67, p 217.

(18) When ^1H NMR deprotonation studies were conducted in THF with 1 equiv each of **1.1I** and $\text{LiN}(\text{SiMe}_3)_2$, **1.1I** exhibited approximately 50% deprotonation. Under similar conditions, **1.1a** exhibited 10% deprotonation. See McGrew, G. I.; Temaismithi, J.; Carroll, P. J.; Walsh, P. J. *Angew. Chem., Int. Ed.* **2010**, 49, 5541.

(19) Early reports on palladium–triphenylphosphine catalyzed allylic substitution reactions: (a) Atkins, K. E.; Walker, W. E.; Manyik, R. M. *Tetrahedron Lett.* **1970**, 3821. (b) Hata, G.; Takahashi, K.; Miyake, A. *J. Chem. Soc., Chem. Comm.* **1970**, 1392. (c) Trost, B. M.; Fullerton, T. J. *J. Am. Chem. Soc.* **1973**, 95, 292. Recent report by our group: (d) Hussain, M. M.; Walsh, P. J. *Angew. Chem., Int. Ed.* **2010**, 49, 1834.

(20) (a) Dreher, S. D.; Dormer, P. G.; Sandrock, D. L.; Molander, G. A. *J. Am. Chem. Soc.* **2008**, 130, 9257. (b) Dreher, S. D.; Lim, S.-E.; Sandrock, D. L.; Molander, G. A. *J. Org. Chem.* **2009**, 74, 3626. (c) Sandrock, D. L.; Jean-Gerard, L.; Chen, C.-Y.; Dreher, S. D.; Molander, G. A. *J. Am. Chem. Soc.* **2010**, 132, 17108. (d) Molander, G. A.; Argintaru, O. A.; Aron, I.; Dreher, S. D. *Org. Lett.* **2010**, 12, 5783. (e) Molander, G. A.; Trice, S. L. J.; Dreher, S. D. *J. Am. Chem. Soc.* **2010**, 132, 17701.

(21) (a) Gossage, R. A.; Jastrzebski, J. T. B. H.; van Koten, G. *Angew. Chem., Int. Ed.* **2005**, 44, 1448. (b) Jones, A. C.; Sanders, A. W.; Bevan, M. J.; Reich, H. J. *J. Am. Chem. Soc.* **2007**, 129, 3492. (c) Gessner, V. H.; Daschlein, C.; Strohmam, C. *Chem.–Eur. J.* **2009**, 15, 3320.

(22) (a) Traylor, T. G.; Stewart, K. J.; Goldberg, M. J. *J. Am. Chem. Soc.* **1984**, 106, 4445. (b) Traylor, T. G.; Stewart, K. J. *J. Am. Chem. Soc.* **1986**, 108, 6977. (c) Traylor, T. G.; Goldberg, M. J. *J. Am. Chem. Soc.* **1987**, 109, 3968.

(23) Early reports on Pd-catalyzed cross-coupling of (η^6 -chloroarene)Cr(CO)₃ compounds: (a) Villemin, D.; Schigeko, E. *J. Organomet. Chem.* **1985**, 293, C10. (b) Carpentier, J. F.; Castanet, Y.; Brocard, J.; Mortreux, A.; Petit, F. *Tetrahedron Lett.* **1991**, 32, 4705. (c) Carpentier, J. F.; Castanet, Y.; Brocard, J.; Mortreux, A.; Petit, F. *Tetrahedron Lett.* **1992**, 33, 2001. (d) Uemura, M.; Nishimura, H.; Hayashi, T. *Tetrahedron Lett.* **1993**, 34, 107. (e) Uemura, M.; Nishimura, H.; Kamikawa, K.; Nakayama, K.; Hayashi, Y. *Tetrahedron Lett.* **1994**, 35, 1909. (f) Uemura, M.; Nishimura, H.; Hayashi, T. *J. Organomet. Chem.* **1994**, 473, 129. (g) Carpentier, J. F.; Finet, E.; Castanet, Y.; Brocard, J.; Mortreux, A. *Tetrahedron Lett.* **1994**, 35, 4995.

(24) (a) You, S.-L.; Zhu, X.-Z.; Luo, Y.-M.; Hou, X.-L.; Dai, L.-X. *J. Am. Chem. Soc.* **2001**, 123, 7471. (b) Pretot, R.; Pfaltz, A. *Angew. Chem., Int. Ed.* **1998**, 37, 323.

(25) (a) Trost, B. M.; Toste, F. D. *J. Am. Chem. Soc.* **1999**, 121, 4545. (b) Butts, C. P.; Filali, E.; Lloyd-Jones, G. C.; Norrby, P.-O.; Sale, D. A.; Schramm, Y. *J. Am. Chem. Soc.* **2009**, 131, 9945.

(26) (a) Bravo-Altamirano, K.; Montchamp, J.-L. *Org. Lett.* **2006**, 8, 4169. (b) Usui, I.; Schmidt, S.; Breit, B. *Org. Lett.* **2009**, 11, 1453. In these papers, only linear products were reported without mentioning branched products.

(27) (a) Cavallini, G.; Massarani, E.; Nardi, D.; Mauri, L.; Barzaghi, F.; Mantegazza, P. *J. Am. Chem. Soc.* **1959**, 81, 2564. (b) Attwood, D. *J. Pharm. Pharmacol.* **1976**, 28, 407. (c) Tobe, A.; Yoshida, Y.; Ikoma, H.; Tonomura, S.; Kikumoto, R. *Arzneim. Forsch., Drug. Res.* **1981**, 31-2, 1278. (d) Ohizumi, Y.; Takahashi, M.; Tobe, A. *Br. J. Pharmacol.* **1982**, 75, 377. (e) Hattori, H.; Yamamoto, S.; Iwata, M.; Takashima, E.; Yamada, T.; Suzuki, O. *J. Chromatogr.-Biomed.* **1992**, 581, 213. (f) Li, J. J.; Johnson, D. S.; Sliskovic, D. R.; Roth, B. D. *Contemporary Drug Synthesis*; Wiley-Interscience: 2004; p. 221 (Zyrtec).

- (28) (a) Oster, G.; Nishijima, Y. *J. Am. Chem. Soc.* **1956**, *78*, 1581. (b) Bomberger, D. C.; Gwinn, J. E.; Boughton, R. L. *Wastes from Manufacture of Dyes and Pigments*; US EPA-600/2-84-III, US. Government Printing Office: Washington, DC.
- (29) Randall, D.; Lee, S. *The Polyurethanes Book*; Wiley: New York, 2003.
- (30) Bouquillon, S.; Muzart, J. *Eur. J. Org. Chem.* **2001**, 3301.
- (31) Zima, A.; Hosek, J.; Treml, J.; Muselik, J.; Suchy, P.; Prazanova, G.; Lopes, A.; Zemlicka, M. *Molecules* **2010**, *15*, 6035.
- (32) Murakami, S.; Kijima, H.; Isobe, Y.; Muramatsu, M.; Aihara, H.; Otomo, S.; Baba, K.; Kozawa, M. *J. Pharm. Pharmacol.* **1990**, *42*, 723.
- (33) (a) Van Tamelen, E. E.; Carlson, J. G.; Russell, R. K.; Zawacky, S. R. *J. Am. Chem. Soc.* **1981**, *103*, 4615. (b) Van Tamelen, E. E.; Zawacky, S. R.; Russel, R. K.; Carlson, J. G. *J. Am. Chem. Soc.* **1983**, *105*, 142. (c) Kim, M. B.; Shaw, J. T. *Org. Lett.* **2010**, *12*, 3324.
- (34) *Ortho*-palladation: (a) Cope, A. C.; Friedrich, E. C. *J. Am. Chem. Soc.* **1968**, *90*, 909. (b) Dupont, J.; Consorti, C. S.; Spencer, J. *Chem. Rev.* **2005**, *105*, 2527. (c) Vicente, J.; Saura-Llamas, I.; Palin, M. G.; Jones, P. G.; Ramirez de Arellano, M. C. *Organometallics* **1997**, *16*, 826. *Ortho*-arylation: (d) Daugulis, O.; Lazareva, A. *Org. Lett.* **2006**, *8*, 5211.
- (35) Trost, B. M.; Verhoeven, T. R. *J. Org. Chem.* **1976**, *41*, 3215.
- (36) Matsushita, H.; Negishi, E. *J. Chem. Soc., Chem. Comm.* **1982**, 160.
- (37) Trost, B. M.; Malhotra, S.; Olson, D. E.; Maruniak, A.; Du Bois, J. *J. Am. Chem. Soc.* **2009**, *131*, 4190.
- (38) Bourque, L. E.; Cleary, P. A.; Woerpel, K. A. *J. Am. Chem. Soc.* **2007**, *129*, 12602.
- (39) Mowery, M. E.; DeShong P. *J. Org. Chem.* **1999**, *64*, 1684.
- (40) Alonso, E.; Guijarro, D.; Martinez, P.; Ramon, D. J.; Yus, M. *Tetrahedron* **1999**, *55*, 11027.

- (41) Weix, D. J.; Markovic, D.; Ueda, M.; Hartwig, J. F. *Org. Lett.* **2009**, *11*, 2944.
- (42) Watson, I. D. G.; Yudin, A. K. *J. Am. Chem. Soc.* **2005**, *127*, 17516.
- (43) Trost, B. M.; Malhotra, S.; Chan, W. H. *J. Am. Chem. Soc.* **2011**, *133*, 7328.
- (44) Tseng, C. C.; Paisley, S. D.; Goering, H. L. *J. Org. Chem.* **1986**, *51*, 2884.
- (45) Fontana, G.; Lubineau, A.; Scherrmann, M.-C. *Org. Biomol. Chem.* **2005**, *3*, 1375.
- (46) Chudek, J. A.; Hunter, G.; Mackay, R. L.; Kremminger, P.; Schlogl, K.; Weissensteiner, W. *J. Chem. Soc. Dalton Trans.* **1990**, 2001.
- (47) Brown, D. A.; Raju, J. R. *J. Chem. Soc. A* **1966**, 1617.
- (48) Fritz, H. P.; Kreiter, C. G. *J. Organomet. Chem.* **1967**, *7*, 427.
- (49) Jackson, W. R.; Jennings, W. B.; Rennison, S. C.; Spratt, R. *J. Chem. Soc. B* **1969**, 1214.
- (50) Cram, D. J.; Wilkinson, D. I. *J. Am. Chem. Soc.* **1960**, *82*, 5721.
- (51) Cambie, R. C.; Clark, G. R.; Gallagher, S. R.; Rutledge, P. S.; Stone, M. J.; Woodgate, P. D. *J. Organomet. Chem.* **1988**, *342*, 315.
- (52) Blagg, J.; Davies, S. G.; Holman, N. J.; Laughton, C. A.; Mobbs, B. E. *J. Chem. Soc., Perkin Trans. 1* **1986**, 1581.
- (53) Gibson, S. E.; Smith, M. H. *Org. Biomol. Chem.* **2003**, *1*, 676.
- (54) Co, T. T.; Paek, S. W.; Shim, S. C.; Cho, C. S.; Kim, T. J.; Choi, D. W.; Kang, S. O.; Jeong, J. H. *Organometallics* **2003**, *22*, 1475.
- (55) Matsushita H.; Negishi E. *J. Org. Chem.* **1982**, *47*, 4161.
- (56) Li, Y.; Huang, J. S.; Zhou, Z. Y.; Che, C. M. *J. Am. Chem. Soc.* **2001**, *123*, 4843.
- (57) Yasuda, M.; Saito, T.; Ueba, M.; Baba, A. *Angew. Chem., Int. Ed.* **2004**, *43*, 1414.
- (58) (a) Koelsch, C. F.; Richter, H. J. *J. Org. Chem.* **1938**, *3*, 473. (b) Wittig, G.; Klein, A. *Chem. Ber.* **1936**, *69*, 2087.
- (59) Hatano, B.; Nagahashi, K.; Kijima, T. *J. Org. Chem.* **2008**, *73*, 9188.

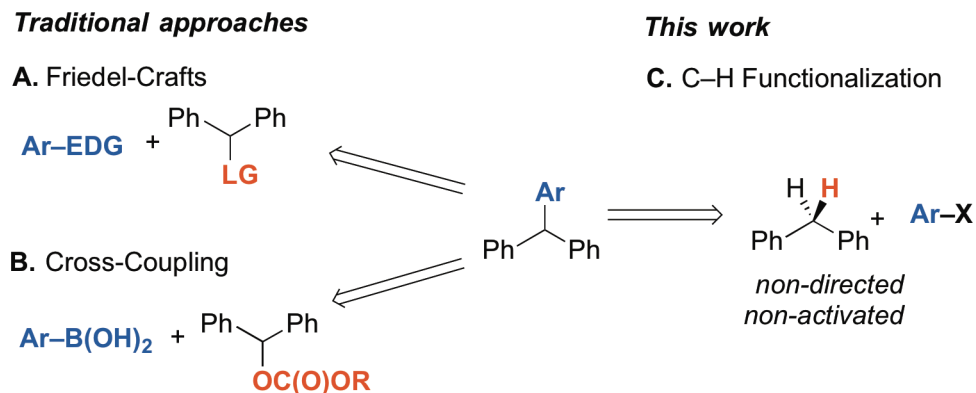
- (60) (a) Trost, B. M.; Verhoeven, T. R. *J. Org. Chem.* **1976**, *41*, 3215. (b) Trost, B. M.; Thaisrivongs, D. A. *J. Am. Chem. Soc.* **2008**, *130*, 14092.
- (61) Sathe, K. M.; Nandi, M.; Amin, S. R.; Puranik, V. G.; Sarkar, A. *Organometallics* **1996**, *15*, 2881.

Chapter 2

Palladium-Catalyzed C(sp³)-H Arylation of Diarylmethanes at Room Temperature: Synthesis of Triarylmethanes via Deprotonative-Cross-Coupling Processes (DCCP)

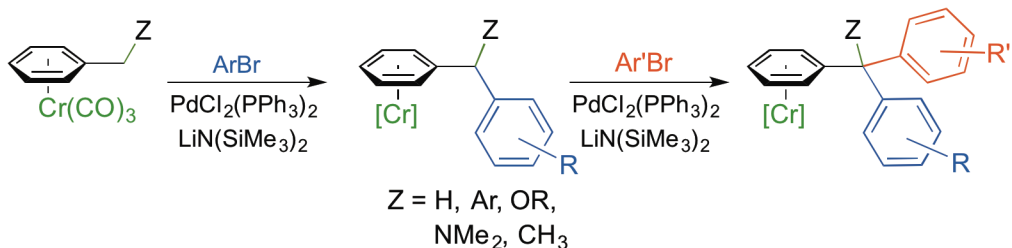
2.1 Introduction

Triarylmethane derivatives are well-known substructures in several areas, including leuco dye precursors,¹ photochromic agents,² and applications in materials science.³ They are also important in medicinal chemistry as antitubercular,⁴ anticancer,⁵ and antiproliferative⁶ agents, among others.^{7,8} For the past decade, advances in the catalytic synthesis of triarylmethanes were largely based on two approaches:⁹ (1) Friedel–Crafts-type arylations of diarylmethanols or diarylmethylamines (Scheme 2.1A)^{10,11} and (2) cross-coupling reactions between diarylmethyl carbonates with arylboronic acids (Scheme 2.1B).¹² Despite the popularity of these methods, both have drawbacks. Friedel–Crafts-type arylations typically have significant electronic and steric limitations, being largely limited to electron-rich and unhindered nucleophiles. Additionally, mixtures of regioisomeric products are often obtained. Cross-coupling methods require prefunctionalization of the coupling partners and occasionally give moderate yield, complicated by formation of homocoupling byproducts.^{12a}



Scheme 2.1 Synthetic approaches to triarylmethanes: (A) Friedel–Crafts reaction, (B) cross-coupling, and (C) non-directed C(sp³)–H arylation (EDG=electron donating group, LG=leaving group)

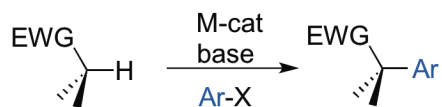
We recently introduced a novel approach toward the catalytic synthesis of di- and triarylmethanes based on an η^6 -arene-activation strategy. Initial studies employed readily available (η^6 -PhCH₂Z)Cr(CO)₃ complexes (Z = Ph, H, OR, NR₂, Scheme 2.2).¹³ Arylations of η^6 -coordinated toluene, diphenylmethane, benzyl ethers, and benzylamines were readily achieved. Although proof-of-concept of this approach was demonstrated, the stoichiometric use of chromium precludes large-scale applications of this chemistry. As outlined in Scheme 2.1C, we envisioned a chromium-free direct arylation approach involving C(sp³)–H bonds of diphenylmethane derivatives.



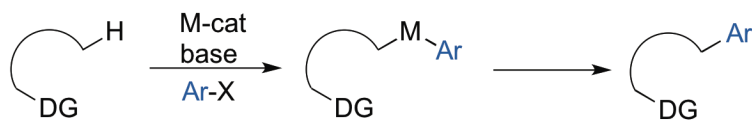
Scheme 2.2 Cross-coupling of (η^6 -C₆H₅-CH₂Z)Cr(CO)₃ complexes with aryl bromides

Although metal-catalyzed cross-coupling reactions to form C–C bonds have become a mainstay in organic synthesis,¹⁴ metal-catalyzed direct arylation reactions of C(sp³)–H bonds possess distinct advantages.^{15,16} Compared with traditional cross-coupling reactions with prefunctionalized partners (Scheme 2.1B), C–H arylation reactions are efficient, atom-economical, and minimize the costs of prefunctionalization. Great progress has been made in direct arylations of activated C(sp³)–H bonds α to electron-withdrawing groups, such as ketones, esters, and amides, among others (Scheme 2.3A).¹⁵ In contrast, much less success has been achieved with the more challenging functionalization of non- or weakly acidic C(sp³)–H bonds. To facilitate reactions at the unactivated C(sp³)–H bonds (those with $pK_a > 30$ ^{16d}), chemists have relied heavily on substrates with appropriately placed directing groups to steer reactivity (Scheme 2.3B).^{16a–d} Although this approach avoids classical prefunctionalization of substrates, the addition and removal of directing groups often offsets any gain in synthetic efficiency provided by the direct C(sp³)–H functionalization. To date, intermolecular arylation of C(sp³)–H bonds *in the absence of* directing groups remains a formidable challenge.¹⁷

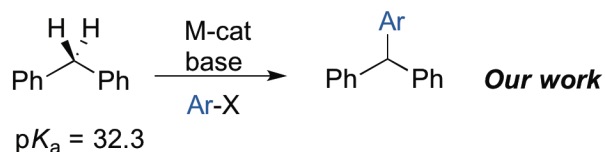
A. Activated C(sp³)–H bond alpha to an EWG ($pK_a < 30$)



B. Directed arylation of unactivated C(sp³)–H bond ($pK_a > 30$)



C. Non-directed arylation of unactivated C(sp³)–H bond ($pK_a > 30$)



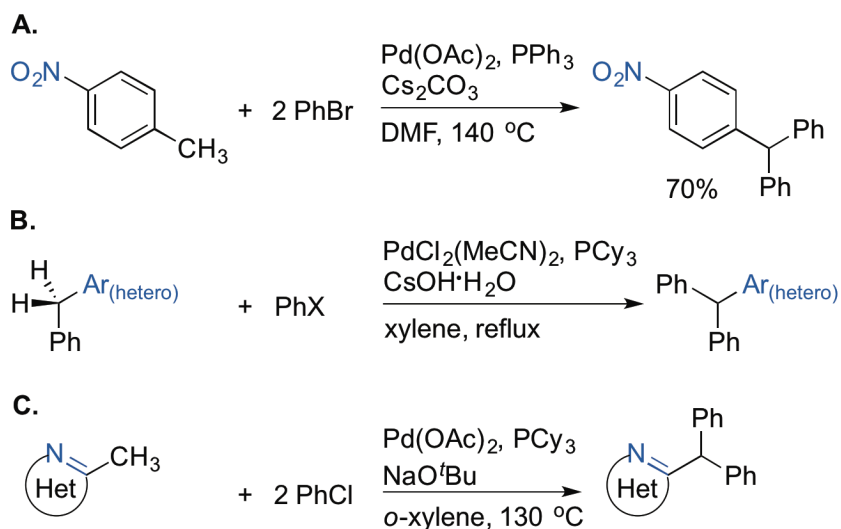
Scheme 2.3 Catalytic C(sp³)-H arylations

To streamline the synthesis of triarylmethanes, we set out to develop a general *room-temperature* directing-group-free method employing simple *diarylmethane* derivatives. To increase the practicality and utility of the method, we restricted our efforts to in situ metallation of the substrate via C-H deprotonation under catalytic cross-coupling conditions, and will refer to these transformations as deprotonative-cross-coupling processes (DCCP) (Scheme 2.3C). Herein we report a palladium-catalyzed DCCP that fulfills these requirements. The advantages of this method are: mild and reversible substrate deprotonation simply by mixing diarylmethanes with KN(SiMe₃)₂, good functional group tolerance and chemoselectivity, nearly stoichiometric ratios of coupling partners for most substrates (down to 1.2:1), and commercial availability of Pd source and ligand.

2.2 Results and Discussion

The first objective towards developing DCCPs is to identify conditions for the deprotonation of diphenylmethane (Ph₂CH₂). Diphenylmethane is weakly acidic, with a pK_a of 32.3 in DMSO.¹⁸ The benzylic C-H bonds in diphenylmethane have traditionally been deprotonated with *n*-BuLi at -78 °C¹⁹ or NaNH₂ and KNH₂ in liquid ammonia.^{20,21} These conditions were viewed as cumbersome and impractical because of the low temperature and strongly basic media. We therefore focused on identifying conditions for the reversible in situ deprotonation of diphenylmethane that would be mild and compatible with the catalyst, reagents, and products in the DCCP. The second challenge is the discovery of catalysts suitable for cross-coupling processes at room temperature.

Prior reports on coupling with diarylmethane derivatives have employed various activation strategies to decrease the pK_a of the substrates. As mentioned above, we activated benzylic C–H bonds through coordination to the $\text{Cr}(\text{CO})_3$ (Scheme 2.2).^{13,22} Miura has employed substrates bearing strong electron-withdrawing groups on the aryl ring, as exemplified by 4-nitrotoluene (pK_a 20.4, Scheme 2.4A).²³ 2-Benzyl- (Scheme 2.4B) and 2-methyl heteroarenes (Scheme 2.4C) are significantly more acidic than diphenylmethane, and have been successfully employed in DCCPs.^{17a,c} Deprotonation of these substrates can be facilitated by binding of the substrates' nitrogen to Lewis acidic species in solution. All three approaches required high temperatures (typically 130–150 °C). However, these methods fail with diarylmethane substrates such as 3-benzylpyridine and diphenylmethane itself.



Scheme 2.4 DCCP with activated benzylic C–H bonds

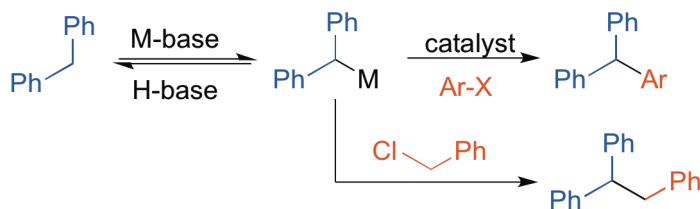
2.2.1 Development of Room-Temperature Deprotonation/Benylation of Diphenylmethane

We decided to separate the challenges of identifying the deprotonation conditions from the development and optimization of the catalyst. We, therefore, first

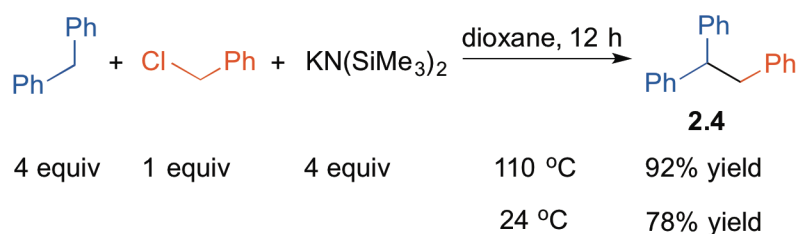
examined diphenylmethane deprotonation step to determine the suitability of the substrate/base combinations. As a surrogate for the transmetallation step in the DCCP, we began with a deprotonation/benzylation reaction employing benzyl chloride (Scheme 2.5). A large number of variables for reagents and conditions were to be simultaneously examined, including: (1) base strength, (2) base nucleophilicity, (3) choice of main-group counterion (M = Li, Na, K), (4) stoichiometry, (5) solvent, (6) concentration and (7) temperature. Based on our previous experience with the DCCP of (η^6 -PhCH₂Z)Cr(CO)₃ complexes,^{13,22} the choice of base would be critical for both deprotonation and cross-coupling. To perform this study in the most efficient manner, we employed low-barrier microscale high-throughput experimentation (HTE)²⁴ techniques.ⁱ Using 12 diverse bases [LiN(SiMe₃)₂, NaN(SiMe₃)₂, KN(SiMe₃)₂, LiO-*t*-Bu, NaO-*t*-Bu, KO-*t*-Bu, LDA, LiH, KH, LiOH, KOH, and K₂CO₃] revealed that the combination of 4 equiv of diphenylmethane and 4 equiv of KN(SiMe₃)₂ with 1 equiv of benzyl chloride in dioxane at 110 °C was the most promising. Translation of this lead to laboratory scale (0.1 mmol) under the same conditions showed excellent reproducibility and rendered the benzylation product **2.4** in 92% yield (Scheme 2.6). Surprisingly, results of the HTE experiments indicated the *only* base leading to in situ deprotonation/benzylation product was KN(SiMe₃)₂. Neither LiN(SiMe₃)₂, NaN(SiMe₃)₂, nor MO-*t*-Bu (M = Li, Na, K) showed any reactivity (on both microscale or laboratory scale). Decreasing the reaction temperature from 110 °C to 24 °C resulted in 78% yield of **2.4** (Scheme 2.6). Note that benzyl chloride did not react with bulky KN(SiMe₃)₂ on the timescale of the benzylation of diphenylmethane. Unlike bases previously used to deprotonate diphenylmethane (*n*-

ⁱ HTE screens in this chapter were performed in collaboration with Dr. Ana Bellomo at Penn/Merck Laboratory for High-Throughput Experimentation.

BuLi, NaNH₂, and KNH₂), KN(SiMe₃)₂ has a high likelihood of compatibility with catalyst, reagents, and products in catalytic DCCP (Scheme 2.5).²⁵



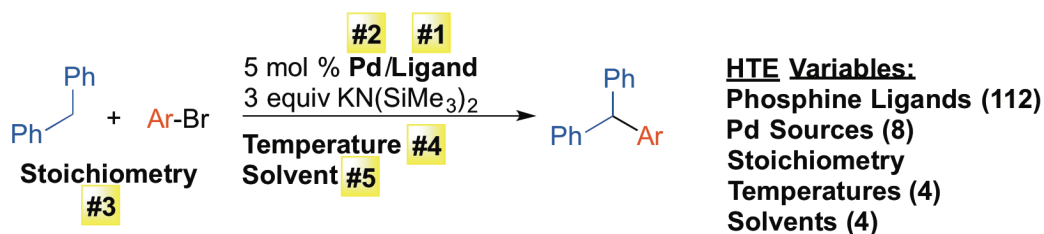
Scheme 2.5 Benzylation used as surrogate for the transmetalation step in DCCP



Scheme 2.6 Deprotonation/benylation of diphenylmethane by KN(SiMe₃)₂

2.2.2 Development and Optimization of Palladium-Catalyzed DCCP of C(sp³)-H of Diarylmethanes

We next turned our attention to the development of a Pd-catalyzed DCCP of C(sp³)-H of diarylmethanes. Essential to accomplish this goal was the rapid identification of reagents and conditions from HTE on a 10 μmol scale. These efforts are summarized in Scheme 2.7, where the variables examined with cumulative HTE are numbered (see “2.4 Experimental Section” for details).

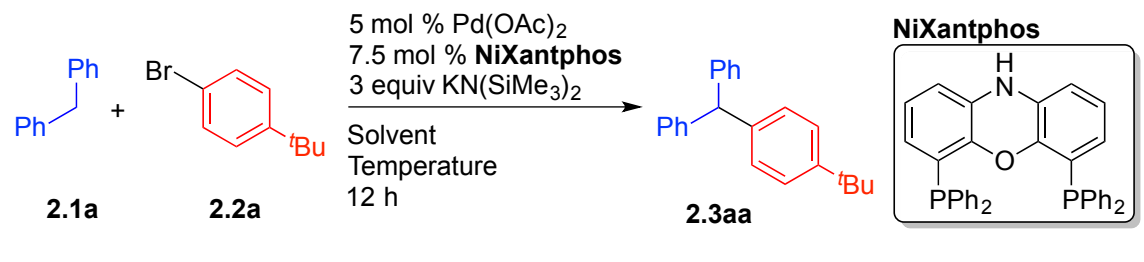


Scheme 2.7 HTE variables in Pd-catalyzed DCCP of diarylmethanes

We initially evaluated the reaction of diphenylmethane (**2.1a**) with 1-bromo-4-*tert*-butylbenzene (**2.2a**) using 112 sterically and electronically diverse, mono- and bidentate phosphine ligands and different Pd(0) and Pd(II) sources on a 10 μ mol scale at 110 °C (see “2.4 Experimental Section” for details). To our surprise, only one ligand from the entire collection, NiXantphos²⁶ (see Table 2.1 for the structure), afforded an excellent HPLC assay yield (AY) of the corresponding DCCP product **2.3aa** (93% AY from Pd(PPh₃)₂Cl₂/NiXantphos and 100% AY from Pd(OAc)₂/NiXantphos). These microscale reactions were successfully translated to laboratory scale (0.1 mmol) under the same conditions.

Although the combination of Pd(OAc)₂ and NiXantphos as precatalyst afforded the triarylmethane product **2.3aa** in excellent yield in the presence of 4 equiv of diphenylmethane (**2.1a**), 1 equiv of aryl bromide (**2.2a**), and 3 equiv of KN(SiMe₃)₂ in dioxane at 110 °C (Table 2.1, entry 1), further optimization was desired to reduce the equivalents of diphenylmethane and the reaction temperature.

Table 2.1 Optimization of Pd-catalyzed DCCP of **2.1a**^a

					
entry	2.1a:2.2a	solvent	temp (°C)	yield (%) ^b	HTE yield (%) ^c
1	4.0:1.0	dioxane	110	>95	100

2	2.0:1.0	dioxane	110	91	99
3	1.2:1.0	dioxane	110	77	77
4	1.2:1.0	dioxane	24	53	55
5	1.2:1.0	CPME	24	>95 (95 ^d)	96

^aReactions conducted on a 0.1 mmol scale using 1 equiv of **2.2a**, 3 equiv of KN(SiMe₃)₂, and **2.1a** at 0.1 M. ^bYield determined by ¹H NMR spectroscopy of the crude reaction mixture. ^cHPLC assay yield of HTE conducted on a 10 μmol scale. ^dIsolated yield after chromatographic purification.

Reducing the equivalents of diphenylmethane from 4 to 2 and 1.2 in dioxane at 110 °C resulted in a drop in triarylmethane yield from >95% to 77% (entries 2–3). Furthermore, the reaction at 24 °C gave moderate yield compared with that at 110 °C (entry 4 vs 3). To reduce both the equivalents of diphenylmethane and reaction temperature without compromising the yield, four ethereal solvents [dioxane, THF, 2-MeTHF and CPME (cyclopentyl methyl ether)] and three temperatures (24, 50, and 70 °C) were examined. The best result was obtained when CPME was used as solvent, where the triarylmethane **2.3aa** was generated in >95% yield from 1.2 equiv of diphenylmethane, 1 equiv of aryl bromide **2.2a**, and 3 equiv of KN(SiMe₃)₂ at 24 °C (entry 5). The triarylmethane **2.3aa** was ultimately isolated on laboratory scale in 95% yield after flash chromatography (entry 5).

Control experiments conducted in the absence of any reagent, ligand, or palladium from the reaction mixture above resulted in no product. These optimized conditions were carried forward in the next phase of the project, which focused on the determination of the scope of diarylmethane derivatives in Pd-catalyzed DCCP.

2.2.3 Scope of Diarylmethanes in Palladium-Catalyzed DCCP

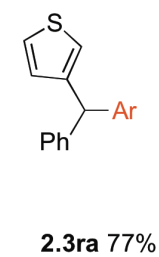
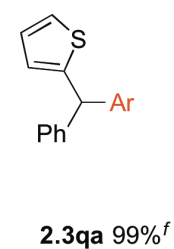
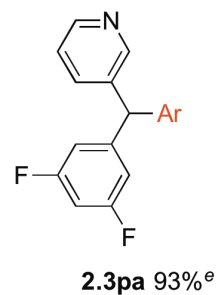
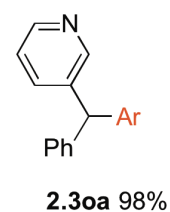
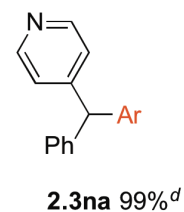
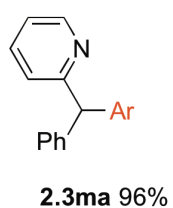
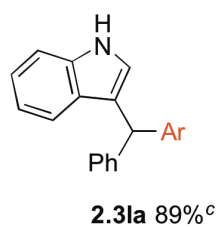
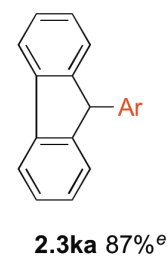
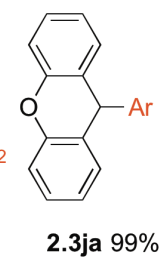
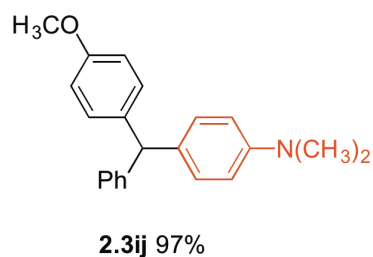
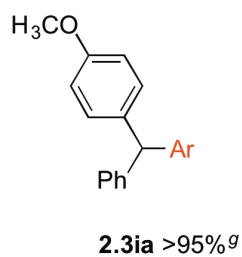
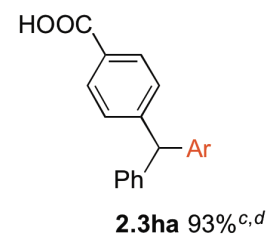
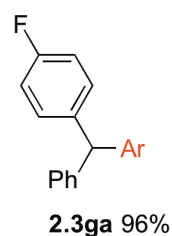
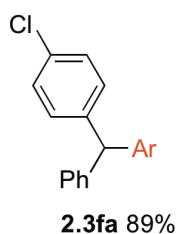
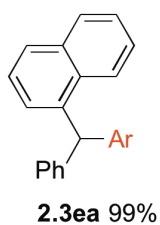
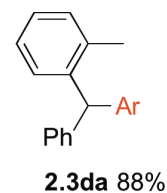
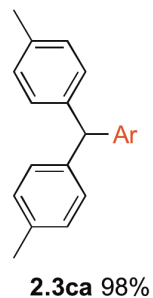
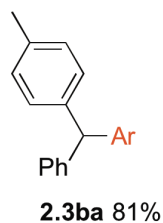
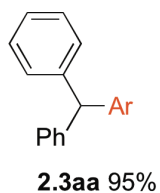
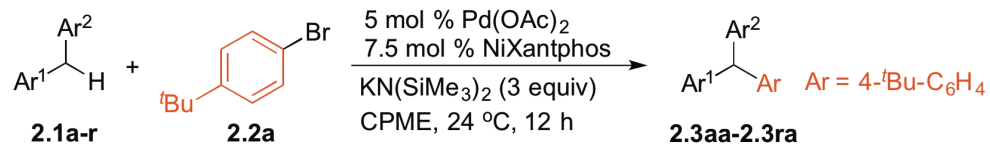
The scope of the DCCP with various diarylmethanes and 1-bromo-4-*tert*-butylbenzene (**2.2a**) is presented in Table 2.2. These reactions were conducted at 24 °C, except where noted. Substrates bearing various substituents on the diarylmethane exhibited excellent reactivity. Alkyl groups (**2.3ba**, **2.3ca**, **2.3da**), *ortho*-substituents (**2.3da**, **2.3ea**), electron-withdrawing (**2.3fa**, **2.3ga**), and electron-donating groups (**2.3ij**) were all well tolerated. Although 4-methoxydiphenylmethane (**2.1i**) reacted with **2.2a** to give >95% conversion to the desired triarylmethane product **2.3ia** (as determined by ¹H NMR of the crude reaction mixture), **2.3ia** was inseparable from the starting diarylmethane (**2.1i**) by flash chromatography. The reaction of **2.1i** with 4-bromo-*N,N*-dimethylaniline (**2.2j**) afforded the desired triarylmethane product **2.3ij** in 97% isolated yield. Interestingly, 4-benzylbenzoic acid (**2.1h**) proved to be a suitable substrate, providing the corresponding product **2.3ha** in 93% yield at 110 °C. In addition to increasing the temperature, an extra equiv of KN(SiMe₃)₂ was necessary to convert the starting acid into a potassium salt.

After demonstrating that our method was compatible with various diarylmethanes with different steric and electronic properties, we examined cyclic diarylmethane analogues. Both xanthene (**2.1j**) and fluorene (**2.1k**) proved to be good substrates, with corresponding products isolated in 99% (**2.3ja**) and 87% (**2.3ka**) yield. Note that the reaction with fluorene (**2.1k**) was run in THF at 85 °C due to solubility issues in CPME at 24 °C.

The next family of substrates examined was heteroaromatic diarylmethane derivatives, which are known for their utility in medicinal chemistry.²⁷ 3-Benzyl-1*H*-indole did not participate in the DCCP with **2.2a** under the optimized conditions, probably due to the decreased acidity of the benzylic hydrogens after deprotonation of the free N–H.^{28a}

Fortunately, DCCP proceeded with the *N*-Boc substrate in the presence of 4 equiv of $\text{KN}(\text{SiMe}_3)_2$ to furnish the indole-containing triarylmethane product **2.3la** in 89% isolated yield. Notably, **2.3la** was isolated in the deprotected 1*H*-indole form. The observed reactivity of 3-benzyl-1*H*-indole and its *N*-Boc analogue suggested that **2.3la** was formed via DCCP with subsequent *N*-Boc deprotection under the reaction conditions. Pyridine substrates bearing benzyl groups on different positions were also examined. Isomeric 2-, 3-, and 4-benzylpyridine substrates all underwent DCCP smoothly to afford high yields of pyridine-containing triarylmethane products (**2.3ma**, **2.3na**, **2.3oa**, **2.3pa**). Although 2- and 4-benzylpyridine were known to participate in Pd-catalyzed DCCP at reflux in xylene, DCCP reactions with 3-benzylpyridine failed in prior studies even under vigorous conditions.^{17a} The lack of reactivity of 3-benzylpyridine under previously reported conditions is likely due to its higher $\text{p}K_a$ (30.1) compared with 2- and 4-benzylpyridines ($\text{p}K_a = 28.2$ and 26.7 , respectively).^{28b} It is noteworthy that 3-benzylpyridine affords the product in 98% yield at 24 °C with our procedure. In addition to 3-benzylpyridine, 3-(3,5-difluorobenzyl)pyridine (**2.1p**) was successfully arylated to afford **2.3pa** in 93% isolated yield. Elevated temperatures were required for 4-benzylpyridine to give **2.3na** (110 °C in CPME) and 3-(3,5-difluorobenzyl)pyridine to furnish **2.3pa**, (85 °C in THF) due to the low solubility of the substrates in CPME at 24 °C. In addition to nitrogen-containing substrates, 2-benzylthiophene (**2.1q**) and 3-benzylthiophene (**2.1r**) underwent DCCP at 24 °C to afford corresponding products **2.3qa** and **2.3ra** in 99% and 77% yield, respectively. To summarize, this method enables the synthesis of a variety of triarylmethanes from diarylmethanes bearing *ortho*-substitution and with electron-donating, electron-withdrawing, and heteroaryl groups.

Table 2.2 Scope of diarylmethanes in Pd-catalyzed DCCP^{a,b}



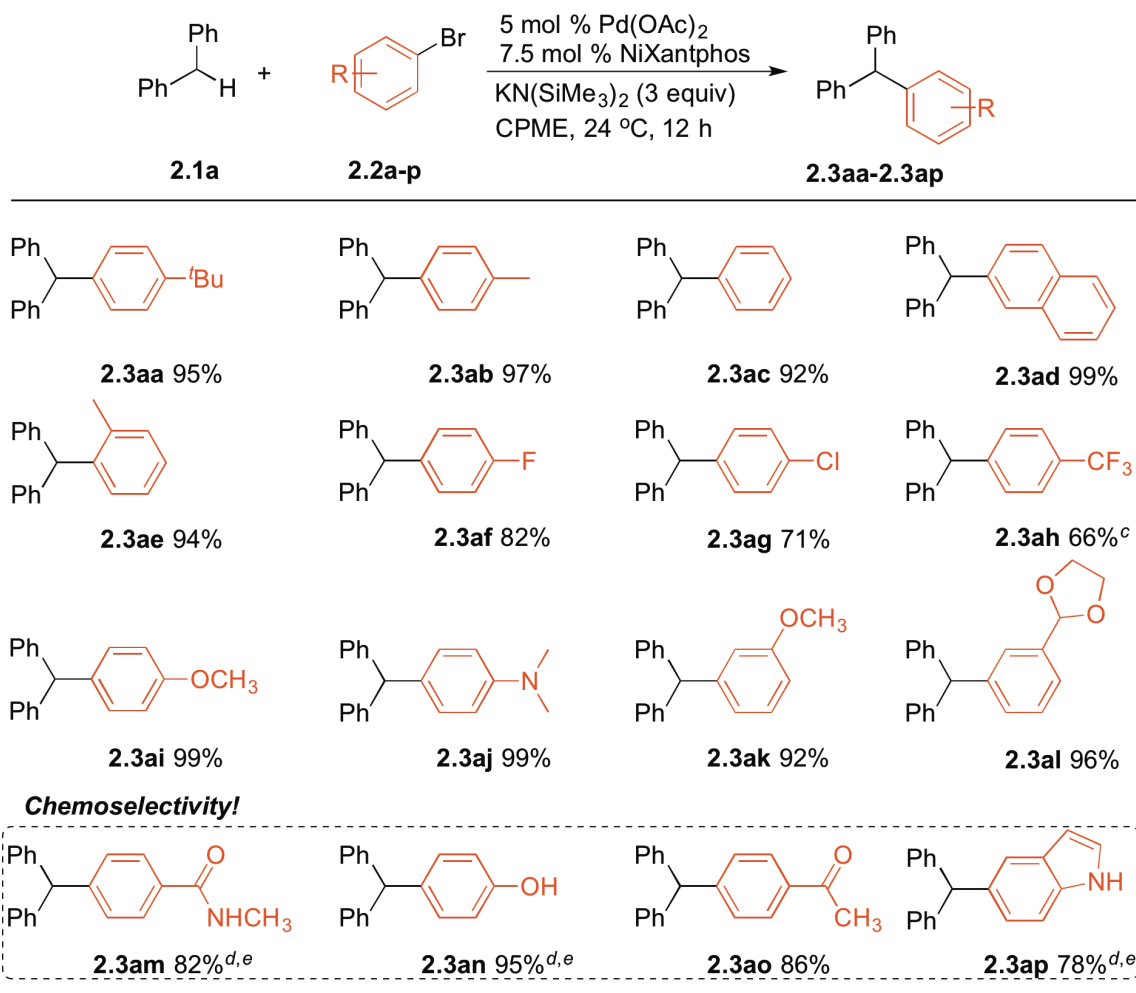
^aReactions conducted on a 0.1 mmol scale using 1 equiv of **2.2a**, 3 equiv of KN(SiMe₃)₂, and 1.2–3 equiv of **2.1** at 0.1 M. ^bIsolated yield after chromatographic purification. ^c4 equiv of KN(SiMe₃)₂. ^d110 °C. ^e85 °C in THF. ^f1.5 equiv of KN(SiMe₃)₂. ^gYield determined by ¹H NMR spectroscopy of the crude reaction mixture.

2.2.4 Scope of Aryl Bromides in Palladium-Catalyzed DCCP

The scope of the DCCP with respect to aryl bromides was next explored with diphenylmethane (**2.1a**) (Table 2.3). Phenyl and 2-naphthyl bromides furnished **2.3ac** and **2.3ad** in 92% and 99% yield, respectively. Aryl bromides bearing various substituents exhibited good to excellent reactivity. Alkyl groups (**2.3aa**, **2.3ab**), *ortho*-methyl (**2.3ae**), electron-withdrawing groups (**2.3af**, **2.3ag**, **2.3ah**), and electron-donating groups (**2.3ai**, **2.3aj**, **2.3ak**) were all well tolerated. 1-Bromo-4-chlorobenzene (**2.2g**) reacted with **2.1a** to produce **2.3ag** as the exclusive product in 71% isolated yield. No products derived from Ar–Cl oxidative addition were observed. The difference in reactivity of C–Cl and C–Br bonds in **2.2g** is in accordance with previous studies on oxidative addition of haloarenes.²⁹ To demonstrate the advantage of the mild conditions of our method over the previous deprotonation conditions using *n*-BuLi, NaNH₂, and KNH₂, we then tested substrates bearing sensitive functional groups. As shown in Table 2.3 remarkable chemoselectivity is observed with aryl bromides containing acetal, amide, phenol, acetyl, and 1*H*-indole moieties, which all underwent DCCP, delivering the corresponding functionalized products in 78–96% yield (**2.3al**–**2.3ap**). Ketones are well known to undergo 1,2-carbonyl addition reactions with reactive organometallics. 4-Bromoacetophenone might be expected to participate in competitive aldol chemistry³⁰ and α -arylation of the enolate derived from deprotonation¹⁵ under the basic conditions of the reaction (p*K*_a of acetophenone in DMSO: 24.7³¹). Yet the triarylmethane **2.3ao** was

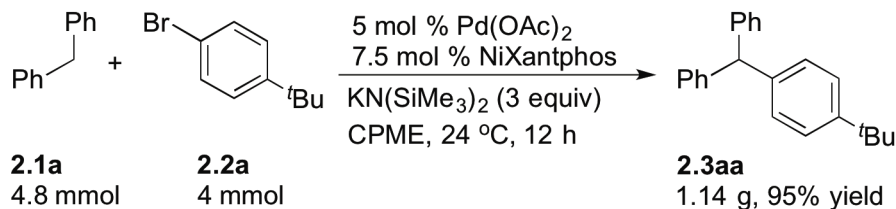
produced in 86% yield. Phenols are known to undergo O- and C(sp²)-H arylation³² while 1*H*-indoles have been reported to react via N-arylation (Buchwald-Hartwig coupling),³³ C-2-, and C-3-arylation³⁴ in the presence of palladium catalysts and bases. Our method exhibits orthogonal chemoselectivity with arylation taking place selectively at the benzylic C(sp³)-H bonds. These functional groups present opportunities to functionalize the triarylmethane products further. It is noteworthy that for 4-bromo-*N*-methylbenzamide (**2.2m**), 4-bromophenol (**2.2n**) and 5-bromoindole (**2.2p**), an extra equiv of KN(SiMe₃)₂ as well as elevated temperature (110 °C) were employed to raise the yield to 82% (**2.3am**), 95% (**2.3an**) and 78% (**2.3ap**), respectively. For substrates giving less than 80% yield in Table 3 (**2.3ag**, **2.3ah**, **2.3ap**), ¹H NMR of the reaction mixture after work-up and removal of volatiles showed no byproduct formation. The DCCP products were easily separated from the unreacted diphenylmethane by flash chromatography.

Table 2.3 Scope of aryl bromides in Pd-catalyzed DCCP^{a,b}

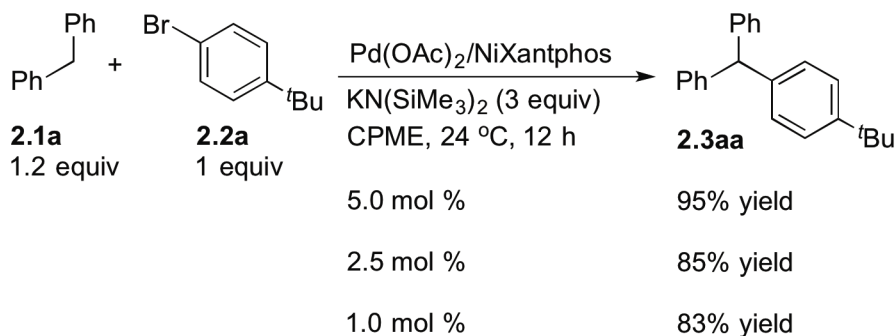


^aReactions conducted on a 0.1 mmol scale using 1 equiv of aryl bromide, 3 equiv of KN(SiMe₃)₂, and 1.2–3 equiv of diphenylmethane at 0.1 M. ^bIsolated yield after chromatographic purification. ^c2 equiv of KN(SiMe₃)₂. ^d4 equiv of KN(SiMe₃)₂. ^e110 °C.

To illustrate the practical utility of our method, we examined its scalability by conducting the reaction of **2.1a** with **2.2a** on a 4 mmol scale, which afforded 1.14 grams of **2.3aa** (95% isolated yield, Scheme 2.8). We were also able to reduce the catalyst loading to 1.0 mol % with only a minor drop in yield (Scheme 2.9).



Scheme 2.8 Gram-scale DCCP of **2.1a** with **2.2a**



Scheme 2.9 Variation of the catalyst loading in DCCP

2.3 Conclusions

We have developed the first general, high-yielding, and scalable method for the palladium-catalyzed C(sp³)-H arylation of diarylmethanes at room temperature. This method circumvents the traditional low-temperature deprotonation conditions with strong bases and the high temperature cross-coupling conditions employed previously with more acidic, activated diarylmethane substrates. Our DCCP affords a variety of triarylmethane derivatives, a class of compounds with various applications and biological activity. Additionally, the DCCP exhibits remarkable chemoselectivity in the presence of substrates that are known to undergo O-, N-, enolate-, and C(sp²)-H arylation.

The development of the DCCP was accomplished by solving two challenging interdependent problems: (1) to identify deprotonation conditions for diphenylmethane (pK_a 32.3) and related weakly acidic derivatives that would be amenable to catalysis,

and (2) to find a catalyst that would be compatible with the deprotonation conditions and promote the cross-coupling. Our approach to these two challenges was to separate them by employing a deprotonation/benzylation protocol as a surrogate for the deprotonation/transmetalation of the desired catalytic cycle. Interestingly, only a single base, $\text{KN}(\text{SiMe}_3)_2$, of the 12 examined, worked for the benzylation. Once the base had been identified, a search for a catalyst was conducted by screening 112 phosphine ligands and several palladium sources. The use of the HTE tools enabled rapid identification of the $\text{Pd}(\text{OAc})_2/\text{NiXantphos}$ combination as an excellent catalyst system for DCCP at room temperature. In hindsight, it is unlikely that we would have identified a reasonable catalyst system given that a single base/ligand combination was found to be successful. This translates to 1 out of 1344 combinations (12 bases \times 112 ligands) of the two most important variables.

The broad scope and mild conditions of the DCCP outlined herein make it a valuable contribution to applications in non-directed transition metal-catalyzed arylation of $\text{C}(\text{sp}^3)\text{-H}$ bonds for the synthesis of triarylmethanes. Preliminary mechanistic studies to understand how the $\text{Pd}(\text{OAc})_2/\text{NiXantphos}$ combination promotes the room-temperature DCCP of diarylmethanes are described in Chapter 3.

2.4 Experimental Section

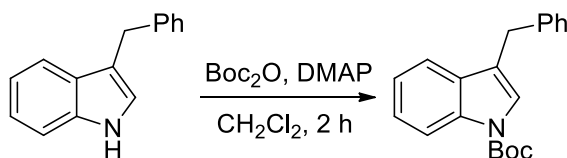
General Methods. All reactions were performed under nitrogen using oven-dried glassware and standard Schlenk or vacuum line techniques. Air- and moisture-sensitive solutions were handled under nitrogen and transferred via syringe. Anhydrous CPME, dioxane, and 2-MeTHF were purchased from Sigma-Aldrich and used as solvent without further purification. Unless otherwise stated, reagents were commercially available and used as purchased without further purification. Chemicals were obtained from Sigma-

Aldrich, Acros, TCI America or Matrix Scientific, and solvents were purchased from Fisher Scientific. The progress of the reactions was monitored by thin-layer chromatography using Whatman Partisil K6F 250 μm precoated 60 Å silica gel plates and visualized by short-wavelength ultraviolet light as well as by treatment with ceric ammonium molybdate (CAM) stain or iodine. Silica gel (230–400 mesh, Silicycle) was used for flash chromatography. The ^1H NMR and $^{13}\text{C}\{^1\text{H}\}$ NMR spectra were obtained using a Brüker AM-500 Fourier-transform NMR spectrometer at 500 and 125 MHz, respectively. Chemical shifts are reported in units of parts per million (ppm) downfield from tetramethylsilane (TMS), and all coupling constants are reported in hertz. The infrared spectra were obtained with KBr plates using a Perkin-Elmer Spectrum 100 Series FTIR spectrometer. High-resolution mass spectrometry (HRMS) data were obtained on a Waters LC–TOF mass spectrometer (model LCT-XE Premier) using chemical ionization (CI) or electrospray ionization (ESI) in positive or negative mode, depending on the analyte. Melting points were determined on a Unimelt Thomas–Hoover melting point apparatus and are uncorrected.

Preparation of Diarylmethanes.

Compounds **2.1q**³⁵ and **2.1r**³⁶ were prepared according to literature procedures.

2.1l – *N*-*tert*-butyl 3-benzylindole carboxylate:

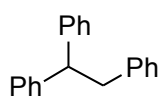


To a solution of 3-benzyl-1*H*-indole (829 mg, 4.0 mmol) and DMAP (48.9 mg, 0.4 mmol) in CH_2Cl_2 (8 mL) was added $(\text{Boc})_2\text{O}$ (1.31 g, 6.0 mmol) at 24 °C, and the solution was stirred for 2 h at this temperature. The resulting mixture was concentrated in vacuo.

Silica gel chromatography using 10% to 20% EtOAc/hexanes afforded 1.21 g (98% yield) of the desired compound as a white solid. $R_f = 0.25$ (EtOAc:hexanes = 1:9). The NMR spectral data match the previously published data.³⁷

Procedure and Characterization for the Deprotonation/Benylation of Diphenylmethane.

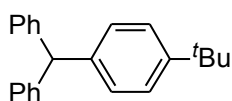
General Procedure A. An oven-dried 10 mL reaction vial equipped with a stir bar was charged with $\text{KN}(\text{SiMe}_3)_2$ (79.8 mg, 0.40 mmol, 4 equiv) under a nitrogen atmosphere followed by 1 mL of dry dioxane, and the reaction mixture was stirred for 5 min at 24 °C. Diphenylmethane (66.9 μL , 0.40 mmol, 4 equiv) was added to the reaction mixture followed by benzyl chloride (11.5 μL , 0.1 mmol, 1 equiv). The reaction mixture was stirred for 12 h at 24 °C (or 110 °C). The reaction mixture was quenched with two drops of H_2O , diluted with 3 mL of ethyl acetate, and filtered over a pad of MgSO_4 and silica. The pad was rinsed with additional ethyl acetate, and the solution was concentrated in vacuo. The crude material was loaded onto a silica gel column and purified by flash chromatography.



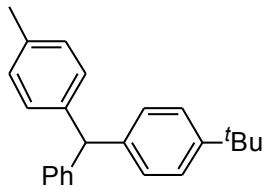
2.4 – 1,1,2-Triphenylethane: The reaction was performed following General Procedure A with diphenylmethane (**2.1a**) (66.9 μL , 0.40 mmol), $\text{KN}(\text{SiMe}_3)_2$ (79.8 mg, 0.40 mmol) and benzyl chloride (11.5 μL , 0.1 mmol) in 1 mL of dioxane at 110 °C. The crude material was purified by flash chromatography on silica gel (eluted with hexanes to EtOAc:hexanes = 5:95) to give the product (23.8 mg, 92% yield) as a colorless oil. $R_f = 0.25$ (hexanes). The NMR spectral data match the previously published data.³⁸

Procedure and Characterization for the Pd-Catalyzed DCCP of Diarylmethanes.

General Procedure B. An oven-dried 10 mL reaction vial equipped with a stir bar was charged with $\text{KN}(\text{SiMe}_3)_2$ (59.8 mg, 0.30 mmol, 3 equiv) under a nitrogen atmosphere. A solution (from a stock solution) of $\text{Pd}(\text{OAc})_2$ (1.12 mg, 0.0050 mmol) and NiXantphos (4.14 mg, 0.0075 mmol) in 1 mL of dry CPME was taken up by syringe and added to the reaction vial. After stirring for 5 min at 24 °C, diphenylmethane (20.1 μL , 0.12 mmol, 1.2 equiv) was added to the reaction mixture followed by 1-bromo-4-*tert*-butylbenzene (17.3 μL , 0.1 mmol, 1 equiv). Note that the diarylmethane or aryl bromide in a solid form was added to the reaction vial prior to $\text{KN}(\text{SiMe}_3)_2$. The reaction mixture was stirred for 12 h at 24 °C, quenched with two drops of H_2O , diluted with 3 mL of ethyl acetate, and filtered over a pad of MgSO_4 and silica. The pad was rinsed with additional ethyl acetate, and the solution was concentrated in vacuo. The crude material was loaded onto a silica gel column and purified by flash chromatography.

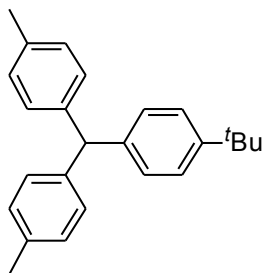


2.3aa – (4-*tert*-Butylphenyl)diphenylmethane: The reaction was performed following General Procedure B with **2.1a** (20.1 μL , 0.12 mmol), $\text{KN}(\text{SiMe}_3)_2$ (59.8 mg, 0.30 mmol) and **2.2a** (17.3 μL , 0.1 mmol). The crude material was purified by flash chromatography on silica gel (eluted with hexanes to EtOAc:hexanes = 2:98) to give the product (28.5 mg, 95% yield) as a white solid. R_f = 0.33 (hexanes); ^1H NMR (500 MHz, CDCl_3): δ 7.32 – 7.23 (m, 6H), 7.21 – 7.16 (m, 2H), 7.12 (d, J = 7.0 Hz, 4H), 7.03 (d, J = 8.5 Hz, 2H), 5.50 (s, 1H), 1.29 (s, 9H) ppm; $^{13}\text{C}\{^1\text{H}\}$ NMR (125 MHz, CDCl_3): δ 149.2, 144.4, 140.9, 129.7, 129.2, 128.5, 126.4, 125.4, 56.6, 34.6, 31.6 ppm; IR (thin film): 3060, 3026, 2963, 2903, 2868, 1599, 1515, 1494, 1450, 1270, 1031, 736, 701, 608 cm^{-1} ; HRMS calc'd for $\text{C}_{23}\text{H}_{24}^+$ 300.1878, observed 300.1867 $[\text{M}]^+$.



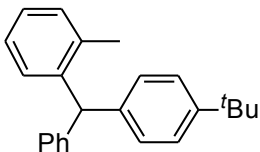
2.3ba – (4-*tert*-Butylphenyl)(4-methylphenyl)phenylmethane:

The reaction was performed following General Procedure B with **2.1b** (22.1 μL , 0.12 mmol), $\text{KN}(\text{SiMe}_3)_2$ (59.8 mg, 0.30 mmol) and **2.2a** (17.3 μL , 0.1 mmol). The crude material was purified by flash chromatography on silica gel (eluted with hexanes to EtOAc:hexanes = 2:98) to give the product (25.5 mg, 81% yield) as a colorless oil. $R_f = 0.33$ (hexanes); ^1H NMR (500 MHz, CDCl_3): δ 7.31 – 7.16 (m, 5H), 7.12 (d, $J = 7.5$ Hz, 2H), 7.08 (d, $J = 8.0$ Hz, 2H), 7.02 (t, $J = 8.0$ Hz, 4H), 5.47 (s, 1H), 2.31 (s, 3H), 1.29 (s, 9H) ppm; $^{13}\text{C}\{^1\text{H}\}$ NMR (125 MHz, CDCl_3): δ 149.1, 144.6, 141.4, 141.2, 135.9, 129.6, 129.5, 129.18, 129.16, 128.4, 126.3, 125.3, 56.3, 34.6, 31.6, 21.2 ppm; IR (thin film): 3025, 2963, 2903, 2868, 1511, 1493, 1451, 1020, 701 cm^{-1} ; HRMS calc'd for $\text{C}_{24}\text{H}_{26}^+$ 314.2035, observed 314.2037 $[\text{M}]^+$.



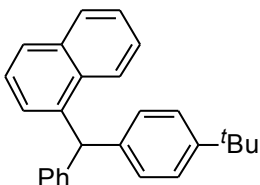
2.3ca – (4-*tert*-Butylphenyl)bis(4-methylphenyl)methane:

The reaction was performed following General Procedure B with **2.1c** (60.1 μL , 0.30 mmol), $\text{KN}(\text{SiMe}_3)_2$ (59.8 mg, 0.30 mmol) and **2.2a** (17.3 μL , 0.1 mmol). The crude material was purified by flash chromatography on silica gel (eluted with hexanes to EtOAc:hexanes = 2:98) to give the product (32.1 mg, 98% yield) as a white solid. $R_f = 0.25$ (hexanes); m.p. = 94–96 $^\circ\text{C}$; ^1H NMR (500 MHz, CDCl_3): δ 7.27 (d, $J = 8.5$ Hz, 2H), 7.07 (d, $J = 8.0$ Hz, 4H), 7.05 – 6.98 (m, 6H), 5.42 (s, 1H), 2.30 (s, 6H), 1.29 (s, 9H) ppm; $^{13}\text{C}\{^1\text{H}\}$ NMR (125 MHz, CDCl_3): δ 149.0, 141.6, 141.4, 135.8, 129.5, 129.14, 129.11, 125.3, 55.9, 34.6, 31.6, 21.2 ppm; IR (thin film): 2962, 2923, 2867, 1510, 1462, 1363, 1269, 1109, 1021, 808, 765 cm^{-1} .



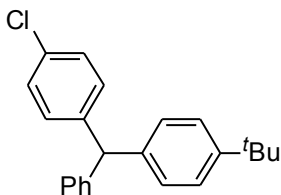
2.3da – (4-*tert*-Butylphenyl)(2-methylphenyl)phenylmethane:

The reaction was performed following General Procedure B with **2.1d** (54.7 μL , 0.30 mmol), $\text{KN}(\text{SiMe}_3)_2$ (59.8 mg, 0.30 mmol) and **2.2a** (17.3 μL , 0.1 mmol). The crude material was purified by flash chromatography on silica gel (eluted with hexanes to EtOAc:hexanes = 2:98) to give the product (27.6 mg, 88% yield) as a colorless oil. $R_f = 0.35$ (hexanes); ^1H NMR (500 MHz, CDCl_3): δ 7.31 – 7.04 (m, 10H), 6.97 (d, $J = 8.5$ Hz, 2H), 6.84 (d, $J = 7.5$ Hz, 1H), 5.63 (s, 1H), 2.22 (s, 3H), 1.29 (s, 9H) ppm; $^{13}\text{C}\{^1\text{H}\}$ NMR (125 MHz, CDCl_3): δ 149.1, 143.8, 142.9, 140.4, 136.8, 130.5, 129.8, 129.6, 129.4, 128.4, 126.5, 126.3, 125.9, 125.3, 53.2, 34.6, 31.6, 20.2 ppm; IR (thin film): 3060, 3025, 2963, 2904, 2868, 1493, 1461, 1363, 1269, 756, 734, 701 cm^{-1} ; HRMS calc'd for $\text{C}_{24}\text{H}_{26}^+$ 314.2035, observed 314.2022 $[\text{M}]^+$.



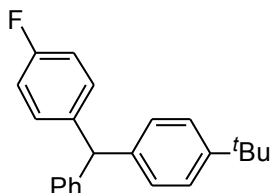
2.3ea – (4-*tert*-Butylphenyl)(1-naphthyl)phenylmethane:

The reaction was performed following General Procedure B with **2.1e** (26.2 mg, 0.12 mmol), $\text{KN}(\text{SiMe}_3)_2$ (59.8 mg, 0.30 mmol) and **2.2a** (17.3 μL , 0.1 mmol). The crude material was purified by flash chromatography on silica gel (eluted with hexanes to EtOAc:hexanes = 1:99) to give the product (35.0 mg, 99% yield) as a colorless oil. $R_f = 0.15$ (hexanes); ^1H NMR (500 MHz, CDCl_3): δ 8.00 (d, $J = 8.0$ Hz, 1H), 7.84 (d, $J = 9.0$ Hz, 1H), 7.73 (d, $J = 8.5$ Hz, 1H), 7.46 – 7.33 (m, 3H), 7.30 – 7.17 (m, 5H), 7.12 (d, $J = 7.0$ Hz, 2H), 7.02 (d, $J = 8.0$ Hz, 2H), 6.97 (d, $J = 7.0$ Hz, 1H), 6.24 (s, 1H), 1.29 (s, 9H) ppm; $^{13}\text{C}\{^1\text{H}\}$ NMR (125 MHz, CDCl_3): δ 149.3, 144.2, 140.7, 140.4, 134.1, 132.2, 129.8, 129.5, 128.9, 128.6, 127.8, 127.4, 126.5, 126.2, 125.6, 125.5, 124.6, 52.9, 34.6, 31.6 ppm; IR (thin film): 2962, 2867, 1509, 1493, 1394, 1268, 1019, 789, 781, 726, 702 cm^{-1} .



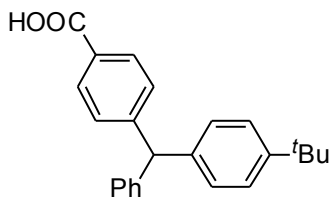
2.3fa – (4-*tert*-Butylphenyl)(4-chlorophenyl)phenylmethane:

The reaction was performed following General Procedure B with **2.1f** (22.0 μL , 0.12 mmol), $\text{KN}(\text{SiMe}_3)_2$ (59.8 mg, 0.30 mmol) and **2.2a** (17.3 μL , 0.1 mmol). The crude material was purified by flash chromatography on silica gel (eluted with hexanes to EtOAc:hexanes = 2:98) to give the product (29.8 mg, 89% yield) as a colorless oil. R_f = 0.35 (hexanes); ^1H NMR (500 MHz, CDCl_3): δ 7.33 – 7.18 (m, 7H), 7.10 (d, J = 7.5 Hz, 2H), 7.05 (d, J = 8.5 Hz, 2H), 7.00 (d, J = 8.5 Hz, 2H), 5.47 (s, 1H), 1.30 (s, 9H) ppm; $^{13}\text{C}\{^1\text{H}\}$ NMR (125 MHz, CDCl_3): δ 149.5, 143.9, 143.0, 140.5, 132.3, 131.0, 129.6, 129.1, 128.6, 126.6, 125.5, 56.0, 34.6, 31.6 ppm; IR (thin film): 3026, 2963, 2903, 2868, 1489, 1364, 1269, 1090, 1015, 818, 702 cm^{-1} ; HRMS calc'd for $\text{C}_{23}\text{H}_{23}\text{Cl}^+$ 334.1488, observed 334.1436 $[\text{M}]^+$.



2.3ga – (4-*tert*-Butylphenyl)(4-fluorophenyl)phenylmethane:

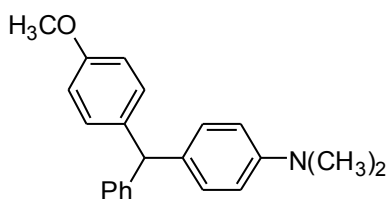
The reaction was performed following General Procedure B with **2.1g** (20.5 μL , 0.12 mmol), $\text{KN}(\text{SiMe}_3)_2$ (59.8 mg, 0.30 mmol) and **2.2a** (17.3 μL , 0.1 mmol). The crude material was purified by flash chromatography on silica gel (eluted with hexanes to EtOAc:hexanes = 2:98) to give the product (30.6 mg, 96% yield) as a colorless oil. R_f = 0.33 (hexanes); ^1H NMR (500 MHz, CDCl_3): δ 7.32 – 7.18 (m, 5H), 7.13 – 6.89 (m, 8H), 5.48 (s, 1H), 1.30 (s, 9H) ppm; $^{13}\text{C}\{^1\text{H}\}$ NMR (125 MHz, CDCl_3): δ 161.6 (d, J = 243 Hz), 149.4, 144.2, 140.8, 140.1 (d, J = 3 Hz), 131.1 (d, J = 8 Hz), 129.6, 129.1, 128.6, 126.6, 125.5, 115.2 (d, J = 21 Hz), 55.9, 34.6, 31.6 ppm; IR (thin film): 3027, 2963, 2904, 2869, 1602, 1507, 1494, 1224, 1158, 824, 701 cm^{-1} ; HRMS calc'd for $\text{C}_{23}\text{H}_{23}\text{F}^+$ 318.1784, observed 318.1774 $[\text{M}]^+$.



2.3ha – 4-((4-*tert*-Butylphenyl)(phenyl)methyl)benzoic acid:

The reaction was performed following General Procedure B with **2.1h** (25.5 mg, 0.12 mmol), $\text{KN}(\text{SiMe}_3)_2$ (79.8 mg, 0.40 mmol) and **2.2a** (17.3 μL , 0.1 mmol) at 110 °C.

The reaction was quenched with 50 μL of 37% hydrochloric acid instead of with two drops of H_2O . The crude material was purified by flash chromatography on silica gel (eluted with EtOAc:hexanes = 3:7 to 4:6) to give the product (32.0 mg, 93% yield) as a white solid. $R_f = 0.50$ (EtOAc:hexanes = 4:6); m.p. = 75–78 °C; ^1H NMR (500 MHz, CDCl_3): δ 8.02 (d, $J = 8.0$ Hz, 2H), 7.33 – 7.26 (m, 4H), 7.26 – 7.20 (m, 3H), 7.11 (d, $J = 7.5$ Hz, 2H), 7.02 (d, $J = 8.5$ Hz, 2H), 5.57 (s, 1H), 1.30 (s, 9H) ppm; $^{13}\text{C}\{^1\text{H}\}$ NMR (125 MHz, CDCl_3): δ 172.4, 150.8, 149.7, 143.4, 140.0, 130.5, 129.8, 129.6, 129.2, 128.7, 127.6, 126.8, 125.6, 56.7, 34.6, 31.6 ppm; IR (thin film): 2964, 2672, 2550, 1694, 1608, 1423, 1288, 1180, 1019, 737, 702 cm^{-1} ; HRMS calc'd for $\text{C}_{24}\text{H}_{23}\text{O}_2^-$ 343.1698, observed 343.1697 $[\text{M}-\text{H}]^-$.

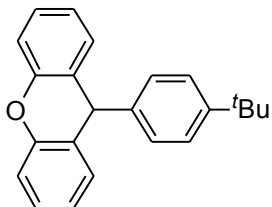


2.3ij – (4-*N,N*-Dimethylphenyl)(4-methoxyphenyl)phenylmethane:

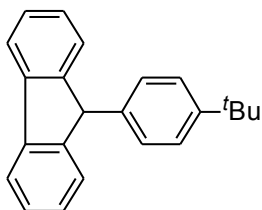
The reaction was performed following General Procedure B with **2.1i** (57.4 μL , 0.30 mmol), $\text{KN}(\text{SiMe}_3)_2$ (59.8 mg, 0.30 mmol) and

2.2j (19.8 mg, 0.099 mmol). The crude material was purified by flash chromatography on silica gel (eluted with hexanes to EtOAc:hexanes = 5:95) to give the product (30.5 mg, 97% yield) as a colorless oil. $R_f = 0.25$ (EtOAc:hexanes = 5:95); ^1H NMR (500 MHz, CDCl_3): δ 7.28 – 7.15 (m, 3H), 7.11 (d, $J = 7.0$ Hz, 2H), 7.03 (d, $J = 9.0$ Hz, 2H), 6.96 (d, $J = 8.5$ Hz, 2H), 6.80 (d, $J = 8.5$ Hz, 2H), 6.66 (d, $J = 8.5$ Hz, 2H), 5.41 (s, 1H), 3.76 (s, 3H), 2.90 (s, 6H) ppm; $^{13}\text{C}\{^1\text{H}\}$ NMR (125 MHz, CDCl_3): δ 158.0, 149.2, 145.2, 137.1,

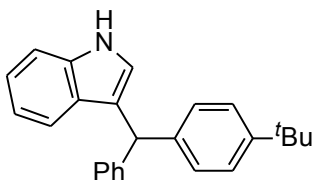
132.5, 130.5, 130.1, 129.5, 128.4, 126.2, 113.7, 112.7, 55.4, 55.3, 40.9 ppm; IR (thin film): 2951, 2834, 1611, 1509, 1450, 1348, 1247, 1176, 1034, 812, 700 cm^{-1} ; HRMS calc'd for $\text{C}_{22}\text{H}_{24}\text{NO}^+$ 318.1858, observed 318.1848 $[\text{MH}]^+$.



2.3ja - 9-(4-*tert*-Butylphenyl)xanthene: The reaction was performed following General Procedure B with **2.1j** (27.3 mg, 0.15 mmol), $\text{KN}(\text{SiMe}_3)_2$ (59.8 mg, 0.30 mmol) and **2.2a** (17.3 μL , 0.1 mmol). The crude material was purified by flash chromatography on silica gel (eluted with hexanes to EtOAc:hexanes = 2:98) to give the product (31.3 mg, 99% yield) as a white solid. R_f = 0.17 (hexanes); m.p. = 136–140 $^\circ\text{C}$; ^1H NMR (500 MHz, CDCl_3): δ 7.28 – 7.22 (m, 2H), 7.22 – 7.16 (m, 2H), 7.14 – 7.05 (m, 6H), 7.00 – 6.94 (m, 2H), 5.21 (s, 1H), 1.26 (s, 9H) ppm; $^{13}\text{C}\{^1\text{H}\}$ NMR (125 MHz, CDCl_3): δ 151.4, 149.5, 143.6, 129.9, 128.00, 127.98, 125.8, 125.0, 123.4, 116.7, 44.2, 34.6, 31.5 ppm; IR (thin film): 2960, 2925, 2866, 1577, 1481, 1452, 1261, 745 cm^{-1} ; HRMS calc'd for $\text{C}_{22}\text{H}_{23}\text{O}^+$ 315.1749, observed 315.1745 $[\text{MH}]^+$.

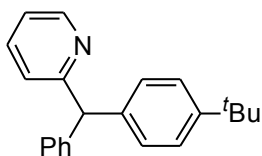


2.3ka - 9-(4-*tert*-Butylphenyl)fluorene: The reaction was performed following General Procedure B with **2.1k** (33.2 mg, 0.20 mmol), $\text{KN}(\text{SiMe}_3)_2$ (59.8 mg, 0.30 mmol) and **2.2a** (17.3 μL , 0.1 mmol) at 85 $^\circ\text{C}$ in THF. The crude material was purified by flash chromatography on silica gel (eluted with hexanes to EtOAc:hexanes = 2:98) to give the product (26.0 mg, 87% yield) as a white solid. R_f = 0.30 (hexanes). The NMR spectral data match the previously published data.³⁹



2.3la – 3-((4-*tert*-Butylphenyl)(phenyl)methyl)-1*H*-indole:

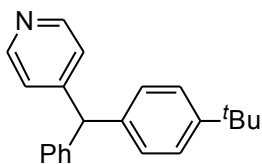
The reaction was performed following General Procedure B with **2.1I** (36.9 mg, 0.12 mmol), $\text{KN}(\text{SiMe}_3)_2$ (79.8 mg, 0.40 mmol) and **2.2a** (17.3 μL , 0.1 mmol). The reaction was quenched with 50 μL of 37% hydrochloric acid instead of with two drops of H_2O to ensure complete removal of the Boc group. The crude material was purified by flash chromatography on silica gel (eluted with hexanes to EtOAc:hexanes = 1:9) to give the product (30.2 mg, 89% yield) as a pale yellow oil. $R_f = 0.50$ (EtOAc:hexanes = 1:9); ^1H NMR (500 MHz, CDCl_3): δ 7.91 (s, br, 1H), 7.33 (d, $J = 7.5$ Hz, 1H), 7.30 – 7.12 (m, 11H), 6.98 (m, 1H), 6.58 (m, 1H), 5.63 (s, 1H), 1.29 (s, 9H) ppm; $^{13}\text{C}\{^1\text{H}\}$ NMR (125 MHz, CDCl_3): δ 149.1, 144.4, 141.0, 136.9, 129.2, 128.7, 128.4, 127.3, 126.3, 125.3, 124.2, 122.2, 120.4, 120.2, 119.5, 111.2, 48.5, 34.6, 31.6 ppm; IR (thin film): 3420, 3057, 2963, 2902, 2867, 1513, 1493, 1456, 1267, 1094, 742, 703 cm^{-1} ; HRMS calc'd for $\text{C}_{25}\text{H}_{24}\text{N}^+$ 338.1909, observed 338.1896 $[\text{M}-\text{H}]^+$.



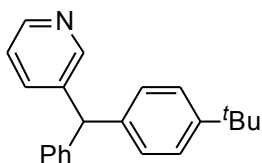
2.3ma – (4-*tert*-Butylphenyl)(2-pyridyl)phenylmethane:

The reaction was performed following General Procedure B with **2.1m** (19.3 μL , 0.12 mmol), $\text{KN}(\text{SiMe}_3)_2$ (59.8 mg, 0.30 mmol) and **2.2a** (17.3 μL , 0.1 mmol). The crude material was purified by flash chromatography on silica gel (eluted with hexanes to EtOAc:hexanes = 5:95 to 1:9) to give the product (28.8 mg, 96% yield) as a colorless oil. $R_f = 0.30$ (EtOAc:hexanes = 1:9); ^1H NMR (500 MHz, CDCl_3): δ 8.59 (m, 1H), 7.61 – 7.55 (td, $J = 7.5$ Hz, 1.5 Hz, 1H), 7.32 – 7.25 (m, 4H), 7.23 – 7.16 (m, 3H), 7.13 – 7.05 (m, 4H), 5.66 (s, 1H), 1.29 (s, 9H) ppm; $^{13}\text{C}\{^1\text{H}\}$ NMR (125 MHz, CDCl_3): δ 163.7, 149.7, 149.4, 143.1, 139.8, 136.6, 129.6, 129.1, 128.6, 126.6, 125.5, 123.9, 121.5, 59.2, 34.6, 31.6 ppm; IR (thin film): 2962, 2903, 1587, 1495,

1468, 1432, 748, 701 cm^{-1} ; HRMS calc'd for $\text{C}_{22}\text{H}_{24}\text{N}^+$ 302.1909, observed 302.1898 $[\text{MH}]^+$.

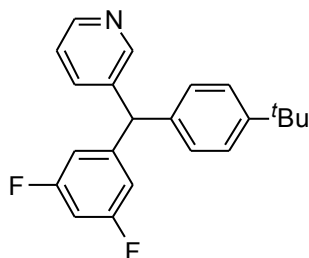


2.3na - (4-*tert*-Butylphenyl)(4-pyridyl)phenylmethane: The reaction was performed following General Procedure B with **2.1n** (19.1 μL , 0.12 mmol), $\text{KN}(\text{SiMe}_3)_2$ (59.8 mg, 0.30 mmol) and **2.2a** (17.3 μL , 0.1 mmol) at 110 $^\circ\text{C}$. The crude material was purified by flash chromatography on silica gel (eluted with hexanes to EtOAc:hexanes = 2:8 to 3:7) to give the product (29.8 mg, 99% yield) as a colorless oil. $R_f = 0.33$ (EtOAc:hexanes = 3:7); ^1H NMR (500 MHz, CDCl_3): δ 8.50 (d, $J = 6.0$ Hz, 2H), 7.34 – 7.21 (m, 5H), 7.10 (d, $J = 7.5$ Hz, 2H), 7.07 – 6.98 (m, 4H), 5.46 (s, 1H), 1.30 (s, 9H) ppm; $^{13}\text{C}\{^1\text{H}\}$ NMR (125 MHz, CDCl_3): δ 153.2, 150.0, 149.9, 142.6, 139.1, 129.5, 129.1, 128.7, 127.0, 125.7, 124.8, 56.0, 34.6, 31.5 ppm; IR (thin film): 3027, 2963, 2904, 2868, 1594, 1514, 1494, 1412, 818, 702 cm^{-1} ; HRMS calc'd for $\text{C}_{22}\text{H}_{24}\text{N}^+$ 302.1909, observed 302.1911 $[\text{MH}]^+$.



2.3oa - (4-*tert*-Butylphenyl)(3-pyridyl)phenylmethane: The reaction was performed following General Procedure B with **2.1o** (19.3 μL , 0.12 mmol), $\text{KN}(\text{SiMe}_3)_2$ (59.8 mg, 0.30 mmol) and **2.2a** (17.3 μL , 0.1 mmol). The crude material was purified by flash chromatography on silica gel (eluted with hexanes to EtOAc:hexanes = 2:8 to 3:7) to give the product (29.6 mg, 98% yield) as a colorless oil. $R_f = 0.50$ (EtOAc:hexanes = 3:7); ^1H NMR (500 MHz, CDCl_3): δ 8.50 – 8.41 (m, 2H), 7.44 – 7.38 (m, 1H), 7.35 – 7.27 (m, 4H), 7.27 – 7.17 (m, 2H), 7.11 (d, $J = 7.0$ Hz, 2H), 7.02 (d, $J = 8.0$ Hz, 2H), 5.51 (s, 1H), 1.30 (s, 9H) ppm; $^{13}\text{C}\{^1\text{H}\}$ NMR (125 MHz, CDCl_3): δ 151.1, 149.7, 147.9, 143.1, 139.8, 139.7, 136.9, 129.5, 129.1, 128.7, 126.8, 125.6, 123.4, 54.2, 34.6, 31.6 ppm; IR (thin film): 3027, 2963,

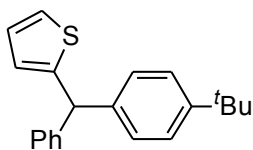
2903, 2868, 1574, 1515, 1495, 1476, 1421, 1026, 716, 702 cm^{-1} ; HRMS calc'd for $\text{C}_{22}\text{H}_{24}\text{N}^+$ 302.1909, observed 302.1911 $[\text{MH}]^+$.



2.3pa – **(4-*tert*-Butylphenyl)(3-pyridyl)(3,5-**

difluorophenyl)methane: The reaction was performed following General Procedure B with **2.1p** (41.0 mg, 0.20 mmol), $\text{KN}(\text{SiMe}_3)_2$ (59.8 mg, 0.30 mmol) and **2.2a** (17.3 μL , 0.1 mmol)

at 85 $^\circ\text{C}$ in THF. The crude material was purified by flash chromatography on silica gel (eluted with hexanes to EtOAc:hexanes = 1:9 to 2:8) to give the product (31.4 mg, 93% yield) as a colorless oil. R_f = 0.20 (EtOAc:hexanes = 2:8); ^1H NMR (500 MHz, CDCl_3): δ 8.50 (dd, J = 5.0 Hz, 1.0 Hz, 1H), 8.41 (d, J = 2.0 Hz, 1H), 7.41 – 7.38 (m, 1H), 7.34 (d, J = 8.5 Hz, 2H), 7.26 – 7.22 (m, 1H), 7.00 (d, J = 8.0 Hz, 2H), 6.72 – 6.60 (m, 3H), 5.47 (s, 1H), 1.31 (s, 9H) ppm; $^{13}\text{C}\{^1\text{H}\}$ NMR (125 MHz, CDCl_3): δ 163.3 (d, J = 247 Hz), 163.2 (d, J = 247 Hz), 150.9, 150.4, 148.4, 147.2 (t, J = 8 Hz), 138.5, 138.4, 136.7, 128.9, 125.9, 123.6, 112.5 (d, J = 19 Hz), 112.4 (d, J = 19 Hz), 102.5 (t, J = 25 Hz), 53.8, 34.7, 31.5 ppm; IR (thin film): 3030, 2964, 2905, 2869, 1623, 1597, 1459, 1317, 1118, 1026, 992, 847, 716 cm^{-1} ; HRMS calc'd for $\text{C}_{22}\text{H}_{22}\text{NF}_2^+$ 338.1720, observed 338.1715 $[\text{MH}]^+$.

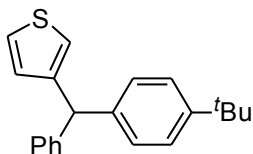


2.3qa – **(4-*tert*-Butylphenyl)(2-thienyl)phenylmethane:** The

reaction was performed following General Procedure B with **2.1q** (20.9 mg, 0.12 mmol), $\text{KN}(\text{SiMe}_3)_2$ (29.9 mg, 0.15 mmol) and **2.2a**

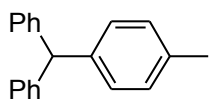
(17.3 μL , 0.1 mmol). The crude material was purified by flash chromatography on silica gel (eluted with hexanes) to give the product (30.5 mg, 99% yield) as a colorless oil. R_f = 0.22 (hexanes); ^1H NMR (500 MHz, CDCl_3): δ 7.32 – 7.27 (m, 4H), 7.24 – 7.17 (m, 4H), 7.13 (d, J = 8.0 Hz, 2H), 6.94 – 6.90 (m, 1H), 6.71 – 6.68 (m, 1H), 5.64 (s, 1H), 1.30 (s,

9H) ppm; $^{13}\text{C}\{^1\text{H}\}$ NMR (125 MHz, CDCl_3): δ 149.7, 148.4, 144.3, 140.9, 129.0, 128.59, 128.56, 126.8, 126.7, 126.5, 125.5, 124.6, 51.9, 34.6, 31.6 ppm; IR (thin film): 3061, 3027, 2962, 2903, 2868, 1514, 1494, 1452, 1364, 1269, 700 cm^{-1} ; HRMS calc'd for $\text{C}_{21}\text{H}_{22}\text{S}^+$ 306.1442, observed 306.1427 $[\text{M}]^+$.

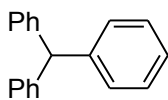


2.3ra - (4-*tert*-Butylphenyl)(3-thienyl)phenylmethane: The

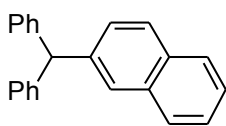
reaction was performed following General Procedure B with **2.1r** (26.1 mg, 0.15 mmol), $\text{KN}(\text{SiMe}_3)_2$ (59.8 mg, 0.30 mmol) and **2.2a** (17.3 μL , 0.1 mmol). The crude material was purified by flash chromatography on silica gel (eluted with hexanes) to give the product (23.6 mg, 77% yield) as a colorless oil. $R_f = 0.35$ (hexanes); ^1H NMR (500 MHz, CDCl_3): δ 7.32 – 7.24 (m, 5H), 7.23 – 7.19 (m, 1H), 7.18 – 7.15 (m, 2H), 7.07 (d, $J = 8.0$ Hz, 2H), 6.88 (dd, $J = 5.0$ Hz, 1.0 Hz, 1H), 6.76 – 6.72 (m, 1H), 5.47 (s, 1H), 1.30 (s, 9H) ppm; $^{13}\text{C}\{^1\text{H}\}$ NMR (125 MHz, CDCl_3): δ 149.4, 145.4, 144.3, 140.9, 129.2, 129.0, 128.7, 128.5, 126.6, 125.6, 125.4, 122.9, 52.4, 34.6, 31.6 ppm; IR (thin film): 3026, 2962, 2902, 2867, 1514, 1494, 1451, 1269, 835, 782, 701 cm^{-1} ; HRMS calc'd for $\text{C}_{21}\text{H}_{23}\text{S}^+$ 307.1520, observed 307.1514 $[\text{MH}]^+$.



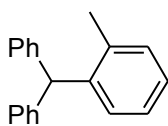
2.3ab - (4-Methylphenyl)diphenylmethane: The reaction was performed following General Procedure B with **2.1a** (20.1 μL , 0.12 mmol), $\text{KN}(\text{SiMe}_3)_2$ (59.8 mg, 0.30 mmol) and **2.2b** (12.3 μL , 0.1 mmol). The crude material was purified by flash chromatography on silica gel (eluted with hexanes to EtOAc:hexanes = 2:98) to give the product (25.1 mg, 97% yield) as a colorless oil. $R_f = 0.38$ (hexanes). The NMR spectral data match the previously published data.⁴⁰



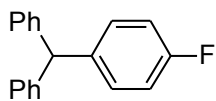
2.3ac – Triphenylmethane: The reaction was performed following General Procedure B with **2.1a** (20.1 μL , 0.12 mmol), $\text{KN}(\text{SiMe}_3)_2$ (59.8 mg, 0.30 mmol) and **2.2c** (10.7 μL , 0.1 mmol). The crude material was purified by flash chromatography on silica gel (eluted with hexanes to EtOAc:hexanes = 2:98) to give the product (22.5 mg, 92% yield) as a white solid. $R_f = 0.40$ (hexanes). The NMR spectral data match the previously published data.⁴¹



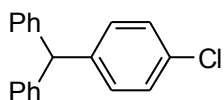
2.3ad – (2-Naphthyl)diphenylmethane: The reaction was performed following General Procedure B with **2.1a** (20.1 μL , 0.12 mmol), $\text{KN}(\text{SiMe}_3)_2$ (59.8 mg, 0.30 mmol) and **2.2d** (20.7 mg, 0.1 mmol). The crude material was purified by flash chromatography on silica gel (eluted with hexanes to EtOAc:hexanes = 1:99) to give the product (29.5 mg, 99% yield) as a white solid. $R_f = 0.30$ (hexanes); ^1H NMR (500 MHz, CDCl_3): δ 7.81 – 7.67 (m, 3H), 7.49 – 7.40 (m, 3H), 7.32 – 7.26 (m, 5H), 7.26 – 7.20 (m, 2H), 7.18 – 7.13 (m, 4H), 5.70 (s, 1H) ppm; $^{13}\text{C}\{^1\text{H}\}$ NMR (125 MHz, CDCl_3): δ 143.9, 141.7, 133.6, 132.4, 129.8, 128.6, 128.3, 128.1, 128.0, 127.8, 126.6, 126.2, 125.8, 57.2 ppm; IR (thin film): 3083, 3058, 3025, 2923, 1600, 1493, 1450, 1030, 814, 747, 722, 699 cm^{-1} ; HRMS calc'd for $\text{C}_{23}\text{H}_{19}^+$ 295.1487, observed 295.1486 $[\text{MH}]^+$.



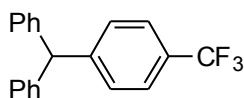
2.3ae – (2-Methylphenyl)diphenylmethane: The reaction was performed following General Procedure B with **2.1a** (50.2 μL , 0.30 mmol), $\text{KN}(\text{SiMe}_3)_2$ (59.8 mg, 0.30 mmol) and **2.2e** (12.0 μL , 0.1 mmol). The crude material was purified by flash chromatography on silica gel (eluted with hexanes to EtOAc:hexanes = 2:98) to give the product (24.2 mg, 94% yield) as a white solid. $R_f = 0.40$ (hexanes). The NMR spectral data match the previously published data.⁴⁰



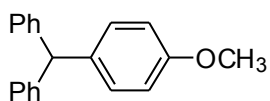
2.3af – (4-Fluorophenyl)diphenylmethane: The reaction was performed following General Procedure B with **2.1a** (50.2 μL , 0.30 mmol), $\text{KN}(\text{SiMe}_3)_2$ (59.8 mg, 0.30 mmol) and **2.2f** (11.0 μL , 0.1 mmol). The crude material was purified by flash chromatography on silica gel (eluted with hexanes to EtOAc:hexanes = 2:98) to give the product (21.3 mg, 82% yield) as a white solid. R_f = 0.33 (hexanes). The NMR spectral data match the previously published data.⁴²



2.3ag – (4-Chlorophenyl)diphenylmethane: The reaction was performed following General Procedure B with **2.1a** (50.2 μL , 0.30 mmol), $\text{KN}(\text{SiMe}_3)_2$ (59.8 mg, 0.30 mmol) and **2.2g** (19.1 mg, 0.1 mmol). The crude material was purified by flash chromatography on silica gel (eluted with hexanes to EtOAc:hexanes = 2:98) to give the product (19.7 mg, 71% yield) as a colorless oil. R_f = 0.30 (hexanes). The NMR spectral data match the previously published data.⁴⁰

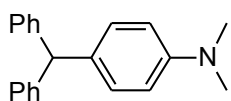


2.3ah – (4-Trifluoromethylphenyl)diphenylmethane: The reaction was performed following General Procedure B with **2.1a** (50.2 μL , 0.30 mmol), $\text{KN}(\text{SiMe}_3)_2$ (39.9 mg, 0.20 mmol) and **2.2h** (14.0 μL , 0.1 mmol). The crude material was purified by flash chromatography on silica gel (eluted with hexanes to EtOAc:hexanes = 2:98) to give the product (20.5 mg, 66% yield) as a colorless oil. R_f = 0.33 (hexanes). The NMR spectral data match the previously published data.⁴⁰

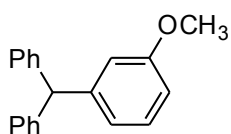


2.3ai – (4-Methoxyphenyl)diphenylmethane: The reaction was performed following General Procedure B with **2.1a** (20.1 μL , 0.12 mmol), $\text{KN}(\text{SiMe}_3)_2$ (59.8 mg, 0.30 mmol) and **2.2i** (12.5 μL , 0.1 mmol). The crude

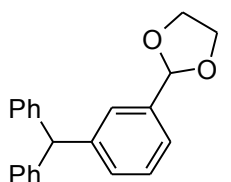
material was purified by flash chromatography on silica gel (eluted with hexanes to EtOAc:hexanes = 5:95) to give the product (27.4 mg, 99% yield) as a colorless oil. R_f = 0.25 (hexanes). The NMR spectral data match the previously published data.⁴⁰



2.3aj – (N,N-Dimethylaminophenyl)diphenylmethane: The reaction was performed following General Procedure B with **2.1a** (20.1 μ L, 0.12 mmol), $\text{KN}(\text{SiMe}_3)_2$ (59.8 mg, 0.30 mmol) and **2.2j** (20.2 mg, 0.101 mmol). The crude material was purified by flash chromatography on silica gel (eluted with EtOAc:hexanes = 5:95) to give the product (29.4 mg, 99% yield) as a white solid. R_f = 0.30 (EtOAc:hexanes = 5:95). The NMR spectral data match the previously published data.⁴³

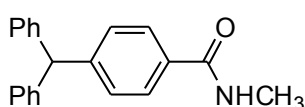


2.3ak – (3-Methoxyphenyl)diphenylmethane: The reaction was performed following General Procedure B with **2.1a** (50.2 μ L, 0.30 mmol), $\text{KN}(\text{SiMe}_3)_2$ (59.8 mg, 0.30 mmol) and **2.2k** (12.7 μ L, 0.1 mmol). The crude material was purified by flash chromatography on silica gel (eluted with hexanes to EtOAc:hexanes = 5:95) to give the product (25.2 mg, 92% yield) as a colorless oil. R_f = 0.25 (hexanes). The NMR spectral data match the previously published data.⁴⁴



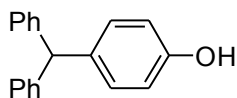
2.3al – 2-(3-Benzhydrylphenyl)-1,3-dioxolane: The reaction was performed following General Procedure B with **2.1a** (20.1 μ L, 0.12 mmol), $\text{KN}(\text{SiMe}_3)_2$ (59.8 mg, 0.30 mmol) and **2.2l** (15.1 μ L, 0.1 mmol). The crude material was purified by flash chromatography on silica gel (eluted with EtOAc:hexanes = 5:95 to 1:9) to give the product (30.4 mg, 96% yield) as a white solid.

$R_f = 0.30$ (EtOAc:hexanes = 1:9); m.p. = 72–74 °C; $^1\text{H NMR}$ (500 MHz, CDCl_3): δ 7.38 – 7.15 (m, 9H), 7.13 – 7.06 (m, 5H), 5.72 (s, 1H), 5.56 (s, 1H), 4.12 – 3.91 (m, 4H) ppm; $^{13}\text{C}\{^1\text{H}\}$ NMR (125 MHz, CDCl_3): δ 144.2, 143.9, 138.0, 130.5, 129.7, 128.6, 128.5, 128.0, 126.5, 124.6, 104.0, 65.5, 57.0 ppm; IR (thin film): 3060, 3025, 2885, 1599, 1494, 1450, 1387, 1223, 1151, 1079, 1030, 966, 737, 700 cm^{-1} ; HRMS calc'd for $\text{C}_{22}\text{H}_{21}\text{O}_2^+$ 317.1542, observed 317.1542 $[\text{MH}]^+$.



2.3am – **4-(Diphenylmethyl)-N-methylbenzamide**: The

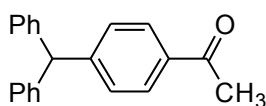
reaction was performed following General Procedure B with **2.1a** (50.2 μL , 0.30 mmol), $\text{KN}(\text{SiMe}_3)_2$ (79.8 mg, 0.40 mmol) and **2.2m** (21.4 mg, 0.1 mmol) at 110 °C. The reaction was quenched with 50 μL of 37% hydrochloric acid instead of with two drops of H_2O . The crude material was purified by flash chromatography on silica gel (eluted with hexanes to EtOAc:hexanes = 4:6 to 6:4) to give the product (24.8 mg, 82% yield) as a colorless oil. $R_f = 0.5$ (EtOAc:hexanes = 7:3); $^1\text{H NMR}$ (500 MHz, CDCl_3): δ 7.66 (d, $J = 8.5$ Hz, 2H), 7.32 – 7.26 (m, 4H), 7.24 – 7.20 (m, 2H), 7.16 (d, $J = 8.0$ Hz, 2H), 7.08 (d, $J = 7.5$ Hz, 4H), 6.23 (m, br, 1H), 5.57 (s, 1H), 2.97 (d, $J = 5.0$ Hz, 3H) ppm; $^{13}\text{C}\{^1\text{H}\}$ NMR (125 MHz, CDCl_3): δ 168.3, 147.7, 143.4, 132.9, 129.8, 129.6, 128.6, 127.1, 126.8, 56.8, 27.0 ppm; IR (thin film): 3322, 3060, 3026, 1636, 1552, 1503, 1495, 1311, 756, 735, 700 cm^{-1} ; HRMS calc'd for $\text{C}_{21}\text{H}_{20}\text{NO}^+$ 302.1545, observed 302.1548 $[\text{MH}]^+$.



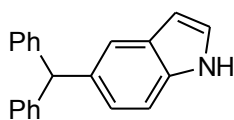
2.3an – **(4-Hydroxyphenyl)diphenylmethane**: The reaction was

performed following General Procedure B with **2.1a** (50.2 μL , 0.30 mmol), $\text{KN}(\text{SiMe}_3)_2$ (79.8 mg, 0.40 mmol) and **2.2m** (21.4 mg, 0.1 mmol) at 110 °C. The reaction was quenched with 50 μL of 37% hydrochloric acid instead of with two drops of

H₂O. The crude material was purified by flash chromatography on silica gel (eluted with hexanes to EtOAc:hexanes = 1:9 to 2:8) to give the product (25.0 mg, 95% yield) as a white solid. $R_f = 0.33$ (EtOAc:hexanes = 2:8). The NMR spectral data match the previously published data.⁴⁵



2.3ao – (4-Acetyldiphenylmethyl)benzene: The reaction was performed following General Procedure B with **2.1a** (50.2 μ L, 0.30 mmol), KN(SiMe₃)₂ (59.8 mg, 0.30 mmol) and **2.2o** (20.2 mg, 0.101 mmol). The reaction was quenched with 50 μ L of 37% hydrochloric acid instead of with two drops of H₂O. The crude material was purified by flash chromatography on silica gel (eluted with EtOAc:hexanes = 5:95 to 1:9) to give the product (24.5 mg, 86% yield) as a white solid. $R_f = 0.33$ (EtOAc:hexanes = 1:9). The NMR spectral data match the previously published data.⁴⁶



2.3ap – 5-(Diphenylmethyl)-1H-indole: The reaction was performed following General Procedure B with **2.1a** (33.4 μ L, 0.20 mmol), KN(SiMe₃)₂ (79.8 mg, 0.40 mmol) and **2.2p** (19.6 mg, 0.1 mmol) at 110 °C. The reaction was quenched with 50 μ L of 37% hydrochloric acid instead of with two drops of H₂O. The crude material was purified by flash chromatography on silica gel (eluted with hexanes to EtOAc:hexanes = 5:95 to 2:8) to give the product (22.1 mg, 78% yield) as a colorless oil. $R_f = 0.25$ (EtOAc:hexanes = 1:9); ¹H NMR (500 MHz, CDCl₃): δ 8.06 (s, br, 1H), 7.34 – 7.23 (m, 6H), 7.23 – 7.11 (m, 7H), 7.00 (d, $J = 8.5$ Hz, 1H), 6.45 (m, 1H), 5.67 (s, 1H) ppm; ¹³C{¹H} NMR (125 MHz, CDCl₃): δ 145.0, 135.8, 134.6, 129.8, 128.4, 128.1, 126.3, 124.6, 124.4, 121.5, 111.0, 102.9, 57.1 ppm; IR (thin film): 3425, 3058,

3024, 2924, 1599, 1493, 1473, 1451, 1343, 1090, 1030, 751, 728, 700 cm^{-1} ; HRMS calc'd for $\text{C}_{21}\text{H}_{16}\text{N}^+$ 282.1283, observed 282.1283 $[\text{M}-\text{H}]^+$.

Representative Microscale High-throughput Experimentation for Base & Catalyst Identification.

General Experimental. The experimental procedures in this work were similar to those reported.⁴⁷ Parallel synthesis was accomplished in an MBraun glovebox operating with a constant N_2 -purge (oxygen typically <5 ppm). The experimental design was accomplished using Accelrys Library Studio. Screening reactions were carried out in 1 mL vials (30 mm height \times 8 mm diameter) in a 96-well plate aluminum reactor block. Liquid chemicals were dosed using multi-channel or single-channel pipettors. Solid chemicals were dosed manually as solutions or slurries in appropriate solvents. Undesired additional solvent was removed using a GeneVac system located inside the glovebox. The reactions were heated and stirred on a heating block with a tumble-stirrer (V&P Scientific) using 1.98 mm diameter \times 4.80 mm length parylene stir bars. The tumble stirring mechanism helped to insure uniform stirring throughout the 96-well plate. The reactions were sealed in the 96-well plate during reaction. Below each reactor vial in the aluminum 96-well plate was a 0.062 mm thick silicon-rubber gasket. Directly above the glass vial reactor tops was a Teflon perfluoroalkoxy copolymer resin sealing gasket and above that, two more 0.062 mm thick silicon-rubber gaskets. The entire assembly was compressed between an aluminum top and the reactor base with 9 evenly-placed screws.

Set up:

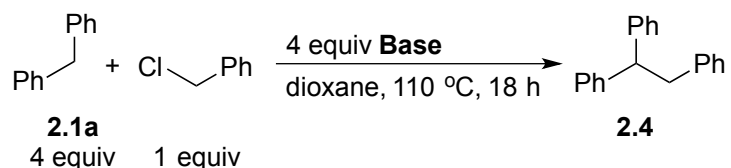
Experiments were set up inside a glovebox under a nitrogen atmosphere. A 96-well aluminum block containing 1 mL glass vials was predosed manually with $\text{Pd}(\text{OAc})_2$ (0.5

μmol) and NiXantphos ($1 \mu\text{mol}$) in THF. The solvent was evacuated to dryness using a GeneVac vacuum centrifuge, and $\text{KN}(\text{SiMe}_3)_2$ ($30 \mu\text{mol}$) in THF was added to the ligand/catalyst mixture. The solvent was removed on the GeneVac, and a parylene stir bar was then added to each reaction vial. 1-Bromo-4-*tert*-butylbenzene ($10 \mu\text{mol}/\text{reaction}$), diphenylmethane ($12 \mu\text{mol}/\text{reaction}$) and biphenyl ($1 \mu\text{mol}/\text{reaction}$) (used as an internal standard to measure HPLC yields) were then dosed together into each reaction vial as a solution in CPME ($100 \mu\text{L}$, 0.1 M). The 96-well plate was then sealed and stirred for 18 h at $110 \text{ }^\circ\text{C}$.

Work up:

Upon opening the plate to air, $500 \mu\text{L}$ of acetonitrile was syringed into each vial. The plate was then covered again and the vials stirred for 20 min to extract the product and to ensure good homogenization. Into a separate 96-well LC block was added $700 \mu\text{L}$ of acetonitrile, followed by $40 \mu\text{L}$ of the diluted reaction mixtures. The LC block was then sealed with a silicon-rubber storage mat, and mounted on HPLC instrument modified with an autosampler for analysis.

(1) Base Screening:

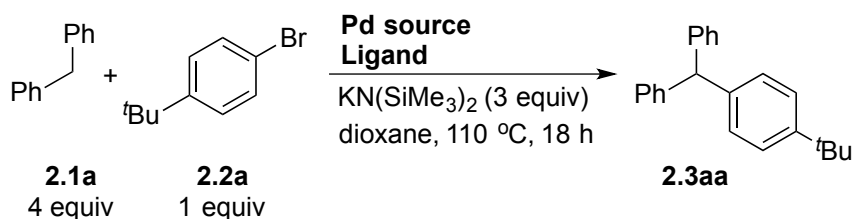


12 Bases: $\text{LiN}(\text{SiMe}_3)_2$, $\text{NaN}(\text{SiMe}_3)_2$, $\text{KN}(\text{SiMe}_3)_2$, LiO^tBu , KO^tBu , NaO^tBu , LDA, LiH, KH, LiOH, KOH, and K_2CO_3 .

The lead hit from the screening was $\text{KN}(\text{SiMe}_3)_2$, giving 90% assay yield of the desired benzylation product **2.4**. A scale-up reaction on a 0.1 mmol scale using General

Procedure A for the deprotonation/benylation of diphenylmethane proved successful with isolation of the benzylation product **2.4** in 92% yield.

(2) Ligand Screening:



Ligand was used in a 4:1 ratio relative to Pd for monodentate ligands and 2:1 ratio for bidentate ligands.

2a. $\text{PdCl}_2(\text{PPh}_3)_2$ (5 mol %) was used to test 96 sterically and electronically diverse, mono- and bidentate phosphine ligands (ligands **1–96** from Table 2.4 below).

2b. 4 Pd sources [$\text{PdCl}_2(\text{PPh}_3)_2$, $\text{Pd}(\text{OAc})_2$, $\text{PdCl}_2(\text{CH}_3\text{CN})_2$, and $\text{Pd}_2(\text{dba})_3$] and 2 catalyst loadings (5 and 10 mol %) were screened with 16 sterically and electronically diverse, mono- and bidentate phosphine (ligands **97–112** from Tables 2.5 and 2.6 below).

The lead hit from the screening was the combination of $\text{PdCl}_2(\text{PPh}_3)_2$ (5 mol %) and **NiXantphos** (10 mol %), giving 93% assay yield of the desired DCCP product **2.3aa**. A scale-up reaction on a 0.1 mmol scale using the same procedure as HTE proved successful with isolation of **2.3aa** in 94% yield.

Table 2.4 HTE using ligands **1–96**

	Ligand libraries (1–96)	2.3aa AY (%)
1	2-Di-tert-butylphosphino-2',4',6'-triisopropylbiphenyl (tBu-XPhos)	18.5
2	2-(Dicyclohexylphosphino)-2'-methylbiphenyl (MePhos)	31.0

3	2-(Di- <i>t</i> -butylphosphino)-2'-methylbiphenyl (tBu-MePhos)	30.1
4	2-(Dicyclohexylphosphino)biphenyl (Cy-JohnPhos)	29.4
5	2-Di- <i>t</i> -butylphosphino-2'-(<i>N,N</i> -dimethylamino)biphenyl (tBu-DavePhos)	41.9
6	Racemic-2-(di- <i>t</i> -butylphosphino)-1,1'-binaphthyl	24.1
7	1-[2-[Bis(<i>t</i> -butyl)phosphino]phenyl]-3,5-diphenyl-1H-pyrazole (TrippyPhos)	50.4
8	5-(Di- <i>t</i> -butylphosphino)-1', 3', 5'-triphenyl-1'H-[1,4']bipyrazole (BippyPhos)	22.1
9	Dicyclohexyl-[2-(<i>o</i> -tolyl)indol-1-yl]phosphane	40.4
10	Di- <i>t</i> -butyl(2,2-diphenyl-1-methyl-1-cyclopropyl)phosphine (cBRIDP [MoPhos])	23.8
11	Dicyclohexyl-(1-methyl-2,2-diphenyl-cyclopropyl)phosphane (Cy-cBRIDP)	24.1
12	Dicyclohexyl-(1-methyl-2,2-diphenyl-vinyl)phosphane (Cy-vBRIDP)	23.7
13	<i>N</i> -phenyl-2-(dicyclohexylphosphino)pyrrole (cataCXium PCy)	24.8
14	<i>N</i> -phenyl-2-(di- <i>t</i> -butylphosphino)pyrrole (cataCXium PtB)	43.2
15	Dicyclohexyl-(1-phenylindol-2-yl)phosphane (cataCXium PInCy)	27.5
16	Di- <i>t</i> -butyl-(1-phenylindol-2-yl)phosphane (cataCXium PIntB)	35.2
17	1-(2-Methoxyphenyl)-2-(dicyclohexylphosphino)pyrrole (cataCXium POMeCy)	32.3
18	Di- <i>t</i> -butyl-[1-(2-methoxyphenyl)pyrrol-2-yl]phosphane (cataCXium POMeTB)	80.9
19	1-(2,4,6-Trimethylphenyl)-2-(dicyclohexylphosphino)imidazole (cataCXium PICy)	34.1
20	Di-(2-pyridyl)(dicyclohexylphosphino)amine (cataCXium KCy)	37.9
21	Di-(2-pyridyl)(diphenylphosphino)amine (cataCXium KPh)	45.2
22	(9-Butylfluoren-9-yl)-dicyclohexyl-phosphonium tetrafluoroborate (cataCXium FBu)	16.2
23	Dicyclohexyl-(9-phenethylfluoren-9-yl)phosphonium tetrafluoroborate (cataCXium FPrPh)	19.1
24	(9-Benzylfluoren-9-yl)-dicyclohexyl-phosphane; trifluoroborane; hydrofluoride (cataCXium FBn)	14.7
25	Trimethylphosphonium tetrafluoroborate	27.8
26	Triethylphosphonium tetrafluoroborate	17.7
27	Triisopropylphosphonium tetrafluoroborate	49.8
28	Tricyclohexylphosphonium tetrafluoroborate	45.1

29	Tribenzylphosphine	2.2
30	Di- <i>t</i> -butylmethylphosphonium tetrafluoroborate	40.4
31	<i>t</i> -Butyldicyclohexylphosphine	64.4
32	Di- <i>t</i> -butylcyclohexylphosphine	34.1
33	Benzyl-di-1-adamantylphosphine (cataCXium ABn)	31.0
34	Di- <i>t</i> -butylneopentylphosphonium tetrafluoroborate	36.2
35	(<i>Z</i>)-1- <i>t</i> -butyl-2,3,6,7-tetrahydro-1H-phosphepinium tetrafluoroborate (Ellman ligand)	9.1
36	1,3,5-Triaza-7-phosphaadamantane	39.7
37	Di- <i>t</i> -butylphenylphosphonium tetrafluoroborate	24.9
38	Dicyclohexylphenylphosphine	14.3
39	(<i>o</i> -Tolyl)dicyclohexylphosphine	41.7
40	Dicyclohexyl-(2,4,6-trimethylphenyl)phosphine	41.5
41	Dicyclohexyl-(2,6-diisopropylphenyl)phosphine	59.1
42	1-Dicyclohexylphosphino-4-dimethylaminobenzene	40.7
43	1,3,5,7-Tetramethyl-8-phenyl-2,4,6-trioxa-8-phosphatricyclo[3.3.1.1 ^{3,7}]decane	50.7
44	2-(Dicyclohexylphosphino)benzophenone	48.5
45	2'-(Dicyclohexylphosphino)acetophenone ethylene ketal	51.0
46	1-Di- <i>i</i> -propylphosphino-2-(<i>N,N</i> -dimethylamino)-1H-indene	50.1
47	11-Dicyclohexylphosphino-12-phenyl-9,10-ethenoanthracene (KitPhos)	38.1
48	11-Dicyclohexylphosphino-12-(2-methoxyphenyl)-9,10-ethenoanthracene (<i>o</i> - Meo-Kitphos)	33.2
49	Triphenylphosphine	37.9
50	Tri- <i>o</i> -tolylphosphine	46.0
51	Trimesitylphosphine	46.5
52	Tri(2-furyl)phosphine	65.9
53	Tris(2-methoxyphenyl)phosphine	53.3
54	Tris(4-methoxyphenyl)phosphine	50.2
55	Tris(2,4,6-trimethoxyphenyl)phosphine	34.7
56	Tris(4-fluorophenyl)phosphine	33.0

57	Tris(pentafluorophenyl)phosphine	0
58	Tris[3,5-bis(trifluoromethyl)phenyl]phosphine	22.1
59	Tri(1-naphthyl)phosphine	51.3
60	1,2-Bis(diphenylphosphino)ethane monooxide	5.6
61	Cyclohexyldiphenylphosphine	50.2
62	<i>t</i> -Butyldiphenylphosphine	54.5
63	Benzoyldiphenylphosphine	2.6
64	4-(Dimethylamino)phenyldiphenylphosphine	49.1
65	Diphenyl-2-pyridylphosphine	29.7
66	2-(1,1-Dimethylpropyl)-6-(diphenylphosphino)pyridine (AlpyPhos)	40.1
67	2-(Diphenylphosphino)-6-(2,4,6-triphenylphenyl)pyridine (ArpyPhos)	26.1
68	1-Diphenylphosphino-2-(<i>N,N</i> -dimethylamino)-1H-indene	42.7
69	2-(Diphenylphosphino)-2'-(<i>N,N</i> -dimethylamino)biphenyl (Ph-DavePhos)	45.6
70	Tris(2,4-di- <i>tert</i> -butylphenyl)phosphite	65.0
71	(1,1'-Ferrocenediyl)phenylphosphine (1,1'-(PhP)-ferrocene)	7.4
72	1,4-Bis(diphenylphosphino)butane monooxide	2.3
73	Bis(diphenylphosphino)methane	1.8
74	1,2-Bis(diphenylphosphino)ethane (dppe [diphos])	4.5
75	1,3-Bis(diphenylphosphino)propane (dppp)	0
76	1,4-Bis(diphenylphosphino)butane (dppb)	10.2
77	1,5-Bis(diphenylphosphino)pentane (dpppe)	16.3
78	1,8-Bis(diphenylphosphino)octane (dppo)	22.6
79	1,2-Bis(dipentafluorophenylphosphino)ethane	6.5
80	1,2-Bis(di-2-pyridylphosphino)ethane	7.8
81	1,2-Bis(diphenylphosphinomethyl)benzene	3.6
82	1,2-Bis(diphenylphosphino)benzene (dppbz)	2.7
83	1,8-Bis(diphenylphosphanyl)naphthalene	47.4
84	1,2,3,4-(Diphenylphosphinomethyl)cyclopentane (Tedicyp)	3.3
85	Bis(2-diphenylphosphinophenyl)ether (DPEPhos)	21.4
86	2,2'-Bis(diphenylphosphino)benzophenone (dppb)	18.3

87	9,9-Dimethyl-4,5-bis(diphenylphosphino)xanthene (Xantphos)	37.2
88	4,6-Bis(diphenylphosphino)phenoxazine (NiXantphos)	93.2
89	(S)-(+)-2,2'-Bis(diphenylphosphino)-1,1'-binaphthyl ((S)-BINAP)	2.3
90	(R)-(+)-2,2'-bis(di-p-tolylphosphino)-1,1'-binaphthyl ((R)-Tol-BINAP)	3.5
91	2,2'-Bis(diphenylphosphino)-1,1'-biphenyl (Biphep)	1.7
92	3,3'-Bis(diphenylphosphino)-5,5',6,6',7,7',8,8'-octahydro[2,2']binaphthalene hemichloroform adduct (Cy-Nu-Biphep)	1.1
93	6,6'-Bis(diphenylphosphino)-1,1',3,3'-tetrahydro[5,5']biisobenzofuran (Thf-Nu-Biphep)	1.6
94	Tetramethyl 6,6'-bis(diphenylphosphino)-1,1',3,3'-tetrahydro[5,5']biindenyl- 2,2',2,2'-tetracarboxylate	11.5
95	2-(Diphenylphosphino)ethylamine	7.6
96	2-[2-(Diphenylphosphino)ethyl]pyridine	27.5

1–24: Monodentate dialkylbiaryl phosphine ligands; **25–48:** Monodentate trialkyl and dialkylaryl phosphine ligands; **49–72:** Monodentate triaryl and diarylalkylphosphine ligands; **73–96:** Bidentate electron-poor phosphine ligands.

Table 2.5 HTE using ligands **97–112** and PdCl₂(PPh₃)₂

	Ligand libraries (97–112)	PdCl ₂ (PPh ₃) ₂	
		5 mol %	10 mol %
97	2-Dicyclohexylphosphino-2',4',6'-tri- <i>i</i> -propyl-1,1'-biphenyl (XPhos)	41.0	52.1
98	2-Dicyclohexylphosphino-2',6'-dimethoxy-1,1'-biphenyl (SPhos)	49.5	52.9
99	2-(Di- <i>t</i> -butylphosphino)biphenyl (JohnPhos)	38.5	24.9
100	2-Dicyclohexylphosphino-2'-(<i>N,N</i> -dimethylamino)biphenyl (DavePhos)	35.9	44.5
101	2-Dicyclohexylphosphino-2',6'-di- <i>i</i> -propoxy-1,1'-biphenyl (RuPhos)	46.7	55.7
102	2-Di- <i>t</i> -butylphosphino-3,4,5,6-tetramethyl-2',4',6'-triisopropyl-1,1'- biphenyl (Me-4- <i>t</i> Bu-XPhos)	62.6	80.6
103	Dicyclohexyl-[3,6-dimethoxy-2-(2,4,6-	21.9	27.7

triisopropylphenyl]phenyl]phosphane (BrettPhos)			
104	Butyldi-1-adamantylphosphine (cataCXium A)	18.9	28.6
105	1,2,3,4,5-Pentaphenyl-1'-(di- <i>t</i> -butylphosphino)ferrocene (QPhos)	30.3	37.4
106	Tri- <i>t</i> -butylphosphonium tetrafluoroborate	25.8	36.2
107	(4-(<i>N,N</i> -dimethylamino)phenyl)di- <i>t</i> -butyl phosphine (AmPhos)	30.6	39.9
108	1,1'-Bis(di- <i>t</i> -butylphosphino)ferrocene (dtbpf)	17.4	20.7
109	1,1'-Bis(diphenylphosphino)ferrocene (dppf)	4.0	3.8
110	1,1'-Bis(diisopropylphosphino)ferrocene (dippf)	11.7	11.5
111	(<i>R</i>)-(+)-2,2'-Bis(diphenylphosphino)-1,1'-binaphthyl ((<i>R</i>)-BINAP)	2.4	2.0
112	(<i>R</i>)-(-)-1-[(<i>S</i>)-2-(Dicyclohexylphosphino)ferrocenyl]ethyl-di- <i>t</i> -butylphosphine (JosiPhos SL-J009-1)	47.6	49.0

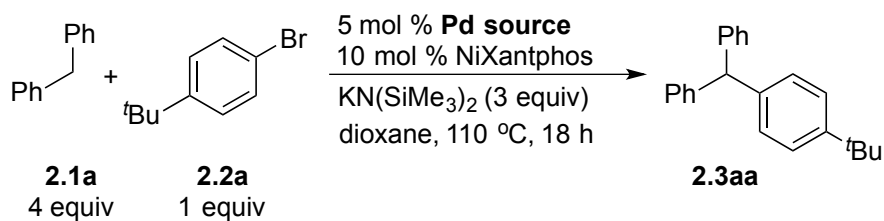
97–108: Monodentate phosphine ligands; **109–112:** Bidentate and monodentate phosphine ligands.

Table 2.6 HTE using ligands **1, 14, 28, 50, 75, 76, 85, 87, 97–112** and 3 Pd sources

Ligand	Pd(OAc) ₂		PdCl ₂ (CH ₃ CN) ₂		Pd ₂ (dba) ₃	
	5 mol %	10 mol %	5 mol %	10 mol %	2.5 mol %	5 mol %
1	0	3.6	3.6	5.0	0	0
14	6.1	7.0	6.9	7.4	3.3	5.7
28	37.5	61.7	41.4	84.7	31.9	39.3
50	12.9	17.6	14.5	14.5	0	14.1
75	0	0.6	0	20.2	0	0
76	5.2	5.8	8.4	2.9	3.0	0
85	43.4	41.3	47.3	55.5	35.8	27.8
87	67.5	69.6	65.9	69.9	24.5	64.1
97	41.0	52.1	41.1	49.7	28.3	37.2
98	49.5	52.9	36.8	40.9	27.0	24.2
99	38.5	24.9	12.2	13.9	6.3	8.1
100	35.9	44.5	22.0	11.1	15.4	15.1

101	46.7	55.7	21.1	21.2	12.3	14.0
102	62.6	80.6	0	4.5	0	0
103	21.9	27.7	7.6	8.6	4.1	13.5
104	18.9	28.6	8.9	12.4	7.2	9.8
105	30.3	37.4	13.6	11.7	12.1	7.8
106	25.8	36.2	6.7	11.1	10.0	3.3
107	30.6	39.9	16.7	22.6	13.2	15.6
108	17.4	20.7	52.3	52.9	36.2	37.8
109	4.0	3.8	13.8	25.3	29.4	0
110	11.7	11.5	19.3	31.4	18.0	0
111	2.4	2.0	2.4	33.8	1.8	9.5
112	47.6	49.0	49.2	42.6	45.6	52.2

(3) Pd Source Screening:



6 Pd sources: $\text{PdCl}_2(\text{PPh}_3)_2$, $\text{Pd}(\text{OAc})_2$, $\text{PdCl}_2(\text{CH}_3\text{CN})_2$, $[\text{Pd}(\text{allyl})\text{Cl}]_2$, $\text{Pd}(\text{COD})\text{Cl}_2$, and $\text{Pd}_2(\text{dba})_3$.

Table 2.7 HTE using 6 Pd sources

Entry	Catalyst	Ligand	AY (%)
1	$\text{PdCl}_2(\text{PPh}_3)_2$	no ligand added	46
2	$\text{PdCl}_2(\text{PPh}_3)_2$	NiXantphos	93
3	$\text{Pd}(\text{OAc})_2$	no ligand added	no reaction
4	$\text{Pd}(\text{OAc})_2$	NiXantphos	100
5	$\text{PdCl}_2(\text{CH}_3\text{CN})_2$	no ligand added	no reaction

6	PdCl ₂ (CH ₃ CN) ₂	NiXantphos	90
7	Pd ₂ (dba) ₃	no ligand added	no reaction
8	Pd ₂ (dba) ₃	NiXantphos	88
9	Pd(COD)Cl ₂	no ligand added	no reaction
10	Pd(COD)Cl ₂	NiXantphos	96
11	[Pd(allyl)Cl] ₂	no ligand added	no reaction
12	[Pd(allyl)Cl] ₂	NiXantphos	91

The lead hit from the screening was the combination of **Pd(OAc)₂** (5 mol %) and **NiXantphos** (10 mol %), giving 100% assay yield of the desired DCCP product **2.3aa**. A scale-up reaction on a 0.1 mmol scale using General Procedure B for the Pd-Catalyzed DCCP of **2.1a** proved successful with > 95% yield of **2.3aa** determined by ¹H NMR spectroscopy of the crude reaction mixture.

2.5 References

- (1) (a) Ryss, P.; Zollinger, H. *Fundamentals of the Chemistry and Application of Dyes*; Wiley-Interscience: New York, 1972. (b) Katritzky, A. R.; Gupta, V.; Garot, C.; Stevens, C. V.; Gordeev, M. F. *Heterocycles* **1994**, *38*, 345. (c) Muthyala, R.; Katritzky, A. R.; Lan, X. F. *Dyes Pigm.* **1994**, *25*, 303.
- (2) (a) Aldag, R. *Photochromism: Molecules and Systems*; Dürr, H., Bouas-Laurent, H., Eds.; Elsevier: London, 1990. (b) Irie, M. *J. Am. Chem. Soc.* **1983**, *105*, 2078.
- (3) (a) Herron, N.; Johansson, G. A.; Radu, N. S.; U.S. Patent Application 2005/0187364, Aug 25, 2005. (b) Xu, Y. Q.; Lu, J. M.; Li, N. J.; Yan, F.; Xia, X. W.; Xu, Q. F. *Eur. Polym. J.* **2008**, *44*, 2404.
- (4) (a) Das, S. K.; Panda, G.; Chaturvedi, V.; Manju, Y. S.; Galkwad, A. K.; Sinha, S. *Bioorg. Med. Chem. Lett.* **2007**, *17*, 5586. (b) Panda, G.; Shagufta; Mishra, J. K.;

Chaturvedi, V.; Srivastava, A. K.; Srivastava, R.; Srivastava, B. S. *Bioorg. Med. Chem.* **2004**, *12*, 5269. (c) Parai, M. K.; Panda, G.; Chaturvedi, V.; Manju, Y. K.; Sinha, S. *Bioorg. Med. Chem. Lett.* **2008**, *18*, 289.

(5) (a) Shagufta; Srivastava, A. K.; Sharma, R.; Mishra, R.; Balapure, A. K.; Murthy, P. S. R.; Panda, G. *Bioorg. Med. Chem.* **2006**, *14*, 1497. (b) Palchaudhuri, R.; Hergenrother, P. J. *Bioorg. Med. Chem. Lett.* **2008**, *18*, 5888. (c) Palchaudhuri, R.; Nesterenko, V.; Hergenrother, P. J. *J. Am. Chem. Soc.* **2008**, *130*, 10274. (d) Risberg, K.; Guldvik, I. J.; Palchaudhuri, R.; Xi, Y. G.; Ju, J. F.; Fodstad, O.; Hergenrother, P. J.; Andersson, Y. *J. Immunother.* **2011**, *34*, 438.

(6) Al-Qawasmeh, R. A.; Lee, Y.; Cao, M. Y.; Gu, X. P.; Vassilakos, A.; Wright, J. A.; Young, A. *Bioorg. Med. Chem. Lett.* **2004**, *14*, 347.

(7) For reviews: (a) Duxbury, D. F. *Chem. Rev.* **1993**, *93*, 381. (b) Shchepinov, M. S.; Korshun, V. A. *Chem. Soc. Rev.* **2003**, *32*, 170. (c) Nair, V.; Thomas, S.; Mathew, S. C.; Abhilash, K. G. *Tetrahedron* **2006**, *62*, 6731.

(8) (a) Schnitzer, R. J.; Hawking, F. *Experimental Chemotherapy*; Academic Press: New York, 1963; Vol. *I*. (b) Greene, T. W.; Wuts, P. G. M. *Protective Groups in Organic Synthesis*, 3rd ed.; Wiley: New York, 1999. (c) Wulff, H.; Miller, M. J.; Hansel, W.; Grissmer, S.; Cahalan, M. D.; Chandy, K. G. *Proc. Natl. Acad. Sci. U.S.A.* **2000**, *97*, 8151. (d) Hernandez, A. I.; Balzarini, J.; Karlsson, A.; Camarasa, M. J.; Perez-Perez, M. *J. Med. Chem.* **2002**, *45*, 4254. (e) Ellsworth, B. A.; Ewing, W. R.; Jurica, E.; U.S. Patent Application 2011/0082165 A1, Apr 7, 2011. (f) Mullen, L. M. A.; Duchowicz, P. R.; Castro, E. A. *Chemom. Intell. Lab. Syst.* **2011**, *107*, 269. (g) Rodriguez, D.; Ramesh, C.; Henson, L. H.; Wilmeth, L.; Bryant, B. K.; Kadavakollu, S.; Hirsch, R.; Montoya, J.; Howell, P. R.; George, J. M.; Alexander, D.; Johnson, D. L.; Arterburn, J. B.; Shuster, C. *B. Bioorg. Med. Chem.* **2011**, *19*, 5446.

(9) For anodic oxidation routes to triarylmethanes, see: (a) Okajima, M.; Soga, K.; Nokami, T.; Suga, S.; Yoshida, J. *Org. Lett.* **2006**, *8*, 5005. (b) Nokami, T.; Watanabe, T.; Musya, N.; Suehiro, T.; Morofuji, T.; Yoshida, J. *Tetrahedron* **2011**, *67*, 4664. For metal-free Friedel–Crafts reactions: (c) Katritzky, A. R.; Toader, D. *J. Org. Chem.* **1997**, *62*, 4137 and references therein.

(10) (a) Roberts, R. M.; Elkhawaga, A. M.; Sweeney, K. M.; Elzohry, M. F. *J. Org. Chem.* **1987**, *52*, 1591. (b) Ramesh, C.; Banerjee, J.; Pal, R.; Das, B. *Adv. Synth. Catal.* **2003**, *345*, 557. (c) Yadav, J. S.; Reddy, B. V. S.; Sunitha, S. *Adv. Synth. Catal.* **2003**, *345*, 349. (d) Nair, V.; Abhilash, K. G.; Vidya, N. *Org. Lett.* **2005**, *7*, 5857. (e) Esquivias, J.; Arrayas, R. G.; Carretero, J. C. *Angew. Chem., Int. Ed.* **2006**, *45*, 629. (f) Nair, V.; Vidya, N.; Abhilash, K. G. *Synthesis* **2006**, 3647. (g) Lin, S. H.; Lu, X. Y. *J. Org. Chem.* **2007**, *72*, 9757. (h) Podder, S.; Choudhury, J.; Roy, U. K.; Roy, S. *J. Org. Chem.* **2007**, *72*, 3100. (i) Alonso, I.; Esquivias, J.; Gomez-Arrayas, R.; Carretero, J. C. *J. Org. Chem.* **2008**, *73*, 6401. (j) Li, G. J.; Wang, E. J.; Chen, H. Y.; Li, H. F.; Liu, Y. H.; Wang, P. G. *Tetrahedron* **2008**, *64*, 9033. (k) Li, Z. X.; Duan, Z.; Kang, J. X.; Wang, H. Q.; Yu, L. J.; Wu, Y. J. *Tetrahedron* **2008**, *64*, 1924. (l) Liu, C. R.; Li, M. B.; Yang, C. F.; Tian, S. K. *Chem. Commun.* **2008**, 1249. (m) Wang, Z. Y.; Sun, X. Y.; Wu, J. *Tetrahedron* **2008**, *64*, 5013.

(11) (a) Shi reported a Fe-catalyzed cross dehydrogenative coupling via a Friedel–Crafts-type mechanism. However, 6 equiv of diphenylmethane are necessary to render high conversions, and the cross-coupling partners are limited to substituted anisoles: Li, Y. Z.; Li, B. J.; Lu, X. Y.; Lin, S.; Shi, Z. J. *Angew. Chem., Int. Ed.* **2009**, *48*, 3817. (b) Han reported a Pd-catalyzed arylation of diphenylmethyl acetate with heteroarenes: Yuan, F. Q.; Gao, L. X.; Han, F. S. *Chem. Commun.* **2011**, *47*, 5289.

(12) (a) A single example is demonstrated in: Molander, G. A.; Elia, M. D. *J. Org. Chem.* **2006**, *71*, 9198. (b) Yu, J. Y.; Kuwano, R. *Org. Lett.* **2008**, *10*, 973. (c) We became aware of a report on synthesis of enantioenriched triarylmethanes by stereospecific cross-coupling reactions of diarylmethanol derivatives with aryl Grignard reagents while this manuscript was in press. See Taylor, B. L. H.; Harris, M. R.; Jarvo, E. R. *Angew. Chem., Int. Ed.* **2012**, *51*, 7790.

(13) McGrew, G. I.; Temaismithi, J.; Carroll, P. J.; Walsh, P. J. *Angew. Chem., Int. Ed.* **2010**, *49*, 5541.

(14) (a) Dugger, R. W.; Ragan, J. A.; Ripin, D. H. B. *Org. Process Res. Dev.* **2005**, *9*, 253. (b) Busacca, C. A.; Fandrick, D. R.; Song, J. J.; Senanayake, C. H. *Adv. Synth. Catal.* **2011**, *353*, 1825. (c) Magano, J.; Dunetz, J. R. *Chem. Rev.* **2011**, *111*, 2177.

(15) For reviews on arylation of activated C(sp³)-H bonds: (a) Bellina, F.; Rossi, R. *Chem. Rev.* **2010**, *110*, 1082. (b) Johansson, C. C. C.; Colacot, T. J. *Angew. Chem., Int. Ed.* **2010**, *49*, 676. (c) Culkin, D. A.; Hartwig, J. F. *Acc. Chem. Res.* **2003**, *36*, 234.

(16) For recent reviews on C(sp³)-H arylation: (a) Tobisu, M.; Chatani, N. *Angew. Chem., Int. Ed.* **2006**, *45*, 1683. (b) Jazzar, R.; Hitce, J.; Renaudat, A.; Sofack-Kreutzer, J.; Baudoin, O. *Chem. –Eur. J.* **2010**, *16*, 2654. (c) Wasa, M.; Engle, K. M.; Yu, J.-Q. *Isr. J. Chem.* **2010**, *50*, 605. (d) Baudoin, O. *Chem. Soc. Rev.* **2011**, *40*, 4902. (e) Bergman, R. G. *Nature* **2007**, *446*, 391. (f) Chen, X.; Engle, K. M.; Wang, D. H.; Yu, J.-Q. *Angew. Chem., Int. Ed.* **2009**, *48*, 5094. (g) Daugulis, O.; Do, H. Q.; Shabashov, D. *Acc. Chem. Res.* **2009**, *42*, 1074. (h) Lyons, T. W.; Sanford, M. S. *Chem. Rev.* **2010**, *110*, 1147. (i) Sun, C. L.; Li, B. J.; Shi, Z. J. *Chem. Rev.* **2011**, *111*, 1293. For recent reviews on general C-H arylation: (j) Yu, J.-Q.; Giri, R.; Chen, X. *Org. Biomol. Chem.* **2006**, *4*, 4041. (k) Kakiuchi, F.; Kochi, T. *Synthesis* **2008**, 3013. (l) Ackermann, L.; Vicente, R.; Kapdi, A. R. *Angew. Chem., Int. Ed.* **2009**, *48*, 9792. (m) McGlacken, G. P.; Bateman, L. M. *Chem.*

Soc. Rev. **2009**, *38*, 2447. (n) Ackermann, L. *Chem. Commun.* **2010**, *46*, 4866. (o) Scheuermann, C. J. *Chem. –Asian J.* **2010**, *5*, 436. (p) Ackermann, L. *Chem. Rev.* **2011**, *111*, 1315. (q) Wencel-Delord, J.; Droge, T.; Liu, F.; Glorius, F. *Chem. Soc. Rev.* **2011**, *40*, 4740. (r) Yeung, C. S.; Dong, V. M. *Chem. Rev.* **2011**, *111*, 1215.

(17) (a) Niwa, T.; Yorimitsu, H.; Oshima, K. *Org. Lett.* **2007**, *9*, 2373. (b) Burton, P. M.; Morris, J. A. *Org. Lett.* **2010**, *12*, 5359. (c) Song, G. Y.; Su, Y.; Gong, X.; Han, K. L.; Li, X. W. *Org. Lett.* **2011**, *13*, 1968. (d) Duez, S.; Steib, A. K.; Manolikakes, S. M.; Knochel, P. *Angew. Chem., Int. Ed.* **2011**, *50*, 7686. (e) Mousseau, J. J.; Larivee, A.; Charette, A. B. *Org. Lett.* **2008**, *10*, 1641. (f) Chen, J.-J.; Onogi, S.; Hsieh, Y.-C.; Hsiao, C.-C.; Higashibayashi, S.; Sakurai, H.; Wu, Y.-T. *Adv. Synth. Catal.* **2012**, *354*, 1551.

(18) Bordwell, F. G.; Matthews, W. S.; Vanier, N. R. *J. Am. Chem. Soc.* **1975**, *97*, 442.

(19) Reports on deprotonation with *n*-BuLi since 2000: (a) Hamashima, Y.; Kanai, M.; Shibasaki, M. *J. Am. Chem. Soc.* **2000**, *122*, 7412. (b) Hirano, T.; Li, W.; Abrams, L.; Krusic, P. J.; Ottaviani, M. F.; Turro, N. J. *J. Org. Chem.* **2000**, *65*, 1319. (c) Grotjahn, D. B.; Collins, L. S. B.; Wolpert, M.; Bikzhanova, G. A.; Lo, H. C.; Combs, D.; Hubbard, J. L. *J. Am. Chem. Soc.* **2001**, *123*, 8260. (d) Mladenova, G.; Chen, L.; Rodriguez, C. F.; Siu, K. W. M.; Johnston, L. J.; Hopkinson, A. C.; Lee-Ruff, E. *J. Org. Chem.* **2001**, *66*, 1109. (e) Varela, J. A.; Pena, D.; Goldfuss, B.; Polborn, K.; Knochel, P. *Org. Lett.* **2001**, *3*, 2395. (f) Banerjee, M.; Emond, S. J.; Lindeman, S. V.; Rathore, R. *J. Org. Chem.* **2007**, *72*, 8054. (g) Wan, S.; Gunaydin, H.; Houk, K. N.; Floreancig, P. E. *J. Am. Chem. Soc.* **2007**, *129*, 7915. (h) Tanaka, Y.; Kanai, M.; Shibasaki, M. *J. Am. Chem. Soc.* **2010**, *132*, 8862. (i) Cacciuttolo, B.; Poulain-Martini, S.; Dunach, E. *Eur. J. Org. Chem.* **2011**, 3710. (j) Clausen, D. J.; Wan, S. Y.; Floreancig, P. E. *Angew. Chem., Int. Ed.* **2011**, *50*, 5178.

- (20) (a) Kofron, W. G.; Mathew, J. *J. Org. Chem.* **1976**, *41*, 114. (b) Okamoto, A.; Snow, M. S.; Arnold, D. R. *Tetrahedron* **1986**, *42*, 6175. (c) Fischer, E.; Larsen, J.; Christensen, J. B.; Fourmigue, M.; Madsen, H. G.; Harrit, N. *J. Org. Chem.* **1996**, *61*, 6997.
- (21) (a) Popielarz, R.; Arnold, D. R. *J. Am. Chem. Soc.* **1990**, *112*, 3068. (b) Elz, S.; Kramer, K.; Leschke, C.; Schunack, W. *Eur. J. Med. Chem.* **2000**, *35*, 41. (c) Elz, S.; Kramer, K.; Pertz, H. H.; Detert, H.; ter Laak, A. M.; Kuhne, R.; Schunack, W. *J. Med. Chem.* **2000**, *43*, 1071.
- (22) Zhang, J.; Stanciu, C.; Wang, B.; Hussain, M. M.; Da, C.-S.; Carroll, P. J.; Dreher, S. D.; Walsh, P. J. *J. Am. Chem. Soc.* **2011**, *133*, 20552.
- (23) (a) Inoh, J.; Satoh, T.; Pivsa-Art, S.; Miura, M.; Nomura, M. *Tetrahedron Lett.* **1998**, *39*, 4673. (b) pK_a of benzylic C–H bonds of 4-nitrotoluene, 20.4: Bordwell, F. G.; Algrim, D.; Vanier, N. R. *J. Org. Chem.* **1977**, *42*, 1817.
- (24) (a) Dreher, S. D.; Dormer, P. G.; Sandrock, D. L.; Molander, G. A. *J. Am. Chem. Soc.* **2008**, *130*, 9257. (b) Dreher, S. D.; Lim, S. E.; Sandrock, D. L.; Molander, G. A. *J. Org. Chem.* **2009**, *74*, 3626. (c) Molander, G. A.; Argintaru, O. A.; Aron, I.; Dreher, S. D. *Org. Lett.* **2010**, *12*, 5783. (d) Molander, G. A.; Trice, S. L. J.; Dreher, S. D. *J. Am. Chem. Soc.* **2010**, *132*, 17701. (e) Sandrock, D. L.; Jean-Gerard, L.; Chen, C. Y.; Dreher, S. D.; Molander, G. A. *J. Am. Chem. Soc.* **2010**, *132*, 17108.
- (25) (a) Nicolaou, K. C.; Shi, G. Q.; Gunzner, J. L.; Gartner, P.; Yang, Z. *J. Am. Chem. Soc.* **1997**, *119*, 5467. (b) Urgaonkar, S.; Verkade, J. G. *Adv. Synth. Catal.* **2004**, *346*, 611. (c) Durbin, M. J.; Willis, M. C. *Org. Lett.* **2008**, *10*, 1413. (d) Inamoto, K.; Hasegawa, C.; Kawasaki, J.; Hiroya, K.; Doi, T. *Adv. Synth. Catal.* **2010**, *352*, 2643. (e) Trost, B. M.; Dogra, K.; Franzini, M. *J. Am. Chem. Soc.* **2004**, *126*, 1944. (f) Kawatsura, M.; Ata, F.; Hayase, S.; Itoh, T. *Chem. Commun.* **2007**, 4283. (g) Gerber, R.; Frech, C. M. *Chem.–Eur. J.* **2011**, *17*, 11893.

- (26) van der Veen, L. A.; Keeven, P. H.; Schoemaker, G. C.; Reek, J. N. H.; Kamer, P. C. J.; van Leeuwen, P. W. N. M.; Lutz, M.; Spek, A. L. *Organometallics* **2000**, *19*, 872.
- (27) Li, J. J.; Johnson, D. S.; Sliskovic, D. R.; Roth, B. D. *Contemporary Drug Synthesis*; Wiley-Interscience: 2004.
- (28) (a) pK_a of indole N–H bond, 21.0: Bordwell, F. G.; Drucker, G. E.; Fried, H. E. *J. Org. Chem.* **1981**, *46*, 632. (b) Bordwell, F. G. *Acc. Chem. Res.* **1988**, *21*, 456.
- (29) (a) Portnoy, M.; Milstein, D. *Organometallics* **1993**, *12*, 1665. (b) Alcazar-Roman, L. M.; Hartwig, J. F.; Rheingold, A. L.; Liable-Sands, L. M.; Guzei, I. A. *J. Am. Chem. Soc.* **2000**, *122*, 4618. (c) Littke, A. F.; Fu, G. C. *Angew. Chem., Int. Ed.* **2002**, *41*, 4176. (d) Barrios-Landeros, F.; Hartwig, J. F. *J. Am. Chem. Soc.* **2005**, *127*, 6944. (e) Barrios-Landeros, F.; Carrow, B. P.; Hartwig, J. F. *J. Am. Chem. Soc.* **2009**, *131*, 8141. (f) Schoenebeck, F.; Houk, K. N. *J. Am. Chem. Soc.* **2010**, *132*, 2496.
- (30) Seminal publications on aldol reaction: (a) Kane, R. *J. Prakt. Chem.* **1838**, *15*, 129. (b) Kane, R. *Ann. Phys. Chem. Ser. 2* **1838**, *44*, 475.
- (31) pK_a of acetophenone in DMSO, 24.7: Matthews, W. S.; Bares, J. E.; Bartmess, J. E.; Bordwell, F. G.; Cornforth, F. J.; Drucker, G. E.; Margolin, Z.; McCallum, R. J.; McCollum, G. J.; Vanier, N. R. *J. Am. Chem. Soc.* **1975**, *97*, 7006.
- (32) For examples of Pd-catalyzed direct arylation of phenols: (a) Bates, R. W.; Gabel, C. J.; Ji, J. H.; Ramadevi, T. *Tetrahedron* **1995**, *51*, 8199. (b) Kawamura, Y.; Satoh, T.; Miura, M.; Nomura, M. *Chem. Lett.* **1999**, 961. (c) Kataoka, N.; Shelby, Q.; Stambuli, J. P.; Hartwig, J. F. *J. Org. Chem.* **2002**, *67*, 5553. (d) Burgos, C. H.; Barder, T. E.; Huang, X. H.; Buchwald, S. L. *Angew. Chem., Int. Ed.* **2006**, *45*, 4321. (e) Hu, T. J.; Schulz, T.; Torborg, C.; Chen, X. R.; Wang, J.; Beller, M.; Huang, J. *Chem. Commun.* **2009**, 7330. (f) Beydoun, K.; Doucet, H. *Catal. Sci. Technol.* **2011**, *1*, 1243. (g) Platon, M.; Cui, L. C.; Mom, S.; Richard, P.; Saeys, M.; Hierso, J. C. *Adv. Synth. Catal.* **2011**, *353*, 3403. (h)

Xiao, B.; Gong, T. J.; Liu, Z. J.; Liu, J. H.; Luo, D. F.; Xu, J.; Liu, L. *J. Am. Chem. Soc.* **2011**, *133*, 9250.

(33) For examples of Pd-catalyzed N-arylation of indoles: (a) Hartwig, J. F.; Kawatsura, M.; Hauck, S. I.; Shaughnessy, K. H.; Alcazar-Roman, L. M. *J. Org. Chem.* **1999**, *64*, 5575. (b) Old, D. W.; Harris, M. C.; Buchwald, S. L. *Org. Lett.* **2000**, *2*, 1403. (c) Grasa, G. A.; Viciu, M. S.; Huang, J. K.; Nolan, S. P. *J. Org. Chem.* **2001**, *66*, 7729.

(34) For examples of Pd-catalyzed C-2- and C-3-arylation of indoles: (a) Lane, B. S.; Sames, D. *Org. Lett.* **2004**, *6*, 2897. (b) Lane, B. S.; Brown, M. A.; Sames, D. *J. Am. Chem. Soc.* **2005**, *127*, 8050. (c) Deprez, N. R.; Kalyani, D.; Krause, A.; Sanford, M. S. *J. Am. Chem. Soc.* **2006**, *128*, 4972. (d) Djakovitch, L.; Dufaud, V.; Zaidi, R. *Adv. Synth. Catal.* **2006**, *348*, 715. (e) Toure, B. B.; Lane, B. S.; Sames, D. *Org. Lett.* **2006**, *8*, 1979. (f) Wang, X.; Gribkov, D. V.; Sames, D. *J. Org. Chem.* **2007**, *72*, 1476. (g) Bellina, F.; Benelli, F.; Rossi, R. *J. Org. Chem.* **2008**, *73*, 5529. (h) Yang, S. D.; Sun, C. L.; Fang, Z.; Li, B. H.; Li, Y. Z.; Shi, Z. *J. Angew. Chem., Int. Ed.* **2008**, *47*, 1473. (i) Zhao, J. L.; Zhang, Y. H.; Cheng, K. *J. Org. Chem.* **2008**, *73*, 7428. (j) Liang, Z. J.; Yao, B. B.; Zhang, Y. H. *Org. Lett.* **2010**, *12*, 3185.

(35) Engel, J. F. Insecticidal Perhaloalkylvinylcyclopropanecarboxylates US Patent US4332815 (A1), 1982.

(36) Henry, N.; Enguehard-Gueiffier, C.; They, I.; Gueiffier, A. *Eur. J. Org. Chem.* **2008**, 4824.

(37) Fuwa, H.; Sasaki, M. *Org. Biomol. Chem.* **2007**, *5*, 2214.

(38) Fessard, T. C.; Motoyoshi, H.; Carreira, E. M. *Angew. Chem., Int. Ed.* **2007**, *46*, 2078.

(39) Robinson, P. D.; McLean, A. W.; Meyers, C. Y. *Acta Cryst.* **2003**, *C59*, o539.

(40) Yu, J-Y; Kuwano, R. *Org. Lett.* **2008**, *10*, 973.

- (41) Aoyama, T.; Kubota, S.; Takido, T.; Kodomari, M. *Chem. Lett.* **2011**, *40*, 484.
- (42) Prakash, G. K. S.; Panja, C.; Shakhmin, A.; Shah, E.; Mathew, T.; Olah, G. A. *J. Org. Chem.* **2009**, *74*, 8659.
- (43) Cho, B. P.; Blankenship, L. R.; Moody, J. D.; Doerge, D. R.; Beland, F. A.; Culp, S. *J. Tetrahedron* **2000**, *56*, 7379.
- (44) Bandaranayake, W. M.; Riggs, N. V. *Aust. J. Chem.* **1981**, *34*, 115.
- (45) Li, H.; Li, W.; Liu, W.; He, Z.; Li, Z. *Angew. Chem., Int. Ed.* **2011**, *50*, 2975.
- (46) Alexander, C.; Feast, W. J. *Synthesis* **1992**, 735.
- (47) Dreher, S. D.; Dormer, P. G.; Sandrock, D. L.; Molander, G. A. *J. Am. Chem. Soc.* **2008**, *130*, 9257.

Chapter 3

NiXantphos: A Deprotonatable Ligand for Room Temperature Palladium-Catalyzed Cross-Couplings of Aryl Chlorides

3.1 Introduction

The past 15 years have witnessed the development of phosphine ligands used for palladium-catalyzed cross-couplings with aryl chlorides.¹ Among them, sterically bulky and electron-rich alkylphosphine ligands have proved particularly successful and have been widely applied in synthesis.² Simple triarylphosphine ligands are generally ineffective for oxidative addition of unactivated aryl chlorides to Pd(0), in part due to their reduced electron-donating ability. Yet, aryl chlorides are arguably the most useful substrates among aryl halides and pseudohalides, because of their low cost and wide availability. To date, few reports document the use of triarylphosphine ligands for cross-couplings with unactivated aryl chlorides, most of which require higher temperatures (≥ 60 °C), and typically give moderate yields with narrow substrate scope.^{3a–i} In 2005, the Buchwald group reported that a sterically hindered monodentate triarylphosphine ligand, 2-diphenylphosphino-2',4',6'-triisopropylbiphenyl, promoted Suzuki–Miyaura couplings of aryl chlorides at room temperature to 40 °C in excellent yields.^{3j}

Mechanistic studies on oxidative addition of aryl chlorides to Pd(0) bearing bulky electron-rich phosphine ligands have been recently reported: the Hartwig group, as well as others, demonstrated that oxidative addition of aryl chlorides to Pd(0) proceeds via a monoligated palladium species, LPd(0) (L = monodentate phosphine).⁴ This mechanistic picture is consistent with the inability of chelating phosphines to add aryl chlorides oxidatively at low temperature. The two reasonable pathways for oxidative addition of

aryl chlorides with bidentate phosphines are dissociation of one of the phosphorus centers of a bidentate chelating phosphine or direct oxidative addition without dissociation of a phosphorus center, both of which are high in energy.^{4e–g} As a result, palladium complexes with chelating bidentate ligands typically catalyze cross-couplings of unactivated aryl chlorides only at elevated temperatures.⁵ In 1993, the Milstein group reported the oxidative addition of aryl chlorides to Pd(P[^]P), which was generated from Pd(P[^]P)₂ [P[^]P = a bidentate phosphine, in this case, 1,3-bis(diisopropylphosphino)propane (dipp)].⁶ Despite the bulky and strongly donating phosphorus centers, the oxidative addition was conducted at 90 °C to achieve complete conversion in 2 h. In 2003, a similar observation was reported by the Hartwig group for the room temperature oxidative addition of aryl tosylates to Pd(P[^]P)₂ (P[^]P = PPF*t*-Bu and CyPF*t*-Bu).⁷ We are not aware of examples of palladium catalysts based on *bidentate phosphine* ligands for efficient room temperature cross-coupling reactions with unactivated aryl chlorides.

Herein we report unprecedented reactivity employing a *deprotonatable chelating arylidiphosphine* ligand, NiXantphos,⁸ for the room temperature palladium-catalyzed cross-coupling reaction of unactivated aryl chlorides. Surprisingly, comparison of an extensive array of ligands revealed that the heterobimetallic (M–NiXantphos)Pd catalyst system (M = alkali metal)⁹ outperformed all the other mono- and bidentate ligands in deprotonative cross-coupling reactions with aryl chlorides.

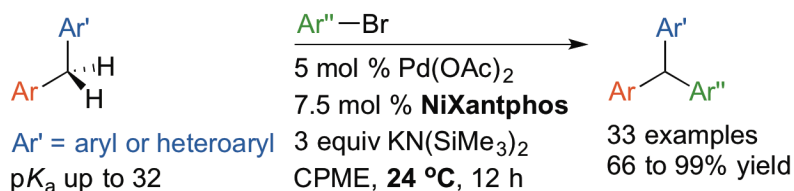
3.2 Results and Discussion

3.2.1 Initial Studies with NiXantphos

We recently initiated a program in the catalytic functionalization of weakly acidic sp³-hybridized C–H bonds. We have categorized these reactions as deprotonative

cross-coupling processes (DCCP), because they involve initial reversible deprotonation of the C–H by base without the participation of the catalyst. The catalyst promotes the subsequent functionalization of the deprotonated species. Thus, DCCP is mechanistically distinct from C–H activation/functionalization processes.

Substrates we reported to undergo DCCP include diarylmethanes, allyl benzenes, sulfoxides, sulfones, amides and η^6 -arene complexes of toluene derivatives and benzylic amines.^{10–12} Diphenylmethane ($pK_a = 32.3$ ¹³) and diarylmethane derivatives were arylated at room temperature with *aryl bromides* in the presence of $\text{KN}(\text{SiMe}_3)_2$ and a palladium catalyst bearing van Leeuwen’s NiXantphos⁸ (Scheme 3.1, see Scheme 3.2 for the structure of NiXantphos).^{11a} This method facilitates rapid access to a wide variety of sterically and electronically diverse triarylmethanes, a class of compounds with various applications and interesting biological activity.^{14–18}

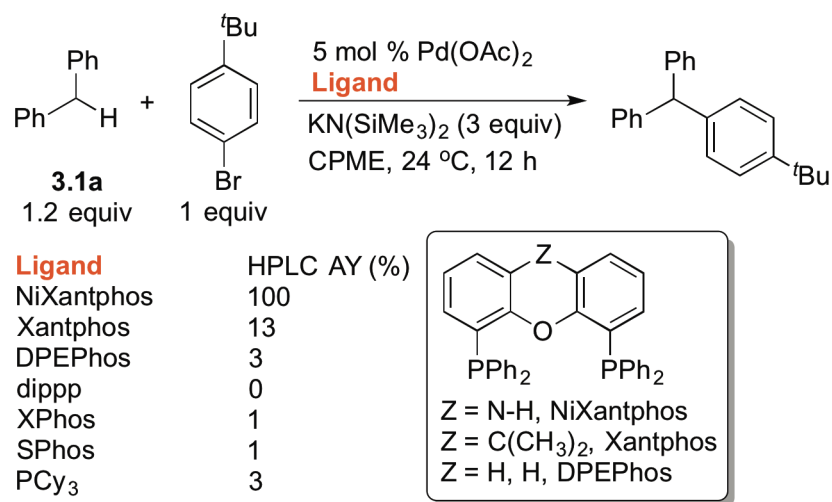


Scheme 3.1 DCCP of diarylmethanes with aryl bromides

Interestingly, when we examined various ligands for the cross-coupling of diphenylmethane (**3.1a**) with 1-bromo-4-*tert*-butylbenzene at room temperature using microscale high-throughput experimentation (HTE,¹⁹ Scheme 3.2),ⁱ the NiXantphos-based catalyst showed superior performance over dippp as well as the other bidentate ligands sharing similar bite angles (see “3.4 Experimental Section” for details).⁸ The

ⁱ HTE screens in this chapter were performed in collaboration with Dr. Ana Bellomo at Penn/Merck Laboratory for High-Throughput Experimentation.

NiXantphos-based catalyst also outperformed monodentate alkylphosphine ligands. The dominance of NiXantphos over the structurally similar Xantphos begged the question: Why is NiXantphos so active under these reaction conditions? We hypothesized that the presence of a somewhat acidic N–H under the basic reaction conditions would result in deprotonation and that the resultant heterobimetallic system might exhibit cooperative reactivity. We then set out to determine the validity of this hypothesis, starting with a deprotonation study.



^aHTE conducted on a 10 μmol scale at 0.1 M. AY = assay yield.

Scheme 3.2 Selected HTE results of the cross-coupling of **3.1a** with 1-bromo-4-*tert*-butylbenzene^a

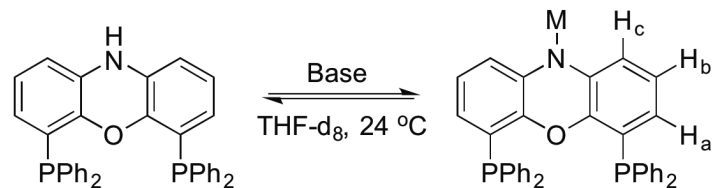
3.2.2 Deprotonation of NiXantphos

3.2.2.1 Solution Studiesⁱⁱ

ⁱⁱ Deprotonation experiments (Table 3.1) were performed in collaboration with Dr. Ana Bellomo at Penn/Merck Laboratory for High-Throughput Experimentation.

NiXantphos has a phenoxazine core, with a pK_a around 22,¹³ and should be deprotonated by $\text{KN}(\text{SiMe}_3)_2$ under the reaction conditions in Scheme 3.2. The ^1H and $^{31}\text{P}\{^1\text{H}\}$ NMR spectra of NiXantphos were recorded in THF-d_8 at room temperature before and after combination with 1.5–6 equiv of $\text{MN}(\text{SiMe}_3)_2$ ($\text{M} = \text{Li}, \text{K}$). After 1.5 equiv of $\text{MN}(\text{SiMe}_3)_2$ were added the ^1H NMR spectrum of the resulting solution displayed significant shifts in the phenoxazine hydrogens (H_a , H_b and H_c , Table 3.1). A distinct upfield shift, Δ , of -0.75 ppm of H_a was observed in the presence of 1.5 equiv of $\text{KN}(\text{SiMe}_3)_2$ (entry 2 vs 1). Similarly, H_c exhibited a smaller shift ($\Delta = -0.59$ ppm) as did H_b ($\Delta = -0.46$ ppm). ^1H NMR chemical shifts did not change upon further addition of $\text{KN}(\text{SiMe}_3)_2$ to NiXantphos (entries 3 and 4 vs 2). Similar shifts were observed in the ^1H NMR spectrum of the phenoxazine hydrogens of NiXantphos in the presence of 1.5 equiv of $\text{LiN}(\text{SiMe}_3)_2$ (entry 5). These observations indicated that deprotonation was complete with 1.5 equiv of $\text{MN}(\text{SiMe}_3)_2$ ($\text{M} = \text{Li}, \text{K}$). Interestingly, a very small shift was observed in the $^{31}\text{P}\{^1\text{H}\}$ NMR spectra of the PPh_2 moiety of NiXantphos after addition of $\text{MN}(\text{SiMe}_3)_2$ (Table 3.1), suggesting (1) the countercation is not bound to the phosphorus centers (also see Figure 3.1a), and (2) the anionic phenoxazine backbone does not render the phosphorus centers significantly more electron-rich (see Section 3.2.2.2 for DFT calculations).

Table 3.1 ^1H and $^{31}\text{P}\{^1\text{H}\}$ NMR studies of NiXantphos deprotonated by base^a



Entry	Base (equiv)	H_b	H_c	H_a	PPh_2
1	none	6.52	6.32	5.91	-18.99
2	$KN(SiMe_3)_2$ (1.5)	6.06	5.73	5.16	-18.69
3	$KN(SiMe_3)_2$ (3)	6.03	5.70	5.14	-18.69
4	$KN(SiMe_3)_2$ (6)	6.04	5.70	5.15	-18.68
5	$LiN(SiMe_3)_2$ (1.5)	6.07	5.75	5.22	-18.45

^aReactions conducted on a 0.04 mmol scale with 1 equiv of NiXantphos and 1.5–6 equiv of $MN(SiMe_3)_2$ ($M = Li, K$) in 0.75 mL of THF- d_8 in a J. Young NMR tube at room temperature, chemical shifts reported in ppm, referenced to the proteo internal standard.

3.2.2.2 DFT Calculations with NiXantphos and Relevant Bidentate Phosphinesⁱⁱⁱ

In reported work, the electron-donating ability of mono- and bidentate phosphine ligands has been assessed using Density Functional Theory (DFT). For example, Spokoyny and Buchwald correlated computed partial charges of B9-connected trivalent aryl and alkyl phosphinoboranes with the electronic properties of their resulting carbonyl complexes.²⁰ To probe the experimental observations for the Pd–NiXantphos system, DFT calculations were performed to assess the electronic structures of the ligands. Gas phase geometry optimizations were performed at the B3LYP level of theory with the 6-31 G* basis set for all atoms using Gaussian '09. Natural Bond Orbital (NBO) analyses of

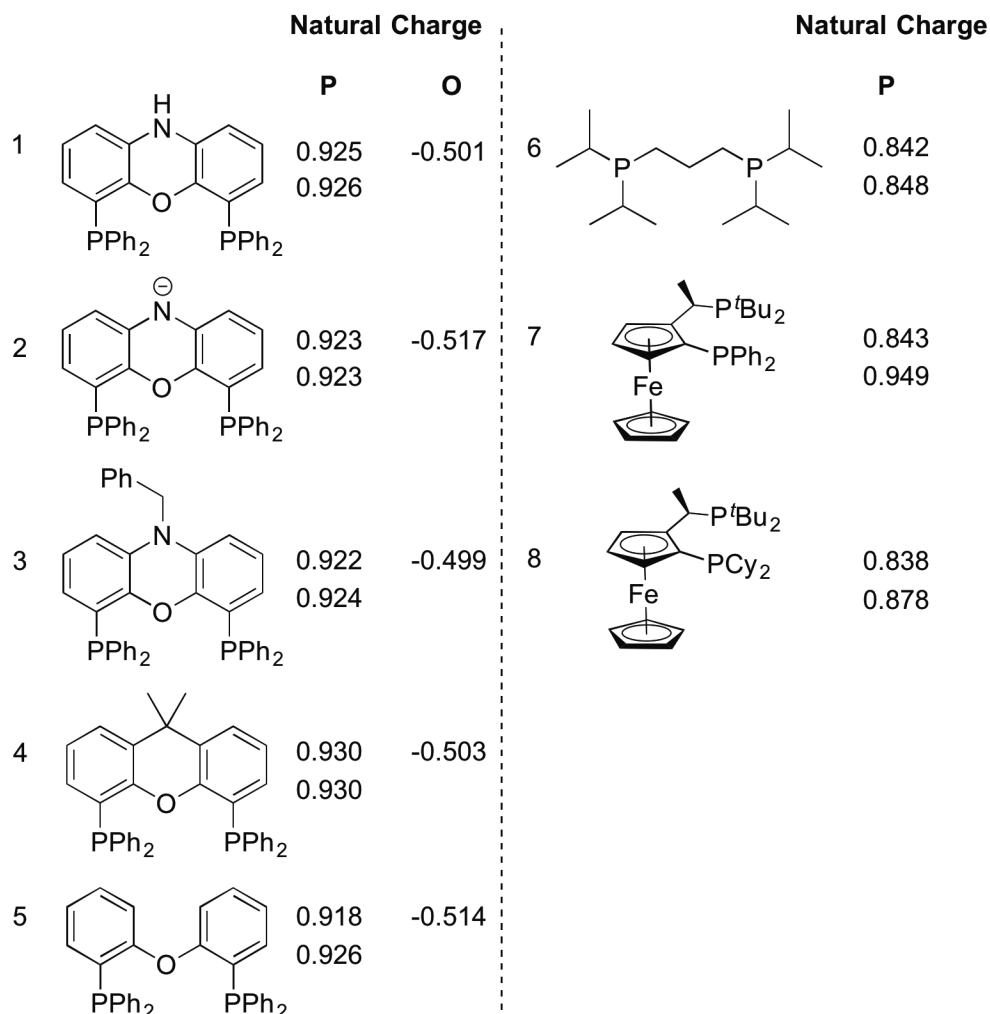
ⁱⁱⁱ DFT calculations (Table 3.2) were performed in collaboration with Haolin Yin at Penn.

the resulting structures afforded comparisons of atomic natural charges (Table 3.2 and also see “3.4 Experimental Section”).

Computations for the 5 ligands: neutral NiXantphos, the deprotonated NiXantphos anion, *N*-Bn-NiXantphos, Xantphos and DPEPhos, and three related bidentate phosphines: P[^]P = dippp, PPF*t*-Bu and CyPF*t*-Bu, were performed. The results suggested that both the phosphorus atoms and the oxygen atom in the deprotonated NiXantphos anion exhibited comparable natural charges to those in the other 4 structurally similar ligands (Table 3.2). In particular, only small ranges of natural charges, $q_P = 0.918$ to 0.930 and $q_O = -0.499$ to -0.517 , were observed, suggesting the electronic structure at the phosphorus and oxygen atoms is largely unchanged upon deprotonation of NiXantphos.

The calculations also suggested the three alkyl-substituted bidentate phosphine ligands: P[^]P, PPF*t*-Bu and CyPF*t*-Bu, were significantly more electron-rich than the Xantphos family of ligands. Overall, the calculations disfavor the possibility that the oxygen atom in the deprotonated NiXantphos is electron-rich, suggesting it is not likely to play a critical role in the oxidative addition of aryl chlorides (see Section 3.2.3).

Table 3.2 Calculated natural charges for members of the Xantphos ligand family and relevant bidentate phosphines



3.2.2.3 Structures of Deprotonated NiXantphos

We were curious how deprotonation would impact the structure of the NiXantphos ligand and how the main group metal would interact with the ligand framework. Bala and co-workers reported the crystal structure of neutral NiXantphos, where the phenoxazine is essentially planar.²¹ We synthesized the metallated ligand, K-NiXantphos by combination of 1 equiv of NiXantphos with 1 equiv of KN(SiMe₃)₂ in Et₂O at room temperature under a nitrogen atmosphere. Upon addition of KN(SiMe₃)₂, K-NiXantphos rapidly precipitated from Et₂O as a yellow solid, and was isolated by

vacuum filtration. ^1H and $^{31}\text{P}\{^1\text{H}\}$ NMR spectra of the isolated K–NiXantphos in THF- d_8 were identical to those obtained in situ from combination of NiXantphos with $\text{KN}(\text{SiMe}_3)_2$ in THF- d_8 (Table 3.1, entry 3).

We obtained diffraction-quality single-crystals of K–NiXantphos in the *absence* and *presence* of 18-crown-6 for a structural study. As illustrated in Figure 3.1a, $[\text{K}(\text{THF})_3\text{-NiXantphos}]_2$ is a dimer in the solid state and the deprotonated phenoxazine ring exhibits a dihedral angle of 1.9° between the two benzo groups, similar to that observed in neutral NiXantphos. The reddish-orange crown ether adduct, $\text{K}(\text{THF})(18\text{-crown-6})\text{-NiXantphos}$, was found to be a monomer in the solid state (Figure 3.1b). A change in geometry of the phenoxazine ring was observed with deprotonation: a dihedral angle of 16.4° between the two benzo rings. The K–N distances were 2.808(3) Å and 2.857(3) Å in the dimer (Figure 3.1a), and 2.885(2) Å in the monomer (Figure 3.1b).

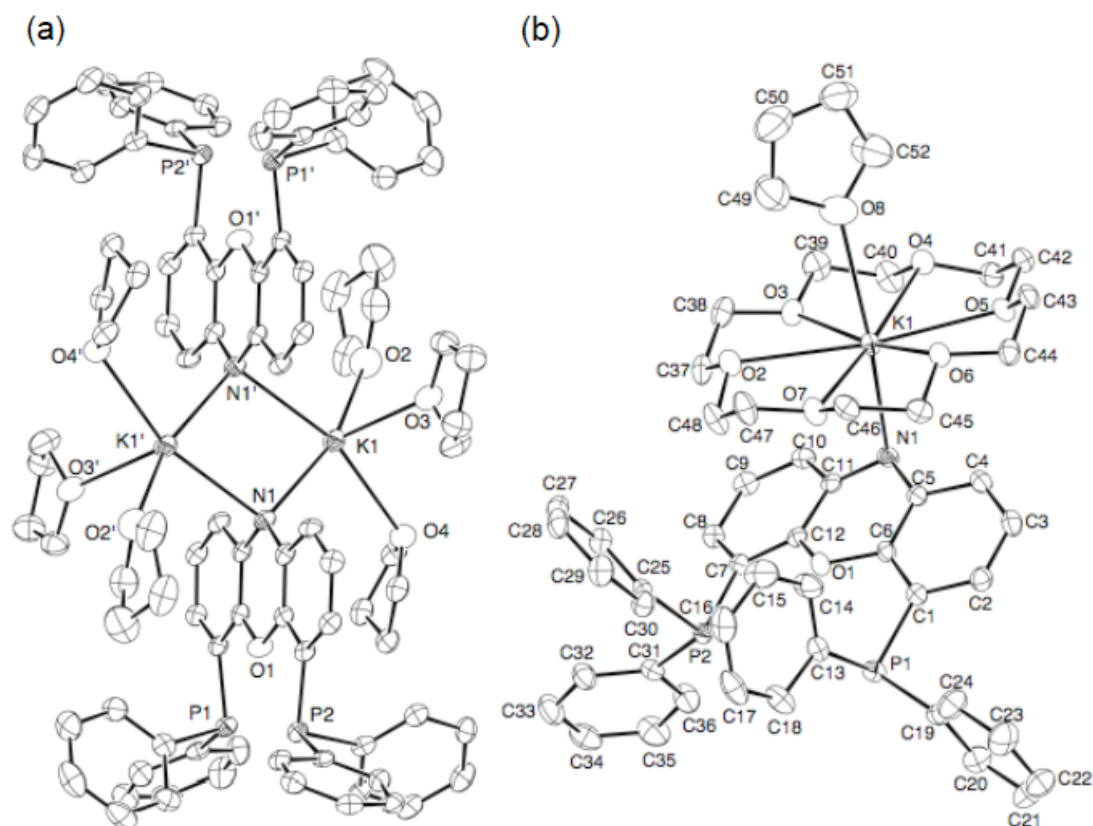


Figure 3.1 (a) ORTEP diagram of $[K(THF)_3-NiXantphos]_2$ with 50% probability thermal ellipsoids displayed. Hydrogen atoms omitted for clarity. $N1-K1 = 2.808(3) \text{ \AA}$, $N1-K1' = 2.857(3) \text{ \AA}$, $P1 \cdots P2$ distance = 4.245 \AA . (b) ORTEP diagram of $K(THF)(18\text{-crown-}6)-NiXantphos$ with 50% probability thermal ellipsoids displayed. Hydrogen atoms omitted for clarity. $N1-K1 = 2.885(2) \text{ \AA}$, $P1 \cdots P2$ distance = 4.301 \AA

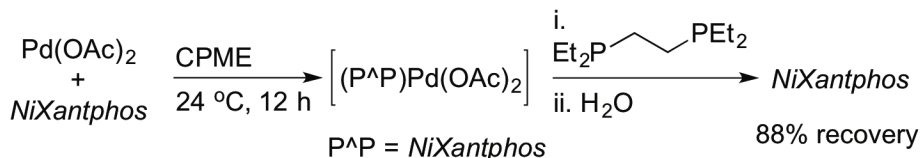
3.2.2.4 Probing *NiXantphos* *N*-Arylation^{iv}

The above studies confirm that *NiXantphos* is deprotonated in the presence of $MN(SiMe_3)_2$ ($M = Li, K$). Thus, under the DCCP reaction conditions (Scheme 3.2) we

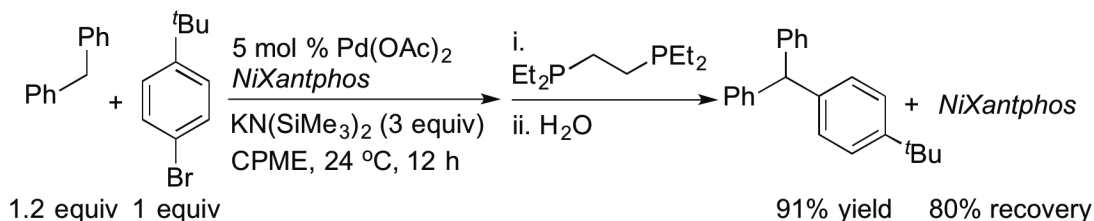
^{iv} Ligand exchange/recovery experiments (Scheme 3.3) were performed in collaboration with Dr. Ana Bellomo at Penn/Merck Laboratory for High-Throughput Experimentation.

were concerned that the deprotonated NiXantphos could be N-arylated via Buchwald–Hartwig amination of aryl halides.²² To address this concern, we needed to displace the NiXantphos-derived products from palladium after the DCCP. For this purpose, an excess of 1,2-bis(diethylphosphino)ethane (depe), a more basic and tighter binding phosphine, was examined for this ligand exchange/NiXantphos recovery experiment. As shown in Scheme 3.3A, palladium acetate was stirred with NiXantphos for 12 h at room temperature, resulting in coordination of NiXantphos, as determined by ³¹P{¹H} NMR spectroscopy. Treatment of the complex with 8 equiv of depe followed by filtration over a pad of silica and flash chromatography resulted in 88% recovered NiXantphos (Scheme 3.3A). To determine whether the deprotonated NiXantphos was N-arylated after the cross-coupling reaction with aryl bromide, we performed the DCCP in Scheme 3.3B then carried out a ligand exchange/recovery procedure. We recovered 80% of NiXantphos after flash chromatography (average of two runs). No N-arylated NiXantphos was observed (Scheme 3.3B), suggesting the catalyst does not undergo N-arylation.

A. Ligand exchange/recovery process (control)



B. Cross-coupling followed by ligand exchange/recovery process



Scheme 3.3 Ligand exchange and recovery of NiXantphos

3.2.3 Oxidative Addition with Aryl Chlorides

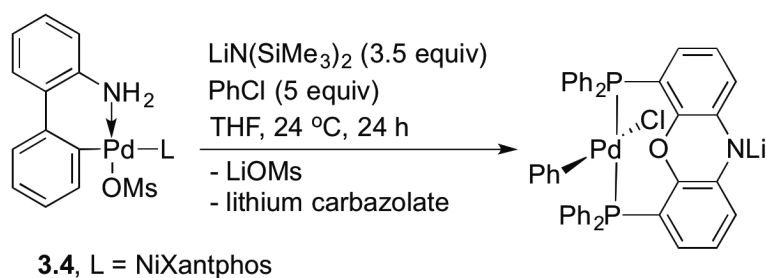
Based on the studies in Sections 3.2.1 and 3.2.2, NiXantphos was deprotonated to generate the metallated ligand, K-NiXantphos, but it was not N-arylated under the DCCP reaction conditions. While the potassium atom was positioned away from the oxygen and the phosphorus atoms in the solid state structures, we wondered if its presence could facilitate the activation of less reactive aryl chlorides, either by cooperative reactivity with the palladium^{9,23} or by an electrostatic effect caused by the presence of the charged potassium and nitrogen atoms near the site of oxidative addition.²⁴ Such interactions could be envisioned to facilitate oxidative additions with less reactive aryl chlorides. Based on this supposition, we set out to study the oxidative addition of chlorobenzene to our heterobimetallic catalyst system.

The oxidative addition of aryl bromides to (Xantphos)Pd(dba) (dba = dibenzylideneacetone) has been previously studied.²⁵ In these studies, combination of 1 equiv of Pd(dba)₂ (or 0.5 equiv of Pd₂dba₃) with 1 equiv of Xantphos generated (Xantphos)Pd(dba) in situ.²⁶ In the presence of 4-bromobenzonitrile, this intermediate reacted at room temperature to afford (Xantphos)Pd(4-C₆H₄CN)(Br) in 80% yield.^{25a} Higher temperature was required (80 °C) for reaction with less reactive bromobenzene to afford (Xantphos)Pd(C₆H₅)(Br).^{25b} We used the same procedure for the oxidative addition studies with chlorobenzene (**3.2b**, 5 equiv) to in situ generated (Xantphos)Pd(dba) and neutral (NiXantphos)Pd(dba) at 24 and 80 °C. Under these conditions no oxidative addition products were detected. These results suggested that Xantphos and neutral NiXantphos were not effective ligands for oxidative addition of aryl chlorides to palladium(0). We also mixed in situ generated (NiXantphos)Pd(dba) with 1 equiv of KN(SiMe₃)₂ and 5 equiv of chlorobenzene (**3.2b**) at 24 °C, but the reaction gave

multiple products, as judged by $^{31}\text{P}\{^1\text{H}\}$ NMR spectroscopy, probably because of interference with dba.

The Buchwald group demonstrated an oxidative addition of chlorobenzene to a $\text{LPd}(0)$ (L = a monodentate phosphine) complex, which was in situ generated by combination of their first-generation chloride precatalyst with 1 equiv of base.²⁷ Other groups also reported on palladacycles used as precatalysts for cross-coupling reactions with aryl chlorides.²⁸ The Buchwald group recently reported their third-generation precatalysts, wherein a dimeric 2-aminobiphenylpalladium methanesulfonate complex can be treated with a range of phosphine ligands (including sterically bulky ligands and bidentate ligands) to provide methanesulfonate precatalysts.²⁹ To determine the reactivity of our palladium catalyst system based on deprotonated NiXantphos in the absence of dba, we combined 1 equiv of the methanesulfonate precatalyst **3.4** (see Scheme 3.4 for the structure) with 3.5 equiv of $\text{LiN}(\text{SiMe}_3)_2$ and 5 equiv of chlorobenzene (**3.2b**) in THF at 24 °C (Scheme 3.4). We propose that the first equiv of $\text{LiN}(\text{SiMe}_3)_2$ deprotonates the NH_2 moiety to induce the reductive elimination, affording carbazole and $(\text{NiXantphos})\text{Pd}(0)$.²⁷ The second and third equiv of $\text{LiN}(\text{SiMe}_3)_2$ deprotonate carbazole ($\text{p}K_a = 19.9$) and $(\text{NiXantphos})\text{Pd}(0)$ ($\text{p}K_a \sim 22$).¹³ The room temperature oxidative addition of chlorobenzene reached about 75% conversion in 6 h and near completion in 24 h, as judged by a singlet at 2.6 ppm in $^{31}\text{P}\{^1\text{H}\}$ NMR spectrum for the oxidative addition product. The singlet is due to the rapid exchange between *cis*- and *trans*-chelation modes of the wide bite angle NiXantphos ligand (114°)⁸ in solution, as also observed with $(\text{Xantphos})\text{Pd}(\text{Ar})(\text{Br})$.³⁰ The oxidative addition product, $(\text{Li-NiXantphos})\text{Pd}(\text{Ph})(\text{Cl})$, is generated along with byproducts lithium mesylate and lithium carbazolate, rendering the isolation of the Pd-containing product challenging (Scheme 3.4). Nevertheless, single-crystals of the neutral $(\text{NiXantphos})\text{Pd}(\text{Ph})(\text{Cl})$ were

obtained by vapor diffusion of pentane into a concentrated THF solution of the reaction mixture (Figure 3.2). The solid state structure shows a slightly distorted square planar geometry with *trans* phosphorus atoms. This *trans*-chelating mode of NiXantphos is similar to that of Xantphos: Xantphos is *trans*-chelating in all reported solid state structures of (Xantphos)Pd(Ar)(halide) complexes to date.³⁰ A larger dihedral angle between the two benzo groups of the phenoxazine ring system was observed in (NiXantphos)Pd(Ph)(Cl): 27.8° vs 1.9° in Figure 3.1a and 16.4° in Figure 3.1b.



Scheme 3.4 Oxidative addition of chlorobenzene (**3.2b**) using **3.4**

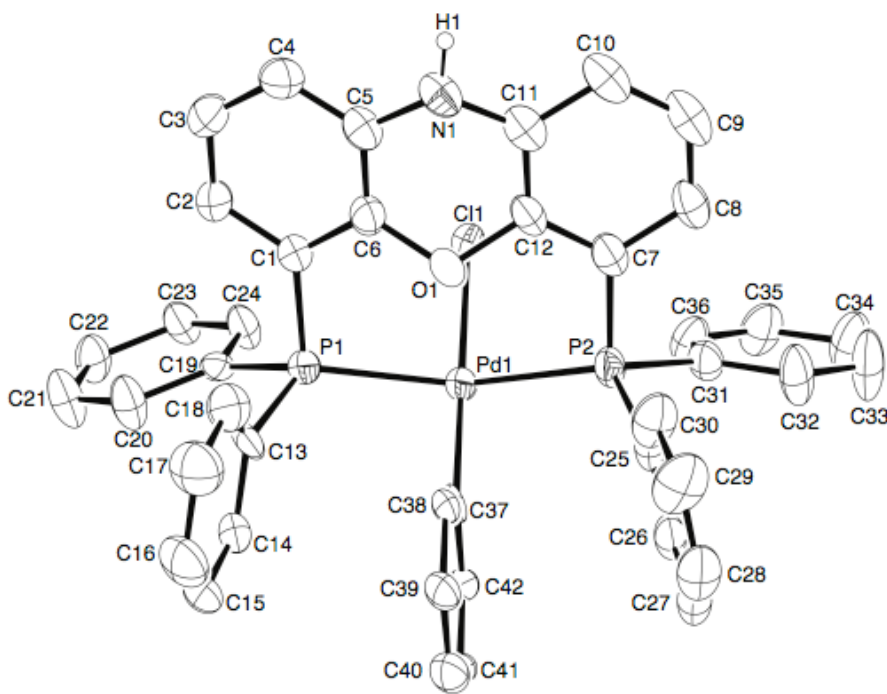


Figure 3.2 ORTEP diagram of (NiXantphos)Pd(Ph)(Cl) with 50% probability thermal ellipsoids displayed. Hydrogen atoms omitted for clarity. Pd1–P1 = 2.3168(9) Å, Pd1–P2 = 2.3083(8) Å, Pd1–C37 = 2.048(2) Å, Pd1–Cl1 = 2.4348(8) Å, P1···P2 distance = 4.454 Å, Pd1···O1 distance = 2.686 Å, C37–Pd1–Cl1 angle = 178.70°, P1–Pd1–P2 angle = 148.76°

The same reactivity was also observed when KN(SiMe₃)₂ was used in place of LiN(SiMe₃)₂ in the oxidative addition of chlorobenzene: the reaction neared completion after 24 h, as judged by a singlet at 2.8 ppm in ³¹P{¹H} NMR spectrum. The results of these experiments are counterintuitive given that oxidative addition of aryl chlorides has been shown to proceed via a PdL₁ pathway. Bidentate ligands typically require significantly higher temperatures because they react via the less favorable PdL₂ pathway. Thus, the observation that a *bidentate triarylphosphine* derivative can activate aryl chlorides at room temperature is unexpected and highlights the novel characteristics of this heterobimetallic catalyst system under the basic DCCP conditions. The oxidative addition studies lay the foundation for aryl chlorides to undergo room temperature cross-coupling reactions catalyzed by Pd–NiXantphos.

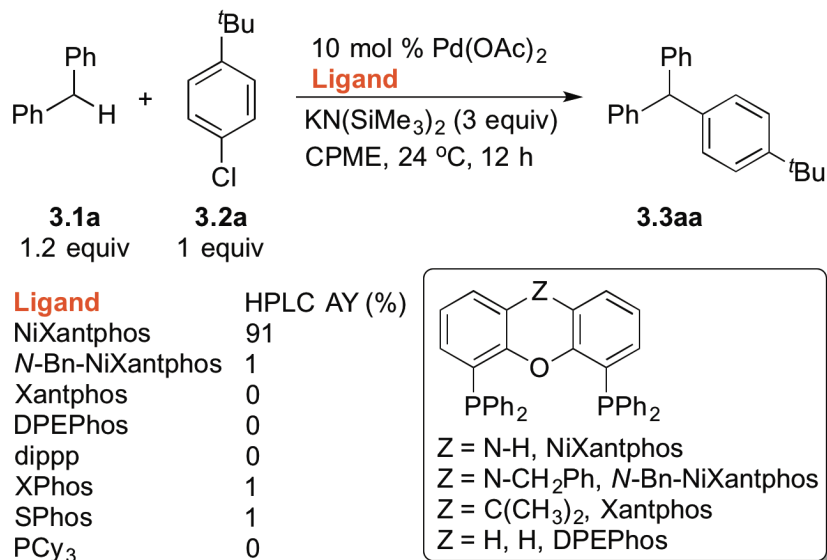
By directly employing K–NiXantphos as a ligand, attempts to synthesize the corresponding palladium compounds (K–NiXantphos)Pd(dba), (K–NiXantphos)PdCl₂ and (K–NiXantphos)Pd(OAc)₂ were unsuccessful. Upon mixing 1 equiv of K–NiXantphos with the corresponding palladium sources [0.5 equiv of Pd₂dba₃, 1 equiv of (norbornadiene)PdCl₂, or 1 equiv of Pd(OAc)₂] we observed multiple products as judged by ³¹P{¹H} NMR spectroscopy. It is possible that K–NiXantphos could undergo rapid transmetallation with Pd(II) or react with dba. Furthermore, combination of 0.5 equiv of Pd₂dba₃ with 2 equiv of neutral NiXantphos in THF (or toluene) resulted in

precipitation of a greenish yellow solid. The identity of the precipitate was confirmed as Pd(NiXantphos)₂ by HRMS analysis. Unfortunately, Pd(NiXantphos)₂ was insoluble in common organic solvents. A similar synthetic route was reported for Pd(Xantphos)₂ by the Buchwald group, and its poor solubility was also noted.²⁶

3.2.4 Development of DCCP with Aryl Chlorides

Based on the preliminary studies in Section 3.2.3, we carried out a ligand comparison experiment employing 1-*tert*-butyl-4-chlorobenzene (**3.2a**) as the cross-coupling partner under reaction conditions related to our previous DCCP of aryl bromides (Scheme 3.5). The comparison was performed on a 10 μmol scale. To probe our hypothesis that the deprotonation of NiXantphos is responsible for the exceptional reactivity in the oxidative addition of aryl chlorides, we synthesized and tested *N*-benzyl NiXantphos, which cannot undergo deprotonation.⁸

In agreement with our hypothesis, excellent HPLC assay yield (AY) of the product **3.3aa** was observed using 10 mol % Pd–NiXantphos. In contrast, catalysts generated from *N*-Bn-NiXantphos showed <2% conversion and Xantphos did not generate detectable amounts of products (Scheme 3.5). Other ligands known to participate in coupling reactions with aryl chlorides showed little or no reactivity in this cross-coupling process.



^aConducted on a 10 μ mol scale at 0.1 M.

Scheme 3.5 Selected results of the cross-coupling of **3.1a** with **3.2a**^a

Considering the structural similarity of NiXantphos, *N*-Bn-NiXantphos and Xantphos, as well as the fact that NiXantphos was deprotonated by KN(SiMe₃)₂ under the DCCP reaction conditions, the data in Scheme 3.5 support the hypothesis that K-NiXantphos forms the active palladium catalyst to “turn on” the cross-couplings with aryl chloride **3.2a** at room temperature, while the neutral *N*-Bn-NiXantphos and Xantphos do not (Figure 3.3).

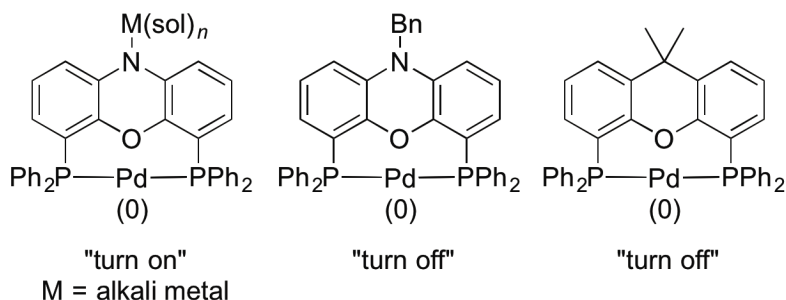
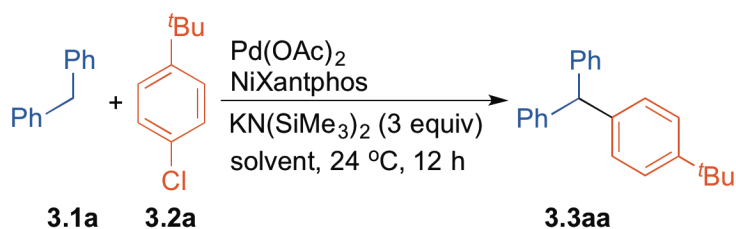


Figure 3.3 Proposed “turn on” form of palladium(0) bearing a deprotonated NiXantphos and the “turn off” form of palladium(0) bearing a neutral *N*-Bn-NiXantphos or Xantphos for the DCCP with aryl chlorides

3.2.5 Optimization of DCCP with Diphenylmethane and Aryl Chloride **3.2a**

The results in Scheme 3.5 provided an excellent starting point for the C–C bond formation from diphenylmethane (**3.1a**) and aryl chloride **3.2a** at room temperature. A 91% assay yield (HPLC) was obtained at 10 mol % catalyst loading on microscale. This microscale reaction was successfully translated to laboratory scale (0.1 mmol) under the same conditions (Table 3.3, entry 1, 87% assay yield). In further agreement with the data in Scheme 3, Pd–Xantphos catalyst system did not render any product **3aa** under the same conditions either at 24 or 80 °C. Considering 10 mol % catalyst loading was relatively high, further optimization on laboratory scale was desired for the room temperature DCCP.

Table 3.3 Optimization of Pd–NiXantphos-catalyzed DCCP of **3.1a** with **3.2a**^a



entry	3.1a : 3.2a	Pd (mol %)	solvent	concentration	yield (%) ^b
				(M)	
1	1.2:1.0	10	CPME	0.1	87
2	1.2:1.0	10	DME	0.1	61

3	1.2:1.0	10	2-MeTHF	0.1	78
4	1.2:1.0	10	THF	0.1	>95
5	1.2:1.0	10	dioxane	0.1	25
6	1.2:1.0	10	MTBE	0.1	10
7	1.2:1.0	5	THF	0.1	79
8	1.2:1.0	5	THF	0.2	88
9 ^c	1.2:1.0	5	THF	0.2	76
10	1.0:2.0	5	THF	0.2	>95 (99 ^d)
11	1.0:2.0	2.5	THF	0.2	(81 ^d)

^aReactions conducted on a 0.1 mmol scale using **3.1a**, **3.2a** and 3 equiv of KN(SiMe₃)₂ at 24 °C. ^bYield determined by ¹H NMR spectroscopy of the crude reaction mixture. ^c5 mol % the methanesulfonate precatalyst **3.4** was used in place of Pd(OAc)₂/NiXantphos. ^dIsolated yield after chromatographic purification.

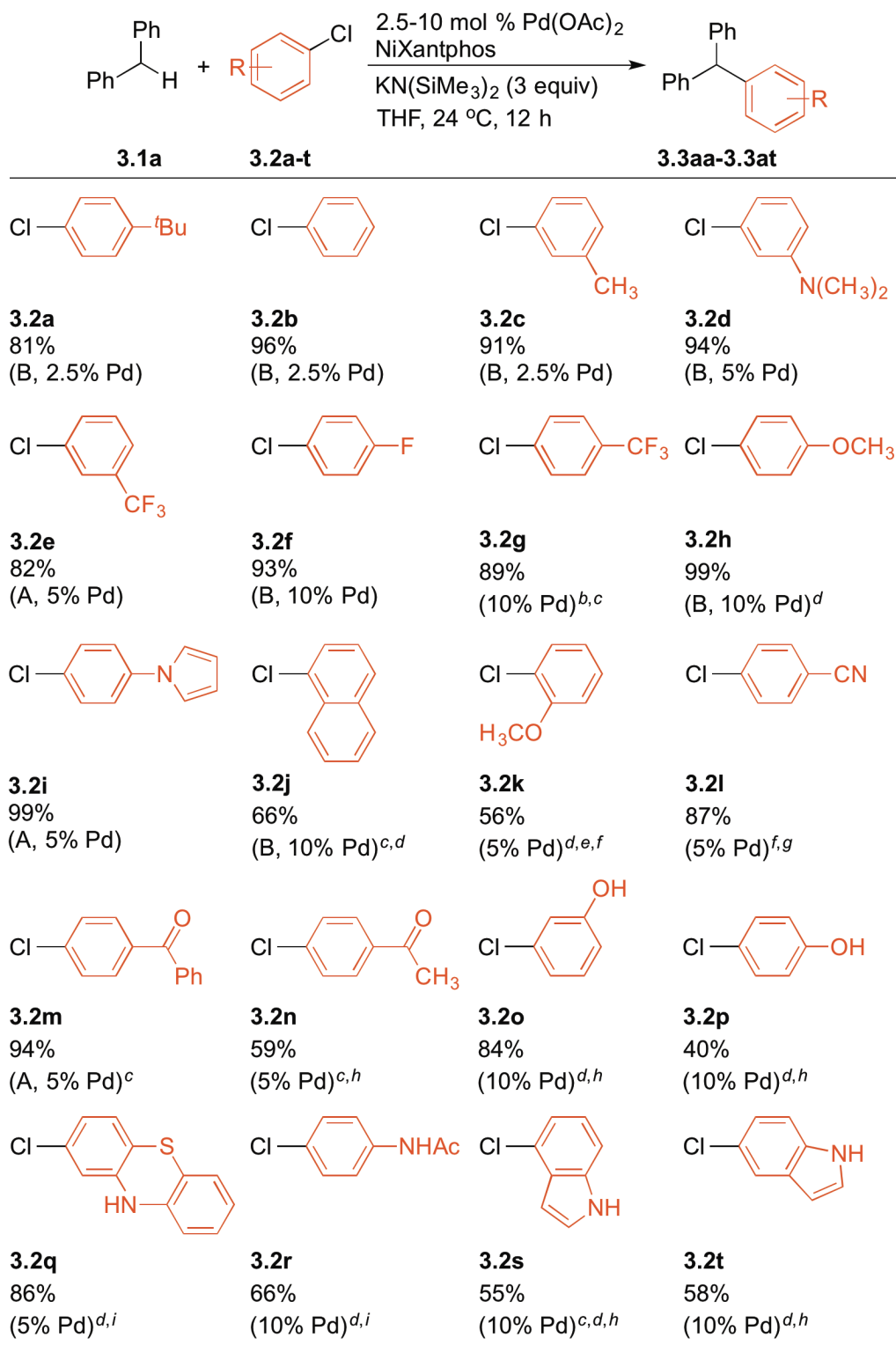
We next examined 5 additional ethereal solvents [DME, 2-MeTHF, THF, dioxane, and MTBE (methyl *tert*-butyl ether)] in the presence of 1.2 equiv of diphenylmethane (**3.1a**), 1 equiv of 1-*tert*-butyl-4-chlorobenzene (**3.2a**), and 3 equiv of KN(SiMe₃)₂ at 0.1 M and 24 °C (entries 2–6). Dioxane and MTBE (entries 5 and 6) afforded <25% yield of product **3.3aa** due to solubility issues of the reactants at 24 °C. The lead result was obtained when THF was used as solvent, where the triarylmethane **3.3aa** was generated in >95% yield (entry 4). Reduction of the catalyst loading from 10 to 5 mol % while increasing the reaction concentration from 0.1 to 0.2 M in THF resulted in only a minor loss in yield (entries 7 and 8 vs 4). Under otherwise identical conditions, a similar yield (76%, entry 9) was obtained using 5 mol % of the methanesulfonate precatalyst **3.4** in place of Pd(OAc)₂/NiXantphos (entry 9 vs 8). Considering the commercial availability of

both Pd(OAc)₂ and NiXantphos, we continued with the Pd(OAc)₂/NiXantphos catalyst system for further optimization. Switching the limiting reagent from aryl chloride **3.2a** to diphenylmethane **3.1a** resulted in >95% yield of the triarylmethane product **3.3aa** with 5 mol % catalyst loading in THF at 0.2 M at 24 °C (entry 10). Compound **3.3aa** was ultimately isolated in 99% yield after flash chromatography. Further reducing the catalyst loading to 2.5 mol % rendered **3.3aa** in 81% isolated yield (entry 11). These optimized conditions were carried forward in the next phase, which focused on the determination of the scope of aryl chlorides in Pd–NiXantphos-catalyzed DCCP.

3.2.6 Scope of Aryl Chlorides in DCCP with Diphenylmethane

In previous reports, we demonstrated that a large range of sterically and electronically diverse hetero- and non-heteroaryl-containing diarylmethane derivatives readily undergo DCCP with *aryl bromides* to afford an array of triarylmethane products.¹¹ In the current study, the scope of Pd–NiXantphos-catalyzed DCCP using a variety of aryl chlorides with a model diarylmethane substrate (**3.1a**) is presented in Table 3.4.

Table 3.4 Scope of aryl chlorides in Pd–NiXantphos-catalyzed DCCP with **3.1a**^a



^aReactions conducted on a 0.1 mmol scale using 1.2 equiv of **3.1a**, 3 equiv of KN(SiMe₃)₂, and 1 equiv of **3.2** (conditions A) or 1 equiv of **3.1a**, 3 equiv of KN(SiMe₃)₂,

and 2 equiv of **3.2** (conditions B) using 2.5–10 mol % Pd(OAc)₂ and NiXantphos (Pd:L = 1:2) in THF at 0.2 M at 24 °C. Isolated yield after chromatographic purification. ^b**3.1a**:KN(SiMe₃)₂:**3.2** = 4:2:1. ^cCPME was used as solvent. ^d80 °C. ^e**3.1a**:KN(SiMe₃)₂:**3.2** = 1:3:3. ^f2-MeTHF was used as solvent. ^g**3.1a**:KN(SiMe₃)₂:**3.2** = 1.2:4:1. ^h**3.1a**:KN(SiMe₃)₂:**3.2** = 3:4:1. ⁱ**3.1a**:KN(SiMe₃)₂:**3.2** = 1:5:2.

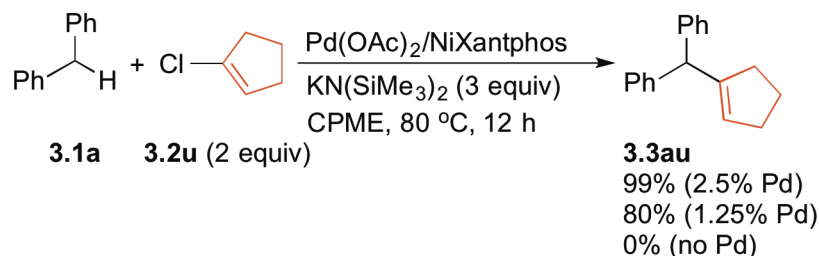
In general, fair to excellent reactivity was exhibited by aryl chlorides bearing various substituents (**3.2a–k**). At least one combination from (1) the two ratios of reagents [diphenylmethane (**3.1a**) : KN(SiMe₃)₂ : aryl chloride (**3.2**) = 1.2:3:1 (conditions A) and 1:3:2 (conditions B)] and (2) the three ethereal solvents (THF, CPME and 2-MeTHF) at 2.5–10 mol % catalyst loading successfully delivered the desired DCCP products in 56–99% yields (average yield: 86% for 11 aryl chlorides, **3.2a–k**). Both 4-*tert*-butylphenyl and phenyl chloride furnished **3.3aa** and **3.3ab** in 81% and 96% yield, respectively, at 2.5 mol % palladium loading. Methyl (**3.2c**), *N,N*-dimethylamino (**3.2d**), and trifluoromethyl (**3.2e**) groups at the *meta* position were all well-tolerated (**3.3ac–3.3ae** in 82–94% yields). Excellent yields were obtained using aryl chlorides bearing both electron-withdrawing CF₃ and 4-F groups (**3.2e–g**) and electron-donating 4-OMe and 4-(*N*-pyrrolyl) groups (**3.2h**, **3.2i**). The sterically more hindered 1-chloronaphthalene and 2-chloroanisole (**3.2j**, **3.2k**) also participated in DCCP to produce the desired products. These substrates, however, required higher temperature (80 °C) to give 66% (**3.3aj**) and 56% (**3.3ak**) yield, respectively.

We next tested aryl chloride substrates bearing sensitive functional groups and heteroaryl groups (**3.2l–t**). As shown in Table 3.4, remarkable chemoselectivity was demonstrated with aryl chlorides containing cyano, keto, acetyl, phenol, phenothiazine, acetamide, and 1*H*-indole moieties, all of which underwent DCCP delivering the

corresponding functionalized triarylmethane products without observation of byproducts (**3.3al–3.3at**). Nitriles and ketones are well known to undergo 1,2-addition reactions with reactive organometallics, while 4'-chloroacetophenone can participate in competitive aldol³¹ and α -arylation³² reactions under the basic reaction conditions (pK_a of acetophenone: 24.7¹³). Yet the triarylmethane products (**3.3al**, **3.3am**, **3.3an**) were produced in 59–94% yields. Challenging classes of substrates bearing acidic O–H and N–H bonds (**3.2o–t**) were next examined. Phenols are known to undergo O- and C(sp²)–H arylation,³³ while 1*H*-indoles (and anilines) have been reported to react via N-arylation (Buchwald–Hartwig coupling),^{22,34} C-2-, and C-3-arylation³⁵ in the presence of palladium catalysts and bases. Our method exhibits orthogonal chemoselectivity with DCCP taking place exclusively at the benzylic C(sp³)–H of diphenylmethane (**3.1a**) and the C(sp²)–Cl of aryl chlorides **3.2o–t**. These functional groups and heteroaryl groups present opportunities to functionalize the triarylmethane products further. Note that for each equiv of aryl chloride bearing acidic protons (**3.2n–t**), an extra equivalent of KN(SiMe₃)₂ was employed. For substrates giving less than 80% yield (**3.2n**, **3.2p**, **3.2r–2t**), ¹H NMR of the reaction mixture after work-up showed only remaining starting materials and product. No byproduct formation was observed. Attempts to push these reactions to completion, however, were unsuccessful. Unfortunately, 3-chloropyridine, 2- and 3-chlorothiophene failed to give the DCCP products in reasonable yield (<10%).

After demonstrating that aryl chloride substrates bearing sensitive functional groups and heteroaryl groups (**3.2l–t**) were viable cross-coupling partners in Pd–NiXantphos-catalyzed DCCP with diphenylmethane (**3.1a**), an unactivated alkenyl chloride **3.2u** was tested (Scheme 3.6). Vinyl chloride **3.2u** participated in DCCP to afford **3au** in 99% yield at 2.5 mol % catalyst loading at 80 °C. Even at 1.25 mol % catalyst loading under identical conditions, **3.3au** was produced in 80% yield. These

results indicate the Pd–NiXantphos catalyst can oxidatively add unactivated alkenyl chlorides. It is also interesting that the product did not isomerize, suggesting that deprotonation of the product did not occur.



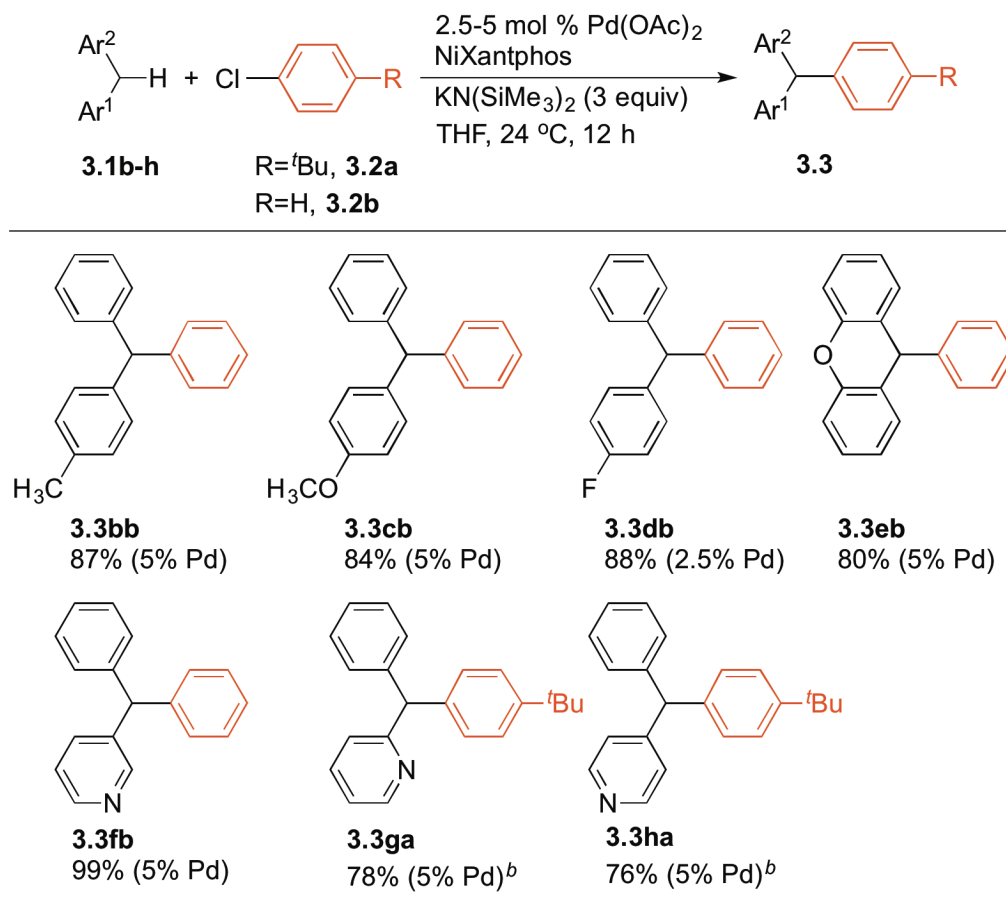
Scheme 3.6 DCCP of **3.1a** with alkenyl chloride **3.2u**

As shown in Table 3.4, both the synthetic utility and the remarkable chemoselectivity of the Pd–NiXantphos-catalyzed C–C cross-coupling method with a large variety of aryl chlorides have been demonstrated. Several aspects are noteworthy: (1) 3- and 4-chlorophenols (**3.2o**, **3.2p**) reacted with **3.1a** to give the DCCP products in 84% and 40% yield, respectively. Given that these phenols are deprotonated by $\text{KN(SiMe}_3)_2$ to give phenoxides under the reaction conditions, these results suggest that the Pd–NiXantphos catalyst system is able to undergo oxidative addition with very electron-rich $\text{C(sp}^2\text{)}-\text{Cl}$ bonds (such as those in phenoxides). (2) 2-Chlorophenothiazine (**3.2q**) produced the DCCP product in 86% yield without observation of N-arylation byproduct. Since **3.2q** has a phenothiazine core, which is structurally similar to the phenoxazine core in NiXantphos, this result supports our earlier conclusion based on the ligand exchange/recovery experiments that NiXantphos was not N-arylated during the reaction.

3.2.7 Scope of Diarylmethanes in DCCP

The scope of the DCCP with respect to diarylmethanes was next explored with aryl chlorides (**3.2a**, **3.2b**) (Table 3.5).

Table 3.5 Scope of diarylmethanes in Pd–NiXantphos-catalyzed DCCP^a



^aReactions conducted on a 0.1 mmol scale using 1 equiv of **3.1**, 3 equiv of $\text{KN}(\text{SiMe}_3)_2$, and 2 equiv of **3.2** with 2.5–5 mol % $\text{Pd}(\text{OAc})_2$ and NiXantphos (Pd:L = 1:2) in THF at 0.2 M at 24 °C. Isolated yield after chromatographic purification. ^b $\text{LiN}(\text{SiMe}_3)_2$ was used as base instead of $\text{KN}(\text{SiMe}_3)_2$.

Substrates bearing various substituents on the diarylmethane exhibited excellent reactivity at 2.5–5 mol % catalyst loading at room temperature. Alkyl (**3.3bb**), electron-

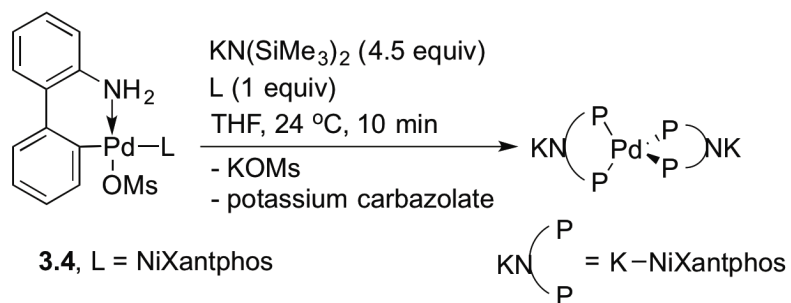
donating (**3.3cb**), and electron-withdrawing groups (**3.3db**) were all well-tolerated. Heteroaryl-containing diarylmethane analogues proved to be good substrates, with corresponding products isolated in 76–99% isolated yields (**3.3eb**, **3.3fb**, **3.3ga**, **3.3ha**). Note that although 3-benzylpyridine required $\text{KN}(\text{SiMe}_3)_2$ as base to promote DCCP (**3.3fb**), a weaker base, $\text{LiN}(\text{SiMe}_3)_2$, successfully promoted DCCP with the more acidic 2- and 4-benzylpyridines ($\text{p}K_a = 28.2$ and 26.7 , respectively)¹³ to deliver **3.3ga** and **3.3ha** in good yields.

3.2.8 Identification of the Catalyst Resting State and Counteraction Effects

To determine the resting state of the palladium catalyst in our DCCP reactions, we conducted the catalytic reaction with diphenylmethane (**3.1a**), chlorobenzene (**3.2b**) and $\text{KN}(\text{SiMe}_3)_2$ as base in the presence of 10 mol % of the methanesulfonate precatalyst **3.4** in THF in a sealed J. Young NMR tube at room temperature. The only species observed by $^{31}\text{P}\{^1\text{H}\}$ NMR spectroscopy over the course of the DCCP (12 h) was $\text{Pd}(\text{K-NiXantphos})_2$, as judged by a singlet at -1.3 ppm in $^{31}\text{P}\{^1\text{H}\}$ NMR spectrum. Using 10 mol % $\text{Pd}(\text{OAc})_2$ and 20 mol % NiXantphos gave the same dominant catalyst resting state 10 min after addition of **3.1a**, **3.2b** and $\text{KN}(\text{SiMe}_3)_2$ at room temperature. The catalyst resting state suggests that ligand dissociation and/or oxidative addition is turnover limiting. The Hartwig group has reported the identification of $\text{Pd}(\text{P}^{\wedge}\text{P})_2$ complexes ($\text{P}^{\wedge}\text{P}$ = a chelating diphosphine ligand such as BINAP and DPPF) as the dominant resting state in the Pd- $\text{P}^{\wedge}\text{P}$ -catalyzed amination of aryl bromides.^{7b} The turnover limiting step was dissociation of BINAP from $\text{Pd}(\text{BINAP})_2$ when BINAP was used as ligand, while the combination of ligand dissociation and irreversible oxidative addition were the turnover limiting steps in the catalytic process when DPPF was used as ligand.

$\text{Pd}(\text{K-NiXantphos})_2$ was independently prepared from combination of 1 equiv of the methanesulfonate precatalyst **3.4** with 4.5 equiv of $\text{KN}(\text{SiMe}_3)_2$ and 1 equiv of NiXantphos ligand in THF at 24 °C under a nitrogen atmosphere (Scheme 3.7). We propose that the in situ generated coordinatively unsaturated $(\text{K-NiXantphos})\text{Pd}(0)$ reacts rapidly with 1 equiv of K-NiXantphos. The formation of $\text{Pd}(\text{K-NiXantphos})_2$ was complete in 10 min as judged by disappearance of **3.4** and appearance of a new singlet at -1.3 ppm in $^{31}\text{P}\{^1\text{H}\}$ NMR spectrum. Single-crystals of $\text{Pd}(\text{K-NiXantphos})_2$ were obtained by crystallization from THF at 24 °C and found to be extremely sensitive, and sample decomposition during mounting could not be avoided. Although the quality of the structure precludes detailed discussion of the metrics, it does serve to establish the connectivity {see Figure 3.4 for a drawing of the structure and Figure 3.5 for the structure of $[\text{PdK}_2(\text{THF})_4(\text{NiXantphos})_2]_{\infty}$ }. In the solid state $\text{Pd}(\text{K-NiXantphos})_2$ exhibits a polymeric structure in which the Pd(0) center adopts a slightly distorted tetrahedral geometry. The PdL_2 units are linked together by bridging potassium-nitrogen interactions, similar to those observed in the structure of K-NiXantphos (Figure 3.1a). The P-Pd-P angle containing two phosphorus atoms of the same K-NiXantphos ligand is $113.22(7)^\circ$. The other P-Pd-P angles are $102.91(12)^\circ$, $106.78(7)^\circ$ and $113.54(12)^\circ$. The deprotonated phenoxazine ring exhibits a dihedral angle of 23.1° between the two benzo groups of the heterocyclic framework. In contrast to the solid state polymeric structure, the hydrodynamic radius (r_H) of $\text{Pd}(\text{K-NiXantphos})_2$, as measured by diffusion-ordered ^1H NMR spectroscopy (DOSY) in THF- d_8 , was consistent with a monomer (see “3.4 Experimental Section” for details).^v

^v DOSY experiments were performed in collaboration with Jerome R. Robinson at Penn.



Scheme 3.7 Synthesis of $\text{Pd}(\text{K-NiXantphos})_2$

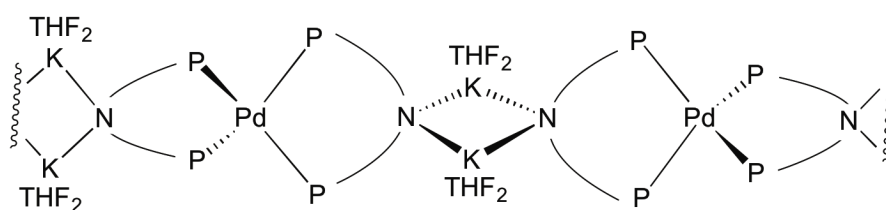


Figure 3.4 Drawing of the solid state structure of polymeric $\text{Pd}(\text{K-NiXantphos})_2$ illustrating the connectivity

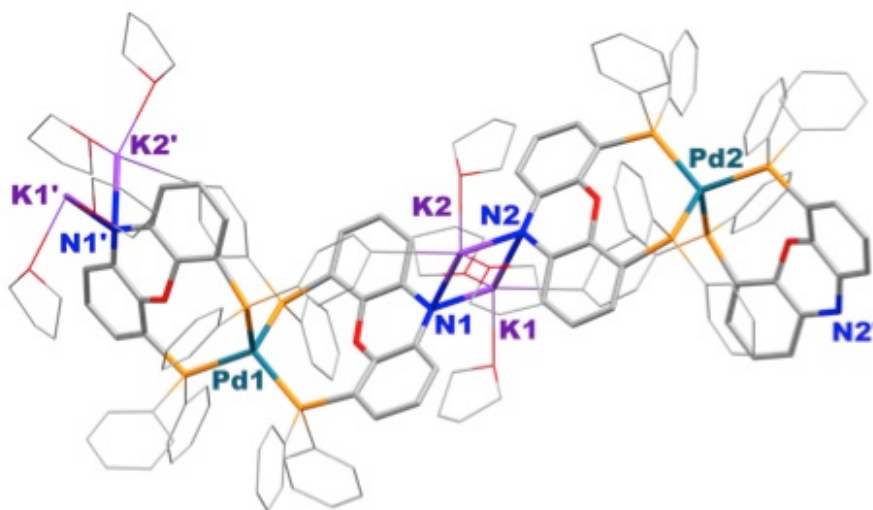
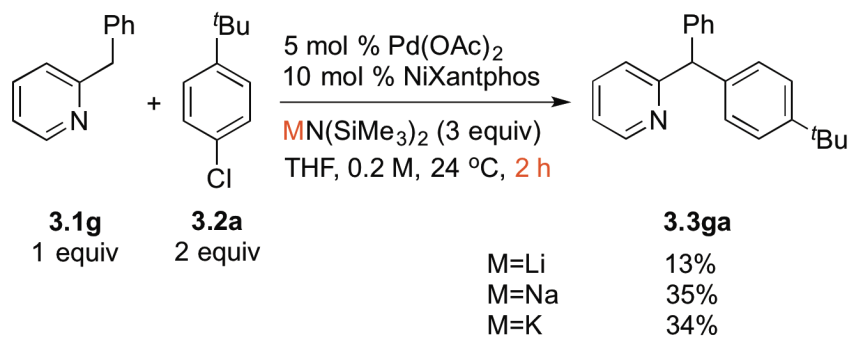


Figure 3.5 Structure of polymeric $[\text{PdK}_2(\text{THF})_4(\text{NiXantphos})_2]_\infty$. Coordinated THF molecules and phenyl groups from NiXantphos are shown in wireframe and hydrogen atoms are omitted for clarity

To compare the catalytic reactivity using different counteranions (Li, Na vs K), we carried out our DCCP reactions under standard conditions with 2-benzylpyridine (**3.1g**) and 1-*tert*-butyl-4-chlorobenzene (**3.2a**) using the following 3 bases: LiN(SiMe₃)₂, NaN(SiMe₃)₂ and KN(SiMe₃)₂. We have previously demonstrated that DCCP of diphenylmethane (**3.1a**) with aryl bromides is readily promoted by KN(SiMe₃)₂ but the reaction fails when NaN(SiMe₃)₂ or LiN(SiMe₃)₂ is used in the absence of additives. In contrast, DCCP of the more acidic substrate 2-benzylpyridine (**3.1g**) can be promoted by MN(SiMe₃)₂ (M = Li, Na, K).^{11b} Assay yields of the product **3.3ga** at 2 h from the DCCP reactions employing 3 bases MN(SiMe₃)₂ (M = Li, Na, K) are illustrated in Scheme 3.8 (average of two runs). The impact of the counteranion on the catalytic reaction follows the trend: K ≈ Na > Li. At this point, it is difficult to draw conclusions from these data, because the main group metal is involved in the deprotonation of the substrate and catalyst, and in each step of catalytic cycle.

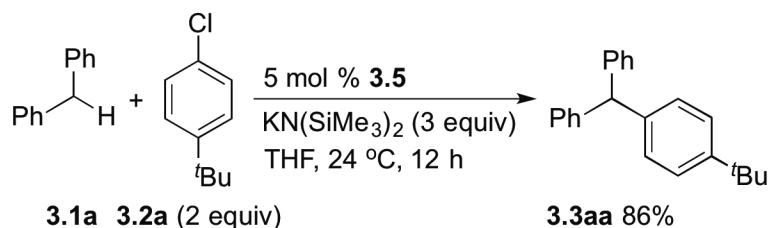


Yield determined by ¹H NMR of the crude reaction mixture.

Scheme 3.8 Impact of the counteranion on the catalytic reaction

Finally, we wanted to determine if the oxidative addition product was a competent intermediate in the catalytic reaction. As mentioned in Scheme 3.4, isolation of (Li-NiXantphos)Pd(Ph)(Cl) from the byproducts of its synthesis was challenging.

Instead, we synthesized a neutral oxidative addition species, (NiXantphos)Pd(4-C₆H₄CN)(Br) (**3.5**) in 88% yield, following the procedure for the preparation of (Xantphos)Pd(4-C₆H₄CN)(Br).^{25a} Subjecting 5 mol % **3.5** to the catalytic reaction resulted in 86% isolated yield of the DCCP product **3.3aa** (Scheme 3.9), suggesting that the oxidative addition species as a competent intermediate.



Scheme 3.9 DCCP catalyzed by **3.5**

3.3 Conclusions

Based on a large number of studies, it was widely accepted that palladium complexes based on *bidentate triarylphosphines* would not oxidatively add unactivated aryl chlorides at room temperature and could not, therefore, catalyze coupling processes with aryl chloride substrates. In this report we have disclosed an exception to this paradigm by demonstrating that under basic reaction conditions the heterobimetallic Pd(M-NiXantphos)-based catalyst system readily activates aryl chlorides at room temperature and successfully promotes the arylation of diphenylmethane derivatives.

The advantages of the Pd-NiXantphos catalyst system are: (1) mild conditions (room temperature) for cross-coupling reactions with unactivated aryl chlorides, (2) greater air- and oxidative-stability of NiXantphos relative to alkylphosphines (many of which are of high sensitivity and/or pyrophoric), (3) superior catalytic performance to all the other mono- and bidentate ligands examined in this report, and (4) commercial availability of palladium source and ligand.

A dramatic difference in the catalytic performance was observed between NiXantphos (91% AY) and its structurally similar analogues *N*-Bn-NiXantphos (1% AY) and Xantphos (0% AY), supporting our hypothesis that the oxidative addition is facilitated with NiXantphos because the heterobimetallic Pd–ligand catalyst system exhibits greatly enhanced reactivity due to the presence of the main group metal. The DCCP with aryl chlorides affords a variety of triarylmethane products, a class of compounds with applications and biological activity. Additionally, the DCCP exhibits remarkable chemoselectivity in the presence of aryl chloride substrates bearing heteroaryl groups and sensitive functional groups that are known to undergo 1,2-addition, aldol reaction, O-, N-, enolate- α -, and C(sp²)-H arylation reactions.

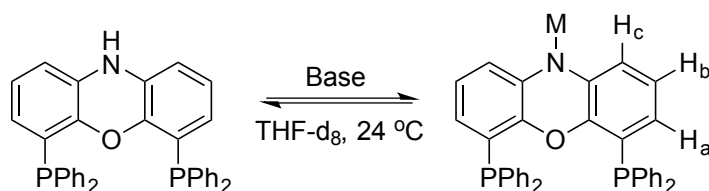
The advantages and importance of the Pd–NiXantphos catalyst system outlined herein make it a valuable contribution to applications in Pd-catalyzed arylation reactions with aryl chlorides under mild conditions. Future work will focus on structural modification of NiXantphos to increase its reactivity and efficiency in catalytic processes.

3.4 Experimental Section

General Methods. All reactions were performed under nitrogen using oven-dried glassware and standard Schlenk or vacuum line techniques. Air- and moisture-sensitive solutions were handled under nitrogen and transferred via syringe. Anhydrous CPME, dioxane, and 2-MeTHF were purchased from Sigma-Aldrich and used as solvent without further purification. Unless otherwise stated, reagents were commercially available and used as purchased without further purification. Chemicals were obtained from Sigma-Aldrich, Acros, TCI America or Alfa Aesar, and solvents were purchased from Fisher Scientific. The progress of the reactions was monitored by thin-layer chromatography using Whatman Partisil K6F 250 μ m precoated 60 Å silica gel plates and visualized by

short-wavelength ultraviolet light as well as by treatment with ceric ammonium molybdate (CAM) stain or iodine. Silica gel (230–400 mesh, Silicycle) was used for flash chromatography. The ^1H NMR and $^{13}\text{C}\{^1\text{H}\}$ NMR spectra were obtained using a Brüker AM-500 Fourier-transform NMR spectrometer at 500 and 125 MHz, respectively. Chemical shifts are reported in units of parts per million (ppm) downfield from tetramethylsilane (TMS), and all coupling constants are reported in hertz. The $^{31}\text{P}\{^1\text{H}\}$ NMR spectra were obtained using a Brüker DMX-360 NMR spectrometer at 145.8 MHz, with chemical shifts reported with respect to calibration with an external standard of phosphoric acid (0 ppm). The infrared spectra were obtained with KBr plates using a Perkin-Elmer Spectrum 100 Series FTIR spectrometer. High-resolution mass spectrometry (HRMS) data were obtained on a Waters LC–TOF mass spectrometer (model LCT-XE Premier) using chemical ionization (CI) or electrospray ionization (ESI) in positive or negative mode, depending on the analyte. Melting points were determined on a Unimelt Thomas–Hoover melting point apparatus and are uncorrected.

^1H and $^{31}\text{P}\{^1\text{H}\}$ NMR Studies of NiXantphos Deprotonated by Base.



The experiments were set up inside a glovebox under a nitrogen atmosphere. NiXantphos (21.4 mg, 0.039 mmol, 1 equiv) and $\text{LiN}(\text{SiMe}_3)_2$ (9.8 mg, 0.059 mmol, 1.5 equiv) or $\text{KN}(\text{SiMe}_3)_2$ (1.5 equiv, 3 equiv, 6 equiv) were weighed in a vial, dissolved in THF- d_8 (0.75 mL) and transferred to a J. Young NMR tube. The solution became yellow immediately. The ^1H and $^{31}\text{P}\{^1\text{H}\}$ NMR spectra were recorded at room temperature.

NiXantphos without base: ^1H NMR (360 MHz, THF- d_8): δ 7.30 – 7.11 (m, 20H), 6.52 (t, J = 7.2 Hz, 2H), 6.32 (dd, J = 7.7, 1.3 Hz, 2H), 5.91 (m, 2H) ppm; $^{31}\text{P}\{^1\text{H}\}$ NMR (145.8 MHz, THF- d_8): δ –18.99 ppm.

NiXantphos with 1.5 equiv $\text{LiN}(\text{SiMe}_3)_2$: ^1H NMR (360 MHz, THF- d_8): δ 7.28 – 7.04 (m, 20H), 6.07 (t, J = 7.6 Hz, 2H), 5.75 (d, J = 7.6 Hz, 2H), 5.22 (d, J = 7.9 Hz, 2H) ppm; $^{31}\text{P}\{^1\text{H}\}$ NMR (145.8 MHz, THF- d_8): δ –18.45 ppm.

NiXantphos with 1.5 equiv $\text{KN}(\text{SiMe}_3)_2$: ^1H NMR (360 MHz, THF- d_8): δ 7.28 – 7.04 (m, 20H), 6.06 (t, J = 7.6 Hz, 2H), 5.73 (d, J = 7.6 Hz, 2H), 5.16 (d, J = 7.2 Hz, 2H) ppm; $^{31}\text{P}\{^1\text{H}\}$ NMR (145.8 MHz, THF- d_8): δ –18.69 ppm.

NiXantphos with 3 equiv $\text{KN}(\text{SiMe}_3)_2$: ^1H NMR (360 MHz, THF- d_8): δ 7.27 – 7.03 (m, 20H), 6.03 (t, J = 7.7 Hz, 2H), 5.70 (dd, J = 7.6, 1.4 Hz, 2H), 5.14 (m, 2H) ppm; $^{31}\text{P}\{^1\text{H}\}$ NMR (145.8 MHz, THF- d_8): δ –18.69 ppm.

NiXantphos with 6 equiv $\text{KN}(\text{SiMe}_3)_2$: ^1H NMR (360 MHz, THF- d_8): δ 7.27 – 7.03 (m, 20H), 6.04 (t, J = 7.6 Hz, 2H), 5.70 (dd, J = 7.6, 1.4 Hz, 2H), 5.15 (m, 2H) ppm; $^{31}\text{P}\{^1\text{H}\}$ NMR (145.8 MHz, THF- d_8): δ –18.68 ppm.

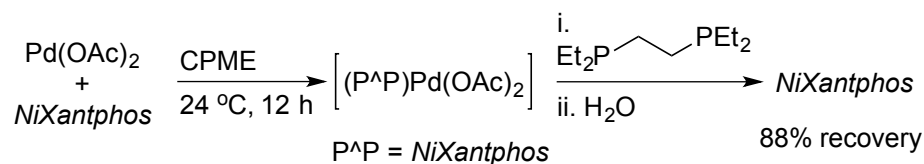
Procedure and Characterization for K-NiXantphos.

The experiments were set up inside a glovebox under a nitrogen atmosphere. To a 20 mL vial containing NiXantphos (110 mg, 0.2 mmol, 1 equiv) dissolved in 10 mL of Et_2O , a solution of $\text{KN}(\text{SiMe}_3)_2$ (40 mg, 0.2 mmol, 1 equiv) in 2 mL of Et_2O was added slowly resulting in rapid precipitation of a yellow solid. After stirring for 2 h, the slurry was filtered through fritted filter and the solid was washed with 3 \times 5 mL Et_2O . Drying under reduced pressure yielded K-NiXantphos as a yellow powder (107 mg, 91% yield). ^1H NMR (500 MHz, THF- d_8): δ 7.23 – 7.04 (m, 20H), 6.03 (t, J = 7.5 Hz, 2H), 5.70 (d, J = 7.5 Hz, 2H), 5.14 (d, J = 7.0 Hz, 2H) ppm; $^{13}\text{C}\{^1\text{H}\}$ NMR (125 MHz, THF- d_8): δ 150.7,

148.2, 140.2, 134.8, 128.4, 128.1, 124.5, 121.0, 118.0, 114.7 ppm; $^{31}\text{P}\{^1\text{H}\}$ NMR (145.8 MHz, THF- d_8): δ -18.63 ppm; IR (thin film): 1566, 1454, 1434, 1405, 742, 695 cm^{-1} . X-ray diffraction-quality single-crystals of $[\text{K}(\text{THF})_3\text{-NiXantphos}]_2$ were obtained by layering a concentrated THF solution of K-NiXantphos with hexanes at -21 °C. X-ray diffraction-quality single-crystals of the reddish-orange crown ether adduct, $\text{K}(\text{THF})(18\text{-crown-6})\text{-NiXantphos}$, were obtained by vapor diffusion of pentane into a concentrated THF solution of K-NiXantphos and 18-crown-6 (1:1) at -21 °C.

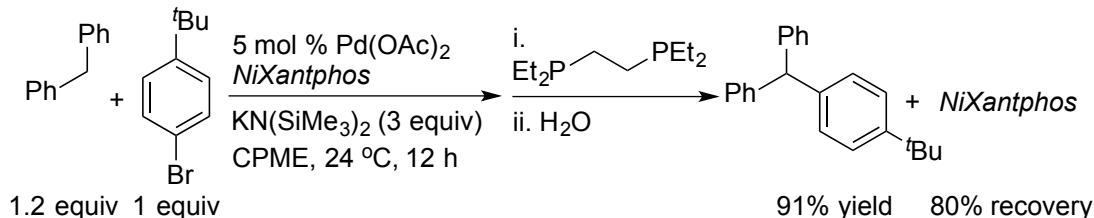
Ligand Exchange and Recovery of NiXantphos.

A. Ligand exchange and recovery process (control)



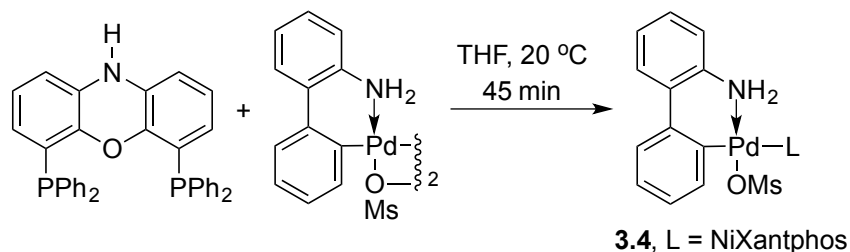
The experiments were set up inside a glovebox under a nitrogen atmosphere. A 20 mL reaction vial equipped with a stir bar was charged with $\text{Pd}(\text{OAc})_2$ (21.0 mg, 0.094 mmol) and NiXantphos (90.4 mg, 0.164 mmol) followed by 19 mL of dry CPME. The reaction mixture was stirred for 12 h at 24 °C, resulting in coordination of NiXantphos to palladium, as judged by a singlet at 3.4 ppm in $^{31}\text{P}\{^1\text{H}\}$ NMR spectrum. 1,2-bis(diethylphosphino)ethane (depe, 180 μL , 0.771 mmol, depe:NiXantphos = 5:1) was added into the reaction mixture. The reaction mixture was stirred for another 40 min at 24 °C. The reaction was quenched with H_2O , diluted with ethyl acetate, and filtered over a pad of silica. The pad was rinsed with additional ethyl acetate, and the solution was concentrated in vacuo. The crude material was loaded onto a silica gel column and purified by flash chromatography to afford NiXantphos (80 mg, 88% recovery).

B. Cross-coupling followed by ligand exchange and recovery process



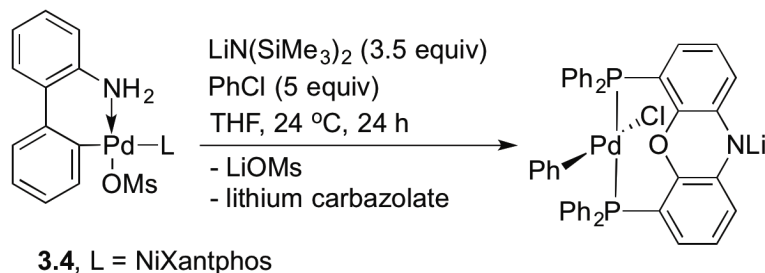
The experiments were set up inside a glovebox under a nitrogen atmosphere. An 8 mL reaction vial equipped with a stir bar was charged with KN(SiMe₃)₂ (329 mg, 1.65 mmol, 3 equiv). A solution of Pd(OAc)₂ (6.2 mg, 0.028 mmol, 5 mol %) and NiXantphos (30.0 mg, 0.054 mmol, 10 mol %) in 6 mL of dry CPME was taken up by syringe and added to the reaction vial. After stirring for 5 min at 24 °C, diphenylmethane (110 μL, 0.66 mmol, 1.2 equiv) was added to the reaction mixture followed by 1-bromo-4-*tert*-butylbenzene (95 μL, 0.55 mmol, 1 equiv). The reaction mixture was stirred for 12 h at 24 °C, before 1,2-bis(diethylphosphino)ethane (depe, 103 μL, 0.44 mmol, depe:NiXantphos = 8:1) was added into the reaction mixture. The reaction mixture was stirred for another 40 min at 24 °C. The reaction was quenched with H₂O, diluted with ethyl acetate, and filtered over a pad of silica. The pad was rinsed with additional ethyl acetate, and the solution was concentrated in vacuo. The crude material was loaded onto a silica gel column and purified by flash chromatography to afford the triarylmethane product **3.3aa** (91% yield) and NiXantphos (24 mg, 80% recovery).

Procedure and Characterization for the Methanesulfonate Precatalyst **3.4**.



To a 50 mL flask under a nitrogen atmosphere was added degassed anhydrous THF (10.4 mL) followed by μ -mesylate dimer (2.00 g, 2.84 mmol) and NiXantphos (1.04 g, 1.41 mmol). The reaction was aged for 45 minutes after which time the slurry was treated with MTBE (10 mL) and aged for an additional 30 minutes. The slurry was collected by filtration and the product washed with MTBE (2 \times 5 mL). The product was dried for 13 hours by pulling N₂ through the cake (1.1 g, 85%). Note: The peaks in the NMR spectra appear broad due to the fluxional nature of the complex. ¹H NMR (400 MHz, CD₂Cl₂): δ 8.99 (1H, br. s), 7.45 – 7.39 (2H, br. m), 7.27 – 7.14 (19H, m), 7.00 – 6.94 (6H, br. m), 6.81 – 6.67 (3H, br. m), 6.44 (2H, br. s), 6.25 – 6.22 (1H, br. m), 4.48 (2H, br. s), 2.64 (3H, s); ³¹P NMR (162.0 MHz, CDCl₃): δ 14.27 (br. s), 3.70 (br. s).

Procedure and Characterization for Oxidative Addition of Chlorobenzene to (M-NiXantphos)Pd(0).



The experiments were set up inside a glovebox under a nitrogen atmosphere. Complex **3.4** (9.2 mg, 0.01 mmol, 1 equiv) was added to a J. Young NMR tube followed by chlorobenzene (5.1 μ L, 0.05 mmol, 5 equiv). LiN(SiMe₃)₂ (5.9 mg, 0.035 mmol, 3.5 equiv) was weighed in a vial, dissolved in THF (500 μ L) and transferred to the NMR tube. The solution became reddish-orange immediately. The progress of the reaction was monitored by ³¹P{¹H} NMR spectroscopy. The room temperature oxidative addition of chlorobenzene reached about 75% conversion in 6 h and near completion in 24 h, as

judged by a singlet at 2.6 ppm in $^{31}\text{P}\{^1\text{H}\}$ NMR spectrum for the oxidative addition product, (Li-NiXantphos)Pd(Ph)(Cl) (a singlet at 2.8 ppm for (K-NiXantphos)Pd(Ph)(Cl) from using $\text{KN}(\text{SiMe}_3)_2$ as base in place of $\text{LiN}(\text{SiMe}_3)_2$). The oxidative addition product was generated along with byproducts lithium mesylate and lithium carbazolate, rendering the isolation of the Pd-containing product challenging. Nevertheless, X-ray diffraction-quality single-crystals of the protonated (NiXantphos)Pd(Ph)(Cl) were obtained by vapor diffusion of pentane into a concentrated THF solution of the reaction mixture at $-21\text{ }^\circ\text{C}$.

Procedure and Characterization for Pd(NiXantphos)₂.

The title compound was prepared according to literature procedure.³⁶ The experiments were set up inside a glovebox under a nitrogen atmosphere. NiXantphos (197.2 mg, 0.358 mmol) and $\text{Pd}_2(\text{dba})_3$ (83.7 mg, 0.091 mmol) were weighed into a 40 mL reaction vial. Toluene (30 mL) was added, and the reaction mixture was stirred for 4 h. The solution was then filtered into another 40 mL vial to remove an insoluble greenish solid. This solution was concentrated to 20 mL and allowed to rest overnight so that any extra palladium black would settle. The resulting solution was filtered again and finally concentrated to dryness. The yellow solid was washed with toluene (5×5 mL) and hexanes (5×5 mL) to remove dibenzylideneacetone and excess NiXantphos, and dried under reduced pressure. The identity of the yellow solid was confirmed as Pd(NiXantphos)₂ by HRMS analysis, and the characteristic isotope pattern was observed. HRMS calc'd for $\text{C}_{72}\text{H}_{55}\text{N}_2\text{O}_2\text{P}_4\text{Pd}^+$ 1209.2249, observed 1209.2277 $[\text{MH}]^+$. Unfortunately, it was insoluble in common organic solvent. A similar synthetic route was reported for Pd(Xantphos)₂ by the Buchwald group, and its poor solubility was also noted.³⁶

Procedure, Characterization and Catalytic Reactivity for (NiXantphos)Pd(4-C₆H₄CN)(Br) (3.5).

Synthesis of 3.5.

The title compound was prepared according to literature procedure.³⁷ The experiments were set up inside a glovebox under a nitrogen atmosphere. A solution of Pd₂dba₃ (22.9 mg, 0.025 mmol, 0.05 mmol Pd, 1 equiv Pd), NiXantphos (27.6 mg, 0.05 mmol, 1 equiv), and 4-bromobenzonitrile (45.5 mg, 0.25 mmol, 5 equiv) in dry THF (1.5 mL) was stirred at room temperature for 12 h. The reaction was filtered through fritted filter. 10 mL of pentane was then added to the residue, and the orange resulting precipitate was allowed to form upon standing for 1 day at -21 °C. The solid was then filtered, washed with 3 × 10 mL Et₂O. Drying under reduced pressure yielded **3.5** as an orange powder (36.9 mg, 88% yield). ¹H NMR (500 MHz, CD₂Cl₂): δ 7.51 – 7.25 (m, 12H), 7.25 – 7.07 (m, 8H), 6.91 – 6.62 (m, 8H), 6.41 – 6.29 (m, 2H), 6.27 (s, 1H) ppm; ¹³C{¹H} NMR (125 MHz, CD₂Cl₂): δ 169.0, 147.0, 135.6, 135.5, 135.1, 130.8, 130.6, 128.9, 128.4, 126.2, 125.1, 122.0, 120.4, 117.2, 104.6 ppm (observed complexity due to P-C splitting); ³¹P{¹H} NMR (145.8 MHz, CD₂Cl₂): δ 7.2 ppm; IR (thin film): 3259, 3052, 2219, 1567, 1452, 1434, 1394, 1174, 1094, 811, 738, 692 cm⁻¹. The identity of the orange solid was confirmed as (NiXantphos)Pd(4-C₆H₄CN)(Br) by HRMS analysis, and the characteristic isotope pattern was observed. HRMS calc'd for C₄₃H₃₁N₂OP₂Pd⁺ 759.0946, observed 759.0946 [M-Br]⁺.

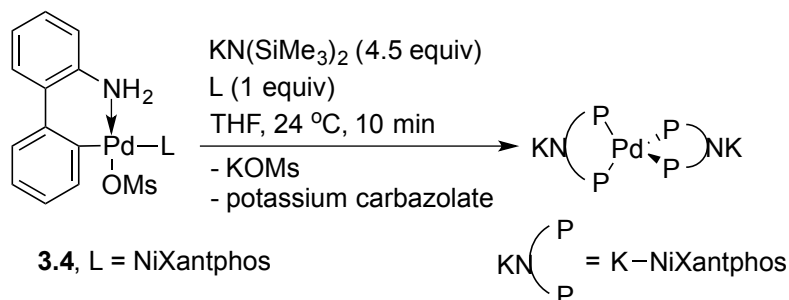
Catalytic reactivity of 3.5.

The reaction was performed following General Procedure I with **3.1a** (16.7 μL, 0.1 mmol, 1 equiv), KN(SiMe₃)₂ (59.8 mg, 0.30 mmol, 3 equiv) and **3.2a** (33.4 μL, 0.2 mmol, 2 equiv) in the presence of 5 mol % **3.5** in THF at 24 °C. The crude material was purified

by flash chromatography on silica gel (eluted with hexanes to EtOAc:hexanes = 2:98) to give the product **3aa** (25.8 mg, 86% yield) as a white solid. Also see “**3.3aa – (4-tert-Butylphenyl)diphenylmethane**” in “Procedure and Characterization for the Pd-Catalyzed DCCP of Aryl Chlorides”.

Procedure, Characterization and DOSY NMR Measurements for Pd(K-NiXantphos)₂.

Synthesis of Pd(K-NiXantphos)₂.



The experiments were set up inside a glovebox under a nitrogen atmosphere. NiXantphos (5.5 mg, 0.01 mmol, 1 equiv) and complex **3.4** (9.2 mg, 0.01 mmol, 1 equiv) were added to a J. Young NMR tube. KN(SiMe₃)₂ (9.0 mg, 0.045 mmol, 4.5 equiv) was weighed in a vial, dissolved in THF (500 μL) and transferred to the NMR tube. The solution became reddish-orange immediately. The progress of the reaction was monitored by ³¹P{¹H} NMR spectroscopy. The formation of Pd(K-NiXantphos)₂ was complete in 10 min, as judged by disappearance of **3.4** and appearance of a new singlet at -1.3 ppm in ³¹P{¹H} NMR spectrum. The reaction mixture was set undisturbed for 12 h. X-ray diffraction-quality single-crystals of Pd[K(THF)₂(NiXantphos)]₂ were obtained under these conditions. The crystalline product was then filtered and washed with 3 × 10 mL Et₂O. Drying under reduced pressure yielded the product as a yellow crystalline solid (9.9 mg, 63% isolated yield). ¹H NMR (500 MHz, THF-d₈): δ 7.03 (m, 16H), 6.84 (m, 8H),

6.67 (m, 16H), 6.06 (m, 4H), 5.76 (m, 4H), 5.48 (m, 4H) ppm; $^{31}\text{P}\{^1\text{H}\}$ NMR (145.8 MHz, THF- d_8): δ -1.3 ppm.

^1H DOSY NMR.

The NMR experiments for the determination of the self-diffusion coefficients and hydrodynamic radii were performed at 300 K on a Brüker Avance DRX 600 MHz spectrometer equipped with a 5 mm TXI probe with a z-axis gradient coil. The gradient system was calibrated with a doped water sample. Data were systematically accumulated by linearly varying the diffusion gradients from 95% to 5% for 16 gradient increment values. Data processing was accomplished with Brüker TOPSPIN 1.3 DOSY software and Brüker TOPSPIN 1.3 T1/T2 software, with representative 2D spectra processed using MestReNova v. 7.0.3. Diffusion coefficients (D_o) were obtained after fitting area data to the Stejskal-Tanner expression with the Brüker TOPSPIN 1.3 T1/T2 software and the reported D_o is an average value calculated from the different NMR responses within the same compound. Similarly, standard deviations associated with values of D_o were calculated from differences in D_o in the same sample using different NMR responses. The experiments were run in THF- d_8 (~16 mM for NiXantphos, ~2 mM for Pd[K(THF) $_2$ (NiXantphos)] $_2$) with 5.0 μL tetramethylsilane (TMS) and ~1.2 mg ferrocene (Fc) used as internal standards. The hydrodynamic radii [$r_H(\text{sample})$] of NiXantphos and Pd[K(THF) $_2$ (NiXantphos)] $_2$ were determined following equation 1:

$$r_H(\text{sample}) = \left(\frac{D_o(\text{reference})}{D_o(\text{sample})} \right) \times r_H(\text{reference}) \quad (1)$$

where $D_o(\text{reference})$ was the diffusion coefficient for the corresponding internal standard, $D_o(\text{sample})$ was the diffusion coefficient of the sample, and $r_H(\text{reference})$ was the hydrodynamic radii of the internal references. Equation 1 was used to minimize errors

between samples due to variations in viscosity and temperature, and is derived from the Stokes–Einstein equation 2:^{38,39}

$$D_o = \frac{kT}{6r_H\pi\eta} \quad (2)$$

where D_o is the diffusion coefficient, k is the Boltzmann constant, T is temperature, r_H is the hydrodynamic radius, and η is the viscosity of the solution. The theoretical hydrodynamic radii ($r_{H(\text{theo})}$) were determined from their reported crystal structures, taking the centroid of the molecule and measuring the distance to the furthest point in the molecule.

Table 3.6 Collected diffusion data from ^1H DOSY NMR experiments for NiXantphos and $\text{Pd}[\text{K}(\text{THF})_2(\text{NiXantphos})]_2$

Compound	D_o ($\times 10^{-6} \text{ cm}^2 \text{ s}^{-1}$)			$r_{H(\text{theo})}$			% Error	
				$r_{H(\text{exp})}$	$r_{H(\text{exp})}$	$r_{H(\text{avg})}$		
	TMS	Fc	Sample ^a	(Å) ^b	(Å) ^c	(Å) ^d		
				Monomer				
				(Å) ^e				
NiXantphos	21.35	17.47	7.856(9)	6.43(8)	6.20(8)	6.32(11)	7.3295(5)	13.8
$\text{Pd}[\text{K}(\text{THF})_2(\text{NiXantphos})]_2$	21.83	17.88	6.467(54)	7.98(66)	7.71(64)	7.85(101)	8.5945(2)	8.7

a – Average of observable ^1H peaks corresponding to the compound. *b* – Based on $r_{H(\text{theo})}$ for TMS. *c* – Based on $r_{H(\text{theo})}$ for Fc. *d* – Average of $r_{H(\text{theo})}$ for both TMS and Fc. *e* – $r_{H(\text{theo})}$ determined from crystal structures; see Figure 3.6a–d. *f* – Standard deviation in parenthesis.

Table 3.7 Acquisition parameters for 2D- ^1H DOSY

Compound	D20 (ms)	P30 (μ s)	NS	D20 (ms)	P30 (μ s)	NS
	Fc, TMS			Sample		
NiXantphos	60	1000	8	120	1000	8
Pd[K(THF) ₂ (NiXantphos)] ₂	60	1000	8	140	1000	64

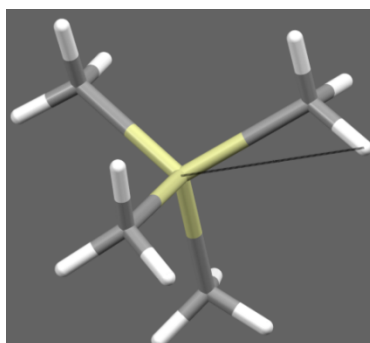


Figure 3.6a Points used for determination of $r_{\text{H(theo)}}$ (2.376(6) Å) from the crystal structure of TMS (CSD ref = TIVWOL)

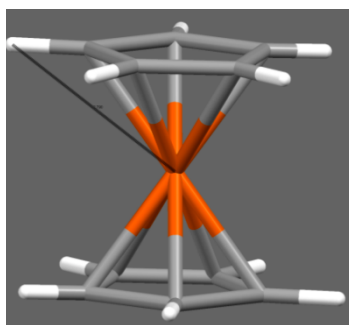


Figure 3.6b Points used for determination of $r_{\text{H(theo)}}$ (2.790(2) Å) from the crystal structure of Fc (CSD ref = FEROCF)

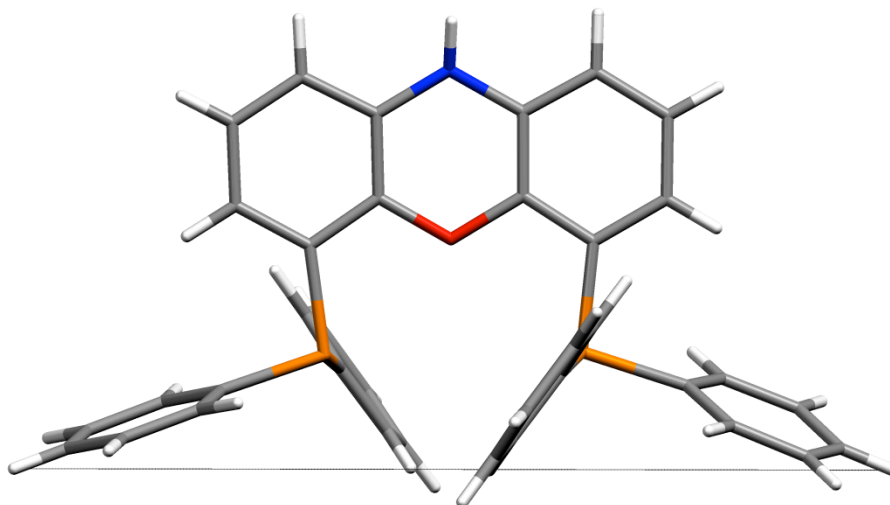


Figure 3.6c Points used for determination of $r_{\text{H}(\text{theo})}$ (7.3295(4) Å) taken from the crystal structure of NiXantphos (CSD ref = KIXFAZ)

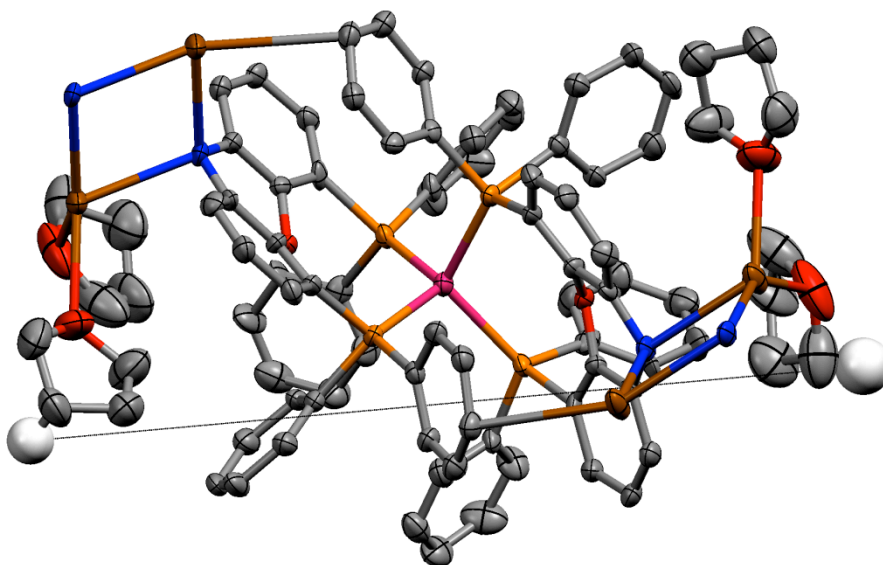


Figure 3.6d Points used for determination of $r_{\text{H}(\text{theo})}$ (8.5945(2) Å) from the crystal structure of Pd[K(THF)₂(NiXantphos)]₂

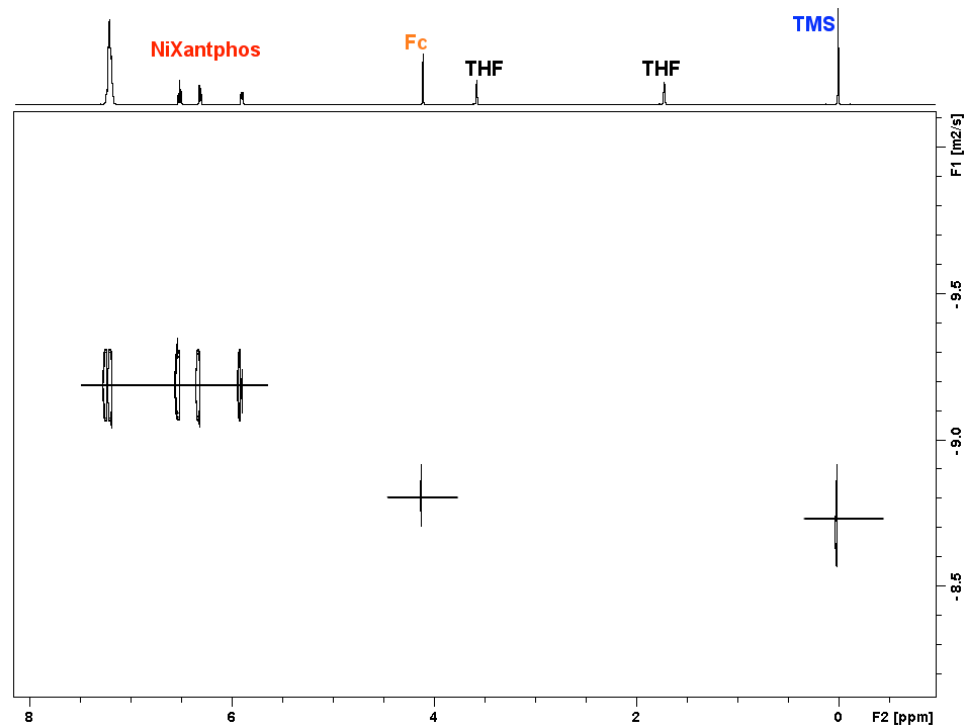


Figure 3.7a 2D-¹H DOSY NMR spectrum of NiXantphos and internal references at 300

K in THF-d₈

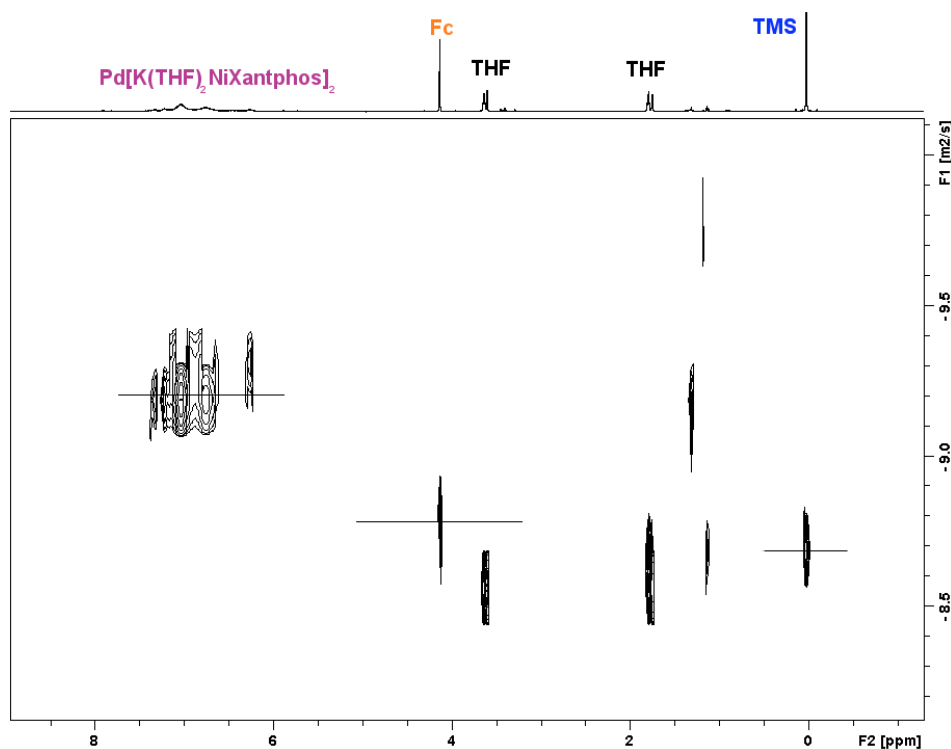


Figure 3.7b 2D-¹H DOSY NMR spectrum of Pd[K(THF)₂(NiXantphos)]₂ and internal references at 300 K in THF-d₈

Identification of the Catalyst Resting State.

The experiments were set up inside a glovebox under a nitrogen atmosphere. An oven-dried 20 mL vial equipped with a stir bar was charged with complex **3.4** (9.2 mg, 0.01 mmol, 10 mol %) and KN(SiMe₃)₂ (59.8 mg, 0.30 mmol, 3 equiv). 0.5 mL of dry THF was taken up by syringe and added to the reaction vial, followed by diphenylmethane (**3.1a**, 16.7 μL, 0.1 mmol, 1 equiv) and chlorobenzene (**3.2b**, 20.4 μL, 0.2 mmol, 2 equiv). After stirring for 5 min at 24 °C, the orange reaction mixture was transferred to a J. Young NMR tube. The reaction mixture was monitored by ³¹P{¹H} NMR spectroscopy for 12 h at 24 °C. The only species observed by ³¹P{¹H} NMR spectroscopy for the DCCP reaction was Pd(K-NiXantphos)₂ throughout the reaction time (12 h), as judged by a

singlet at -1.3 ppm in $^{31}\text{P}\{^1\text{H}\}$ NMR spectrum. Using 10 mol % $\text{Pd}(\text{OAc})_2$ and 20 mol % NiXantphos as the precatalyst system gave the same dominant catalyst resting state within 10 minutes after addition of **3.1a**, **3.2b** and $\text{KN}(\text{SiMe}_3)_2$ at room temperature.

Counteraction Effects.

To compare the catalytic reactivity using different counteractions (Li, Na vs K), we carried out our DCCP reactions under standard conditions with 2-benzylpyridine (**3.1g**) and 1-*tert*-butyl-4-chlorobenzene (**3.2a**) using the following 3 bases: $\text{LiN}(\text{SiMe}_3)_2$, $\text{NaN}(\text{SiMe}_3)_2$ and $\text{KN}(\text{SiMe}_3)_2$. The reaction was performed following General Procedure I with **3.1g** (16.1 μL , 0.1 mmol, 1 equiv), $\text{MN}(\text{SiMe}_3)_2$ (M = Li, Na, K) (0.30 mmol, 3 equiv) and **3.2a** (33.4 μL , 0.2 mmol, 2 equiv) in the presence of 5 mol % Pd catalyst in THF at 24 °C. The assay yields were recorded at 2 h (average of two runs).

Base	Assay yield (%)
$\text{LiN}(\text{SiMe}_3)_2$	13.3
$\text{NaN}(\text{SiMe}_3)_2$	35.1
$\text{KN}(\text{SiMe}_3)_2$	34.2

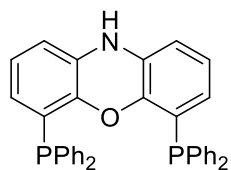
Details on DFT Calculations.

A. Computational Details.

Gaussian '09 Rev. A.02 was used for all electronic structure calculations with B3LYP hybrid DFT method.^{40a} The 6-31 G* basis set was employed for all atoms. The geometry optimizations were performed on gas phase structures. Frequency calculations, performed on each optimized structure, found no imaginary frequencies to confirm that the optimized structures were minima. Bonding analyses were performed using NBO 3.1.^{40b}

		Natural Charge				Natural Charge	
		P	O			P	
1		0.925 0.926	-0.501	6		0.842 0.848	
2		0.923 0.923	-0.517	7		0.843 0.949	
3		0.922 0.924	-0.499	8		0.838 0.878	
4		0.930 0.930	-0.503				
5		0.918 0.926	-0.514				

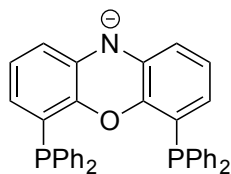
B. Cartesian coordinates for phosphine ligand optimized geometries.



C	-1.27425500	3.41391300	-0.14815900
C	-2.50554100	4.05808600	-0.27045700
H	-2.53181100	5.13810100	-0.39695800
C	-3.68764700	3.31757100	-0.21744700
H	-4.64331700	3.82643000	-0.30621200
C	-3.64638200	1.93579800	-0.05802700
H	-4.57008400	1.36987300	-0.01961500
C	-2.41727700	1.25801500	0.05477700
C	-1.24484700	2.01936600	0.01882800
C	1.13526900	2.02082300	-0.16757600
C	2.30262900	1.26065100	-0.28606400
C	3.49600000	1.93328000	-0.61232100
H	4.41570600	1.36763200	-0.70932000
C	3.50588500	3.31028800	-0.81348000
H	4.43341300	3.81561800	-1.06740400
C	2.33072000	4.05285200	-0.68353800
H	2.33560900	5.13057000	-0.83049100
C	1.13682200	3.41303100	-0.34991500
C	-4.03365200	-1.05847100	0.59715400
C	-4.48474700	-1.07678900	1.92799800
H	-3.80147800	-0.79902000	2.72752000
C	-5.79173900	-1.45311100	2.23739300

H	-6.12277600	-1.45654800	3.27281500
C	-6.66680400	-1.83894900	1.21983200
H	-7.68252000	-2.14332400	1.45888200
C	-6.22757100	-1.84026000	-0.10517500
H	-6.90203100	-2.14428700	-0.90192000
C	-4.92287600	-1.45045900	-0.41534800
H	-4.59412800	-1.45583800	-1.45022200
C	-1.94272100	-1.19246700	-1.39128000
C	-2.16134200	-0.44880500	-2.56059200
H	-2.54693000	0.56414100	-2.49202700
C	-1.88469000	-0.99706300	-3.81496900
H	-2.05743000	-0.40549900	-4.71076100
C	-1.39149800	-2.29840800	-3.92070600
H	-1.17697900	-2.72358300	-4.89781200
C	-1.16849200	-3.04856400	-2.76440100
H	-0.77700000	-4.06002900	-2.83660500
C	-1.43356400	-2.49571400	-1.51177800
H	-1.23799800	-3.07913300	-0.61525200
C	3.88559400	-1.13242300	-0.49276800
C	4.12081100	-1.51744900	-1.82362700
H	3.30907400	-1.46676000	-2.54590600
C	5.37691600	-1.97034700	-2.22803500
H	5.54007700	-2.25978000	-3.26308800
C	6.41662500	-2.06539500	-1.30096800
H	7.39338500	-2.42801900	-1.61073900

C	6.19281400	-1.70109600	0.02802700
H	6.99650500	-1.77803500	0.75623000
C	4.93885200	-1.23574400	0.42906600
H	4.77780700	-0.95609500	1.46587000
C	2.12283900	-0.75693800	1.76569000
C	1.64066900	-1.97242700	2.27693200
H	1.30284200	-2.74505600	1.59058100
C	1.58034300	-2.19703100	3.65225500
H	1.20445800	-3.14480400	4.02908500
C	1.98766400	-1.20083800	4.54146100
H	1.93289400	-1.37013400	5.61377000
C	2.45789600	0.01686200	4.04693400
H	2.77231600	0.79887700	4.73375000
C	2.52775900	0.23669600	2.66978800
H	2.89616700	1.18779100	2.29647400
N	-0.06125900	4.11132000	-0.16175400
H	-0.08904500	5.06556600	-0.49363200
O	-0.03445500	1.36186100	0.17934100
P	-2.26169100	-0.57455400	0.32757100
P	2.16202300	-0.57969100	-0.07933700

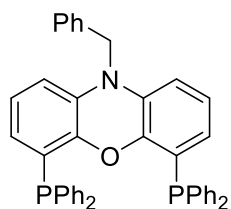


P	-2.23926600	-0.54277200	-0.13291600
---	-------------	-------------	-------------

P	2.23936900	-0.54280000	0.13332800
O	0.00008800	1.32479700	0.00000900
N	0.00013700	4.18297200	-0.00061600
C	-2.37606800	1.29736800	-0.08604200
C	-3.61257500	1.99393300	-0.10240000
H	-4.54513600	1.44181400	-0.14053400
C	-3.60932000	3.38539300	-0.08645600
H	-4.55596800	3.92441400	-0.10130500
C	-2.41363900	4.10425400	-0.05205800
H	-2.40992300	5.19126500	-0.04092300
C	-1.15379400	3.46108000	-0.02954000
C	-1.19373900	2.03392700	-0.04284800
C	2.37625700	1.29731700	0.08569700
C	3.61277500	1.99384400	0.10171900
H	4.54532400	1.44170800	0.13996200
C	3.60957500	3.38530000	0.08528200
H	4.55624400	3.92428800	0.09988300
C	2.41391300	4.10418500	0.05070200
H	2.41022100	5.19118900	0.03918000
C	1.15405400	3.46103500	0.02850300
C	1.19393400	2.03389900	0.04235500
C	-3.92521800	-1.03089600	-0.75058100
C	-4.19793300	-0.80359100	-2.11263800
H	-3.45672800	-0.29673100	-2.72636400
C	-5.40098700	-1.20997100	-2.68586800

H	-5.58951800	-1.01374900	-3.73917300
C	-6.35921700	-1.87334400	-1.91371800
H	-7.29601200	-2.19816700	-2.36092800
C	-6.10013900	-2.11536100	-0.56509700
H	-6.83871600	-2.62786300	0.04816800
C	-4.89782400	-1.69493000	0.01153300
H	-4.71879700	-1.88239500	1.06578900
C	-2.34865900	-1.01613700	1.66249500
C	-2.81407500	-0.15765500	2.67017800
H	-3.14732000	0.84128000	2.40402000
C	-2.84387200	-0.57353100	4.00277700
H	-3.20303700	0.10769600	4.77119900
C	-2.41259100	-1.85518900	4.35154600
H	-2.43277100	-2.17567800	5.39090000
C	-1.94264500	-2.71795600	3.35958900
H	-1.59154400	-3.71341900	3.62250500
C	-1.90396500	-2.29639300	2.02948000
H	-1.51215700	-2.96302300	1.26458900
C	2.34832600	-1.01686200	-1.66192300
C	2.81338100	-0.15872400	-2.67006800
H	3.14659600	0.84034600	-2.40439800
C	2.84285500	-0.57511200	-4.00251500
H	3.20174500	0.10585500	-4.77129600
C	2.41160500	-1.85694600	-4.35067200
H	2.43153100	-2.17783200	-5.38990800

C	1.94201800	-2.71937500	-3.35825100
H	1.59094200	-3.71497300	-3.62068300
C	1.90366100	-2.29730200	-2.02829500
H	1.51213800	-2.96368000	-1.26304300
C	3.92544800	-1.03075400	0.75077300
C	4.89808100	-1.69463200	-0.01143500
H	4.71895100	-1.88216800	-1.06566300
C	6.10053900	-2.11483000	0.56506900
H	6.83913600	-2.62722100	-0.04826500
C	6.35973100	-1.87272200	1.91365100
H	7.29663900	-2.19736000	2.36075700
C	5.40147000	-1.20950500	2.68589800
H	5.59008700	-1.01323200	3.73917900
C	4.19827400	-0.80336800	2.11279600
H	3.45703000	-0.29665300	2.72659500

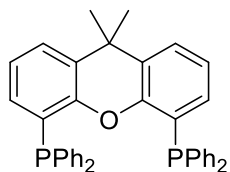


C	-2.56140700	0.50684400	-0.72027700
C	-3.53812500	1.50780800	-0.75528400
H	-4.58387600	1.23964600	-0.85537900
C	-3.17183900	2.85091200	-0.64050400
H	-3.94098300	3.61708100	-0.68146000

C	-1.84142300	3.20905400	-0.45678300
H	-1.56976200	4.25451800	-0.36322700
C	-0.83815600	2.22480900	-0.38352600
C	-1.21973400	0.88773600	-0.53349500
C	-0.56426400	-1.39444400	-0.33860300
C	0.46519900	-2.28922000	-0.03184900
C	0.13304800	-3.64782700	0.12651400
H	0.91313200	-4.36324100	0.36106800
C	-1.18331500	-4.07350000	-0.00705900
H	-1.43262700	-5.12200800	0.12983800
C	-2.19862200	-3.16412100	-0.31436900
H	-3.22526300	-3.50498900	-0.38927600
C	-1.89695900	-1.81147400	-0.50543900
C	0.99454200	4.44035600	-0.37678600
C	1.18474300	4.92205700	-1.68363400
H	1.28983800	4.21510300	-2.50373600
C	1.24701800	6.29108700	-1.94210100
H	1.38926500	6.64311200	-2.96072100
C	1.14179400	7.20584600	-0.89204600
H	1.20095500	8.27316200	-1.08900300
C	0.96906100	6.74149800	0.41266300
H	0.89153800	7.44741400	1.23596600
C	0.89266800	5.37047100	0.66885500
H	0.75625000	5.02396900	1.68868000
C	1.17561700	2.39183400	1.66227200

C	0.12759200	2.47488800	2.59222200
H	-0.88449100	2.66727000	2.24820600
C	0.37182000	2.30932900	3.95686000
H	-0.45182400	2.37508100	4.66360900
C	1.66761000	2.06135000	4.41375400
H	1.85625700	1.93203700	5.47644600
C	2.71812500	1.97216500	3.49888900
H	3.72825600	1.76947100	3.84537100
C	2.47113500	2.12851900	2.13461200
H	3.28938300	2.03423900	1.42529700
C	3.10728900	-3.09519700	0.77012900
C	3.18541000	-3.28718800	2.16029800
H	2.69476200	-2.58029400	2.82576300
C	3.88814400	-4.36588800	2.69722000
H	3.93275700	-4.49967000	3.77511000
C	4.54491600	-5.26213100	1.85135500
H	5.10264400	-6.09730400	2.26718500
C	4.48896000	-5.07466500	0.46932900
H	5.00253600	-5.76544300	-0.19490100
C	3.77368700	-4.00216700	-0.06791800
H	3.73825600	-3.86802400	-1.14472800
C	2.75136100	-1.42468500	-1.56362100
C	3.82293600	-0.54845400	-1.79786400
H	4.25852000	-0.00177900	-0.96517100
C	4.32739400	-0.36187700	-3.08507400

H	5.15804600	0.32040800	-3.24637000
C	3.75619300	-1.03868400	-4.16412000
H	4.14172800	-0.88821300	-5.16923600
C	2.68195500	-1.90351300	-3.94734800
H	2.22951600	-2.43035600	-4.78397500
C	2.18439000	-2.09692800	-2.65718800
H	1.34863400	-2.77276800	-2.50052600
N	-2.86498200	-0.85813500	-0.86981700
O	-0.21926800	-0.06777400	-0.51992900
P	0.97236800	2.59510800	-0.17041800
P	2.17520700	-1.59763300	0.19051000
C	-4.12676900	-1.27518900	-1.45530900
H	-4.41682600	-0.51627500	-2.19248000
H	-3.93729600	-2.19211800	-2.02714800
C	-5.28496100	-1.51127600	-0.48962300
C	-6.53185600	-1.88771500	-1.00881500
C	-5.14511600	-1.36918700	0.89345500
C	-7.61509700	-2.11850000	-0.16305200
H	-6.65454500	-2.00104200	-2.08472300
C	-6.23047500	-1.60009600	1.74313600
H	-4.18407700	-1.07721900	1.30567400
C	-7.46696300	-1.97507800	1.21929900
H	-8.57496100	-2.40979000	-0.58162200
H	-6.10513900	-1.48569700	2.81664900
H	-8.31036500	-2.15461800	1.88052200

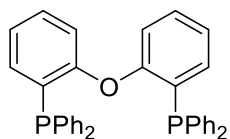


P	2.10153500	-0.68647600	-0.76772300
C	-0.00000200	3.91240000	0.89480400
C	-0.00002100	5.43215500	0.65341700
C	-0.00000500	3.65729600	2.43039400
C	2.30559300	1.12017500	-0.38867700
C	1.18546400	1.86121000	0.03162400
C	1.23843200	3.23598200	0.29905400
C	2.45561100	3.89160100	0.08347600
C	3.57980300	3.19337700	-0.35180200
C	3.50679500	1.81908200	-0.57093300
C	2.24701900	-1.46030600	0.91172300
C	2.64243200	-0.78034200	2.07288500
C	2.72306100	-1.44821400	3.29699400
C	2.41846500	-2.80740700	3.37809500
C	2.02308200	-3.49568900	2.22923400
C	1.92906900	-2.82501700	1.01053000
C	3.75338200	-1.10033500	-1.51021900
C	4.88811700	-1.48481500	-0.77879900
C	6.07778800	-1.81455800	-1.43110300
C	6.15498000	-1.76030600	-2.82412100
C	5.03357000	-1.38085000	-3.56426500

C	3.84188700	-1.06305700	-2.91190400
O	0.00000300	1.16669000	0.19448500
H	2.53469900	4.95788300	0.26565100
H	4.51756200	3.71916400	-0.50898700
H	4.38934300	1.28098500	-0.89927200
H	2.89112100	0.27548500	2.02190000
H	3.02902100	-0.90438700	4.18740900
H	2.48326800	-3.32625600	4.33098500
H	1.77796300	-4.55330900	2.28415200
H	1.60334400	-3.36472900	0.12418700
H	4.84038400	-1.53050100	0.30508200
H	6.94613900	-2.11340400	-0.84903600
H	7.08162900	-2.01868200	-3.33013000
H	5.08275800	-1.34341800	-4.64955800
H	2.96559000	-0.78860900	-3.49493300
H	0.00000100	5.67458000	-0.41456700
H	0.87536000	5.89910200	1.11418000
H	0.00000800	2.58596900	2.65407300
H	0.89028300	4.10224000	2.89010900
C	-1.23843000	3.23597700	0.29905500
H	-0.87544500	5.89907000	1.11413400
H	-0.89030600	4.10221900	2.89010400
C	-1.18545900	1.86120600	0.03162500
C	-2.45560700	3.89159700	0.08347900
C	-2.30558800	1.12017100	-0.38867600

C	-3.57980000	3.19337300	-0.35179900
H	-2.53469300	4.95788000	0.26565700
P	-2.10153100	-0.68648000	-0.76772300
C	-3.50679100	1.81907800	-0.57093100
H	-4.51755900	3.71916000	-0.50898300
C	-2.24702100	-1.46031000	0.91172200
C	-3.75337600	-1.10033600	-1.51022400
H	-4.38933900	1.28098000	-0.89927100
C	-2.64243400	-0.78034500	2.07288400
C	-1.92907600	-2.82502200	1.01052900
C	-4.88811300	-1.48481600	-0.77880700
C	-3.84187700	-1.06305500	-2.91191000
C	-2.72306700	-1.44821800	3.29699300
H	-2.89111900	0.27548300	2.02189900
C	-2.02309400	-3.49569500	2.22923300
H	-1.60335200	-3.36473600	0.12418700
C	-6.07778200	-1.81455700	-1.43111500
H	-4.84038300	-1.53050400	0.30507300
C	-5.03355900	-1.38084600	-3.56427400
H	-2.96557800	-0.78860700	-3.49493500
C	-2.41847600	-2.80741300	3.37809300
H	-3.02902700	-0.90439000	4.18740700
H	-1.77797900	-4.55331600	2.28415000
C	-6.15497100	-1.76030300	-2.82413400
H	-6.94613500	-2.11340400	-0.84905200

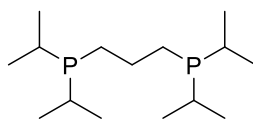
H	-5.08274400	-1.34341200	-4.64956600
H	-2.48328300	-3.32626200	4.33098300
H	-7.08161900	-2.01867600	-3.33014600



P	2.69390900	0.11811700	-0.98661200
P	-2.37012500	0.53443000	-0.37997400
O	0.09350400	-1.01046700	-0.23550900
C	2.39828300	-1.14305900	0.34240400
C	2.11491100	1.68642800	-0.18698900
C	-2.11272700	-1.16342900	-1.08751900
C	-4.12321900	0.88721400	-0.88004700
C	-0.84354900	-1.75301300	-0.93158300
C	1.08881100	-1.62930300	0.50189700
C	-2.52158000	0.16580700	1.43128600
C	4.54081800	0.30137700	-0.92519900
C	3.11028100	-2.71969900	2.06394300
H	3.90627300	-3.14309400	2.67028100
C	-0.53268100	-2.98694800	-1.50393100
H	0.45886700	-3.40680300	-1.37204000
C	3.40030800	-1.70980700	1.14565900
H	4.42177200	-1.35796200	1.04383100
C	1.92284300	1.85124700	1.19283400

H	2.11799400	1.02346000	1.86823100
C	-2.76746800	-3.10268900	-2.41788300
H	-3.52514500	-3.62543600	-2.99493300
C	-5.25905200	0.60237400	-0.10704900
H	-5.14931700	0.11044600	0.85428600
C	5.23219700	1.18437700	-0.08119600
H	4.68029800	1.80812800	0.61558100
C	-1.50212500	-3.66232600	-2.24554200
H	-1.25912100	-4.62186500	-2.69402000
C	0.78120000	-2.62711800	1.42818400
H	-0.24743900	-2.95417700	1.53870100
C	-3.06215000	-1.86380500	-1.84468900
H	-4.04819200	-1.43292500	-1.98456100
C	-6.53377500	0.95267200	-0.55745100
H	-7.40183900	0.72816000	0.05748500
C	-6.69592300	1.58636300	-1.79039500
H	-7.68900700	1.85801000	-2.13882700
C	1.47567700	3.06994700	1.70797700
H	1.33216900	3.18038700	2.78007700
C	6.62457700	1.27525900	-0.13241100
H	7.14322800	1.96769800	0.52604600
C	1.21673300	4.14245300	0.85254600
H	0.86879400	5.09046700	1.25470400
C	1.79902500	-3.17638600	2.20604100
H	1.56273900	-3.95355600	2.92782100

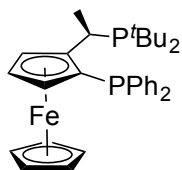
C	-2.15870600	1.18649700	2.32332600
H	-1.78960800	2.13103300	1.93169100
C	1.83828400	2.76901400	-1.03742100
H	1.95861200	2.65088600	-2.11176500
C	-2.69169800	-0.22607900	4.21311300
H	-2.75609300	-0.37857100	5.28739000
C	-2.96131100	-1.05995700	1.95681700
H	-3.23892600	-1.86571400	1.28272000
C	-2.24929000	0.99542600	3.70323900
H	-1.96541400	1.79754700	4.37981500
C	5.28278600	-0.48061400	-1.82651100
H	4.76251200	-1.15370600	-2.50436100
C	1.40069000	3.98931700	-0.52305600
H	1.19233900	4.81632500	-1.19689300
C	-3.04456700	-1.25472000	3.33681800
H	-3.38794500	-2.20949600	3.72771200
C	7.34968500	0.48184500	-1.02346900
H	8.43342500	0.55518200	-1.06254100
C	-4.30057100	1.54084000	-2.11204400
H	-3.43008700	1.79133000	-2.71434100
C	-5.57442800	1.87779700	-2.56960800
H	-5.68999400	2.37825200	-3.52763800
C	6.67496800	-0.39951600	-1.87021900
H	7.23079100	-1.01518300	-2.57281900



C	-1.33012100	0.06577600	0.49028200
H	-1.27292400	0.93703900	1.15606500
H	-1.41988100	-0.81383200	1.14291800
C	-0.03308200	-0.01000800	-0.33461300
H	0.03957100	0.88351000	-0.96552500
H	-0.07145200	-0.85880400	-1.02857200
C	1.21632100	-0.14586300	0.55161600
H	1.26803100	0.67980000	1.27539000
H	1.12651900	-1.06379600	1.14622400
P	2.83682500	-0.28740400	-0.40680300
P	-2.88193400	0.26503500	-0.56582600
C	3.86153500	-1.10210700	0.97481700
C	3.47846700	1.50447600	-0.37523100
C	-3.60188700	-1.48552300	-0.49692500
C	-4.01923000	1.20675500	0.62789700
H	3.84697000	1.71977600	0.63876600
H	3.56957700	-0.63149200	1.92556000
H	-5.00434100	1.15483800	0.14416200
H	-3.65440300	-1.81015100	0.55180300
C	5.37710500	-0.92757400	0.80093200
C	3.51724000	-2.60028500	1.03982500
C	4.63770000	1.65800500	-1.37674200
C	2.38257000	2.52786700	-0.71338600

C	-5.01866000	-1.50900200	-1.09188800
C	-2.68745500	-2.46298100	-1.25313300
C	-4.15221000	0.63831700	2.04812300
C	-3.60895100	2.68928400	0.65809400
H	-2.56407000	-2.16211000	-2.30064400
H	-1.69093800	-2.52953000	-0.80373100
H	-3.11924100	-3.47224600	-1.24508900
H	-5.72181900	-0.89513500	-0.51869300
H	-5.01856700	-1.14169300	-2.12551400
H	-5.41164800	-2.53383800	-1.10387100
H	-4.32359200	3.27478900	1.25063100
H	-2.62110100	2.82750700	1.11560500
H	-3.57161000	3.11695400	-0.34954100
H	-4.51487400	-0.39496100	2.04958500
H	-3.19397500	0.65757400	2.58030200
H	-4.86258500	1.23579200	2.63520400
H	1.57353100	2.53902900	0.02300700
H	2.81157700	3.53770100	-0.74574100
H	1.94197100	2.32965000	-1.69830900
H	5.05419600	2.67282200	-1.32757700
H	5.45419800	0.95404400	-1.19453900
H	4.28386200	1.49104300	-2.40102300
H	5.68928900	0.11783400	0.88452800
H	5.91133600	-1.49089500	1.57713600
H	5.71528400	-1.30814600	-0.17093800

H	3.82222400	-3.10944700	0.11793900
H	4.04329500	-3.07754600	1.87676100
H	2.44617500	-2.78338300	1.17916100

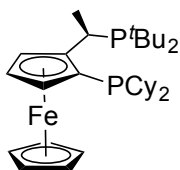


Fe	1.38840500	-2.01755900	-0.67454700
P	0.88561700	1.19760800	1.16040800
P	-2.70592400	0.33324800	0.61495300
C	-1.60930700	-0.63391000	-0.64624400
H	-1.22529200	0.21082800	-1.22685300
C	-0.42429800	-1.25512400	0.06770300
C	0.69983400	-0.58081200	0.68607900
C	1.49984700	-1.59475500	1.32219400
H	2.41506400	-1.41287200	1.86865900
C	0.89302500	-2.86345800	1.11444500
H	1.27280900	-3.81729400	1.45791500
C	-0.27500800	-2.65729900	0.32695000
H	-0.93886500	-3.43472300	-0.02680800
C	1.60362300	-1.69631600	-2.70670600
H	0.96108200	-1.09680400	-3.33848800
C	1.44249700	-3.08782700	-2.43559900
H	0.64954800	-3.72193300	-2.81035900
C	2.50206100	-3.49402600	-1.57147300

H	2.64822200	-4.48851000	-1.16988500
C	3.31786300	-2.35392100	-1.30570800
H	4.19258900	-2.32868400	-0.66912000
C	2.76601400	-1.24420900	-2.00952600
H	3.15974800	-0.23763900	-2.00509700
C	-4.06317600	1.16208400	-0.49128700
C	-5.23242600	0.28848000	-0.98448400
H	-5.89448300	0.88846500	-1.62572000
H	-5.84232900	-0.08721300	-0.15782900
H	-4.90064000	-0.57157700	-1.57206300
C	-4.63596900	2.34115500	0.33163800
H	-5.32705200	2.92285800	-0.29458300
H	-3.83968100	3.01263600	0.66913000
H	-5.19237700	2.01150000	1.21203300
C	-3.34500200	1.78902500	-1.70753600
H	-4.04560300	2.44802100	-2.23802800
H	-2.99652000	1.04267300	-2.42697400
H	-2.48621300	2.39821200	-1.40401600
C	-3.52865700	-0.94085600	1.81522500
C	-2.44351000	-1.27574100	2.86621000
H	-2.87596800	-1.92734400	3.63903200
H	-2.07181100	-0.37018000	3.35713400
H	-1.58878500	-1.79916700	2.43233900
C	-4.67283900	-0.23439000	2.57319400
H	-4.99609100	-0.87202100	3.40751100

H	-5.55102100	-0.05458400	1.94660600
H	-4.34884200	0.72208100	2.99829100
C	-4.06088700	-2.25625700	1.21706900
H	-4.56100800	-2.84043900	2.00328800
H	-3.24966600	-2.87712300	0.82705600
H	-4.78685600	-2.09509800	0.41506700
C	0.67707200	2.21594900	-0.37124300
C	0.79737400	1.73931300	-1.68405900
H	1.01703200	0.69029500	-1.83857500
C	0.62712400	2.59471600	-2.77525000
H	0.72189100	2.20580400	-3.78629700
C	0.34044900	3.94514100	-2.56922300
H	0.20942800	4.61189400	-3.41745200
C	0.21547800	4.43333000	-1.26634100
H	-0.01428600	5.48220800	-1.09725400
C	0.37372600	3.57415300	-0.17830300
H	0.25535600	3.95791300	0.83230900
C	2.72278700	1.31851700	1.44301400
C	3.17235100	1.12629200	2.76002800
H	2.44944600	0.91370900	3.54450500
C	4.52943300	1.21144500	3.07653200
H	4.85675700	1.05381000	4.10109200
C	5.46012400	1.51564600	2.08192700
H	6.51624300	1.59336500	2.32675400
C	5.02523200	1.73389900	0.77297800

H	5.74307100	1.98426700	-0.00432400
C	3.66916700	1.63453300	0.45621500
H	3.34422800	1.82121500	-0.56280100
C	-2.25229000	-1.60363700	-1.65495900
H	-1.48061900	-2.00123100	-2.32568200
H	-2.99615200	-1.09745500	-2.27377900
H	-2.74657400	-2.45300400	-1.17970000



Fe	-0.98362600	-2.25187100	-1.06038100
P	-1.07014200	1.05145900	0.56308200
P	2.81118500	0.43720000	0.55039100
C	-2.74072400	-2.92858800	-0.21199400
H	-3.52749900	-2.31132000	0.19648400
C	-2.64121800	-3.36025300	-1.56568700
H	-3.33070700	-3.11441400	-2.36313500
C	-1.45869600	-4.14820200	-1.69178600
H	-1.09045600	-4.60302800	-2.60235500
C	-0.82996600	-4.20656000	-0.41330100
H	0.09380700	-4.72127100	-0.18555700
C	-1.61838600	-3.44971600	0.50201900
H	-1.40530500	-3.30222800	1.55258800
C	-0.57838200	-0.21885000	-0.69746300

C	0.63788400	-1.00489900	-0.59799800
C	0.81512600	-1.68400400	-1.84471200
H	1.61771100	-2.37018700	-2.08289500
C	-0.25479600	-1.33186000	-2.71980000
H	-0.40330100	-1.70284900	-3.72627600
C	-1.12133100	-0.45389900	-2.00978600
H	-2.04434300	-0.04129400	-2.39106000
C	1.57938500	-1.04939800	0.58897300
H	0.97580400	-0.74117000	1.44836100
C	2.09913500	-2.46614300	0.88870100
H	1.26098800	-3.11677900	1.15984500
H	2.80283500	-2.46799100	1.72369000
H	2.60336200	-2.92264600	0.03393800
C	4.21583800	0.08410100	-0.73091800
C	3.60655100	0.41877000	-2.11247800
H	4.37845300	0.31368600	-2.88814200
H	3.23608500	1.44905100	-2.14361500
H	2.77696900	-0.24119200	-2.37564000
C	4.82103000	-1.33062200	-0.78610500
H	5.66177000	-1.34286100	-1.49509100
H	4.09614000	-2.06869600	-1.14013400
H	5.20268700	-1.66686600	0.18147800
C	5.35095300	1.10509200	-0.49542500
H	6.04509800	1.07061400	-1.34641300
H	5.93492100	0.89467800	0.40478300

H	4.96841600	2.12951900	-0.42564200
C	3.56049200	0.43536800	2.34399000
C	4.71259000	-0.53629800	2.66313400
H	5.00247900	-0.42329500	3.71788500
H	5.60593000	-0.33811100	2.06436500
H	4.43663600	-1.58409000	2.51538000
C	2.40568600	0.17500100	3.33749900
H	2.74304900	0.42134000	4.35347300
H	2.09076000	-0.87337000	3.34802800
H	1.52840600	0.79494000	3.11937700
C	4.04929100	1.88159100	2.59832400
H	4.39911400	1.97497100	3.63602500
H	3.24116800	2.60477600	2.44750600
H	4.87904000	2.16653600	1.94644300
C	-1.14046200	2.66533400	-0.43637800
H	-1.60897600	3.34751200	0.29005300
C	0.27560200	3.21661900	-0.70513300
H	0.79123300	2.55943100	-1.41863500
H	0.87445000	3.19371700	0.21122200
C	0.21936500	4.64695100	-1.27007600
H	-0.18790200	5.32050600	-0.50080800
H	1.23541400	5.00222500	-1.48671100
C	-0.65389700	4.73613800	-2.53023300
H	-0.17337000	4.17125300	-3.34294000
H	-0.72554900	5.77660800	-2.87312800

C	-2.05426900	4.15734200	-2.28059900
H	-2.64316100	4.17155800	-3.20745400
H	-2.59035300	4.79365000	-1.56039900
C	-1.97250100	2.72118000	-1.73263600
H	-2.98279200	2.32245900	-1.57612600
H	-1.49627100	2.08787400	-2.49036400
C	-2.90128800	0.69685300	0.93933400
H	-3.37877300	0.22945800	0.06613000
C	-2.95600500	-0.28730900	2.12995200
H	-2.39267200	-1.19637900	1.89876000
H	-2.44510800	0.17725500	2.98561100
C	-4.39644600	-0.63624600	2.53861200
H	-4.38631100	-1.32591900	3.39275800
H	-4.89780700	-1.16833100	1.71581800
C	-5.19672400	0.62755400	2.88076600
H	-4.77372600	1.08706800	3.78632000
H	-6.23791000	0.37232300	3.11649900
C	-5.14279000	1.63844700	1.72803400
H	-5.66491200	2.56328100	2.00641000
H	-5.68078000	1.22703000	0.86082300
C	-3.69776400	1.96707300	1.30931400
H	-3.19138600	2.48287100	2.13969600
H	-3.72441200	2.67346500	0.47371900

Representative Microscale High-throughput Experimentation.

General Experimental.

The experimental procedures in this work were similar to those reported.⁴¹ Parallel synthesis was accomplished in an MBraun glovebox operating with a constant N₂-purge (oxygen typically <5 ppm). The experimental design was accomplished using Accelrys Library Studio. Screening reactions were carried out in 1 mL vials (30 mm height × 8 mm diameter) in a 96-well plate aluminum reactor block. Liquid chemicals were dosed using multi-channel or single-channel pipettors. Solid chemicals were dosed manually as solutions or slurries in appropriate solvents. Undesired additional solvent was removed using a GeneVac system located inside the glovebox. The reactions were heated and stirred on a heating block with a tumble-stirrer (V&P Scientific) using 1.98 mm diameter × 4.80 mm length parylene stir bars. The tumble stirring mechanism helped to insure uniform stirring throughout the 96-well plate. The reactions were sealed in the 96-well plate during reaction. Below each reactor vial in the aluminum 96-well plate was a 0.062 mm thick silicon-rubber gasket. Directly above the glass vial reactor tops was a Teflon perfluoroalkoxy copolymer resin sealing gasket and above that, two more 0.062 mm thick silicon-rubber gaskets. The entire assembly was compressed between an aluminum top and the reactor base with 9 evenly-placed screws.

Set up:

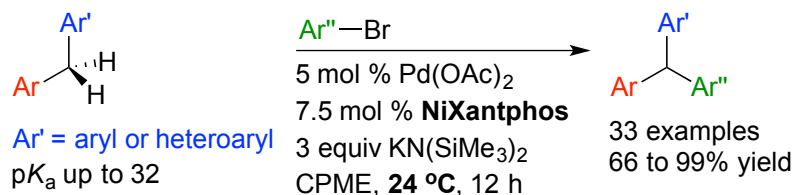
Experiments were set up inside a glovebox under a nitrogen atmosphere. A 96-well aluminum block containing 1 mL glass vials was predosed with Pd(OAc)₂ (1 μmol) and Ligand (Ligand was used in a 4:1 ratio relative to Pd for monodentate ligands and 2:1 ratio for bidentate ligands) in THF. The solvent was evacuated to dryness using a Genevac vacuum centrifuge, and KN(SiMe₃)₂ (30 μmol) in THF was added to the ligand/catalyst mixture. The solvent was removed on the Genevac, and a parylene stir bar was then added to each reaction vial. 1-*tert*-Butyl-4-chlorobenzene (10

$\mu\text{mol}/\text{reaction}$), diphenylmethane ($12 \mu\text{mol}/\text{reaction}$) and biphenyl ($1 \mu\text{mol}/\text{reaction}$) (used as an internal standard to measure HPLC yields) were then dosed together into each reaction vial as a solution in CPME ($100 \mu\text{L}$, 0.1 M). The 96-well plate was then sealed and stirred for 18 h at $24 \text{ }^\circ\text{C}$.

Work up:

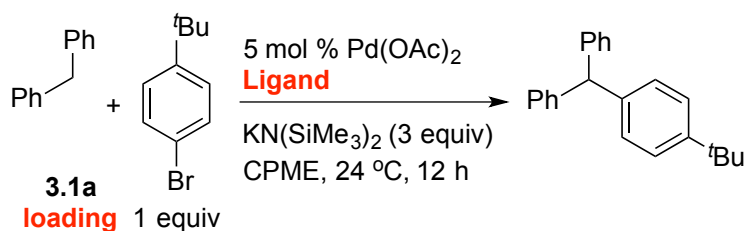
Upon opening the plate to air, $500 \mu\text{L}$ of acetonitrile was pipetted into each vial. The plate was then covered again and the vials stirred for 20 min to extract the product and to ensure good homogenization. Into a separate 96-well LC block was added $700 \mu\text{L}$ of acetonitrile, followed by $40 \mu\text{L}$ of the diluted reaction mixtures. The LC block was then sealed with a silicon-rubber storage mat, and mounted on HPLC instrument for analysis.

(1) Ligand screening for the cross-coupling of diphenylmethane with 1-bromo-4-*tert*-butylbenzene.



NiXantphos was found to be the best ligand from the 112 ligands examined. See HTE details in Tables 2.4, 2.5, 2.6 and 2.7.

(2) Ligand comparison for the cross-coupling of diphenylmethane with 1-bromo-4-*tert*-butylbenzene.



Ligands examined (×7): NiXantphos, Xantphos, DPEPhos, dippp, XPhos, SPhos, PCy₃.

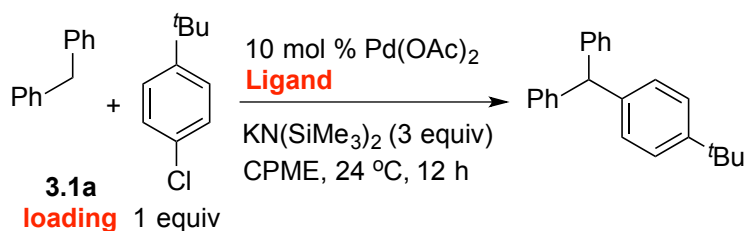
3.1a loadings examined (×2): 1.2 equiv, 3 equiv.

The lead hits from the screening were the combination of **1.2 equiv** of **3.1a** and **NiXantphos**, and the combination of **3 equiv** of **3.1a** and **NiXantphos**, both giving 100% assay yield of the desired DCCP product **3.3aa**.

Table 3.8 HTE with 1-bromo-4-*tert*-butylbenzene using 7 ligands and 2 **3.1a** loadings

Ligand	3.1a loading	
	1.2 equiv	3 equiv
NiXantphos	100	100
Xantphos	13	16
DPEPhos	3	7
dipp	0	0
XPhos	1	2
SPhos	1	2
PCy ₃	3	2

(3) Ligand comparison for the cross-coupling of diphenylmethane with 1-*tert*-butyl-4-chlorobenzene.



Ligands examined (×8): NiXantphos, *N*-Bn-NiXantphos, Xantphos, DPEPhos, dippp, XPhos, SPhos, PCy₃.

3.1a loadings examined ($\times 3$): 1.2 equiv, 2 equiv, 3 equiv.

The lead hits from the screening were the combination of **1.2 equiv** of **3.1a** and **NiXantphos**, giving 91% assay yield of the desired DCCP product **3.3aa**.

Table 3.9 HTE with 1-bromo-4-*tert*-butylbenzene using 8 ligands and 3 **3.1a** loadings

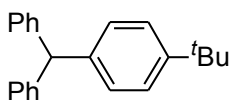
Ligand	3.1a loading		
	1.2 equiv	2 equiv	3 equiv
NiXantphos	91	85	64
<i>N</i> -Bn-NiXantphos	1	2	1
Xantphos	0	0	0
DPEPhos	0	0	0
dipp	0	0	0
XPhos	1	3	2
SPhos	1	3	2
PCy ₃	0	0	0

Procedure and Characterization for the Pd-Catalyzed DCCP of Aryl Chlorides.

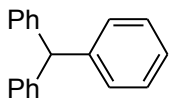
General Procedure I. An oven-dried 10 mL reaction vial equipped with a stir bar was charged with KN(SiMe₃)₂ (59.8 mg, 0.30 mmol, 3 equiv) under a nitrogen atmosphere. A solution (from a stock solution) of Pd(OAc)₂ (0.56 mg, 0.0025 mmol, 2.5 mol %) and NiXantphos (2.76 mg, 0.0050 mmol, 5 mol %) in 0.5 mL of dry THF was taken up by syringe and added to the reaction vial. After stirring for 5 min at 24 °C, diphenylmethane (16.7 μ L, 0.1 mmol, 1 equiv) was added to the reaction mixture followed by 1-*tert*-butyl-4-chlorobenzene (33.4 μ L, 0.2 mmol, 2 equiv). Note that the aryl chloride in a solid form was added to the reaction vial prior to KN(SiMe₃)₂. The reaction mixture was stirred for

12 h at 24 °C, quenched with three drops of H₂O, diluted with 3 mL of ethyl acetate, and filtered over a pad of MgSO₄ and silica. The pad was rinsed with additional ethyl acetate, and the solution was concentrated in vacuo. The crude material was loaded onto a silica gel column and purified by flash chromatography.

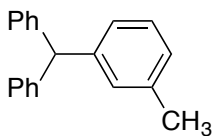
General Procedure II. Under a nitrogen atmosphere a solution (from a stock solution) of Pd(OAc)₂ (1.12 mg, 0.0050 mmol, 5 mol %) and NiXantphos (5.52 mg, 0.010 mmol, 10 mol %) in 0.5 mL of dry THF was taken up by syringe and added to an oven-dried 10 mL reaction vial equipped with a stir bar. The solvent was removed under reduced pressure, and KN(SiMe₃)₂ (59.8 mg, 0.30 mmol, 3 equiv) was then added to the reaction vial followed by 0.5 mL of dry CPME (or 2-MeTHF). After stirring for 5 min at 24 °C, diphenylmethane (16.7 μL, 0.1 mmol, 1 equiv) was added to the reaction mixture followed by 1-*tert*-butyl-4-chlorobenzene (33.4 μL, 0.2 mmol, 2 equiv). Note that the aryl chloride in a solid form was added to the reaction vial prior to KN(SiMe₃)₂. The reaction mixture was stirred for 12 h at 24 °C, quenched with three drops of H₂O, diluted with 3 mL of ethyl acetate, and filtered over a pad of MgSO₄ and silica. The pad was rinsed with additional ethyl acetate, and the solution was concentrated in vacuo. The crude material was loaded onto a silica gel column and purified by flash chromatography.



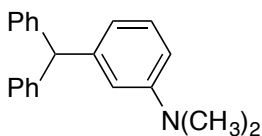
3.3aa – (4-*tert*-Butylphenyl)diphenylmethane: The reaction was performed following General Procedure I with **3.1a** (16.7 μL, 0.1 mmol, 1 equiv), KN(SiMe₃)₂ (59.8 mg, 0.30 mmol, 3 equiv) and **3.2a** (33.4 μL, 0.2 mmol, 2 equiv) in the presence of 2.5 mol % Pd catalyst in THF at 24 °C. The crude material was purified by flash chromatography on silica gel (eluted with hexanes to EtOAc:hexanes = 2:98) to give the product (24.3 mg, 81% yield) as a white solid. R_f = 0.33 (hexanes); The NMR spectral data match the previously published data.⁴²



3.3ab – Triphenylmethane: The reaction was performed following General Procedure I with **3.1a** (16.7 μL , 0.1 mmol, 1 equiv), $\text{KN}(\text{SiMe}_3)_2$ (59.8 mg, 0.30 mmol, 3 equiv) and **3.2b** (20.4 μL , 0.2 mmol, 2 equiv) in the presence of 2.5 mol % Pd catalyst in THF at 24 $^\circ\text{C}$. The crude material was purified by flash chromatography on silica gel (eluted with hexanes to EtOAc:hexanes = 2:98) to give the product (23.4 mg, 96% yield) as a white solid. $R_f = 0.40$ (hexanes). The NMR spectral data match the previously published data.⁴²

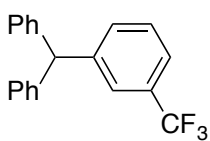


3.3ac – (3-Methylphenyl)diphenylmethane: The reaction was performed following General Procedure I with **3.1a** (16.7 μL , 0.1 mmol, 1 equiv), $\text{KN}(\text{SiMe}_3)_2$ (59.8 mg, 0.30 mmol, 3 equiv) and **3.2c** (23.6 μL , 0.2 mmol, 2 equiv) in the presence of 2.5 mol % Pd catalyst in THF at 24 $^\circ\text{C}$. The crude material was purified by flash chromatography on silica gel (eluted with hexanes to EtOAc:hexanes = 2:98) to give the product (23.5 mg, 91% yield) as a white solid. $R_f = 0.30$ (hexanes); m.p. data for the title compound have been reported;⁴³ ^1H NMR (500 MHz, CDCl_3): δ 7.30 – 7.25 (m, 4H), 7.22 – 7.14 (m, 3H), 7.14 – 7.09 (m, 4H), 7.02 (d, $J = 7.5$ Hz, 1H), 6.95 (s, 1H), 6.90 (d, $J = 8.0$ Hz, 1H), 5.51 (s, 1H), 2.28 (s, 3H) ppm; $^{13}\text{C}\{^1\text{H}\}$ NMR (125 MHz, CDCl_3): δ 144.2, 144.0, 138.1, 130.4, 129.7, 128.5, 128.4, 127.3, 126.7, 126.4, 57.0, 21.7 ppm; IR (thin film): 3084, 3060, 3025, 2921, 1600, 1494, 1450, 1031, 774, 748, 730, 699 cm^{-1} ; HRMS calc'd for $\text{C}_{20}\text{H}_{18}^+$ 258.1409, observed 258.1404 $[\text{M}]^+$.

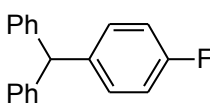


3.3ad – (3-Dimethylaminophenyl)diphenylmethane: The reaction was performed following General Procedure I with **3.1a**

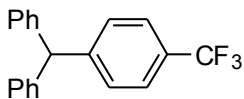
(16.7 μL , 0.1 mmol, 1 equiv), $\text{KN}(\text{SiMe}_3)_2$ (59.8 mg, 0.30 mmol, 3 equiv) and **3.2d** (27.9 μL , 0.2 mmol, 2 equiv) in the presence of 5 mol % Pd catalyst in THF at 24 $^\circ\text{C}$. The crude material was purified by flash chromatography on silica gel (eluted with EtOAc:hexanes = 2:98) to give the product (27.0 mg, 94% yield) as a colorless oil. R_f = 0.30 (EtOAc:hexanes = 5:95). The NMR spectral data match the previously published data.⁴⁴



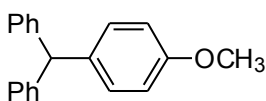
3.3ae – (3-Trifluoromethylphenyl)diphenylmethane: The reaction was performed following General Procedure I with **3.1a** (20.1 μL , 0.12 mmol, 1.2 equiv), $\text{KN}(\text{SiMe}_3)_2$ (59.8 mg, 0.30 mmol, 3 equiv) and **3.2e** (13.6 μL , 0.1 mmol, 1 equiv) in the presence of 5 mol % Pd catalyst in THF at 24 $^\circ\text{C}$. The crude material was purified by flash chromatography on silica gel (eluted with hexanes to EtOAc:hexanes = 2:98) to give the product (25.6 mg, 82% yield) as a colorless oil. R_f = 0.30 (hexanes). The ^1H NMR spectrum matches the previously published report.⁴⁵ The ^{13}C NMR spectrum of the title compound was not reported before. $^{13}\text{C}\{^1\text{H}\}$ NMR (125 MHz, CDCl_3): δ 145.1, 143.2, 133.0, 130.9 (q, J = 32 Hz), 129.6, 129.0, 128.8, 126.9, 126.3 (q, J = 4 Hz), 124.4 (q, J = 273 Hz), 123.5 (q, J = 4 Hz), 56.8 ppm.



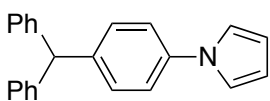
3.3af – (4-Fluorophenyl)diphenylmethane: The reaction was performed following General Procedure I with **3.1a** (16.7 μL , 0.1 mmol, 1 equiv), $\text{KN}(\text{SiMe}_3)_2$ (59.8 mg, 0.30 mmol, 3 equiv) and **3.2f** (21.3 μL , 0.2 mmol, 2 equiv) in the presence of 10 mol % Pd catalyst in THF at 24 $^\circ\text{C}$. The crude material was purified by flash chromatography on silica gel (eluted with hexanes to EtOAc:hexanes = 2:98) to give the product (24.4 mg, 93% yield) as a white solid. R_f = 0.33 (hexanes). The NMR spectral data match the previously published data.⁴²



3.3ag – (4-Trifluoromethylphenyl)diphenylmethane: The reaction was performed following General Procedure II with **3.1a** (66.9 μL , 0.40 mmol, 4 equiv), $\text{KN}(\text{SiMe}_3)_2$ (39.9 mg, 0.20 mmol, 2 equiv) and **3.2g** (14.0 μL , 0.1 mmol, 1 equiv) in the presence of 10 mol % Pd catalyst in CPME at 24 °C. The crude material was purified by flash chromatography on silica gel (eluted with hexanes to EtOAc:hexanes = 2:98) to give the product (27.8 mg, 89% yield) as a colorless oil. R_f = 0.33 (hexanes). The NMR spectral data match the previously published data.⁴²

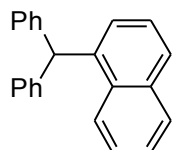


3.3ah – (4-Methoxyphenyl)diphenylmethane: The reaction was performed following General Procedure I with **3.1a** (16.7 μL , 0.1 mmol, 1 equiv), $\text{KN}(\text{SiMe}_3)_2$ (59.8 mg, 0.30 mmol, 3 equiv) and **3.2h** (24.5 μL , 0.2 mmol, 2 equiv) in the presence of 10 mol % Pd catalyst in THF at 80 °C. The crude material was purified by flash chromatography on silica gel (eluted with hexanes to EtOAc:hexanes = 5:95) to give the product (27.4 mg, 99% yield) as a colorless oil. R_f = 0.25 (hexanes). The NMR spectral data match the previously published data.⁴²

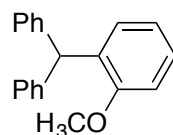


3.3ai – (4-(N-Pyrrolyl)phenyl)diphenylmethane: The reaction was performed following General Procedure I with **3.1a** (20.1 μL , 0.12 mmol, 1.2 equiv), $\text{KN}(\text{SiMe}_3)_2$ (59.8 mg, 0.30 mmol, 3 equiv) and **3.2i** (17.8 mg, 0.1 mmol, 1 equiv) in the presence of 5 mol % Pd catalyst in THF at 24 °C. The crude material was purified by flash chromatography on silica gel (eluted with hexanes to EtOAc:hexanes = 5:95) to give the product (30.9 mg, 99% yield) as a white solid. R_f = 0.40 (EtOAc:hexanes = 5:95); m.p. = 104–106 °C; ^1H NMR (500 MHz, CDCl_3): δ 7.33 – 7.27 (m, 6H), 7.26 – 7.20 (m, 2H), 7.18 – 7.11 (m, 6H), 7.05 (t, J = 2.2 Hz, 2H), 6.32 (t, J

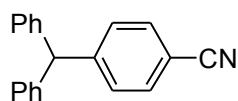
= 2.2 Hz, 2H), 5.56 (s, 1H) ppm; $^{13}\text{C}\{^1\text{H}\}$ NMR (125 MHz, CDCl_3): δ 143.9, 141.6, 139.3, 130.7, 129.6, 128.6, 126.7, 120.6, 119.5, 110.5, 56.5 ppm; IR (thin film): 3025, 1519, 1491, 1329, 1070, 725, 700 cm^{-1} ; HRMS calc'd for $\text{C}_{23}\text{H}_{20}\text{N}^+$ 310.1596, observed 310.1602 $[\text{MH}]^+$.



3.3aj – (1-Naphthyl)diphenylmethane: The reaction was performed following General Procedure II with **3.1a** (16.7 μL , 0.1 mmol, 1 equiv), $\text{KN}(\text{SiMe}_3)_2$ (59.8 mg, 0.30 mmol, 3 equiv) and **3.2j** (27.3 μL , 0.2 mmol, 2 equiv) in the presence of 10 mol % Pd catalyst in CPME at 80 $^\circ\text{C}$. The crude material was purified by flash chromatography on silica gel (eluted with hexanes to EtOAc:hexanes = 3:97) to give the product (19.5 mg, 66% yield) as a white solid. R_f = 0.33 (hexanes). The NMR spectral data match the previously published data.⁴⁶

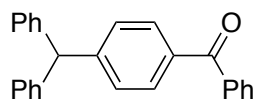


3.3ak – (2-Methoxyphenyl)diphenylmethane: The reaction was performed following General Procedure II with **3.1a** (16.7 μL , 0.1 mmol, 1 equiv), $\text{KN}(\text{SiMe}_3)_2$ (59.8 mg, 0.30 mmol, 3 equiv) and **3.2k** (38.1 μL , 0.3 mmol, 3 equiv) in the presence of 5 mol % Pd catalyst in 2-MeTHF at 80 $^\circ\text{C}$. The crude material was purified by flash chromatography on silica gel (eluted with hexanes to EtOAc:hexanes = 2:98) to give the product (15.3 mg, 56% yield) as a white solid. R_f = 0.40 (EtOAc:hexanes = 5:95). The NMR spectral data match the previously published data.⁴⁷

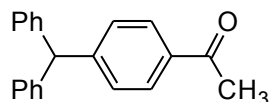


3.3al – (4-Cyanophenyl)diphenylmethane: The reaction was performed following General Procedure II with **3.1a** (20.1 μL , 0.12 mmol, 1.2 equiv), $\text{KN}(\text{SiMe}_3)_2$ (79.8 mg, 0.40 mmol, 4 equiv) and **3.2l** (13.8 mg, 0.1

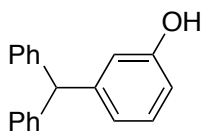
mmol, 1 equiv) in the presence of 5 mol % Pd catalyst in 2-MeTHF at 24 °C. The crude material was purified by flash chromatography on silica gel (eluted with hexanes to EtOAc:hexanes = 2:98) to give the product (23.4 mg, 87% yield) as a colorless oil. $R_f = 0.25$ (hexanes). The NMR spectral data match the previously published data.⁴⁶



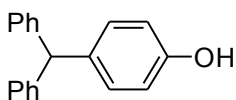
3.3am – 4-Benzhydrylbenzophenone: The reaction was performed following General Procedure II with **3.1a** (20.1 μL , 0.12 mmol, 1.2 equiv), $\text{KN}(\text{SiMe}_3)_2$ (59.8 mg, 0.30 mmol, 3 equiv) and **3.2m** (21.7 mg, 0.1 mmol, 1 equiv) in the presence of 5 mol % Pd catalyst in CPME at 24 °C. The crude material was purified by flash chromatography on silica gel (eluted with EtOAc:hexanes = 5:95 to 10:90) to give the product (32.9 mg, 94% yield) as a white solid. $R_f = 0.25$ (EtOAc:hexanes = 5:95). The ^1H NMR spectrum matches the previously published report.⁴⁸ The ^{13}C NMR spectrum of the title compound was not reported before. $^{13}\text{C}\{^1\text{H}\}$ NMR (125 MHz, CDCl_3): δ 196.6, 149.1, 143.3, 137.9, 135.9, 132.5, 130.5, 130.2, 129.64, 129.60, 128.7, 128.4, 126.8, 57.1 ppm.



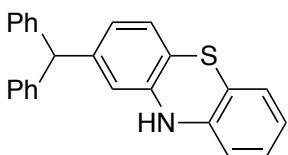
3.3an – (4-Acetylphenyl)diphenylmethane: The reaction was performed following General Procedure II with **3.1a** (50.2 μL , 0.3 mmol, 3 equiv), $\text{KN}(\text{SiMe}_3)_2$ (79.8 mg, 0.40 mmol, 4 equiv) and **3.2n** (13.0 μL , 0.1 mmol, 1 equiv) in the presence of 5 mol % Pd catalyst in CPME at 24 °C. The crude material was purified by flash chromatography on silica gel (eluted with hexanes to EtOAc:hexanes = 5:95) to give the product (16.9 mg, 59% yield) as a white solid. $R_f = 0.33$ (EtOAc:hexanes = 1:9). The NMR spectral data match the previously published data.⁴²



3.3ao – (3-Hydroxyphenyl)diphenylmethane: The reaction was performed following General Procedure I with **3.1a** (50.2 μL , 0.3 mmol, 3 equiv), $\text{KN}(\text{SiMe}_3)_2$ (79.8 mg, 0.40 mmol, 4 equiv) and **3.2o** (10.6 μL , 0.1 mmol, 1 equiv) in the presence of 10 mol % Pd catalyst in THF at 80 °C. The crude material was purified by flash chromatography on silica gel (eluted with CH_2Cl_2) to give the product (21.9 mg, 84% yield) as a white solid. $R_f = 0.35$ (EtOAc:hexanes = 2:8); m.p. = 103–104 °C; The measured m.p. data for the title compound match the previously published data;⁴⁹ ^1H NMR (500 MHz, CDCl_3): δ 7.32 – 7.23 (m, 4H), 7.23 – 7.18 (m, 2H), 7.17 – 7.04 (m, 5H), 6.74 – 6.63 (m, 2H), 6.58 – 6.48 (m, 1H), 5.49 (s, 1H), 4.59 (s, 1H) ppm; $^{13}\text{C}\{^1\text{H}\}$ NMR (125 MHz, CDCl_3): δ 155.7, 146.1, 143.8, 129.7, 129.6, 128.5, 126.6, 122.3, 116.6, 113.5, 56.8 ppm; IR (thin film): 3400 (broad OH stretch), 3025, 1598, 1494, 1452, 698 cm^{-1} ; HRMS calc'd for $\text{C}_{19}\text{H}_{16}\text{O}^+$ 260.1201, observed 260.1212 $[\text{M}]^+$.

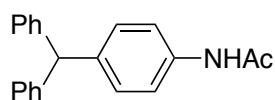


3.3ap – (4-Hydroxyphenyl)diphenylmethane: The reaction was performed following General Procedure I with **3.1a** (50.2 μL , 0.3 mmol, 3 equiv), $\text{KN}(\text{SiMe}_3)_2$ (79.8 mg, 0.40 mmol, 4 equiv) and **3.2p** (12.9 mg, 0.1 mmol, 1 equiv) in the presence of 10 mol % Pd catalyst in THF at 80 °C. The crude material was purified by flash chromatography on silica gel (eluted with EtOAc:hexanes = 5:95 to 1:9) to give the product (10.4 mg, 40% yield) as a white solid. $R_f = 0.33$ (EtOAc:hexanes = 2:8). The NMR spectral data match the previously published data.⁴²

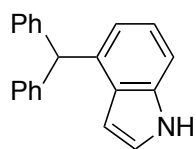


3.3aq – 2-Benzhydrylphenothiazine: The reaction was performed following General Procedure I with **3.1a** (16.7 μL , 0.1 mmol, 1 equiv), $\text{KN}(\text{SiMe}_3)_2$ (99.7 mg, 0.50 mmol, 5 equiv) and **3.2q** (46.7 mg, 0.2 mmol, 2 equiv) in the presence of 5 mol % Pd catalyst in THF at

80 °C. The crude material was purified by flash chromatography on silica gel (eluted with EtOAc:hexanes = 5:95) to give the product (31.4 mg, 86% yield) as a white solid. R_f = 0.50 (EtOAc:hexanes = 1:9); m.p. = 175–178 °C; ^1H NMR (500 MHz, CDCl_3): δ 7.31 – 7.25 (m, 4H), 7.23 – 7.18 (m, 2H), 7.13 – 7.05 (m, 4H), 6.95 (t, J = 7.5 Hz, 2H), 6.88 (d, J = 7.5 Hz, 1H), 6.79 (t, J = 7.5 Hz, 1H), 6.58 (dd, J = 7.5, 1.5 Hz, 1H), 6.46 (d, J = 7.5 Hz, 1H), 6.25 (d, J = 1.5 Hz, 1H), 5.67 (s, 1H), 5.39 (s, 1H) ppm; $^{13}\text{C}\{^1\text{H}\}$ NMR (125 MHz, CDCl_3): δ 143.9, 143.6, 141.82, 141.79, 129.6, 128.6, 127.5, 127.1, 126.8, 126.7, 124.1, 122.8, 118.5, 116.3, 115.8, 114.7, 56.4 ppm; IR (thin film): 3383 (broad NH stretch), 3024, 1567, 1462, 1431, 1305, 743, 700 cm^{-1} ; HRMS calc'd for $\text{C}_{25}\text{H}_{19}\text{NS}^+$ 365.1238, observed 365.1228 $[\text{M}]^+$.

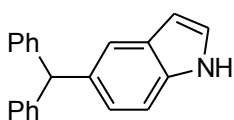


3.3ar – N-(4-Benzhydrylphenyl)acetamide: The reaction was performed following General Procedure I with **3.1a** (16.7 μL , 0.1 mmol, 1 equiv), $\text{KN}(\text{SiMe}_3)_2$ (99.7 mg, 0.50 mmol, 5 equiv) and **3.2r** (33.9 mg, 0.2 mmol, 2 equiv) in the presence of 10 mol % Pd catalyst in THF at 80 °C. The crude material was purified by flash chromatography on silica gel (eluted with EtOAc:hexanes = 3:7 to 1:1) to give the product (19.9 mg, 66% yield) as a white solid. R_f = 0.60 (EtOAc). The NMR spectral data match the previously published data.⁴⁷

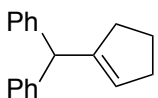


3.3as – 4-Benzhydryl-1H-indole: The reaction was performed following General Procedure II with **3.1a** (50.2 μL , 0.3 mmol, 3 equiv), $\text{KN}(\text{SiMe}_3)_2$ (79.8 mg, 0.40 mmol, 4 equiv) and **3.2s** (12.0 μL , 0.1 mmol, 1 equiv) in the presence of 10 mol % Pd catalyst in CPME at 80 °C. The crude material was purified by flash chromatography on silica gel (eluted with EtOAc:hexanes = 1:9) to give the product (15.5 mg, 55% yield) as a colorless oil. R_f = 0.12 (EtOAc:hexanes = 1:9);

^1H NMR (500 MHz, CDCl_3): δ 8.11 (s, br, 1H), 7.30 – 7.23 (m, 5H), 7.22 – 7.15 (m, 6H), 7.12 – 7.06 (m, 2H), 6.64 (d, J = 7.5 Hz, 1H), 6.32 (m, 1H), 5.94 (s, 1H) ppm; $^{13}\text{C}\{^1\text{H}\}$ NMR (125 MHz, CDCl_3): δ 143.9, 136.4, 136.0, 129.7, 128.4, 127.7, 126.4, 123.9, 122.1, 120.6, 109.8, 102.0, 54.8 ppm; IR (thin film): 3419 (broad NH stretch), 3024, 1598, 1494, 1344, 1078, 753, 700 cm^{-1} ; HRMS calc'd for $\text{C}_{21}\text{H}_{18}\text{N}^+$ 284.1439, observed 284.1453 $[\text{MH}]^+$.

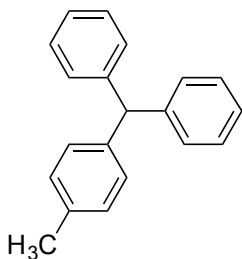


3.3at – 5-Benzhydryl-1H-indole: The reaction was performed following General Procedure I with **3.1a** (50.2 μL , 0.3 mmol, 3 equiv), $\text{KN}(\text{SiMe}_3)_2$ (79.8 mg, 0.40 mmol, 4 equiv) and **3.2t** (15.2 mg, 0.1 mmol, 1 equiv) in the presence of 10 mol % Pd catalyst in THF at 80 $^\circ\text{C}$. The crude material was purified by flash chromatography on silica gel (eluted with hexanes to EtOAc:hexanes = 5:95 to 1:9) to give the product (16.4 mg, 58% yield) as a colorless oil. The NMR spectral data match the previously published data.⁴²

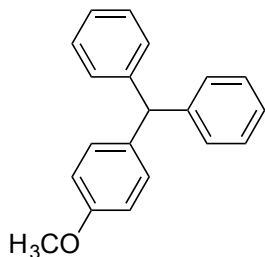


3.3au – 1-Benzhydrylcyclopent-1-ene: The reaction was performed following General Procedure II with **3.1a** (16.7 μL , 0.1 mmol, 1 equiv), $\text{KN}(\text{SiMe}_3)_2$ (59.8 mg, 0.30 mmol, 3 equiv) and **3.2u** (19.8 μL , 0.2 mmol, 2 equiv) in the presence of 2.5 mol % Pd catalyst in CPME at 80 $^\circ\text{C}$. The crude material was purified by flash chromatography on silica gel (eluted with hexanes to EtOAc:hexanes = 0.5:99.5) to give the product (23.4 mg, 99% yield) as a colorless oil. R_f = 0.40 (hexanes); ^1H NMR (500 MHz, CDCl_3): δ 7.30 – 7.24 (m, 4H), 7.21 – 7.14 (m, 6H), 5.18 (m, 1H), 4.75 (s, 1H), 2.34 (m, 2H), 2.25 (m, 2H), 1.90 (m, 2H) ppm; $^{13}\text{C}\{^1\text{H}\}$ NMR (125 MHz, CDCl_3): δ 146.9, 143.2, 129.1, 128.6, 128.4, 126.4, 53.9, 35.2, 32.6, 24.0 ppm; IR (thin film): 3025, 2949,

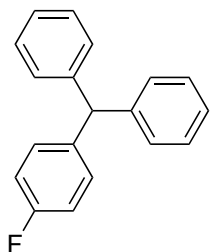
2846, 1598, 1495, 1450, 1031, 744, 701 cm^{-1} ; HRMS calc'd for $\text{C}_{18}\text{H}_{17}^+$ 233.1330, observed 233.1325 $[\text{M}-\text{H}]^+$.



3.3bb – (4-Methylphenyl)diphenylmethane: The reaction was performed following General Procedure I with **3.1b** (18.8 μL , 0.1 mmol, 1 equiv), $\text{KN}(\text{SiMe}_3)_2$ (59.8 mg, 0.30 mmol, 3 equiv) and **3.2b** (20.4 μL , 0.2 mmol, 2 equiv) in the presence of 5 mol % Pd catalyst in THF at 24 $^\circ\text{C}$. The crude material was purified by flash chromatography on silica gel (eluted with hexanes to EtOAc:hexanes = 1:99) to give the product (22.4 mg, 87% yield) as a colorless oil. R_f = 0.25 (hexanes). The NMR spectral data match the previously published data.⁴²

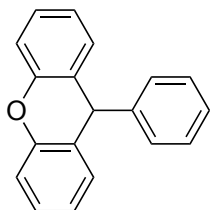


3.3cb – (4-Methoxyphenyl)diphenylmethane: The reaction was performed following General Procedure I with **3.1c** (18.9 μL , 0.1 mmol, 1 equiv), $\text{KN}(\text{SiMe}_3)_2$ (59.8 mg, 0.30 mmol, 3 equiv) and **3.2b** (20.4 μL , 0.2 mmol, 2 equiv) in the presence of 5 mol % Pd catalyst in THF at 24 $^\circ\text{C}$. The crude material was purified by flash chromatography on silica gel (eluted with hexanes to EtOAc:hexanes = 2:98) to give the product (23.0 mg, 84% yield) as a colorless oil. R_f = 0.25 (EtOAc:hexanes = 2:98). The NMR spectral data match the previously published data.⁴²



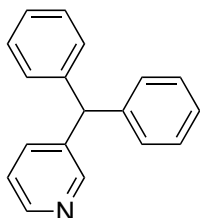
3.3db – (4-Fluorophenyl)diphenylmethane: The reaction was performed following General Procedure I with **3.1d** (18.6 μL , 0.1 mmol, 1 equiv), $\text{KN}(\text{SiMe}_3)_2$ (59.8 mg, 0.30 mmol, 3 equiv) and **3.2b** (20.4 μL , 0.2 mmol, 2 equiv) in the presence of 2.5 mol % Pd catalyst in THF at

24 °C. The crude material was purified by flash chromatography on silica gel (eluted with hexanes to EtOAc:hexanes = 2:98) to give the product (22.9 mg, 88% yield) as a white solid. R_f = 0.33 (hexanes). The NMR spectral data match the previously published data.⁴²



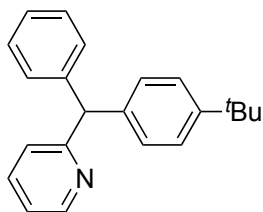
3.3eb – 9-Phenyl-9H-xanthene: The reaction was performed following General Procedure I with **3.1e** (18.2 mg, 0.1 mmol, 1 equiv), $\text{KN}(\text{SiMe}_3)_2$ (59.8 mg, 0.30 mmol, 3 equiv) and **3.2b** (20.4 μL , 0.2 mmol, 2 equiv) in the presence of 5 mol % Pd catalyst in THF at 24 °C.

The crude material was purified by flash chromatography on silica gel (eluted with hexanes to EtOAc:hexanes = 5:95) to give the product (20.6 mg, 80% yield) as a white solid. R_f = 0.33 (EtOAc:hexanes = 2:98). The NMR spectral data match the previously published data.⁵⁰



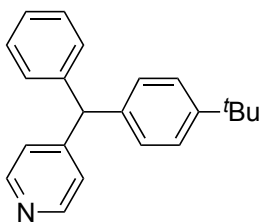
3.3fb – (3-Benzhydryl)pyridine: The reaction was performed following General Procedure I with **3.1f** (16.1 μL , 0.1 mmol, 1 equiv), $\text{KN}(\text{SiMe}_3)_2$ (59.8 mg, 0.30 mmol, 3 equiv) and **3.2b** (20.4 μL , 0.2 mmol, 2 equiv) in the presence of 5 mol % Pd catalyst in THF at 24 °C.

The crude material was purified by flash chromatography on silica gel (eluted with EtOAc:hexanes = 2:8) to give the product (24.6 mg, 99% yield) as a white solid. R_f = 0.2 (EtOAc:hexanes = 2:98). The NMR spectral data match the previously published data.⁴⁷



3.3ga – (4-tert-Butylphenyl)(2-pyridyl)phenylmethane: The reaction was performed following General Procedure I with **3.1g** (16.1 μL , 0.1 mmol, 1 equiv), $\text{LiN}(\text{SiMe}_3)_2$ (50.2 mg, 0.30 mmol, 3

equiv) and **3.2a** (33.4 μL , 0.2 mmol, 2 equiv) in the presence of 5 mol % Pd catalyst in THF at 24 °C. The crude material was purified by flash chromatography on silica gel (eluted with EtOAc:hexanes = 5:95 to 1:9) to give the product (23.5 mg, 78% yield) as a colorless oil. R_f = 0.30 (EtOAc:hexanes = 1:9). The NMR spectral data match the previously published data.⁴²



3.3ha – (4-*tert*-Butylphenyl)(4-pyridyl)phenylmethane: The reaction was performed following General Procedure I with **3.1h** (15.9 μL , 0.095 mmol, 1 equiv), $\text{LiN}(\text{SiMe}_3)_2$ (50.2 mg, 0.30 mmol, 3 equiv) and **3.2a** (33.4 μL , 0.2 mmol, 2 equiv) in the presence of 5 mol % Pd catalyst in THF at 24 °C. The crude material was purified by flash chromatography on silica gel (eluted with EtOAc:hexanes = 2:8) to give the product (21.7 mg, 76% yield) as a colorless oil. R_f = 0.20 (EtOAc:hexanes = 2:8). The NMR spectral data match the previously published data.⁴²

3.5 References

- (1) (a) Littke, A. F.; Fu, G. C. *Angew. Chem., Int. Ed.* **2002**, *41*, 4176. (b) Whitcombe, N. J.; Hii, K. K.; Gibson, S. E. *Tetrahedron* **2001**, *57*, 7449. (c) Bedford, R. B.; Cazin, C. S. J.; Holder, D. *Coord. Chem. Rev.* **2004**, *248*, 2283.
- (2) (a) Fu, G. C. *Acc. Chem. Res.* **2008**, *41*, 1555. (b) Martin, R.; Buchwald, S. L. *Acc. Chem. Res.* **2008**, *41*, 1461. (c) Surry, D. S.; Buchwald, S. L. *Angew. Chem., Int. Ed.* **2008**, *47*, 6338. (d) Christmann, U.; Vilar, R. N. *Angew. Chem., Int. Ed.* **2005**, *44*, 366.
- (3) Suzuki coupling at 70 °C: (a) Liu, S.-Y.; Choi, M. J.; Fu, G. C. *Chem. Commun.* **2001**, 2408. Suzuki coupling at 60 °C, 5 examples with moderate yields (\leq 57% by GC): (b) Pickett, T. E.; Richards, C. J. *Tetrahedron Lett.* **2001**, *42*, 3767. (c) Pickett, T. E.; Roca,

F. X.; Richards, C. J. *J. Org. Chem.* **2003**, *68*, 2592. Suzuki coupling at 90 °C, 2 examples with moderate yields ($\leq 57\%$ by GC): (d) Pramick, M. R.; Rosemeier, S. M.; Beranek, M. T.; Nickse, S. B.; Stone, J. J.; Stockland, R. A.; Baldwin, S. M.; Kastner, M. E. *Organometallics* **2003**, *22*, 523. Suzuki coupling at ≥ 110 °C: (e) Kwong, F. Y.; Chan, K. S.; Yeung, C. H.; Chan, A. S. C. *Chem. Commun.* **2004**, 2336. Suzuki coupling at ≥ 50 °C and Heck reaction at ≥ 110 °C: (f) Iwasawa, T.; Komano, T.; Tajima, A.; Tokunaga, M.; Obora, Y.; Fujihara, T.; Tsuji, Y. *Organometallics* **2006**, *25*, 4665. Suzuki coupling at ≥ 75 °C (2 examples) and Heck reaction at 120 °C (1 example): (g) Iwasawa, T.; Kamei, T.; Watanabe, S.; Nishiuchi, M.; Kawamura, Y. *Tetrahedron Lett.* **2008**, *49*, 7430. Suzuki coupling at 60 °C: (h) Fujihara, T.; Yoshida, S.; Terao, J.; Tsuji, Y. *Org. Lett.* **2009**, *11*, 2121. Suzuki coupling at ≥ 110 °C: (i) So, C. M.; Chow, W. K.; Choy, P. Y.; Lau, C. P.; Kwong, F. Y. *Chem.-Eur. J.* **2010**, *16*, 7996. (j) Barder, T. E.; Walker, S. D.; Martinelli, J. R.; Buchwald, S. L. *J. Am. Chem. Soc.* **2005**, *127*, 4685.

(4) (a) Barrios-Landeros, F.; Hartwig, J. F. *J. Am. Chem. Soc.* **2005**, *127*, 6944. (b) Barrios-Landeros, F.; Carrow, B. P.; Hartwig, J. F. *J. Am. Chem. Soc.* **2009**, *131*, 8141. (c) Lewis, A. K. de K.; Caddick, S.; Cloke, F. G. N.; Billingham, N. C.; Hitchcock, P. B.; Leonard, J. *J. Am. Chem. Soc.* **2003**, *125*, 10066. (d) Galardon, E.; Ramdeehul, S.; Brown, J. M.; Cowley, A.; Hii, K. K.; Jutand, A. *Angew. Chem., Int. Ed.* **2002**, *41*, 1760. See references on computational studies of oxidative addition of aryl chlorides to Pd(0): (e) Schoenebeck, F.; Houk, K. N. *J. Am. Chem. Soc.* **2010**, *132*, 2496. (f) Senn, H. M.; Ziegler, T. *Organometallics* **2004**, *23*, 2980. (g) Kozuch, S.; Amatore, C.; Jutand, A.; Shaik, S. *Organometallics* **2005**, *24*, 2319. (h) Ahlquist, M.; Norrby, P.-O. *Organometallics* **2007**, *26*, 550.

(5) Reference (1)a and references therein.

- (6) Portnoy, M.; Milstein, D. *Organometallics* **1993**, *12*, 1665. Note that the oxidative addition of 10-fold excess of PhCl to Pd(dipp)₂ required 90 °C to go to completion in 2 h in dioxane. The temperature range of the kinetic measurements was 30–70 °C.
- (7) Aryl tosylates oxidatively add to Pd(chelate)₂: (a) Roy, A. H.; Hartwig, J. F. *J. Am. Chem. Soc.* **2003**, *125*, 8704. Aryl bromides oxidatively add to Pd(chelate)₂: (b) Alcazar-Roman, L. M.; Hartwig, J. F.; Rheingold, A. L.; Liable-Sands, L. M.; Guzei, I. A. *J. Am. Chem. Soc.* **2000**, *122*, 4618. (c) Amatore, C.; Broeker, G.; Jutand, A.; Khalil, F. *J. Am. Chem. Soc.* **1997**, *119*, 5176. (d) Jutand, A.; Hii, K. K.; Thornton-Pett, M.; Brown, J. M. *Organometallics* **1999**, *18*, 5367.
- (8) van der Veen, L. A.; Keeven, P. H.; Schoemaker, G. C.; Reek, J. N. H.; Kamer, P. C. J.; van Leeuwen, P. W. N. M.; Lutz, M.; Spek, A. L. *Organometallics* **2000**, *19*, 872.
- (9) Note that transition metal/main group metal bimetallic activation mode of sp² C–X bonds has rarely been reported. The Nakamura group disclosed that in the reaction of a lithium diorganocuprate(I) with an alkenyl bromide, the sp² C–Br bond was activated by Cu(I) and Li(I) synergistically. See: (a) Yoshikai, N.; Nakamura, E. *J. Am. Chem. Soc.* **2004**, *126*, 12264. (b) Yoshikai, N.; Iida, R.; Nakamura, E. *Adv. Synth. Catal.* **2008**, *350*, 1063. The same group later reported that in nickel-catalyzed cross-coupling reactions of aryl electrophiles and Grignard reagents, the sp² C–X bonds (X=F, Cl, carbamates, phosphates, etc.) were activated via a nickel/magnesium bimetallic cooperative mechanism. See: (c) Yoshikai, N.; Matsuda, H.; Nakamura, E. *J. Am. Chem. Soc.* **2009**, *131*, 9590.
- (10) (a) McGrew, G. I.; Temaismithi, J.; Carroll, P. J.; Walsh, P. J. *Angew. Chem., Int. Ed.* **2010**, *49*, 5541. (b) McGrew, G. I.; Stanciu, C.; Zhang, J.; Carroll, P. J.; Dreher, S. D.; Walsh, P. J. *Angew. Chem., Int. Ed.* **2012**, *51*, 11510. (c) Zhang, J.; Stanciu, C.; Wang,

B.; Hussain, M. M.; Da, C.-S.; Carroll, P. J.; Dreher, S. D.; Walsh, P. J. *J. Am. Chem. Soc.* **2011**, *133*, 20552.

(11) (a) Zhang, J.; Bellomo, A.; Creamer, A. D.; Dreher, S. D.; Walsh, P. J. *J. Am. Chem. Soc.* **2012**, *134*, 13765. (b) Bellomo, A.; Zhang, J.; Trongsirawat, N.; Walsh, P. J. *Chem. Sci.* **2013**, *4*, 849. (c) Hussain, N.; Frensch, G.; Zhang, J.; Walsh, P. J. *Angew. Chem., Int. Ed.* **2014**, *53*, 3693.

(12) (a) Jia, T.; Bellomo, A.; EL Baina, K.; Dreher, S. D.; Walsh, P. J. *J. Am. Chem. Soc.* **2013**, *135*, 3740. (b) Zheng, B.; Jia, T.; Walsh, P. J. *Org. Lett.* **2013**, *15*, 1690. (c) Zheng, B.; Jia, T.; Walsh, P. J. *Org. Lett.* **2013**, *15*, 4190. (d) Zheng, B.; Jia, T.; Walsh, P. J. *Adv. Synth. Catal.* **2014**, *356*, 165. (e) Montel, S.; Jia, T.; Walsh, P. J. *Org. Lett.* **2014**, *16*, 130. (f) Montel, S.; Raffier, L.; He, Y.; Walsh, P. J. *Org. Lett.* **2014**, *16*, 1446.

(13) Bordwell, F. G. *Acc. Chem. Res.* **1988**, *21*, 456.

(14) (a) Ryss, P.; Zollinger, H. *Fundamentals of the Chemistry and Application of Dyes*; Wiley-Interscience: New York, 1972. (b) Katritzky, A. R.; Gupta, V.; Garot, C.; Stevens, C. V.; Gordeev, M. F. *Heterocycles* **1994**, *38*, 345. (c) Muthyala, R.; Katritzky, A. R.; Lan, X. F. *Dyes Pigm.* **1994**, *25*, 303.

(15) (a) Aldag, R. *Photochromism: Molecules and Systems*; Dürr, H., Bouas-Laurent, H., Eds.; Elsevier: London, 1990. (b) Irie, M. *J. Am. Chem. Soc.* **1983**, *105*, 2078. (c) Herron, N.; Johansson, G. A.; Radu, N. S.; U.S. Patent Application 2005/0187364, Aug 25, 2005. (d) Xu, Y. Q.; Lu, J. M.; Li, N. J.; Yan, F.; Xia, X. W.; Xu, Q. F. *Eur. Polym. J.* **2008**, *44*, 2404.

(16) (a) Das, S. K.; Panda, G.; Chaturvedi, V.; Manju, Y. S.; Galkwad, A. K.; Sinha, S. *Bioorg. Med. Chem. Lett.* **2007**, *17*, 5586. (b) Panda, G.; Shagufta; Mishra, J. K.; Chaturvedi, V.; Srivastava, A. K.; Srivastava, R.; Srivastava, B. S. *Bioorg. Med. Chem.* **2004**, *12*, 5269. (c) Parai, M. K.; Panda, G.; Chaturvedi, V.; Manju, Y. K.; Sinha, S.

Bioorg. Med. Chem. Lett. **2008**, *18*, 289. (d) Shagufta; Srivastava, A. K.; Sharma, R.; Mishra, R.; Balapure, A. K.; Murthy, P. S. R.; Panda, G. *Bioorg. Med. Chem.* **2006**, *14*, 1497. (e) Palchaudhuri, R.; Hergenrother, P. J. *Bioorg. Med. Chem. Lett.* **2008**, *18*, 5888. (f) Palchaudhuri, R.; Nesterenko, V.; Hergenrother, P. J. *J. Am. Chem. Soc.* **2008**, *130*, 10274. (g) Risberg, K.; Guldvik, I. J.; Palchaudhuri, R.; Xi, Y. G.; Ju, J. F.; Fodstad, O.; Hergenrother, P. J.; Andersson, Y. *J. Immunother.* **2011**, *34*, 438. (h) Al-Qawasmeh, R. A.; Lee, Y.; Cao, M. Y.; Gu, X. P.; Vassilakos, A.; Wright, J. A.; Young, A. *Bioorg. Med. Chem. Lett.* **2004**, *14*, 347.

(17) For reviews: (a) Duxbury, D. F. *Chem. Rev.* **1993**, *93*, 381. (b) Shchepinov, M. S.; Korshun, V. A. *Chem. Soc. Rev.* **2003**, *32*, 170. (c) Nair, V.; Thomas, S.; Mathew, S. C.; Abhilash, K. G. *Tetrahedron* **2006**, *62*, 6731.

(18) (a) Schnitzer, R. J.; Hawking, F. *Experimental Chemotherapy*; Academic Press: New York, 1963; Vol. I. (b) Greene, T. W.; Wuts, P. G. M. *Protective Groups in Organic Synthesis*, 3rd ed.; Wiley: New York, 1999. (c) Wulff, H.; Miller, M. J.; Hansel, W.; Grissmer, S.; Cahalan, M. D.; Chandy, K. G. *Proc. Natl. Acad. Sci. U.S.A.* **2000**, *97*, 8151. (d) Hernandez, A. I.; Balzarini, J.; Karlsson, A.; Camarasa, M. J.; Perez-Perez, M. J. *J. Med. Chem.* **2002**, *45*, 4254. (e) Ellsworth, B. A.; Ewing, W. R.; Jurica, E. U.S. Patent Application 2011/0082165 A1, Apr 7, 2011. (f) Mullen, L. M. A.; Duchowicz, P. R.; Castro, E. A. *Chemom. Intell. Lab. Syst.* **2011**, *107*, 269. (g) Rodriguez, D.; Ramesh, C.; Henson, L. H.; Wilmeth, L.; Bryant, B. K.; Kadavakollu, S.; Hirsch, R.; Montoya, J.; Howell, P. R.; George, J. M.; Alexander, D.; Johnson, D. L.; Arterburn, J. B.; Shuster, C. B. *Bioorg. Med. Chem.* **2011**, *19*, 5446. (h) Bobko, A. A.; Dhimitruka, I.; Zweier, J. L.; Khramtsov, V. V. *Angew. Chem., Int. Ed.* **2014**, *53*, 2735.

(19) (a) Reetz, M. T.; Kühling, K. M.; Deege, A.; Hinrichs, H.; Belder, D. *Angew. Chem., Int. Ed.* **2000**, *39*, 3891. (b) Trapp, O.; Weber, S. K.; Bauch, S.; Hofstadt, W. *Angew.*

Chem., Int. Ed. **2007**, 46, 7307. (c) Dreher, S. D.; Dormer, P. G.; Sandrock, D. L.; Molander, G. A. *J. Am. Chem. Soc.* **2008**, 130, 9257. (d) Davies, I. W.; Welch, C. J. *Science* **2009**, 325, 701. (e) Robbins, D. W.; Hartwig, J. F. *Science* **2011**, 333, 1423. (f) McNally, A.; Prier, C. K.; MacMillan, D. W. C. *Science* **2011**, 334, 1114. (g) Bellomo, A.; Celebi-Olcum, N.; Bu, X.; Rivera, N.; Ruck, R. T.; Welch, C. J.; Houk, K. N.; Dreher, S. D. *Angew. Chem., Int. Ed.* **2012**, 51, 6912.

(20) (a) Spokoyny, A. M.; Lewis, C. D.; Teverovskiy, G.; Buchwald, S. L. *Organometallics* **2012**, 31, 8478. (b) Spokoyny, A. M.; Machan, C. W.; Clingerman, D. J.; Rosen, M. S.; Wiester, M. J.; Kennedy, R. D.; Stern, C. L.; Sarjeant, A. A.; Mirkin, C. A. *Nat. Chem.* **2011**, 3, 590.

(21) Marimuthu, T.; Bala, M. D.; Friedrich, H. B. *Acta Cryst.* **2008**, E64, o711.

(22) (a) Hartwig, J. F. *Nature* **2008**, 455, 314. (b) Surry, D. S.; Buchwald, S. L. *Chem. Sci.* **2011**, 2, 27. (c) Hartwig, J. F. *Acc. Chem. Res.* **2008**, 41, 1534. (d) Schlummer, B.; Scholz, U. *Adv. Synth. Catal.* **2004**, 346, 1599. (e) Buchwald, S. L.; Mauger, C.; Mignani, G.; Scholz, U. *Adv. Synth. Catal.* **2006**, 348, 23.

(23) Poirier, V.; Roisnel, T.; Carpentier, J.-F.; Sarazin, Y. *Dalton Trans.* **2009**, 9820.

(24) (a) Hoffman, B. M.; Lukoyanov, D.; Dean, D. R.; Seefeldt, L. C. *Acc. Chem. Res.* **2013**, 46, 587. (b) Horn, B.; Pfirrmann, S.; Limberg, C.; Herwig, C.; Braun, B.; Mebs, S.; Metzinger, R. *Z. Anorg. Allg. Chem.* **2011**, 637, 1169. (c) Ding, K.; Pierpont, A. W.; Brennessel, W. W.; Lukat-Rodgers, G.; Rodgers, K. R.; Cundari, T. R.; Bill, E.; Holland, P. L. *J. Am. Chem. Soc.* **2009**, 131, 9471.

(25) (a) Yin, J.; Buchwald, S. L. *J. Am. Chem. Soc.* **2002**, 124, 6043. (b) Fujita, K.-I.; Yamashita, M.; Puschmann, F.; Alvarez-Falcon, M. M.; Incarvito, C. D.; Hartwig, J. F. *J. Am. Chem. Soc.* **2006**, 128, 9044.

(26) Klingensmith, L. M.; Strieter, E. R.; Barder, T. E.; Buchwald, S. L. *Organometallics* **2006**, *25*, 82.

(27) Biscoe, M. R.; Fors, B. P.; Buchwald, S. L. *J. Am. Chem. Soc.* **2008**, *130*, 6686.

(28) See leading references on palladacycles used as precatalysts for cross-coupling reactions with aryl chlorides: (a) Herrmann, W. A.; Brossmer, C.; Ofele, K.; Reisinger, C.-P.; Priermeier, T.; Beller, M.; Fischer, H. *Angew. Chem., Int. Ed. Engl.* **1995**, *34*, 1844. (b) Beller, M.; Fischer, H.; Herrmann, W. A.; Ofele, K.; Brossmer, C. *Angew. Chem., Int. Ed. Engl.* **1995**, *34*, 1848. (c) Schnyder, A.; Indolese, A. F.; Studer, M.; Blaser, H.-U. *Angew. Chem., Int. Ed.* **2002**, *41*, 3668.

(29) (a) Bruno, N. C.; Tudge, M. T.; Buchwald, S. L. *Chem. Sci.* **2013**, *4*, 916. (b) Bruno, N. C.; Buchwald, S. L. *Org. Lett.* **2013**, *15*, 2876.

(30) Note that due to the coordinatively flexible nature of the Xantphos framework, both *cis*- and *trans*-isomers of (Xantphos)Pd(II) complexes are known in literature, depending on the nature of the other substituents bound to the Pd(II) center. In several complexes Xantphos can even have different chelating modes between solid state and solution. Furthermore, (Xantphos)Pd(II) complexes can show equilibrium between *cis*- and *trans*-isomers in solution. (Xantphos)Pd(*acyl*)(halide): (a) Martinelli, J. R.; Watson, D. A.; Freckmann, D. M. M.; Barder, T. E.; Buchwald, S. L. *J. Org. Chem.* **2008**, *73*, 7102. (b) Miloserdov, F. M.; Grushin, V. V. *Angew. Chem., Int. Ed.* **2012**, *51*, 3668. (Xantphos)Pd(*aryl*)(halide) and related (Xantphos)Pd(II) complexes: (c) reference (22)a. (d) reference (22)b. (e) Zuideveld, M. A.; Swenneshuis, B. H. G.; Boele, M. D. K.; Guari, Y.; van Strijdonck, G. P. F.; Reek, J. N. H.; Kamer, P. C. J.; Goubitz, K.; Fraanje, J.; Lutz, M.; Spek, A. L.; van Leeuwen, P. W. N. M. *J. Chem. Soc., Dalton Trans.* **2002**, 2308. (f) Grushin, V. V.; Marshall, W. J. *J. Am. Chem. Soc.* **2006**, *128*, 12644.

(31) Seminal publications on aldol reaction: (a) Kane, R. *J. Prakt. Chem.* **1838**, *15*, 129.

(b) Kane, R. *Ann. Phys. Chem. Ser. 2* **1838**, *44*, 475.

(32) For reviews on arylation of activated C(sp³)-H bonds: (a) Bellina, F.; Rossi, R. *Chem. Rev.* **2010**, *110*, 1082. (b) Johansson, C. C. C.; Colacot, T. J. *Angew. Chem., Int. Ed.* **2010**, *49*, 676. (c) Culkin, D. A.; Hartwig, J. F. *Acc. Chem. Res.* **2003**, *36*, 234. (d) Novák, P.; Martin, R. *Curr. Org. Chem.* **2011**, *15*, 3233. (e) Burtoloso, A. C. B. *Synlett* **2009**, 320.

(33) For examples of Pd-catalyzed direct arylation of phenols: (a) Bates, R. W.; Gabel, C. J.; Ji, J. H.; Ramadevi, T. *Tetrahedron* **1995**, *51*, 8199. (b) Kawamura, Y.; Satoh, T.; Miura, M.; Nomura, M. *Chem. Lett.* **1999**, 961. (c) Kataoka, N.; Shelby, Q.; Stambuli, J. P.; Hartwig, J. F. *J. Org. Chem.* **2002**, *67*, 5553. (d) Burgos, C. H.; Barder, T. E.; Huang, X. H.; Buchwald, S. L. *Angew. Chem., Int. Ed.* **2006**, *45*, 4321. (e) Hu, T. J.; Schulz, T.; Torborg, C.; Chen, X. R.; Wang, J.; Beller, M.; Huang, J. *Chem. Commun.* **2009**, 7330. (f) Beydoun, K.; Doucet, H. *Catal. Sci. Technol.* **2011**, *1*, 1243. (g) Platon, M.; Cui, L. C.; Mom, S.; Richard, P.; Saeys, M.; Hierso, J. C. *Adv. Synth. Catal.* **2011**, *353*, 3403. (h) Xiao, B.; Gong, T. J.; Liu, Z. J.; Liu, J. H.; Luo, D. F.; Xu, J.; Liu, L. *J. Am. Chem. Soc.* **2011**, *133*, 9250.

(34) For examples of Pd-catalyzed N-arylation of indoles: (a) Hartwig, J. F.; Kawatsura, M.; Hauck, S. I.; Shaughnessy, K. H.; Alcazar-Roman, L. M. *J. Org. Chem.* **1999**, *64*, 5575. (b) Old, D. W.; Harris, M. C.; Buchwald, S. L. *Org. Lett.* **2000**, *2*, 1403. (c) Grasa, G. A.; Viciu, M. S.; Huang, J. K.; Nolan, S. P. *J. Org. Chem.* **2001**, *66*, 7729.

(35) For examples of Pd-catalyzed C-2- and C-3-arylation of indoles: (a) Lane, B. S.; Sames, D. *Org. Lett.* **2004**, *6*, 2897. (b) Lane, B. S.; Brown, M. A.; Sames, D. *J. Am. Chem. Soc.* **2005**, *127*, 8050. (c) Deprez, N. R.; Kalyani, D.; Krause, A.; Sanford, M. S. *J. Am. Chem. Soc.* **2006**, *128*, 4972. (d) Djakovitch, L.; Dufaud, V.; Zaidi, R. *Adv. Synth.*

Catal. **2006**, *348*, 715. (e) Toure, B. B.; Lane, B. S.; Sames, D. *Org. Lett.* **2006**, *8*, 1979. (f) Wang, X.; Gribkov, D. V.; Sames, D. *J. Org. Chem.* **2007**, *72*, 1476. (g) Bellina, F.; Benelli, F.; Rossi, R. *J. Org. Chem.* **2008**, *73*, 5529. (h) Yang, S. D.; Sun, C. L.; Fang, Z.; Li, B. H.; Li, Y. Z.; Shi, Z. J. *Angew. Chem., Int. Ed.* **2008**, *47*, 1473. (i) Zhao, J. L.; Zhang, Y. H.; Cheng, K. *J. Org. Chem.* **2008**, *73*, 7428. (j) Liang, Z. J.; Yao, B. B.; Zhang, Y. H. *Org. Lett.* **2010**, *12*, 3185.

(36) Klingensmith, L. M.; Strieter, E. R.; Barder, T. E.; Buchwald, S. L. *Organometallics* **2006**, *25*, 82.

(37) Yin, J.; Buchwald, S. L. *J. Am. Chem. Soc.* **2002**, *124*, 6043.

(38) Li, D.; Kagan, G.; Hopson, R.; Williard, P. G. *J. Am. Chem. Soc.* **2009**, *131*, 5627.

(39) Cabrita, E. J.; Berger, S. *Magn. Reson. Chem.* **2001**, *39*, S142–S148.

(40) (a) Gaussian 09, Revision A.02, M. J. Frisch, G. W. Trucks, H. B. Schlegel, G. E. Scuseria, M. A. Robb, J. R. Cheeseman, G. Scalmani, V. Barone, B. Mennucci, G. A. Petersson, H. Nakatsuji, M. Caricato, X. Li, H. P. Hratchian, A. F. Izmaylov, J. Bloino, G. Zheng, J. L. Sonnenberg, M. Hada, M. Ehara, K. Toyota, R. Fukuda, J. Hasegawa, M. Ishida, T. Nakajima, Y. Honda, O. Kitao, H. Nakai, T. Vreven, J. A. Montgomery, Jr., J. E. Peralta, F. Ogliaro, M. Bearpark, J. J. Heyd, E. Brothers, K. N. Kudin, V. N. Staroverov, R. Kobayashi, J. Normand, K. Raghavachari, A. Rendell, J. C. Burant, S. S. Iyengar, J. Tomasi, M. Cossi, N. Rega, J. M. Millam, M. Klene, J. E. Knox, J. B. Cross, V. Bakken, C. Adamo, J. Jaramillo, R. Gomperts, R. E. Stratmann, O. Yazyev, A. J. Austin, R. Cammi, C. Pomelli, J. W. Ochterski, R. L. Martin, K. Morokuma, V. G. Zakrzewski, G. A. Voth, P. Salvador, J. J. Dannenberg, S. Dapprich, A. D. Daniels, O. Farkas, J. B. Foresman, J. V. Ortiz, J. Cioslowski, and D. J. Fox, Gaussian, Inc., Wallingford CT, 2009. (b) Glendening, E. D.; Reed, A. E.; Carpenter, J. E.; Weinhold, F. NBO Version 3.1.

- (41) Dreher, S. D.; Dormer, P. G.; Sandrock, D. L.; Molander, G. A. *J. Am. Chem. Soc.* **2008**, *130*, 9257.
- (42) Zhang, J.; Bellomo, A.; Creamer, A. D.; Dreher, S. D.; Walsh, P. J. *J. Am. Chem. Soc.* **2012**, *134*, 13765.
- (43) Bistrzycki, A.; Gyr, J. *Chem. Ber.* **1904**, *37*, 1245.
- (44) Zhou, L.; Yang, H.; Wang, P. *J. Org. Chem.* **2011**, *76*, 5873.
- (45) Bordwell, F. G.; Cheng, J.-P.; Satish, A. V.; Twyman, C. L. *J. Org. Chem.* **1992**, *57*, 6542.
- (46) Bellomo, A.; Zhang, J.; Trongsirawat, N.; Walsh, P. J. *Chem. Sci.* **2013**, *4*, 849.
- (47) Xia, Y.; Hu, F.; Liu, Z.; Qu, P.; Ge, R.; Ma, C.; Zhang, Y.; Wang, J. *Org. Lett.* **2013**, *15*, 1784.
- (48) Saito, S.; Ohwada, T.; Shudo, K. *J. Org. Chem.* **1996**, *61*, 8089.
- (49) Bowden, S. T.; Beynon, K. I. *J. Chem. Soc.* **1957**, 4253.
- (50) Yoshida, H.; Watanabe, M.; Fukushima, H.; Ohshita, J.; Kunai, A. *Org. Lett.* **2004**, *6*, 4049.

Chapter 4

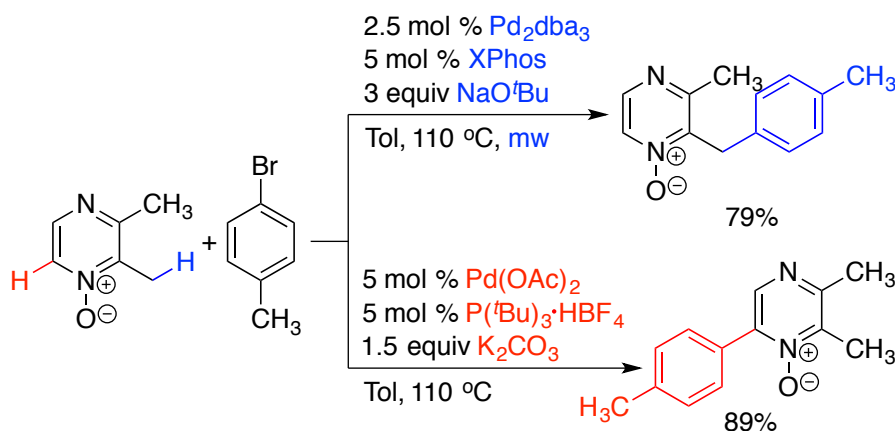
Site-Selective sp^2 and sp^3 C–H Functionalization: Divergent Palladium-Catalyzed C3 and Benzylic Direct Arylation of 2-Substituted Furans

4.1 Introduction

Metal-catalyzed cross-coupling reactions to form C–C bonds are a mainstay in the preparation of small molecules, which have applications ranging from biological studies to treatment of human disease, and have an increasing contribution to the syntheses of complex bioactive targets and natural products.¹⁻³ Traditional cross-coupling methods generally require prefunctionalization of the coupling partners, consisting of an organometallic reagent and an aryl halide or pseudohalide. Compared with traditional cross-coupling methods, catalytic C–H functionalization has emerged as a more efficient and atom-economical synthetic approach in organic synthesis.⁴⁻¹⁷ A particularly appealing and yet challenging aspect of this approach is the selective functionalization of distinct C–H bonds of a substrate, and thus introduction of multiple functional groups at precise locations. How can chemists control site selectivity to form multiple products when more than one type of C–H bond can potentially be functionalized? Most current reports are still limited to achieving single-site reactivity with high yield. Recently a few examples of selective multi-site reactivity have been reported, the majority of which are focused on *regioselective* sp^2 vs sp^2 (such as *ortho* vs *meta* vs *para* position of arenes, C2/C5 vs C3/C4 position of five-membered heteroaromatics, etc.) and sp^3 vs sp^3 (such as α - vs β -arylation of carbonyl compounds) sites.¹⁸⁻²⁰ A common strategy to control multi-site selectivity involves appropriately

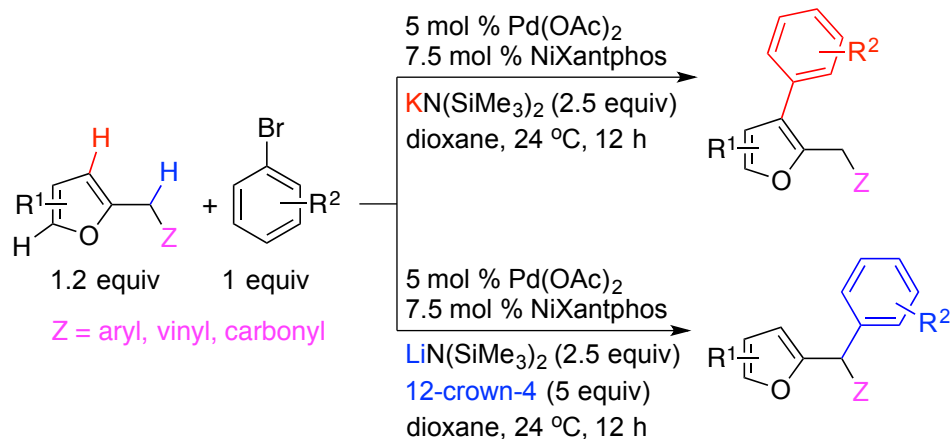
placed directing groups to direct reactivity. The addition and removal of directing groups often offsets any gain in synthetic efficiency provided by the direct functionalization. In contrast, for organic compounds which contain ostensibly unreactive sp^2 and sp^3 C–H bonds, orthogonal *chemoselective* functionalization of sp^2 vs sp^3 sites has received considerably less attention and remains a formidable challenge. From the ubiquity of various types of C–H bonds in organic compounds, it is clear that precise, highly selective, multi-site direct functionalization is one of the most significant challenges facing chemists.

Fagnou and co-workers have described site-selective arylation reactions at both sp^2 and benzylic sp^3 sites of azine and diazine *N*-oxide substrates (Scheme 4.1).²¹⁻²⁴ The multi-site reactivity was achieved using two significantly different sets of reaction conditions, including different Pd sources, ligands, bases, and heating methods (oil bath vs microwave reactor). The origin of multi-site reactivity was ascribed to two different mechanisms of the C–H bond cleavage step: (1) sp^3 C–H bond deprotonation by base, and (2) the palladium-assisted concerted metallation-deprotonation (CMD) pathway for sp^2 C–H bond cleavage.



Scheme 4.1 Site-selective sp^2 and benzylic sp^3 C–H arylation of *N*-oxide

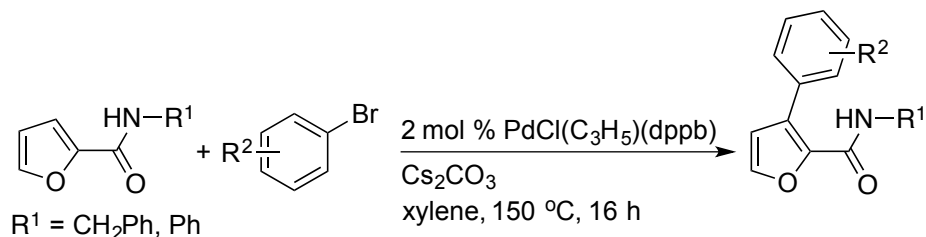
Compared with Fagnou's strategy to screen all reaction parameters, we envision that *chemoselective* functionalization of sp^2 vs sp^3 sites may be controlled by a simpler strategy. Herein, we describe room-temperature palladium-catalyzed site-selective arylation reactions of both sp^2 and sp^3 sites of 2-substituted furan derivatives (Scheme 4.2). Combination of a 2-substituted furan substrate, a $MN(SiMe_3)_2$ base (M = main group counteranion), an aryl bromide and a palladium catalyst $[Pd(OAc)_2/NiXantphos]$ in dioxane at room temperature enables access to either sp^2 or sp^3 C–H arylation products with *complete* site selectivity. Surprisingly, the *complete* site selectivity is governed simply by choice of the main group counteranion M (from $MN(SiMe_3)_2$) while other reaction parameters are exactly the same. Such a subtle change results in exclusive sp^2 C3–H arylation products when $M = K$, and exclusive sp^3 benzylic C–H arylation products when $M = Li, Na$, and crown ether–alkali metal (Li, Na, K) adducts. Under our reaction conditions for site-selective sp^2 C3 and sp^3 benzylic arylations, the traditionally more reactive C5–H bond remains intact, illustrating the complementarity of our chemistry from traditional heteroaromatic functionalizations.^{5,25-31} We also demonstrate that the multi-site reactivity can be performed not only divergently to give monoarylation products at the precise positions, but also sequentially, affording hetero-diarylation products via both an sp^2/sp^3 and an sp^3/sp^2 arylation sequence. Furthermore, a convenient one-pot homo-diarylation protocol is also disclosed.



Scheme 4.2 Counteranion-controlled site-selective sp² C3–H and sp³ benzylic C–H arylation of furans

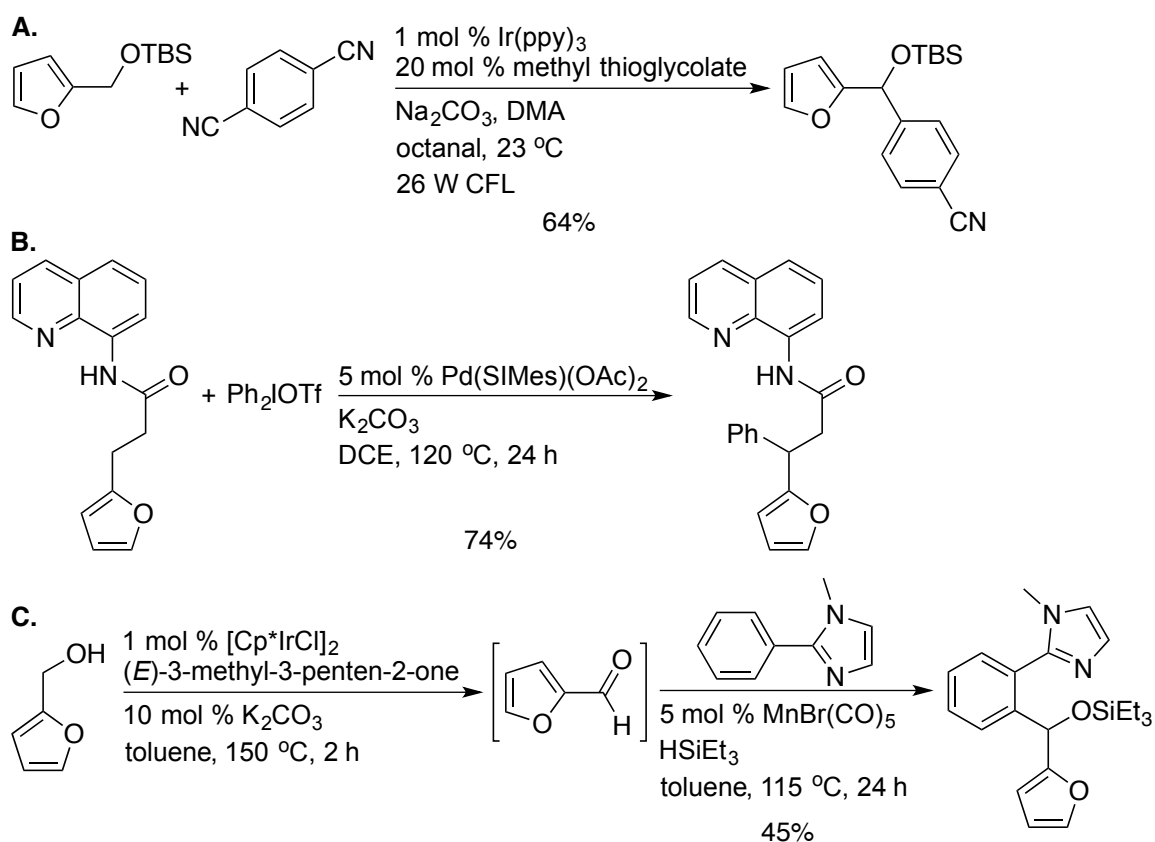
Furans are ubiquitous heterocycles, broadly found in naturally occurring and biologically active compounds.³²⁻³⁷

Background for C3–H arylation of furans: Due to the inherent reactivity of furan derivatives favoring reactions at C2/C5 over C3/C4, catalytic methods for the direct C2/C5–H arylation of furan derivatives have been widely explored.^{5,25-31} The more challenging “direct C3/C4” arylation products are achieved only by “indirect” multi-step synthesis, or by employing 2,5-disubstituted furan substrates or in intramolecular functionalizations where the C2/C5 position is not approachable.³⁸ Recently Doucet and co-workers reported high-temperature (150 °C) C3–H arylation of furan-2-carboxamides, where a secondary amide moiety (CONHR) served as a directing group for the C3 position overriding the C5–H arylation (Scheme 4.3).³⁹



Scheme 4.3 C3–H arylation of furan-2-carboxamides

Background for sp^3 benzylic C–H arylation of furans: To date, only 3 reports provide a single example each of sp^3 benzylic C–H arylation of furan derivatives, via (1) photoredox organocatalysis with TBS-protected furfuryl alcohol (Scheme 4.4A),⁴⁰ (2) palladium catalysis with *N*-3-(2-furyl)propoyl-8-aminoquinoline (Scheme 4.4B),⁴¹ and (3) tandem iridium/manganese catalysis with furfuryl alcohol (Scheme 4.4C).⁴² Our benzylic C–H arylation protocol for furan substrates, such as 2-benzylfuran derivatives, furnishes 2-furan-containing unsymmetrical triarylmethane products (Tables 4.4 and 4.5). These products are traditionally synthesized from Friedel–Crafts-type reactions of furans with unsymmetrical diarylmethanol derivatives.^{43,44}



Scheme 4.4 Example of sp^3 benzylic C–H arylation of furan derivatives

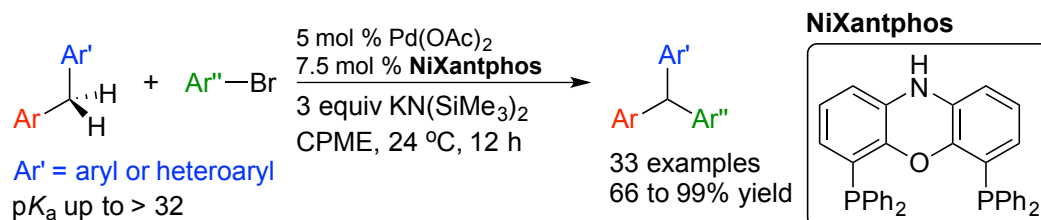
Our work described herein represents a novel, attractive, efficient alternative to gain rapid access to valuable furan-containing compounds that would be otherwise difficult to prepare by the existing protocols.

4.2 Results and Discussion

4.2.1 Initial Studies with 2-Benzylfuran

Our group recently initiated a program for the catalytic functionalization of substrates bearing weakly acidic sp^3 -hybridized C–H bonds via deprotonative cross-coupling processes (DCCP). They involve initial reversible deprotonation of the C–H bond by base, and the catalyst promotes the subsequent functionalization of the deprotonated species. Thus, DCCP is mechanistically distinct from C–H activation processes.

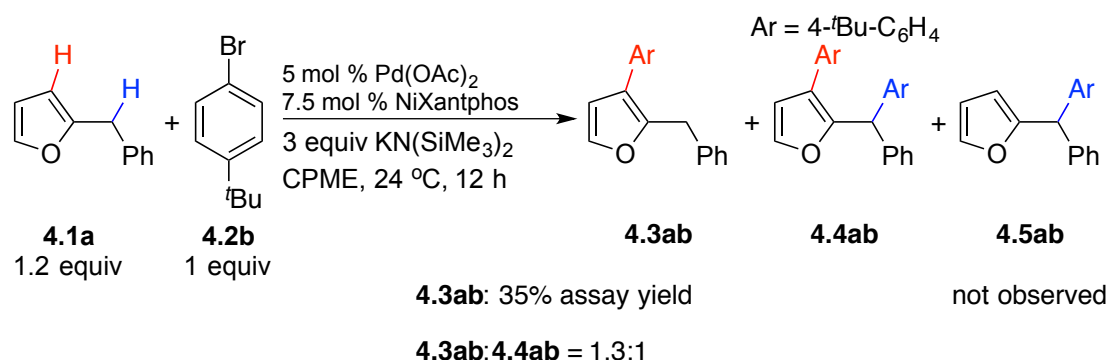
Diphenylmethane ($pK_a = 32.3^{45}$) and diarylmethane derivatives were arylated at room temperature with aryl bromides in the presence of $KN(SiMe_3)_2$ and a palladium catalyst bearing van Leeuwen's NiXantphos⁴⁶ (Scheme 4.5).^{47,48}



Scheme 4.5 DCCP of diarylmethanes with aryl bromides

When we subjected 2-benzylfuran (**4.1a**) and 1-bromo-4-*tert*-butylbenzene (**4.2b**) to the standard DCCP conditions, we were surprised to obtain a 1.3:1 ratio of an “unexpected” C3–H arylation product **4.3ab** (35% assay yield determined by ¹H NMR

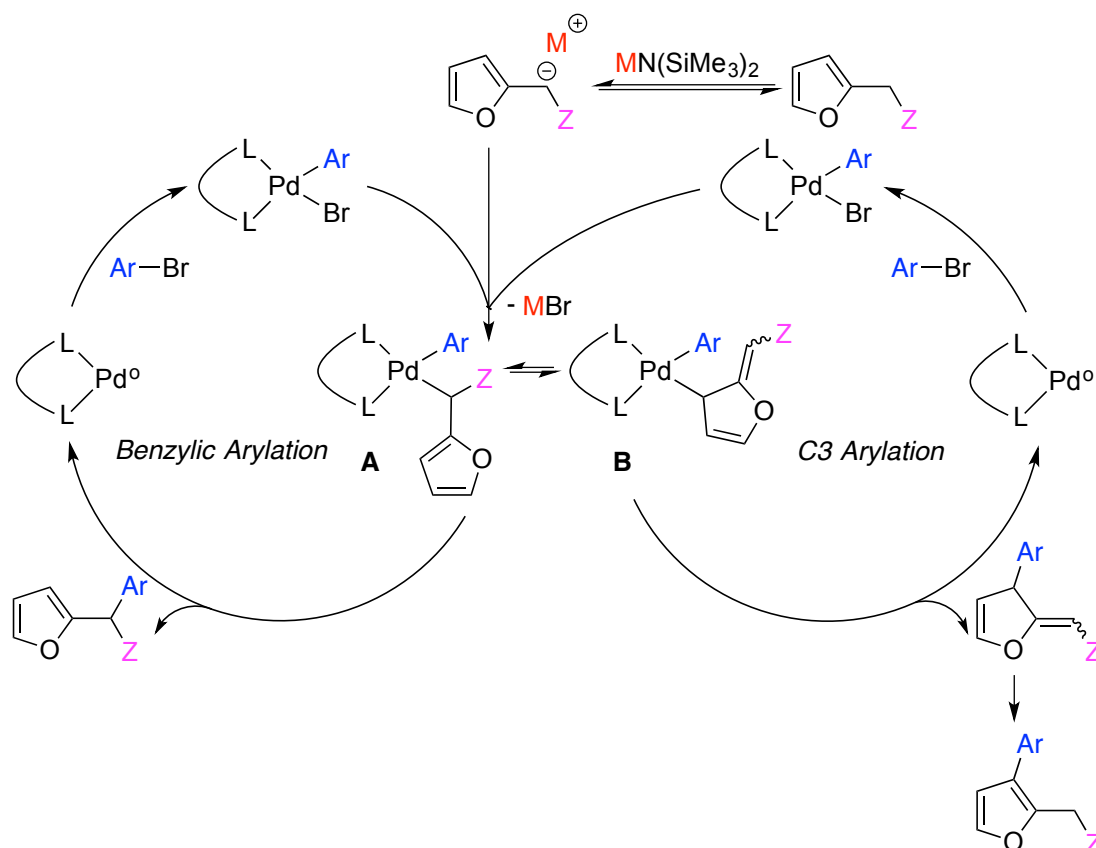
spectroscopy of the crude reaction mixture) to diarylation product **4.4ab**, without formation of the “expected” benzylic arylation product **4.5ab** or the C5–H arylation product (Scheme 4.6). The presence of **4.3ab** and **4.4ab** confirms both C3 and benzylic C–H bonds may undergo arylation reactions, which sheds light on site-selective C3 and benzylic arylations. Furthermore, the absence of the C5–H arylation product strongly suggests that our arylation pathway is different from the well-known furan arylation pathway at the C2/C5 position.



Scheme 4.6 Reaction of **4.1a** with **4.2b** under standard DCCP conditions

Based on the reaction pathway of DCCP,^{47,48} and the preliminary results in Scheme 4.6, we proposed a reaction pathway for the site-selective arylation products **4.3ab** and **4.5ab** (Scheme 4.7). Traditional C2/C5 arylation of furans with aryl halides requires a weak inorganic base, such as carbonate or acetate.^{5,25-31} As shown in Scheme 4.7, we envisioned that a strong base ($MN(SiMe_3)_2$) could reversibly deprotonate a 2-substituted furan substrate, the benzylic C–H bonds of which have a pK_a of 30.2.⁴⁵ Transmetalation of the metallated substrate to palladium generates intermediate **A**. Formation of the benzylic arylation product occurs via reductive elimination of **A** (Scheme 4.7, left). This pathway is similar to that of the palladium-catalyzed enolate arylation chemistry.⁴⁹⁻⁵¹ In contrast, due to the well-known low

aromaticity of furan derivatives,⁵² dearomatization/isomerization of **A** could reversibly form an intermediate **B**, which undergoes reductive elimination followed by rearomatization to afford the C3 arylation product (Scheme 4.7, right). The site selectivity is governed by the equilibrium of **A** and **B** and the relative rates of the reductive elimination step from **A** and **B**.



Scheme 4.7 Reaction pathways of benzylic and C3 arylations

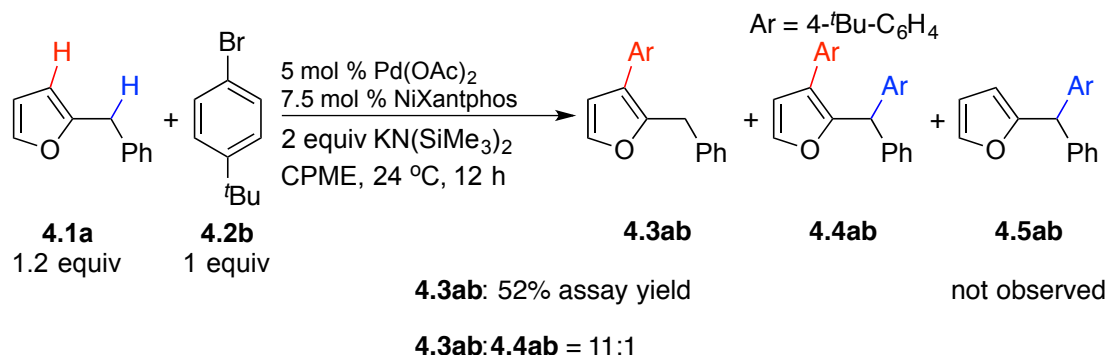
4.2.2 Development and Optimization of Palladium-Catalyzed C3 and Benzylic Arylations

Given that the working model points to a number of variables for reagents and conditions to be examined, we employed low-barrier microscale high-throughput

experimentation (HTE) techniques⁵³⁻⁵⁹ to perform the optimization in the most efficient manner.

First, we evaluated the reaction of 2-benzylfuran (**4.1a**) with 1-bromo-4-*tert*-butylbenzene (**4.2b**) using 23 common mono- and bidentate phosphine ligands on a 10 μ mol scale at 24 and 110 °C (see “4.4 Experimental Section” for details).ⁱ To our surprise, the other 22 ligands from the entire collection afforded <5% HPLC assay yield (AY) of the corresponding C3 arylation product **4.3ab**, without formation of diarylation product **4.4ab** or benzylic arylation product **4.5ab**. Included was the structurally similar bidentate ligand Xantphos, as well as dppf and BINAP, etc. The lead in HTE was NiXantphos as ligand at 24 °C, giving 21% HPLC AY of **4.3ab**. Translation of this lead to laboratory scale (0.1 mmol) under the same conditions rendered **4.3ab** in 35% AY (Scheme 4.6).

We reduced the equivalents of $\text{KN}(\text{SiMe}_3)_2$ from 3 to 2 equiv to decrease the amount of diarylation product **4.4ab**. As expected, **4.3ab** was obtained in 52% AY with an increase in the **4.3ab:4.4ab** ratio to 11:1 (Scheme 4.8).



Scheme 4.8 Reaction of **4.1a** with **4.2b** using 2 equiv of $\text{KN}(\text{SiMe}_3)_2$

ⁱ HTE screens in this section were performed in collaboration with Dr. Ana Bellomo at Penn/Merck Laboratory for High-Throughput Experimentation.

The second HTE survey was carried out to improve the yield of **4.3ab** using 6 palladium sources and 4 ethereal solvents (CPME, dioxane, THF, 2-MeTHF) under otherwise identical conditions as Scheme 4.8. Among the 4 solvents, dioxane proved to be the best solvent for both promoting C3 arylation and inhibiting diarylation. The combination of dioxane as solvent with 3 palladium sources afforded excellent HPLC AY of **4.3ab**: 100% AY from Pd(OAc)₂, 97% AY from Pd(COD)Cl₂, and 99% AY from Pd(NCMe)₂Cl₂. Because Pd(OAc)₂ is the least expensive among the 3 palladium sources, it was chosen to be translated to laboratory scale under the same conditions, affording the C3 arylation product **4.3ab** in 76.9% AY with a good **4.3ab**:**4.4ab** ratio (13.3:1, Table 4.1, entry 1). Increasing the equivalents of KN(SiMe₃)₂ from 2 to 2.5 equiv resulted in an excellent AY of **4.3ab** (92.6%) with an increase in the **4.3ab**:**4.4ab** ratio (14.2:1, entry 2). Compound **4.3ab** was ultimately isolated in 93% yield after flash chromatography. A similar AY (91.0%) was obtained using 3 equiv of KN(SiMe₃)₂ with a minor drop in the **4.3ab**:**4.4ab** ratio (13.6:1, entry 3 vs 2).

Table 4.1 Optimization of Pd-catalyzed C3 arylation of **4.1a**^a

entry	KN(SiMe ₃) ₂ (equiv)	4.3ab (%) ^b	4.3ab : 4.4ab ^b
1	2	76.9	13.3:1
2	2.5	92.6 (93 ^c)	14.2:1

3	3	91.0	13.6:1
---	---	------	--------

^aReactions conducted on a 0.1 mmol scale using 1.2 equiv of **4.1a**, 1 equiv of **4.2b** and KN(SiMe₃)₂ at 0.1 M. ^bYield determined by ¹H NMR spectroscopy of the crude reaction mixture. ^cIsolated yield after chromatographic purification.

After we screened reaction parameters including choice of catalyst (palladium source and ligand), temperature, solvent, and stoichiometry, we were able to obtain excellent reaction conditions for site-selective C3 arylation. This is “unexpected” because the reaction pathway involves dearomatization/isomerization of **A** to form **B**, reductive elimination, and rearomatization (Scheme 4.7, right). In contrast, the “expected” benzylic arylation (Scheme 4.7, left) was not achieved. As outlined in the proposed reaction pathway (Scheme 4.7), we were curious about the impact of the main group counteranions (M) on the dearomatization/isomerization step of **A**. *Do all main group counteranions give C3 arylation products?* Instead of moving on to determine the scope of C3 arylation, we next examined various main group counteranions (M = K, Na, Li with and without the corresponding crown ethers) under the optimized reaction conditions (Table 4.1, entry 2). As depicted in Table 4.2, we were surprised to find that *only the potassium counteranion* promoted site-selective C3 arylation of **4.1a** (Table 4.2, entry 1). In sharp contrast, the potassium counteranion caged with 18-crown-6 (1:2) afforded the benzylic arylation product **4.5ab** as the major product without formation of **4.3ab** (entry 2). Employing NaN(SiMe₃)₂ with and without 15-crown-5 both afforded benzylic arylation **4.5ab** as the major product, along with <5% production of **4.3ab** and **4.4ab** (entries 3 and 4). Interestingly, using LiN(SiMe₃)₂ as base did not promote any arylation reaction (entry 5), probably due to its inability to deprotonate the substrate **4.1a**.⁴⁸ The optimal conditions for **4.5ab** was obtained using LiN(SiMe₃)₂ with 12-crown-

4 (1:2) to afford 91% isolated yield of **4.5ab** with *complete* site-selectivity (entry 6). The results in Table 4.2 suggest the *complete* multi-site selectivity is governed by a simple factor, counteranion and its associated ligand. *The potassium counteranion* promoted the “unexpected” C3 arylation, while *the potassium-18-crown-6 adduct*, other main group counteranions (Na, Li), and their crown ether adducts promoted the “expected” benzylic arylation.

Table 4.2 Main group counteranion-controlled site-selective arylation of **4.1a**

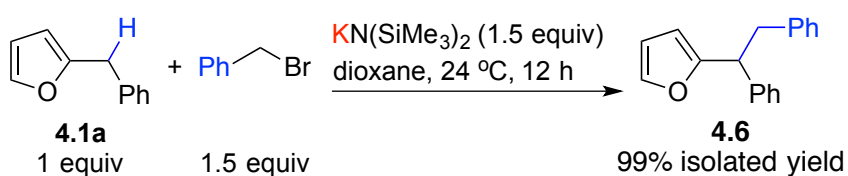
Ar = 4-^tBu-C₆H₄

entry	base	4.3ab (%) ^a	4.4ab (%) ^a	4.5ab (%) ^a
1	KN(SiMe ₃) ₂	92.6	6.5	0
2	KN(SiMe ₃) ₂ :18-crown-6 (1:2)	0	13.1	50.9
3	NaN(SiMe ₃) ₂	< 5	< 5	28.7
4	NaN(SiMe ₃) ₂ :15-crown-5 (1:2)	0	< 5	38.9
5	LiN(SiMe ₃) ₂	0	0	0
6	LiN(SiMe ₃) ₂ :12-crown-4 (1:2)	0	0	94.0 (91) ^b

^aYield was based on 0.1 mmol as determined by ¹H NMR spectroscopy of the crude reaction mixture. ^bIsolated yield after chromatographic purification.

To confirm our proposed C3 arylation pathway, we carried out the following two experiments. Deprotonation/benylation of **4.1a** with benzyl bromide using KN(SiMe₃)₂

as base afforded 99% isolated yield of the benzylation product **4.6** in dioxane at 24 °C (Scheme 4.9). This result shows that the inherent deprotonation site is the benzylic position, and thus the unique role of the potassium countercation for site-selective C3 arylation involves the isomerization of the palladium intermediates after the transmetallation step. Secondly, subjecting 2-methylfuran (pK_a , 43)⁴⁵ as substrate to the optimized reaction conditions (entries 1 and 6) resulted in no arylation product, confirming the necessity of reversible deprotonation.



Scheme 4.9 Deprotonation/benzylation of **4.1a** using $\text{KN(SiMe}_3)_2$

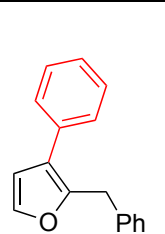
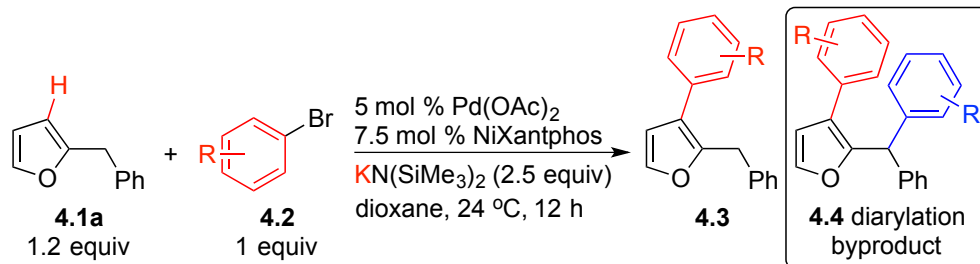
The optimized conditions (entries 1 and 6) were carried forward in the next phase, which focused on the determination of the scope of aryl bromides in Pd–NiXantphos catalyzed C3 and benzylic arylation reactions of furan derivatives.

4.2.3 Scope of Aryl Bromides in Pd–NiXantphos-Catalyzed C3 and Benzylic Arylations of **4.1a**

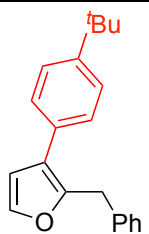
As shown in all cases in Table 4.3, by employing $\text{KN(SiMe}_3)_2$ as base, *complete* C3 selectivity was obtained with a variety of aryl bromides without observation of any benzylic arylation products. Good to excellent selectivity for mono- over diarylation was exhibited (C3:diarylation from 5:1 to > 20:1). All the C3 arylation products were separable from the diarylation byproducts by column chromatography, delivering **4.3aa–4.3ao** in 55–93% isolated yields. Excellent yields were obtained using bromobenzene (**4.2a**) and aryl bromides bearing 4-alkyl (**4.2b**), electron-donating 4-

methoxy and 4-*N,N*-dimethylamino (**4.2c**, **4.2d**) and electron-withdrawing 4-fluoro (**4.2e**) groups, with the C3:diarylation ratios $\geq 11:1$. 1-Bromo-4-chlorobenzene (**4.2f**) reacted with **4.1a** to produce C3 arylation product **4.3af** in 55% isolated yield with the C3:diarylation ratio of 13:1. No products derived from oxidative addition of Ar-Cl to palladium were observed. Trifluoromethyl (**4.2g**), methoxy (**4.2h**), and acetal (**4.2i**) groups at the *meta* position were all well-tolerated (65–77% yields) with moderate to good C3:diarylation ratios ($\geq 5:1$). The sterically hindered 1-bromonaphthalene and 2-bromotoluene (**4.2j**, **4.2k**) also participated in C3 arylation to produce the desired products (**4.3aj**, **4.3ak**) with excellent C3:diarylation ratios ($> 20:1$), probably because the steric bulk from the newly formed aryl groups at C3 position inhibited the second arylation. Aryl bromides containing a functional group such as acetyl (**4.2l**) and a heterocyclic moiety such as benzofuran (**4.2m**) and indole (**4.2n**, **4.2o**) were next examined. In these cases, remarkable C3:diarylation ratios were observed ($> 20:1$), delivering the desired products in 56–80% yields. To summarize, this method enables the synthesis of a wide range of C3 arylated furan derivatives from a variety of sterically and electronically diverse aryl and heteroaryl bromides.

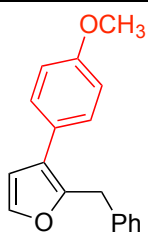
Table 4.3 Scope of aryl bromides in Pd-NiXantphos-catalyzed C3 arylation of **4.1a**^a



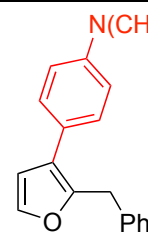
4.3aa 89%
(C3:di = 16:1)



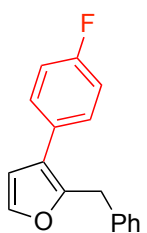
4.3ab 93%
(C3:di = 14:1)



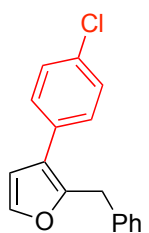
4.3ac 80%
(C3:di = 11:1)



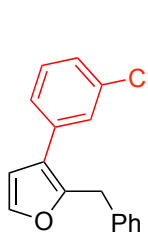
4.3ad 78%^b
(C3:di = 17:1)



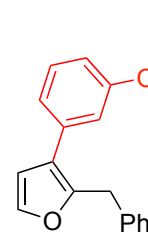
4.3ae 83%
(C3:di > 20:1)



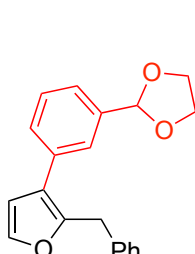
4.3af 55%
(C3:di = 13:1)



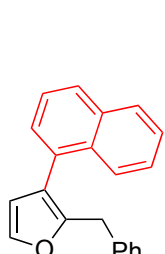
4.3ag 65%
(C3:di = 5:1)



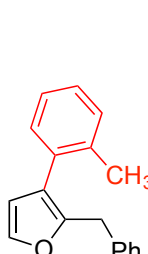
4.3ah 77%
(C3:di = 8:1)



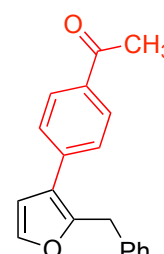
4.3ai 74%^c
(C3:di = 11:1)



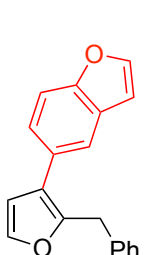
4.3aj 93%
(C3:di > 20:1)



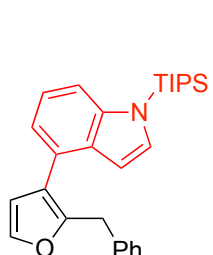
4.3ak 60%^d
(C3:di > 20:1)



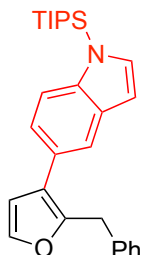
4.3al 80%^e
(C3:di > 20:1)



4.3am 64%
(C3:di > 20:1)



4.3an 56%^f
(C3:di > 20:1)



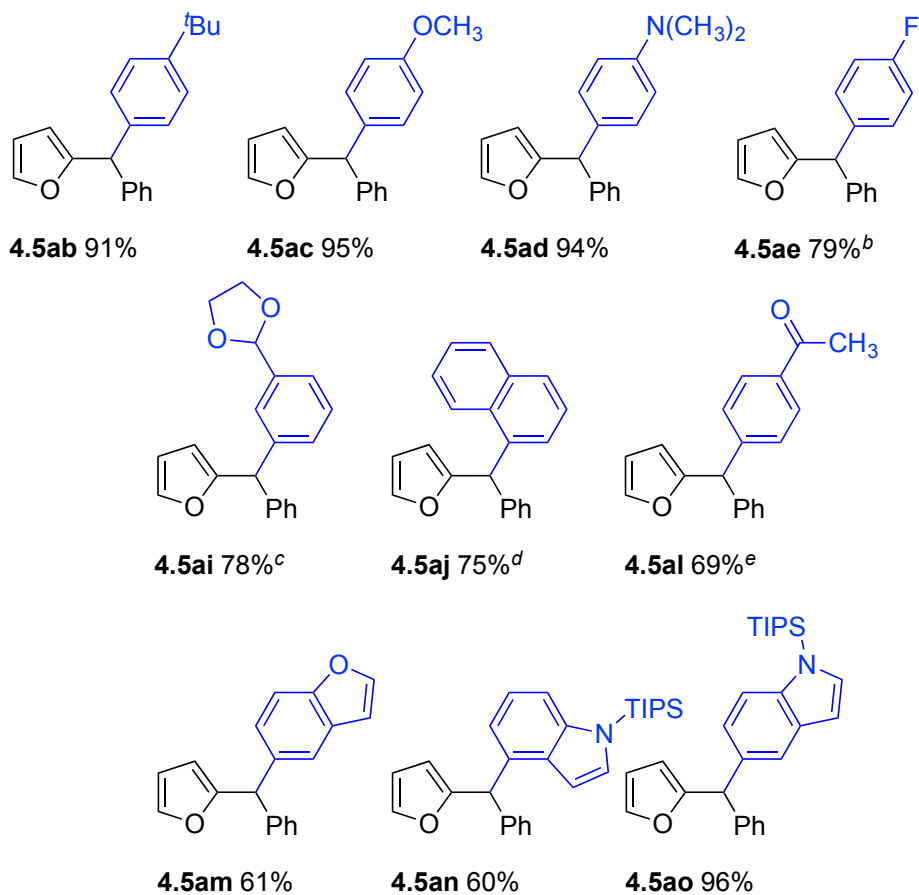
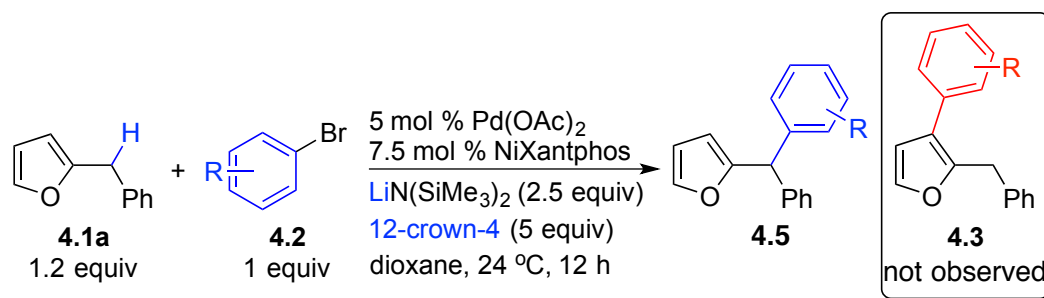
4.3ao 68%^b
(C3:di > 20:1)

^aReactions conducted on a 0.1 mmol scale using 1.2 equiv of **4.1a**, 2.5 equiv of KN(SiMe₃)₂, and 1 equiv of **4.2a–o** at 0.1 M. Isolated yield after chromatographic purification. The C3:diarylation ratios in the parentheses were determined by ¹H NMR spectroscopy of the crude reaction mixture. ^b45 °C. ^c2 equiv of KN(SiMe₃)₂. ^dReaction conducted on a 0.3 mmol scale. ^e3 equiv of KN(SiMe₃)₂. ^f10 mol % Pd(OAc)₂ and 15 mol % NiXantphos.

After demonstrating the scope of aryl bromides in Pd–NiXantphos-catalyzed C3 arylation of **4.1a** in Table 4.3, we next employed LiN(SiMe₃)₂ with 12-crown-4 (1:2) to survey the scope of aryl bromides in benzylic arylation of **4.1a**. As shown in Table 4.4, with the same aryl bromides used as cross-coupling partners, a *complete* reversal in selectivity towards benzylic arylation was observed. Neither C3 arylation nor diarylation products was observed in any case, rendering the exclusive formation of **4.5** in 60–96% yields. Aryl bromides bearing 4-alkyl (**4.2b**), electron-donating 4-methoxy and 4-*N,N*-dimethylamino (**4.2c**, **4.2d**), electron-withdrawing 4-fluoro (**4.2e**) and sterically hindered 1-naphthyl (**4.2j**) groups all proved to be good cross-coupling partners for the benzylic arylation. Furthermore, functional groups such as acetal (**4.2i**), acetyl (**4.2l**) and heterocycles such as benzofuran (**4.2m**) and indole (**4.2n**, **4.2o**) were well tolerated, delivering the corresponding products in 60–96% yields. The presence of these functional groups, and heterocycles including the furan moiety itself, presents opportunities to functionalize both the C3 and benzylic arylated furan derivatives further to synthesize complex molecules.

Table 4.4 Scope of aryl bromides in Pd–NiXantphos-catalyzed benzylic arylation of

4.1a^a



^aReactions conducted on a 0.1 mmol scale using 1.2 equiv of **4.1a**, 2.5 equiv of LiN(SiMe₃)₂, 5 equiv of 12-crown-4, and 1 equiv of **4.2** at 0.1 M. Isolated yield after chromatographic purification. ^b**4.1a**:LiN(SiMe₃)₂:12-crown-4:**4.2** = 2:1.5:3:1.

^c**4.1a**:LiN(SiMe₃)₂:12-crown-4:**4.2** = 2:2:4:1. ^d**4.1a**:LiN(SiMe₃)₂:12-crown-4:**4.2** = 1:2:4:2.

^e**4.1a**:LiN(SiMe₃)₂:12-crown-4:**4.2** = 1.2:3:6:1.

4.2.4 Scope of Furans in Pd-NiXantphos-Catalyzed C3 and Benzylic Arylations

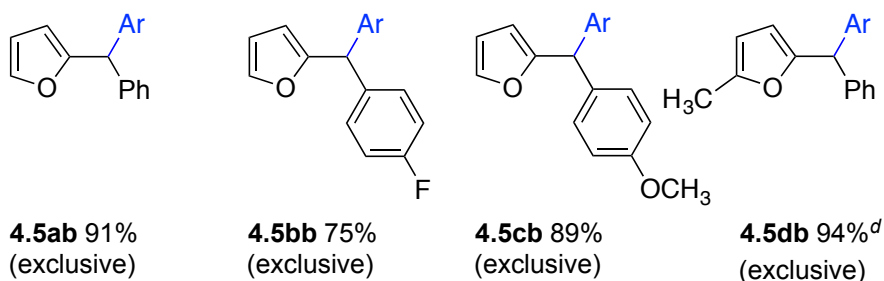
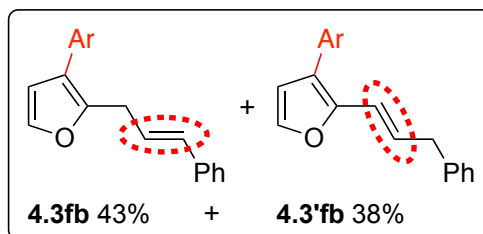
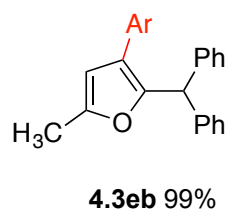
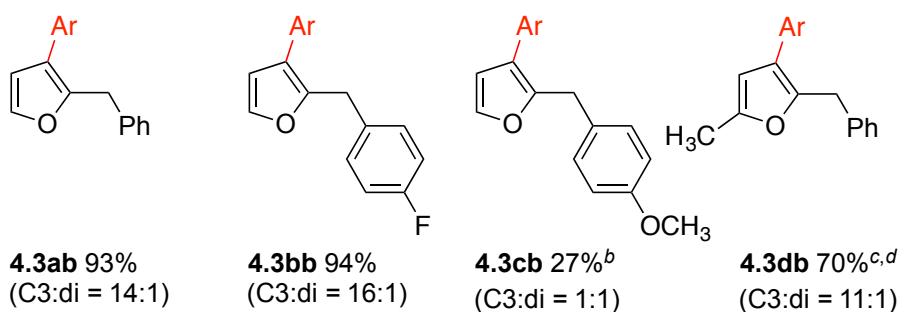
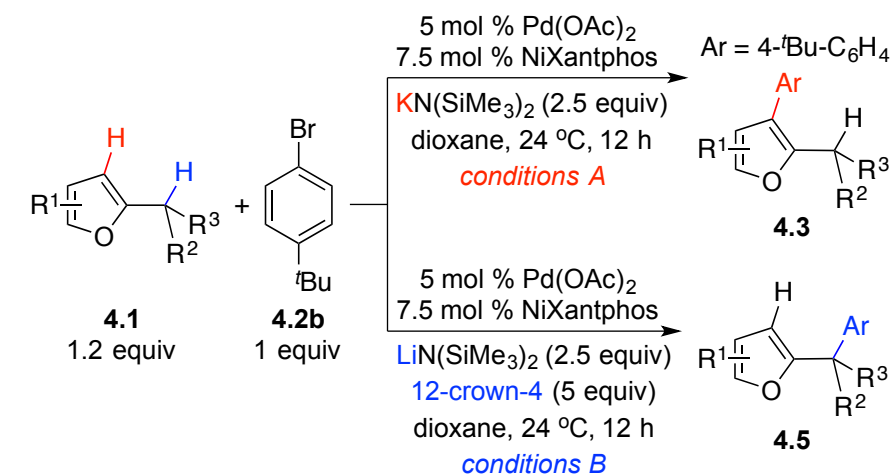
The scope of the C3 and benzylic arylations with respect to the 2-substituted furan derivatives was next explored with aryl bromide **4.2b** (Table 4.5). Again, no isomeric mixture of products from C3 and benzylic arylation was observed in any case. In general, conditions A afforded C3 arylation products **4.3**, which were separable from the diarylation byproducts by column chromatography, while conditions B afforded benzylic arylation products **4.5** exclusively. We studied the impact of electronic effects of the 2-substituent on the C3 and benzylic arylations. Varying the *para*-substituent on the phenyl group from H (**4.1a**) to F (**4.1b**) and OCH₃ (**4.1c**) resulted in excellent isolated yields of the benzylic arylation products (75–91%), suggesting that these 3 substrates were reversibly deprotonated and entered the catalytic cycle. In contrast, while **4.1a** and **4.1b** were able to deliver the C3 arylation products **4.3ab** and **4.3bb** in excellent yields and C3:diarylation ratios, the least acidic substrate **4.1c** gave only 27% AY of **4.3cb** as determined by ¹H NMR spectroscopy of the crude reaction mixture with the C3:diarylation ratio of 1:1, suggesting that under conditions A, half of the initial C3 arylation product **4.3cb** underwent the second arylation to form the byproduct **4.4cb**. In order to examine whether a C5–H bond was necessary for achieving multi-site selectivity, we subjected 2-benzyl-5-methylfuran (**4.1d**), the C5 position of which was blocked, to reaction conditions A and B. Both C3 and benzylic arylation products were obtained with excellent site selectivity. These results suggest that our counteranion-controlled multi-site selectivity does not require the presence of a C5–H bond to steer reactivity for C3 and benzylic arylations, further supporting our proposed working model. In the case of 2-benzhydrylfuran (**4.1e**, Table 4.5, R¹ = 5-CH₃, R² = R³ = Ph), we were concerned that the benzhydryl substituent might hinder deprotonation of the benzylic C–H bond by the bulky base, MN(SiMe₃)₂. However, C3 arylation proceeded smoothly to afford **4.3eb** in 99% isolated yield. This result has also demonstrated the promise of sequential

functionalization of 2-substituted furan derivatives to give hetero-diarylation products via an sp^3/sp^2 arylation sequence. We next examined the reactivity of an (*E*)-cinnamyl substituted furan substrate (**4.1f**). We proposed that the resulting carbanion from the deprotonation of the benzylic C–H bond of **4.1f** would undergo transmetalation to form the η^1 cinnamyl palladium intermediate **A**, and **A** would isomerize to form an η^1 benzyl palladium intermediate (Scheme 4.10). We were concerned that the isomerization process might prevent **A** from forming the productive intermediate, **B**, for C3 arylation (Scheme 4.7). To our surprise, the C3 arylation products (**4.3fb** and **4.3'fb**) were isolated in 81% total yield as isomers (43% and 38%, respectively). Note that **4.3fb** and **4.3'fb** were separable by column chromatography, and the double bond geometry in both was confirmed as *E*. It was not surprising the (*E*)-cinnamyl moiety isomerized to form regioisomers due to a reversible deprotonation/reprotonation process. The (*E*)-double bond in the side chain of the C3 arylation products (**4.3fb** and **4.3'fb**) could be further functionalized to install the C3-arylated furan moiety into complex molecules. In contrast, subjecting 2-(*E*)-cinnamylfuran (**4.1f**) to conditions B formed inseparable mixture of arylation products, as identified by the presence of multiple resonances in the olefinic and *tert*-butyl regions in the ^1H NMR spectrum of the crude reaction mixture. Our group recently reported a ligand-controlled regioselective α -arylation of allylarenes (Scheme 4.11).⁶⁰ In this report, we discovered that the Pd–NiXantphos catalyst system resulted in inseparable mixture of α - and γ -arylation products. Based on our experience, we believe that to achieve a highly regioselective α - and/or γ -arylation of **4.1f** should require a different catalyst.

Table 4.5 Scope of furans in Pd–NiXantphos-catalyzed C3 and benzylic arylations with

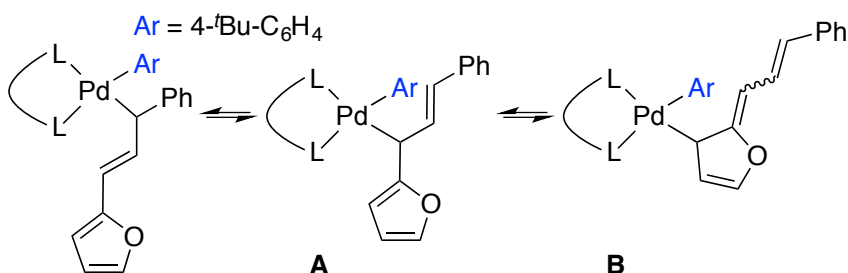
4.2a

232

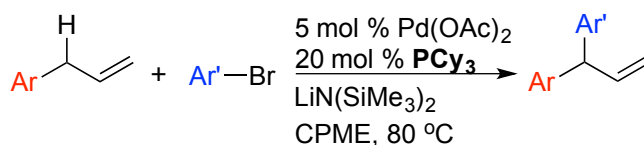


^aReactions conducted on a 0.1 mmol scale using 1.2 equiv of **4.1**, 2.5 equiv of KN(SiMe₃)₂ (conditions A) or 2.5 equiv of LiN(SiMe₃)₂, 5 equiv of 12-crown-4 (conditions B), and 1 equiv of **4.2b** at 0.1 M. Isolated yield after chromatographic purification. Data in the parentheses were determined by ¹H NMR spectroscopy of the crude reaction

mixture. ^bYield determined by ¹H NMR spectroscopy of the crude reaction mixture. ^c2.5 equiv of **4.1**. ^dCPME was used as solvent.



Scheme 4.10 Isomerization of palladium intermediates



Scheme 4.11 Regioselective α -arylation of allylarenes

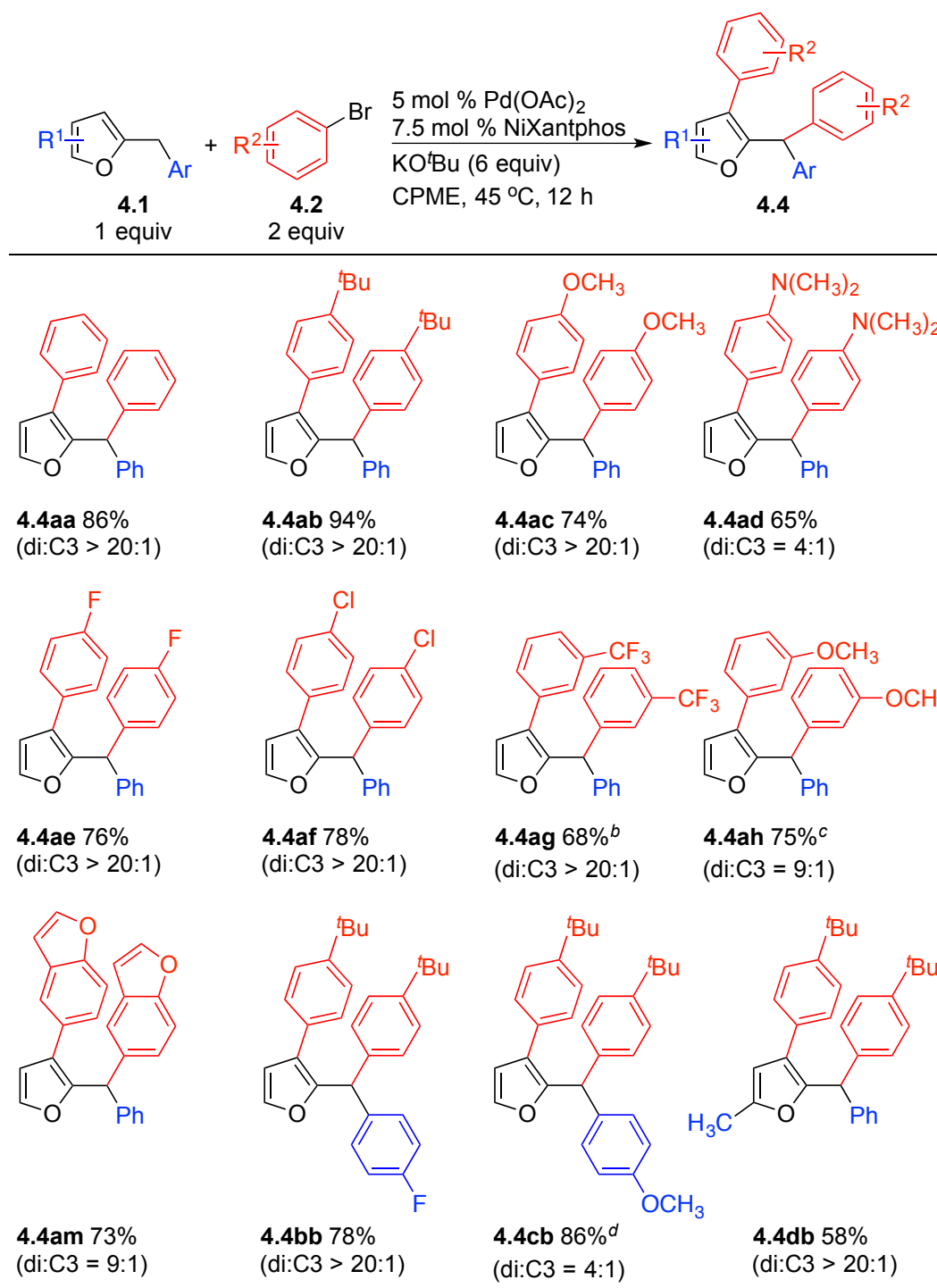
4.2.5 Pd–NiXantphos-Catalyzed Homo-Diarylations

After we established a broad scope of site-selective monoarylation reactions for both C3 and benzylic C–H bonds, we set out to develop a homo-diarylation protocol for the furan derivatives. The optimal diarylation conditions to obtain excellent yield and selectivity for di- over monoarylation were: combination of 1 equiv of furan substrate (**4.1**), 2 equiv of aryl bromide (**4.2**), and 6 equiv of KO^tBu as base in CPME as solvent at 45 °C (Table 4.6).

In all cases in Table 4.6, <5% of benzylic arylation product **4.5** was observed. The reaction conditions afforded the homo-diarylation products **4.4** with good to excellent di:C3 arylation ratios (> 20:1 unless otherwise mentioned), delivering **4.4** in 58–94% yields (76–97% per C–C bond formation). Note that products **4.4** were

separable from the C3 arylation byproducts **4.3** by column chromatography. In general, excellent di-:C3 arylation ratios and good yields of **4.4** were obtained using bromobenzene (**4.2a**) and aryl bromides bearing 4-alkyl (**4.2b**), electron-donating (**4.2c**, **4.2d**) and electron-withdrawing (**4.2e**, **4.2f**, **4.2g**) groups. *meta*-Methoxy group (**4.2h**) and a benzofuran moiety (**4.2m**) were also well-tolerated (75% and 73% yield, respectively) with good di-:C3 arylation ratios (both 9:1). Reaction of **4.1a** with the sterically hindered 1-bromonaphthalene and 2-bromotoluene (**4.2j**, **4.2k**), however, gave 38% assay yield of the C3 arylation product **4.3aj** with <10% formation of the diarylation product **4.4aj**, and gave 63% assay yield of **4.3ak** without formation of **4.4ak**. These two aryl bromides failed to give homo-diarylation products **4.4** due to the steric bulk from the first installed aryl groups at C3 position preventing the second arylation. Besides 2-benzylfuran (**4.1a**), other furan substrates with substituents at C5 and 2-benzyl group all delivered homo-diarylation products in 58–86% yields (**4.4bb**, **4.4cb**, **4.4db**).

Table 4.6 Pd–NiXantphos-catalyzed homo-diarylations



^aReactions conducted on a 0.1 mmol scale using 1 equiv of **4.1**, 6 equiv of KO^tBu, and 2 equiv of **4.2** at 0.1 M. Isolated yield after chromatographic purification. The di:C3 arylation ratios in the parentheses were determined by ¹H NMR spectroscopy of the

crude reaction mixture. ^b2.4 equiv of **4.1**. ^c1.2 equiv of **4.1**. ^d**4.1**:KN(SiMe₃)₂:**4.2** = 1.2:2.5:1 at 24 °C.

4.3 Conclusions

We have developed a room-temperature palladium-catalyzed site-selective arylation reactions of both sp² and sp³ sites of 2-substituted furan derivatives. A 2-substituted furan substrate reacted with an aryl bromide in the presence of a MN(SiMe₃)₂ base (M = main group counteranion) and a palladium catalyst [Pd(OAc)₂/NiXantphos] in dioxane at room temperature to form either sp² or sp³ C–H arylation products with *complete* site selectivity. Surprisingly, the *complete* site selectivity is not governed by reaction parameters such as a catalyst, but simply by choice of the main group counteranion M and crown ether while other reaction parameters are exactly the same. Such a subtle change results in exclusive sp² C3–H arylation products when M = K, and exclusive sp³ benzylic C–H arylation products when M = Li, Na, and crown ether–alkali metal (Li, Na, K) adducts.

Although the origin of the impact of M and crown ether on the site selectivity is not clear, we propose that the heterobimetallic (M–NiXantphos)Pd catalyst system may exhibit an electrostatic effect caused by the presence of the charged M and nitrogen atoms near the reaction site (see Chapter 3 for details), and impact the equilibrium of **A** and **B** and the relative rates of the reductive elimination step from **A** and **B**.

Direct arylation chemistry occurs preferentially at the C2/C5 position of furan derivatives when both C2/C5 and C3/C4 positions are available, due to the inherent reactivity favoring C2/C5 over C3/C4. In contrast to the traditional reaction pathway, our site-selective C–H arylation occurred at both C3 and benzylic sites of 2-substituted furan derivatives, while the more reactive C5–H bond remained intact, differentiating our

chemistry from traditional heteroaromatic functionalizations. No isomeric mixtures of products were observed, which rendered the isolation processes convenient and the products isolated in a pure form.

Our site-selective C–H arylation represents a novel, attractive, efficient protocol to gain rapid access to a variety of valuable furan-containing compounds that would be otherwise difficult to prepare by the existing methods. Functionalized furan derivatives are found widely in naturally occurring and biologically active compounds.

Additionally, we also demonstrate that the multi-site reactivity can be performed not only divergently to give monoarylation products at the precise positions, but also sequentially, affording hetero-diarylation products via both an sp^2/sp^3 and an sp^3/sp^2 arylation sequence. Furthermore, a convenient one-pot homo-diarylation protocol is also disclosed.

We believe the advantages and importance of the unprecedented strategy outlined in this report make it a valuable contribution in this field, and will inspire chemists to explore new strategies for future applications in the precise, highly selective, multi-site direct functionalization.

4.4 Experimental Section

General Methods. All reactions were performed under nitrogen using oven-dried glassware and standard Schlenk or vacuum line techniques. Air- and moisture-sensitive solutions were handled under nitrogen and transferred via syringe. Anhydrous CPME and dioxane were purchased from Sigma-Aldrich and used as solvent without further purification. Unless otherwise stated, reagents were commercially available and used as purchased without further purification. Chemicals were obtained from Sigma-Aldrich, Acros, TCI America or Alfa Aesar, and solvents were purchased from Fisher Scientific.

The progress of the reactions was monitored by thin-layer chromatography using Whatman Partisil K6F 250 μm precoated 60 Å silica gel plates and visualized by short-wavelength ultraviolet light as well as by treatment with ceric ammonium molybdate (CAM) stain or iodine. Silica gel (230–400 mesh, Silicycle) was used for flash chromatography. The ^1H NMR and $^{13}\text{C}\{^1\text{H}\}$ NMR spectra were obtained using a Brüker AM-500 Fourier-transform NMR spectrometer at 500 and 125 MHz, respectively. Chemical shifts are reported in units of parts per million (ppm) downfield from tetramethylsilane (TMS), and all coupling constants are reported in hertz. The infrared spectra were obtained with KBr plates using a Perkin-Elmer Spectrum 100 Series FTIR spectrometer. High-resolution mass spectrometry (HRMS) data were obtained on a Waters LC–TOF mass spectrometer (model LCT-XE Premier) using chemical ionization (CI) or electrospray ionization (ESI) in positive or negative mode, depending on the analyte. Melting points were determined on a Unimelt Thomas–Hoover melting point apparatus and are uncorrected.

Preparation of Furan Derivatives.

4.1a⁶¹, **4.1d**⁶², **4.1e**⁶³ and **4.1f**⁶⁴ were prepared according to literature procedures.

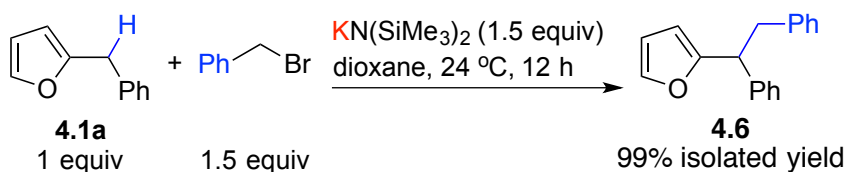
General Procedure A. *n*-BuLi (3.1 mL of a 2.5 M solution in hexanes, 7.7 mmol) was added to a solution of furan (0.53 mL, 7.3 mmol) in THF (10 mL) at 0 °C. The mixture was warmed and stirred for 4 h at 24 °C before benzyl bromide (0.83 mL, 7.0 mmol) was added dropwise. The resulting solution was stirred for 4 h at 24 °C, quenched with saturated aqueous NH_4Cl , and then diluted with 10 mL of Et_2O . The layers were separated and the aqueous layer was extracted with Et_2O (3 \times 10 mL). The organic layers were combined, washed with brine, dried over MgSO_4 , filtered, and concentrated

in vacuo. The crude material was loaded onto a silica gel column and purified by flash chromatography.

4.1b – 2-(4-fluorobenzyl)furan: General Procedure A was applied to furan (0.53 mL, 7.3 mmol), *n*-BuLi (7.7 mmol), and 4-fluorobenzyl bromide (0.87 mL, 7.0 mmol). The crude material was purified by flash chromatography on silica gel (eluted with hexanes) to give the product (1.03 g, 83% yield) as a colorless oil. $R_f = 0.5$ (hexanes); The NMR spectral data match the previously published data.⁶⁵

4.1c – 2-(4-methoxybenzyl)furan: General Procedure A was applied to furan (1.06 mL, 14.6 mmol), NaI (0.47 g, 22 mol %), *n*-BuLi (15.4 mmol), and 4-methoxybenzyl chloride (1.90 mL, 14.0 mmol) in THF (20 mL). The crude material was purified by flash chromatography on silica gel (eluted with EtOAc:hexanes = 2:98) to give the product (1.69 g, 64% yield) as a colorless oil. $R_f = 0.33$ (EtOAc:hexanes = 2:98); The NMR spectral data match the previously published data.⁶⁶

Deprotonation/Benzylation of 4.1a.



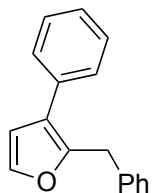
An oven-dried 10 mL reaction vial equipped with a stir bar was charged with KN(SiMe₃)₂ (29.9 mg, 0.15 mmol, 1.5 equiv) followed by 1 mL of dry dioxane under a nitrogen atmosphere. After stirring for 5 min at 24 °C, **4.1a** (15.1 μ L, 0.1 mmol, 1 equiv) was added to the reaction mixture followed by benzyl bromide (17.8 μ L, 0.15 mmol, 1.5 equiv). The reaction mixture was stirred for 12 h at 24 °C, quenched with three drops of

H₂O, diluted with 3 mL of ethyl acetate, and filtered over a pad of MgSO₄ and silica. The pad was rinsed with additional ethyl acetate, and the solution was concentrated in vacuo. The crude material was purified by flash chromatography on silica gel (eluted with EtOAc:hexanes = 1:99) to give the product **4.6** (24.6 mg, 99% yield) as a colorless oil. R_f = 0.33 (EtOAc:hexanes = 2:98); ¹H NMR (500 MHz, CDCl₃): δ 7.34 – 7.30 (m, 1H), 7.27 – 7.10 (m, 8H), 6.99 (d, *J* = 7.0 Hz, 2H), 6.26 (m, 1H), 6.04 (d, *J* = 3.0 Hz, 1H), 4.21 (t, *J* = 7.5 Hz, 1H), 3.44 (dd, *J* = 13.5, 7.5 Hz, 1H), 3.14 (dd, *J* = 13.5, 7.5 Hz, 1H) ppm; ¹³C{¹H} NMR (125 MHz, CDCl₃): δ 157.2, 142.3, 141.6, 139.9, 129.2, 128.6, 128.3, 128.2, 126.8, 126.3, 110.3, 106.2, 47.6, 41.5 ppm; IR (thin film): λ_{max} 3061, 3027, 2928, 1602, 1495, 1453, 1070, 1009, 730, 697 cm⁻¹; HRMS calc'd for C₁₈H₁₆O⁺ 248.1201, observed 248.1203 [M]⁺.

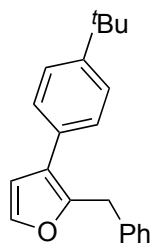
Procedure and Characterization for the Pd-Catalyzed C3 Arylation of 4.1a with Aryl Bromides.

General Procedure B. An oven-dried 10 mL reaction vial equipped with a stir bar was charged with KN(SiMe₃)₂ (49.9 mg, 0.25 mmol, 2.5 equiv) under a nitrogen atmosphere. A solution (from a stock solution) of Pd(OAc)₂ (1.12 mg, 0.0050 mmol, 5 mol %) and NiXantphos (4.14 mg, 0.0075 mmol, 7.5 mol %) in 1 mL of dry dioxane was taken up by syringe and added to the reaction vial. After stirring for 5 min at 24 °C, **4.1a** (18.1 μL, 0.12 mmol, 1.2 equiv) was added to the reaction mixture followed by 1-bromo-4-*tert*-butylbenzene (**4.2b**, 17.3 μL, 0.1 mmol, 1 equiv). Note that the aryl bromide in a solid form was added to the reaction vial prior to KN(SiMe₃)₂. The reaction mixture was stirred for 12 h at 24 °C, quenched with three drops of H₂O, diluted with 3 mL of ethyl acetate, and filtered over a pad of MgSO₄ and silica. The pad was rinsed with additional

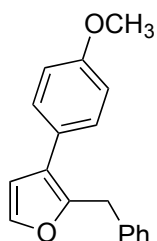
ethyl acetate, and the solution was concentrated in vacuo. The crude material was loaded onto a silica gel column and purified by flash chromatography.



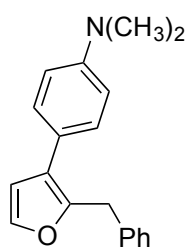
4.3aa – 2-benzyl-3-phenylfuran: The reaction was performed following General Procedure B with **4.1a** (18.1 μ L, 0.12 mmol, 1.2 equiv), $\text{KN}(\text{SiMe}_3)_2$ (49.9 mg, 0.25 mmol, 2.5 equiv) and **4.2a** (10.7 μ L, 0.1 mmol, 1 equiv) in the presence of 5 mol % Pd catalyst. Ratio of C3:di was determined to be 16:1 by ^1H NMR of the crude reaction mixture. The crude material was purified by flash chromatography on silica gel (eluted with hexanes to EtOAc:hexanes = 2:98) to give the product (20.8 mg, 89% yield) as a colorless oil. R_f = 0.3 (hexanes); The NMR spectral data match the previously published data.⁶⁷



4.3ab – 2-benzyl-3-(4-tert-butylphenyl)furan: The reaction was performed following General Procedure B with **4.1a** (18.1 μ L, 0.12 mmol, 1.2 equiv), $\text{KN}(\text{SiMe}_3)_2$ (49.9 mg, 0.25 mmol, 2.5 equiv) and **4.2b** (17.3 μ L, 0.1 mmol, 1 equiv) in the presence of 5 mol % Pd catalyst. Ratio of C3:di was determined to be 14:1 by ^1H NMR of the crude reaction mixture. The crude material was purified by flash chromatography on silica gel (eluted with hexanes to EtOAc:hexanes = 2:98) to give the product (27.0 mg, 93% yield) as a colorless oil. R_f = 0.33 (hexanes); ^1H NMR (500 MHz, CDCl_3): δ 7.43 – 7.36 (m, 3H), 7.36 – 7.27 (m, 4H), 7.24 – 7.18 (m, 3H), 6.55 (d, J = 2.0 Hz, 1H), 4.15 (s, 2H), 1.34 (s, 9H) ppm; $^{13}\text{C}\{^1\text{H}\}$ NMR (125 MHz, CDCl_3): δ 149.8, 149.3, 141.4, 138.8, 131.1, 128.8, 128.6, 127.6, 126.6, 125.8, 122.4, 111.6, 34.7, 33.1, 31.6 ppm; IR (thin film): λ_{max} 3029, 2963, 2867, 1603, 1521, 1495, 1454, 1363, 1269, 1142, 973, 835, 733 cm^{-1} ; HRMS calc'd for $\text{C}_{21}\text{H}_{22}\text{O}^+$ 290.1671, observed 290.1658 $[\text{M}]^+$.

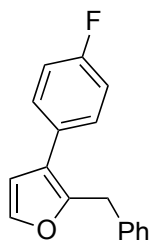


4.3ac – 2-benzyl-3-(4-methoxyphenyl)furan: The reaction was performed following General Procedure B with **4.1a** (18.1 μ L, 0.12 mmol, 1.2 equiv), $\text{KN}(\text{SiMe}_3)_2$ (49.9 mg, 0.25 mmol, 2.5 equiv) and **4.2c** (12.5 μ L, 0.1 mmol, 1 equiv) in the presence of 5 mol % Pd catalyst. Ratio of C3:di was determined to be 11:1 by ^1H NMR of the crude reaction mixture. The crude material was purified by flash chromatography on silica gel (eluted with hexanes to EtOAc:hexanes = 2:98) to give the product (21.2 mg, 80% yield) as a colorless oil. R_f = 0.25 (EtOAc:hexanes = 2:98); ^1H NMR (500 MHz, CDCl_3): δ 7.36 (d, J = 1.5 Hz, 1H), 7.34 – 7.26 (m, 4H), 7.25 – 7.17 (m, 3H), 6.94 – 6.88 (m, 2H), 6.51 (d, J = 2.0 Hz, 1H), 4.11 (s, 2H), 3.81 (s, 3H) ppm; $^{13}\text{C}\{^1\text{H}\}$ NMR (125 MHz, CDCl_3): δ 158.7, 148.9, 141.3, 138.8, 129.1, 128.8, 128.5, 126.59, 126.56, 122.1, 114.3, 111.6, 55.5, 33.0 ppm; IR (thin film): λ_{max} 2931, 2835, 1602, 1517, 1453, 1246, 1176, 1030, 831, 722 cm^{-1} ; HRMS calc'd for $\text{C}_{18}\text{H}_{17}\text{O}_2^+$ 265.1229, observed 265.1223 $[\text{MH}]^+$.

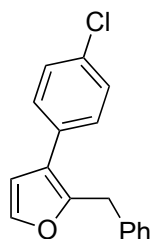


4.3ad – 2-benzyl-3-(4-N,N-dimethylaminophenyl)furan: The reaction was performed following General Procedure B with **4.1a** (18.1 μ L, 0.12 mmol, 1.2 equiv), $\text{KN}(\text{SiMe}_3)_2$ (49.9 mg, 0.25 mmol, 2.5 equiv) and **4.2d** (20.0 mg, 0.1 mmol, 1 equiv) in the presence of 5 mol % Pd catalyst at 45 $^\circ\text{C}$. Ratio of C3:di was determined to be 17:1 by ^1H NMR of the crude reaction mixture. The crude material was purified by flash chromatography on silica gel (eluted with hexanes to EtOAc:hexanes = 5:95) to give the product (21.7 mg, 78% yield) as a white solid. R_f = 0.2 (EtOAc:hexanes = 5:95); m.p. = 70–71 $^\circ\text{C}$; ^1H NMR (500 MHz, CDCl_3): δ 7.35 (d, J = 2.0 Hz, 1H), 7.32 – 7.26 (m, 4H), 7.25 – 7.19 (m, 3H), 6.79 – 6.72 (m, 2H), 6.51 (d, J = 2.0 Hz, 1H), 4.13 (s, 2H), 2.95 (s, 6H) ppm; $^{13}\text{C}\{^1\text{H}\}$ NMR (125 MHz,

CDCl₃): δ 149.6, 148.4, 141.2, 139.1, 128.73, 128.66, 128.55, 126.5, 122.4, 122.2, 112.9, 111.6, 40.8, 33.1 ppm; IR (thin film): λ_{\max} 3029, 2918, 2802, 2358, 1604, 1525, 1494, 1448, 1356, 1226, 1173, 1149, 1064, 821, 741, 723 cm⁻¹; HRMS calc'd for C₁₉H₂₀NO⁺ 278.1545, observed 278.1560 [MH]⁺.

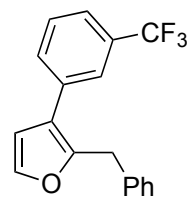


4.3ae – 2-benzyl-3-(4-fluorophenyl)furan: The reaction was performed following General Procedure B with **4.1a** (18.1 μ L, 0.12 mmol, 1.2 equiv), KN(SiMe₃)₂ (49.9 mg, 0.25 mmol, 2.5 equiv) and **4.2e** (11.0 μ L, 0.1 mmol, 1 equiv) in the presence of 5 mol % Pd catalyst. Ratio of C3:di was determined to be > 20:1 by ¹H NMR of the crude reaction mixture. The crude material was purified by flash chromatography on silica gel (eluted with hexanes to EtOAc:hexanes = 2:98) to give the product (20.9 mg, 83% yield) as a colorless oil. R_f = 0.25 (hexanes); ¹H NMR (500 MHz, CDCl₃): δ 7.38 (d, *J* = 2.0 Hz, 1H), 7.35 – 7.27 (m, 4H), 7.24 – 7.15 (m, 3H), 7.09 – 7.02 (m, 2H), 6.50 (d, *J* = 2.0 Hz, 1H), 4.10 (s, 2H) ppm; ¹³C{¹H} NMR (125 MHz, CDCl₃): δ 162.0 (d, *J* = 244.6 Hz), 149.4, 141.5, 138.6, 130.1 (d, *J* = 3.5 Hz), 129.5 (d, *J* = 8.0 Hz), 128.8, 128.5, 126.7, 121.7, 115.8 (d, *J* = 21.1 Hz), 111.6, 32.9 ppm; IR (thin film): λ_{\max} 1601, 1517, 1495, 1454, 1223, 835, 721 cm⁻¹; HRMS calc'd for C₁₇H₁₃OF⁺ 252.0950, observed 252.0953 [M]⁺.

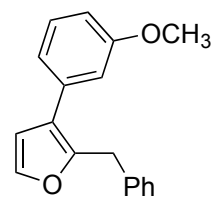


4.3af – 2-benzyl-3-(4-chlorophenyl)furan: The reaction was performed following General Procedure B with **4.1a** (18.1 μ L, 0.12 mmol, 1.2 equiv), KN(SiMe₃)₂ (49.9 mg, 0.25 mmol, 2.5 equiv) and **4.2f** (19.1 mg, 0.1 mmol, 1 equiv) in the presence of 5 mol % Pd catalyst. Ratio of C3:di was determined to be 13:1 by ¹H NMR of the crude reaction mixture. The crude material was purified by flash chromatography on silica gel (eluted with hexanes to EtOAc:hexanes =

2:98) to give the product (14.8 mg, 55% yield) as a colorless oil. $R_f = 0.4$ (EtOAc:hexanes = 2:98); $^1\text{H NMR}$ (500 MHz, CDCl_3): δ 7.39 (d, $J = 1.5$ Hz, 1H), 7.36 – 7.26 (m, 6H), 7.24 – 7.20 (m, 1H), 7.20 – 7.15 (m, 2H), 6.51 (d, $J = 1.5$ Hz, 1H), 4.11 (s, 2H) ppm; $^{13}\text{C}\{^1\text{H}\}$ NMR (125 MHz, CDCl_3): δ 149.7, 141.7, 138.4, 132.8, 132.6, 129.2, 129.0, 128.9, 128.5, 126.7, 121.5, 111.4, 33.0 ppm; IR (thin film): λ_{max} 3029, 2924, 2851, 1603, 1514, 1493, 1453, 1091, 971, 830, 738 cm^{-1} ; HRMS calc'd for $\text{C}_{17}\text{H}_{13}\text{OCl}^+$ 268.0655, observed 268.0647 $[\text{M}]^+$.

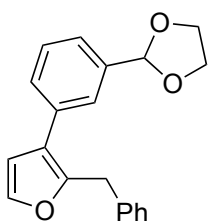


4.3ag – 2-benzyl-3-(3-trifluoromethylphenyl)furan: The reaction was performed following General Procedure B with **4.1a** (18.1 μL , 0.12 mmol, 1.2 equiv), $\text{KN}(\text{SiMe}_3)_2$ (49.9 mg, 0.25 mmol, 2.5 equiv) and **4.2g** (13.9 μL , 0.1 mmol, 1 equiv) in the presence of 5 mol % Pd catalyst. Ratio of C3:di was determined to be 5:1 by $^1\text{H NMR}$ of the crude reaction mixture. The crude material was purified by flash chromatography on silica gel (eluted with hexanes to EtOAc:hexanes = 2:98) to give the product (19.7 mg, 65% yield) as a colorless oil. $R_f = 0.25$ (hexanes); $^1\text{H NMR}$ (500 MHz, CDCl_3): δ 7.62 (s, 1H), 7.56 – 7.50 (m, 2H), 7.50 – 7.45 (m, 1H), 7.41 (d, $J = 2.0$ Hz, 1H), 7.33 – 7.28 (m, 2H), 7.25 – 7.18 (m, 3H), 6.56 (d, $J = 2.0$ Hz, 1H), 4.12 (s, 2H) ppm; $^{13}\text{C}\{^1\text{H}\}$ NMR (125 MHz, CDCl_3): δ 150.3, 141.8, 138.2, 134.9, 131.2 (q, $J = 32$ Hz), 131.1, 129.3, 128.9, 128.5, 126.8, 124.7 (q, $J = 4$ Hz), 124.3 (q, $J = 271$ Hz), 123.6 (q, $J = 4$ Hz), 121.3, 111.3, 33.1 ppm; IR (thin film): λ_{max} 3064, 3031, 2909, 1603, 1517, 1496, 1454, 1334, 1278, 1167, 1124, 1074, 896, 802, 739, 721, 699 cm^{-1} ; HRMS calc'd for $\text{C}_{18}\text{H}_{13}\text{OF}_3^+$ 302.0918, observed 302.0927 $[\text{M}]^+$.



4.3ah – 2-benzyl-3-(3-methoxyphenyl)furan: The reaction was performed following General Procedure B with **4.1a** (18.1 μL , 0.12

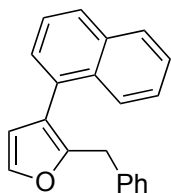
mmol, 1.2 equiv), $\text{KN}(\text{SiMe}_3)_2$ (49.9 mg, 0.25 mmol, 2.5 equiv) and **4.2h** (12.7 μL , 0.1 mmol, 1 equiv) in the presence of 5 mol % Pd catalyst. Ratio of C3:di was determined to be 8:1 by ^1H NMR of the crude reaction mixture. The crude material was purified by flash chromatography on silica gel (eluted with hexanes to EtOAc:hexanes = 2:98) to give the product (20.4 mg, 77% yield) as a colorless oil. $R_f = 0.3$ (EtOAc:hexanes = 2:98); ^1H NMR (500 MHz, CDCl_3): δ 7.38 (d, $J = 1.5$ Hz, 1H), 7.32 – 7.25 (m, 3H), 7.23 – 7.17 (m, 3H), 6.98 (d, $J = 7.5$ Hz, 1H), 6.91 (m, 1H), 6.82 (dd, $J = 8.5, 2.5$ Hz, 1H), 6.54 (d, $J = 1.5$ Hz, 1H), 4.15 (s, 2H), 3.75 (s, 3H) ppm; $^{13}\text{C}\{^1\text{H}\}$ NMR (125 MHz, CDCl_3): δ 160.0, 149.6, 141.5, 138.7, 135.5, 129.8, 128.8, 128.5, 126.6, 122.4, 120.4, 113.5, 112.5, 111.6, 55.4, 33.1 ppm; IR (thin film): λ_{max} 3028, 2833, 1602, 1577, 1494, 1230, 1046, 696 cm^{-1} ; HRMS calc'd for $\text{C}_{18}\text{H}_{16}\text{O}_2^+$ 264.1150, observed 264.1149 $[\text{M}]^+$.



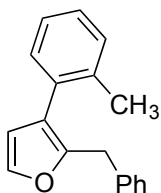
4.3ai – 2-(3-(2-benzylfuran-3-yl)phenyl)-1,3-dioxolane: The reaction was performed following General Procedure B with **4.1a** (18.1 μL , 0.12 mmol, 1.2 equiv), $\text{KN}(\text{SiMe}_3)_2$ (39.9 mg, 0.2 mmol, 2 equiv) and **4.2i** (15.1 μL , 0.1 mmol, 1 equiv) in the presence of 5 mol % Pd catalyst.

Ratio of C3:di was determined to be 11:1 by ^1H NMR of the crude reaction mixture. The crude material was purified by flash chromatography on silica gel (eluted with EtOAc:hexanes = 5:95 to 1:9) to give the product (22.6 mg, 74% yield) as a colorless oil. $R_f = 0.25$ (EtOAc:hexanes = 1:9); ^1H NMR (500 MHz, CDCl_3): δ 7.54 – 7.47 (m, 1H), 7.42 – 7.36 (m, 4H), 7.33 – 7.27 (m, 2H), 7.24 – 7.18 (m, 3H), 6.56 (d, $J = 1.5$ Hz, 1H), 5.82 (s, 1H), 4.16 – 4.00 (m, 6H) ppm; $^{13}\text{C}\{^1\text{H}\}$ NMR (125 MHz, CDCl_3): δ 149.7, 141.5, 138.7, 138.6, 134.3, 128.9, 128.8, 128.7, 128.6, 126.6, 126.1, 125.1, 122.3, 111.5, 103.9, 65.6, 33.1 ppm; IR (thin film): λ_{max} 3028, 2887, 1603, 1515, 1495, 1453, 1374, 1206,

1075, 943, 895, 797, 722, 696, 667 cm^{-1} ; HRMS calc'd for $\text{C}_{20}\text{H}_{19}\text{O}_3^+$ 307.1334, observed 307.1348 $[\text{MH}]^+$.

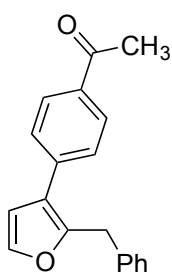


4.3aj – 2-benzyl-3-(1-naphthyl)furan: The reaction was performed following General Procedure B with **4.1a** (18.1 μL , 0.12 mmol, 1.2 equiv), $\text{KN}(\text{SiMe}_3)_2$ (49.9 mg, 0.25 mmol, 2.5 equiv) and **4.2j** (14.0 μL , 0.1 mmol, 1 equiv) in the presence of 5 mol % Pd catalyst. Ratio of C3:di was determined to be > 20:1 by ^1H NMR of the crude reaction mixture. The crude material was purified by flash chromatography on silica gel (eluted with hexanes to EtOAc:hexanes = 2:98) to give the product (26.4 mg, 93% yield) as a white solid. R_f = 0.35 (hexanes); m.p. = 80–82 $^\circ\text{C}$; ^1H NMR (500 MHz, CDCl_3): δ 7.92 (d, J = 8.0 Hz, 1H), 7.89 (d, J = 8.0 Hz, 1H), 7.83 (d, J = 8.5 Hz, 1H), 7.52 – 7.42 (m, 4H), 7.38 (d, J = 7.0 Hz, 1H), 7.26 – 7.20 (m, 2H), 7.19 – 7.14 (m, 1H), 7.12 (d, J = 7.5 Hz, 2H), 6.54 (d, J = 1.5 Hz, 1H), 3.92 (s, 2H) ppm; $^{13}\text{C}\{^1\text{H}\}$ NMR (125 MHz, CDCl_3): δ 151.0, 141.2, 138.7, 134.0, 132.7, 131.9, 128.7, 128.6, 128.5, 128.0, 127.8, 126.5, 126.2, 126.1, 125.6, 120.6, 113.7, 32.9 ppm; IR (thin film): λ_{max} 3060, 2924, 2360, 1734, 1590, 1508, 1495, 1454, 1235, 1135, 1078, 1056, 944, 895, 801, 779, 738, 716, 695, 653 cm^{-1} ; HRMS calc'd for $\text{C}_{21}\text{H}_{16}\text{O}^+$ 284.1201, observed 284.1201 $[\text{M}]^+$.



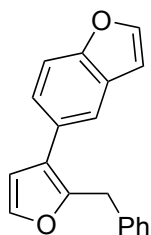
4.3ak – 2-benzyl-3-(2-tolyl)furan: The reaction was performed following General Procedure B with **4.1a** (54.3 μL , 0.36 mmol, 1.2 equiv), $\text{KN}(\text{SiMe}_3)_2$ (149.7 mg, 0.75 mmol, 2.5 equiv) and **4.2k** (36.1 μL , 0.3 mmol, 1 equiv) in the presence of 5 mol % Pd catalyst in dioxane (3 mL). Ratio of C3:di was determined to be > 20:1 by ^1H NMR of the crude reaction mixture. The crude material was purified by flash chromatography on silica gel (eluted with hexanes to

EtOAc:hexanes = 2:98) to give the product (45.0 mg, 60% yield) as a colorless oil. $R_f = 0.2$ (EtOAc:hexanes = 2:98); $^1\text{H NMR}$ (500 MHz, CDCl_3): δ 7.36 (d, $J = 2.0$ Hz, 1H), 7.28 – 7.22 (m, 4H), 7.20 – 7.15 (m, 3H), 7.12 (d, $J = 7.0$ Hz, 2H), 6.38 (d, $J = 1.5$ Hz, 1H), 3.88 (s, 2H), 2.23 (s, 3H) ppm; $^{13}\text{C}\{^1\text{H}\}$ NMR (125 MHz, CDCl_3): δ 150.1, 140.9, 138.8, 137.3, 133.6, 130.6, 130.4, 128.7, 128.6, 127.7, 126.5, 125.9, 121.7, 112.9, 32.7, 20.6 ppm; IR (thin film): λ_{max} 3062, 3028, 2922, 2852, 1603, 1495, 1454, 1140, 1057, 968, 760, 737, 715, 694, 615 cm^{-1} ; HRMS calc'd for $\text{C}_{18}\text{H}_{16}\text{O}^+$ 248.1201, observed 248.1202 $[\text{M}]^+$.



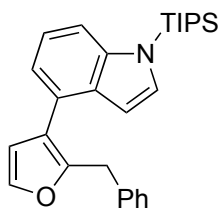
4.3al – 2-benzyl-3-(4-acetylphenyl)furan: The reaction was performed following General Procedure B with **4.1a** (18.1 μL , 0.12 mmol, 1.2 equiv), $\text{KN}(\text{SiMe}_3)_2$ (59.8 mg, 0.3 mmol, 3 equiv) and **4.2l** (19.9 mg, 0.1 mmol, 1 equiv) in the presence of 5 mol % Pd catalyst. Ratio of C3:di was determined to be $> 20:1$ by $^1\text{H NMR}$ of the crude reaction mixture. The

crude material was purified by flash chromatography on silica gel (eluted with EtOAc:hexanes = 5:95 to 1:9) to give the product (22.1 mg, 80% yield) as a colorless oil. $R_f = 0.2$ (EtOAc:hexanes = 1:9); $^1\text{H NMR}$ (500 MHz, CDCl_3): δ 7.96 (d, $J = 8.0$ Hz, 2H), 7.47 (d, $J = 8.5$ Hz, 2H), 7.42 (d, $J = 2.0$ Hz, 1H), 7.34 – 7.28 (m, 2H), 7.27 – 7.18 (m, 3H), 6.59 (d, $J = 1.5$ Hz, 1H), 4.16 (s, 2H), 2.60 (s, 3H) ppm; $^{13}\text{C}\{^1\text{H}\}$ NMR (125 MHz, CDCl_3): δ 197.8, 150.6, 141.9, 139.0, 138.2, 135.5, 129.0, 128.9, 128.5, 127.8, 126.8, 121.7, 111.2, 33.2, 26.8 ppm; IR (thin film): λ_{max} 3029, 2921, 1681, 1605, 1495, 1357, 1270, 957, 840, 724 cm^{-1} ; HRMS calc'd for $\text{C}_{19}\text{H}_{16}\text{O}_2^+$ 276.1150, observed 276.1144 $[\text{M}]^+$.



4.3am – 5-(2-benzylfuran-3-yl)benzofuran: The reaction was performed following General Procedure B with **4.1a** (18.1 μL , 0.12 mmol, 1.2 equiv),

KN(SiMe₃)₂ (49.9 mg, 0.25 mmol, 2.5 equiv) and **4.2m** (12.5 μL, 0.1 mmol, 1 equiv) in the presence of 5 mol % Pd catalyst. Ratio of C3:di was determined to be > 20:1 by ¹H NMR of the crude reaction mixture. The crude material was purified by flash chromatography on silica gel (eluted with EtOAc:hexanes = 2:98) to give the product (17.5 mg, 64% yield) as a colorless oil. R_f = 0.25 (EtOAc:hexanes = 5:95); ¹H NMR (500 MHz, CDCl₃): δ 7.63 (d, *J* = 2.0 Hz, 1H), 7.59 (d, *J* = 2.0 Hz, 1H), 7.50 (d, *J* = 8.5 Hz, 1H), 7.40 (d, *J* = 2.0 Hz, 1H), 7.34 – 7.27 (m, 3H), 7.24 – 7.17 (m, 3H), 6.76 (m, 1H), 6.56 (d, *J* = 1.5 Hz, 1H), 4.15 (s, 2H) ppm; ¹³C{¹H} NMR (125 MHz, CDCl₃): δ 154.2, 149.2, 145.7, 141.4, 138.8, 128.9, 128.8, 128.6, 128.0, 126.6, 124.8, 122.8, 120.5, 112.0, 111.7, 106.8, 32.9 ppm; IR (thin film): λ_{max} 3028, 1602, 1495, 1453, 1235, 1170, 1131, 1030, 882, 813, 736 cm⁻¹; HRMS calc'd for C₁₉H₁₃O₂⁺ 273.0916, observed 273.0924 [M–H]⁺.

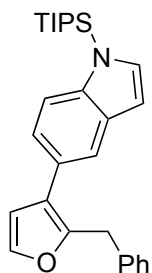


4.3an – 4-(2-benzylfuran-3-yl)-1-(triisopropylsilyl)-1H-indole: The

reaction was performed following General Procedure B with **4.1a** (18.1 μL, 0.12 mmol, 1.2 equiv), KN(SiMe₃)₂ (49.9 mg, 0.25 mmol, 2.5 equiv) and **4.2n** (35.2 mg, 0.1 mmol, 1 equiv) in the presence of

10 mol % Pd(OAc)₂ and 15 mol % NiXantphos. Ratio of C3:di was determined to be > 20:1 by ¹H NMR of the crude reaction mixture. The crude material was purified by flash chromatography on silica gel (eluted with hexanes to EtOAc:hexanes = 2:98) to give the product (23.9 mg, 56% yield) as a colorless oil. R_f = 0.33 (EtOAc:hexanes = 5:95); ¹H NMR (500 MHz, CDCl₃): δ 7.46 (d, *J* = 8.5 Hz, 1H), 7.43 (d, *J* = 1.5 Hz, 1H), 7.29 – 7.25 (m, 3H), 7.22 – 7.17 (m, 3H), 7.16 – 7.11 (m, 1H), 7.04 (d, *J* = 7.0 Hz, 1H), 6.70 (d, *J* = 1.5 Hz, 1H), 6.65 (d, *J* = 3.0 Hz, 1H), 4.11 (s, 2H), 1.72 (septet, *J* = 7.5 Hz, 3H), 1.16 (d, *J* = 7.5 Hz, 18H) ppm; ¹³C{¹H} NMR (125 MHz, CDCl₃): δ 149.8, 141.3, 141.1, 139.2,

131.4, 130.8, 128.7, 128.6, 126.4, 126.3, 122.0, 121.5, 120.3, 113.0, 112.8, 104.5, 33.1, 18.4, 13.1 ppm; IR (thin film): λ_{\max} 2948, 2868, 1603, 1510, 1465, 1422, 1276, 1143, 1075, 1059, 1016, 975, 883, 752, 692, 661 cm^{-1} ; HRMS calc'd for $\text{C}_{28}\text{H}_{36}\text{NOSi}^+$ 430.2566, observed 430.2568 $[\text{MH}]^+$.

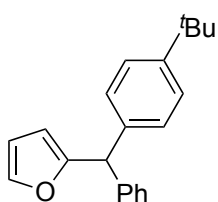


4.3ao – **5-(2-benzylfuran-3-yl)-1-(triisopropylsilyl)-1H-indole**: The reaction was performed following General Procedure B with **4.1a** (18.1 μL , 0.12 mmol, 1.2 equiv), $\text{KN}(\text{SiMe}_3)_2$ (49.9 mg, 0.25 mmol, 2.5 equiv) and **4.2o** (35.2 mg, 0.1 mmol, 1 equiv) in the presence of 5 mol % Pd catalyst at 45 $^\circ\text{C}$. Ratio of C3:di was determined to be > 20:1 by ^1H NMR of the crude reaction mixture. The crude material was purified by flash chromatography on silica gel (eluted with EtOAc:hexanes = 2:98) to give the product (27.9 mg, 68% yield) as a light yellow oil. R_f = 0.17 (EtOAc:hexanes = 2:98); ^1H NMR (500 MHz, CDCl_3): δ 7.64 (d, J = 1.5 Hz, 1H), 7.50 (d, J = 8.5 Hz, 1H), 7.38 (d, J = 1.5 Hz, 1H), 7.33 – 7.28 (m, 2H), 7.26 – 7.16 (m, 5H), 6.61 (d, J = 3.0 Hz, 1H), 6.59 (d, J = 1.5 Hz, 1H), 4.19 (s, 2H), 1.70 (septet, J = 7.5 Hz, 3H), 1.15 (d, J = 7.5 Hz, 18H) ppm; $^{13}\text{C}\{^1\text{H}\}$ NMR (125 MHz, CDCl_3): δ 148.7, 141.1, 140.1, 139.2, 131.98, 131.96, 128.73, 128.65, 126.5, 125.7, 123.5, 122.0, 119.8, 114.1, 112.1, 105.0, 33.1, 18.4, 13.0 ppm; IR (thin film): λ_{\max} 2948, 2868, 1465, 1281, 1141, 883, 724, 689 cm^{-1} ; HRMS calc'd for $\text{C}_{28}\text{H}_{36}\text{NOSi}^+$ 430.2566, observed 430.2553 $[\text{MH}]^+$.

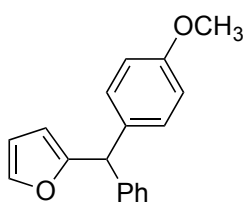
Procedure and Characterization for the Pd-Catalyzed Benzylic Arylation of **4.1a** with Aryl Bromides.

General Procedure C. An oven-dried 10 mL reaction vial equipped with a stir bar was charged with $\text{LiN}(\text{SiMe}_3)_2$ (41.8 mg, 0.25 mmol, 2.5 equiv) and 12-crown-4 (80.9 μL , 0.5

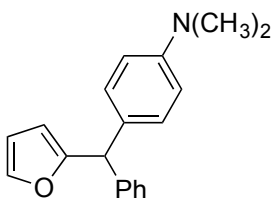
mmol, 5 equiv) under a nitrogen atmosphere. A solution (from a stock solution) of Pd(OAc)₂ (1.12 mg, 0.0050 mmol, 5 mol %) and NiXantphos (4.14 mg, 0.0075 mmol, 7.5 mol %) in 1 mL of dry dioxane was taken up by syringe and added to the reaction vial. After stirring for 5 min at 24 °C, **4.1a** (18.1 μL, 0.12 mmol, 1.2 equiv) was added to the reaction mixture followed by 1-bromo-4-*tert*-butylbenzene (**4.2b**, 17.3 μL, 0.1 mmol, 1 equiv). Note that the aryl bromide in a solid form was added to the reaction vial prior to LiN(SiMe₃)₂. The reaction mixture was stirred for 12 h at 24 °C, quenched with three drops of H₂O, diluted with 3 mL of ethyl acetate, and filtered over a pad of MgSO₄ and silica. The pad was rinsed with additional ethyl acetate, and the solution was concentrated in vacuo. The crude material was loaded onto a silica gel column and purified by flash chromatography.



4.5ab – 2-((4-(*tert*-butyl)phenyl)(phenyl)methyl)furan: The reaction was performed following General Procedure C with **4.1a** (18.1 μL, 0.12 mmol, 1.2 equiv), LiN(SiMe₃)₂ (41.8 mg, 0.25 mmol, 2.5 equiv), 12-crown-4 (80.9 μL, 0.5 mmol, 5 equiv) and **4.2b** (17.3 μL, 0.1 mmol, 1 equiv) in the presence of 5 mol % Pd catalyst. The crude material was purified by flash chromatography on silica gel (eluted with hexanes to EtOAc:hexanes = 2:98) to give the product (26.2 mg, 91% yield) as a light yellow oil. *R_f* = 0.17 (EtOAc:hexanes = 2:98); ¹H NMR (500 MHz, CDCl₃): δ 7.36 (m, 1H), 7.32 – 7.26 (m, 4H), 7.24 – 7.15 (m, 3H), 7.11 – 7.06 (m, 2H), 6.29 (m, 1H), 5.92 (dd, *J* = 3.0, 0.5 Hz, 1H), 5.41 (s, 1H), 1.29 (s, 9H) ppm; ¹³C{¹H} NMR (125 MHz, CDCl₃): δ 157.2, 149.7, 142.2, 142.0, 138.9, 129.0, 128.6, 128.5, 126.9, 125.6, 110.3, 108.4, 50.7, 34.6, 31.6 ppm; IR (thin film): λ_{max} 2962, 1600, 1503, 1452, 1363, 1269, 1011, 806, 732, 702 cm⁻¹; HRMS calc'd for C₂₁H₂₂O⁺ 290.1671, observed 290.1678 [M]⁺.

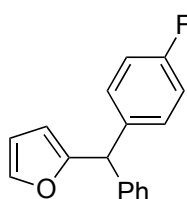


4.5ac – 2-((4-methoxyphenyl)(phenyl)methyl)furan: The reaction was performed following General Procedure C with **4.1a** (18.1 μL , 0.12 mmol, 1.2 equiv), $\text{LiN}(\text{SiMe}_3)_2$ (41.8 mg, 0.25 mmol, 2.5 equiv), 12-crown-4 (80.9 μL , 0.5 mmol, 5 equiv) and **4.2c** (12.5 μL , 0.1 mmol, 1 equiv) in the presence of 5 mol % Pd catalyst. The crude material was purified by flash chromatography on silica gel (eluted with hexanes to EtOAc:hexanes = 2:98) to give the product (25.0 mg, 95% yield) as a pale yellow oil. $R_f = 0.25$ (EtOAc:hexanes = 2:98); ^1H NMR (500 MHz, CDCl_3): δ 7.36 (d, $J = 1.0$ Hz, 1H), 7.31 – 7.26 (m, 2H), 7.24 – 7.19 (m, 1H), 7.18 – 7.13 (m, 2H), 7.11 – 7.05 (m, 2H), 6.87 – 6.79 (m, 2H), 6.29 (m, 1H), 5.89 (d, $J = 3.5$ Hz, 1H), 5.39 (s, 1H), 3.77 (s, 3H) ppm; $^{13}\text{C}\{^1\text{H}\}$ NMR (125 MHz, CDCl_3): δ 158.3, 157.0, 142.1, 141.8, 133.9, 129.6, 128.6, 128.3, 126.6, 113.8, 110.0, 108.0, 55.2, 50.0 ppm; IR (thin film): λ_{max} 2931, 1608, 1510, 1452, 1246, 1174, 1032, 732, 698, 666 cm^{-1} ; HRMS calc'd for $\text{C}_{18}\text{H}_{17}\text{O}_2^+$ 265.1229, observed 265.1231 [MH] $^+$.

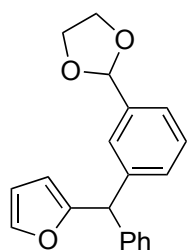


4.5ad – 4-(furan-2-yl(phenyl)methyl)-*N,N*-dimethylaniline: The reaction was performed following General Procedure C with **4.1a** (18.1 μL , 0.12 mmol, 1.2 equiv), $\text{LiN}(\text{SiMe}_3)_2$ (41.8 mg, 0.25 mmol, 2.5 equiv), 12-crown-4 (80.9 μL , 0.5 mmol, 5 equiv) and **4.2d** (20.0 mg, 0.1 mmol, 1 equiv) in the presence of 5 mol % Pd catalyst. The crude material was purified by flash chromatography on silica gel (eluted with hexanes to EtOAc:hexanes = 5:95) to give the product (26.0 mg, 94% yield) as a white solid. $R_f = 0.2$ (EtOAc:hexanes = 5:95); m.p. = 63–64 $^\circ\text{C}$; ^1H NMR (500 MHz, CDCl_3): δ 7.36 (m, 1H), 7.32 – 7.25 (m, 2H), 7.23 – 7.14 (m, 3H), 7.08 – 6.99 (m, 2H), 6.72 – 6.63 (m, 2H), 6.29 (m, 1H), 5.90 (m, 1H), 5.36 (s, 1H), 2.92 (s, 6H) ppm; $^{13}\text{C}\{^1\text{H}\}$ NMR (125 MHz, CDCl_3): δ 157.5, 149.4, 142.5, 141.6,

129.7, 129.3, 128.6, 128.3, 126.4, 112.5, 109.9, 107.8, 49.9, 40.6 ppm; IR (thin film): λ_{\max} 2882, 1613, 1520, 1348, 1162, 1010, 947, 801, 726, 698, 666 cm^{-1} ; HRMS calc'd for $\text{C}_{19}\text{H}_{20}\text{NO}^+$ 278.1545, observed 278.1543 $[\text{MH}]^+$.

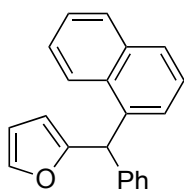


4.5ae – 2-((4-fluorophenyl)(phenyl)methyl)furan: The reaction was performed following General Procedure C with **4.1a** (30.2 μL , 0.2 mmol, 2 equiv), $\text{LiN}(\text{SiMe}_3)_2$ (25.1 mg, 0.15 mmol, 1.5 equiv), 12-crown-4 (48.5 μL , 0.3 mmol, 3 equiv) and **4.2e** (11.0 μL , 0.1 mmol, 1 equiv) in the presence of 5 mol % Pd catalyst. The crude material was purified by flash chromatography on silica gel (eluted with hexanes to EtOAc:hexanes = 1:99) to give the product (19.9 mg, 79% yield) as a colorless oil. R_f = 0.2 (EtOAc:hexanes = 1:99); ^1H NMR (500 MHz, CDCl_3): δ 7.41 – 7.35 (m, 1H), 7.34 – 7.28 (m, 2H), 7.27 – 7.21 (m, 1H), 7.18 – 7.09 (m, 4H), 7.02 – 6.94 (m, 2H), 6.31 (m, 1H), 5.90 (dd, J = 3.0, 0.5 Hz, 1H), 5.43 (s, 1H) ppm; $^{13}\text{C}\{^1\text{H}\}$ NMR (125 MHz, CDCl_3): δ 161.9 (d, J = 243.8 Hz), 156.7, 142.3, 141.8, 137.8 (d, J = 3.1 Hz), 130.4 (d, J = 7.8 Hz), 128.9, 128.7, 127.1, 115.5 (d, J = 21.1 Hz), 110.3, 108.6, 50.3 ppm; IR (thin film): λ_{\max} 3029, 1603, 1506, 1452, 1222, 1157, 1011, 800, 732, 697 cm^{-1} ; HRMS calc'd for $\text{C}_{17}\text{H}_{13}\text{OF}^+$ 252.0950, observed 252.0951 $[\text{M}]^+$.

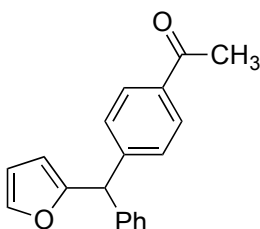


4.5ai – 2-(3-(furan-2-yl(phenyl)methyl)phenyl)-1,3-dioxolane: The reaction was performed following General Procedure C with **4.1a** (30.2 μL , 0.2 mmol, 2 equiv), $\text{LiN}(\text{SiMe}_3)_2$ (33.5 mg, 0.2 mmol, 2 equiv), 12-crown-4 (64.7 μL , 0.4 mmol, 4 equiv) and **4.2i** (15.1 μL , 0.1 mmol, 1 equiv) in the presence of 5 mol % Pd catalyst. The crude material was purified by flash chromatography on silica gel (eluted with EtOAc:hexanes = 5:95 to 1:9) to give the

product (24.0 mg, 78% yield) as a yellow oil. $R_f = 0.25$ (EtOAc:hexanes = 1:9); ^1H NMR (500 MHz, CDCl_3): δ 7.39 – 7.34 (m, 2H), 7.33 – 7.25 (m, 4H), 7.24 – 7.20 (m, 1H), 7.18 – 7.12 (m, 3H), 6.29 (m, 1H), 5.90 (d, $J = 3.5$ Hz, 1H), 5.75 (s, 1H), 5.46 (s, 1H), 4.12 – 3.95 (m, 4H) ppm; $^{13}\text{C}\{^1\text{H}\}$ NMR (125 MHz, CDCl_3): δ 156.4, 141.87, 141.86, 141.5, 138.0, 129.5, 128.7, 128.5, 128.4, 127.0, 126.7, 124.8, 110.0, 108.3, 103.6, 65.2, 50.8 ppm; IR (thin film): λ_{max} 3028, 2954, 2887, 1591, 1495, 1452, 1387, 1154, 1078, 1012, 946, 737, 702 cm^{-1} ; HRMS calc'd for $\text{C}_{20}\text{H}_{19}\text{O}_3^+$ 307.1334, observed 307.1336 $[\text{MH}]^+$.

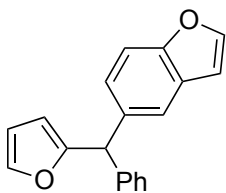


4.5aj – 2-(naphthalen-1-yl(phenyl)methyl)furan: The reaction was performed following General Procedure C with **4.1a** (15.1 μL , 0.1 mmol, 1 equiv), $\text{LiN}(\text{SiMe}_3)_2$ (33.5 mg, 0.2 mmol, 2 equiv), 12-crown-4 (64.7 μL , 0.4 mmol, 4 equiv) and **4.2j** (28.0 μL , 0.2 mmol, 2 equiv) in the presence of 5 mol % Pd catalyst. The crude material was purified by flash chromatography on silica gel (eluted with hexanes to EtOAc:hexanes = 1:99) to give the product (21.3 mg, 75% yield) as a colorless oil. $R_f = 0.2$ (EtOAc:hexanes = 1:99); ^1H NMR (500 MHz, CDCl_3): δ 8.02 – 7.95 (m, 1H), 7.88 – 7.83 (m, 1H), 7.76 (d, $J = 8.0$ Hz, 1H), 7.46 – 7.36 (m, 4H), 7.32 – 7.26 (m, 2H), 7.25 – 7.16 (m, 3H), 7.04 (d, $J = 7.5$ Hz, 1H), 6.30 (m, 1H), 6.22 (s, 1H), 5.82 (d, $J = 3.0$ Hz, 1H) ppm; $^{13}\text{C}\{^1\text{H}\}$ NMR (125 MHz, CDCl_3): δ 156.9, 142.1, 141.7, 137.8, 134.2, 131.8, 129.2, 129.0, 128.7, 127.9, 127.1, 126.9, 126.4, 125.7, 125.5, 124.0, 110.4, 109.3, 47.4 ppm; IR (thin film): λ_{max} 3060, 1598, 1494, 1452, 1396, 1169, 1077, 1010, 787, 723, 699 cm^{-1} ; HRMS calc'd for $\text{C}_{21}\text{H}_{16}\text{O}^+$ 284.1201, observed 284.1202 $[\text{M}]^+$.

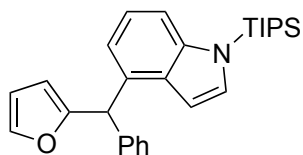


4.5al – 1-(4-(furan-2-yl(phenyl)methyl)phenyl)ethan-1-one: The reaction was performed following General Procedure C with **4.1a** (18.1 μL , 0.12 mmol, 1.2 equiv), $\text{LiN}(\text{SiMe}_3)_2$ (50.2 mg, 0.3 mmol,

3 equiv), 12-crown-4 (97.1 μL , 0.6 mmol, 6 equiv) and **4.2l** (19.9 mg, 0.1 mmol, 1 equiv) in the presence of 5 mol % Pd catalyst. The crude material was purified by flash chromatography on silica gel (eluted with EtOAc:hexanes = 5:95 to 1:9) to give the product (19.0 mg, 69% yield) as a yellow oil. $R_f = 0.2$ (EtOAc:hexanes = 1:9); ^1H NMR (500 MHz, CDCl_3): δ 7.95 – 7.84 (m, 2H), 7.41 – 7.35 (m, 1H), 7.34 – 7.21 (m, 5H), 7.18 – 7.09 (m, 2H), 6.31 (m, 1H), 5.92 (m, 1H), 5.48 (s, 1H), 2.56 (s, 3H) ppm; $^{13}\text{C}\{^1\text{H}\}$ NMR (125 MHz, CDCl_3): δ 197.6, 155.6, 147.2, 142.1, 140.9, 135.7, 128.9, 128.6, 128.53, 128.49, 127.0, 110.1, 108.5, 50.8, 26.5 ppm; IR (thin film): λ_{max} 3029, 1683, 1608, 1358, 1268, 1012, 733, 712 cm^{-1} ; HRMS calc'd for $\text{C}_{19}\text{H}_{16}\text{O}_2^+$ 276.1150, observed 276.1153 $[\text{M}]^+$.



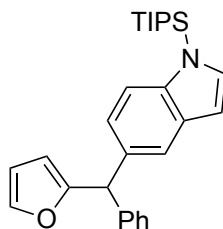
4.5am – 5-(furan-2-yl(phenyl)methyl)benzofuran: The reaction was performed following General Procedure C with **4.1a** (18.1 μL , 0.12 mmol, 1.2 equiv), $\text{LiN}(\text{SiMe}_3)_2$ (41.8 mg, 0.25 mmol, 2.5 equiv), 12-crown-4 (80.9 μL , 0.5 mmol, 5 equiv) and **4.2m** (12.5 μL , 0.1 mmol, 1 equiv) in the presence of 5 mol % Pd catalyst. The crude material was purified by flash chromatography on silica gel (eluted with hexanes to EtOAc:hexanes = 2:98) to give the product (16.7 mg, 61% yield) as a white solid. $R_f = 0.17$ (EtOAc:hexanes = 2:98); m.p. = 71–73 $^\circ\text{C}$; ^1H NMR (500 MHz, CDCl_3): δ 7.58 (d, $J = 2.0$ Hz, 1H), 7.42 (d, $J = 8.5$ Hz, 1H), 7.40 – 7.34 (m, 2H), 7.33 – 7.27 (m, 2H), 7.26 – 7.16 (m, 3H), 7.13 (dd, $J = 8.5$, 2.0 Hz, 1H), 6.68 (m, 1H), 6.31 (m, 1H), 5.91 (dd, $J = 3.0$, 0.5 Hz, 1H), 5.56 (s, 1H) ppm; $^{13}\text{C}\{^1\text{H}\}$ NMR (125 MHz, CDCl_3): δ 157.3, 154.2, 145.5, 142.4, 142.1, 136.7, 129.0, 128.7, 127.8, 126.9, 125.6, 121.4, 111.5, 110.3, 108.5, 106.9, 51.0 ppm; IR (thin film): λ_{max} 3027, 1590, 1494, 1466, 1265, 1110, 1031, 1011, 885, 765, 735, 700 cm^{-1} ; HRMS calc'd for $\text{C}_{19}\text{H}_{14}\text{O}_2^+$ 274.0994, observed 274.0996 $[\text{M}]^+$.



4.5an – 4-(furan-2-yl(phenyl)methyl)-1-(triisopropylsilyl)-

1H-indole: The reaction was performed following General Procedure C with **4.1a** (18.1 μ L, 0.12 mmol, 1.2 equiv),

LiN(SiMe₃)₂ (50.2 mg, 0.3 mmol, 3 equiv), 12-crown-4 (97.1 μ L, 0.6 mmol, 6 equiv) and **4.2n** (35.2 mg, 0.1 mmol, 1 equiv) in the presence of 5 mol % Pd catalyst. The crude material was purified by flash chromatography on silica gel (eluted with hexanes to EtOAc:hexanes = 2:98) to give the product (25.8 mg, 60% yield) as a light yellow oil. R_f = 0.4 (EtOAc:hexanes = 5:95); ¹H NMR (500 MHz, CDCl₃): δ 7.42 – 7.36 (m, 2H), 7.31 – 7.15 (m, 6H), 7.08 – 7.04 (m, 1H), 6.74 (d, J = 7.0 Hz, 1H), 6.49 (d, J = 3.5 Hz, 1H), 6.29 (m, 1H), 5.89 (m, 1H), 5.86 (s, 1H), 1.68 (septet, J = 7.5 Hz, 3H), 1.13 (d, J = 7.5 Hz, 18H) ppm; ¹³C{¹H} NMR (125 MHz, CDCl₃): δ 157.3, 142.1, 141.8, 141.2, 133.6, 131.1, 131.0, 129.1, 128.5, 126.7, 121.4, 119.7, 112.9, 110.3, 108.4, 103.4, 48.9, 18.4, 13.1 ppm; IR (thin film): λ_{max} 2948, 2868, 1465, 1426, 1281, 1148, 1015, 883, 749, 720 cm⁻¹; HRMS calc'd for C₂₈H₃₆NOSi⁺ 430.2566, observed 430.2565 [MH]⁺.



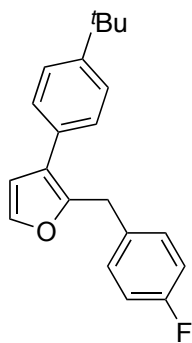
4.5ao – 5-(furan-2-yl(phenyl)methyl)-1-(triisopropylsilyl)-1H-

indole: The reaction was performed following General Procedure C with **4.1a** (18.1 μ L, 0.12 mmol, 1.2 equiv), LiN(SiMe₃)₂ (50.2 mg, 0.3 mmol, 3 equiv), 12-crown-4 (97.1 μ L, 0.6 mmol, 6 equiv) and **4.2o**

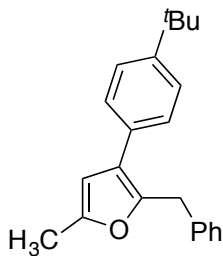
(35.2 mg, 0.1 mmol, 1 equiv) in the presence of 5 mol % Pd catalyst. The crude material was purified by flash chromatography on silica gel (eluted with hexanes to EtOAc:hexanes = 2:98) to give the product (41.1 mg, 96% yield) as a light yellow oil. R_f = 0.4 (EtOAc:hexanes = 5:95); ¹H NMR (500 MHz, CDCl₃): δ 7.40 (d, J = 8.5 Hz, 1H), 7.37 (m, 2H), 7.31 – 7.26 (m, 2H), 7.25 – 7.18 (m, 4H), 6.97 (dd, J = 8.5, 1.5 Hz, 1H), 6.53 (d,

$J = 3.0$ Hz, 1H), 6.29 (m, 1H), 5.92 (d, $J = 3.0$ Hz, 1H), 5.54 (s, 1H), 1.67 (septet, $J = 7.5$ Hz, 3H), 1.12 (d, $J = 7.5$ Hz, 18H) ppm; $^{13}\text{C}\{^1\text{H}\}$ NMR (125 MHz, CDCl_3): δ 158.0, 142.9, 141.9, 140.0, 133.4, 131.71, 131.66, 129.1, 128.5, 126.7, 122.8, 120.6, 113.9, 110.2, 108.3, 105.0, 51.1, 18.4, 13.0 ppm; IR (thin film): λ_{max} 2948, 2868, 1466, 1284, 1144, 1011, 884, 727, 700 cm^{-1} ; HRMS calc'd for $\text{C}_{28}\text{H}_{36}\text{NOSi}^+$ 430.2566, observed 430.2547 $[\text{MH}]^+$.

Procedure and Characterization for the Pd-Catalyzed Furan C3 and Benzylic Arylations with 4.2a

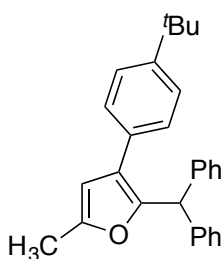


4.3bb – **3-(4-(tert-butyl)phenyl)-2-(4-fluorobenzyl)furan**: The reaction was performed following General Procedure B with **4.1b** (18.7 μL , 0.12 mmol, 1.2 equiv), $\text{KN}(\text{SiMe}_3)_2$ (49.9 mg, 0.25 mmol, 2.5 equiv) and **4.2b** (17.3 μL , 0.1 mmol, 1 equiv) in the presence of 5 mol % Pd catalyst. Ratio of C3:di was determined to be 16:1 by ^1H NMR of the crude reaction mixture. The crude material was purified by flash chromatography on silica gel (eluted with hexanes to EtOAc:hexanes = 2:98) to give the product (29.0 mg, 94% yield) as a colorless oil. $R_f = 0.25$ (hexanes); ^1H NMR (500 MHz, CDCl_3): δ 7.43 – 7.38 (m, 2H), 7.37 (d, $J = 2.0$ Hz, 1H), 7.34 – 7.29 (m, 2H), 7.18 – 7.13 (m, 2H), 7.01 – 6.94 (m, 2H), 6.54 (d, $J = 1.5$ Hz, 1H), 4.11 (s, 2H), 1.34 (s, 9H) ppm; $^{13}\text{C}\{^1\text{H}\}$ NMR (125 MHz, CDCl_3): δ 161.8 (d, $J = 242.9$ Hz), 149.9, 149.0, 141.5, 134.4 (d, $J = 3.1$ Hz), 131.0, 130.0 (d, $J = 8.0$ Hz), 127.6, 125.8, 122.4, 115.6 (d, $J = 21.4$ Hz), 111.7, 34.7, 32.3, 31.6 ppm; IR (thin film): λ_{max} 2963, 1605, 1509, 1223, 835, 734 cm^{-1} ; HRMS calc'd for $\text{C}_{21}\text{H}_{21}\text{OF}^+$ 308.1576, observed 308.1573 $[\text{M}]^+$.



4.3db – **2-benzyl-3-(4-(*tert*-butyl)phenyl)-5-methylfuran**: The reaction was performed following General Procedure B with **4.1d** (43.1 μL , 0.25 mmol, 2.5 equiv), $\text{KN}(\text{SiMe}_3)_2$ (49.9 mg, 0.25 mmol, 2.5 equiv) and **4.2b** (17.3 μL , 0.1 mmol, 1 equiv) in the presence of 5 mol % Pd catalyst in CPME (1 mL). Ratio of C3:di was determined to

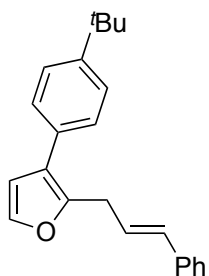
be 11:1 by ^1H NMR of the crude reaction mixture. The crude material was purified by flash chromatography on silica gel (eluted with hexanes to EtOAc:hexanes = 1:99) to give the product (21.3 mg, 70% yield) as a colorless oil. R_f = 0.33 (EtOAc:hexanes = 2:98); ^1H NMR (500 MHz, CDCl_3): δ 7.40 – 7.34 (m, 2H), 7.32 – 7.27 (m, 4H), 7.24 – 7.20 (m, 3H), 6.14 (s, 1H), 4.09 (s, 2H), 2.28 (s, 3H), 1.32 (s, 9H) ppm; $^{13}\text{C}\{^1\text{H}\}$ NMR (125 MHz, CDCl_3): δ 150.8, 149.5, 147.3, 139.3, 131.5, 128.7, 128.5, 127.4, 126.4, 125.7, 123.1, 107.5, 34.7, 33.1, 31.6, 13.8 ppm; IR (thin film): λ_{max} 2962, 1577, 1495, 1453, 1363, 1234, 1096, 1007, 838, 801, 720, 696 cm^{-1} ; HRMS calc'd for $\text{C}_{22}\text{H}_{24}\text{O}^+$ 304.1827, observed 304.1821 [M] $^+$.



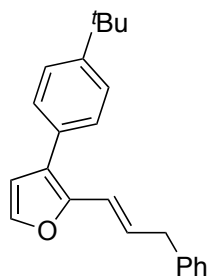
4.3eb – **2-benzhydryl-3-(4-(*tert*-butyl)phenyl)-5-methylfuran**: The reaction was performed following General Procedure B with **4.1e** (29.8 μL , 0.12 mmol, 1.2 equiv), $\text{KN}(\text{SiMe}_3)_2$ (49.9 mg, 0.25 mmol, 2.5 equiv) and **4.2b** (17.3 μL , 0.1 mmol, 1 equiv) in the presence of 5

mol % Pd catalyst. The crude material was purified by flash chromatography on silica gel (eluted with hexanes to EtOAc:hexanes = 2:98) to give the product (38.0 mg, 99% yield) as a colorless viscous oil. R_f = 0.25 (EtOAc:hexanes = 2:98); ^1H NMR (500 MHz, CDCl_3): δ 7.40 – 7.34 (m, 2H), 7.31 – 7.17 (m, 12H), 6.11 (s, 1H), 5.58 (s, 1H), 2.26 (s, 3H), 1.32 (s, 9H) ppm; $^{13}\text{C}\{^1\text{H}\}$ NMR (125 MHz, CDCl_3): δ 151.3, 149.6, 148.7, 142.8, 131.6, 129.2, 128.5, 127.9, 126.6, 125.7, 123.6, 107.8, 48.7, 34.7, 31.6, 13.9 ppm; IR (thin film): λ_{max}

3028, 2963, 1601, 1575, 1494, 1449, 1363, 1269, 1229, 1092, 1032, 1007, 983, 959, 910, 839, 800, 739, 700 cm^{-1} ; HRMS calc'd for $\text{C}_{28}\text{H}_{28}\text{O}^+$ 380.2140, observed 380.2138 $[\text{M}]^+$.

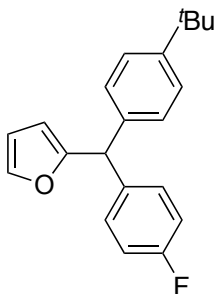


4.3fb – (E)-3-(4-(tert-butyl)phenyl)-2-cinnamylfuran: The reaction was performed following General Procedure B with **4.1f** (21.7 μL , 0.12 mmol, 1.2 equiv), $\text{KN}(\text{SiMe}_3)_2$ (49.9 mg, 0.25 mmol, 2.5 equiv) and **4.2b** (17.3 μL , 0.1 mmol, 1 equiv) in the presence of 5 mol % Pd catalyst. The crude material was purified by flash chromatography on silica gel (eluted with hexanes to EtOAc:hexanes = 1:99) to give the product (13.6 mg, 43% yield) as a colorless oil. $R_f = 0.15$ (hexanes); ^1H NMR (500 MHz, CDCl_3): δ 7.44 – 7.40 (m, 2H), 7.38 (d, $J = 2.0$ Hz, 1H), 7.37 – 7.33 (m, 4H), 7.30 – 7.26 (m, 2H), 7.22 – 7.18 (m, 1H), 6.54 (d, $J = 1.5$ Hz, 1H), 6.45 (d, $J = 16.0$ Hz, 1H), 6.36 (dt, $J = 16.0, 6.0$ Hz, 1H), 3.70 (d, $J = 6.0$ Hz, 2H), 1.34 (s, 9H) ppm; $^{13}\text{C}\{^1\text{H}\}$ NMR (125 MHz, CDCl_3): δ 149.8, 148.9, 141.2, 137.5, 131.8, 131.1, 128.7, 127.6, 127.4, 126.44, 126.40, 125.8, 121.9, 111.6, 34.7, 31.6, 30.8 ppm; IR (thin film): λ_{max} 2962, 1520, 1363, 1269, 1141, 963, 892, 835, 763, 733, 691 cm^{-1} ; HRMS calc'd for $\text{C}_{23}\text{H}_{24}\text{O}^+$ 316.1827, observed 316.1814 $[\text{M}]^+$.



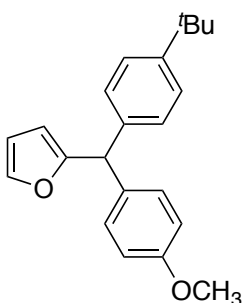
4.3'fb – (E)-3-(4-(tert-butyl)phenyl)-2-(3-phenylprop-1-en-1-yl)furan: The reaction was performed following General Procedure B with **4.1f** (21.7 μL , 0.12 mmol, 1.2 equiv), $\text{KN}(\text{SiMe}_3)_2$ (49.9 mg, 0.25 mmol, 2.5 equiv) and **4.2b** (17.3 μL , 0.1 mmol, 1 equiv) in the presence of 5 mol % Pd catalyst. The crude material was purified by flash chromatography on silica gel (eluted with hexanes to EtOAc:hexanes = 1:99) to

give the product (12.0 mg, 38% yield) as a light yellow oil. $R_f = 0.2$ (hexanes); $^1\text{H NMR}$ (500 MHz, CDCl_3): δ 7.45 – 7.40 (m, 2H), 7.36 – 7.28 (m, 5H), 7.25 – 7.18 (m, 3H), 6.56 – 6.49 (m, 2H), 6.41 (dt, $J = 15.5, 7.0$ Hz, 1H), 3.54 (d, $J = 7.0$ Hz, 2H), 1.35 (s, 9H) ppm; $^{13}\text{C}\{^1\text{H}\}$ NMR (125 MHz, CDCl_3): δ 150.0, 148.2, 141.4, 140.4, 131.0, 129.1, 128.8, 128.7, 128.1, 126.4, 125.8, 122.7, 119.0, 112.5, 39.6, 34.8, 31.6 ppm; IR (thin film): λ_{max} 2962, 1514, 1495, 1453, 1363, 1268, 1148, 963, 891, 835, 736, 699 cm^{-1} ; HRMS calc'd for $\text{C}_{23}\text{H}_{24}\text{O}^+$ 316.1827, observed 316.1815 $[\text{M}]^+$.



4.5bb – 2-((4-(*tert*-butyl)phenyl)(4-fluorophenyl)methyl)furan: The reaction was performed following General Procedure C with **4.1b** (18.7 μL , 0.12 mmol, 1.2 equiv), $\text{LiN}(\text{SiMe}_3)_2$ (41.8 mg, 0.25 mmol, 2.5 equiv), 12-crown-4 (80.9 μL , 0.5 mmol, 5 equiv) and **4.2b** (17.3 μL , 0.1 mmol, 1 equiv) in the presence of 5 mol % Pd catalyst. The

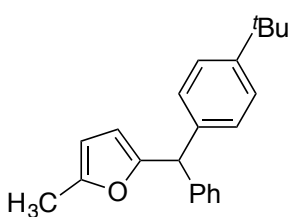
crude material was purified by flash chromatography on silica gel (eluted with hexanes to EtOAc:hexanes = 1:99) to give the product (23.2 mg, 75% yield) as a colorless oil. $R_f = 0.25$ (hexanes); $^1\text{H NMR}$ (500 MHz, CDCl_3): δ 7.39 – 7.34 (m, 1H), 7.34 – 7.27 (m, 2H), 7.17 – 7.10 (m, 2H), 7.10 – 7.03 (m, 2H), 7.01 – 6.93 (m, 2H), 6.30 (m, 1H), 5.90 (d, $J = 3.0$ Hz, 1H), 5.39 (s, 1H), 1.30 (s, 9H) ppm; $^{13}\text{C}\{^1\text{H}\}$ NMR (125 MHz, CDCl_3): δ 161.9 (d, $J = 243.6$ Hz), 157.0, 149.9, 142.2, 138.7, 138.0 (d, $J = 3.0$ Hz), 130.4 (d, $J = 7.9$ Hz), 128.4, 125.6, 115.4 (d, $J = 21.1$ Hz), 110.3, 108.4, 49.9, 34.7, 31.6 ppm; IR (thin film): λ_{max} 2963, 1603, 1508, 1226, 1158, 1011, 842, 818, 735, 579 cm^{-1} ; HRMS calc'd for $\text{C}_{21}\text{H}_{21}\text{OF}^+$ 308.1576, observed 308.1574 $[\text{M}]^+$.



4.5cb – 2-((4-(*tert*-butyl)phenyl)(4-methoxyphenyl)methyl)furan:

The reaction was performed following General Procedure C with

4.1c (21.1 μL , 0.12 mmol, 1.2 equiv), $\text{LiN}(\text{SiMe}_3)_2$ (41.8 mg, 0.25 mmol, 2.5 equiv), 12-crown-4 (80.9 μL , 0.5 mmol, 5 equiv) and **4.2b** (17.3 μL , 0.1 mmol, 1 equiv) in the presence of 5 mol % Pd catalyst. The crude material was purified by flash chromatography on silica gel (eluted with hexanes to EtOAc:hexanes = 2:98) to give the product (28.4 mg, 89% yield) as a colorless oil. $R_f = 0.33$ (EtOAc:hexanes = 5:95); ^1H NMR (500 MHz, CDCl_3): δ 7.39 – 7.34 (m, 1H), 7.32 – 7.27 (m, 2H), 7.13 – 7.05 (m, 4H), 6.88 – 6.81 (m, 2H), 6.29 (m, 1H), 5.90 (d, $J = 3.0$ Hz, 1H), 5.36 (s, 1H), 3.78 (s, 3H), 1.29 (s, 9H) ppm; $^{13}\text{C}\{^1\text{H}\}$ NMR (125 MHz, CDCl_3): δ 158.6, 157.5, 149.6, 142.0, 139.3, 134.4, 129.9, 128.4, 125.5, 114.0, 110.2, 108.2, 55.4, 49.9, 34.6, 31.6 ppm; IR (thin film): λ_{max} 2961, 1610, 1511, 1463, 1248, 1176, 1036, 1010, 807, 733 cm^{-1} ; HRMS calc'd for $\text{C}_{22}\text{H}_{24}\text{O}_2^+$ 320.1776, observed 320.1764 $[\text{M}]^+$.



4.5db – **2-((4-(tert-butyl)phenyl)(phenyl)methyl)-5-**

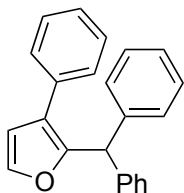
methylfuran: The reaction was performed following General Procedure C with **4.1d** (20.7 μL , 0.12 mmol, 1.2 equiv), $\text{LiN}(\text{SiMe}_3)_2$ (41.8 mg, 0.25 mmol, 2.5 equiv), 12-crown-4 (80.9

μL , 0.5 mmol, 5 equiv) and **4.2b** (17.3 μL , 0.1 mmol, 1 equiv) in the presence of 5 mol % Pd catalyst in CPME (1 mL). The crude material was purified by flash chromatography on silica gel (eluted with hexanes to EtOAc:hexanes = 2:98) to give the product (28.7 mg, 94% yield) as a colorless oil. $R_f = 0.2$ (EtOAc:hexanes = 1:99); ^1H NMR (500 MHz, CDCl_3): δ 7.33 – 7.25 (m, 4H), 7.24 – 7.15 (m, 3H), 7.13 – 7.05 (m, 2H), 5.86 (d, $J = 3.0$ Hz, 1H), 5.75 (d, $J = 3.0$ Hz, 1H), 5.35 (s, 1H), 2.24 (s, 3H), 1.29 (s, 9H) ppm; $^{13}\text{C}\{^1\text{H}\}$ NMR (125 MHz, CDCl_3): δ 155.3, 151.6, 149.5, 142.5, 139.2, 129.0, 128.5 (two carbons), 126.7, 125.5, 109.1, 106.1, 50.8, 34.6, 31.6, 13.9 ppm; IR (thin film): λ_{max} 2962, 1494,

1451, 1219, 1021, 781, 702 cm^{-1} ; HRMS calc'd for $\text{C}_{22}\text{H}_{24}\text{O}^+$ 304.1827, observed 304.1819 $[\text{M}]^+$.

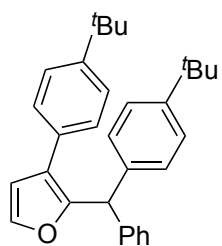
Procedure and Characterization for the Pd-Catalyzed Homo-Diarylation.

General Procedure D. An oven-dried 10 mL reaction vial equipped with a stir bar was charged with KO^tBu (67.3 mg, 0.6 mmol, 6 equiv) under a nitrogen atmosphere. A solution (from a stock solution) of $\text{Pd}(\text{OAc})_2$ (1.12 mg, 0.0050 mmol, 5 mol %) and NiXantphos (4.14 mg, 0.0075 mmol, 7.5 mol %) in 1 mL of dry CPME was taken up by syringe and added to the reaction vial. After stirring for 5 min at 24 °C, **4.1a** (15.1 μL , 0.1 mmol, 1 equiv) was added to the reaction mixture followed by 1-bromo-4-*tert*-butylbenzene (**4.2b**, 34.7 μL , 0.2 mmol, 2 equiv). Note that the aryl bromide in a solid form was added to the reaction vial prior to KO^tBu . The reaction mixture was stirred for 12 h at 45 °C, quenched with three drops of H_2O , diluted with 3 mL of ethyl acetate, and filtered over a pad of MgSO_4 and silica. The pad was rinsed with additional ethyl acetate, and the solution was concentrated in vacuo. The crude material was loaded onto a silica gel column and purified by flash chromatography.



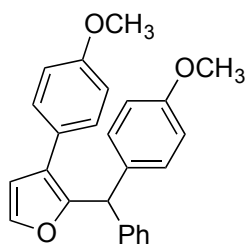
4.4aa – 2-benzhydryl-3-phenylfuran: The reaction was performed following General Procedure D with **4.1a** (15.1 μL , 0.1 mmol, 1 equiv), KO^tBu (67.3 mg, 0.6 mmol, 6 equiv) and **4.2a** (21.3 μL , 0.2 mmol, 2 equiv) in the presence of 5 mol % Pd catalyst. Ratio of di:C3 was determined to be > 20:1 by ^1H NMR of the crude reaction mixture. The crude material was purified by flash chromatography on silica gel (eluted with hexanes to EtOAc:hexanes = 2:98) to give the product (26.6 mg, 86% yield) as a white solid. R_f = 0.13 (hexanes); m.p. = 83–85 °C; ^1H NMR (500 MHz, CDCl_3): δ 7.42 (d, J = 2.0 Hz, 1H), 7.39 – 7.32 (m, 4H), 7.31 – 7.27 (m,

5H), 7.25 – 7.17 (m, 6H), 6.54 (d, $J = 2.0$ Hz, 1H), 5.63 (s, 1H) ppm; $^{13}\text{C}\{^1\text{H}\}$ NMR (125 MHz, CDCl_3): δ 150.8, 142.4, 142.0, 134.1, 129.1, 128.8, 128.6, 128.4, 127.1, 126.8, 123.0, 111.7, 48.7 ppm; IR (thin film): λ_{max} 3060, 3026, 1601, 1515, 1494, 1448, 961, 743, 698 cm^{-1} ; HRMS calc'd for $\text{C}_{23}\text{H}_{19}\text{O}^+$ 311.1436, observed 311.1434 $[\text{MH}]^+$.



4.4ab – **3-(4-(tert-butyl)phenyl)-2-((4-(tert-**

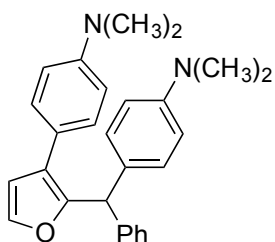
butyl)phenyl)(phenyl)methyl)furan: The reaction was performed following General Procedure D with **4.1a** (15.1 μL , 0.1 mmol, 1 equiv), KO^tBu (67.3 mg, 0.6 mmol, 6 equiv) and **4.2b** (34.7 μL , 0.2 mmol, 2 equiv) in the presence of 5 mol % Pd catalyst. Ratio of di:C3 was determined to be > 20:1 by ^1H NMR of the crude reaction mixture. The crude material was purified by flash chromatography on silica gel (eluted with hexanes to EtOAc:hexanes = 2:98) to give the product (39.5 mg, 94% yield) as a light yellow oil. $R_f = 0.5$ (EtOAc:hexanes = 5:95); ^1H NMR (500 MHz, CDCl_3): δ 7.42 – 7.37 (m, 3H), 7.32 – 7.26 (m, 6H), 7.24 – 7.19 (m, 3H), 7.15 – 7.10 (m, 2H), 6.52 (d, $J = 2.0$ Hz, 1H), 5.62 (s, 1H), 1.33 (s, 9H), 1.29 (s, 9H) ppm; $^{13}\text{C}\{^1\text{H}\}$ NMR (125 MHz, CDCl_3): δ 150.9, 149.8, 149.4, 142.7, 141.7, 139.3, 131.1, 129.2, 128.7, 128.6, 128.0, 126.7, 125.8, 125.5, 122.7, 111.7, 48.2, 34.7, 34.6, 31.6 (two carbons) ppm; IR (thin film): λ_{max} 3028, 2962, 2903, 2867, 1600, 1515, 1363, 1269, 1144, 964, 909, 835, 735, 698 cm^{-1} ; HRMS calc'd for $\text{C}_{31}\text{H}_{34}\text{ONa}^+$ 445.2507, observed 445.2507 $[\text{MNa}]^+$.



4.4ac – **3-(4-methoxyphenyl)-2-((4-**

methoxyphenyl)(phenyl)methyl)furan: The reaction was performed following General Procedure D with **4.1a** (15.1 μL , 0.1 mmol, 1 equiv), KO^tBu (67.3 mg, 0.6 mmol, 6 equiv) and **4.2c** (25.0

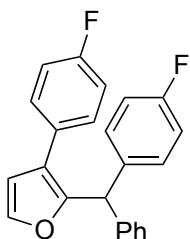
μL , 0.2 mmol, 2 equiv) in the presence of 5 mol % Pd catalyst. Ratio of di:C3 was determined to be > 20:1 by ^1H NMR of the crude reaction mixture. The crude material was purified by flash chromatography on silica gel (eluted with EtOAc:hexanes = 5:95) to give the product (27.4 mg, 74% yield) as a colorless oil. $R_f = 0.33$ (EtOAc:hexanes = 5:95); ^1H NMR (500 MHz, CDCl_3): δ 7.40 (d, $J = 2.0$ Hz, 1H), 7.32 – 7.15 (m, 7H), 7.14 – 7.04 (m, 2H), 6.94 – 6.86 (m, 2H), 6.86 – 6.77 (m, 2H), 6.49 (d, $J = 2.0$ Hz, 1H), 5.54 (s, 1H), 3.81 (s, 3H), 3.77 (s, 3H) ppm; $^{13}\text{C}\{^1\text{H}\}$ NMR (125 MHz, CDCl_3): δ 158.8, 158.4, 150.6, 142.8, 141.7, 134.6, 130.1, 129.4, 129.0, 128.6, 126.7, 126.5, 122.3, 114.3, 114.0, 111.7, 55.5, 55.4, 47.9 ppm; IR (thin film): λ_{max} 2955, 2835, 1608, 1510, 1249, 1178, 1033, 833, 745 cm^{-1} ; HRMS calc'd for $\text{C}_{25}\text{H}_{22}\text{O}_3^+$ 370.1569, observed 370.1565 $[\text{M}]^+$.



4.4ad – 4-(2-((4-(dimethylamino)phenyl)(phenyl)methyl)furan-

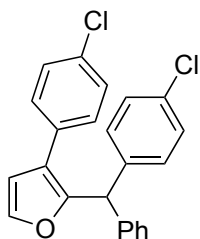
3-yl)-N,N-dimethylaniline: The reaction was performed following General Procedure D with **4.1a** (15.1 μL , 0.1 mmol, 1 equiv), KO^tBu (67.3 mg, 0.6 mmol, 6 equiv) and **4.2d** (40.0 mg, 0.2 mmol,

2 equiv) in the presence of 5 mol % Pd catalyst. Ratio of di:C3 was determined to be 4:1 by ^1H NMR of the crude reaction mixture. The crude material was purified by flash chromatography on silica gel (eluted with EtOAc:hexanes = 5:95 to 1:9) to give the product (25.7 mg, 65% yield) as a yellow oil. $R_f = 0.3$ (EtOAc:hexanes = 1:9); ^1H NMR (500 MHz, CDCl_3): δ 7.36 (d, $J = 2.0$ Hz, 1H), 7.28 – 7.15 (m, 7H), 7.10 – 7.05 (m, 2H), 6.76 – 6.71 (m, 2H), 6.69 – 6.64 (m, 2H), 6.47 (d, $J = 2.0$ Hz, 1H), 5.54 (s, 1H), 2.93 (s, 6H), 2.89 (s, 6H) ppm; $^{13}\text{C}\{^1\text{H}\}$ NMR (125 MHz, CDCl_3): δ 150.7, 149.6, 149.4, 143.4, 141.4, 130.7, 129.8, 129.08, 129.05, 128.4, 126.4, 122.4, 122.3, 112.9, 112.8, 111.6, 47.8, 40.9, 40.8 ppm; IR (thin film): λ_{max} 2885, 2801, 1615, 1523, 1351, 1197, 946, 820, 727 cm^{-1} ; HRMS calc'd for $\text{C}_{27}\text{H}_{28}\text{N}_2\text{O}^+$ 396.2202, observed 396.2183 $[\text{M}]^+$.



4.4ae – 3-(4-fluorophenyl)-2-((4-fluorophenyl)(phenyl)methyl)furan:

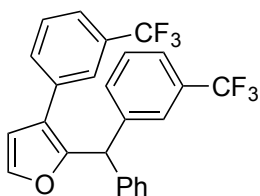
The reaction was performed following General Procedure D with **4.1a** (15.1 μ L, 0.1 mmol, 1 equiv), KO^tBu (67.3 mg, 0.6 mmol, 6 equiv) and **4.2e** (22.0 μ L, 0.2 mmol, 2 equiv) in the presence of 5 mol % Pd catalyst. Ratio of di:C3 was determined to be > 20:1 by ¹H NMR of the crude reaction mixture. The crude material was purified by flash chromatography on silica gel (eluted with hexanes to EtOAc:hexanes = 2:98) to give the product (26.2 mg, 76% yield) as a colorless oil. R_f = 0.3 (EtOAc:hexanes = 2:98); ¹H NMR (500 MHz, CDCl₃): δ 7.42 (d, J = 1.5 Hz, 1H), 7.35 – 7.23 (m, 5H), 7.19 – 7.10 (m, 4H), 7.09 – 7.02 (m, 2H), 7.00 – 6.90 (m, 2H), 6.50 (d, J = 2.0 Hz, 1H), 5.52 (s, 1H) ppm; ¹³C{¹H} NMR (125 MHz, CDCl₃): δ 162.2 (d, J = 244.7 Hz), 161.9 (d, J = 244.1 Hz), 150.5, 142.10, 142.06, 137.9 (d, J = 3.2 Hz), 130.6 (d, J = 7.7 Hz), 129.9 (d, J = 7.9 Hz), 129.0, 128.8, 127.0, 122.1, 115.8 (d, J = 21.4 Hz), 115.5 (d, J = 21.4 Hz), 111.8, 47.9 ppm; IR (thin film): λ_{max} 1601, 1507, 1224, 1158, 837, 745 cm⁻¹; HRMS calc'd for C₂₃H₁₆OF₂⁺ 346.1169, observed 346.1160 [M]⁺.



4.4af – 3-(4-chlorophenyl)-2-((4-chlorophenyl)(phenyl)methyl)furan:

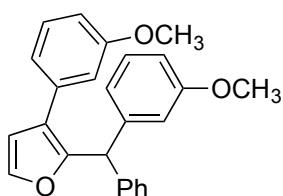
The reaction was performed following General Procedure D with **4.1a** (15.1 μ L, 0.1 mmol, 1 equiv), KO^tBu (67.3 mg, 0.6 mmol, 6 equiv) and **4.2f** (38.2 mg, 0.2 mmol, 2 equiv) in the presence of 5 mol % Pd catalyst. Ratio of di:C3 was determined to be > 20:1 by ¹H NMR of the crude reaction mixture. The crude material was purified by flash chromatography on silica gel (eluted with hexanes to EtOAc:hexanes = 2:98) to give the product (29.4 mg, 78% yield) as a colorless oil. R_f = 0.33 (EtOAc:hexanes = 2:98); ¹H NMR (500 MHz, CDCl₃): δ 7.43 (d, J = 2.0 Hz, 1H), 7.36 – 7.28 (m, 4H), 7.28 – 7.21 (m,

5H), 7.17 – 7.14 (m, 2H), 7.11 – 7.06 (m, 2H), 6.51 (d, $J = 2.0$ Hz, 1H), 5.51 (s, 1H) ppm; $^{13}\text{C}\{^1\text{H}\}$ NMR (125 MHz, CDCl_3): δ 150.5, 142.3, 141.6, 140.6, 133.1, 132.8, 132.3, 130.4, 129.6, 129.1, 129.0, 128.8 (two carbons), 127.2, 122.2, 111.6, 48.2 ppm; IR (thin film): λ_{max} 3027, 1598, 1513, 1491, 1091, 1014, 962, 830, 743, 701 cm^{-1} ; HRMS calc'd for $\text{C}_{23}\text{H}_{16}\text{OCl}_2^+$ 378.0578, observed 378.0569 $[\text{M}]^+$.



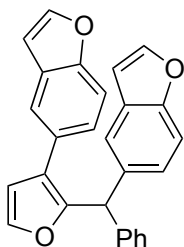
4.4ag – **2-(phenyl(3-(trifluoromethyl)phenyl)methyl)-3-(3-(trifluoromethyl)phenyl)furan**: The reaction was performed following General Procedure D with **4.1a** (36.2 μL , 0.24 mmol, 2.4 equiv), KO^tBu (67.3 mg, 0.6 mmol, 6 equiv) and **4.2g** (27.8 μL , 0.2

mmol, 2 equiv) in the presence of 5 mol % Pd catalyst. Ratio of di:C3 was determined to be > 20:1 by ^1H NMR of the crude reaction mixture. The crude material was purified by flash chromatography on silica gel (eluted with hexanes to EtOAc:hexanes = 2:98) to give the product (30.4 mg, 68% yield) as a colorless oil. $R_f = 0.33$ (EtOAc:hexanes = 2:98); ^1H NMR (500 MHz, CDCl_3): δ 7.61 – 7.52 (m, 2H), 7.52 – 7.36 (m, 7H), 7.36 – 7.30 (m, 2H), 7.30 – 7.25 (m, 1H), 7.21 – 7.14 (m, 2H), 6.57 (d, $J = 1.5$ Hz, 1H), 5.59 (s, 1H) ppm; $^{13}\text{C}\{^1\text{H}\}$ NMR (125 MHz, CDCl_3): δ 150.6, 142.8, 142.6, 141.0, 134.6, 132.5, 131.5, 131.4 (q, $J = 32$ Hz), 131.1 (q, $J = 32$ Hz), 129.4, 129.2, 129.0, 128.9, 127.4, 125.7 (q, $J = 4$ Hz), 125.1 (q, $J = 4$ Hz), 124.3 (q, $J = 271$ Hz), 124.2 (q, $J = 271$ Hz), 124.0 (q, $J = 4$ Hz, two carbons), 122.3, 111.6, 48.8 ppm; IR (thin film): λ_{max} 3064, 3030, 1601, 1515, 1495, 1448, 1331, 1277, 1167, 1126, 1075, 906, 800, 744, 701 cm^{-1} ; HRMS calc'd for $\text{C}_{25}\text{H}_{16}\text{OF}_6^+$ 446.1105, observed 446.1089 $[\text{M}]^+$.



4.4ah – **3-(3-methoxyphenyl)-2-((3-methoxyphenyl)(phenyl)methyl)furan**: The reaction was

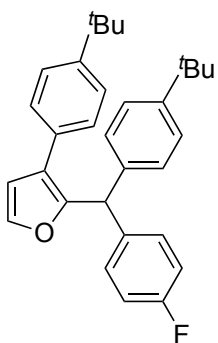
performed following General Procedure D with **4.1a** (18.1 μL , 0.12 mmol, 1.2 equiv), KO^tBu (67.3 mg, 0.6 mmol, 6 equiv) and **4.2h** (25.3 μL , 0.2 mmol, 2 equiv) in the presence of 5 mol % Pd catalyst. Ratio of di:C3 was determined to be 9:1 by ^1H NMR of the crude reaction mixture. The crude material was purified by flash chromatography on silica gel (eluted with EtOAc:hexanes = 5:95) to give the product (27.7 mg, 75% yield) as a yellow oil. R_f = 0.33 (EtOAc:hexanes = 1:9); ^1H NMR (500 MHz, CDCl_3): δ 7.41 (d, J = 2.0 Hz, 1H), 7.31 – 7.26 (m, 3H), 7.23 – 7.18 (m, 4H), 6.94 (d, J = 7.5 Hz, 1H), 6.87 – 6.74 (m, 5H), 6.53 (d, J = 2.0 Hz, 1H), 5.61 (s, 1H), 3.73 (s, 3H), 3.72 (s, 3H) ppm; $^{13}\text{C}\{^1\text{H}\}$ NMR (125 MHz, CDCl_3): δ 160.0, 159.9, 150.9, 143.9, 142.1, 141.9, 135.4, 129.8, 129.6, 129.1, 128.6, 126.8, 122.9, 121.6, 120.8, 115.3, 113.7, 113.0, 111.9, 111.7, 55.4 (two carbons), 48.8 ppm; IR (thin film): λ_{max} 3001, 2937, 2834, 1599, 1489, 1454, 1265, 1231, 1141, 1047, 781, 732, 697 cm^{-1} ; HRMS calc'd for $\text{C}_{25}\text{H}_{23}\text{O}_3^+$ 371.1647, observed 371.1637 $[\text{MH}]^+$.



4.4am – 5-(2-(benzofuran-5-yl(phenyl)methyl)furan-3-yl)benzofuran:

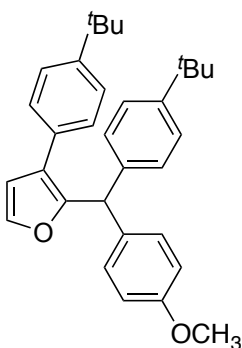
The reaction was performed following General Procedure D with **4.1a** (15.1 μL , 0.1 mmol, 1 equiv), KO^tBu (67.3 mg, 0.6 mmol, 6 equiv) and **4.2m** (25.0 μL , 0.2 mmol, 2 equiv) in the presence of 5 mol % Pd catalyst. Ratio of di:C3 was determined to be 9:1 by ^1H NMR of the crude reaction mixture. The crude material was purified by flash chromatography on silica gel (eluted with hexanes to EtOAc:hexanes = 2:98) to give the product (28.6 mg, 73% yield) as a colorless viscous oil. R_f = 0.33 (EtOAc:hexanes = 5:95); ^1H NMR (500 MHz, CDCl_3): δ 7.62 (d, J = 2.0 Hz, 1H), 7.58 (d, J = 2.0 Hz, 1H), 7.54 (d, J = 1.5 Hz, 1H), 7.49 (d, J = 8.0 Hz, 1H), 7.45 (d, J = 1.5 Hz, 1H), 7.44 – 7.39 (m, 2H), 7.33 – 7.26 (m, 3H), 7.26 – 7.19 (m, 3H), 7.18 – 7.13 (m, 1H), 6.73 (m, 1H), 6.68 (m, 1H), 6.56 (d, J = 2.0 Hz, 1H),

5.74 (s, 1H) ppm; $^{13}\text{C}\{^1\text{H}\}$ NMR (125 MHz, CDCl_3): δ 154.4, 154.1, 151.0, 145.7, 145.5, 142.9, 141.8, 137.1, 129.1, 128.9, 128.6, 128.0, 127.8, 126.8, 125.7, 125.1, 123.1, 121.6, 120.9, 112.2, 111.7, 111.4, 106.9, 106.8, 48.5 ppm; IR (thin film): λ_{max} 3115, 3060, 3026, 1600, 1512, 1494, 1467, 1443, 1264, 1236, 1133, 1111, 1031, 908, 885, 767, 738, 700 cm^{-1} ; HRMS calc'd for $\text{C}_{27}\text{H}_{18}\text{O}_3^+$ 390.1256, observed 390.1273 $[\text{M}]^+$.



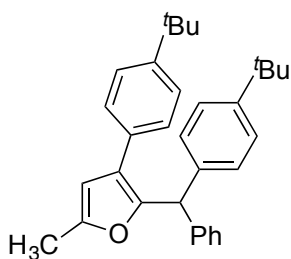
4.4bb – **3-(4-(*tert*-butyl)phenyl)-2-((4-(*tert*-butyl)phenyl)(4-fluorophenyl)methyl)furan**: The reaction was performed following General Procedure D with **4.1b** (15.7 μL , 0.1 mmol, 1 equiv), KO^tBu (67.3 mg, 0.6 mmol, 6 equiv) and **4.2b** (34.7 μL , 0.2 mmol, 2 equiv) in the presence of 5 mol % Pd catalyst. Ratio of di:C3 was determined to be > 20:1 by ^1H NMR of the crude reaction mixture. The crude

material was purified by flash chromatography on silica gel (eluted with hexanes to EtOAc:hexanes = 1:99) to give the product (34.2 mg, 78% yield) as a yellow oil. R_f = 0.33 (EtOAc:hexanes = 2:98); ^1H NMR (500 MHz, CDCl_3): δ 7.42 – 7.37 (m, 3H), 7.33 – 7.25 (m, 4H), 7.19 – 7.07 (m, 4H), 7.00 – 6.92 (m, 2H), 6.52 (d, J = 1.5 Hz, 1H), 5.58 (s, 1H), 1.34 (s, 9H), 1.30 (s, 9H) ppm; $^{13}\text{C}\{^1\text{H}\}$ NMR (125 MHz, CDCl_3): δ 161.8 (d, J = 243.6 Hz), 150.7, 150.0, 149.6, 141.8, 139.2, 138.4 (d, J = 3.0 Hz), 131.0, 130.7 (d, J = 8.0 Hz), 128.6, 128.0, 125.8, 125.6, 122.8, 115.3 (d, J = 21.2 Hz), 111.8, 47.5, 34.8, 34.6, 31.6 ppm; IR (thin film): λ_{max} 2963, 2904, 1604, 1507, 1463, 1363, 1227, 1158, 964, 909, 838, 734 cm^{-1} ; HRMS calc'd for $\text{C}_{31}\text{H}_{33}\text{OF}^+$ 440.2515, observed 440.2508 $[\text{M}]^+$.



4.4cb – **3-(4-(*tert*-butyl)phenyl)-2-((4-(*tert*-butyl)phenyl)(4-methoxyphenyl)methyl)furan**: The reaction was performed following General Procedure D with **4.1c** (21.1 μL , 0.12 mmol, 1.2

equiv), $\text{KN}(\text{SiMe}_3)_2$ (49.9 mg, 0.25 mmol, 2.5 equiv) and **4.2b** (17.3 μL , 0.1 mmol, 1 equiv) in the presence of 5 mol % Pd catalyst at 24 °C. Ratio of di:C3 was determined to be 4:1 by ^1H NMR of the crude reaction mixture. The crude material was purified by flash chromatography on silica gel (eluted with CH_2Cl_2 :hexanes = 1:9 to 2:8) to give the product (19.4 mg, 86% yield) as a colorless oil. $R_f = 0.25$ (EtOAc:hexanes = 5:95); ^1H NMR (500 MHz, CDCl_3): δ 7.42 – 7.37 (m, 3H), 7.33 – 7.26 (m, 4H), 7.17 – 7.08 (m, 4H), 6.86 – 6.80 (m, 2H), 6.52 (d, $J = 1.5$ Hz, 1H), 5.56 (s, 1H), 3.78 (s, 3H), 1.34 (s, 9H), 1.29 (s, 9H) ppm; $^{13}\text{C}\{^1\text{H}\}$ NMR (125 MHz, CDCl_3): δ 158.4, 151.2, 149.8, 149.4, 141.7, 139.7, 134.9, 131.2, 130.2, 128.6, 128.0, 125.7, 125.5, 122.5, 114.0, 111.7, 55.4, 47.4, 34.8, 34.6, 31.6 (two carbons) ppm; IR (thin film): λ_{max} 2962, 2904, 1610, 1511, 1463, 1363, 1249, 1178, 1037, 964, 838, 734 cm^{-1} ; HRMS calc'd for $\text{C}_{32}\text{H}_{37}\text{O}_2^+$ 453.2794, observed 453.2779 $[\text{MH}]^+$.



4.4db – **3-(4-(tert-butyl)phenyl)-2-((4-(tert-butyl)phenyl)(phenyl)methyl)-5-methylfuran:**

The reaction was performed following General Procedure D with **4.1d** (17.2 μL , 0.1 mmol, 1 equiv), KO^tBu (67.3 mg, 0.6 mmol, 6 equiv) and **4.2b** (34.7 μL , 0.2 mmol, 2 equiv) in the presence of 5 mol %

Pd catalyst. Ratio of di:C3 was determined to be > 20:1 by ^1H NMR of the crude reaction mixture. The crude material was purified by flash chromatography on silica gel (eluted with hexanes to EtOAc:hexanes = 1:99) to give the product (25.4 mg, 58% yield) as a yellow oil. $R_f = 0.25$ (EtOAc:hexanes = 1:99); ^1H NMR (500 MHz, CDCl_3): δ 7.38 – 7.35 (m, 2H), 7.31 – 7.25 (m, 6H), 7.25 – 7.18 (m, 3H), 7.16 – 7.12 (m, 2H), 6.10 (s, 1H), 5.54 (s, 1H), 2.28 (s, 3H), 1.33 (s, 9H), 1.30 (s, 9H) ppm; $^{13}\text{C}\{^1\text{H}\}$ NMR (125 MHz, CDCl_3): δ 151.2, 149.6, 149.3, 149.0, 143.1, 139.7, 131.7, 129.2, 128.8, 128.5, 127.9, 126.5, 125.7,

125.4, 123.6, 107.8, 48.2, 34.7, 34.6, 31.62, 31.60, 13.9 ppm; IR (thin film): λ_{\max} 2963, 2904, 2867, 1575, 1513, 1494, 1452, 1363, 1269, 909, 839, 799, 736, 699 cm^{-1} ; HRMS calc'd for $\text{C}_{32}\text{H}_{37}\text{O}_2^+$ 436.2766, observed 436.2773 [M]⁺.

Representative Microscale High-throughput Experimentation.

General Experimental.

The experimental procedures in this work were similar to those reported.⁶⁸ Parallel synthesis was accomplished in an MBraun glovebox operating with a constant N_2 -purge (oxygen typically <5 ppm). The experimental design was accomplished using Accelrys Library Studio. Screening reactions were carried out in 1 mL vials (30 mm height \times 8 mm diameter) in a 96-well plate aluminum reactor block. Liquid chemicals were dosed using multi-channel or single-channel pipettors. Solid chemicals were dosed manually as solutions or slurries in appropriate solvents. Undesired additional solvent was removed using a GeneVac system located inside the glovebox. The reactions were heated and stirred on a heating block with a tumble-stirrer (V&P Scientific) using 1.98 mm diameter \times 4.80 mm length parylene stir bars. The tumble stirring mechanism helped to insure uniform stirring throughout the 96-well plate. The reactions were sealed in the 96-well plate during reaction. Below each reactor vial in the aluminum 96-well plate was a 0.062 mm thick silicon-rubber gasket. Directly above the glass vial reactor tops was a Teflon perfluoroalkoxy copolymer resin sealing gasket and above that, two more 0.062 mm thick silicon-rubber gaskets. The entire assembly was compressed between an aluminum top and the reactor base with 9 evenly-placed screws.

Set up:

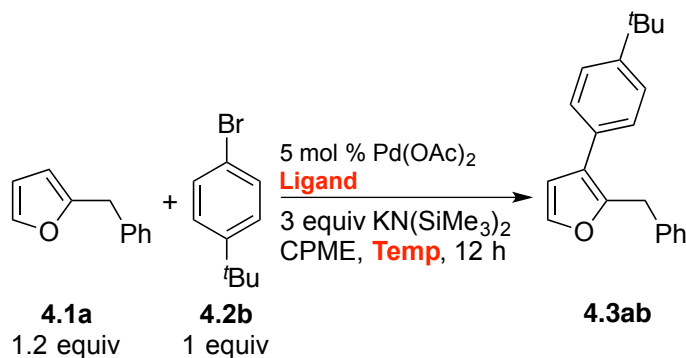
Experiments were set up inside a glovebox under a nitrogen atmosphere. A 96-well aluminum block containing 1 mL glass vials was predosed with $\text{Pd}(\text{OAc})_2$ (0.5 μmol) and

Ligand (Ligand was used in a 4:1 ratio relative to Pd for monodentate ligands and 2:1 ratio for bidentate ligands) in THF. The solvent was evacuated to dryness using a Genevac vacuum centrifuge, and $\text{KN}(\text{SiMe}_3)_2$ (30 μmol) in THF was added to the ligand/catalyst mixture. The solvent was removed on the Genevac, and a parylene stir bar was then added to each reaction vial. 1-Bromo-4-*tert*-butylbenzene (10 μmol /reaction), 2-benzylfuran (12 μmol /reaction) and biphenyl (1 μmol /reaction) (used as an internal standard to measure HPLC yields) were then dosed together into each reaction vial as a solution in CPME (100 μL , 0.1 M). The 96-well plate was then sealed and stirred for 12 h at 24 °C.

Work up:

Upon opening the plate to air, 500 μL of acetonitrile was pipetted into each vial. The plate was then covered again and the vials stirred for 20 min to extract the product and to ensure good homogenization. Into a separate 96-well LC block was added 700 μL of acetonitrile, followed by 40 μL of the diluted reaction mixtures. The LC block was then sealed with a silicon-rubber storage mat, and mounted on HPLC instrument for analysis.

(1) Ligand and temperature screening for C3 arylation of **4.1a** with **4.2b**.



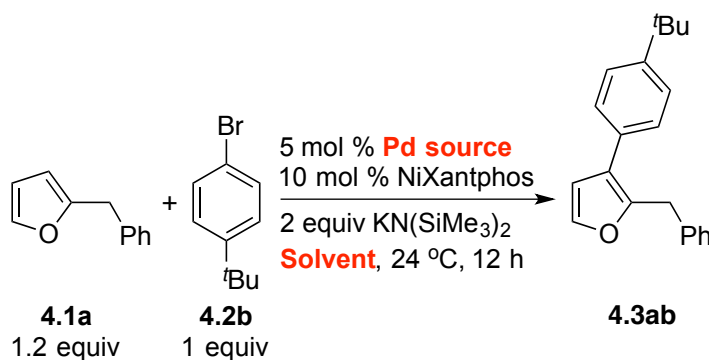
Ligands examined ($\times 24$): XPhos, SPhos, RuPhos, cataCXium A, Dppf, Dtbpf, *t*-Bu-XPhos, P(*o*-Tol)₃, JohnPhos, BrettPhos, PCy₃HBF₄, (*S*)-BINAP, Pt-Bu₃HBF₄, Xantphos,

DavePhos, QPhos, *t*-Bu-BrettPhos, TrippyPhos, BippyPhos, Mor-DalPhos, A-^{ta}Phos, PPh₃, NiXantphos, and no ligand as control.

Temperatures examined (×2): 24 and 110 °C.

The lead hit from the screening was the combination of NiXantphos and 24 °C, giving 21% HPLC AY of **4.3ab**. The other 22 ligands afforded <5% HPLC AY at both temperatures.

(2) Solvent and Pd source screening for C3 arylation of **4.1a** with **4.2b**.



Solvents examined (×4): CPME, dioxane, THF, and 2-MeTHF.

Pd sources examined (×6): Pd(OAc)₂, Pd(COD)Cl₂, Pd(NCMe)₂Cl₂, [Pd(allyl)Cl]₂, Pd₂dba₃, and Pd(PPh₃)₄.

The lead hits from the screening were the combination of dioxane as solvent with 3 palladium sources afforded excellent HPLC AY of **4.3ab**: 100% AY from Pd(OAc)₂, 97% AY from Pd(COD)Cl₂, and 99% AY from Pd(NCMe)₂Cl₂ (Table 4.7).

Table 4.7 HTE using 4 solvents and 6 Pd sources

Pd	Solvent	4.3ab (%)	Pd	Solvent	4.3ab (%)
Pd(OAc) ₂	CPME	55.0	Pd(OAc) ₂	THF	66.7
Pd(COD)Cl ₂	CPME	56.0	Pd(COD)Cl ₂	THF	66.9

Pd(NCMe) ₂ Cl ₂	CPME	75.2	Pd(NCMe) ₂ Cl ₂	THF	72.6
[Pd(allyl)Cl] ₂	CPME	61.8	[Pd(allyl)Cl] ₂	THF	67.0
Pd ₂ dba ₃	CPME	34.3	Pd ₂ dba ₃	THF	57.1
Pd(PPh ₃) ₄	CPME	10.1	Pd(PPh ₃) ₄	THF	9.5
Pd(OAc)₂	dioxane	102.5	Pd(OAc) ₂	2-MeTHF	57.7
Pd(COD)Cl₂	dioxane	96.7	Pd(COD)Cl ₂	2-MeTHF	56.3
Pd(NCMe)₂Cl₂	dioxane	99.4	Pd(NCMe) ₂ Cl ₂	2-MeTHF	68.3
[Pd(allyl)Cl] ₂	dioxane	90.3	[Pd(allyl)Cl] ₂	2-MeTHF	50.6
Pd ₂ dba ₃	dioxane	75.5	Pd ₂ dba ₃	2-MeTHF	40.8
Pd(PPh ₃) ₄	dioxane	1.4	Pd(PPh ₃) ₄	2-MeTHF	4.9

4.5 References

- (1) Dugger, R. W.; Ragan, J. A.; Ripin, D. H. B. *Org. Process Res. Dev.* **2005**, *9*, 253.
- (2) Busacca, C. A.; Fandrick, D. R.; Song, J. J.; Senanayake, C. H. *Adv. Synth. Catal.* **2011**, *353*, 1825.
- (3) Magano, J.; Dunetz, J. R. *Chem. Rev.* **2011**, *111*, 2177.
- (4) Campeau, L.-C.; Fagnou, K. *Chem. Commun.* **2006**, 1253.
- (5) Alberico, D.; Scott, M. E.; Lautens, M. *Chem. Rev.* **2007**, *107*, 174.
- (6) Goj, L. A.; Gunnoe, T. B. *Curr. Org. Chem.* **2005**, *9*, 671.
- (7) Li, B.-J.; Yang, S.-D.; Shi, Z.-J. *Synlett* **2008**, 949.
- (8) Tobisu, M.; Chatani, N. *Angew. Chem., Int. Ed.* **2006**, *45*, 1683.
- (9) Jazzar, R.; Hitce, J.; Renaudat, A.; Sofack-Kreutzer, J.; Baudoin, O. *Chem.–Eur. J.* **2010**, *16*, 2654.
- (10) Wasa, M.; Engle, K. M.; Yu, J.-Q. *Isr. J. Chem.* **2010**, *50*, 605.
- (11) Baudoin, O. *Chem. Soc. Rev.* **2011**, *40*, 4902.

- (12) Girard, S. A.; Knauber, T.; Li, C.-J. *Angew. Chem., Int. Ed.* **2014**, *53*, 74.
- (13) Li, H.; Li, B.-J.; Shi, Z.-J. *Catal. Sci. Technol.* **2011**, *1*, 191.
- (14) Lyons, T. W.; Sanford, M. S. *Chem. Rev.* **2010**, *110*, 1147.
- (15) Chen, X.; Engle, K. M.; Wang, D.-H.; Yu, J.-Q. *Angew. Chem., Int. Ed.* **2009**, *48*, 5094.
- (16) Daugulis, O.; Do, H.-Q.; Shabashov, D. *Acc. Chem. Res.* **2009**, *42*, 1074.
- (17) Mousseau, J. J.; Charette, A. B. *Acc. Chem. Res.* **2013**, *46*, 412.
- (18) Mahatthananchai, J.; Dumas, A. M.; Bode, J. W. *Angew. Chem., Int. Ed.* **2012**, *51*, 10954.
- (19) Neufeldt, S. R.; Sanford, M. S. *Acc. Chem. Res.* **2012**, *45*, 936.
- (20) Roduner, E.; Kaim, W.; Sarkar, B.; Urlacher, V. B.; Pleiss, J.; Gläser, R.; Einicke, W.-D.; Sprenger, G. A.; Beifuß, U.; Klemm, E.; Liebner, C.; Hieronymus, H.; Hsu, S.-F.; Plietker, B.; Laschat, S. *ChemCatChem* **2013**, *5*, 82.
- (21) Campeau, L.-C.; Schipper, D. J.; Fagnou, K. *J. Am. Chem. Soc.* **2008**, *130*, 3266.
- (22) Schipper, D. J.; Campeau, L.-C.; Fagnou, K. *Tetrahedron* **2009**, *65*, 3155.
- (23) Bassoude, I.; Berteina-Raboin, S.; Massip, S.; Leger, J.-M.; Jarry, C.; Essassi, E. M.; Guillaumet, G. *Eur. J. Org. Chem.* **2012**, 2572.
- (24) Zhao, L.; Bruneau, C.; Doucet, H. *Chem. Commun.* **2013**, *49*, 5598.
- (25) Ackermann, L.; Vicente, R.; Kapdi, A. R. *Angew. Chem., Int. Ed.* **2009**, *48*, 9792.
- (26) Chiusoli, G. P.; Catellani, M.; Costa, M.; Motti, E.; Ca', N. D.; Maestri, G. *Coord. Chem. Rev.* **2010**, *254*, 456.
- (27) Bellina, F.; Rossi, R. *Tetrahedron* **2009**, *65*, 10269.
- (28) Messaoudi, S.; Brion, J.-D.; Alami, M. *Eur. J. Org. Chem.* **2010**, 6495.
- (29) Satoh, T.; Miura, M. *Chem. Lett.* **2007**, *36*, 200.
- (30) Bellina, F.; Cauteruccio, S.; Rossi, R. *Curr. Org. Chem.* **2008**, *12*, 774.

- (31) Seregin, I. V.; Gevorgyan, V. *Chem. Soc. Rev.* **2007**, *36*, 1173.
- (32) Boto, A.; Alvarez, L. Furan and its Derivatives in Natural Product Synthesis. In *Heterocycles in Natural Product Synthesis*; Majumdar, K. C., Chattopadhyay, S. K., Eds.; Wiley-VCH: Weinheim, Germany, 2011; p 99.
- (33) Raczko, J.; Jurczak, J. *Stud. Nat. Prod. Chem.* **1995**, *16*, 639.
- (34) Li, J. J. *Heterocyclic Chemistry in Drug Discovery*; John Wiley & Sons, 2013.
- (35) Keay, B. A.; Dibble, P. W. In *Comprehensive Heterocyclic Chemistry II*; Katritzky, A. R., Rees, C. W., Scriven, E. F. V., Eds.; Elsevier: Oxford, 1996; Vol. 2, p 395.
- (36) Donnelly, D. M. X.; Meegan, M. J. In *Comprehensive Heterocyclic Chemistry*; Katritzky, A. R., Rees, C. W., Eds.; Pergamon: Oxford, 1984; Vol. 4, p 657.
- (37) Dean, F. M. *Naturally Occurring Oxygen Ring Compounds*; Butterworths: London, 1963; Chapter 1, p 1.
- (38) Roger, J.; Gottumukkala, A. L.; Doucet, H. *ChemCatChem* **2010**, *2*, 20.
- (39) Larbi, K. S.; Fu, H. Y.; Laidaoui, N.; Beydoun, K.; Miloudi, A.; El Abed, D.; Djabbar, S.; Doucet, H. *ChemCatChem* **2012**, *4*, 815.
- (40) Qvortrup, K.; Rankic, D. A.; MacMillan, D. W. C. *J. Am. Chem. Soc.* **2014**, *136*, 626.
- (41) Pan, F.; Shen, P.-X.; Zhang, L.-S.; Wang, X.; Shi, Z.-J. *Org. Lett.* **2013**, *15*, 4758.
- (42) Kuninobu, Y.; Asanoma, D.; Takai, K. *Synlett* **2010**, 2883.
- (43) Kul'nevich, V. G.; Zhuravlev, S. V. *Chem. Heterocycl. Compd.* **1984**, *20*, 244.
- (44) Gutnov, A. V.; Butin, A. V.; Abaev, V. T.; Krapivin, G. D.; Zavodnik, V. E. *Molecules* **1999**, *4*, 204.
- (45) Bordwell, F. G. *Acc. Chem. Res.* **1988**, *21*, 456.
- (46) van der Veen, L. A.; Keeven, P. H.; Schoemaker, G. C.; Reek, J. N. H.; Kamer, P. C. J.; van Leeuwen, P. W. N. M.; Lutz, M.; Spek, A. L. *Organometallics* **2000**, *19*, 872.

- (47) Zhang, J.; Bellomo, A.; Creamer, A. D.; Dreher, S. D.; Walsh, P. J. *J. Am. Chem. Soc.* **2012**, *134*, 13765.
- (48) Bellomo, A.; Zhang, J.; Trongsirawat, N.; Walsh, P. J. *Chem. Sci.* **2013**, *4*, 849.
- (49) Bellina, F.; Rossi, R. *Chem. Rev.* **2010**, *110*, 1082.
- (50) Johansson, C. C. C.; Colacot, T. J. *Angew. Chem., Int. Ed.* **2010**, *49*, 676.
- (51) Culkin, D. A.; Hartwig, J. F. *Acc. Chem. Res.* **2003**, *36*, 234.
- (52) Balaban, A. T.; Oniciu, D. C.; Katritzky, A. R. *Chem. Rev.* **2004**, *104*, 2777.
- (53) Reetz, M. T.; Kühling, K. M.; Deege, A.; Hinrichs, H.; Belder, D. *Angew. Chem., Int. Ed.* **2000**, *39*, 3891.
- (54) Trapp, O.; Weber, S. K.; Bauch, S.; Hofstadt, W. *Angew. Chem., Int. Ed.* **2007**, *46*, 7307.
- (55) Dreher, S. D.; Dormer, P. G.; Sandrock, D. L.; Molander, G. A. *J. Am. Chem. Soc.* **2008**, *130*, 9257.
- (56) Davies, I. W.; Welch, C. J. *Science* **2009**, *325*, 701.
- (57) Robbins, D. W.; Hartwig, J. F. *Science* **2011**, *333*, 1423.
- (58) McNally, A.; Prier, C. K.; MacMillan, D. W. C. *Science* **2011**, *334*, 1114.
- (59) Bellomo, A.; Celebi-Olcum, N.; Bu, X.; Rivera, N.; Ruck, R. T.; Welch, C. J.; Houk, K. N.; Dreher, S. D. *Angew. Chem., Int. Ed.* **2012**, *51*, 6912.
- (60) Hussain, N.; Frensch, G.; Zhang, J.; Walsh, P. J. *Angew. Chem., Int. Ed.* **2014**, *53*, 3693.
- (61) Wu, H.-J.; Lin, C.-C. *J. Org. Chem.* **1996**, *61*, 3820.
- (62) Wu, H.-J.; Lin, C.-C. *J. Org. Chem.* **1995**, *60*, 7558.
- (63) Li, H.; Li, W.; Liu, W.; He, Z.; Li, Z. *Angew. Chem., Int. Ed.* **2011**, *50*, 2975.
- (64) Yang, Z.; Tang, P.; Gauuan, J. F.; Molino, B. F. *J. Org. Chem.* **2009**, *74*, 9546.
- (65) Zhang, Y.; Feng, M.-T.; Lu, J.-M. *Org. Biomol. Chem.* **2013**, *11*, 2266.

- (66) Chang, S.-T.; Li, Q.; Chiang, R.-T.; Gau, H.-M. *Tetrahedron* **2012**, *68*, 3956.
- (67) Du, X.; Song, F.; Lu, Y.; Chen, H.; Liu, Y. *Tetrahedron* **2009**, *65*, 1839.
- (68) Dreher, S. D.; Dormer, P. G.; Sandrock, D. L.; Molander, G. A. *J. Am. Chem. Soc.* **2008**, *130*, 9257.

Appendix A1. NMR Spectra Relevant to Chapter 1

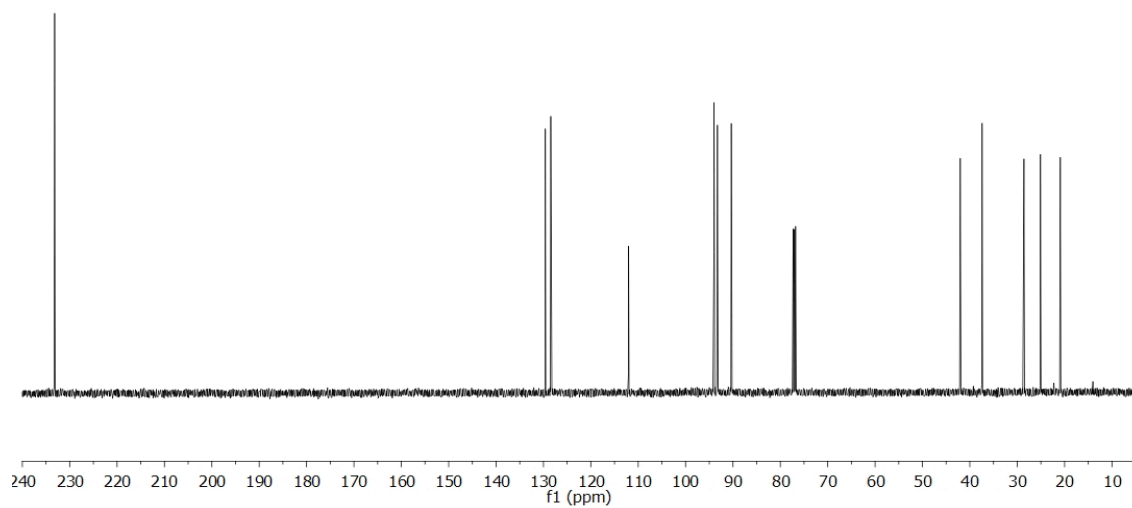
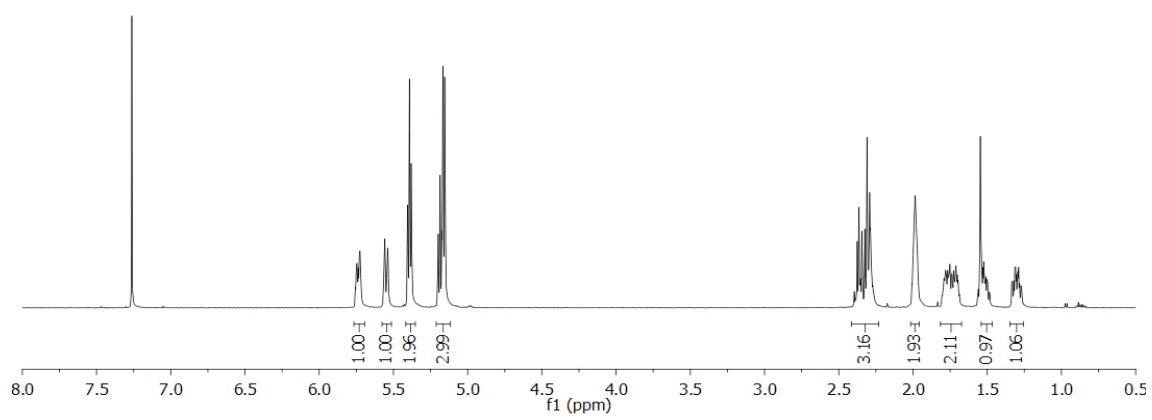
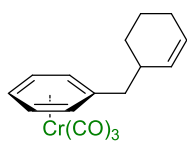


Figure A1.1 500 MHz ¹H and 125 MHz ¹³C{¹H} NMR of **1.3a** in CDCl₃

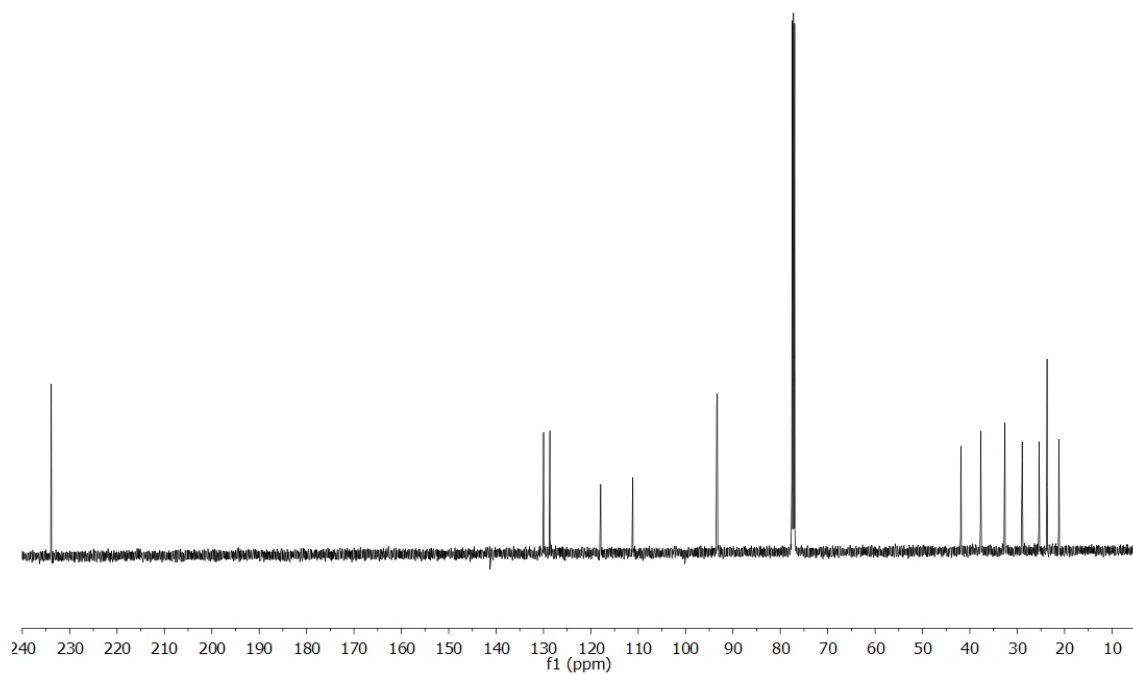
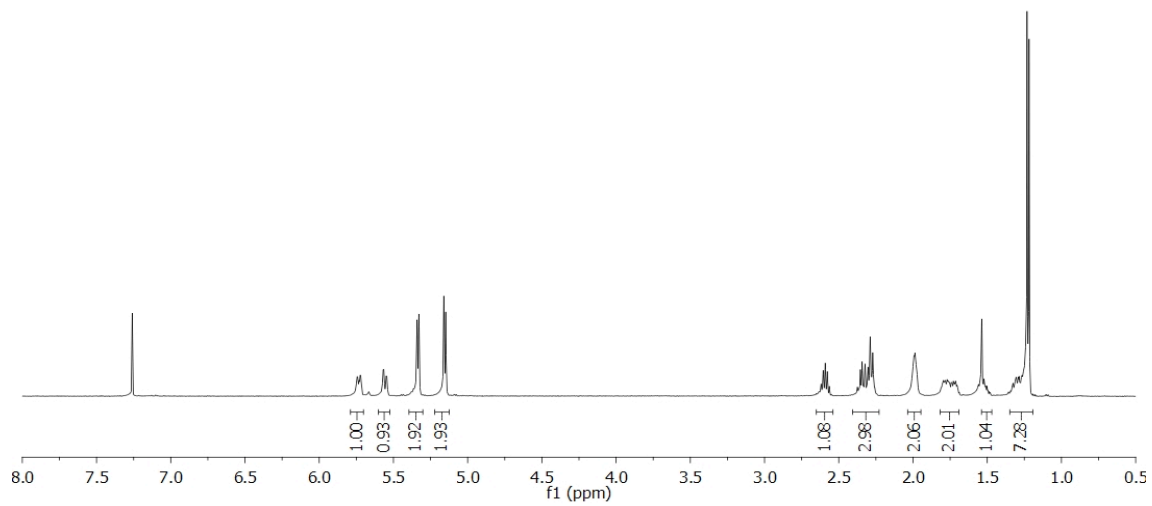
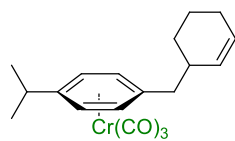


Figure A1.2 500 MHz ^1H and 125 MHz $^{13}\text{C}\{^1\text{H}\}$ NMR of **1.3b** in CDCl_3

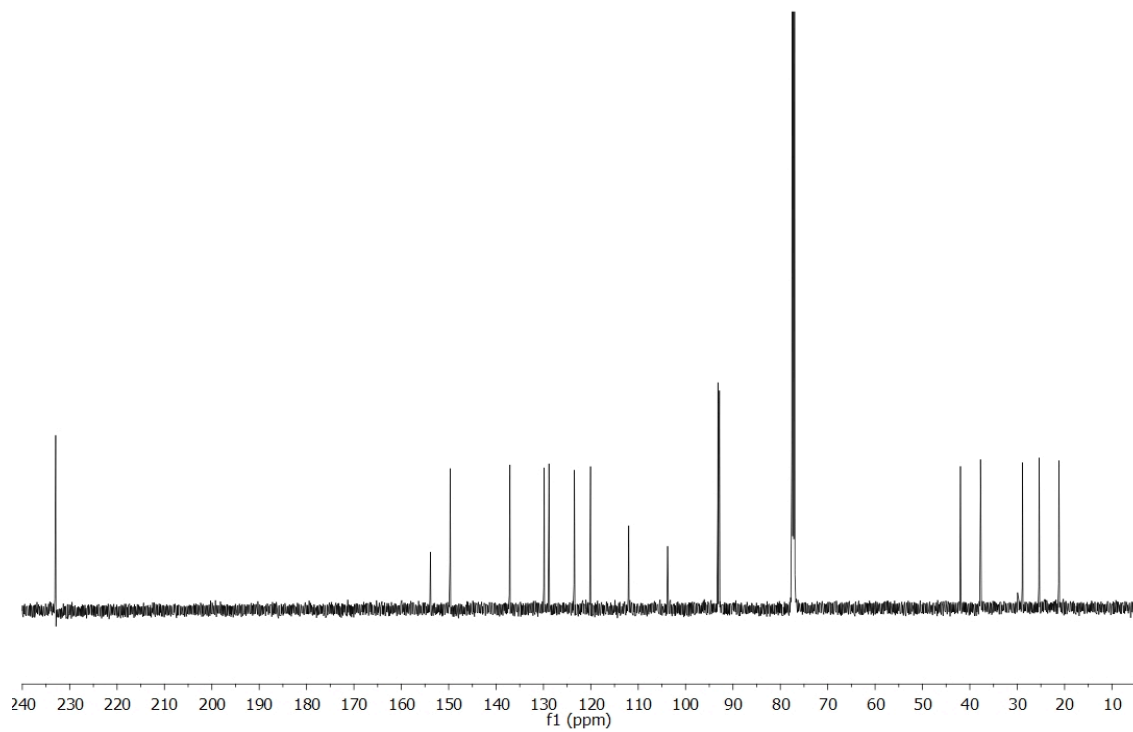
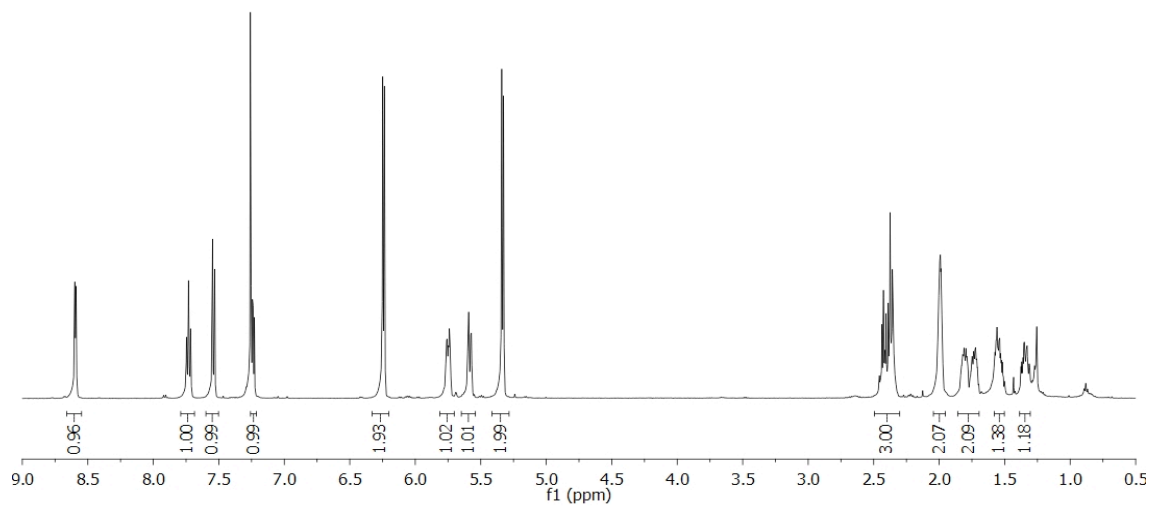
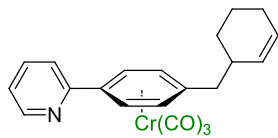


Figure A1.3 500 MHz ^1H and 125 MHz $^{13}\text{C}\{^1\text{H}\}$ NMR of **1.3e** in CDCl_3

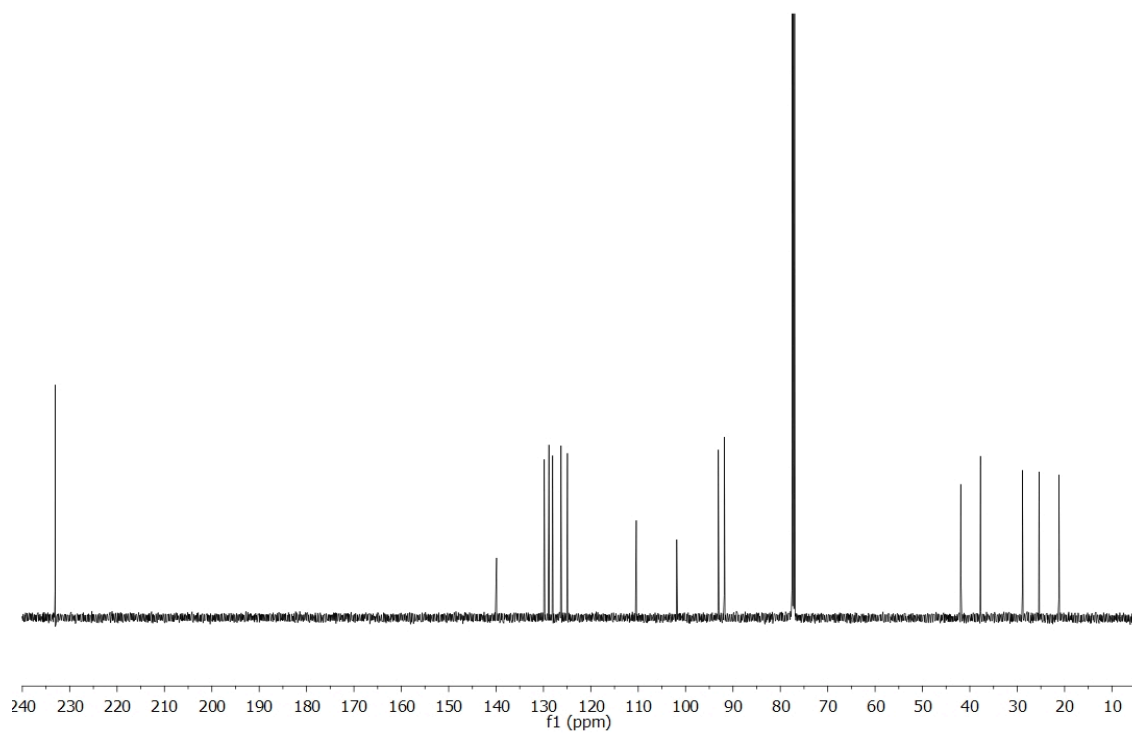
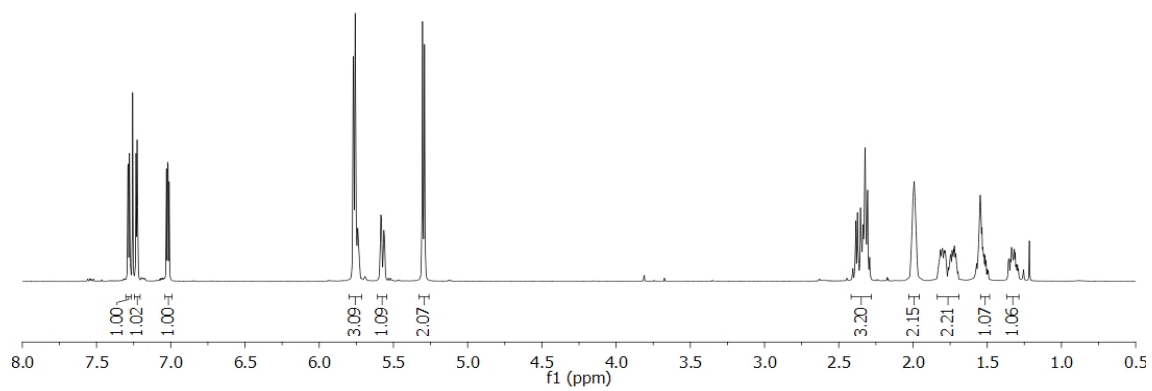
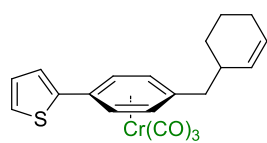


Figure A1.4 500 MHz ^1H and 125 MHz $^{13}\text{C}\{^1\text{H}\}$ NMR of **1.3f** in CDCl_3

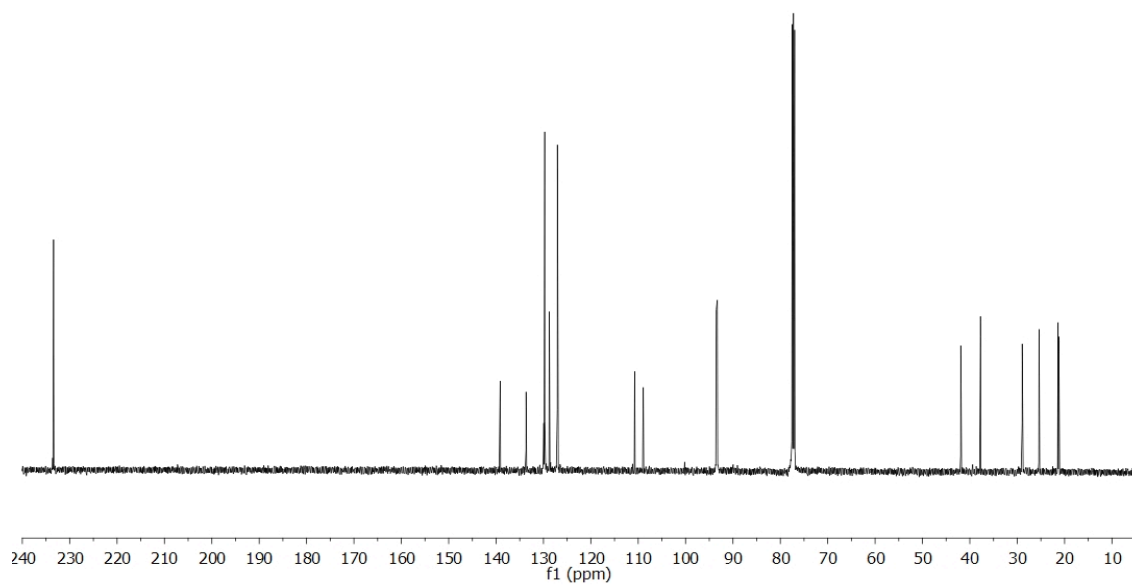
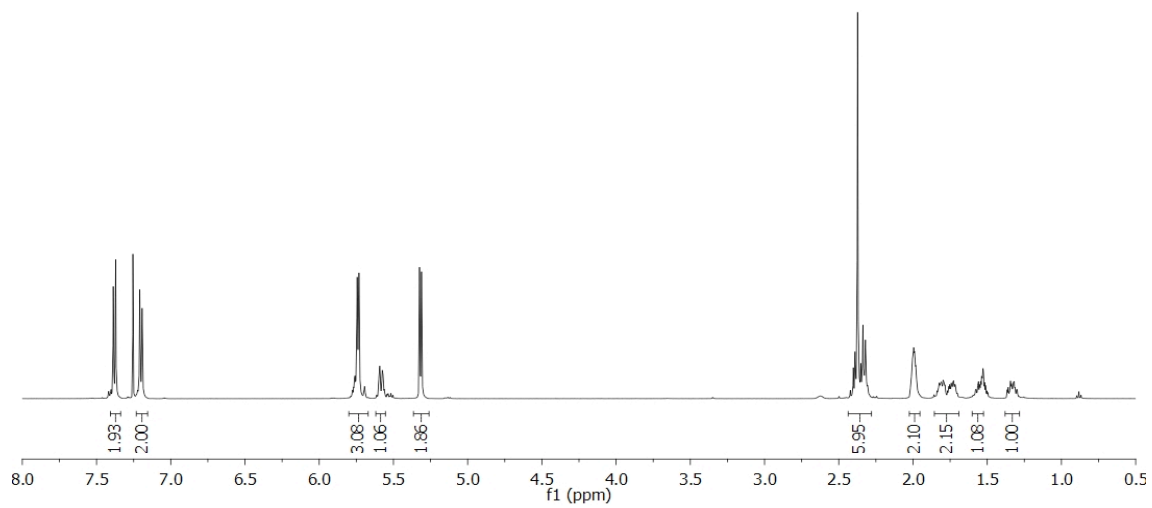
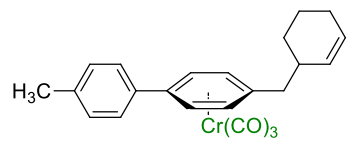


Figure A1.5 500 MHz ^1H and 125 MHz $^{13}\text{C}\{^1\text{H}\}$ NMR of **1.3d** in CDCl_3

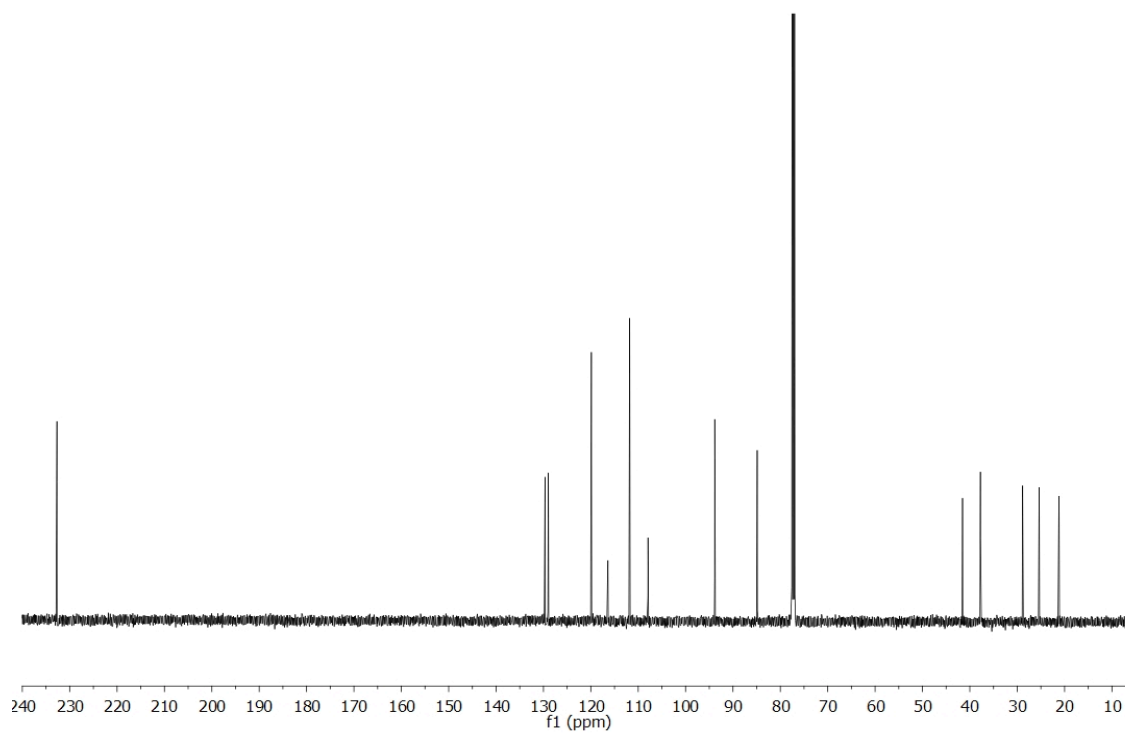
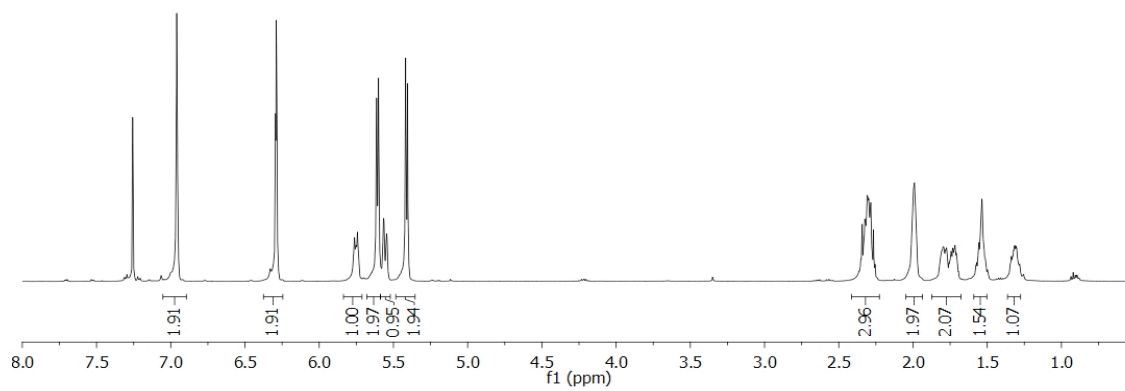
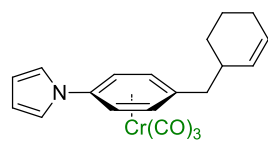


Figure A1.6 500 MHz ¹H and 125 MHz ¹³C{¹H} NMR of **1.3g** in CDCl₃

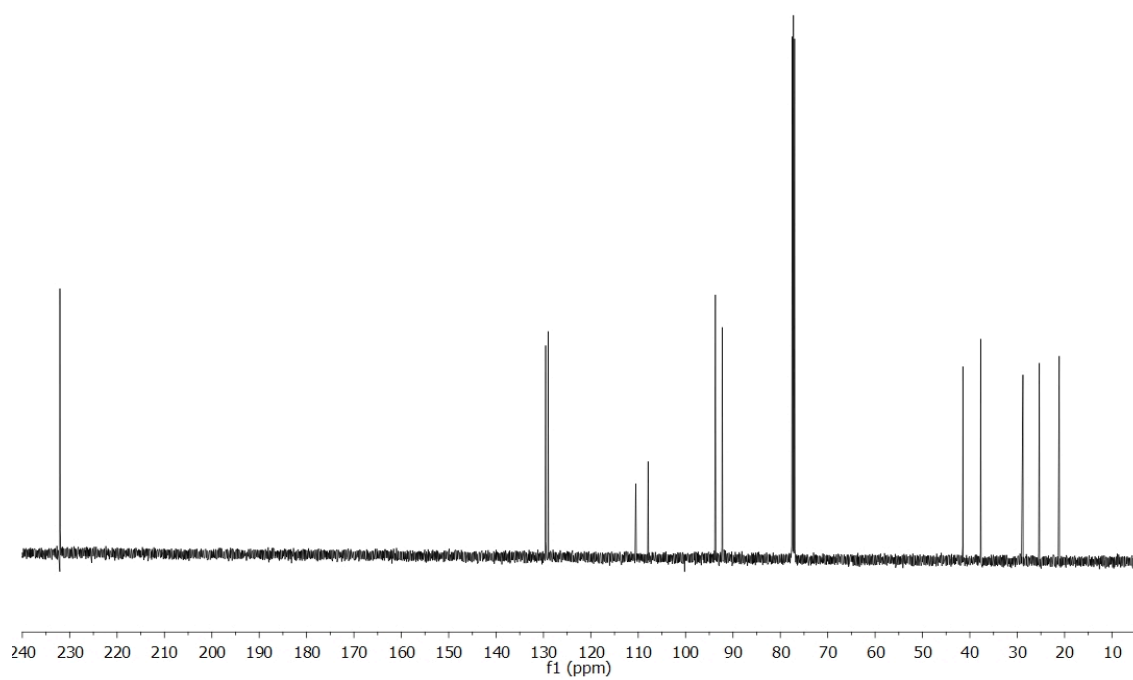
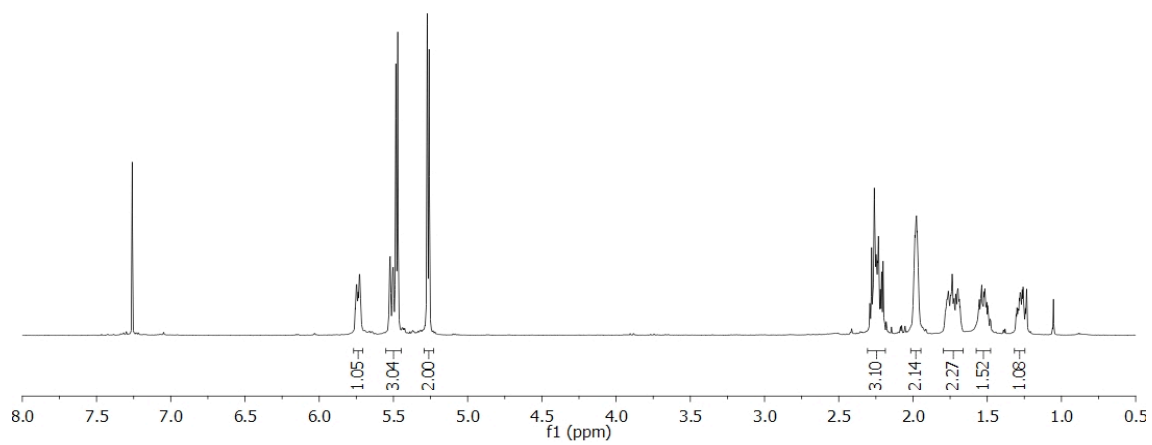
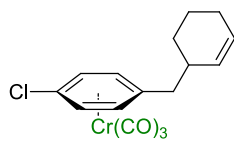


Figure A1.7 500 MHz ^1H and 125 MHz $^{13}\text{C}\{^1\text{H}\}$ NMR of **1.3h** in CDCl_3

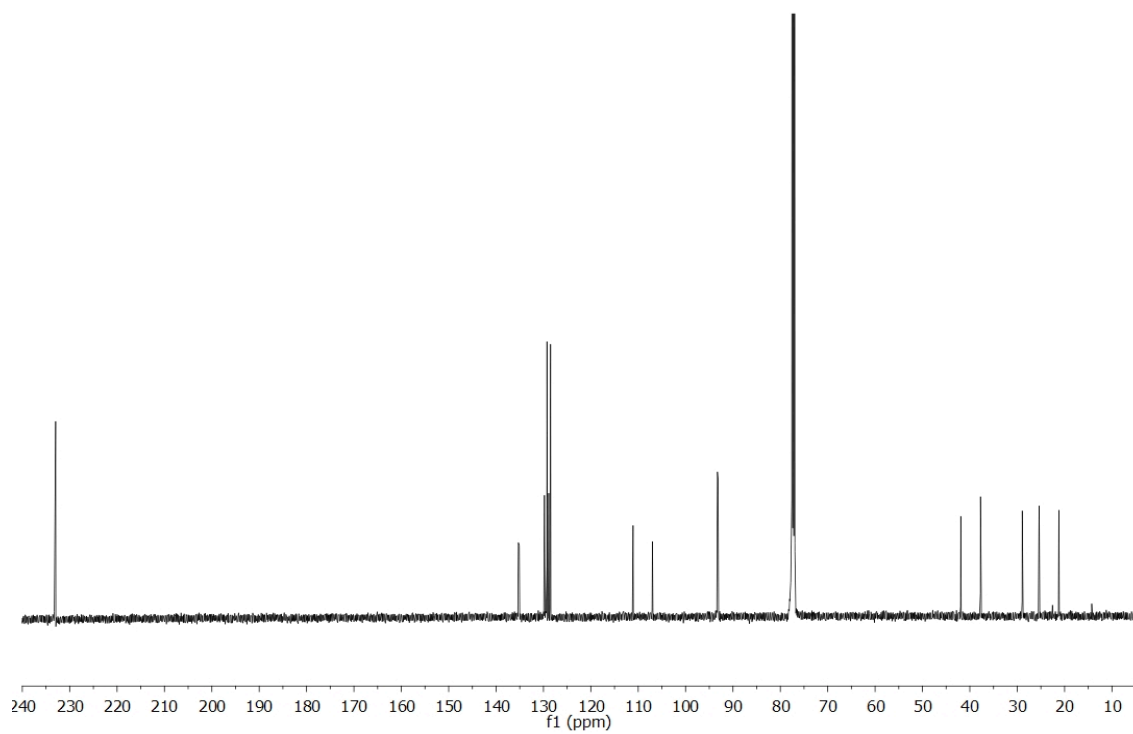
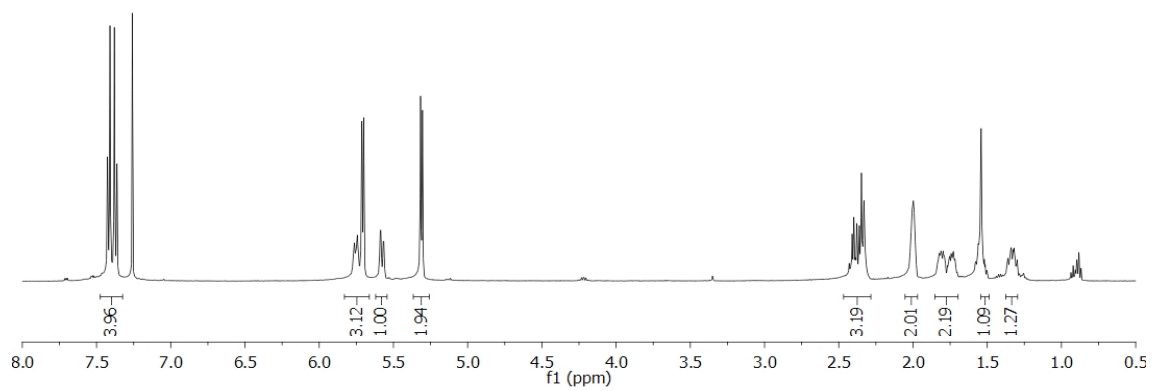
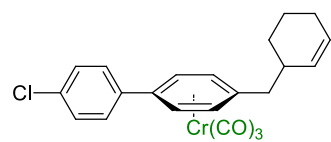


Figure A1.8 500 MHz ^1H and 125 MHz $^{13}\text{C}\{^1\text{H}\}$ NMR of **1.3i** in CDCl_3

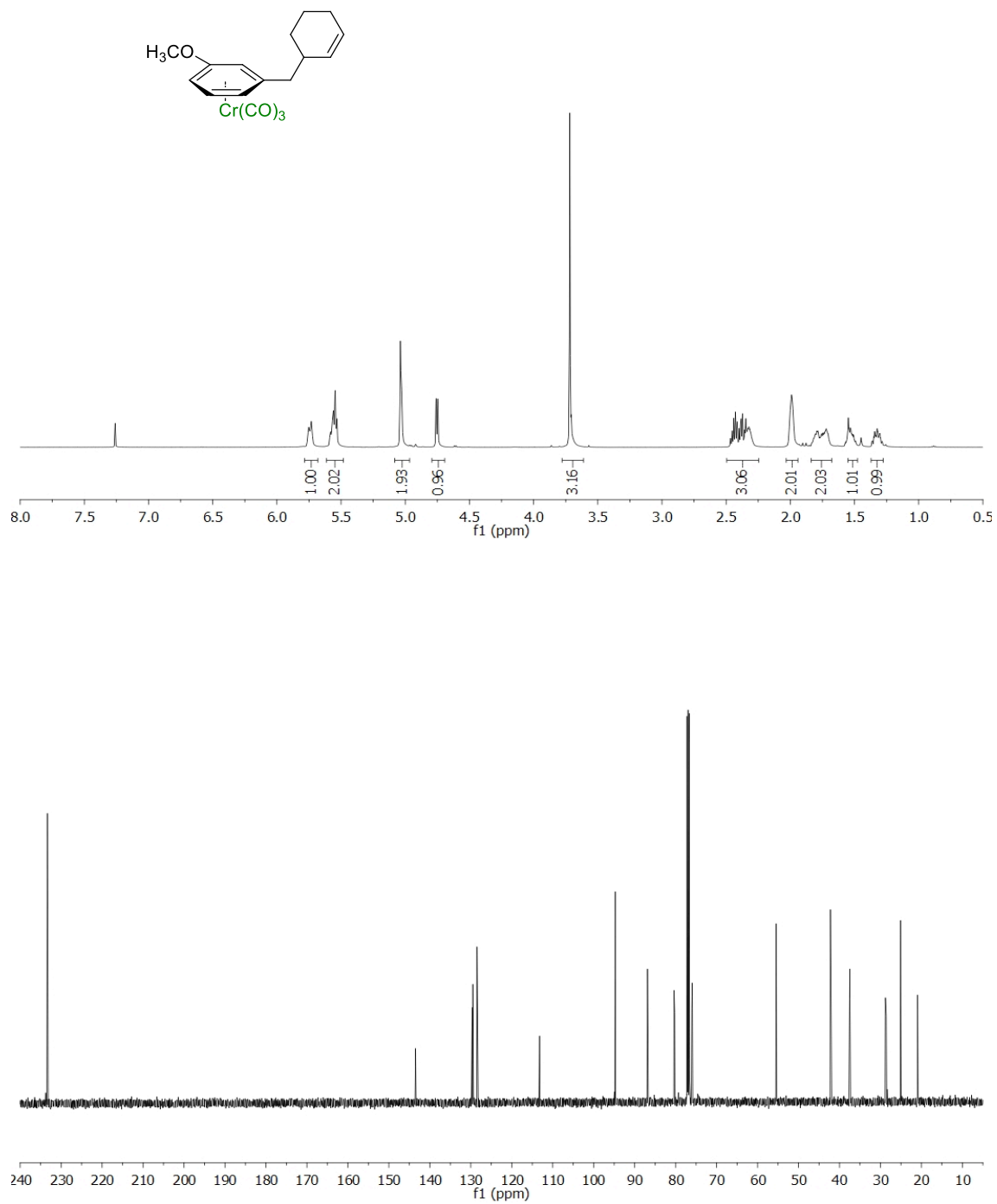


Figure A1.9 500 MHz ^1H and 125 MHz $^{13}\text{C}\{^1\text{H}\}$ NMR of **1.3c** in CDCl_3

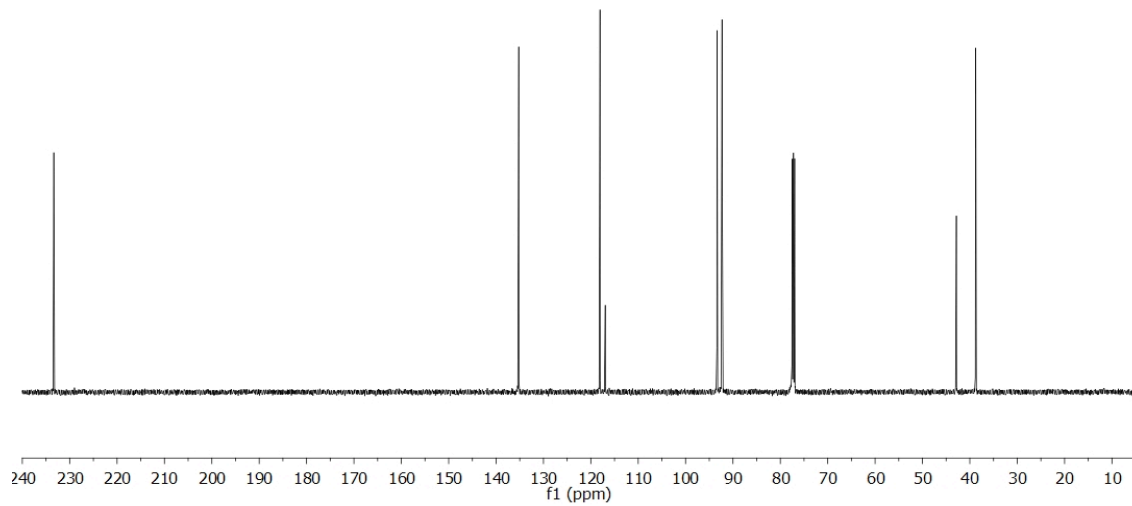
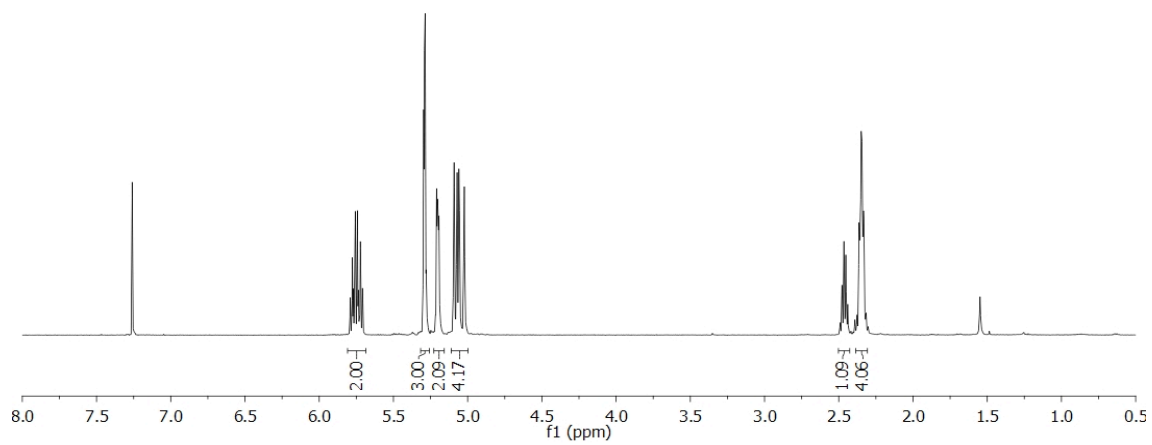
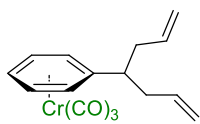


Figure A1.10 500 MHz ^1H and 125 MHz $^{13}\text{C}\{^1\text{H}\}$ NMR of **1.4ad** in CDCl_3

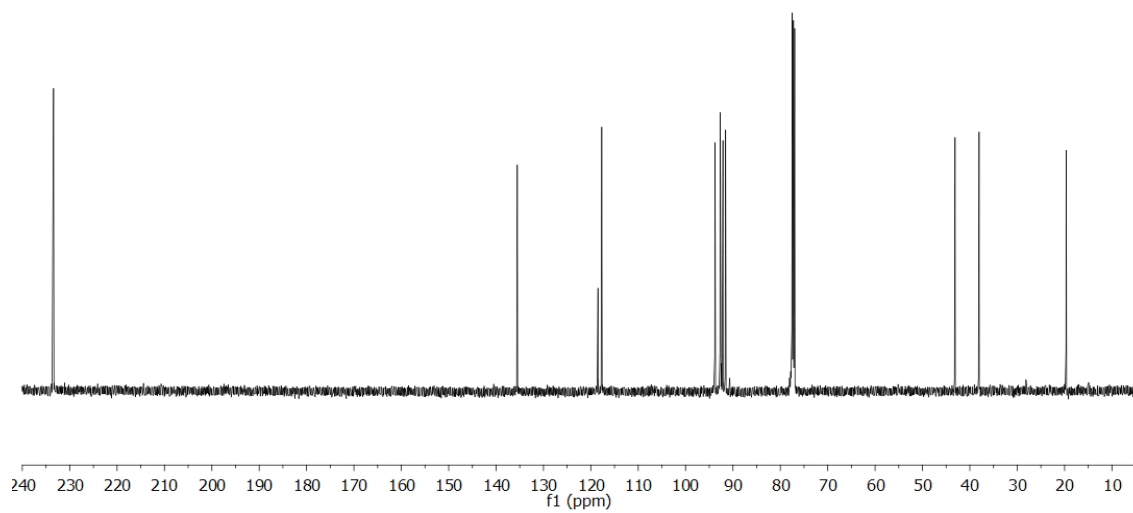
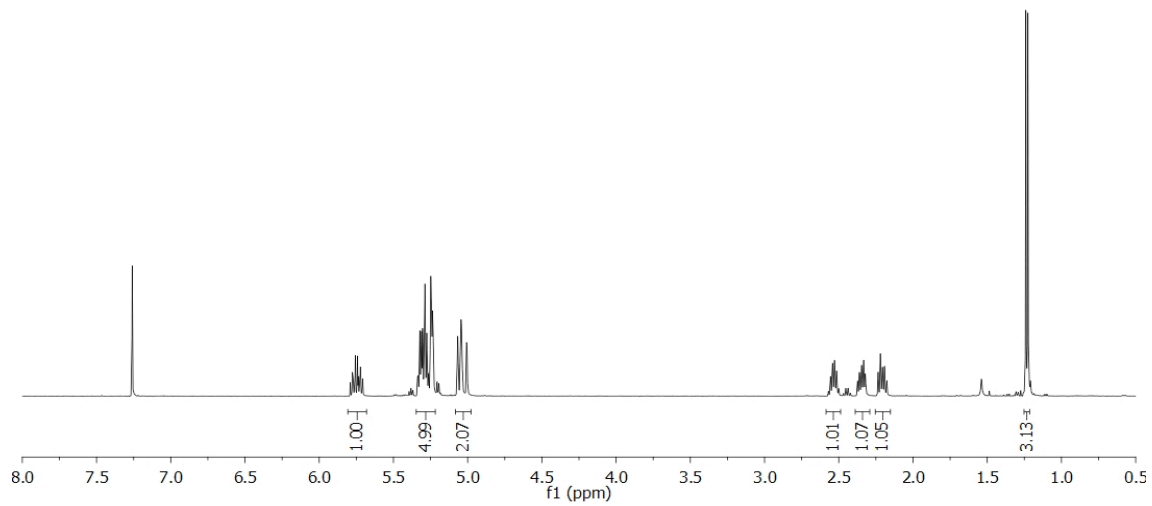
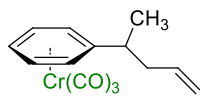


Figure A1.11 500 MHz ¹H and 125 MHz ¹³C{¹H} NMR of **1.4kd** in CDCl₃

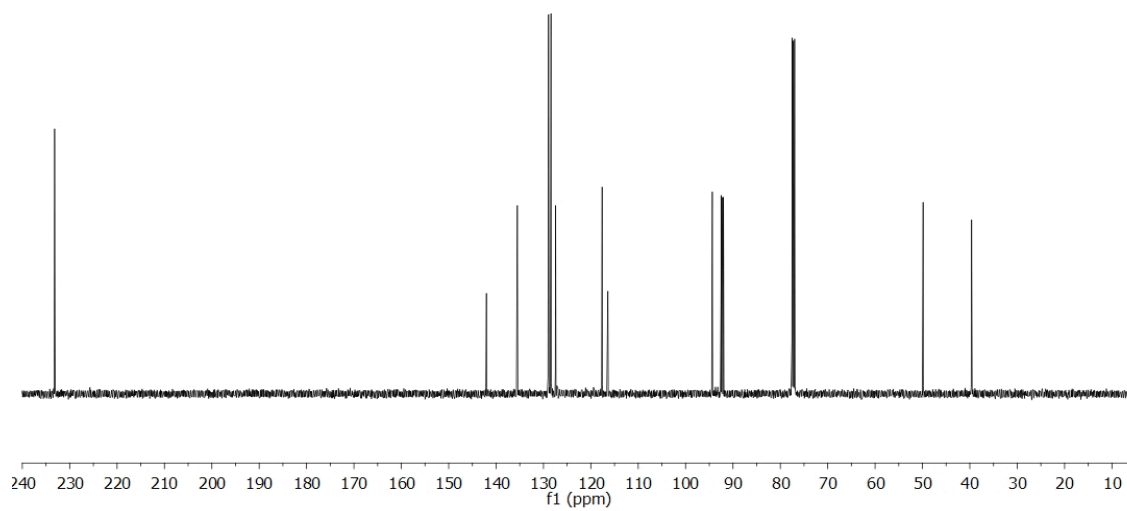
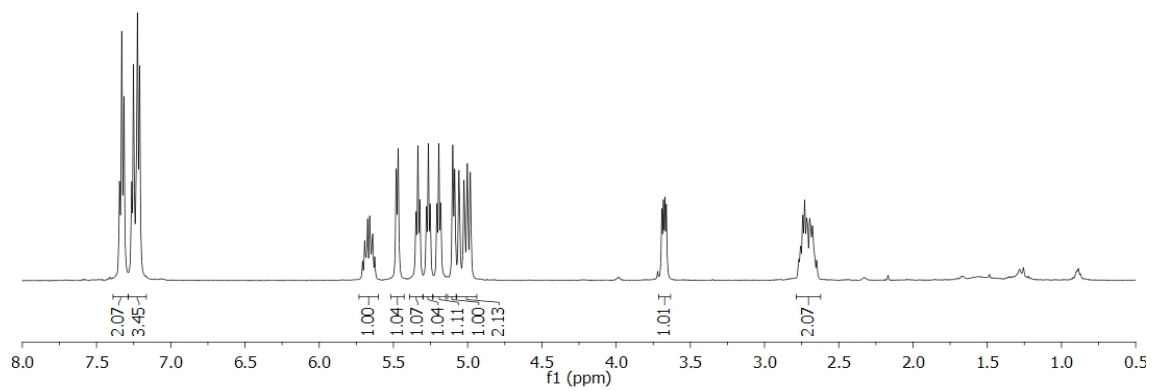
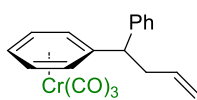


Figure A1.12 500 MHz ^1H and 125 MHz $^{13}\text{C}\{^1\text{H}\}$ NMR of **1.4Id** in CDCl_3

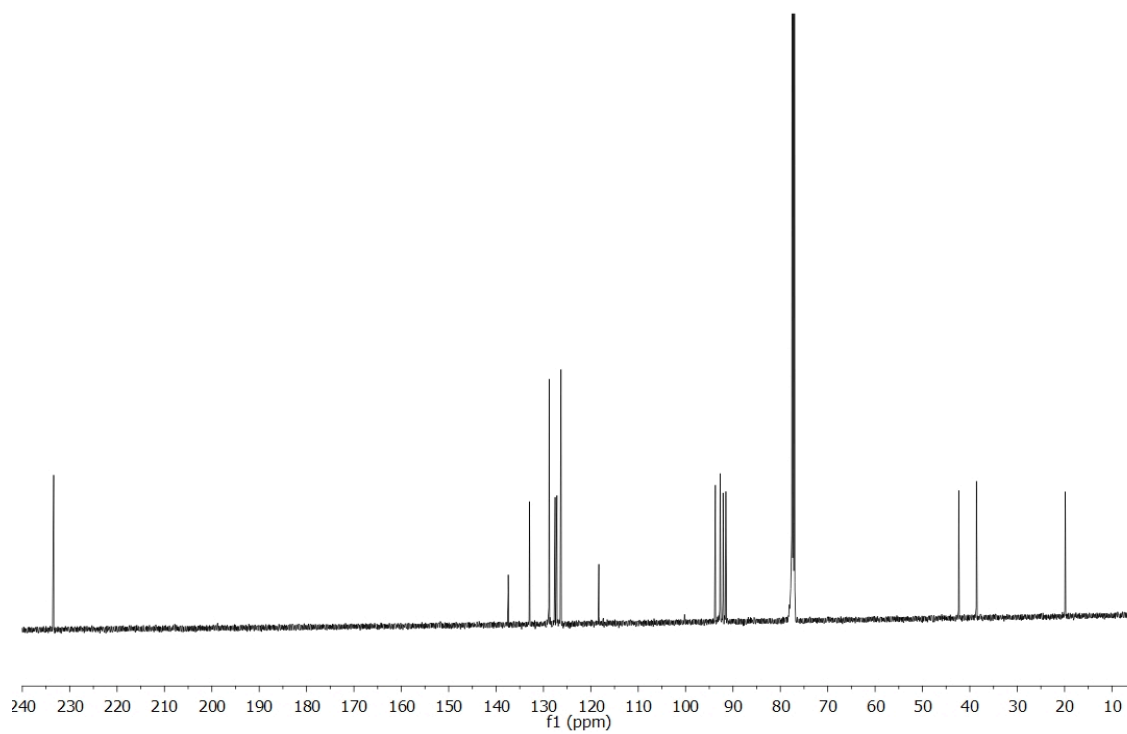
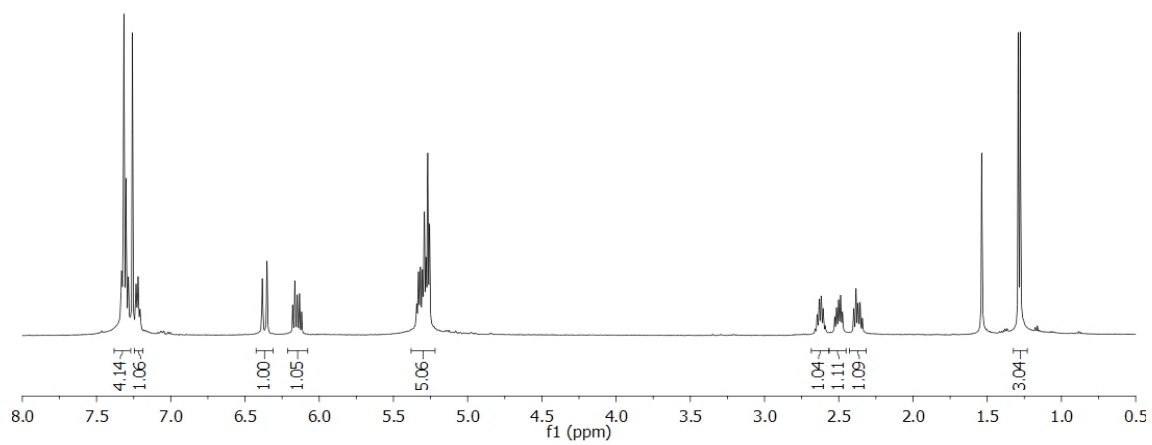
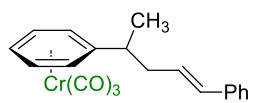


Figure A1.13 500 MHz ¹H and 125 MHz ¹³C{¹H} NMR of **1.4ke** in CDCl₃

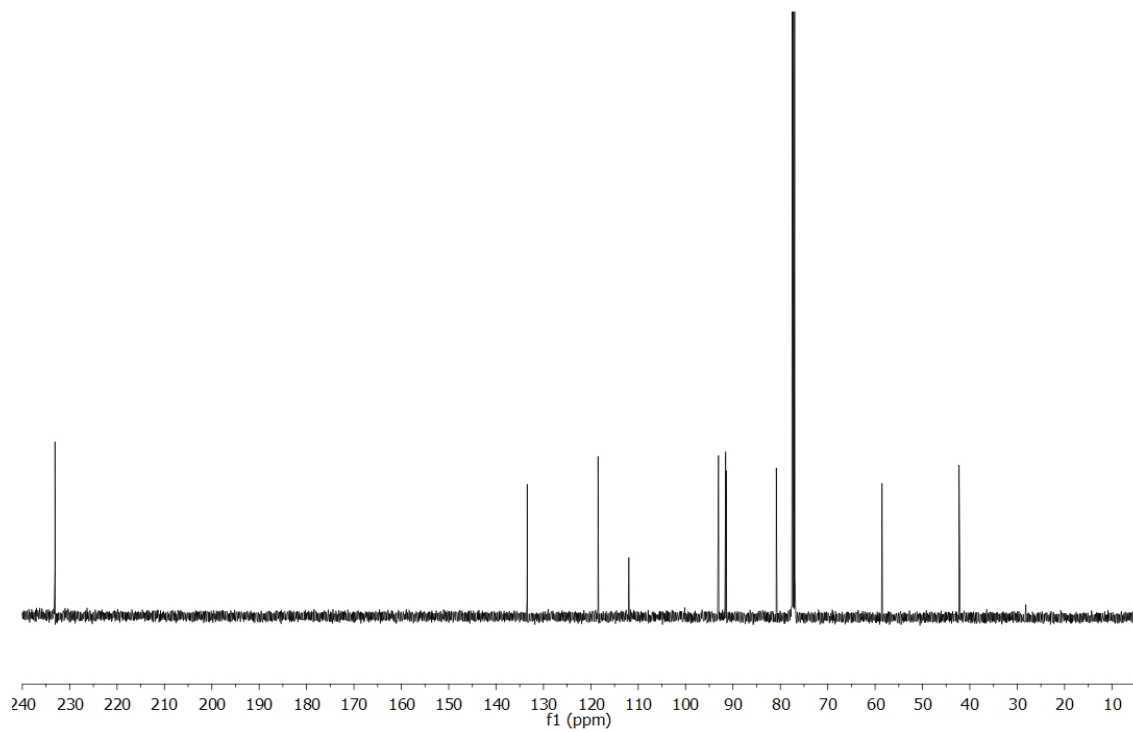
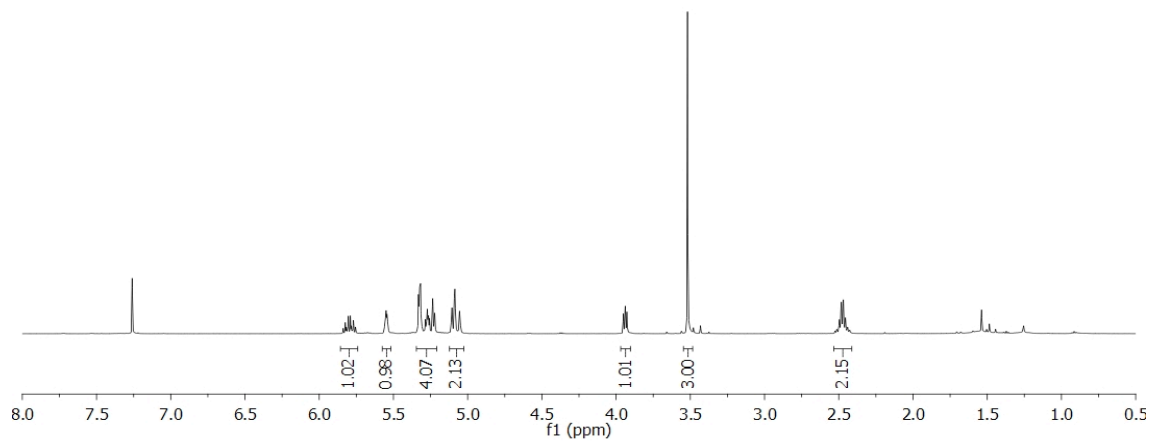
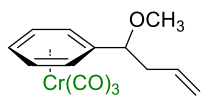


Figure A1.14 500 MHz ¹H and 125 MHz ¹³C{¹H} NMR of **1.4od** in CDCl₃

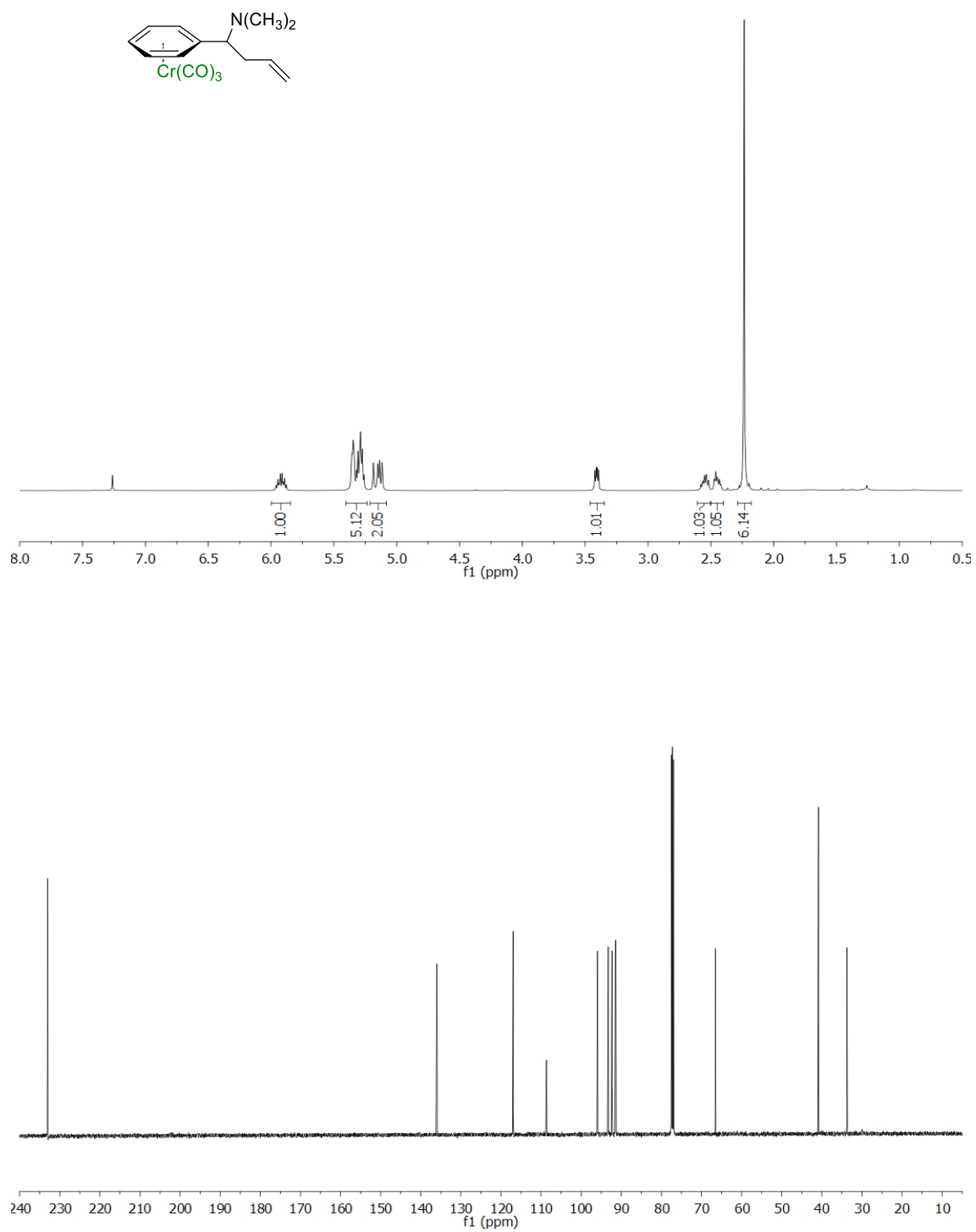


Figure A1.15 500 MHz ^1H and 125 MHz $^{13}\text{C}\{^1\text{H}\}$ NMR of **1.4pd** in CDCl_3

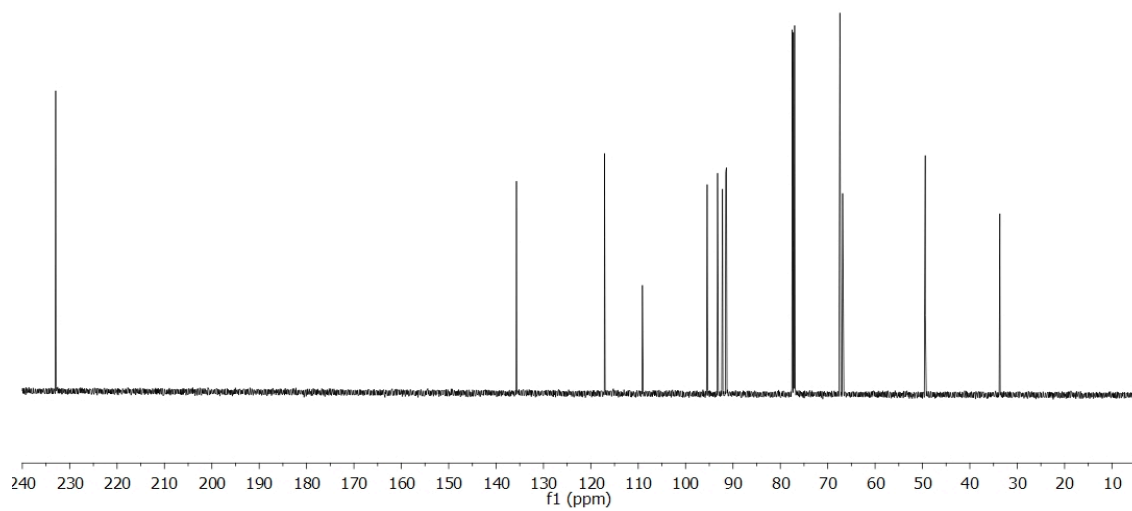
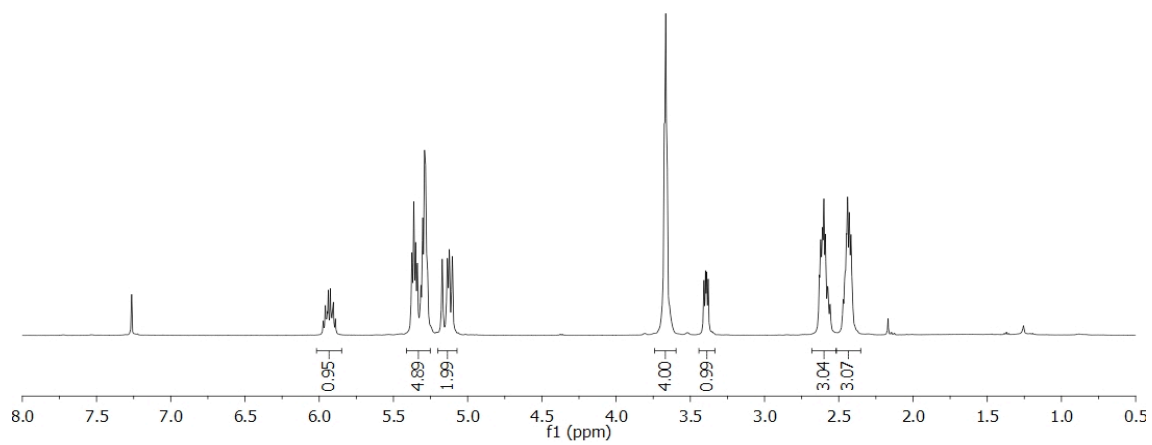
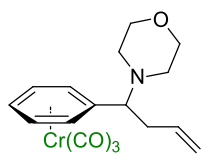


Figure A1.16 500 MHz ¹H and 125 MHz ¹³C{¹H} NMR of **1.4qd** in CDCl₃

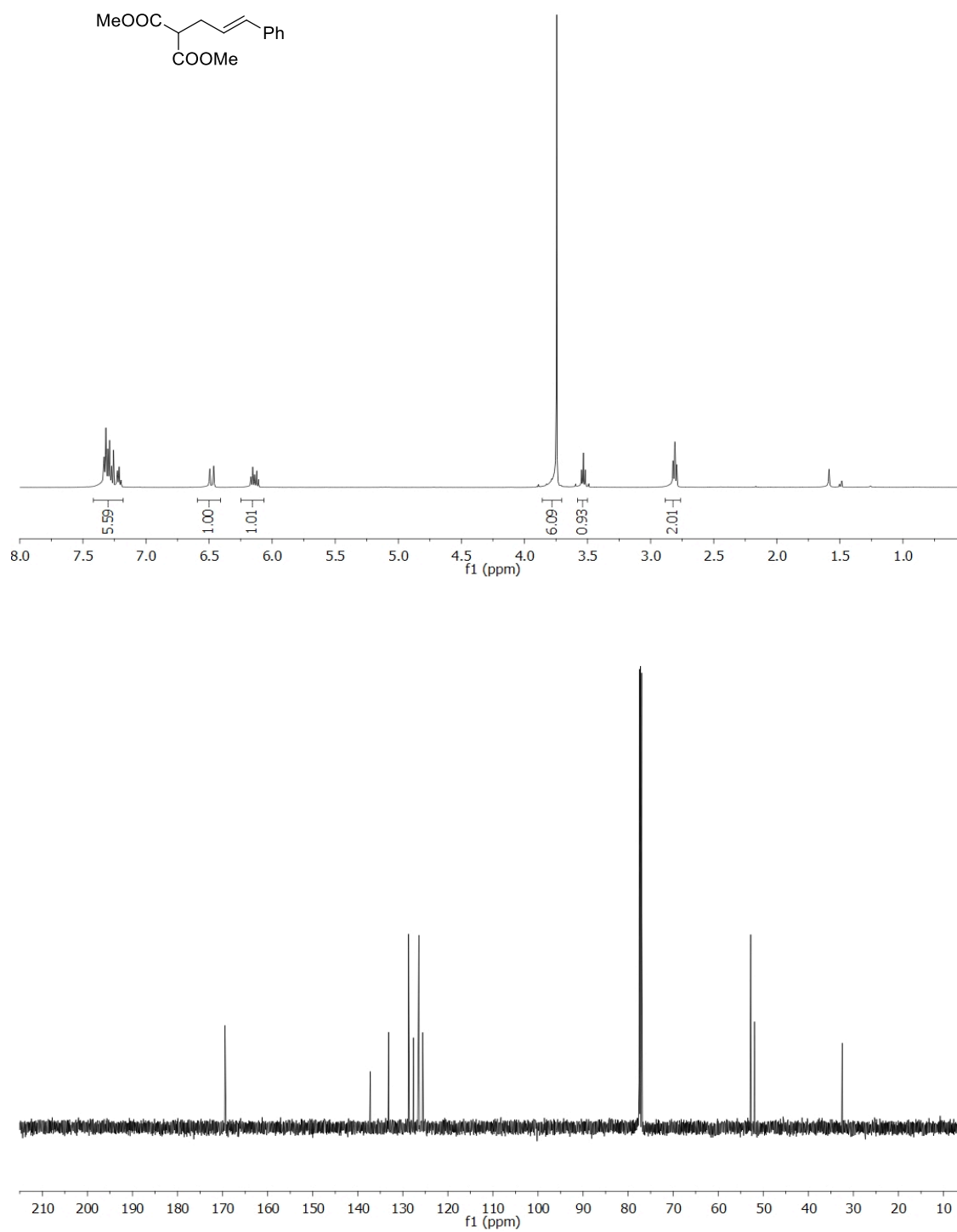


Figure A1.17 500 MHz ^1H and 125 MHz $^{13}\text{C}\{^1\text{H}\}$ NMR of **1.11** in CDCl_3

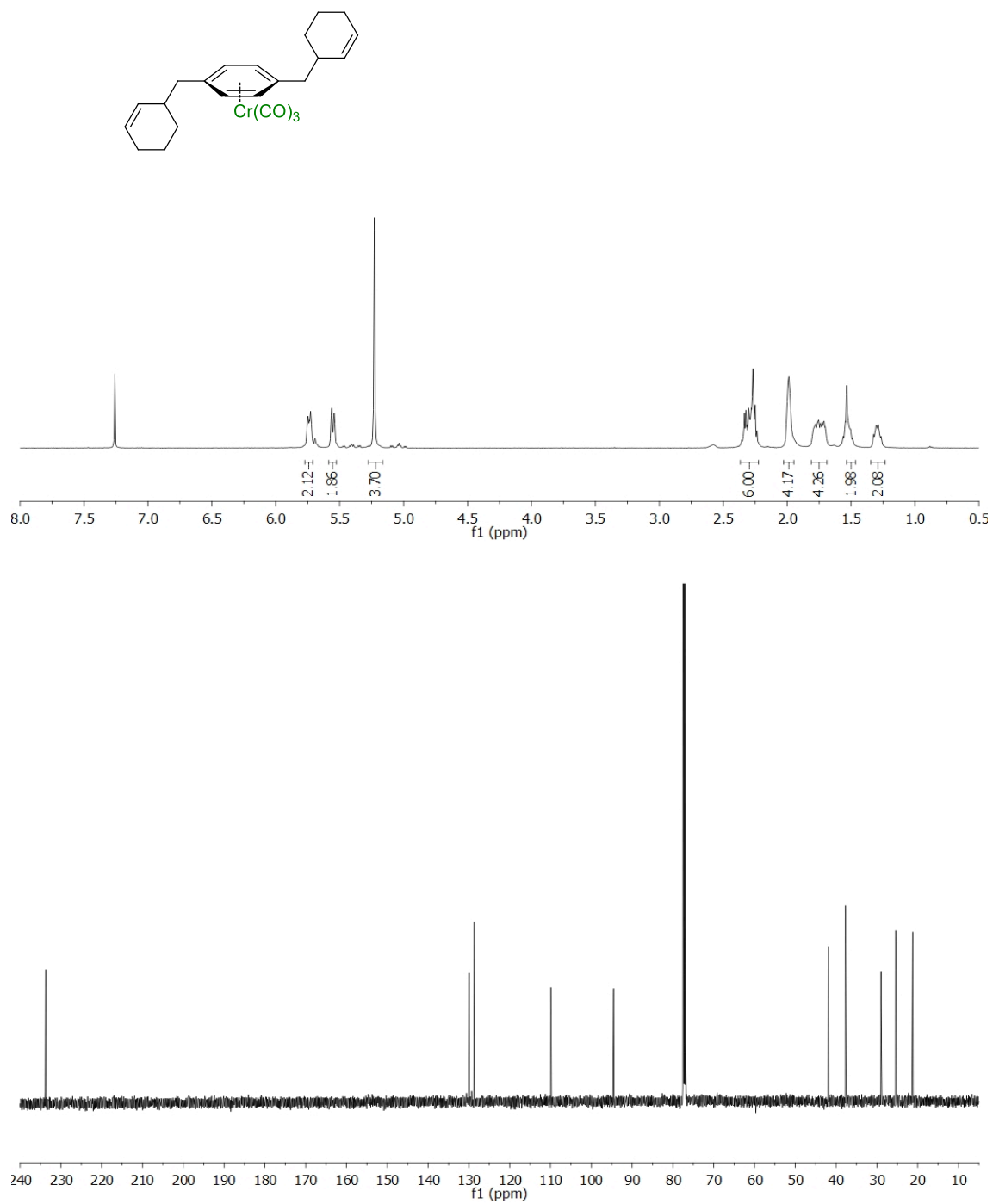


Figure A1.18 500 MHz ^1H and 125 MHz $^{13}\text{C}\{^1\text{H}\}$ NMR of **1.7** in CDCl_3

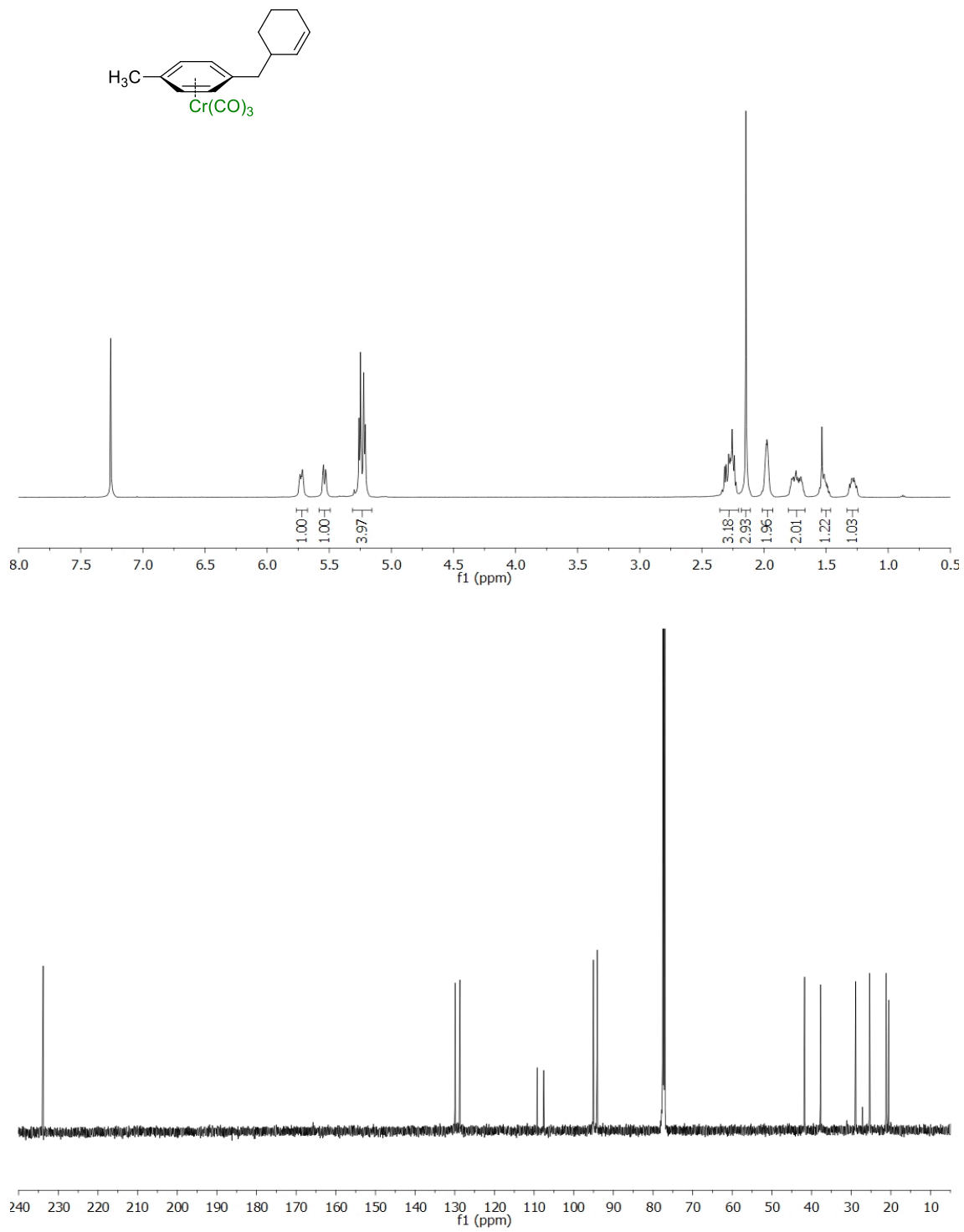


Figure A1.19 500 MHz ^1H and 125 MHz $^{13}\text{C}\{^1\text{H}\}$ NMR of **1.8** in CDCl_3

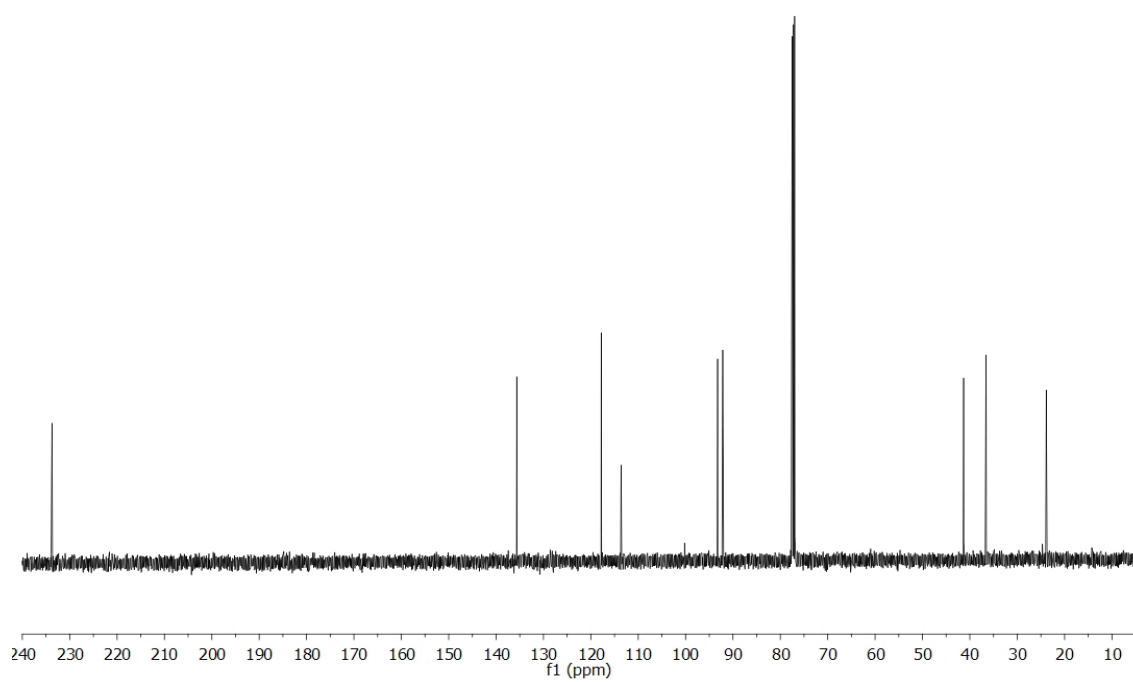
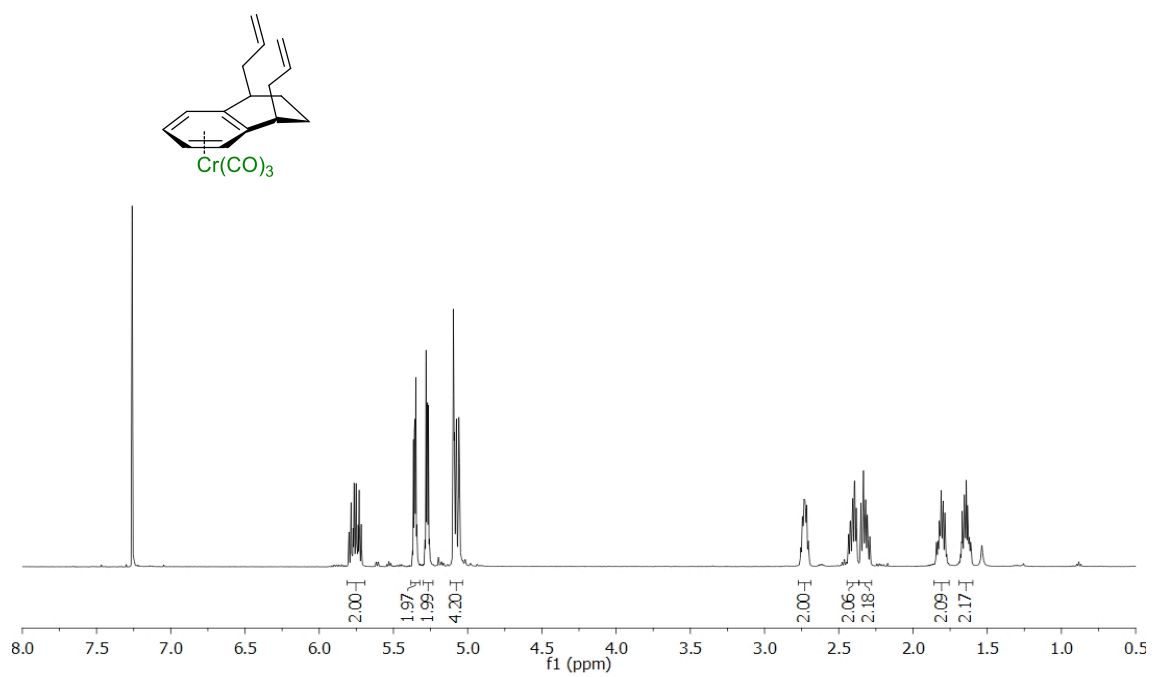


Figure A1.20 500 MHz ^1H and 125 MHz $^{13}\text{C}\{^1\text{H}\}$ NMR of **1.9** in CDCl_3

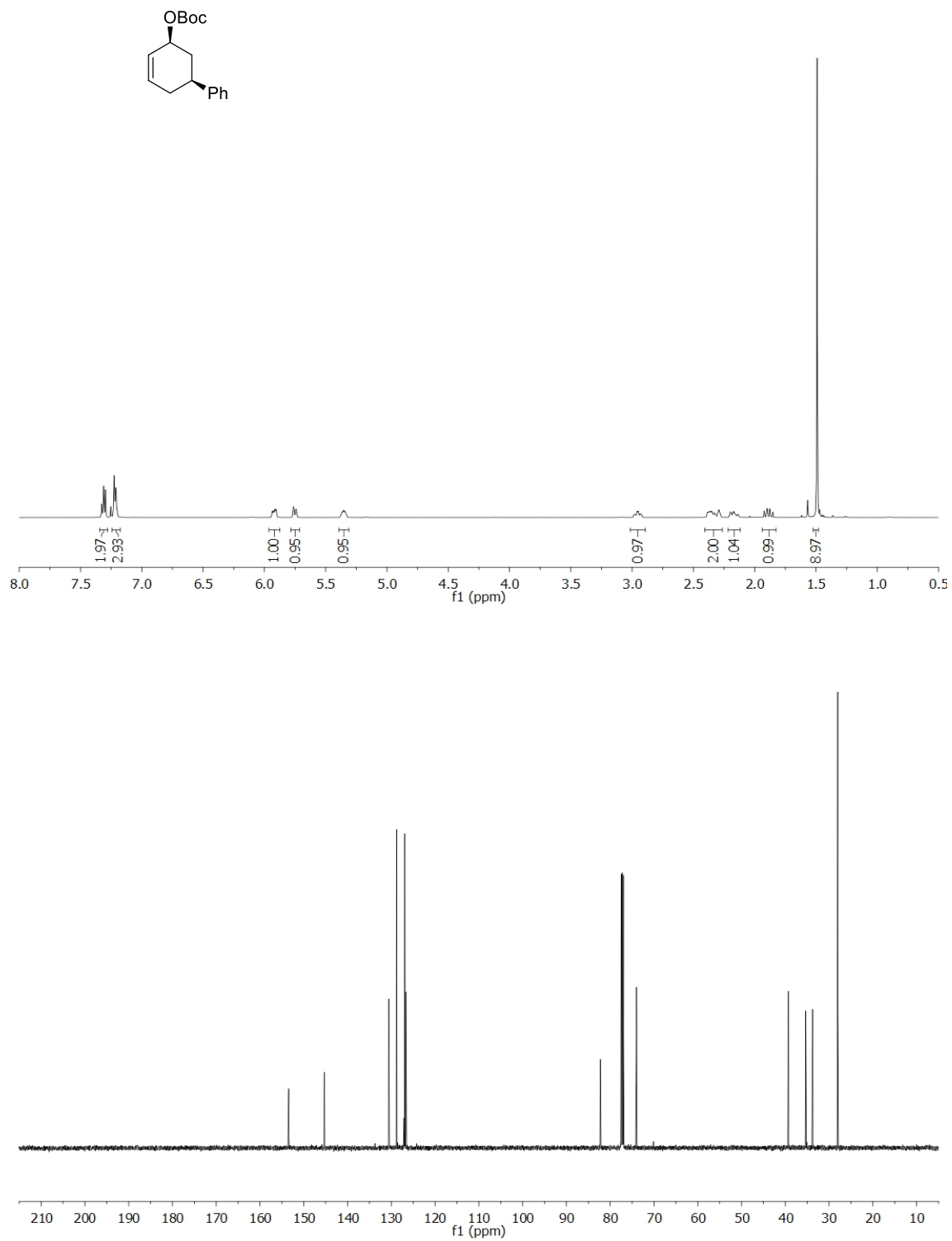


Figure A1.21 500 MHz ^1H and 125 MHz $^{13}\text{C}\{^1\text{H}\}$ NMR of **1.2j** in CDCl_3

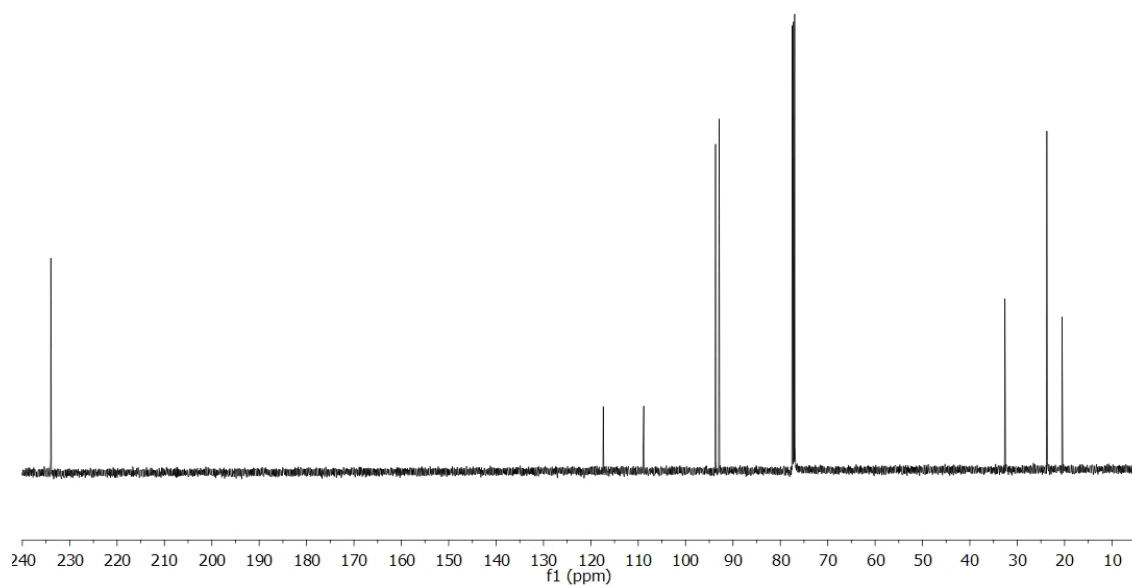
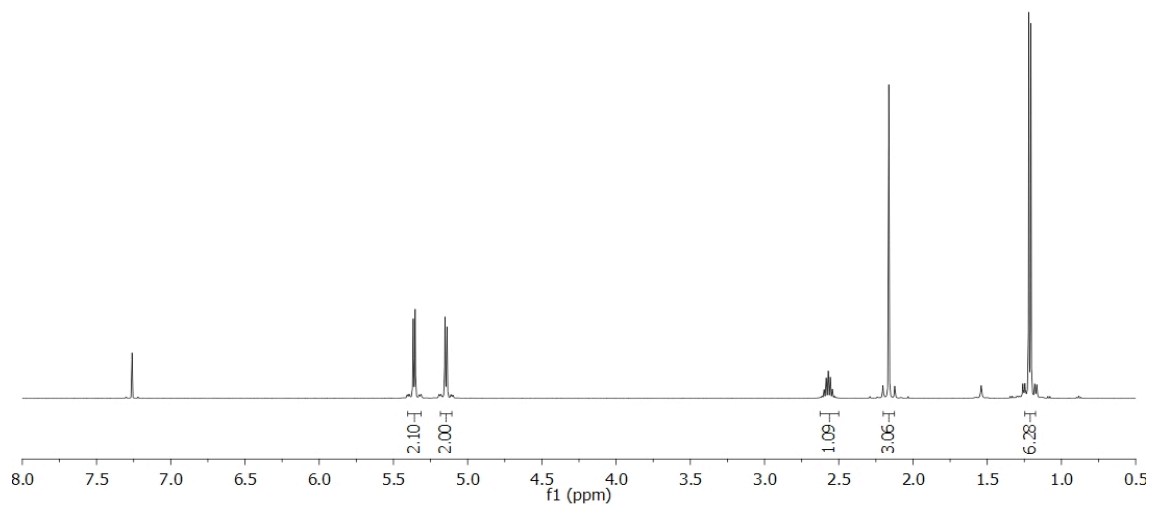
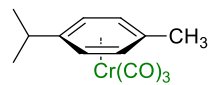


Figure A1.22 500 MHz ¹H and 125 MHz ¹³C{¹H} NMR of **1.1b** in CDCl₃

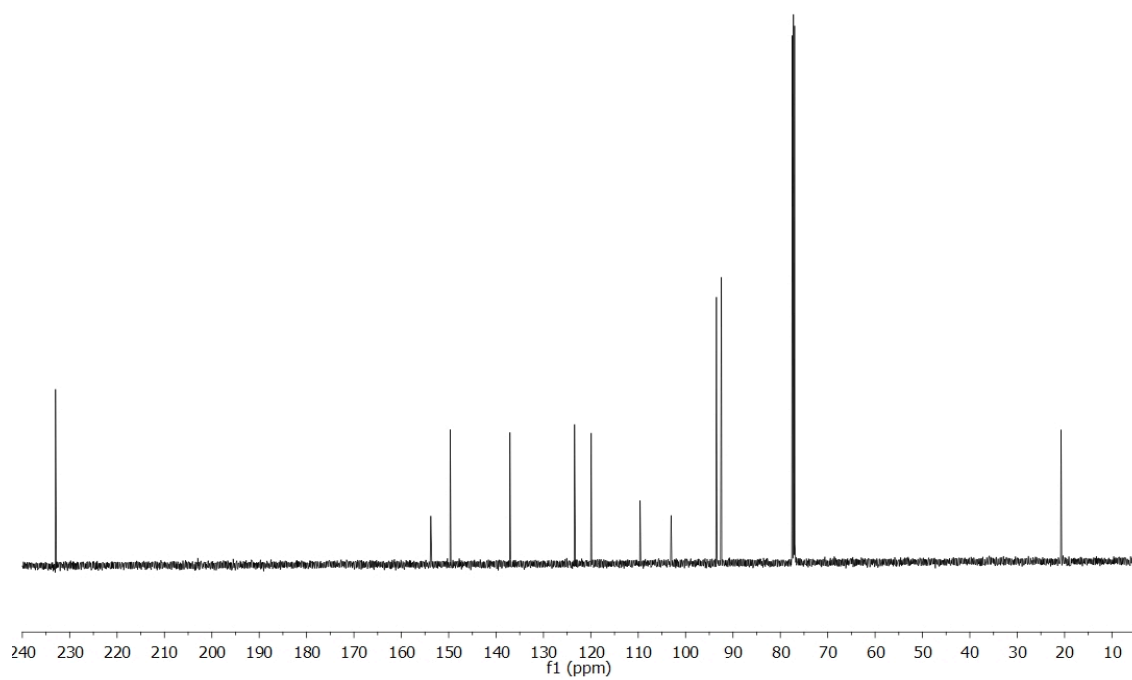
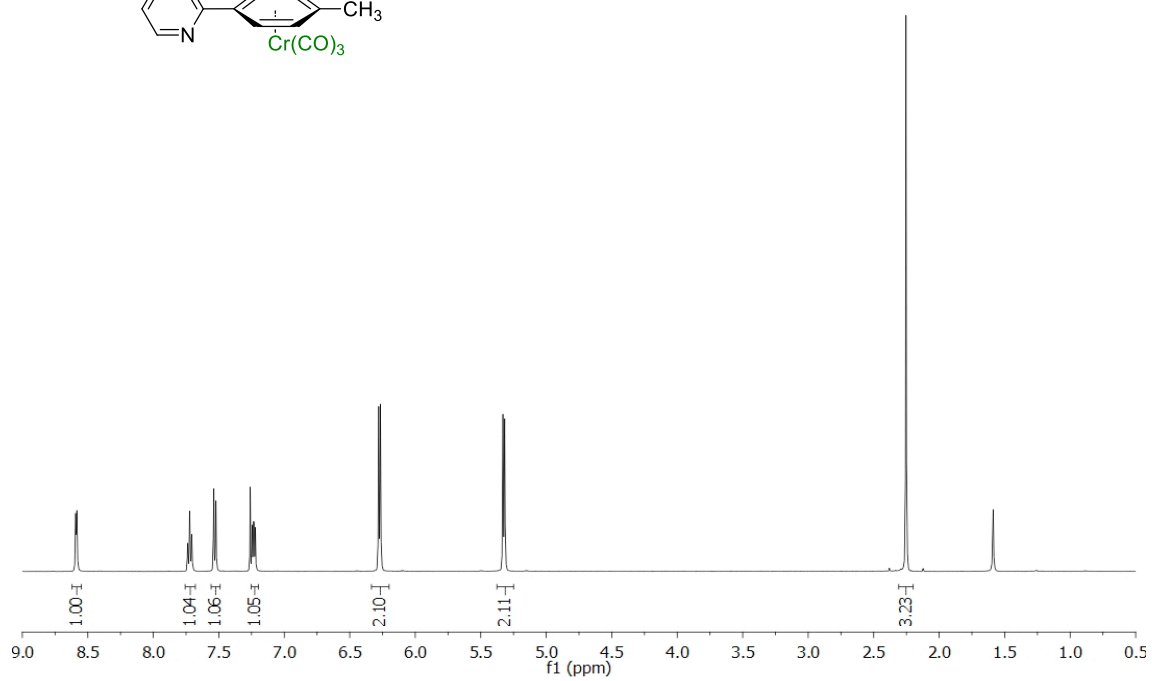
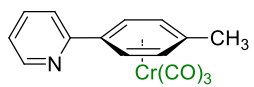


Figure A1.23 500 MHz ¹H and 125 MHz ¹³C{¹H} NMR of **1.1e** in CDCl₃

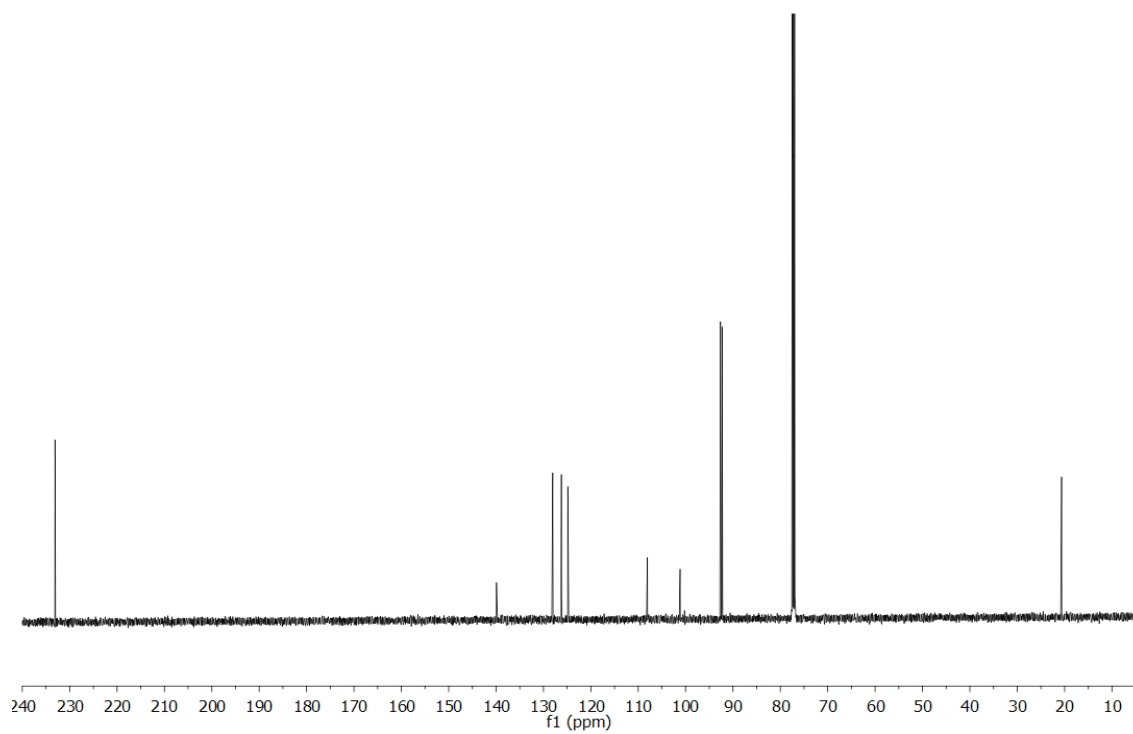
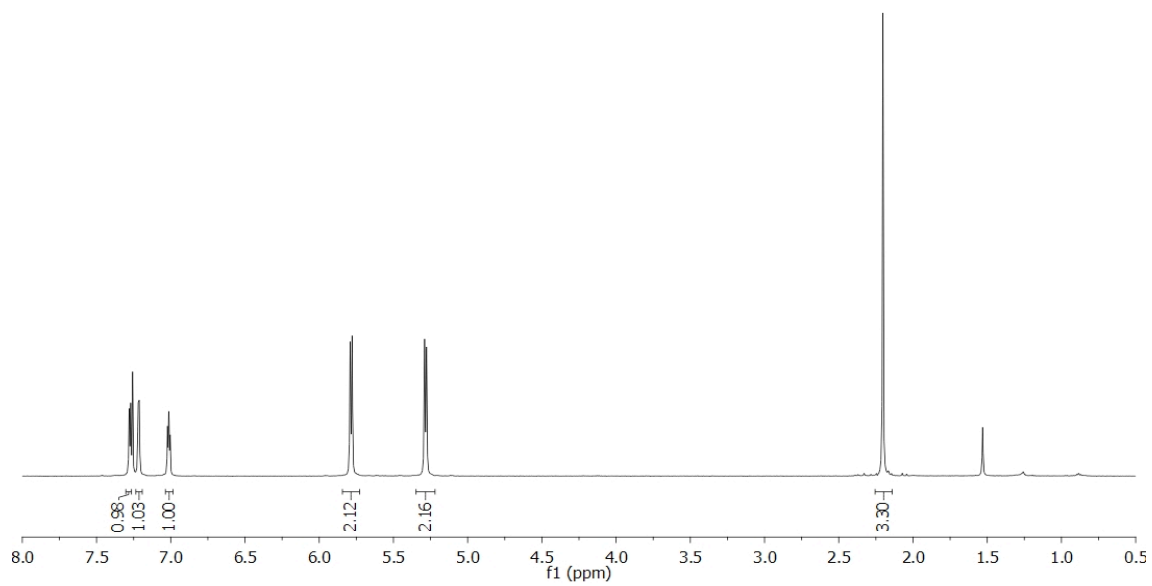
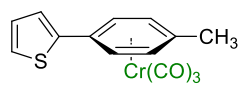


Figure A1.24 500 MHz ¹H and 125 MHz ¹³C{¹H} NMR of 1.1f in CDCl₃

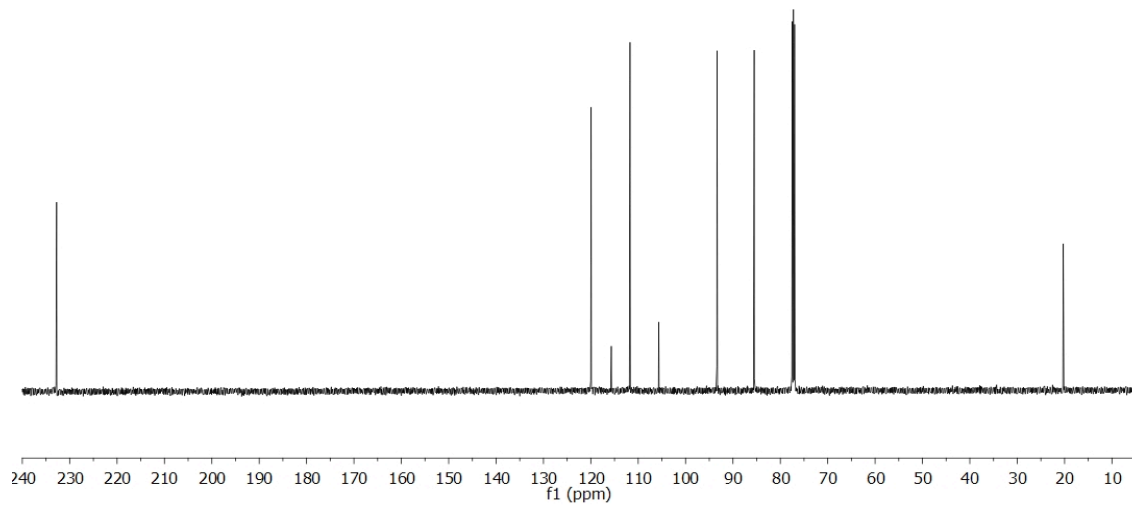
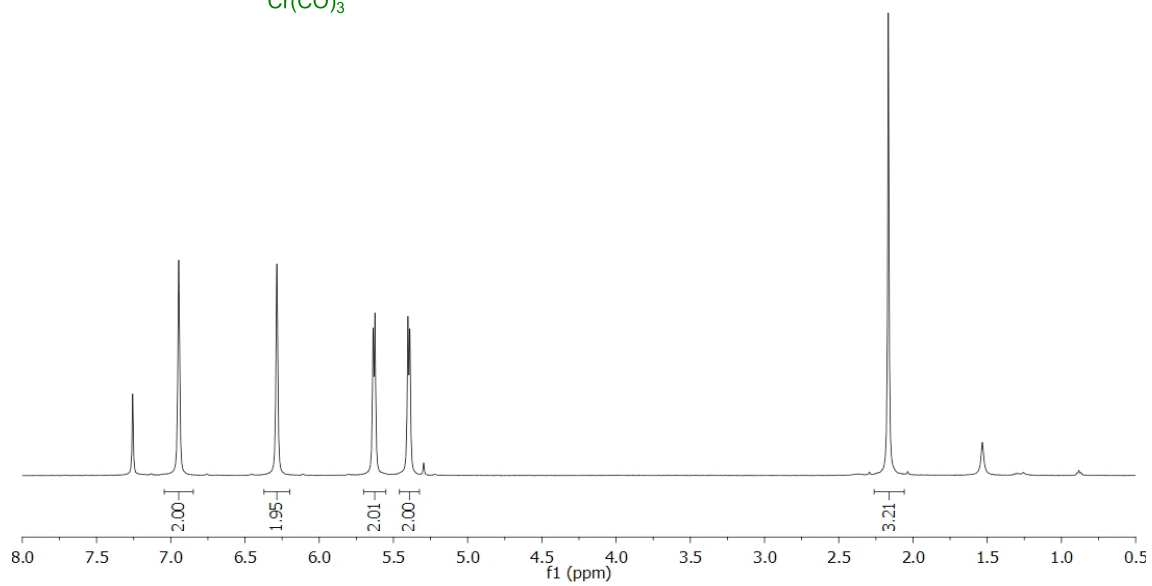
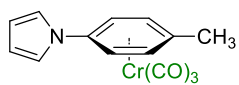


Figure A1.25 500 MHz ^1H and 125 MHz $^{13}\text{C}\{^1\text{H}\}$ NMR of **1.1g** in CDCl_3

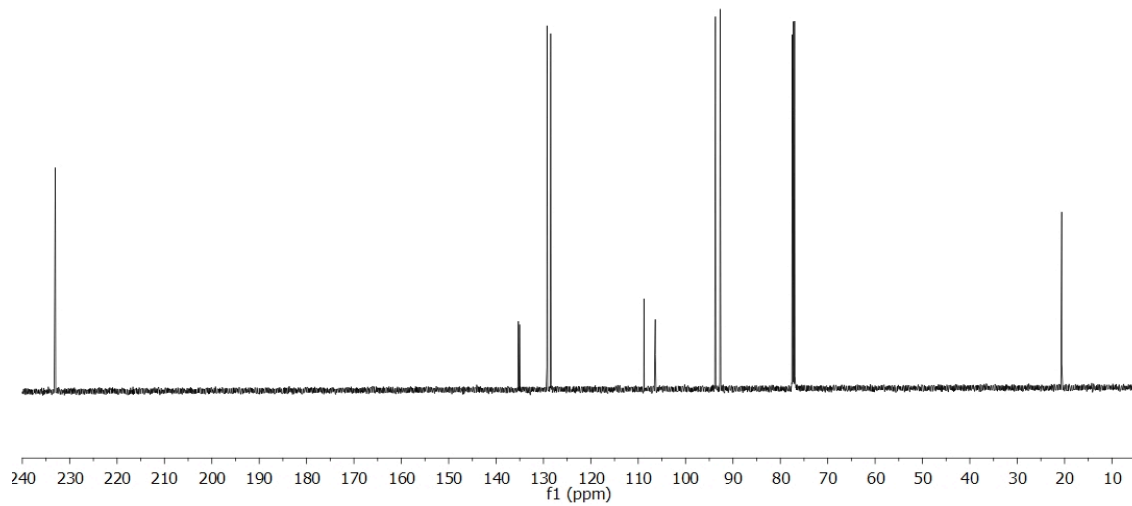
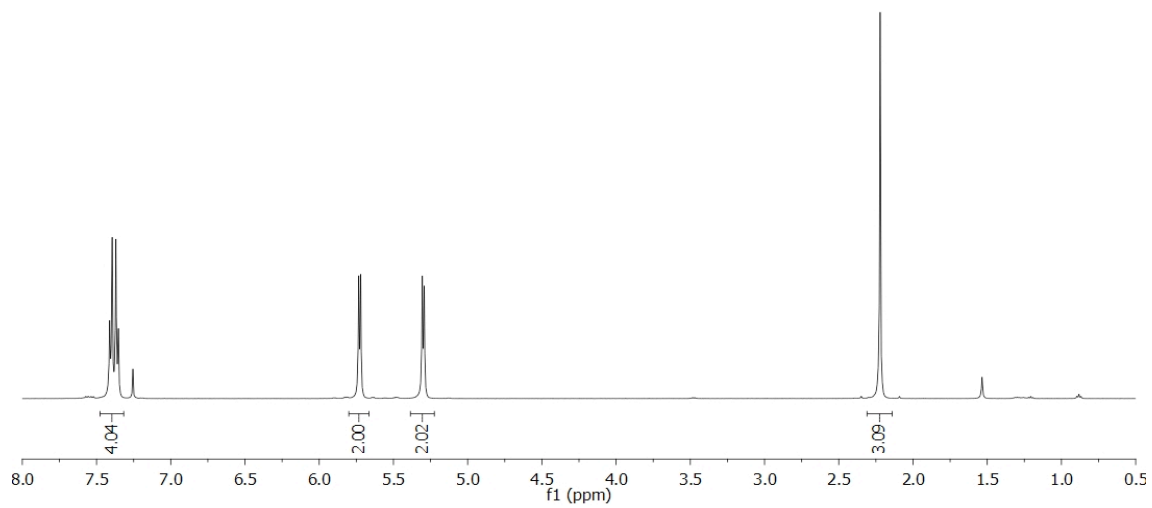
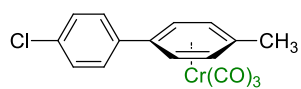


Figure A1.26 500 MHz ¹H and 125 MHz ¹³C{¹H} NMR of **1.1i** in CDCl₃

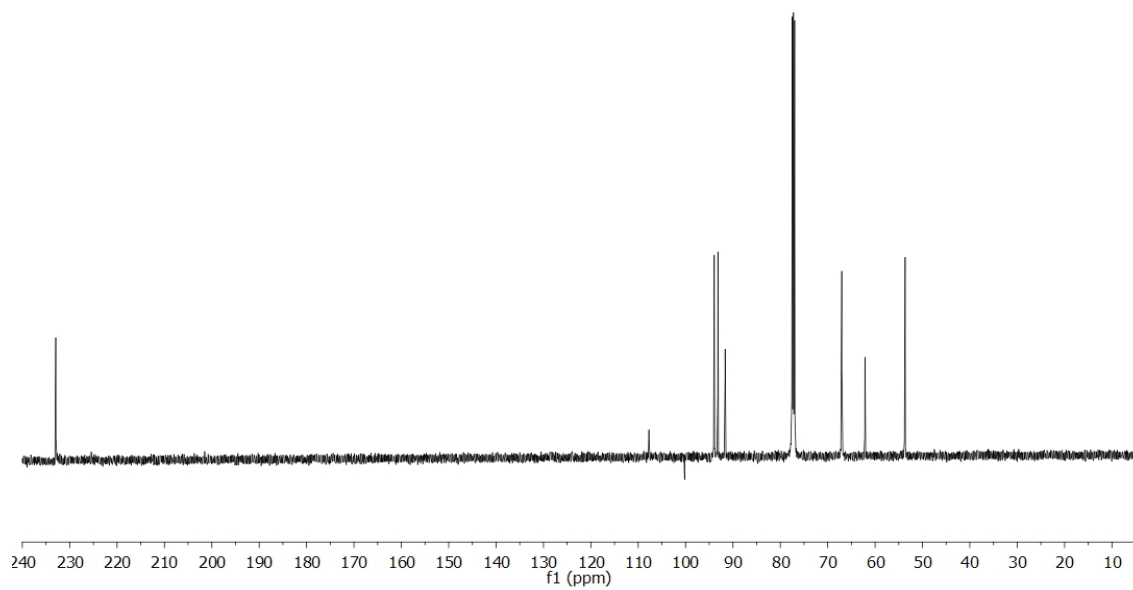
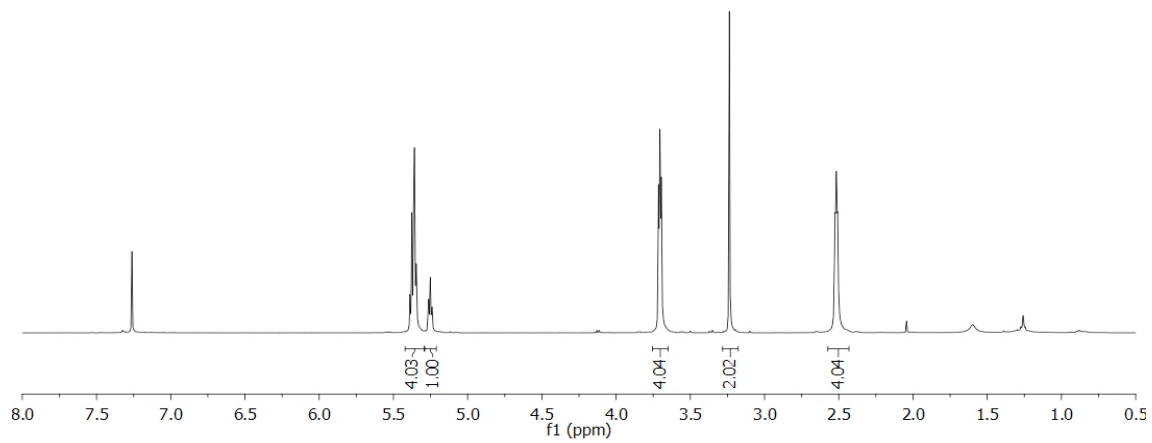
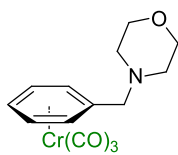


Figure A1.27 500 MHz ^1H and 125 MHz $^{13}\text{C}\{^1\text{H}\}$ NMR of **1.1q** in CDCl_3

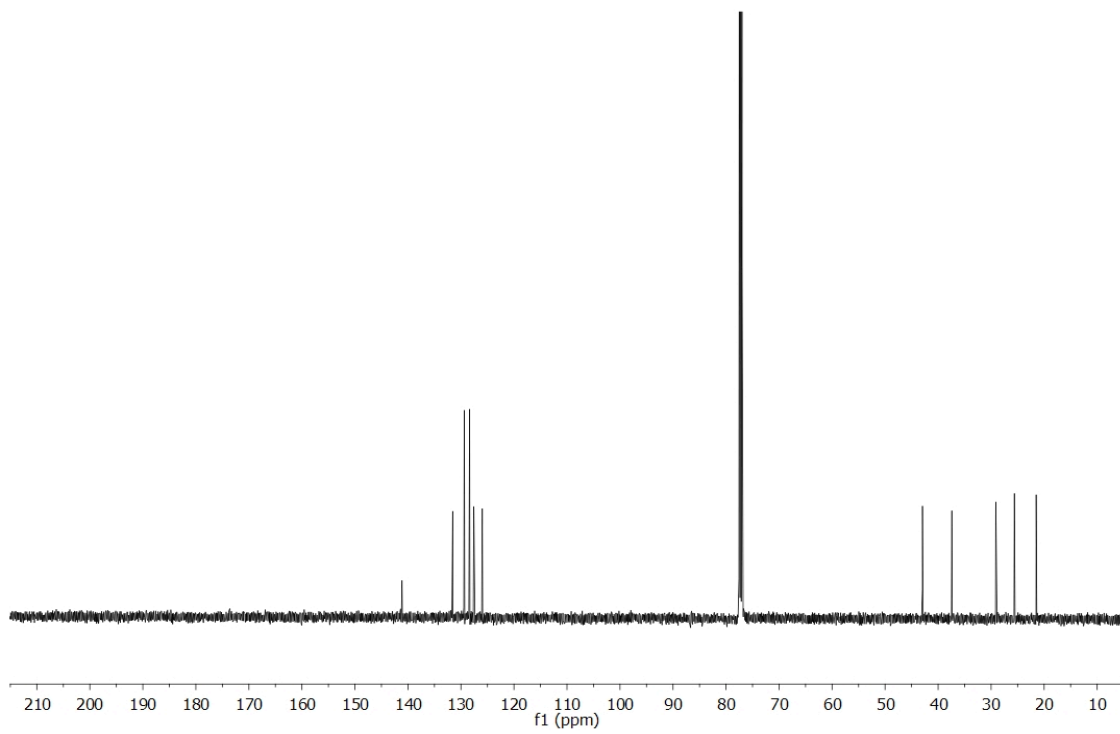
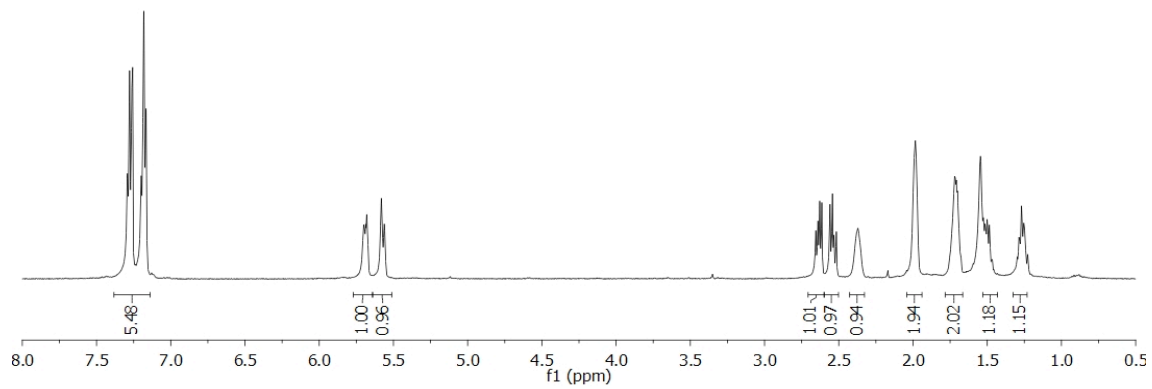
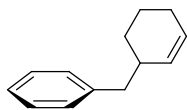


Figure A1.28 500 MHz ^1H and 125 MHz $^{13}\text{C}\{^1\text{H}\}$ NMR of **1.3'a** in CDCl_3

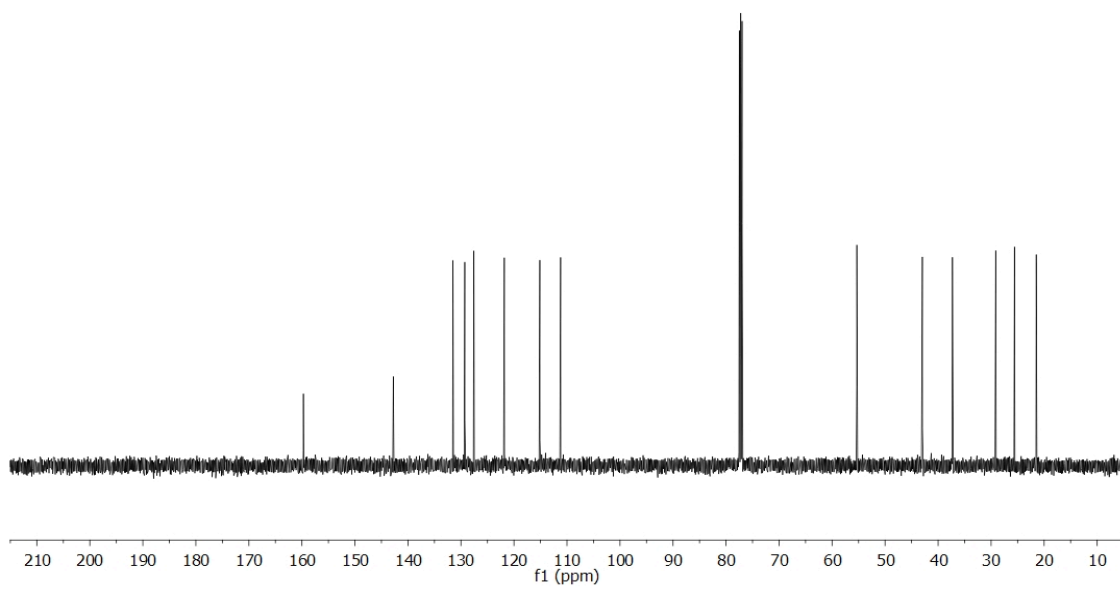
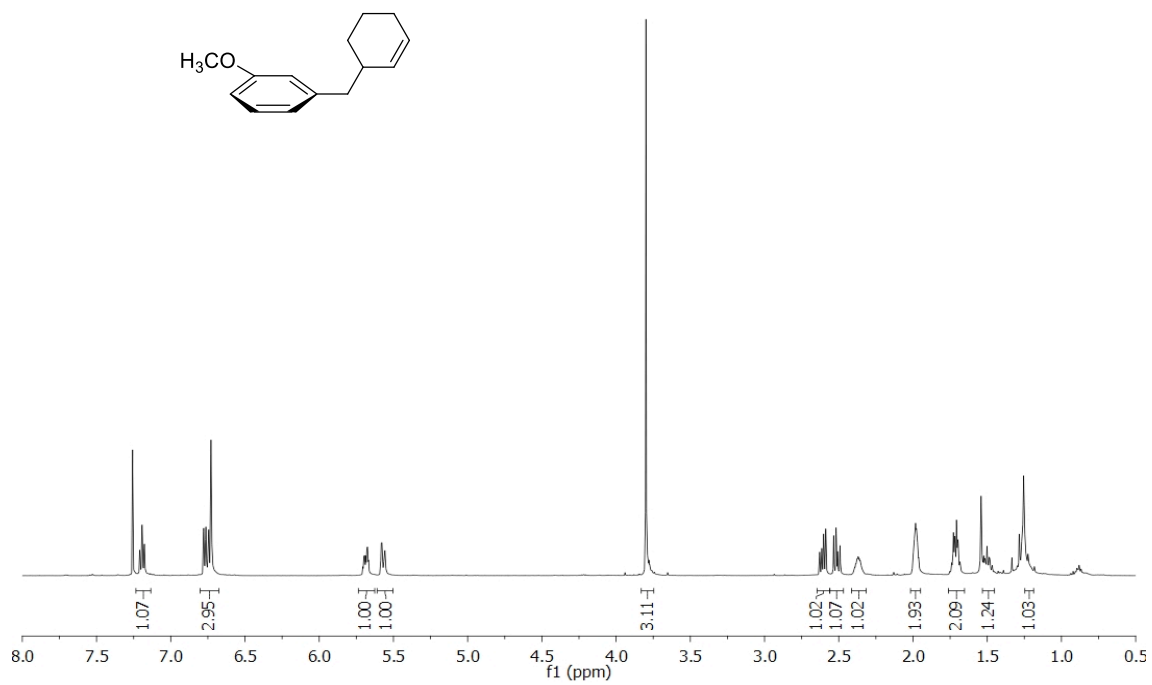


Figure A1.29 500 MHz ^1H and 125 MHz $^{13}\text{C}\{^1\text{H}\}$ NMR of **1.3c** in CDCl_3

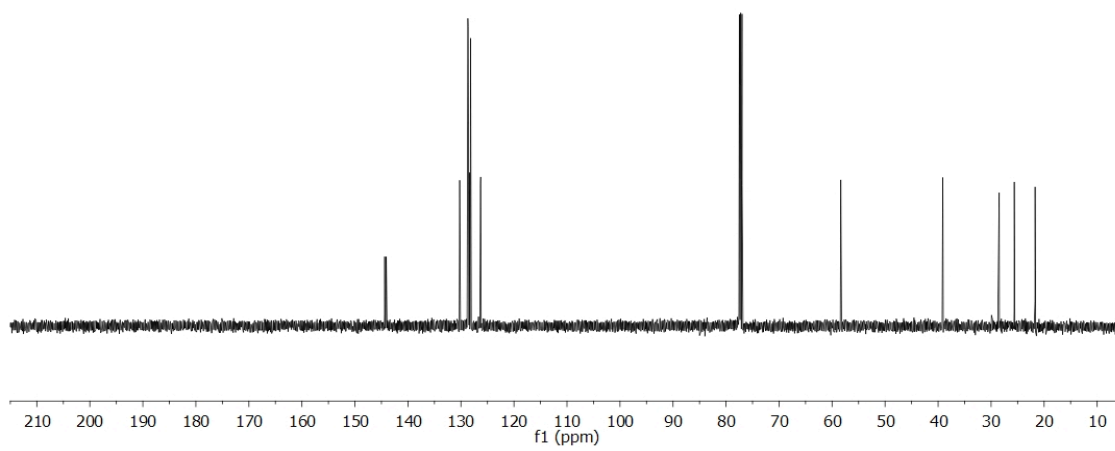
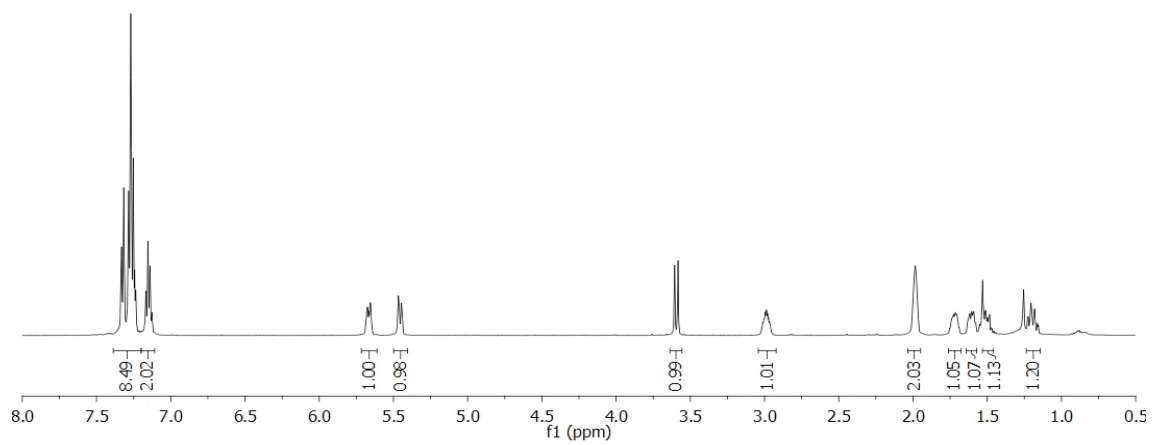
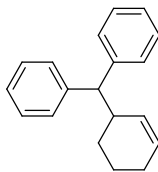


Figure A1.30 500 MHz ^1H and 125 MHz $^{13}\text{C}\{^1\text{H}\}$ NMR of **1.51b** in CDCl_3

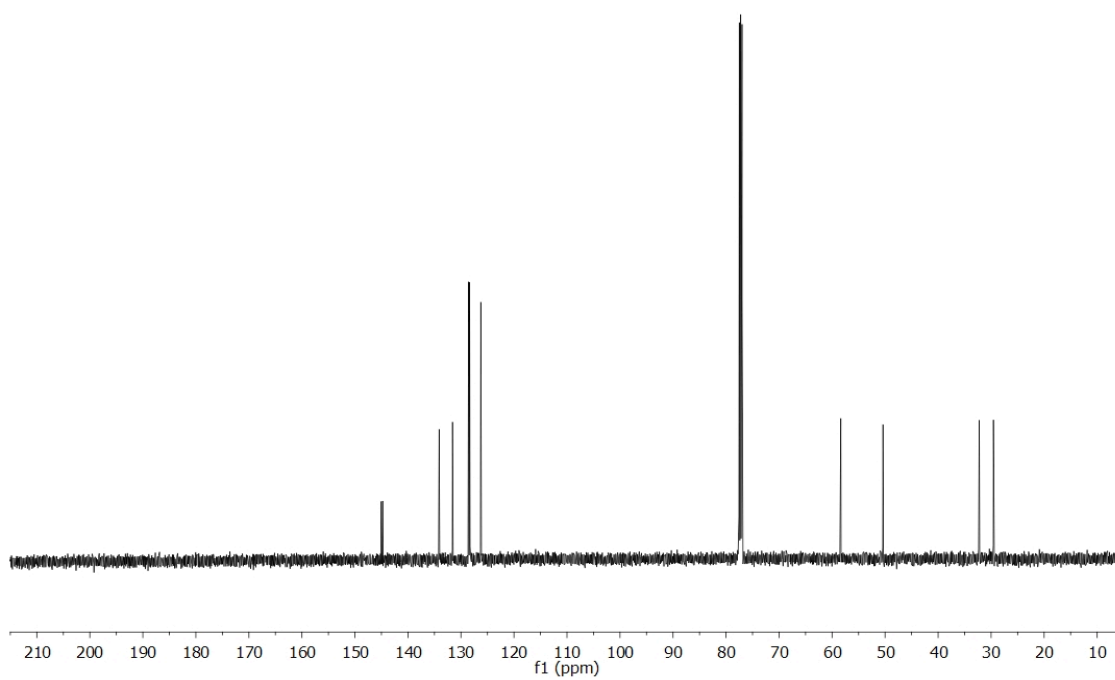
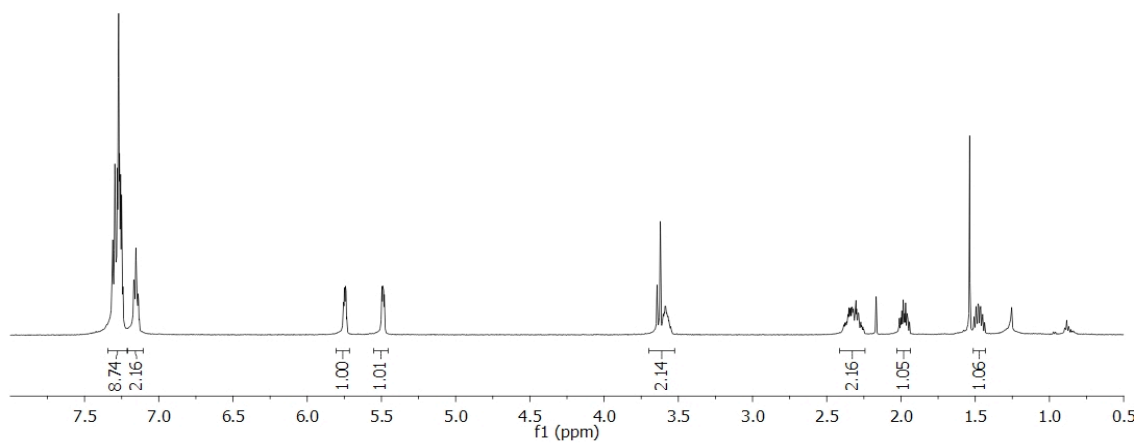
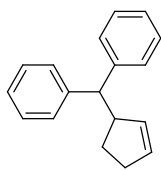


Figure A1.31 500 MHz ^1H and 125 MHz $^{13}\text{C}\{^1\text{H}\}$ NMR of **1.5lg** in CDCl_3

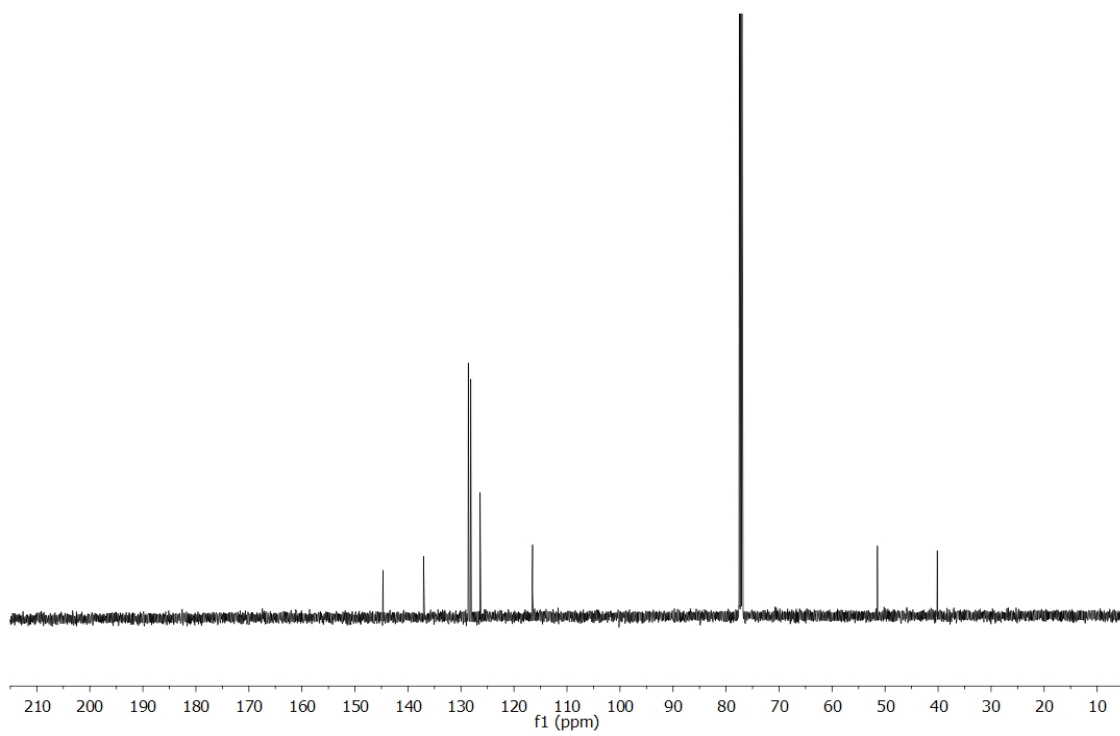
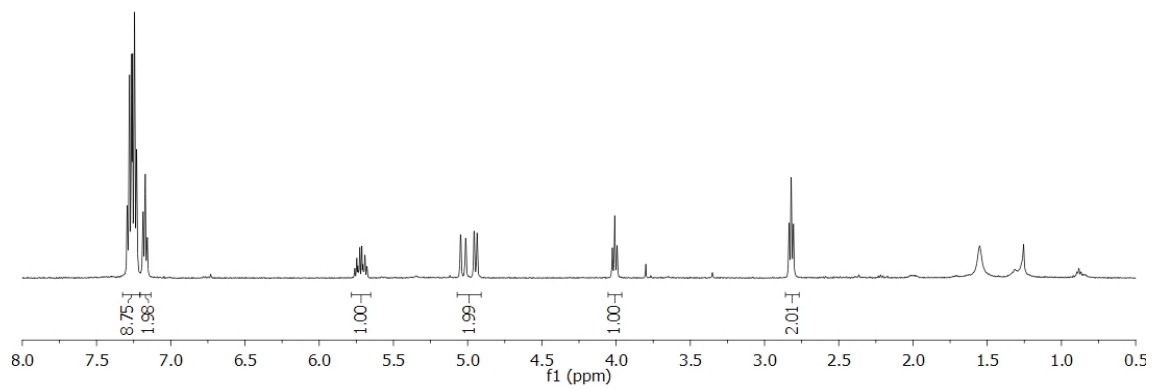
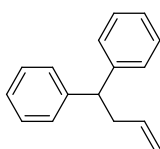


Figure A1.32 500 MHz ^1H and 125 MHz $^{13}\text{C}\{^1\text{H}\}$ NMR of **1.5Id** in CDCl_3

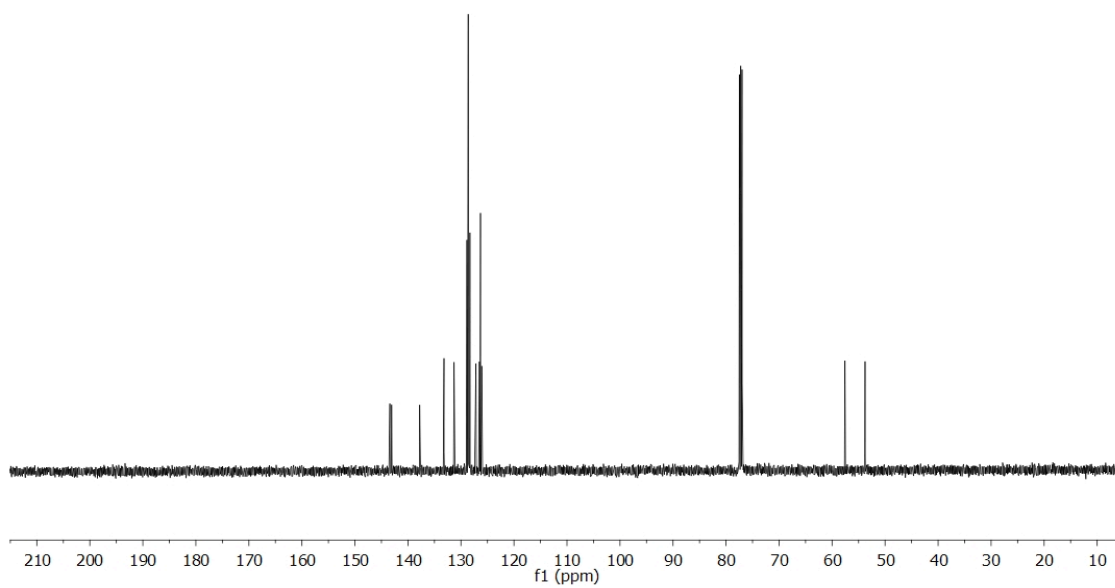
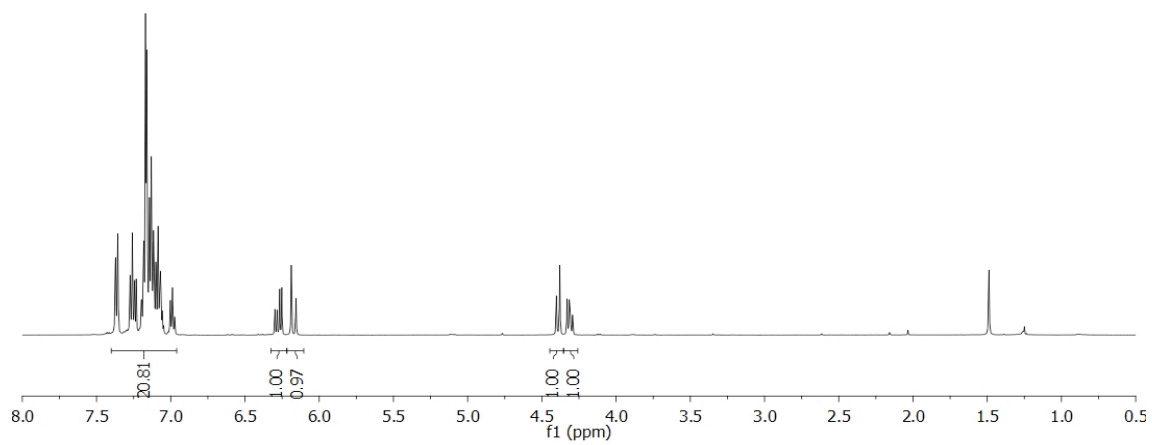
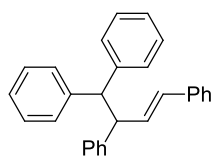
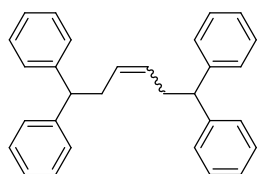


Figure A1.33 500 MHz ^1H and 125 MHz $^{13}\text{C}\{^1\text{H}\}$ NMR of 1.5If in CDCl_3



cis:trans = 2:1

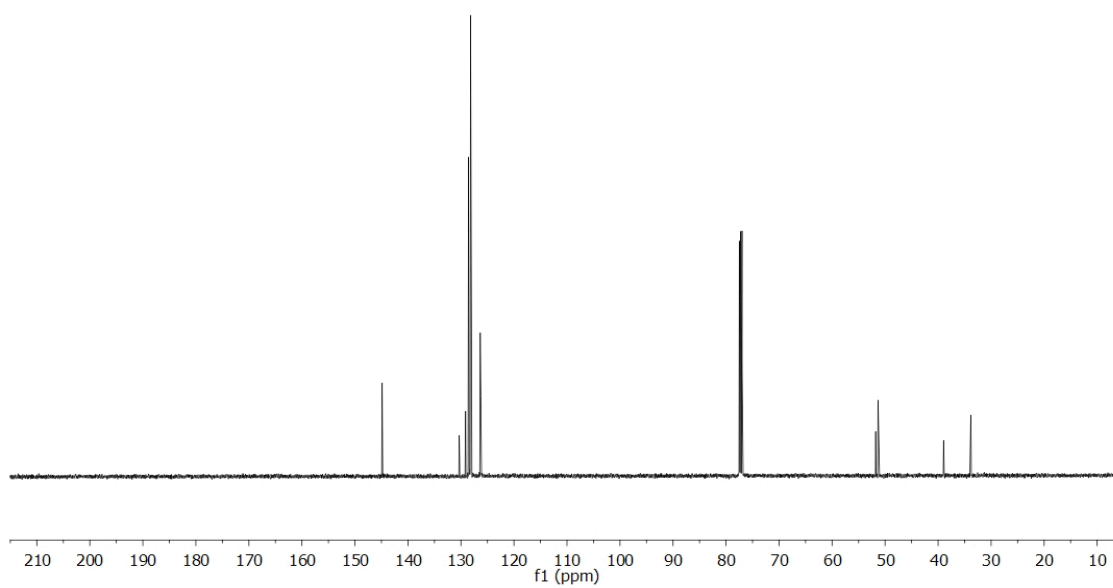
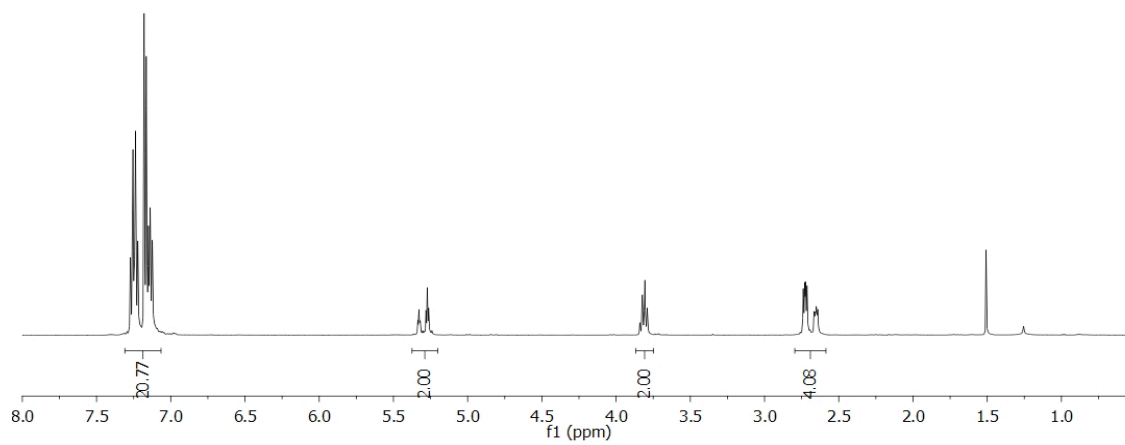


Figure A1.34 500 MHz ^1H and 125 MHz $^{13}\text{C}\{^1\text{H}\}$ NMR of **1.5h** in CDCl_3

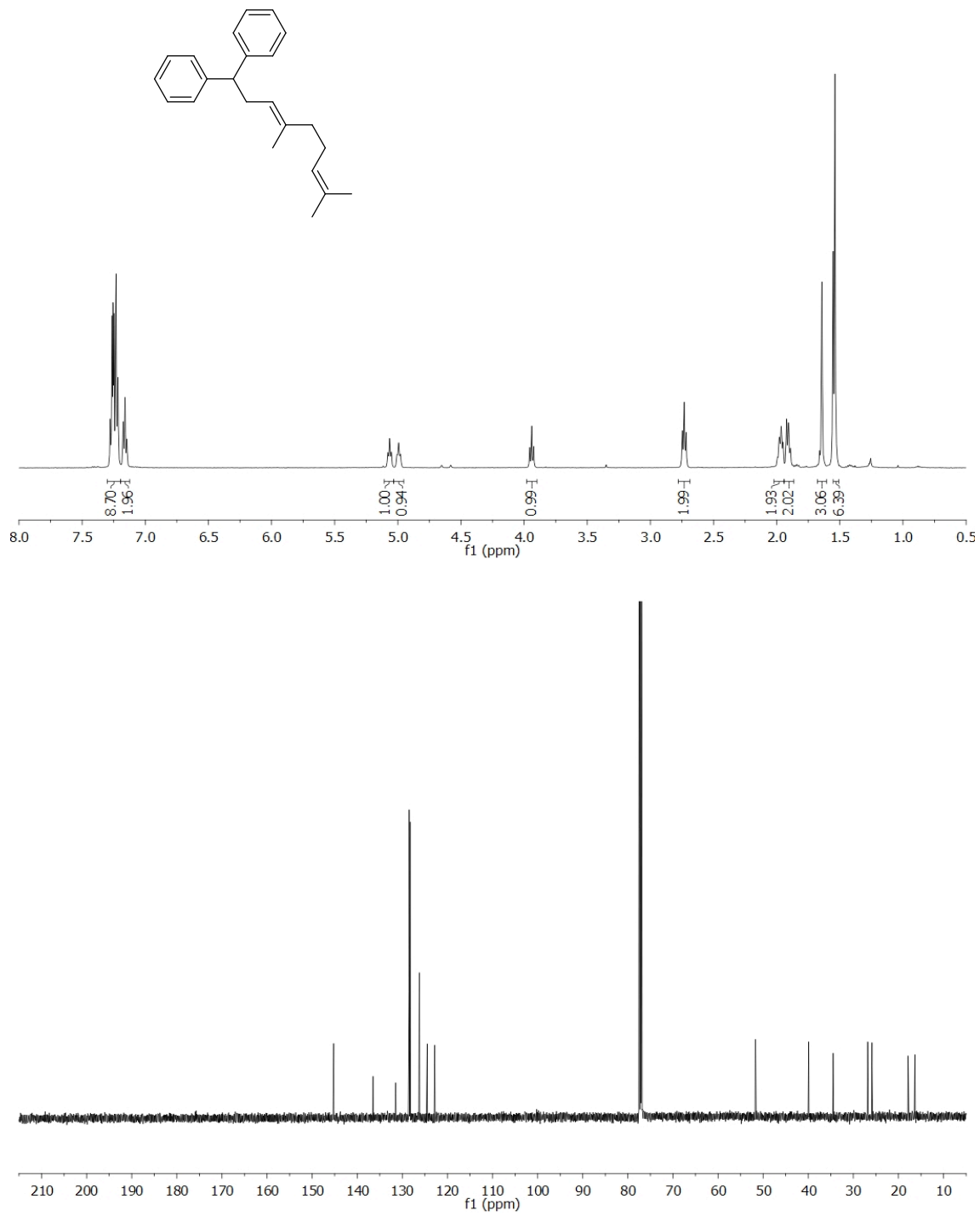


Figure A1.35 500 MHz ^1H and 125 MHz $^{13}\text{C}\{^1\text{H}\}$ NMR of **1.5li** in CDCl_3

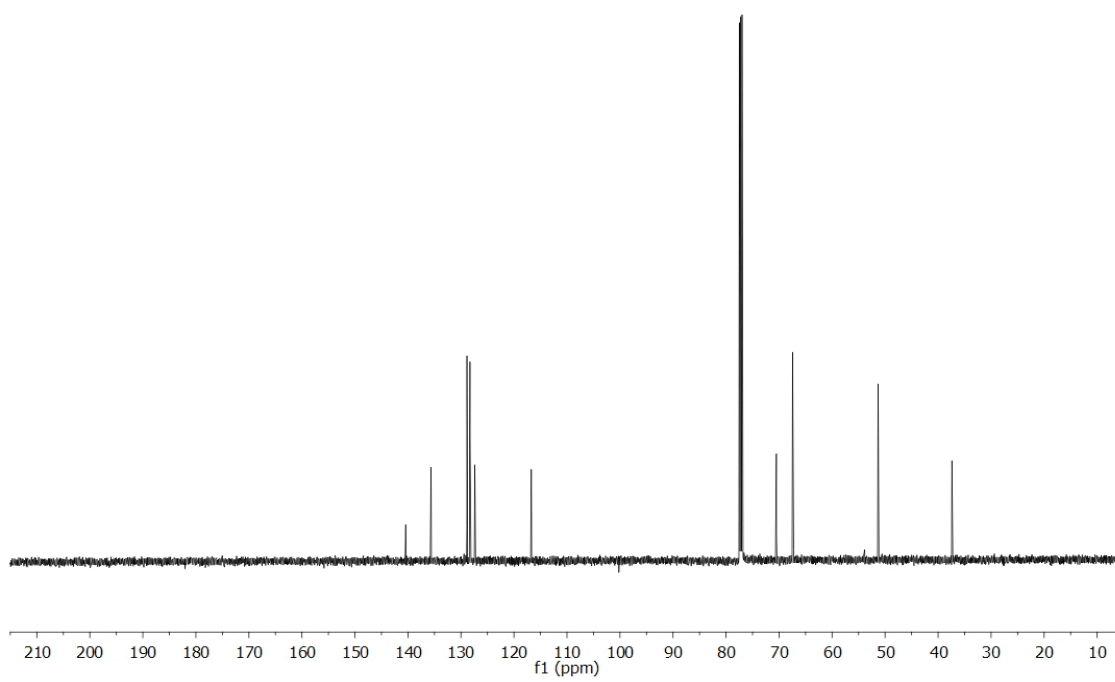
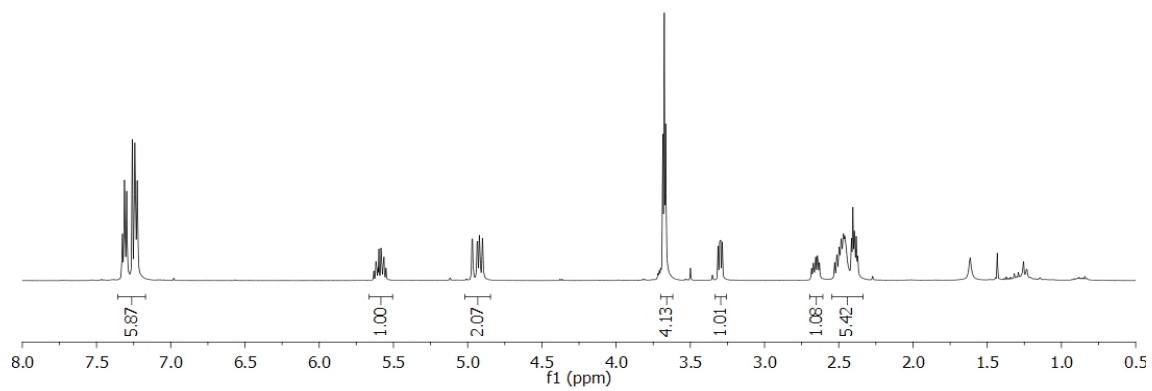
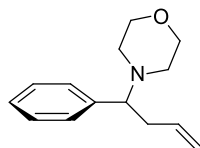


Figure A1.36 500 MHz ^1H and 125 MHz $^{13}\text{C}\{^1\text{H}\}$ NMR of 1.4'qd in CDCl_3

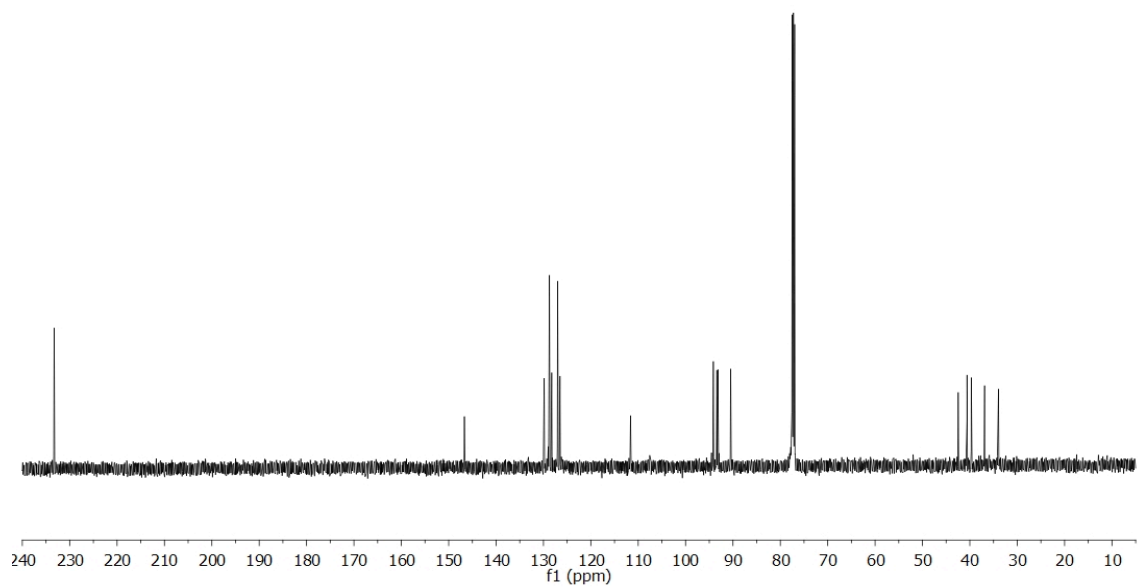
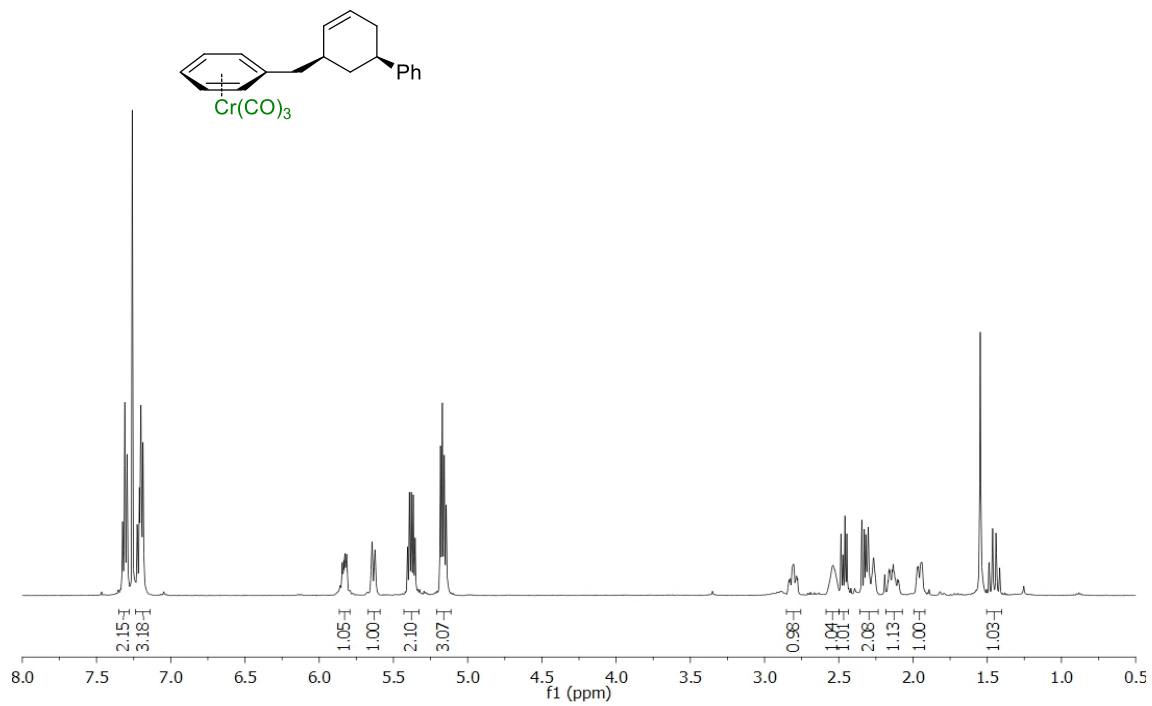


Figure A1.37 500 MHz ^1H and 125 MHz $^{13}\text{C}\{^1\text{H}\}$ NMR of **1.6** in CDCl_3

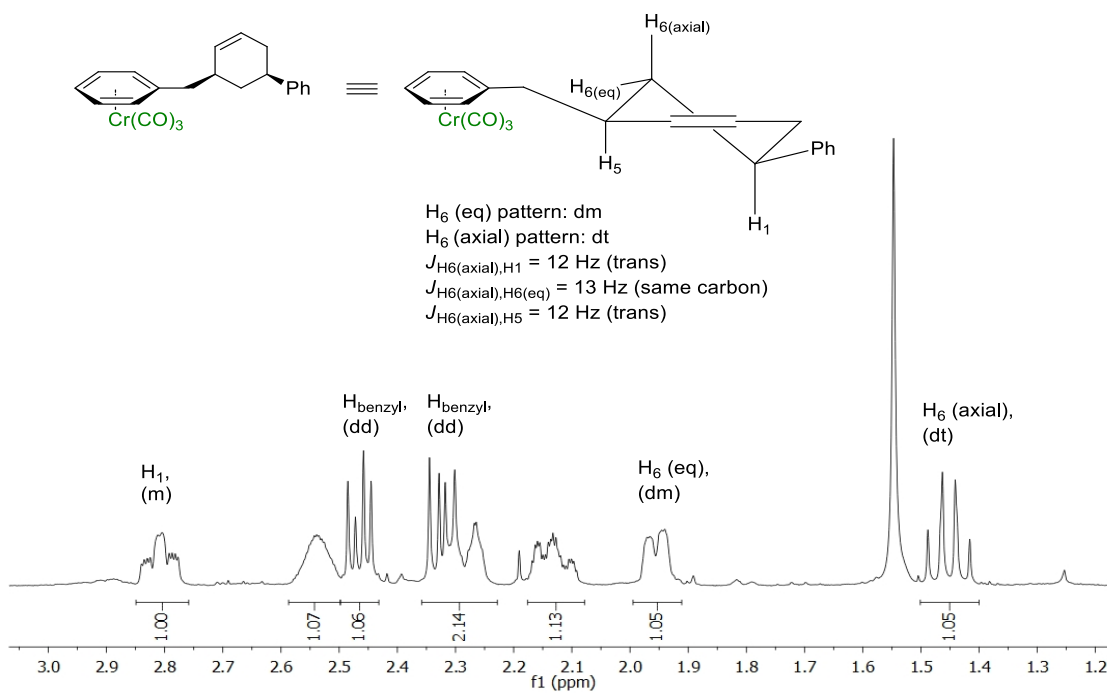


Figure A1.38 Determination of the relative stereochemistry of **1.6**

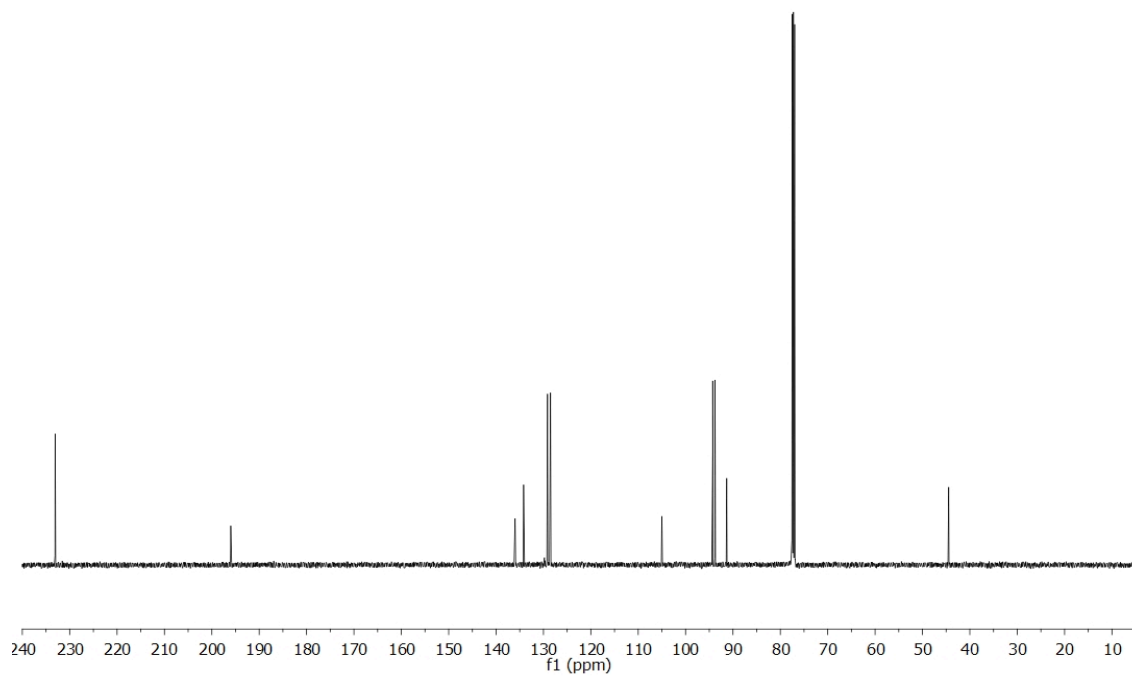
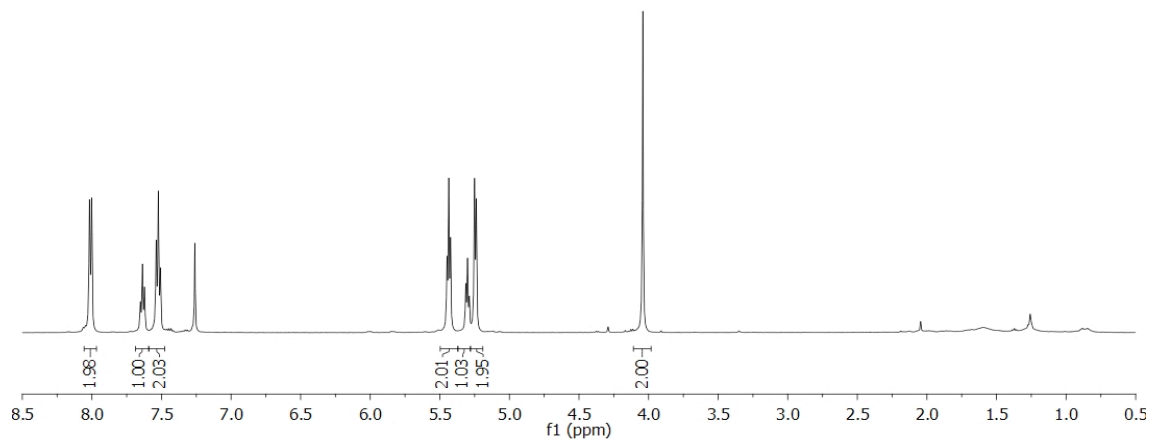
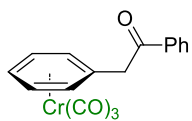


Figure A1.39 500 MHz ^1H and 125 MHz $^{13}\text{C}\{^1\text{H}\}$ NMR of **1.10** in CDCl_3

Appendix A2. NMR Spectra Relevant to Chapter 2

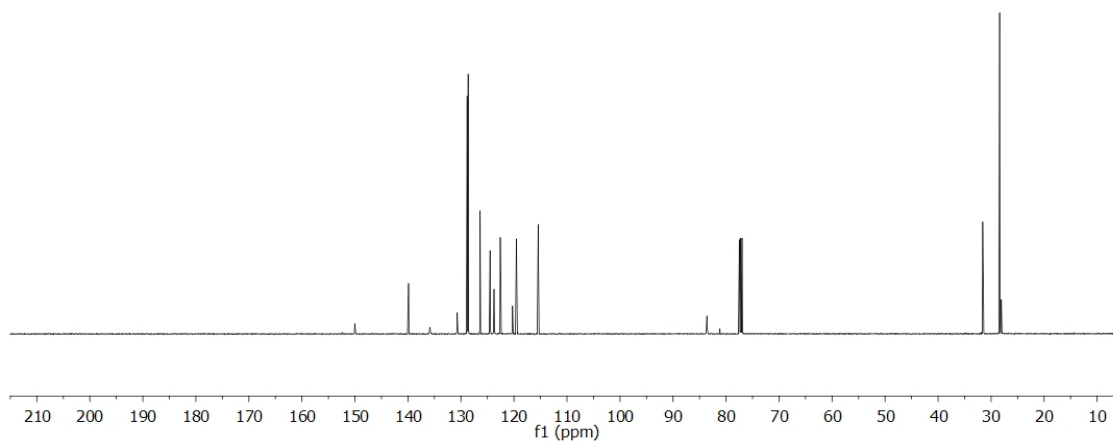
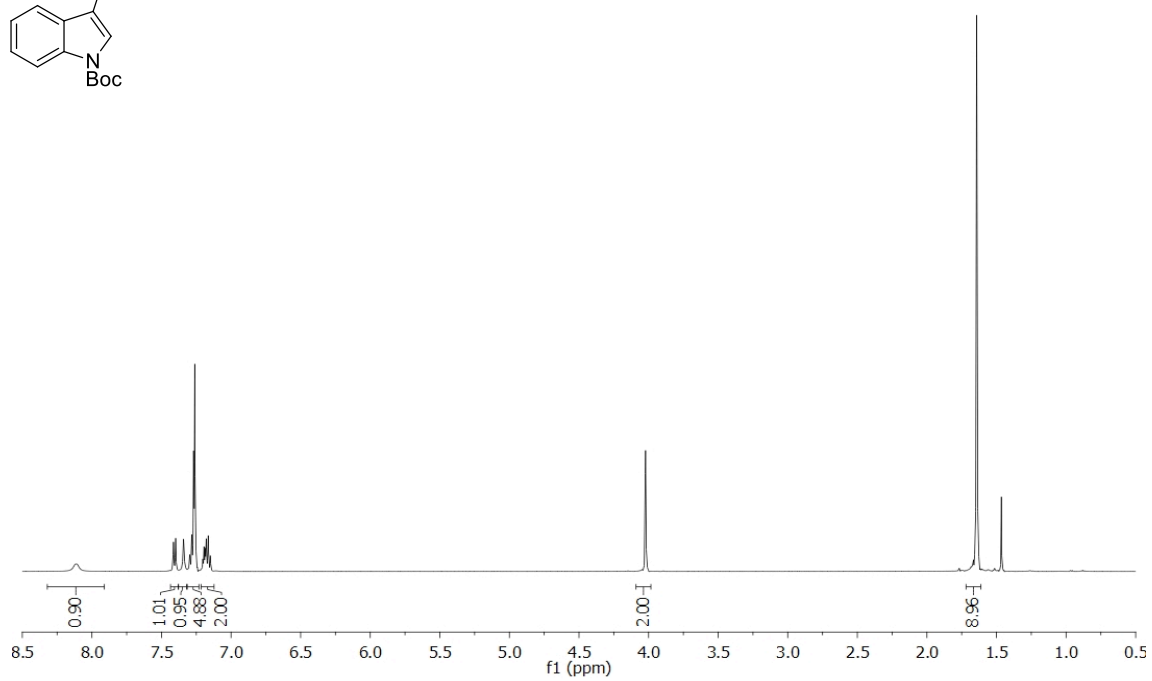
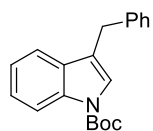


Figure A2.1 500 MHz ^1H and 125 MHz $^{13}\text{C}\{^1\text{H}\}$ NMR of **2.11** in CDCl_3

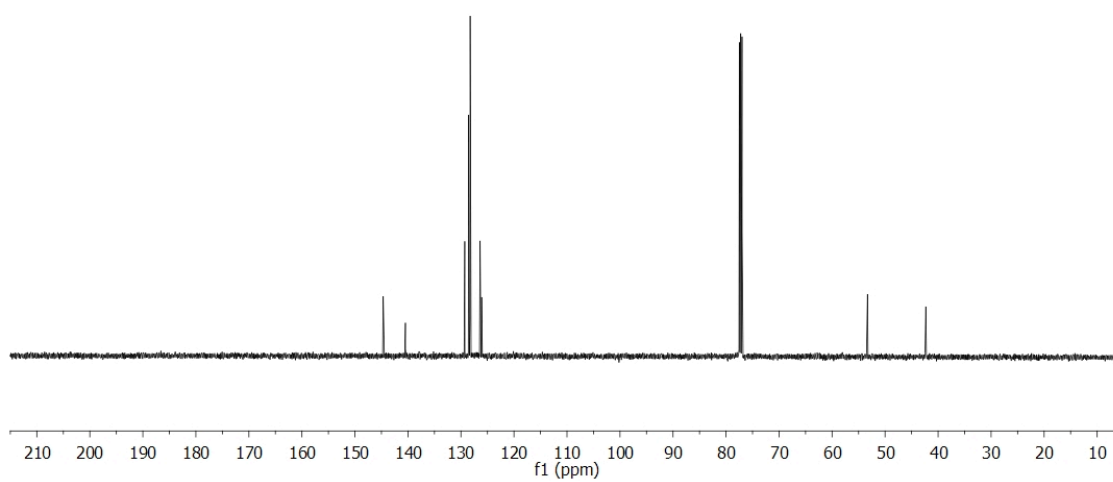
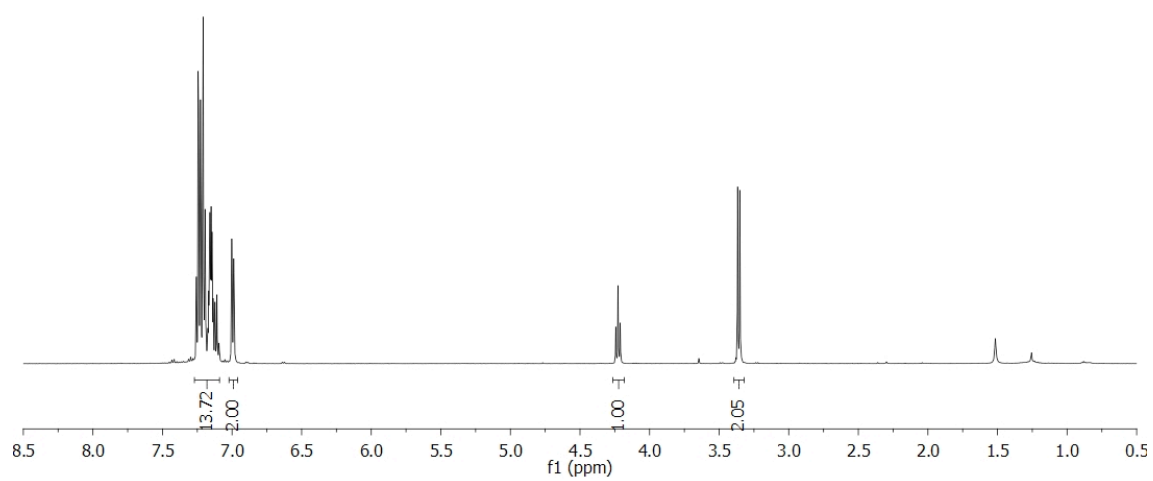
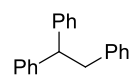


Figure A2.2 500 MHz ^1H and 125 MHz $^{13}\text{C}\{^1\text{H}\}$ NMR of **2.4** in CDCl_3

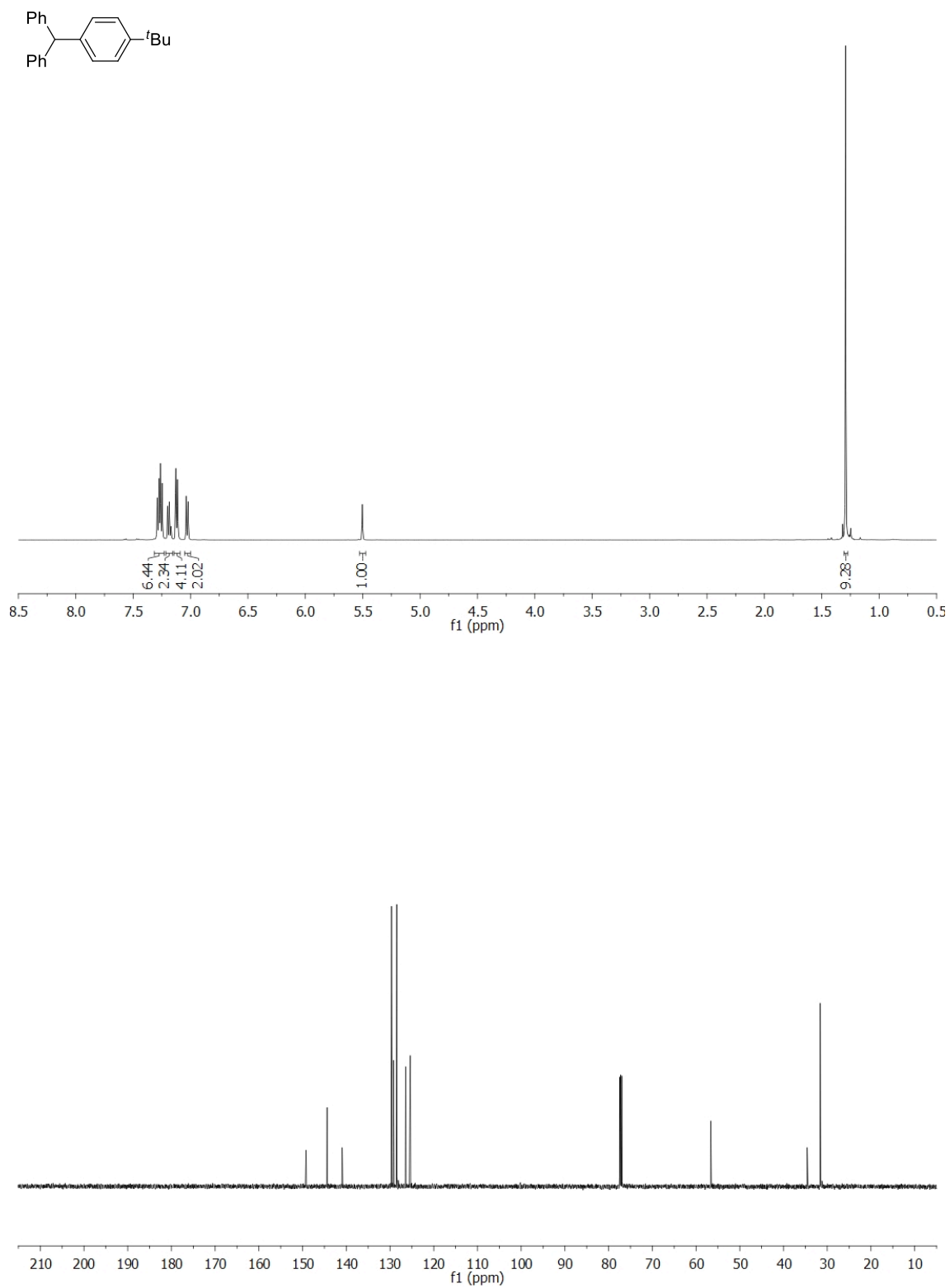


Figure A2.3 500 MHz ^1H and 125 MHz $^{13}\text{C}\{^1\text{H}\}$ NMR of **2.3aa** in CDCl_3

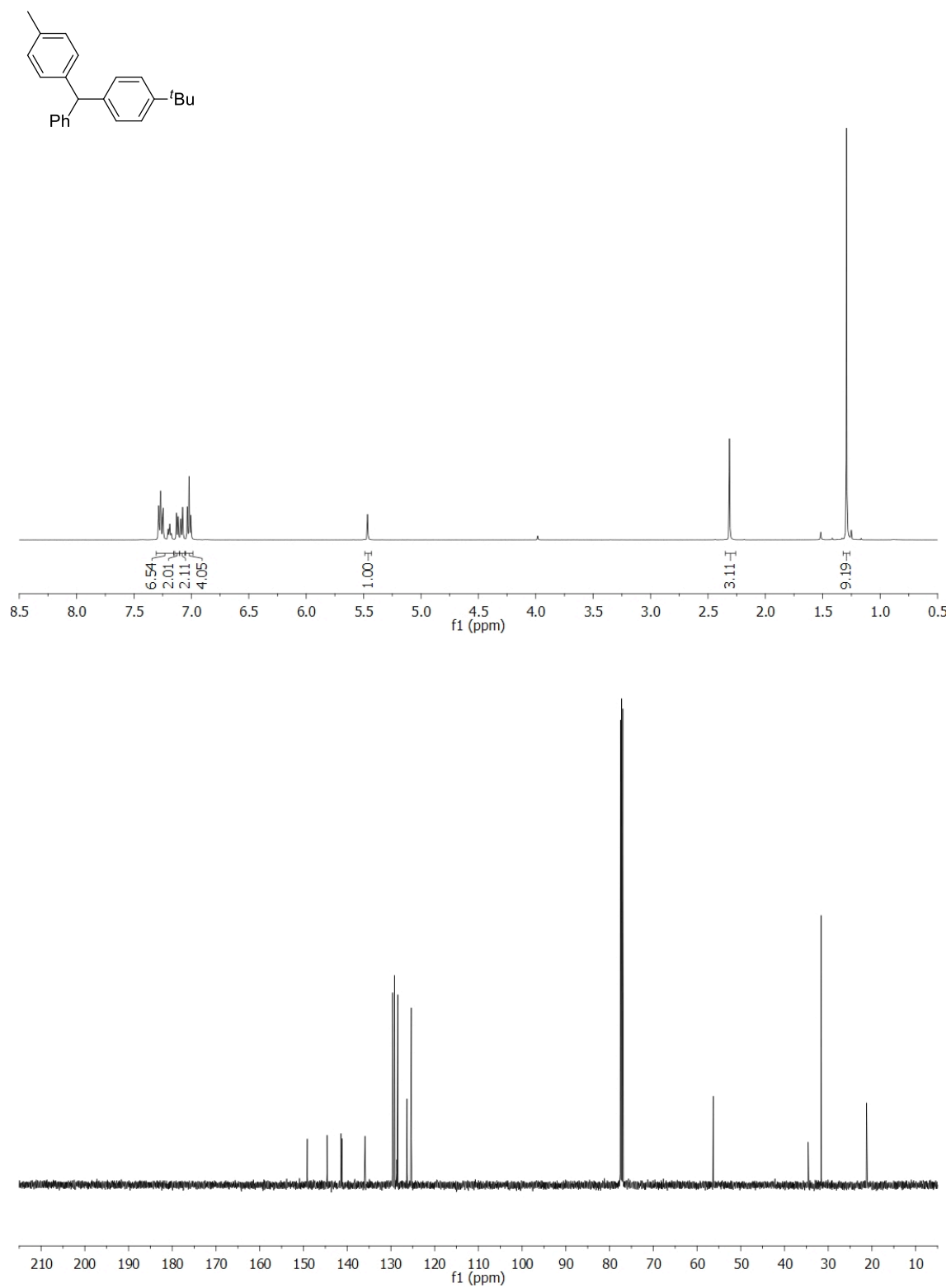


Figure A2.4 500 MHz ^1H and 125 MHz $^{13}\text{C}\{^1\text{H}\}$ NMR of **2.3ba** in CDCl_3

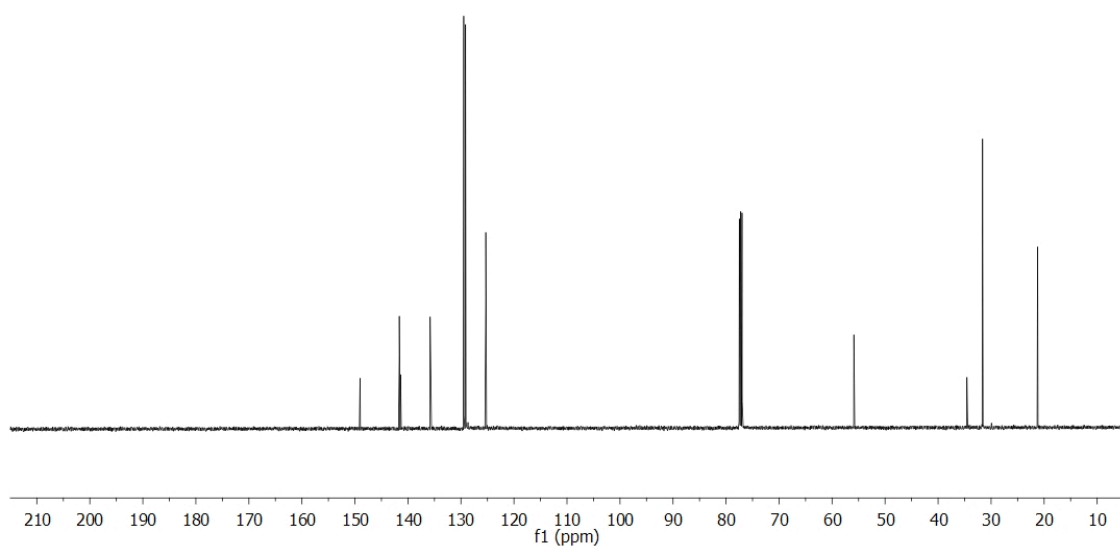
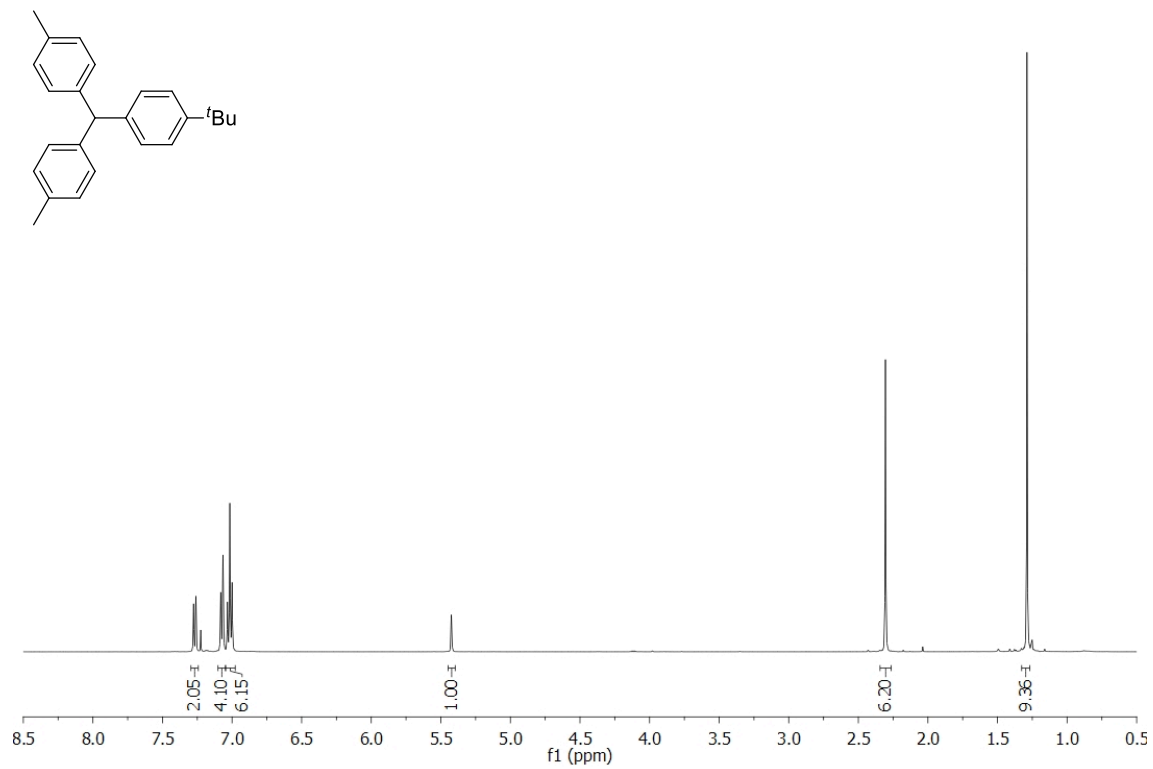


Figure A2.5 500 MHz ^1H and 125 MHz $^{13}\text{C}\{^1\text{H}\}$ NMR of **2.3ca** in CDCl_3

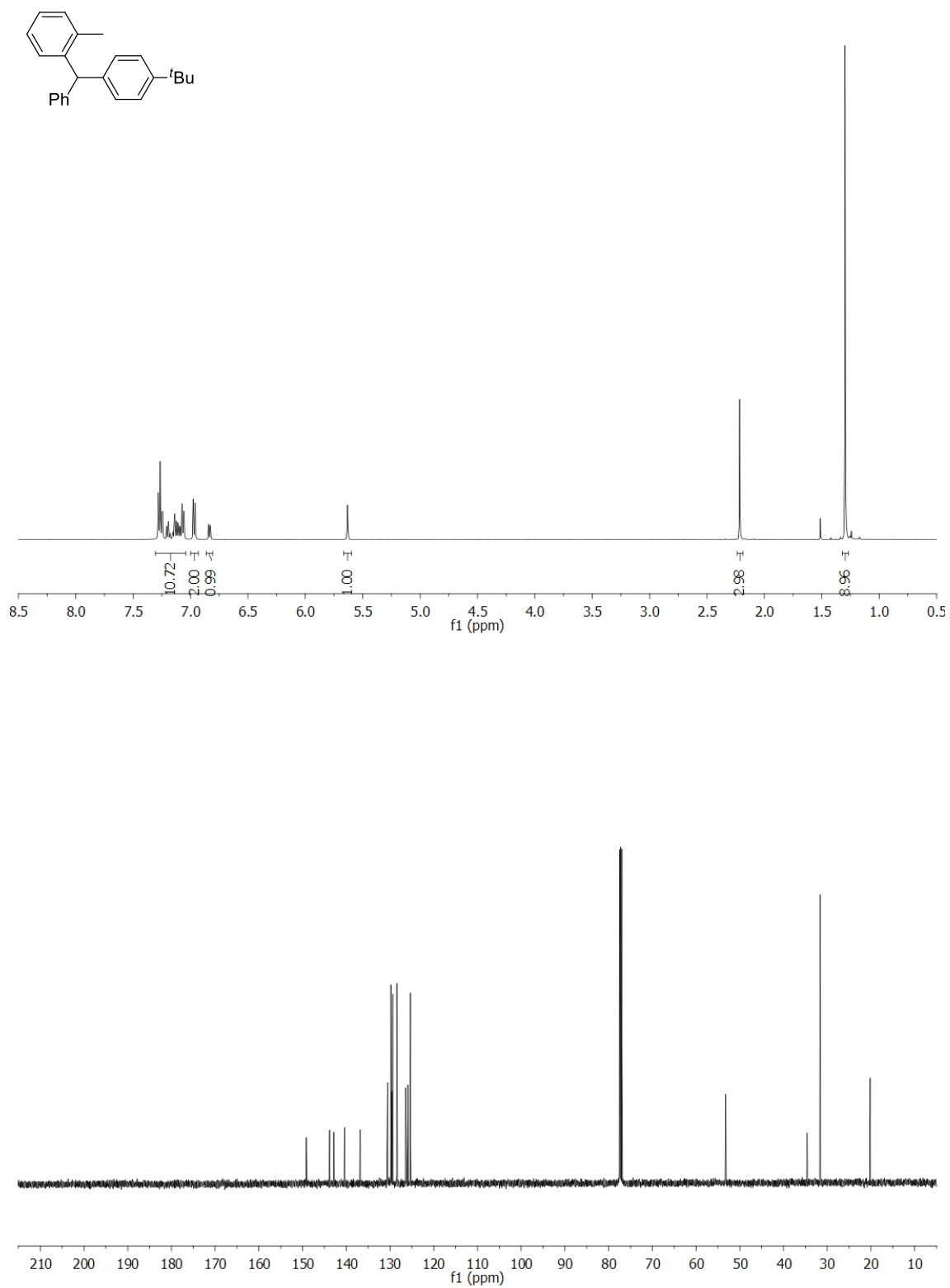


Figure A2.6 500 MHz ^1H and 125 MHz $^{13}\text{C}\{^1\text{H}\}$ NMR of **2.3da** in CDCl_3

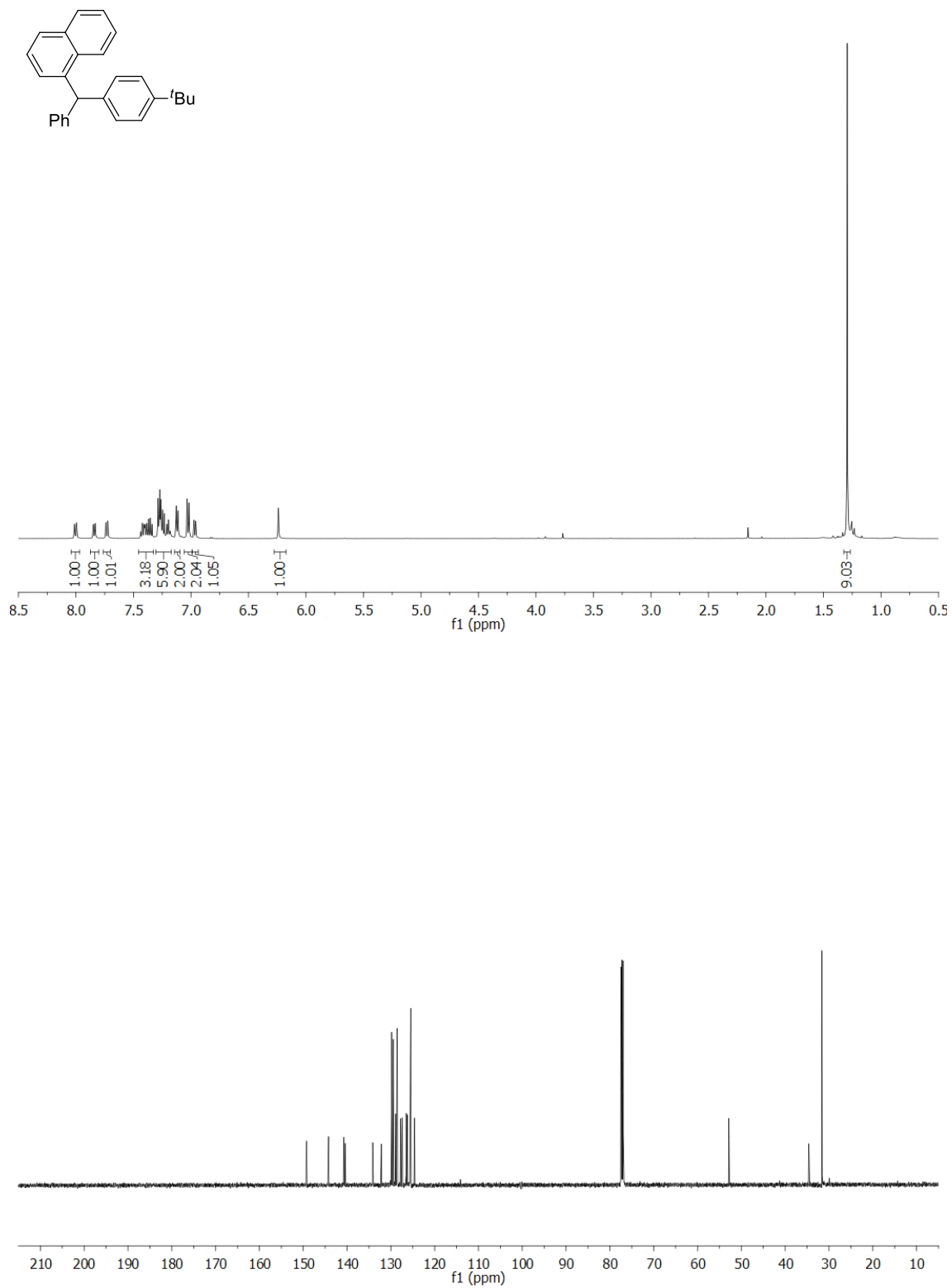


Figure A2.7 500 MHz ^1H and 125 MHz $^{13}\text{C}\{^1\text{H}\}$ NMR of **2.3ea** in CDCl_3

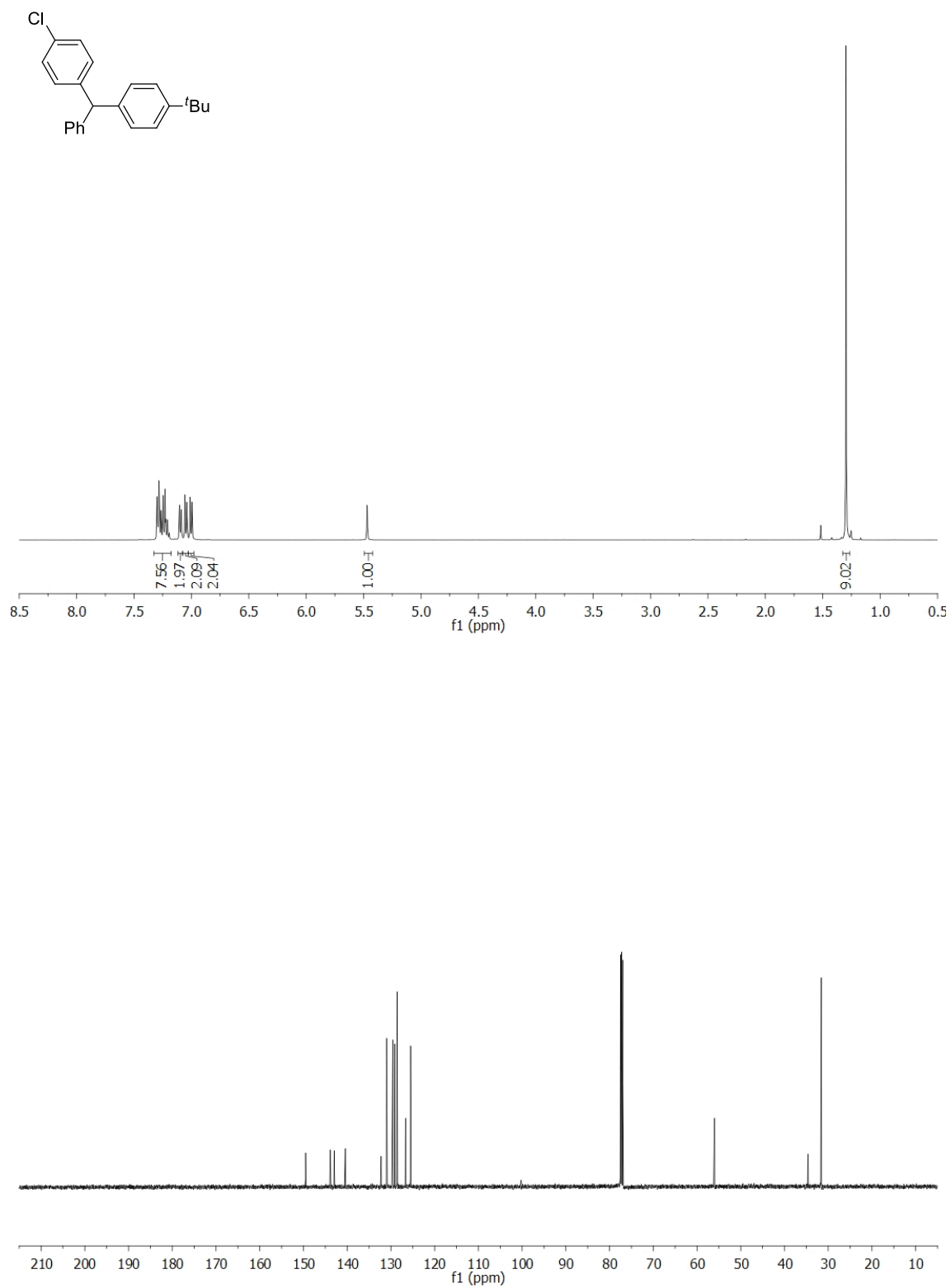


Figure A2.8 500 MHz ^1H and 125 MHz $^{13}\text{C}\{^1\text{H}\}$ NMR of **2.3fa** in CDCl_3

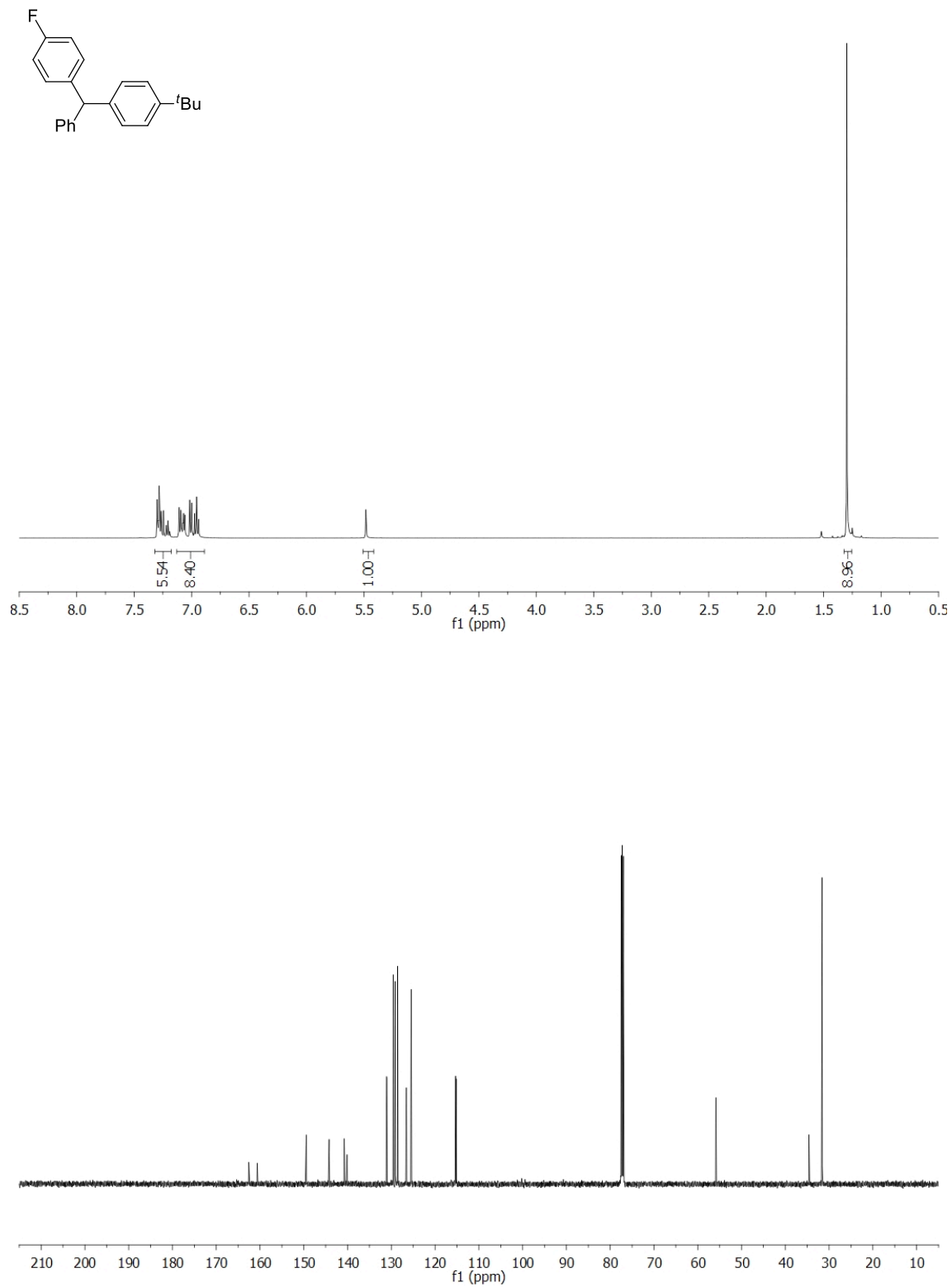


Figure A2.9 500 MHz ^1H and 125 MHz $^{13}\text{C}\{^1\text{H}\}$ NMR of **2.3ga** in CDCl_3

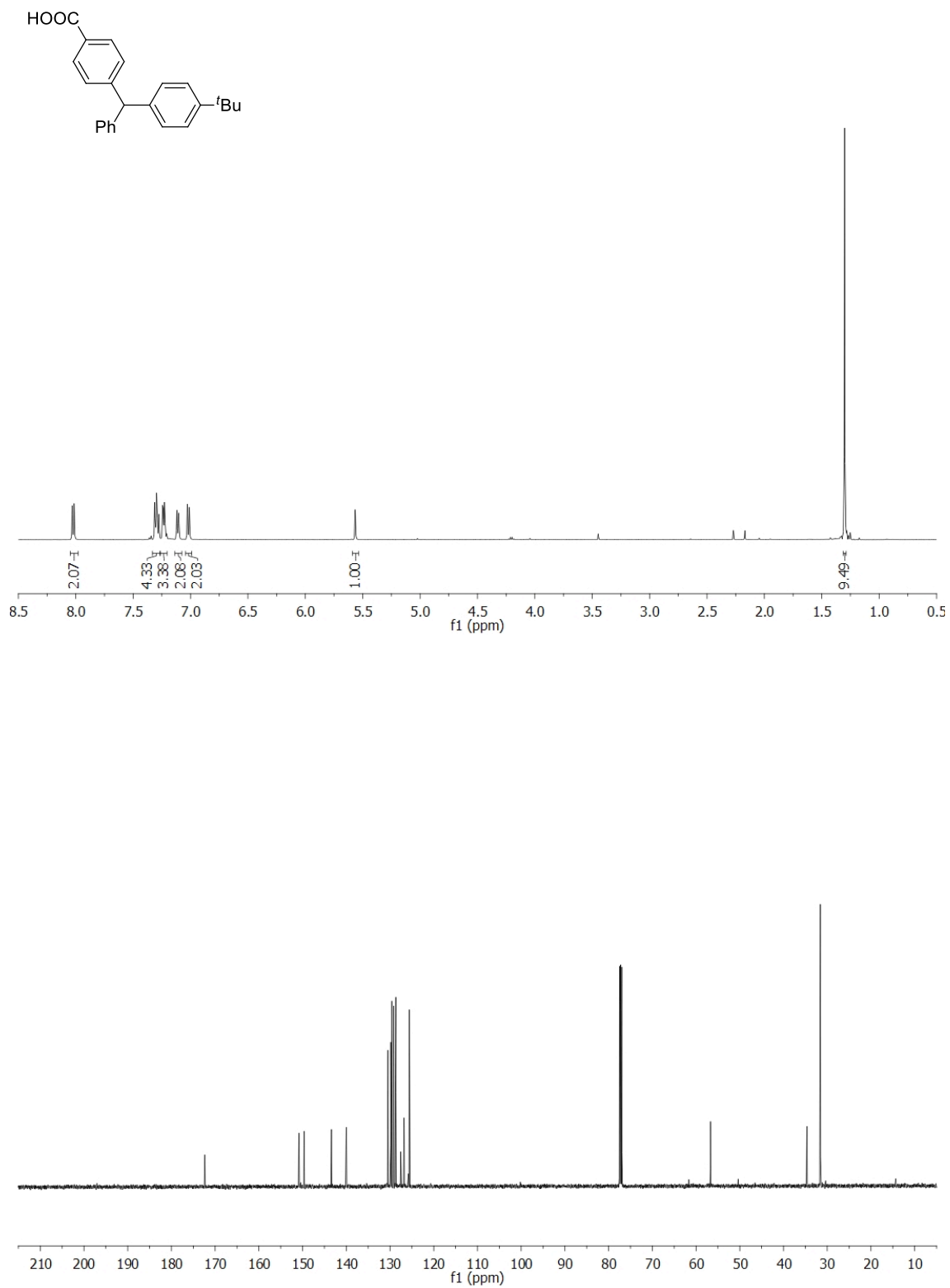


Figure A2.10 500 MHz ¹H and 125 MHz ¹³C{¹H} NMR of **2.3ha** in CDCl₃

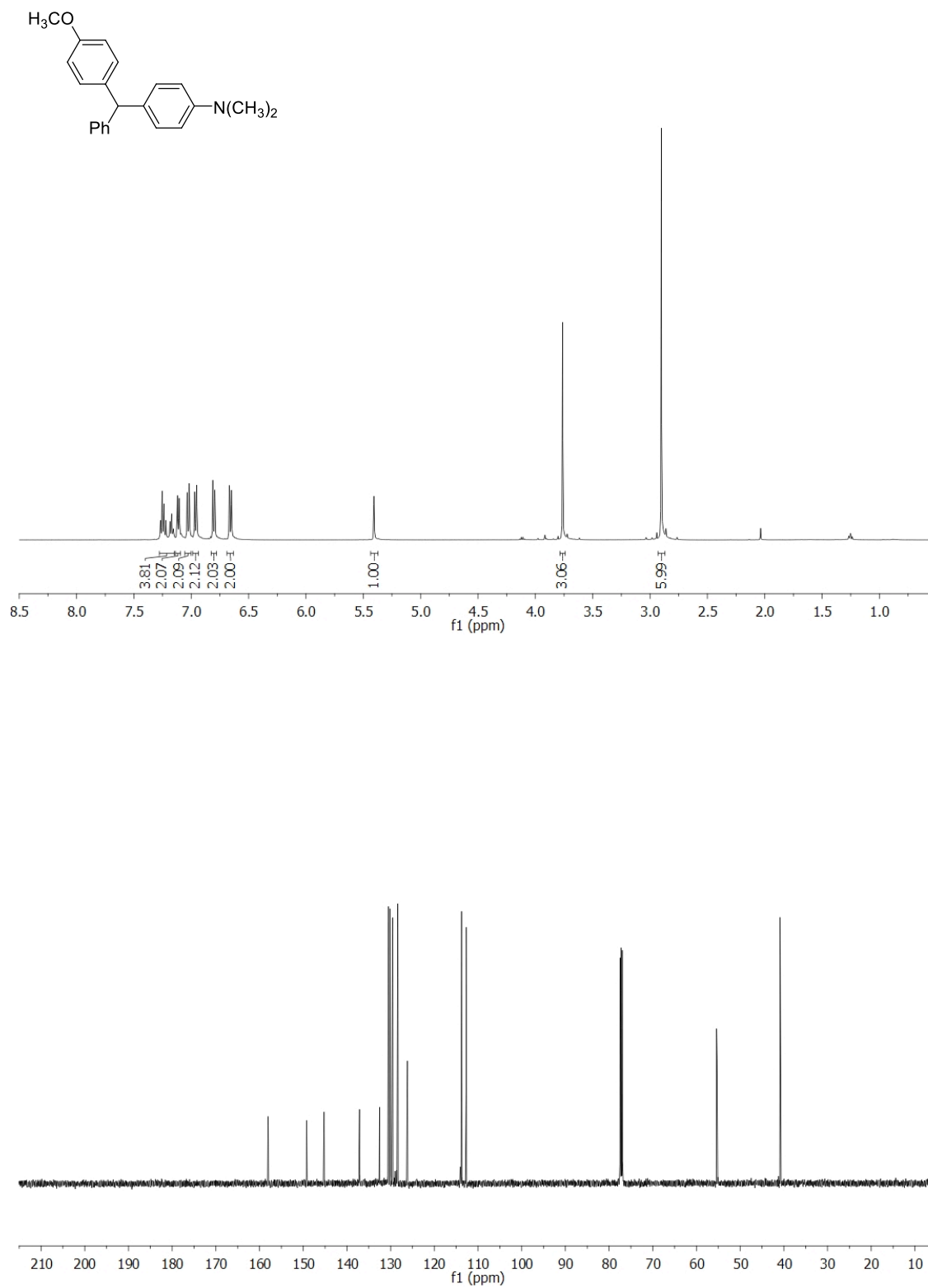


Figure A2.11 500 MHz ^1H and 125 MHz $^{13}\text{C}\{^1\text{H}\}$ NMR of **2.3ij** in CDCl_3

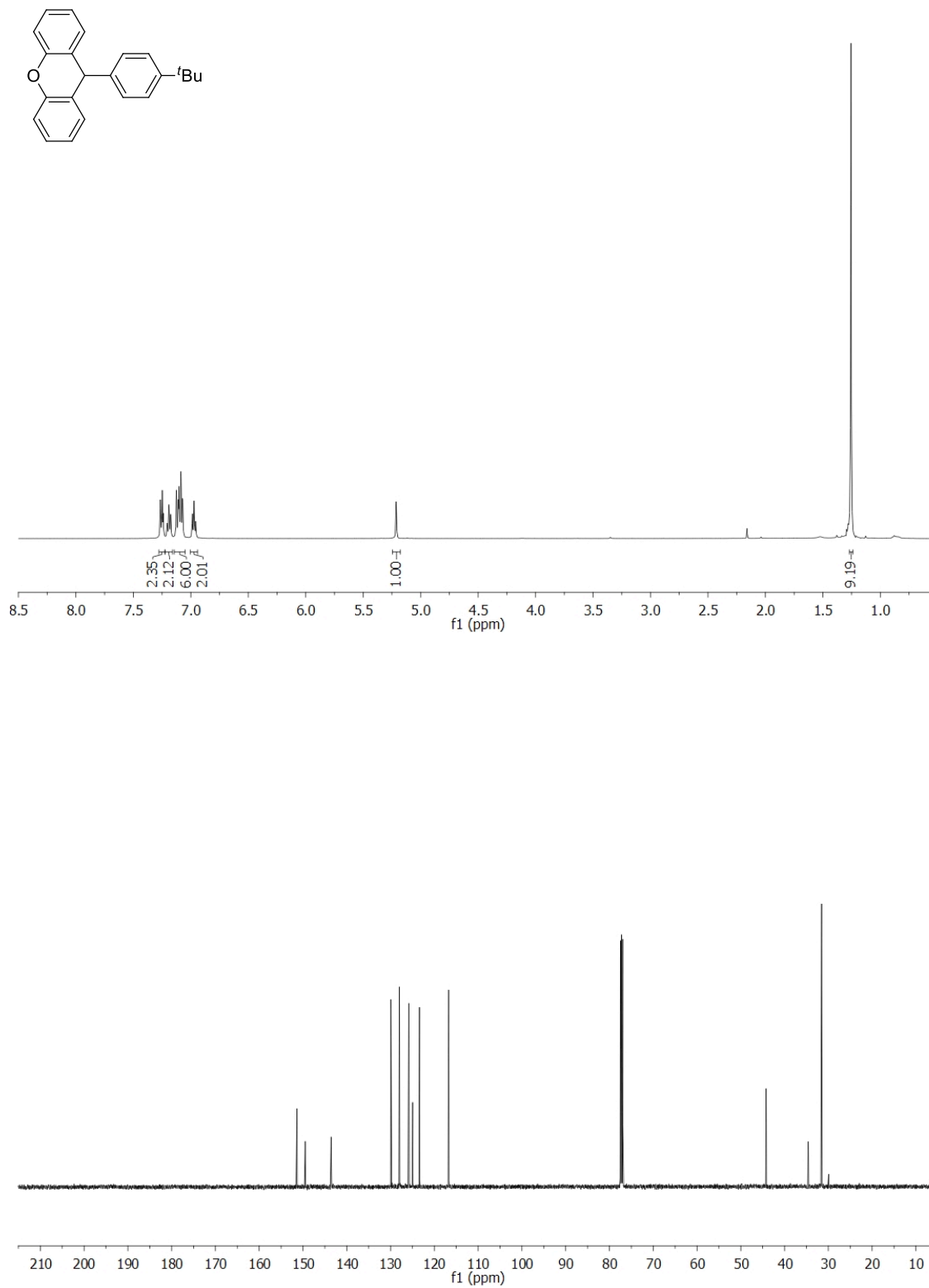


Figure A2.12 500 MHz ^1H and 125 MHz $^{13}\text{C}\{^1\text{H}\}$ NMR of **2.3ja** in CDCl_3

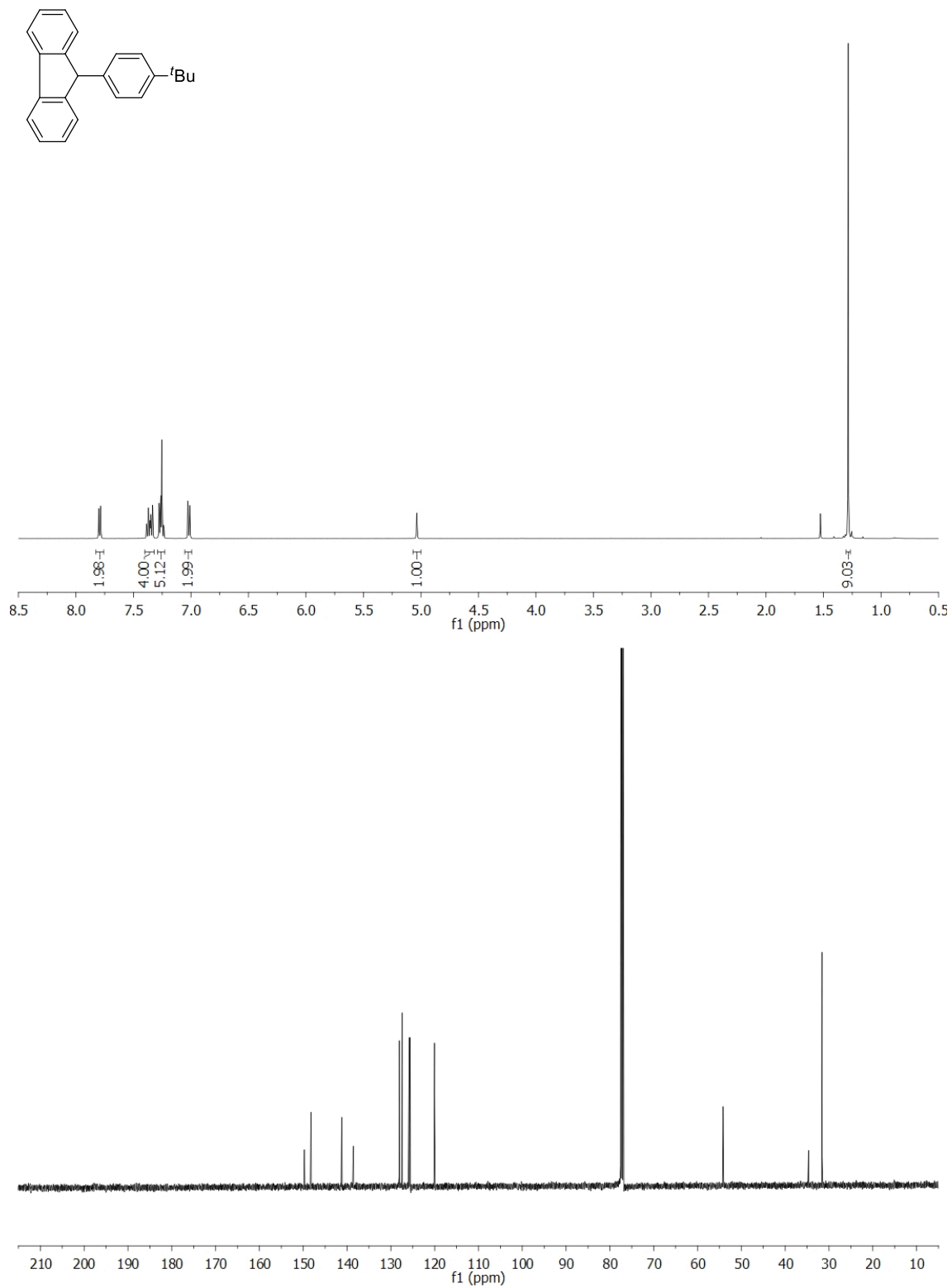


Figure A2.13 500 MHz ^1H and 125 MHz $^{13}\text{C}\{^1\text{H}\}$ NMR of **2.3ka** in CDCl_3

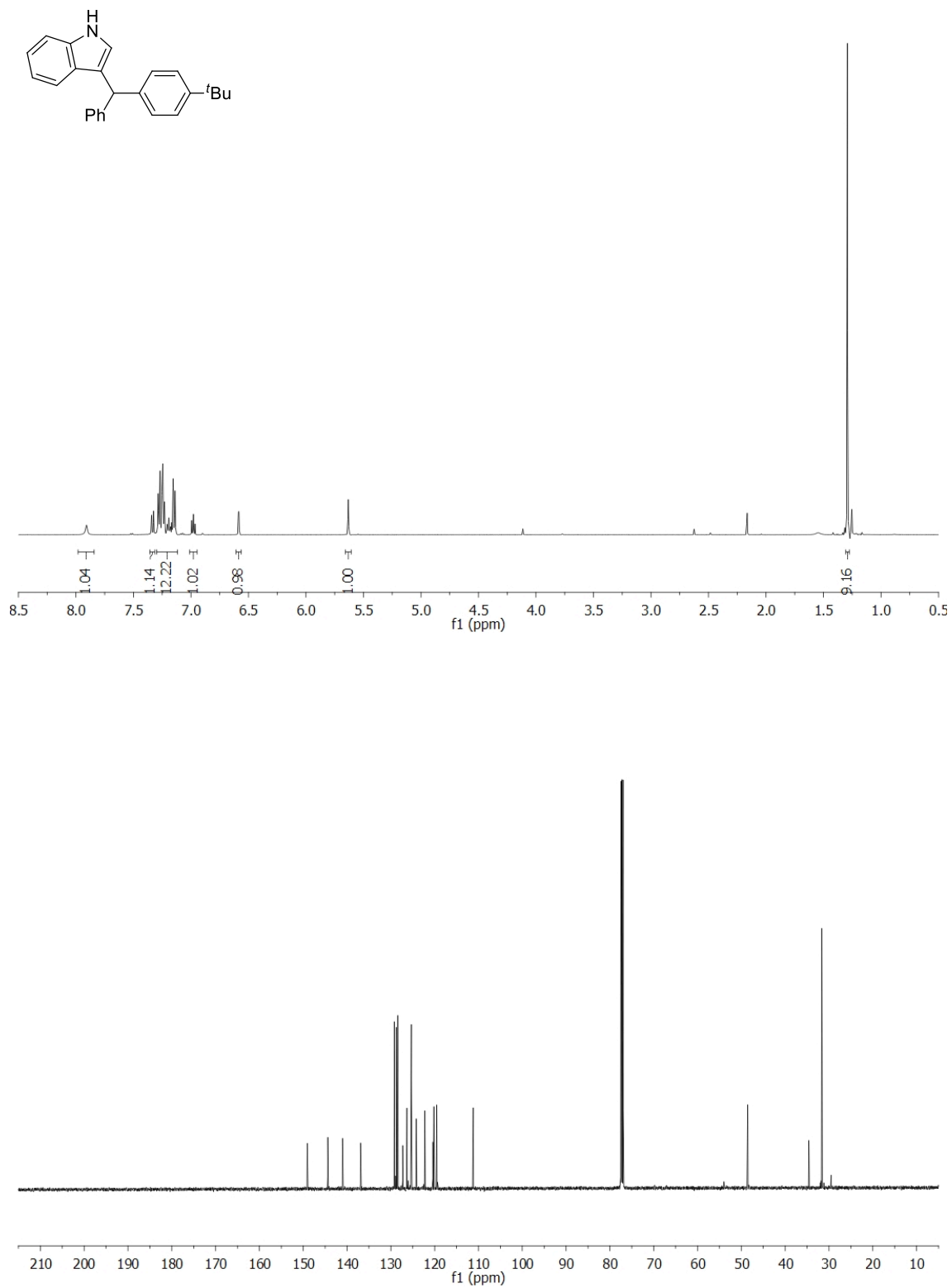


Figure A2.14 500 MHz ^1H and 125 MHz $^{13}\text{C}\{^1\text{H}\}$ NMR of **2.31a** in CDCl_3

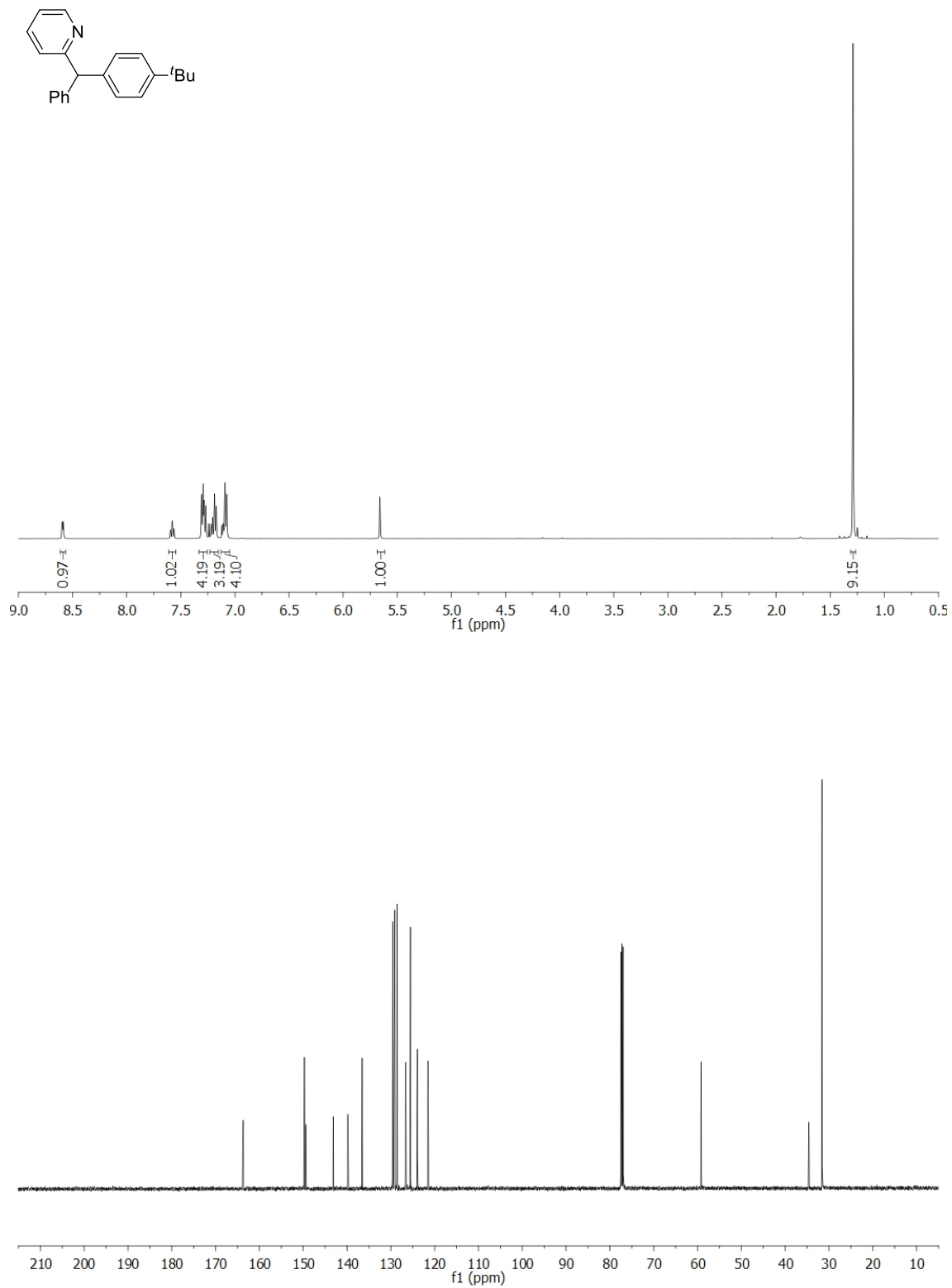


Figure A2.15 500 MHz ^1H and 125 MHz $^{13}\text{C}\{^1\text{H}\}$ NMR of **2.3ma** in CDCl_3

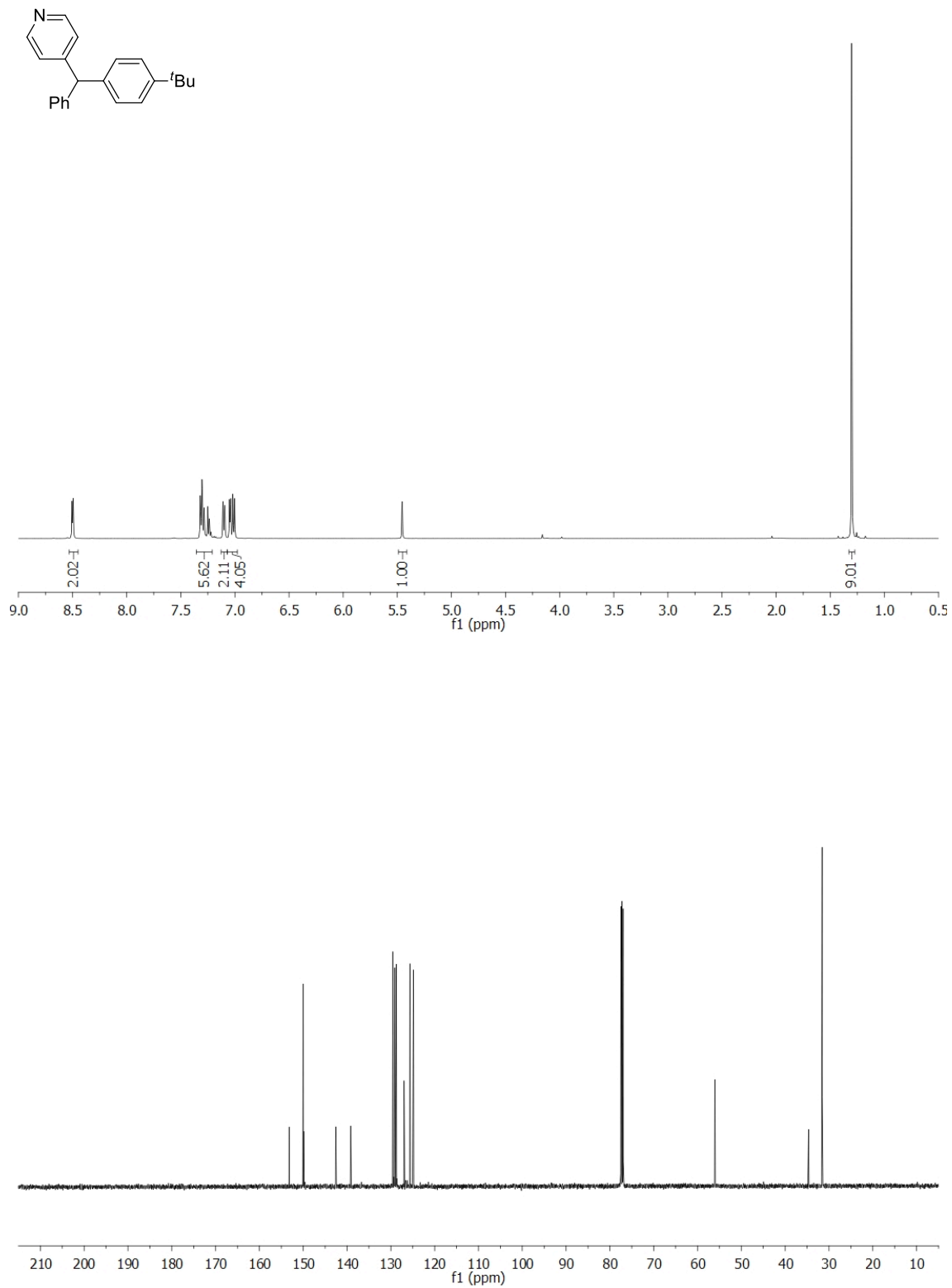


Figure A2.16 500 MHz ^1H and 125 MHz $^{13}\text{C}\{^1\text{H}\}$ NMR of **2.3na** in CDCl_3

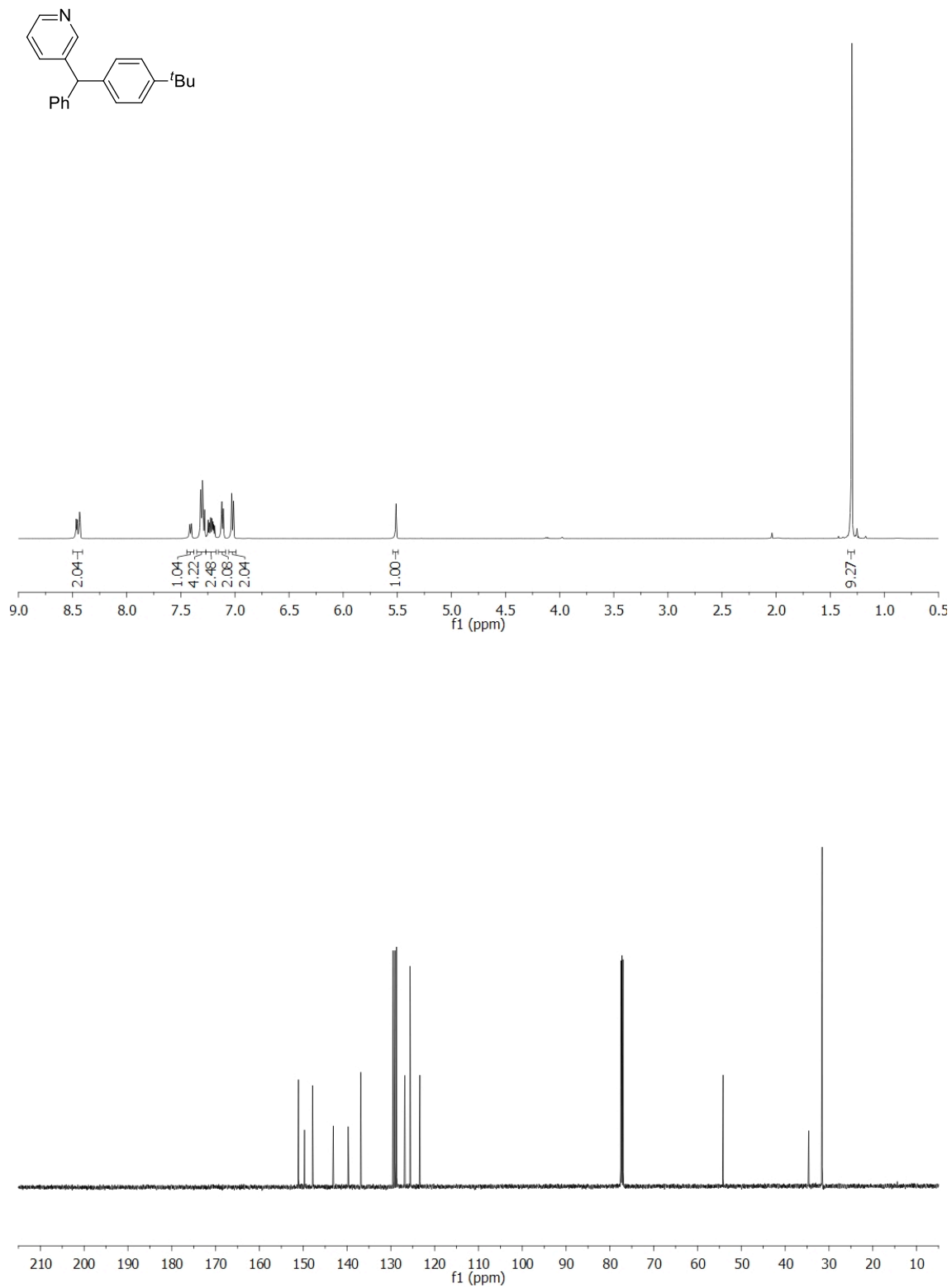


Figure A2.17 500 MHz ^1H and 125 MHz $^{13}\text{C}\{^1\text{H}\}$ NMR of **2.30a** in CDCl_3

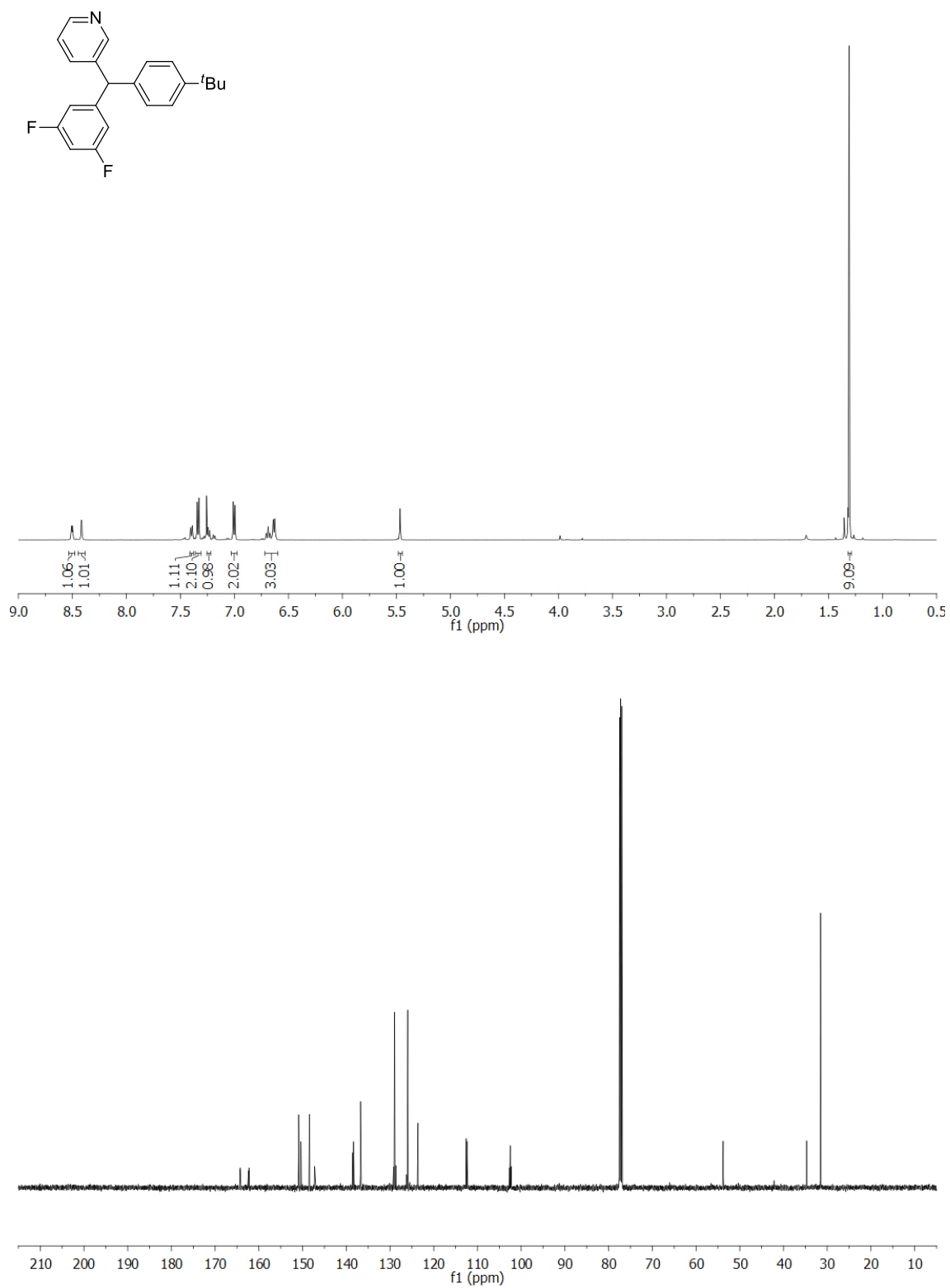


Figure A2.18 500 MHz ^1H and 125 MHz $^{13}\text{C}\{^1\text{H}\}$ NMR of **2.3pa** in CDCl_3

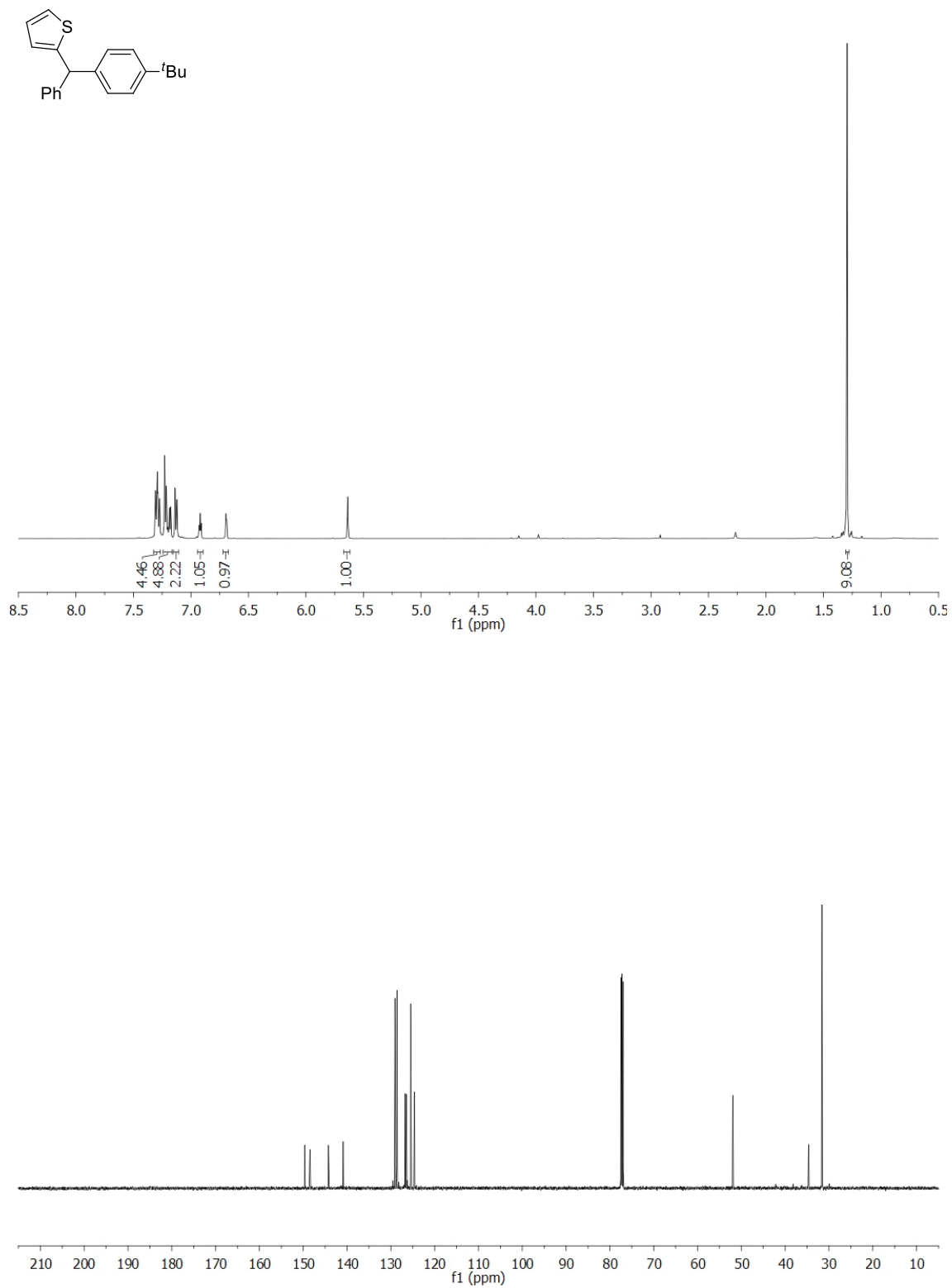


Figure A2.19 500 MHz ^1H and 125 MHz $^{13}\text{C}\{^1\text{H}\}$ NMR of **2.3qa** in CDCl_3

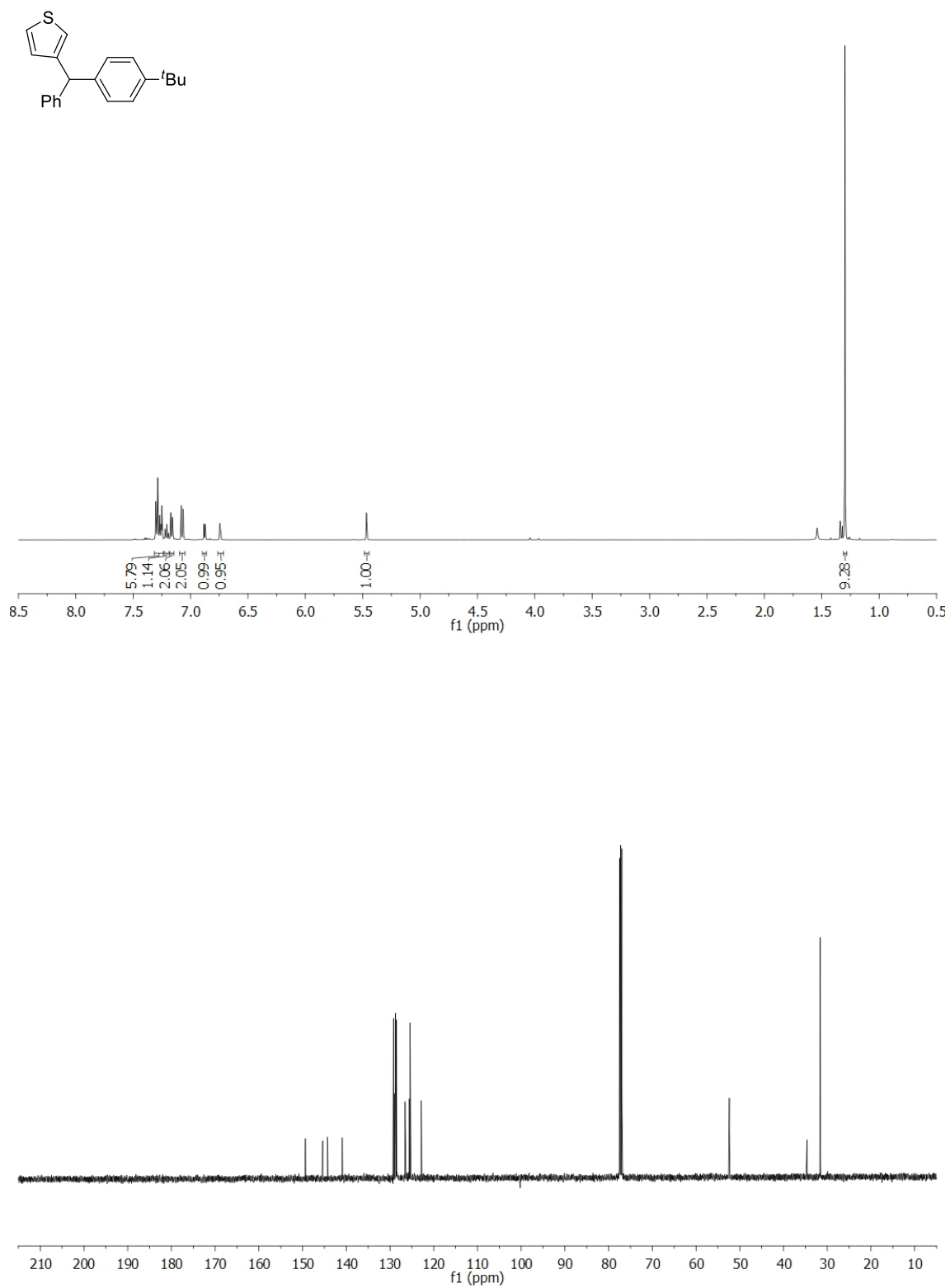


Figure A2.20 500 MHz ¹H and 125 MHz ¹³C{¹H} NMR of **2.3ra** in CDCl₃

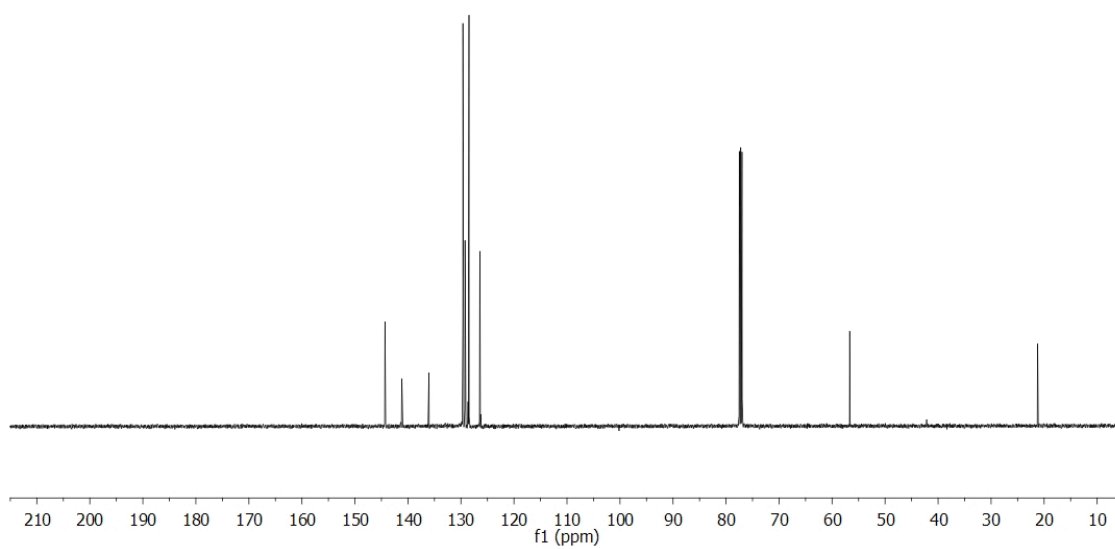
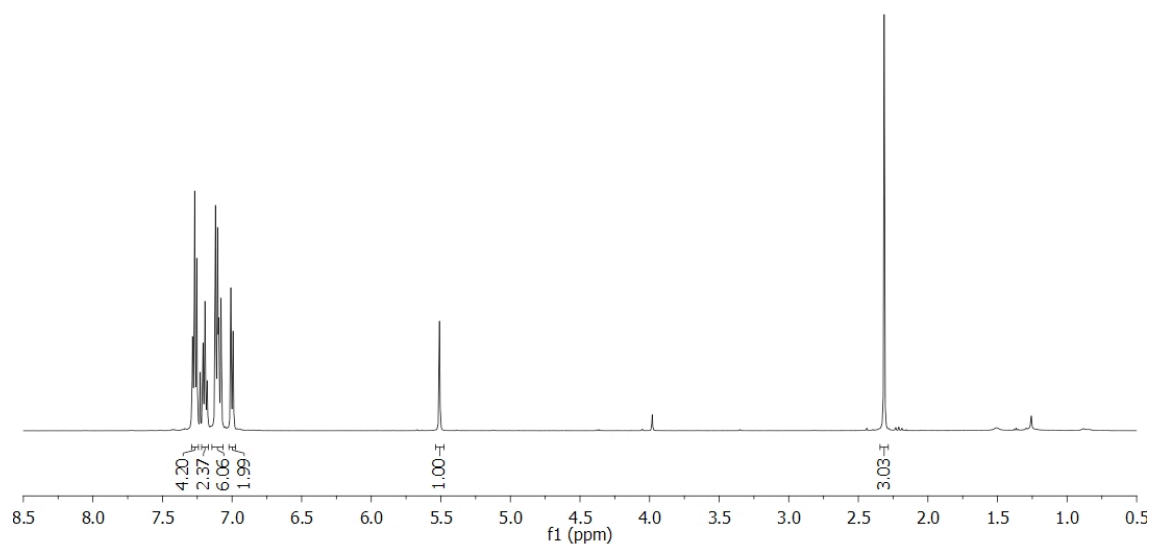
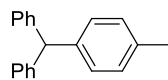


Figure A2.21 500 MHz ¹H and 125 MHz ¹³C{¹H} NMR of **2.3ab** in CDCl₃

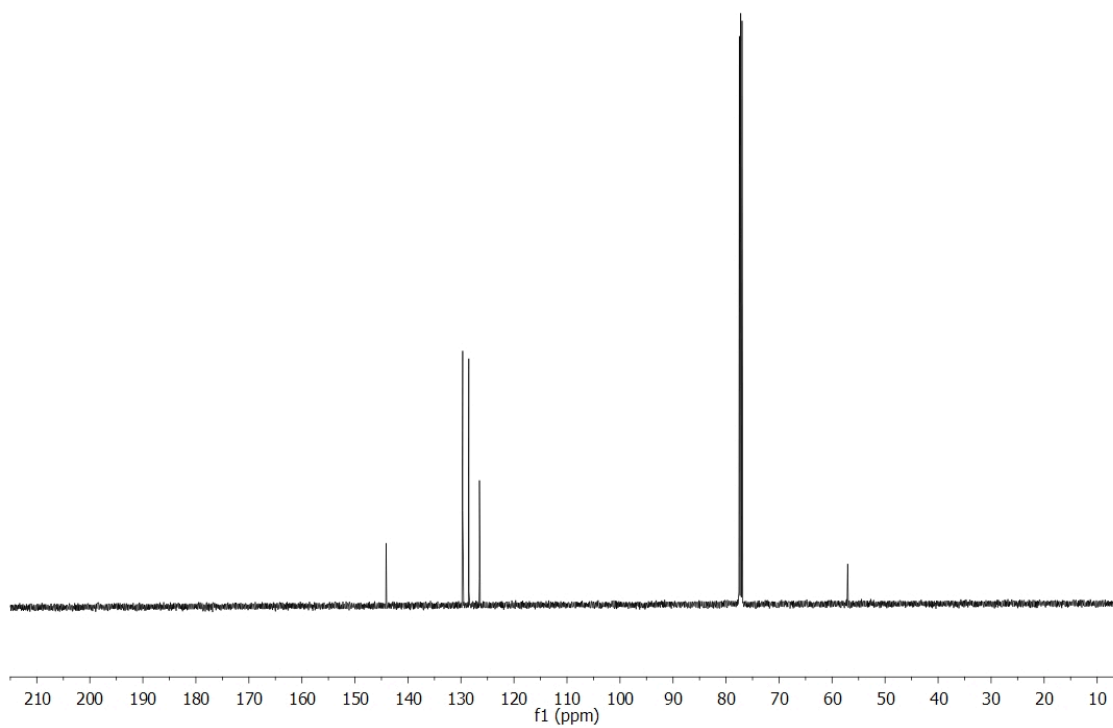
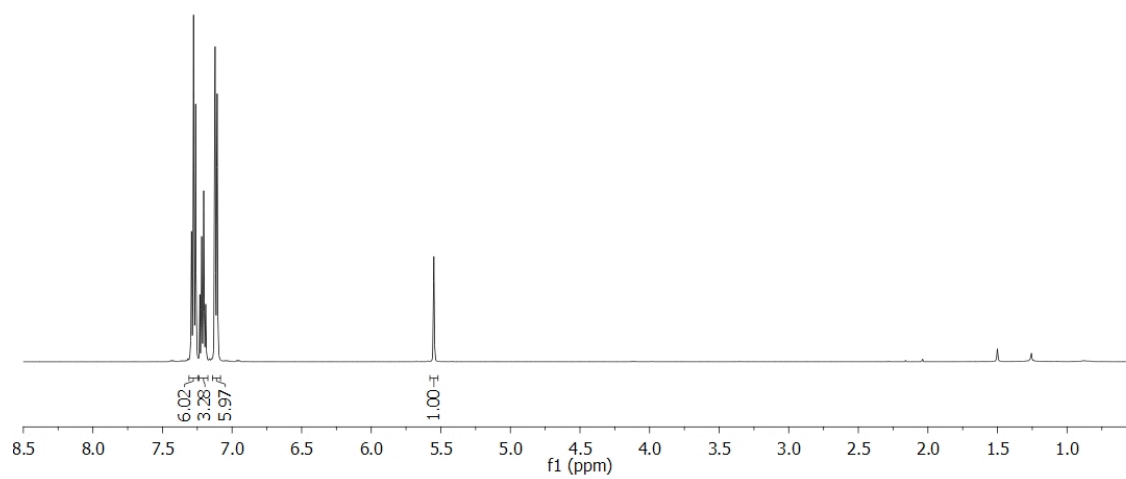
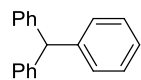


Figure A2.22 500 MHz ^1H and 125 MHz $^{13}\text{C}\{^1\text{H}\}$ NMR of **2.3ac** in CDCl_3

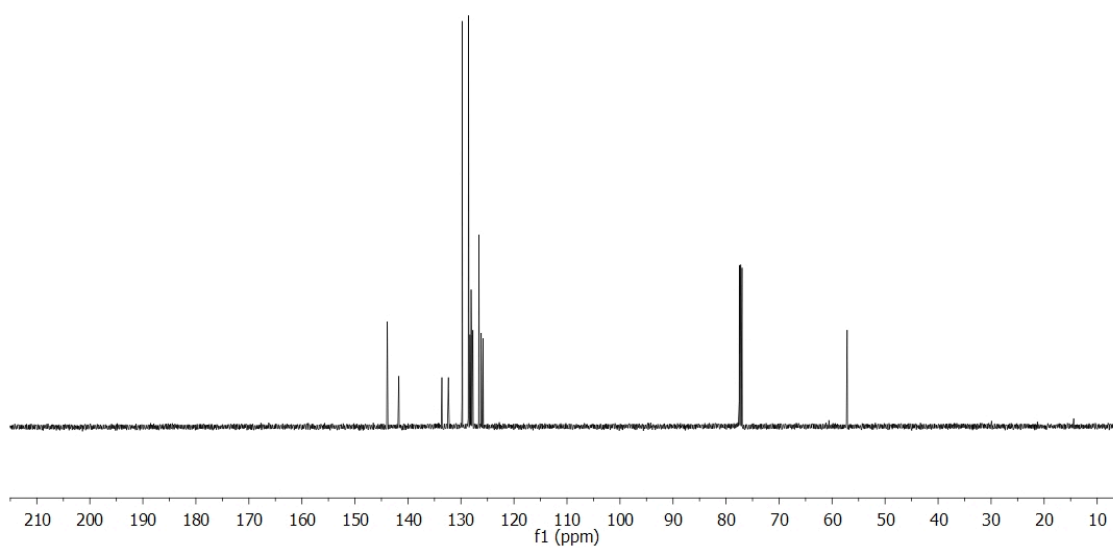
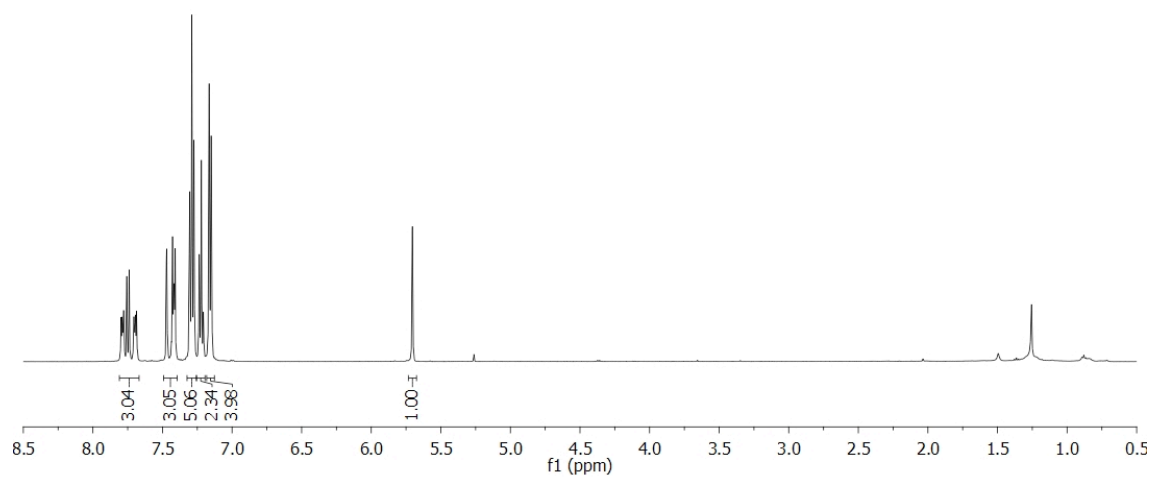
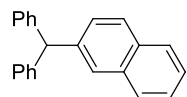


Figure A2.23 500 MHz ^1H and 125 MHz $^{13}\text{C}\{^1\text{H}\}$ NMR of **2.3ad** in CDCl_3

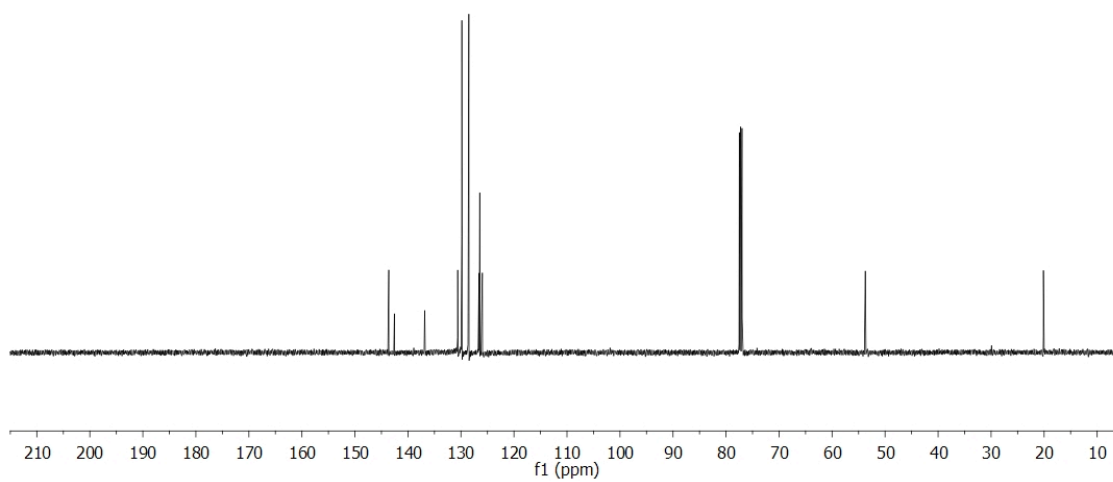
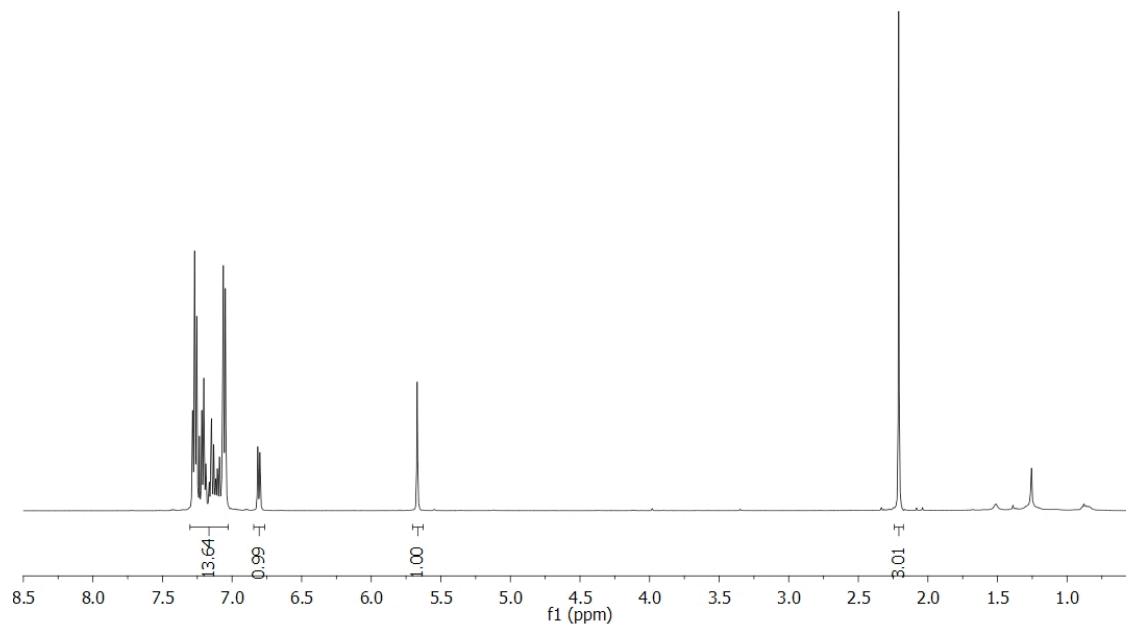
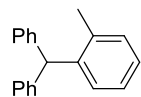


Figure A2.24 500 MHz ^1H and 125 MHz $^{13}\text{C}\{^1\text{H}\}$ NMR of **2.3ae** in CDCl_3

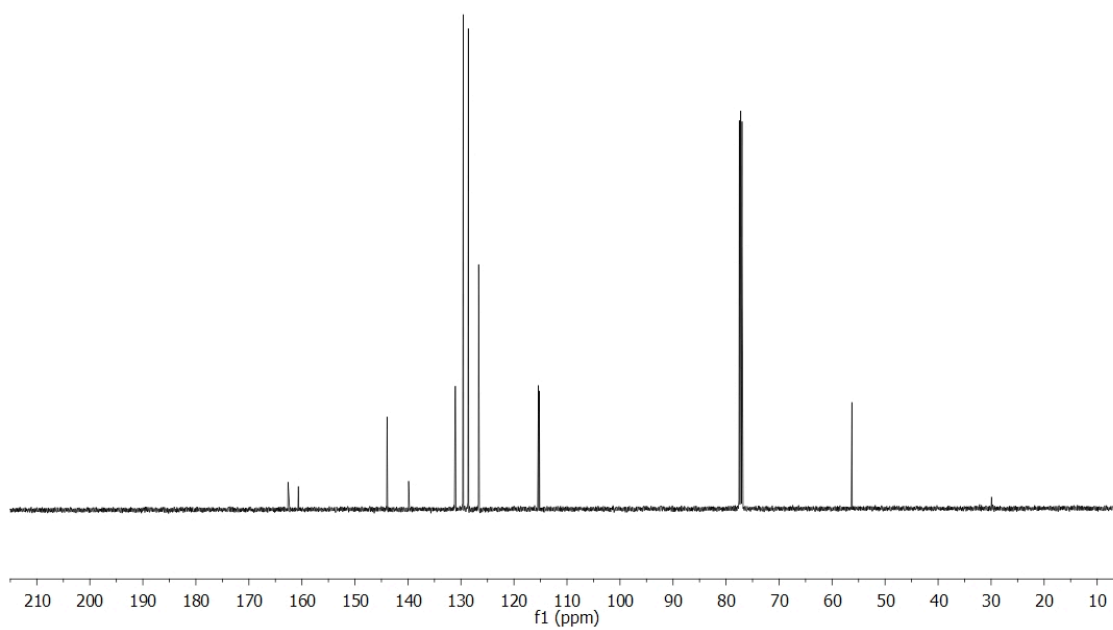
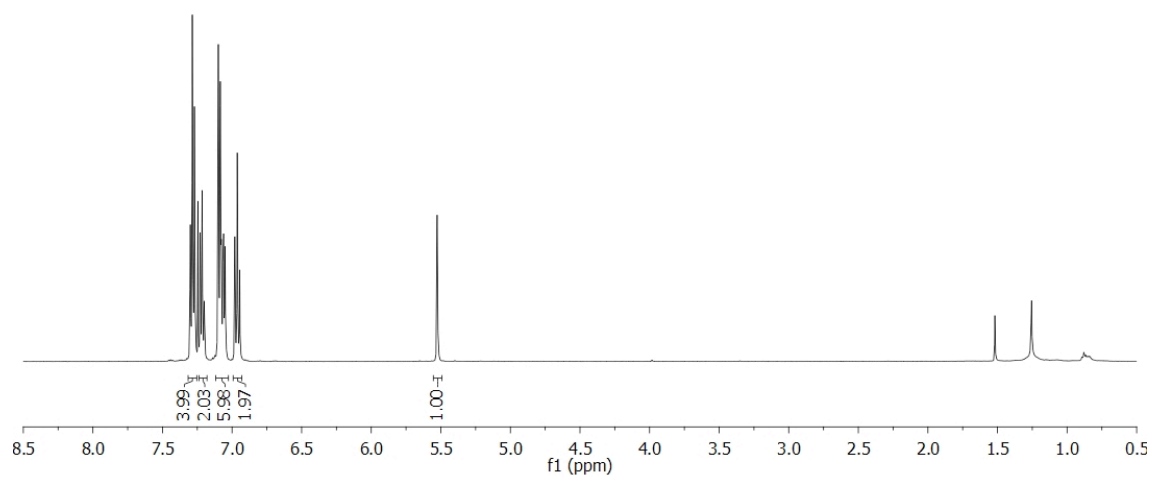
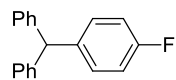


Figure A2.25 500 MHz ^1H and 125 MHz $^{13}\text{C}\{^1\text{H}\}$ NMR of **2.3af** in CDCl_3

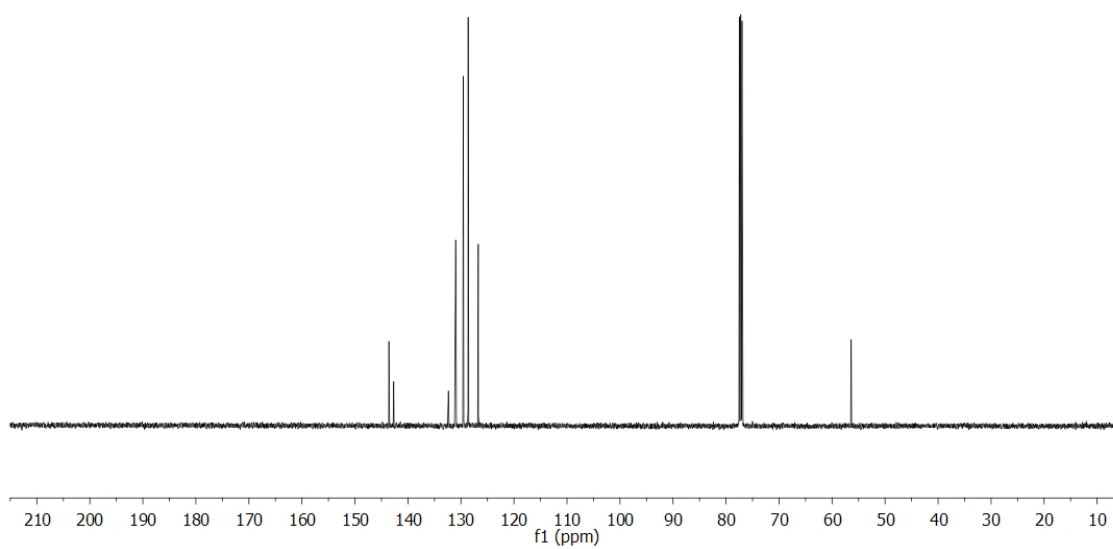
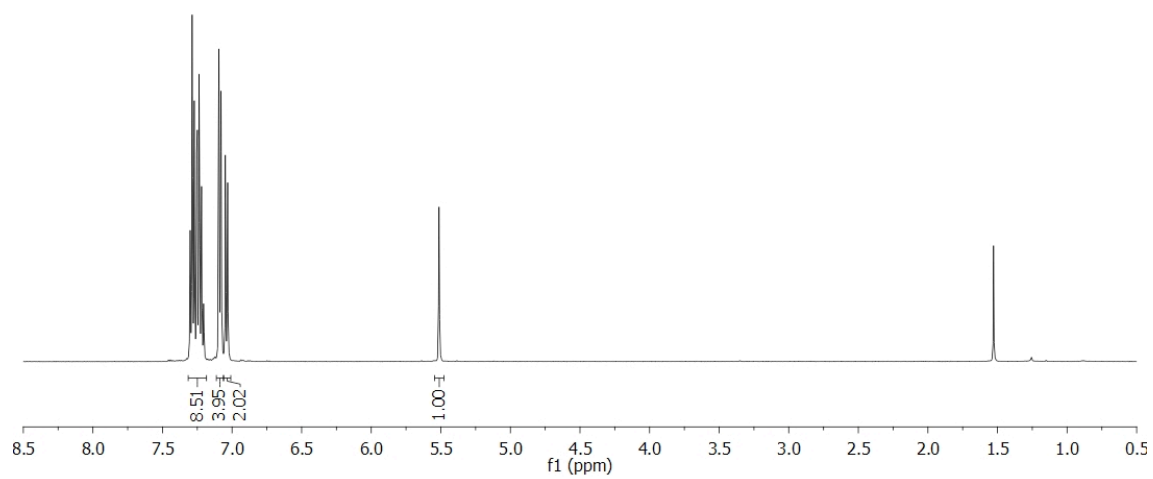
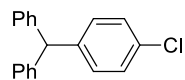


Figure A2.26 500 MHz ^1H and 125 MHz $^{13}\text{C}\{^1\text{H}\}$ NMR of **2.3ag** in CDCl_3

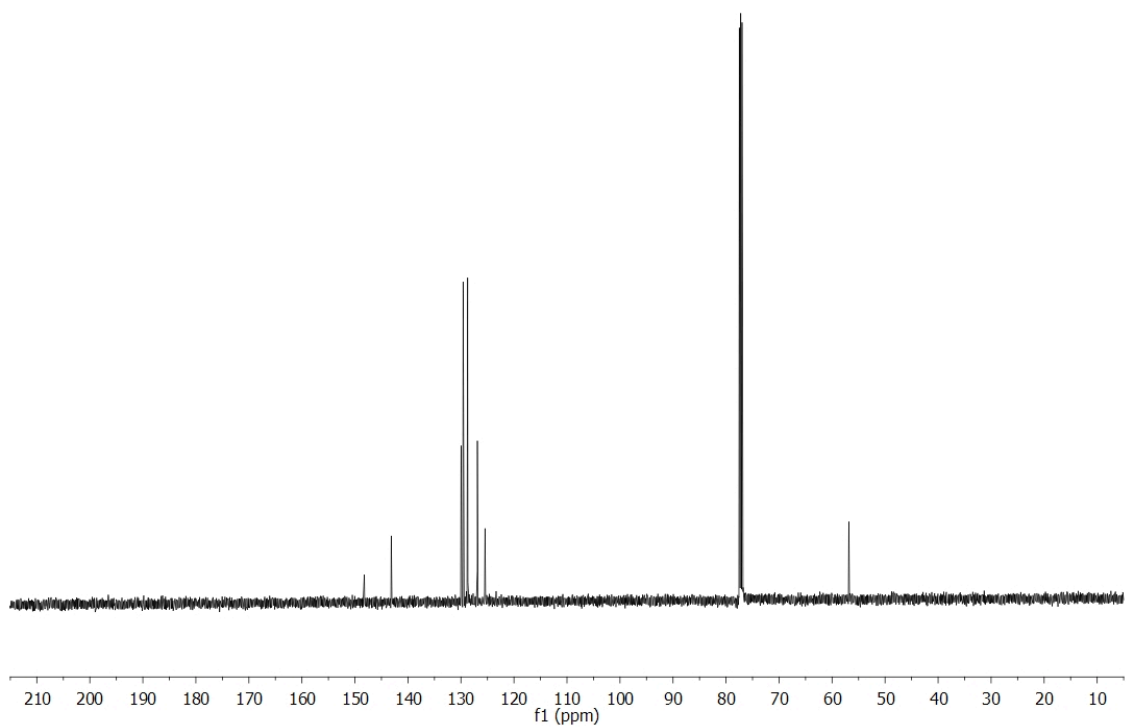
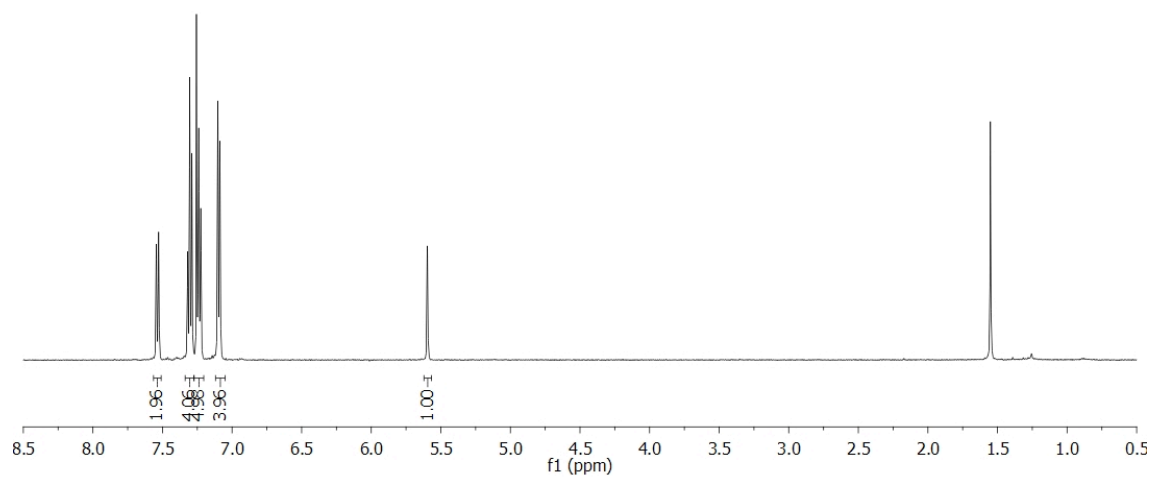
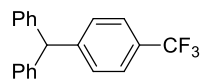


Figure A2.27 500 MHz ¹H and 125 MHz ¹³C{¹H} NMR of 2.3ah in CDCl₃

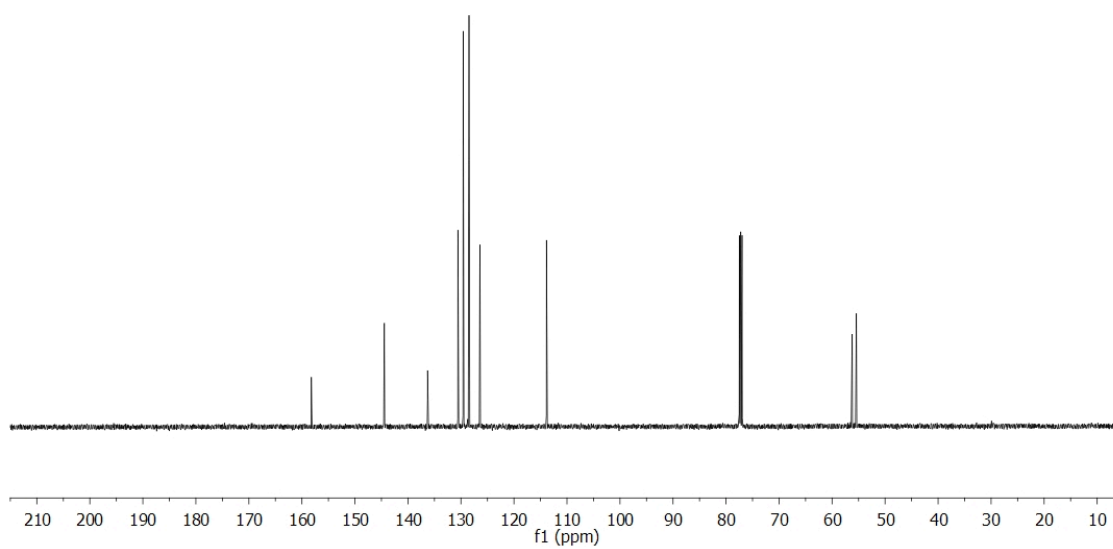
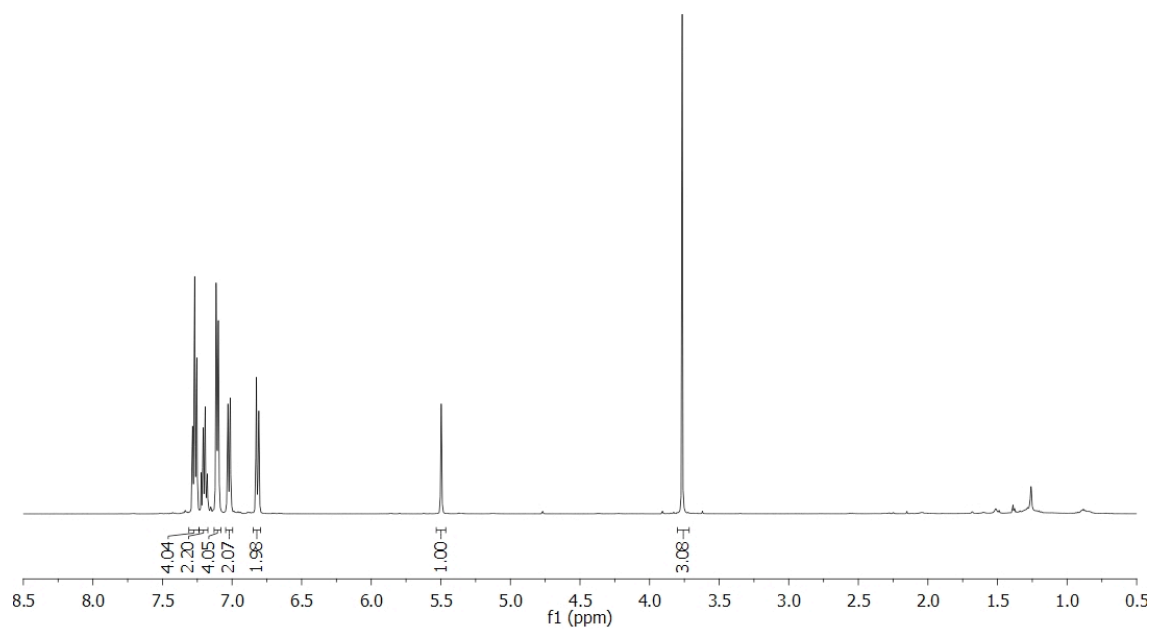
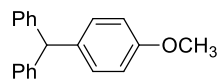


Figure A2.28 500 MHz ^1H and 125 MHz $^{13}\text{C}\{^1\text{H}\}$ NMR of **2.3ai** in CDCl_3

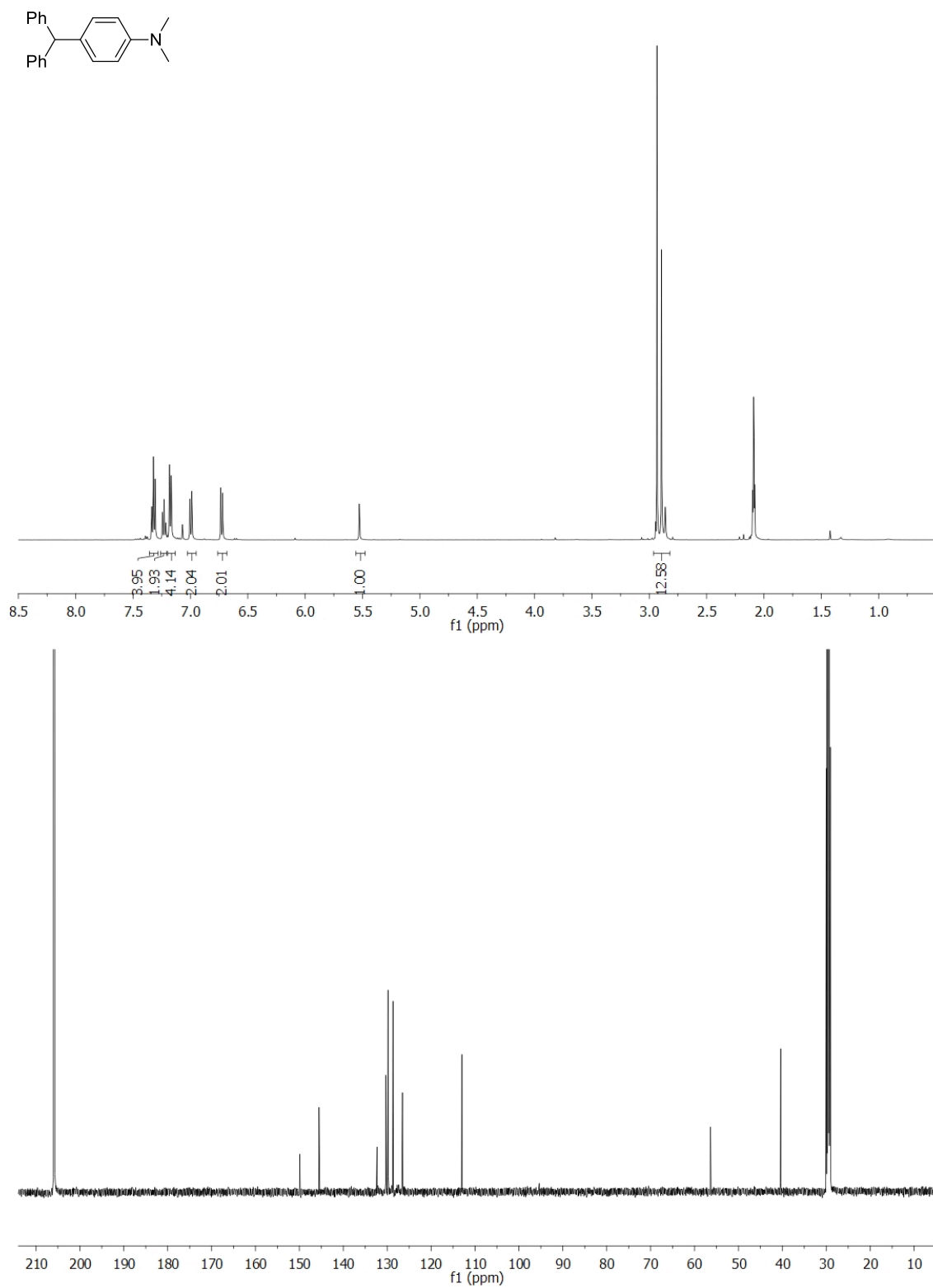


Figure A2.29 500 MHz ^1H and 125 MHz $^{13}\text{C}\{^1\text{H}\}$ NMR of **2.3aj** in acetone- d_6

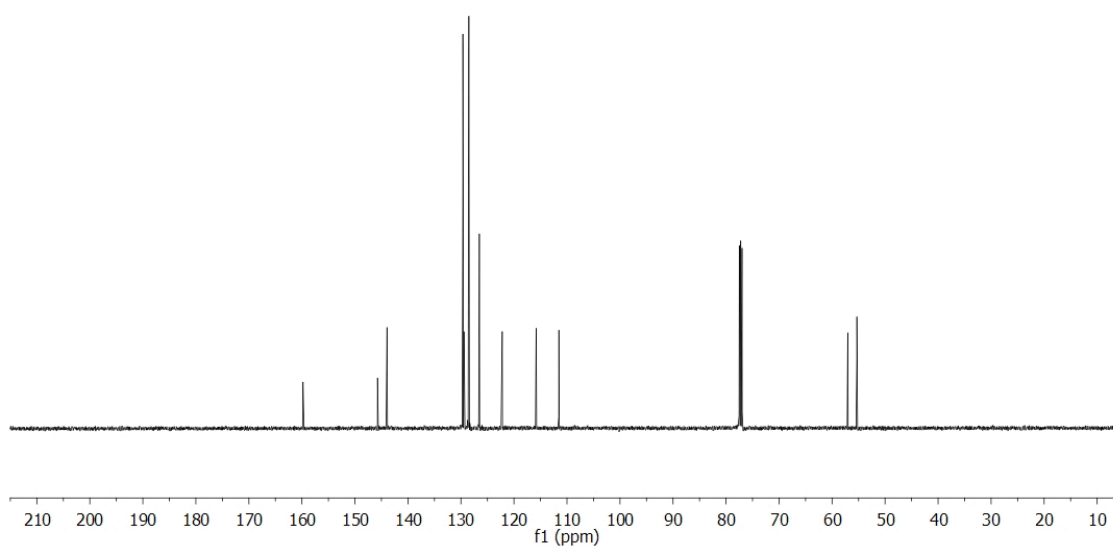
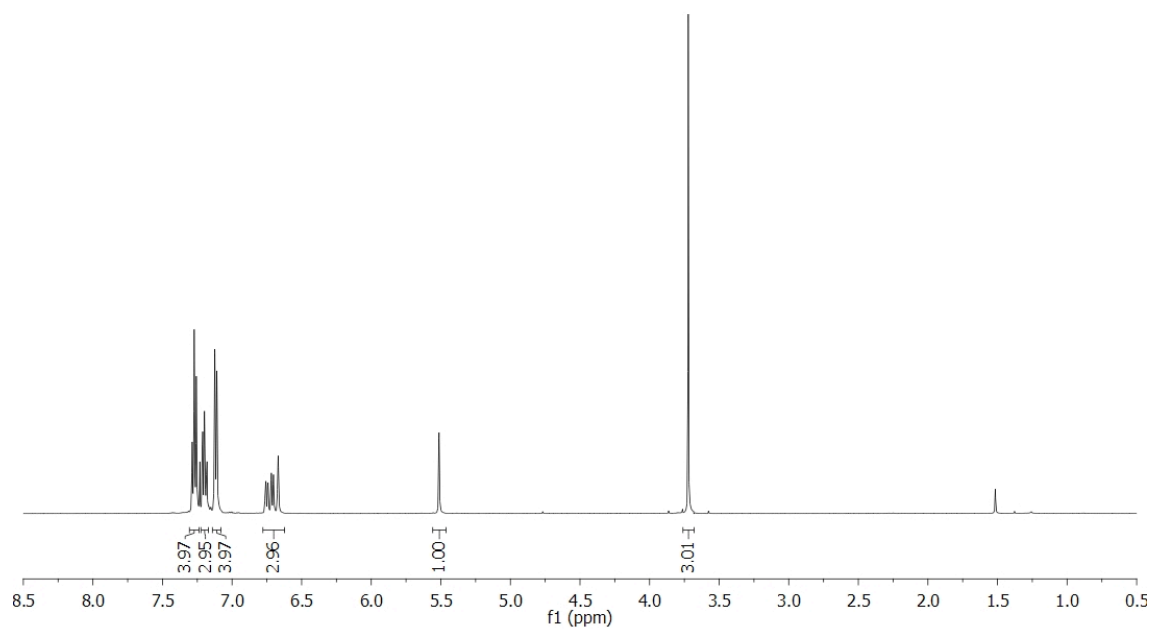
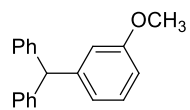


Figure A2.30 500 MHz ^1H and 125 MHz $^{13}\text{C}\{^1\text{H}\}$ NMR of **2.3ak** in CDCl_3

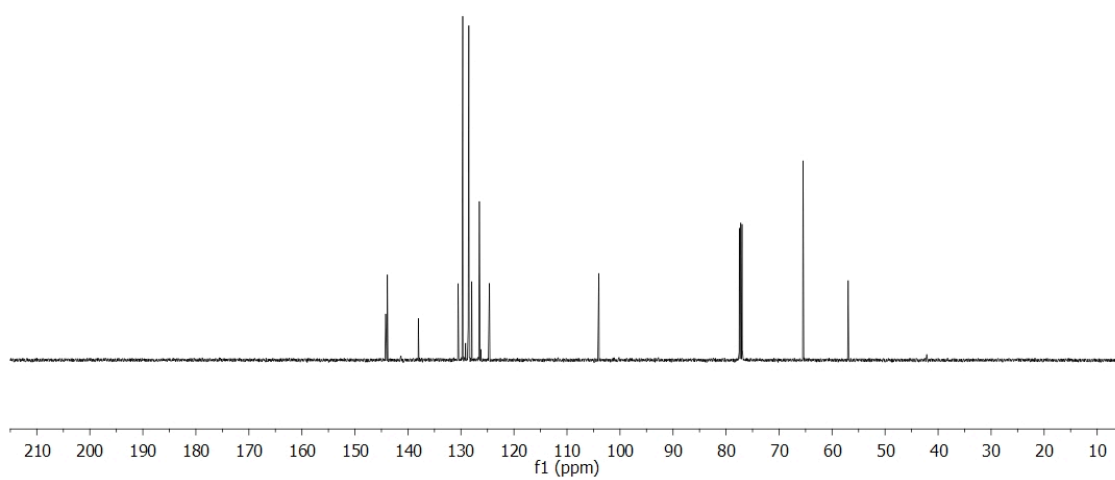
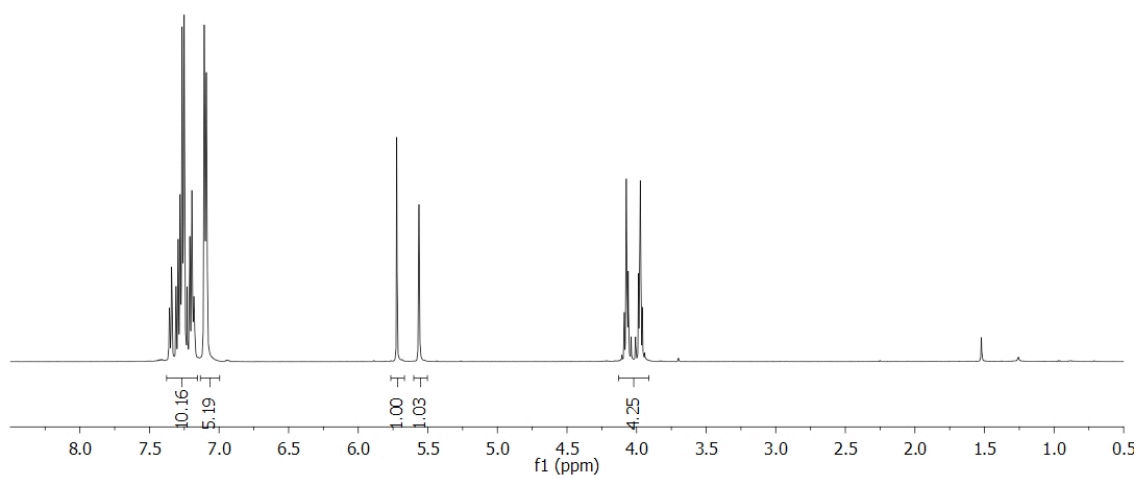
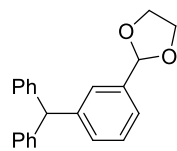


Figure A2.31 500 MHz ¹H and 125 MHz ¹³C{¹H} NMR of **2.3aI** in CDCl₃

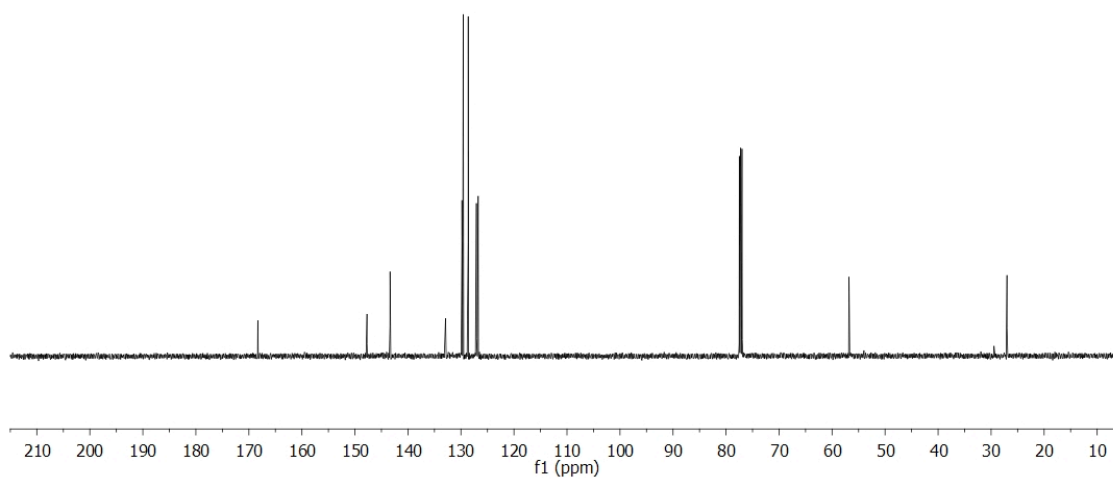
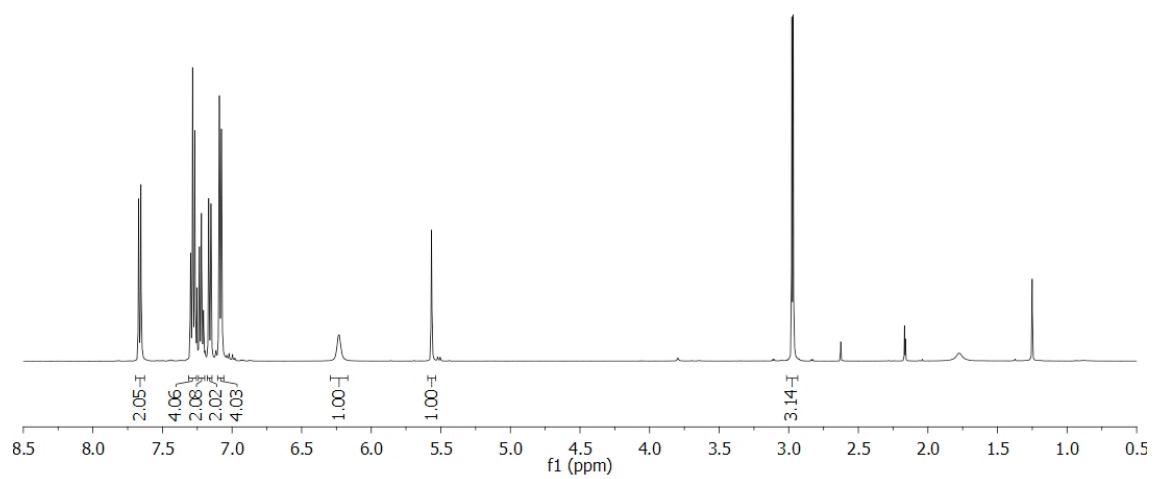
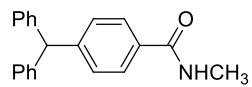


Figure A2.32 500 MHz ^1H and 125 MHz $^{13}\text{C}\{^1\text{H}\}$ NMR of **2.3am** in CDCl_3

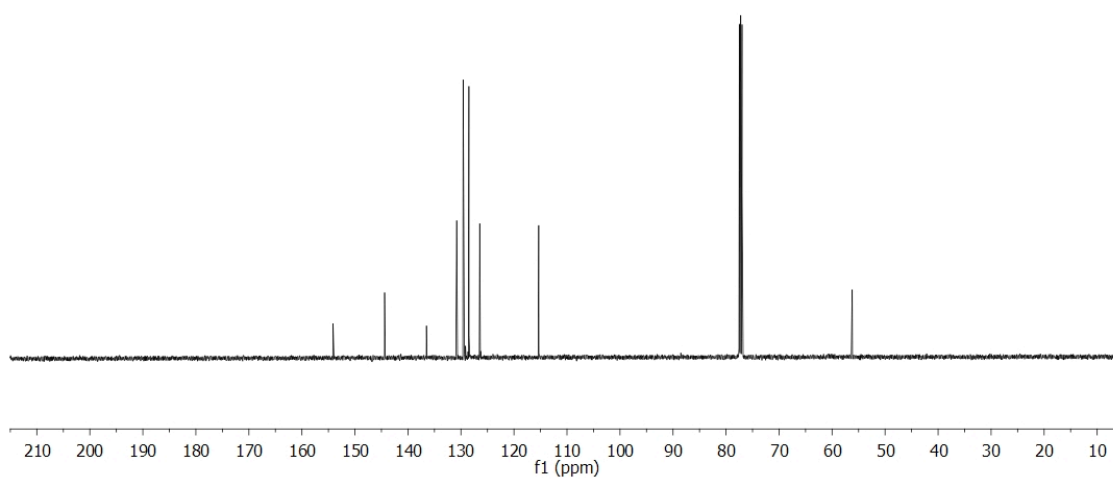
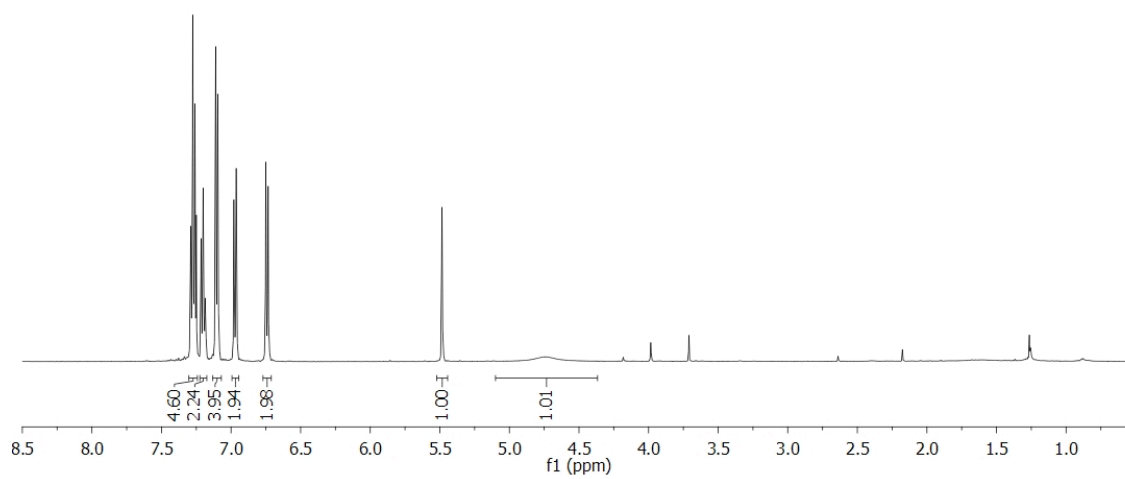
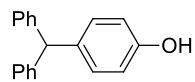


Figure A2.33 500 MHz ¹H and 125 MHz ¹³C{¹H} NMR of **2.3an** in CDCl₃

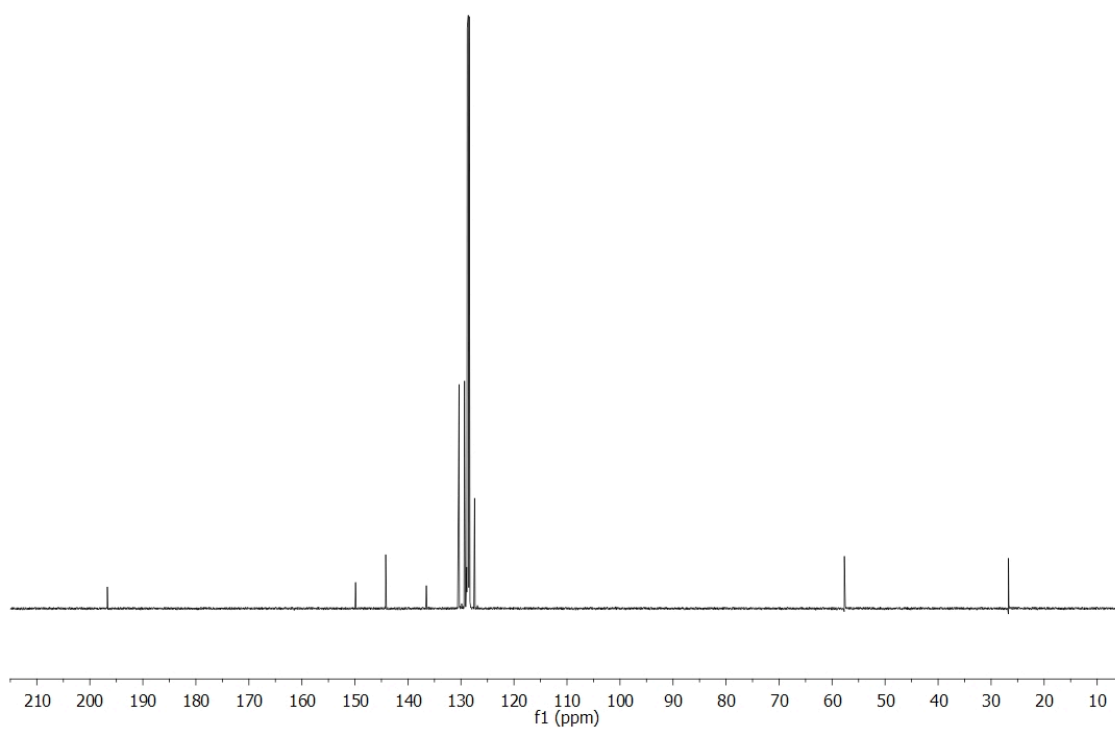
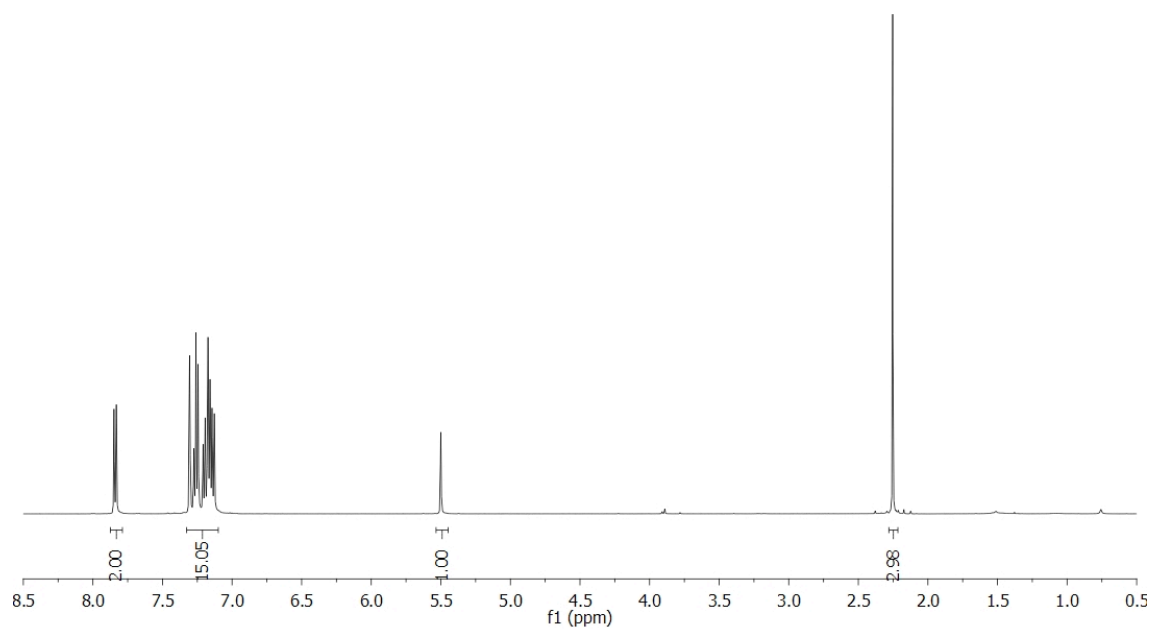
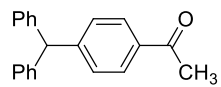


Figure A2.34 500 MHz ^1H and 125 MHz $^{13}\text{C}\{^1\text{H}\}$ NMR of **2.3ao** in C_6D_6

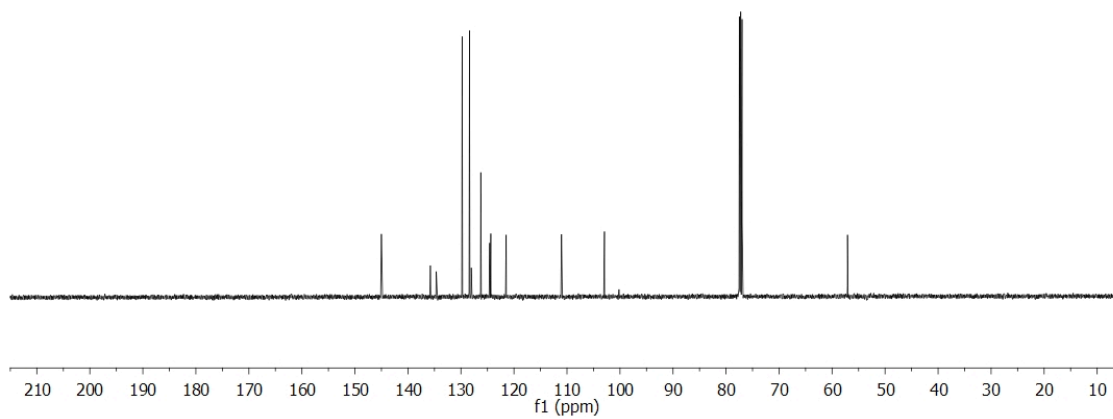
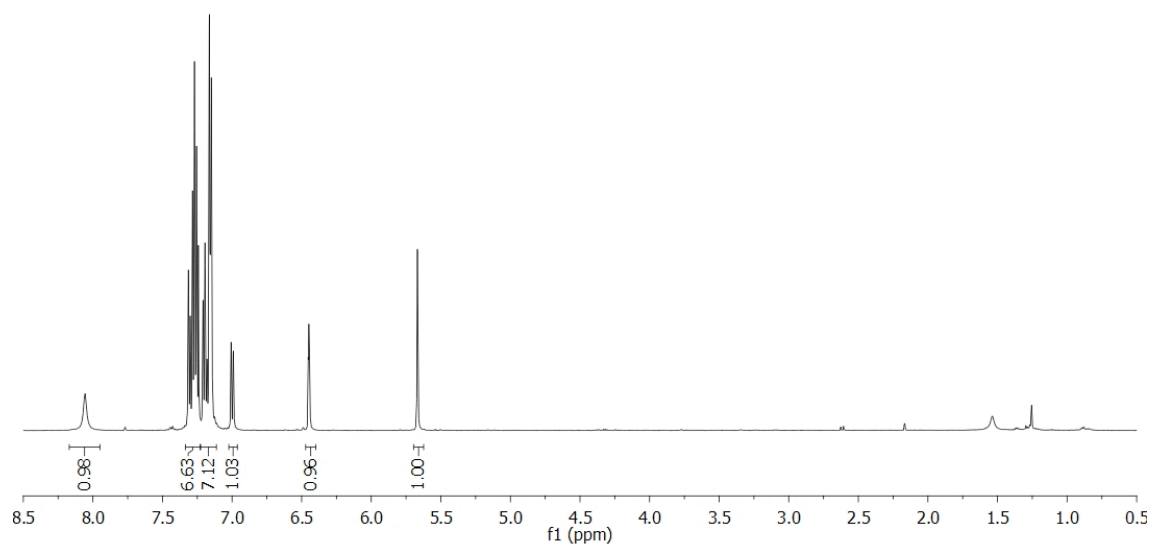
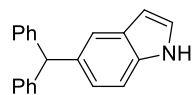


Figure A2.35 500 MHz ^1H and 125 MHz $^{13}\text{C}\{^1\text{H}\}$ NMR of **2.3ap** in CDCl_3

Appendix A3. NMR Spectra Relevant to Chapter 3

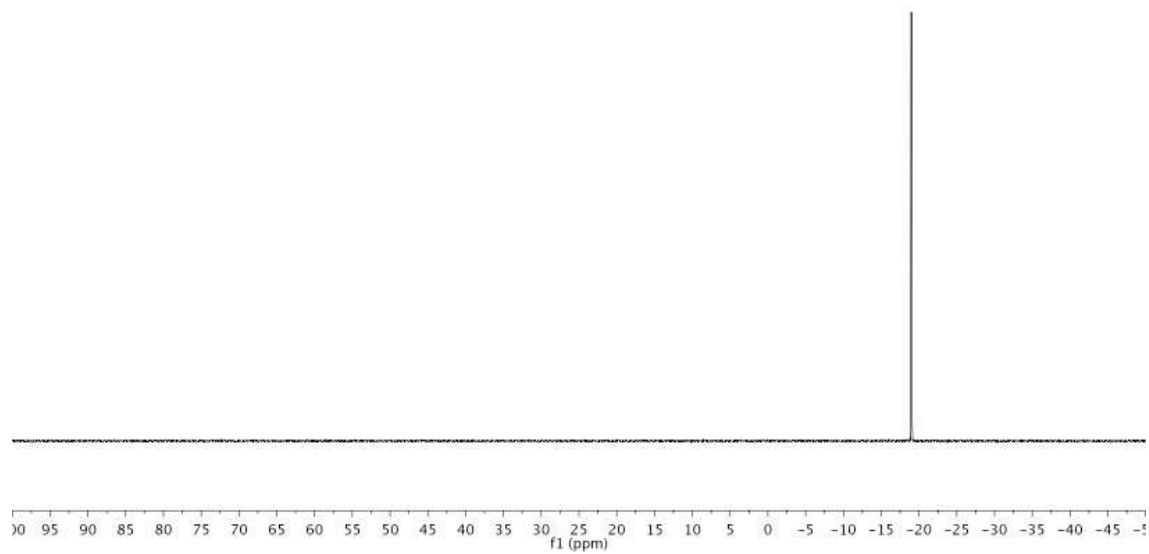
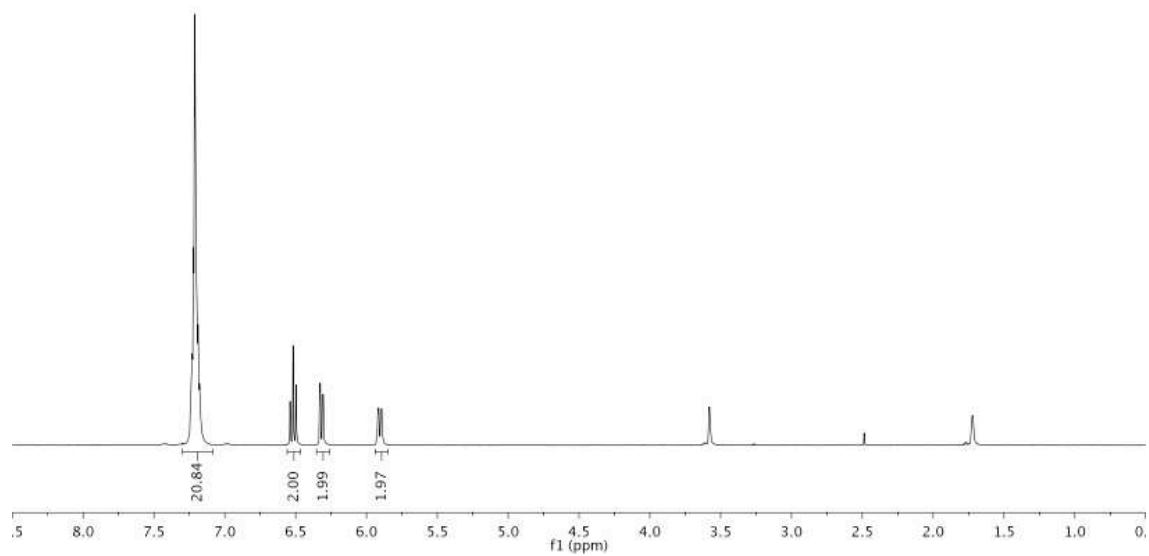


Figure A3.1 500 MHz ¹H and 145.8 MHz ³¹P{¹H} NMR of NiXantphos in THF-d₈
355

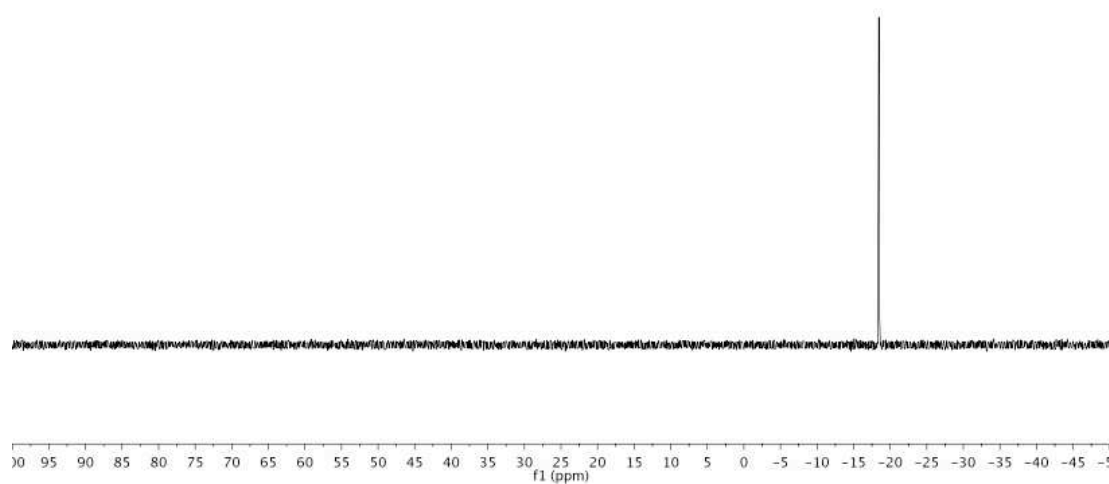
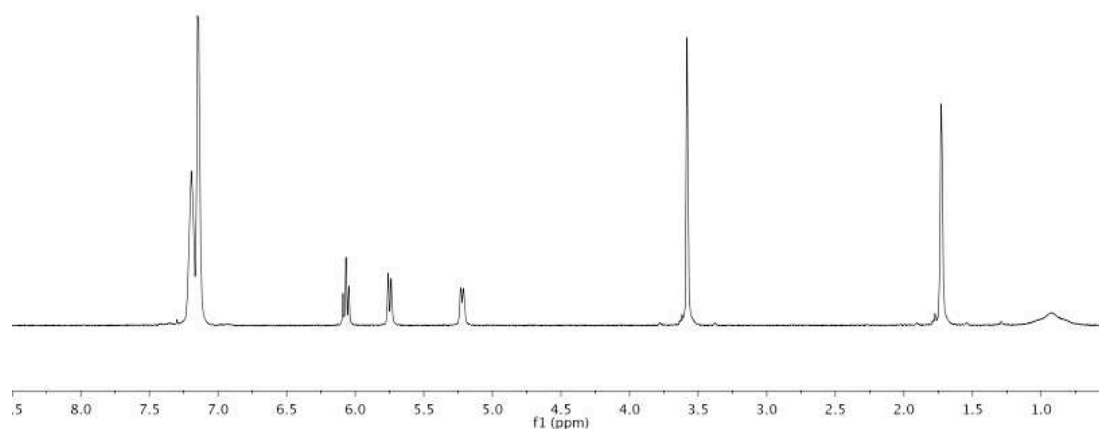


Figure A3.2 500 MHz ^1H and 145.8 MHz $^{31}\text{P}\{^1\text{H}\}$ NMR of NiXantphos with 1.5 equiv $\text{LiN}(\text{SiMe}_3)_2$ in THF-d_8

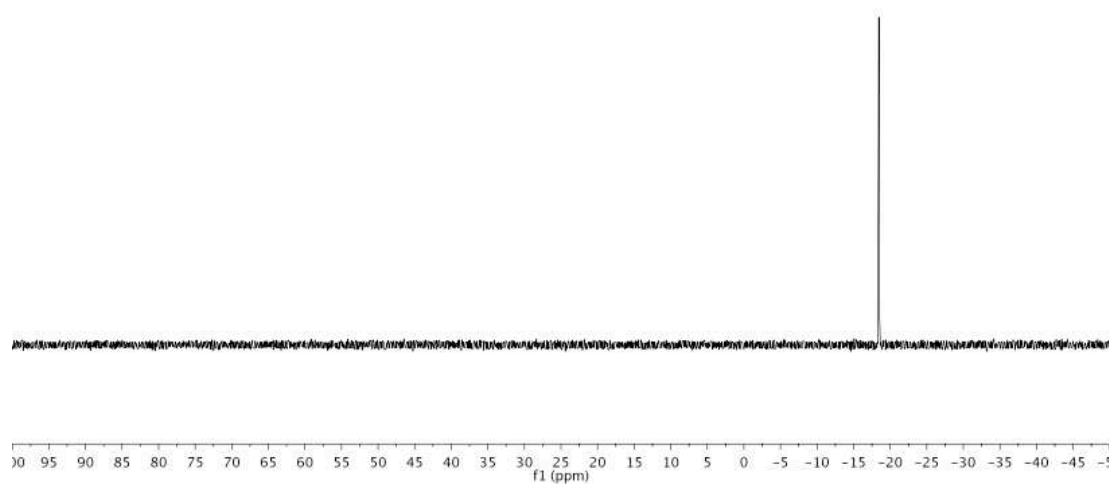
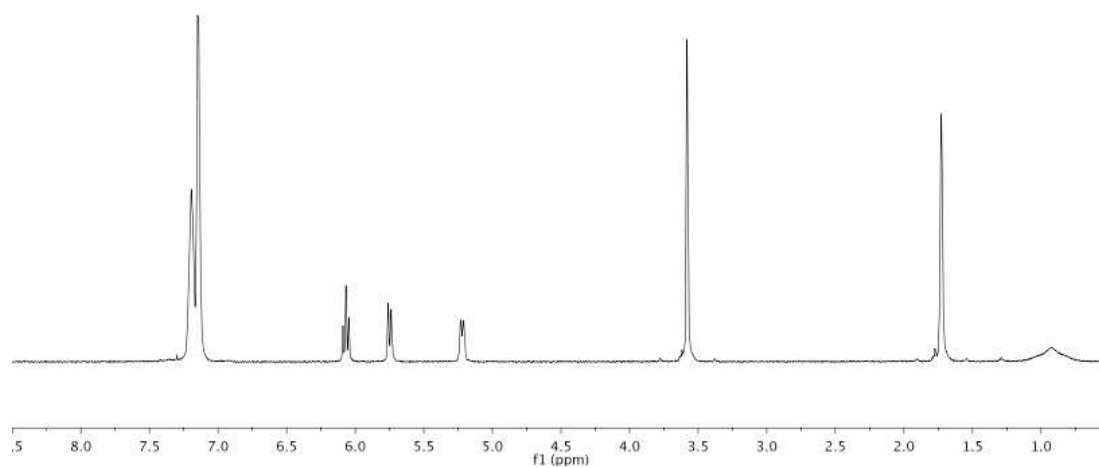


Figure A3.3 500 MHz ^1H and 145.8 MHz $^{31}\text{P}\{^1\text{H}\}$ NMR of NiXantphos with 1.5 equiv $\text{KN}(\text{SiMe}_3)_2$ in THF-d_8

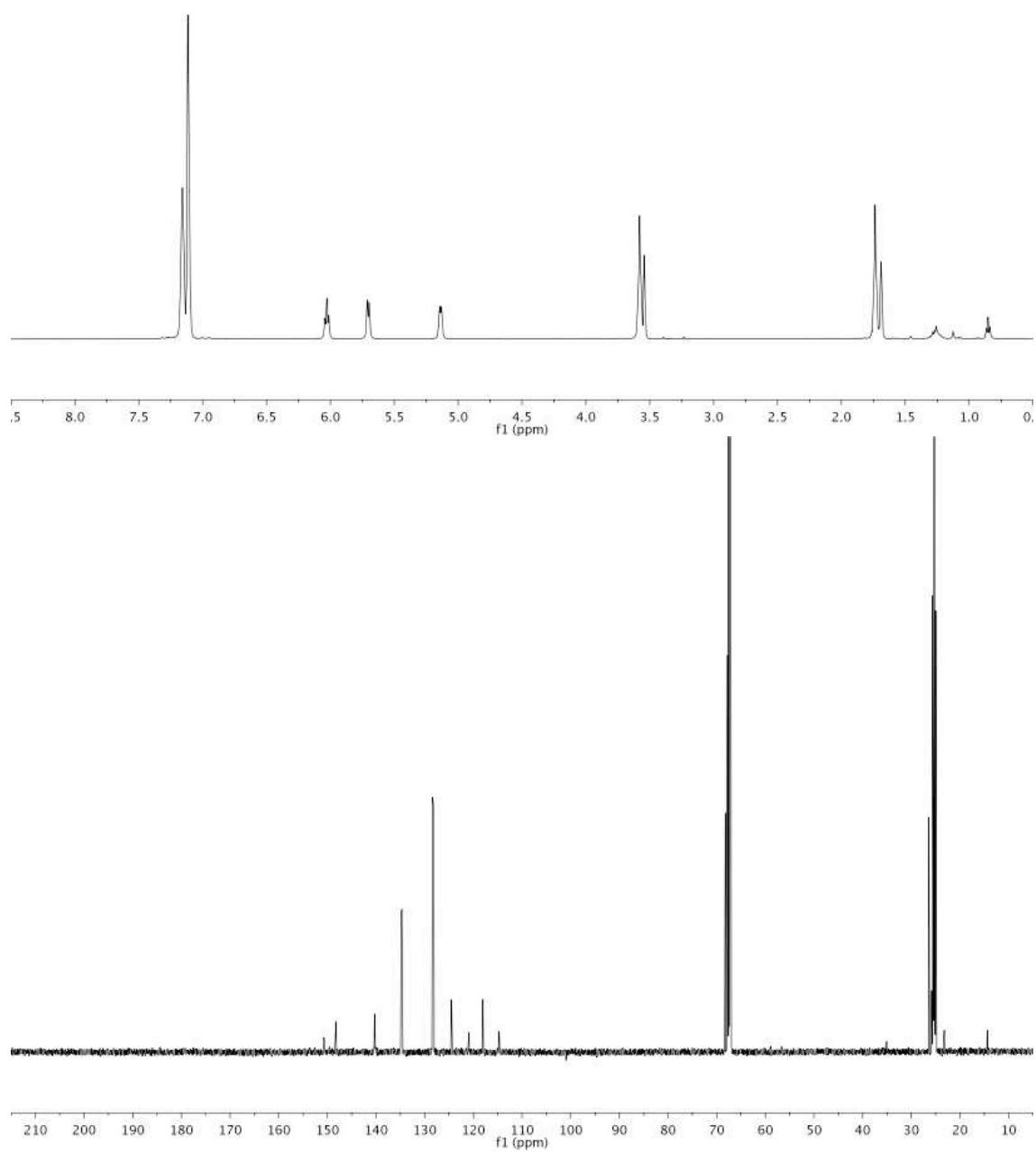


Figure A3.4 500 MHz ¹H and 125 MHz ¹³C{¹H} NMR of K-NiXantphos in THF-d₈

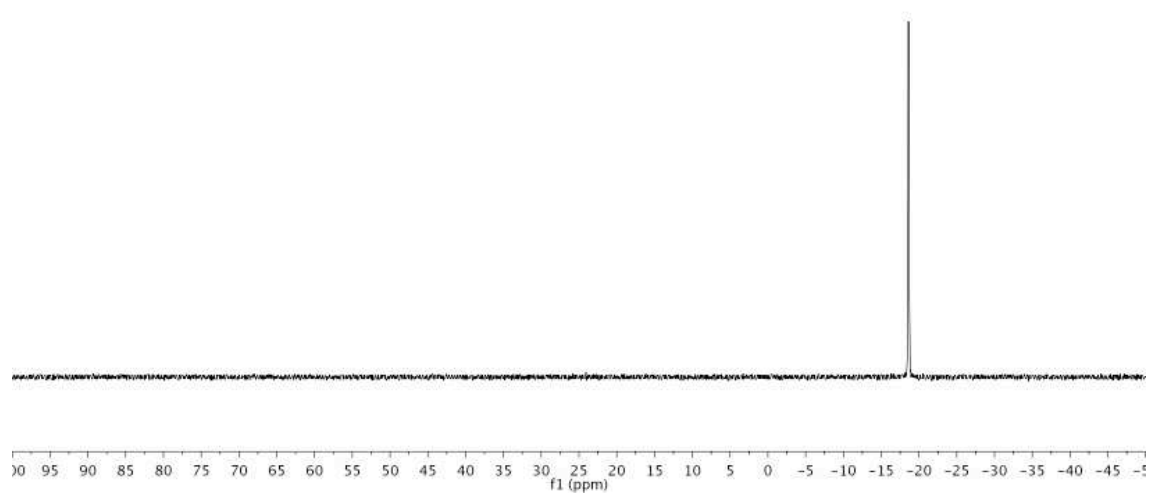


Figure A3.5 145.8 MHz $^{31}\text{P}\{^1\text{H}\}$ NMR of K-NiXantphos in THF- d_8

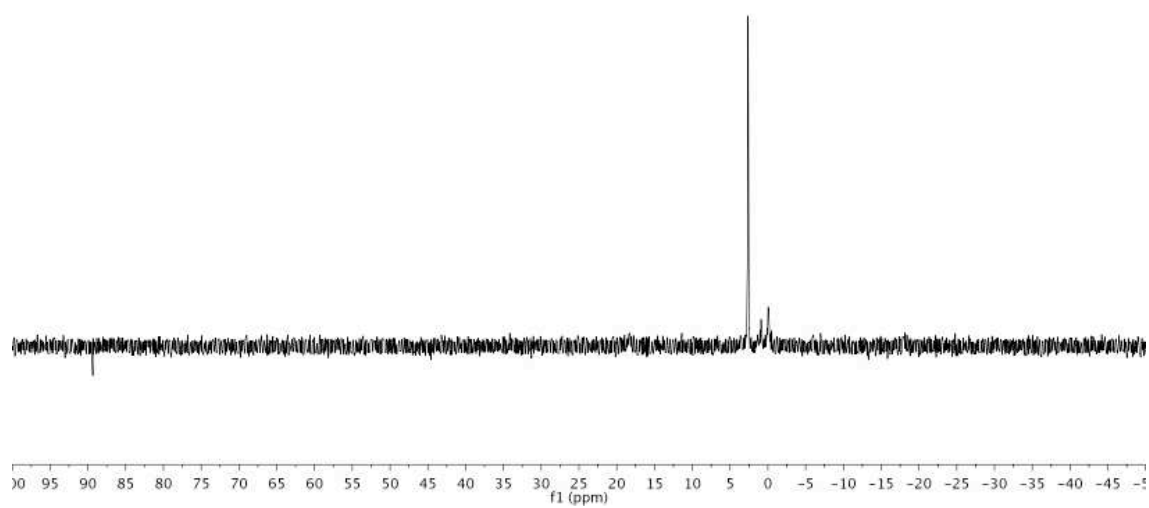


Figure A3.6 145.8 MHz $^{31}\text{P}\{^1\text{H}\}$ NMR of oxidative addition of chlorobenzene to
(Li-NiXantphos)Pd(0) in THF

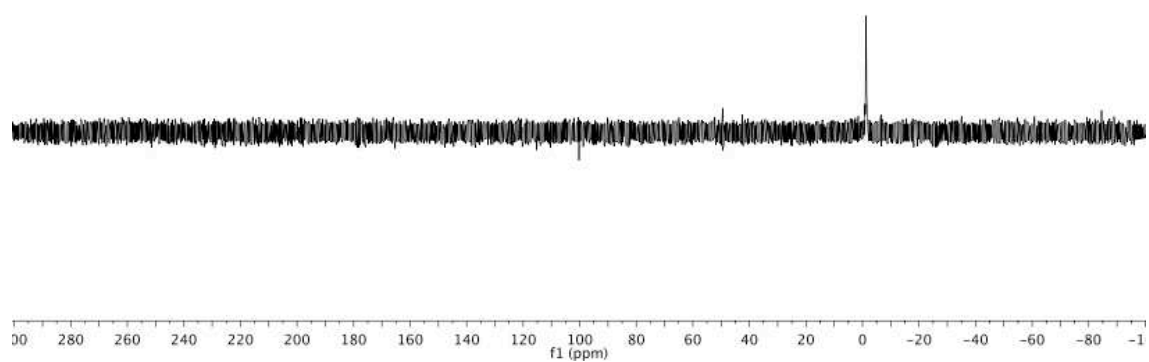
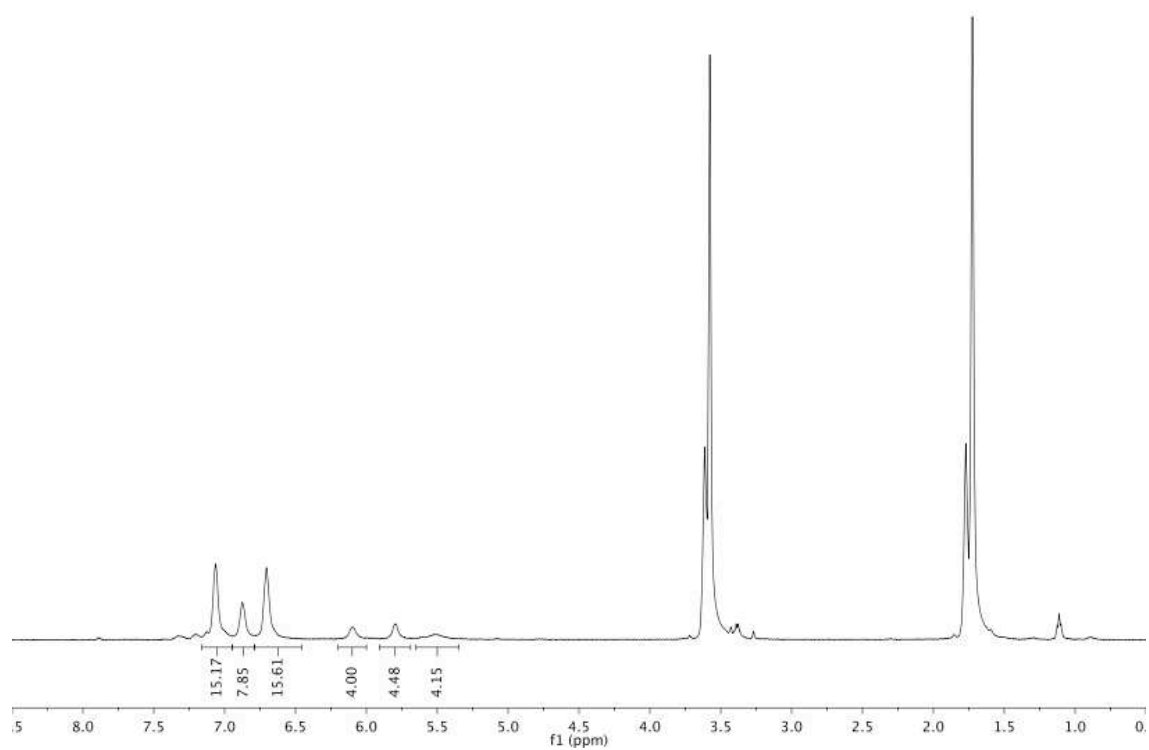


Figure A3.7 500 MHz ^1H and 145.8 MHz $^{31}\text{P}\{^1\text{H}\}$ NMR of $\text{Pd}(\text{K-NiXantphos})_2$ in THF-d_8
361

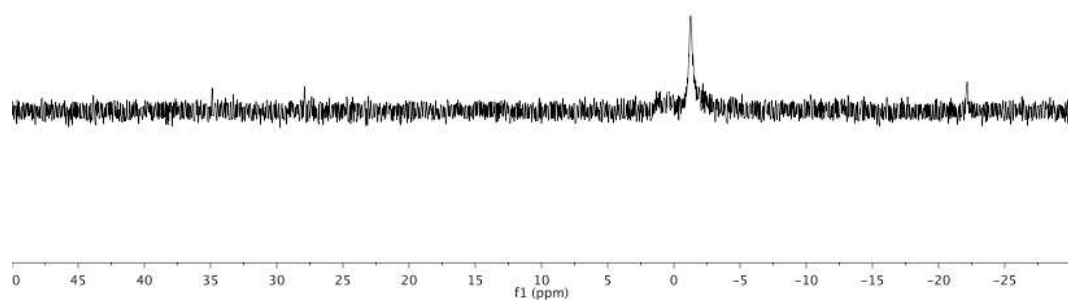
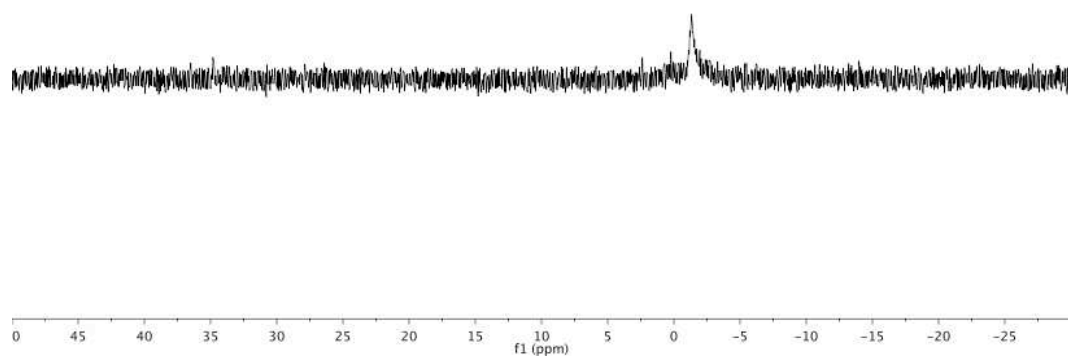


Figure A3.8 145.8 MHz $^{31}\text{P}\{^1\text{H}\}$ NMR of the catalyst resting state in THF after 10 min and 12 h

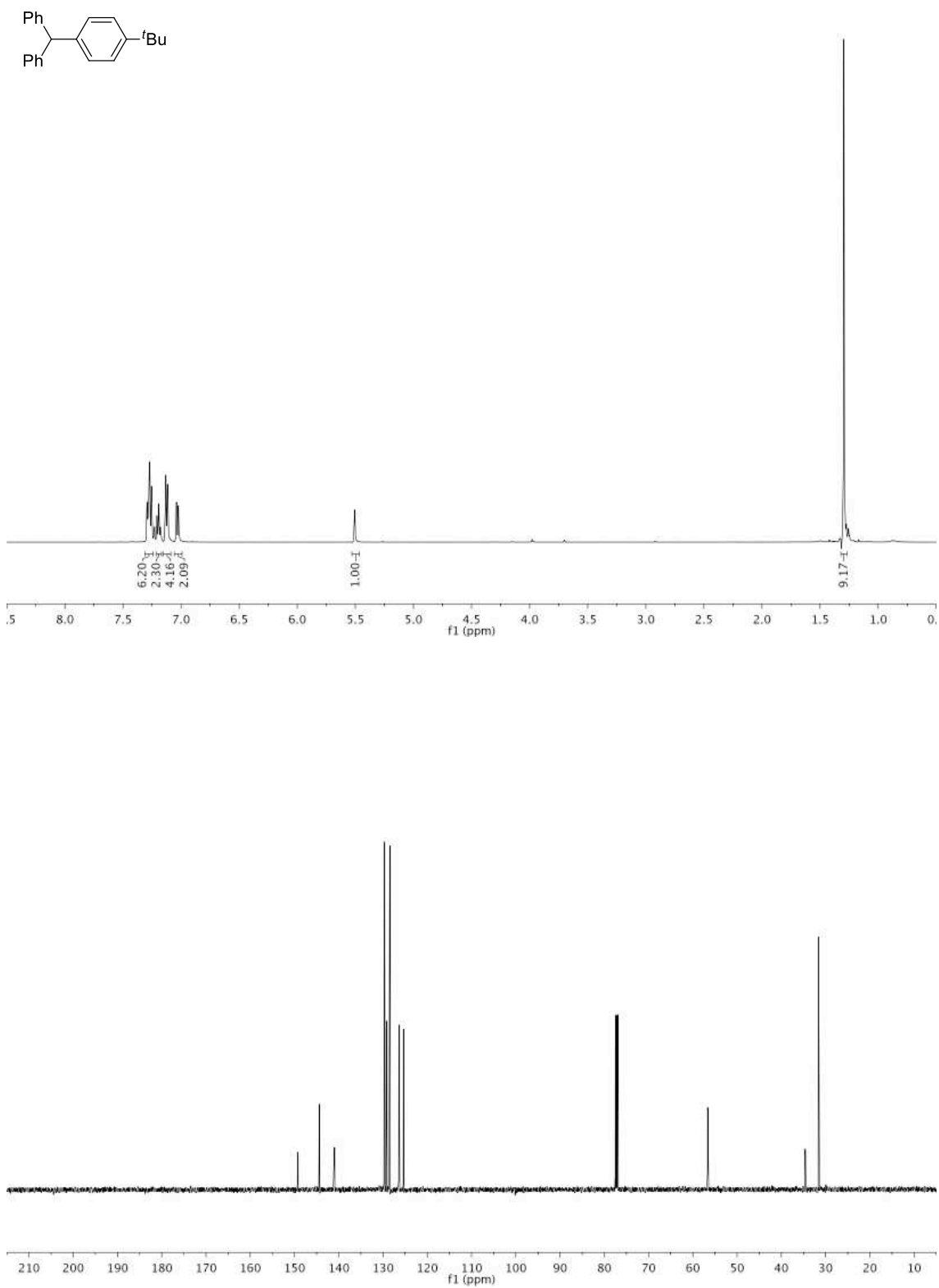


Figure A3.9 500 MHz ^1H and 125 MHz $^{13}\text{C}\{^1\text{H}\}$ NMR of **3.3aa** in CDCl_3

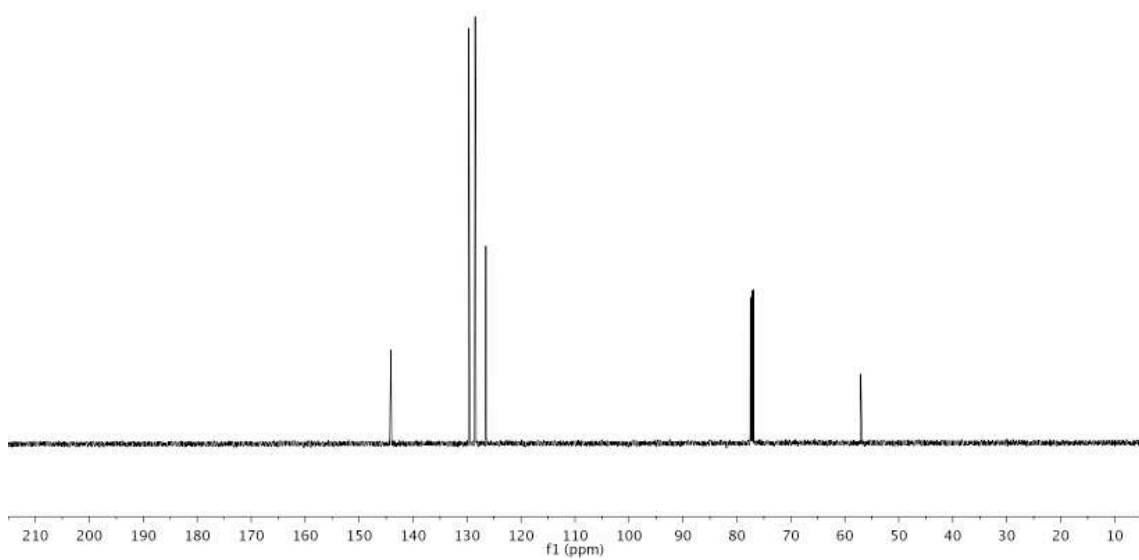
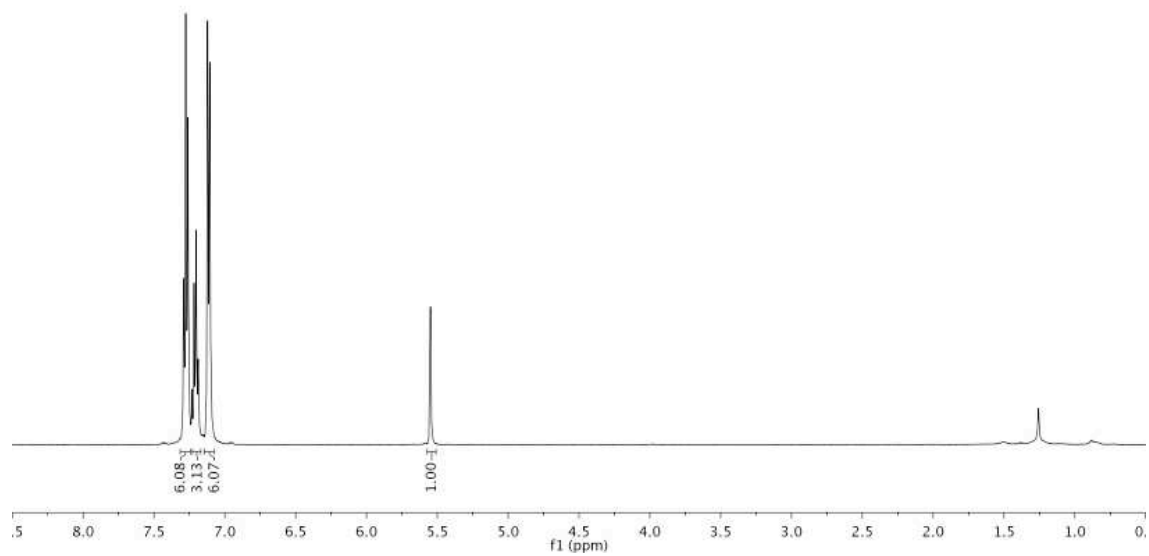
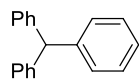


Figure A3.10 500 MHz ^1H and 125 MHz $^{13}\text{C}\{^1\text{H}\}$ NMR of **3.3ab** in CDCl_3

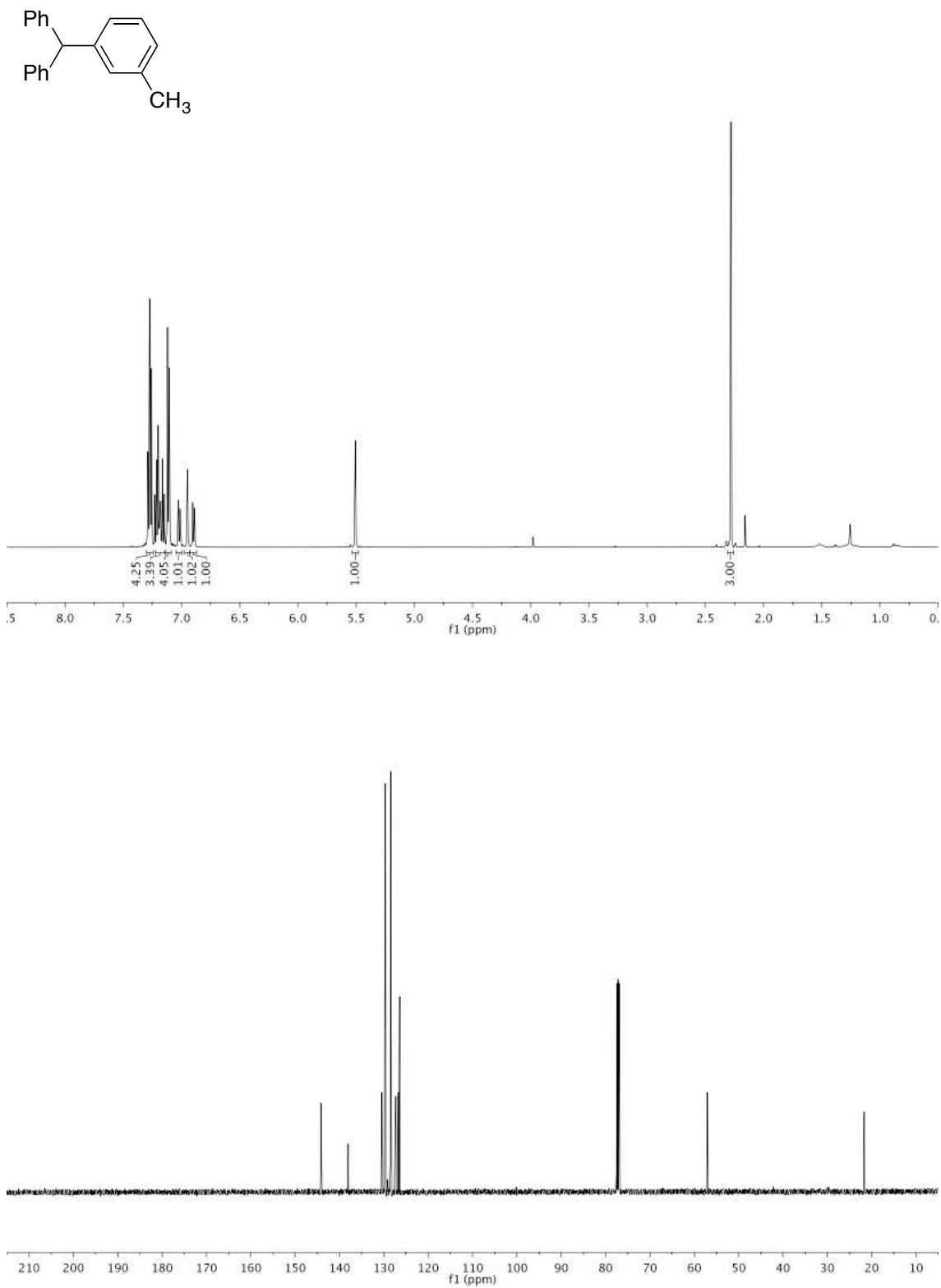


Figure A3.11 500 MHz ^1H and 125 MHz $^{13}\text{C}\{^1\text{H}\}$ NMR of **3.3ac** in CDCl_3

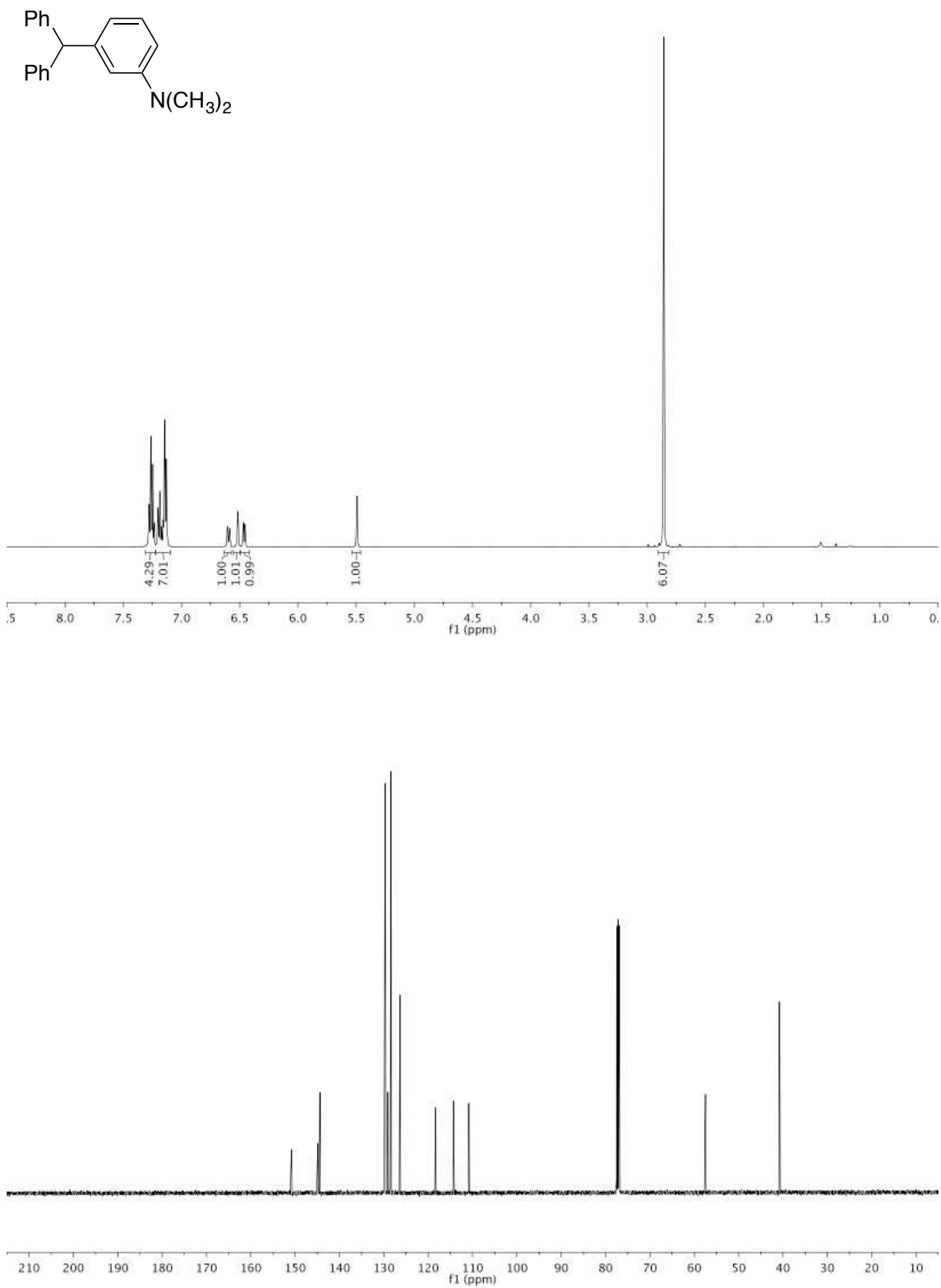


Figure A3.12 500 MHz ^1H and 125 MHz $^{13}\text{C}\{^1\text{H}\}$ NMR of **3.3ad** in CDCl_3

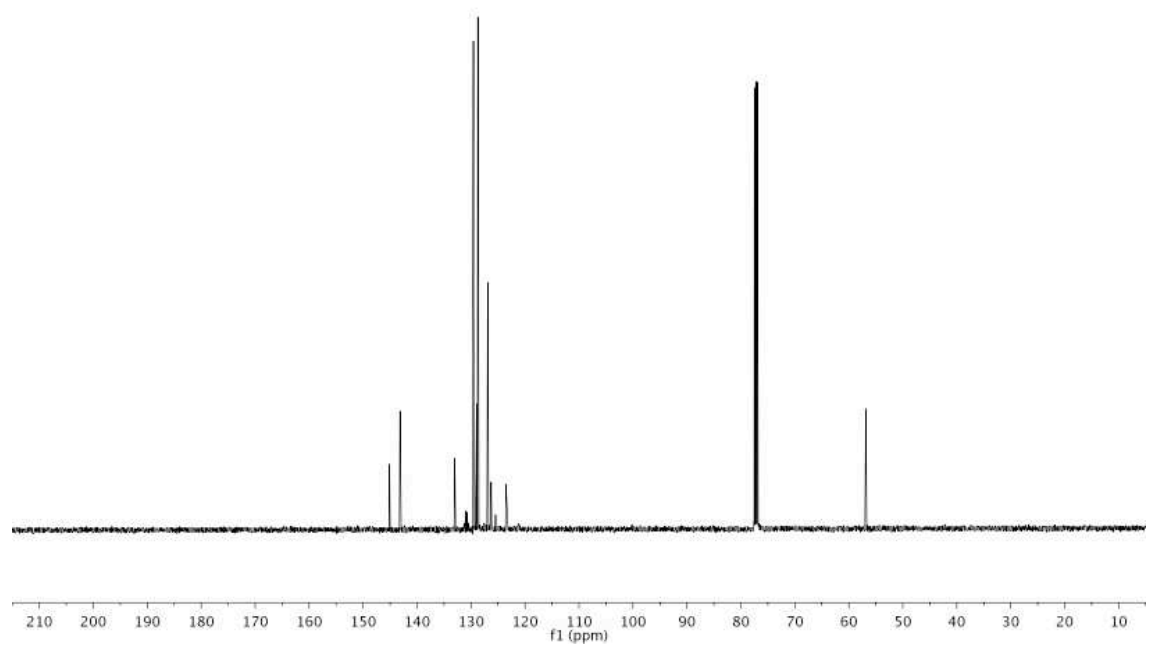
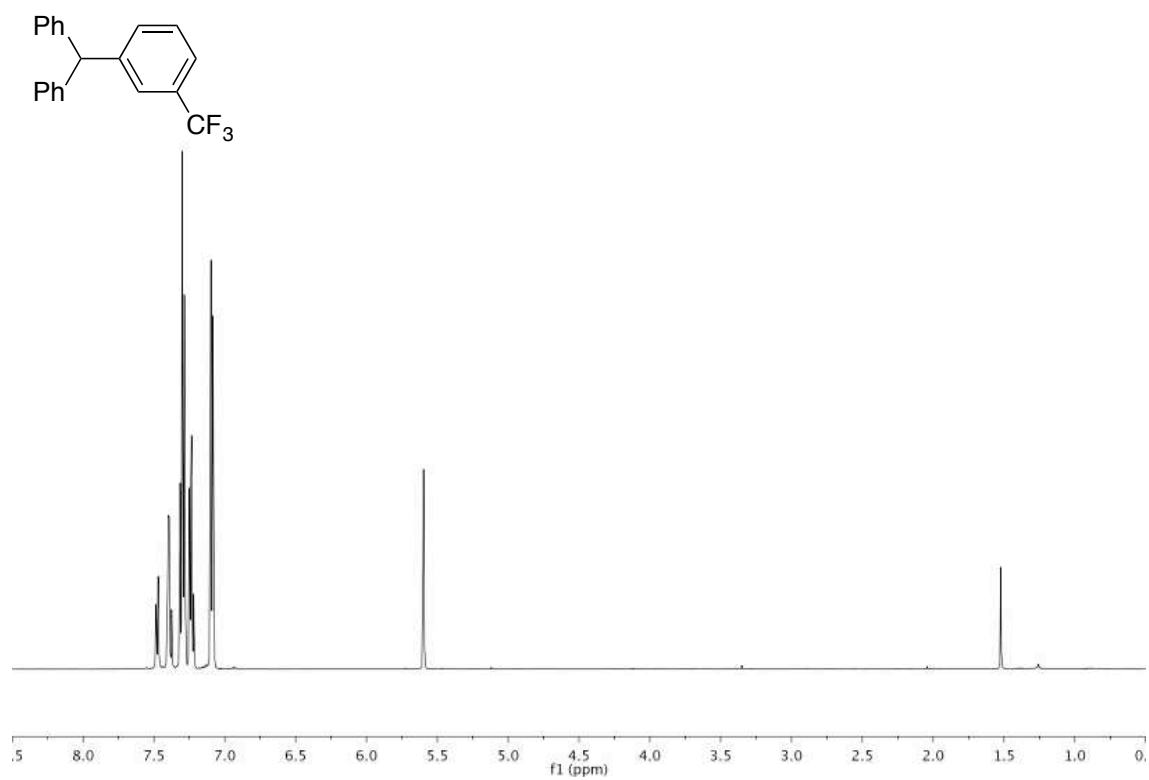


Figure A3.13 500 MHz ¹H and 125 MHz ¹³C{¹H} NMR of **3.3ae** in CDCl₃

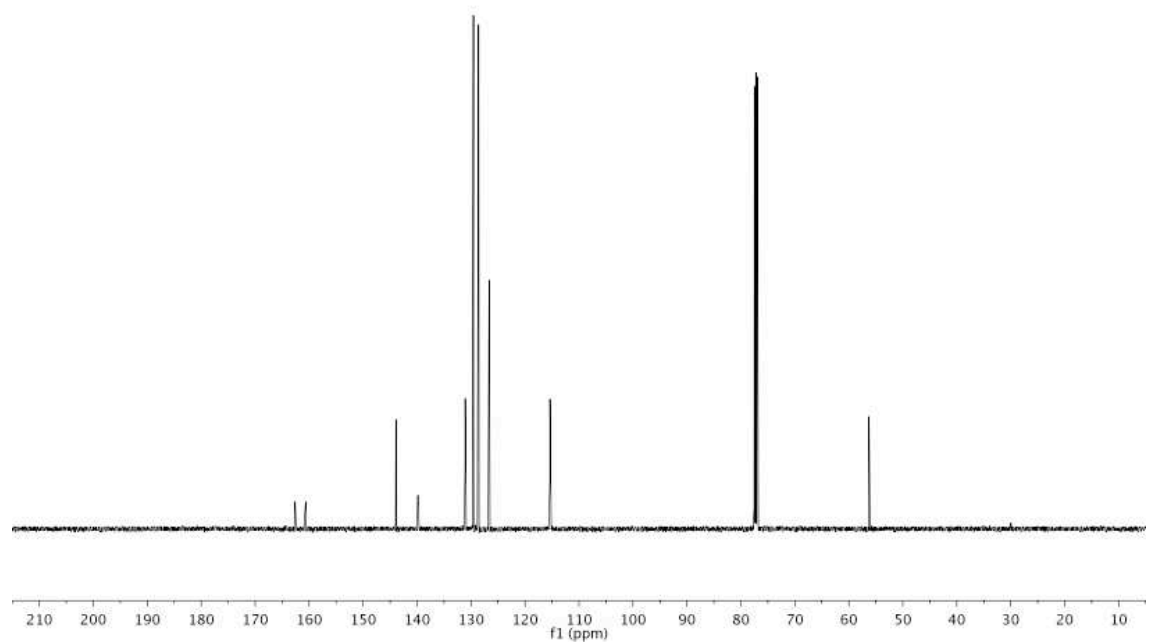
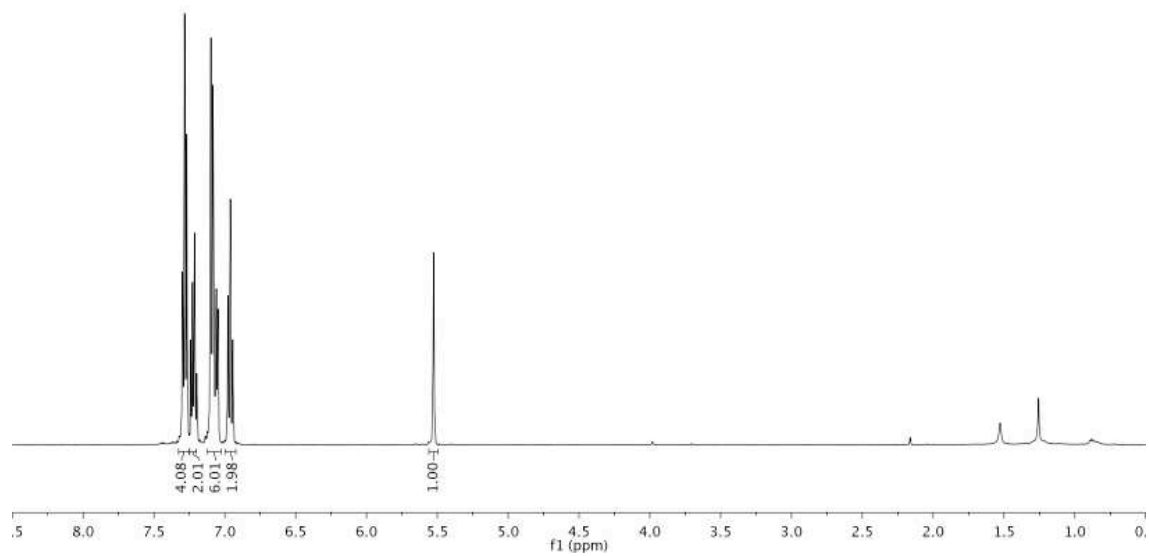
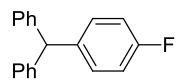


Figure A3.14 500 MHz ^1H and 125 MHz $^{13}\text{C}\{^1\text{H}\}$ NMR of **3.3af** in CDCl_3

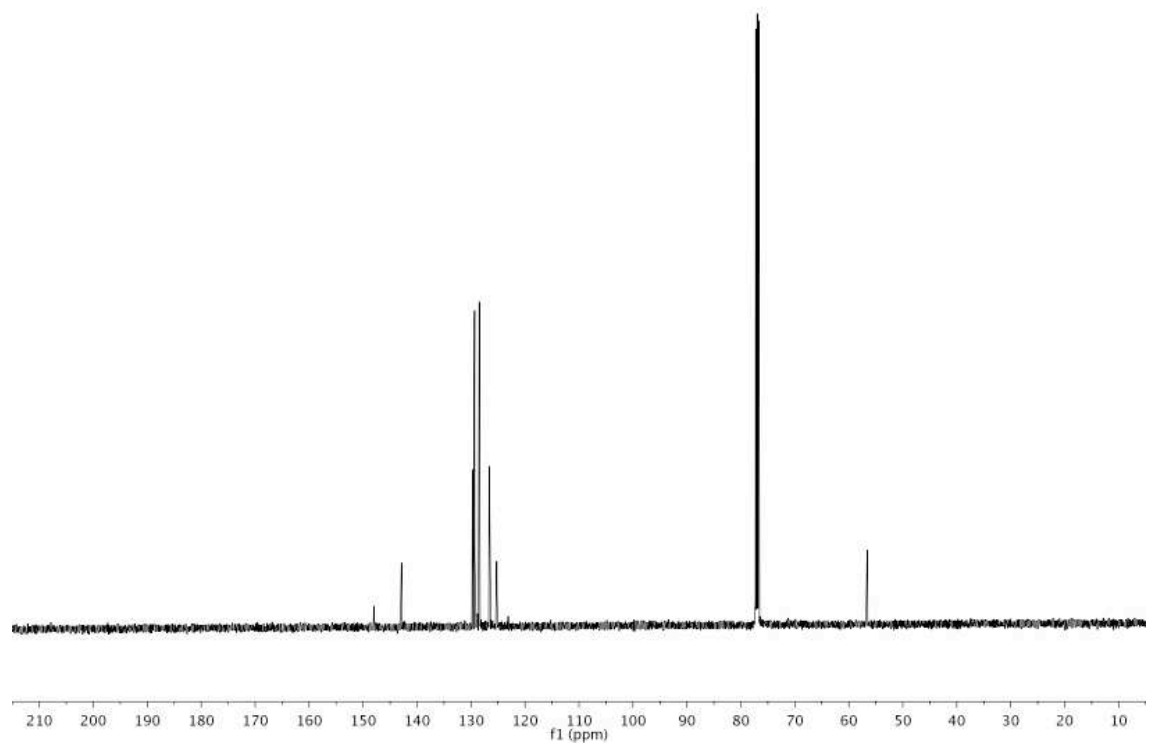
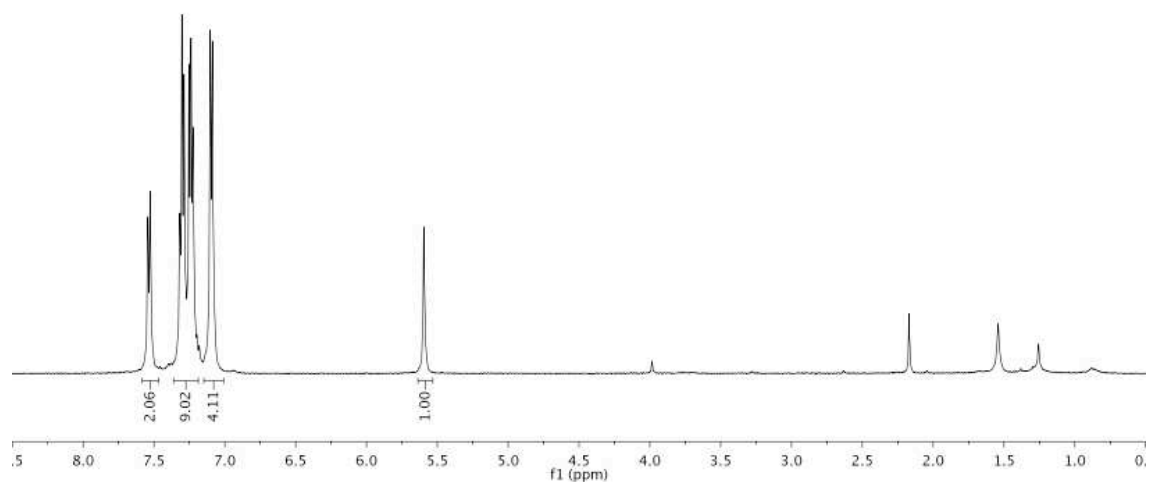
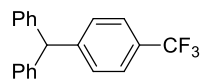


Figure A3.15 500 MHz ^1H and 125 MHz $^{13}\text{C}\{^1\text{H}\}$ NMR of **3.3ag** in CDCl_3

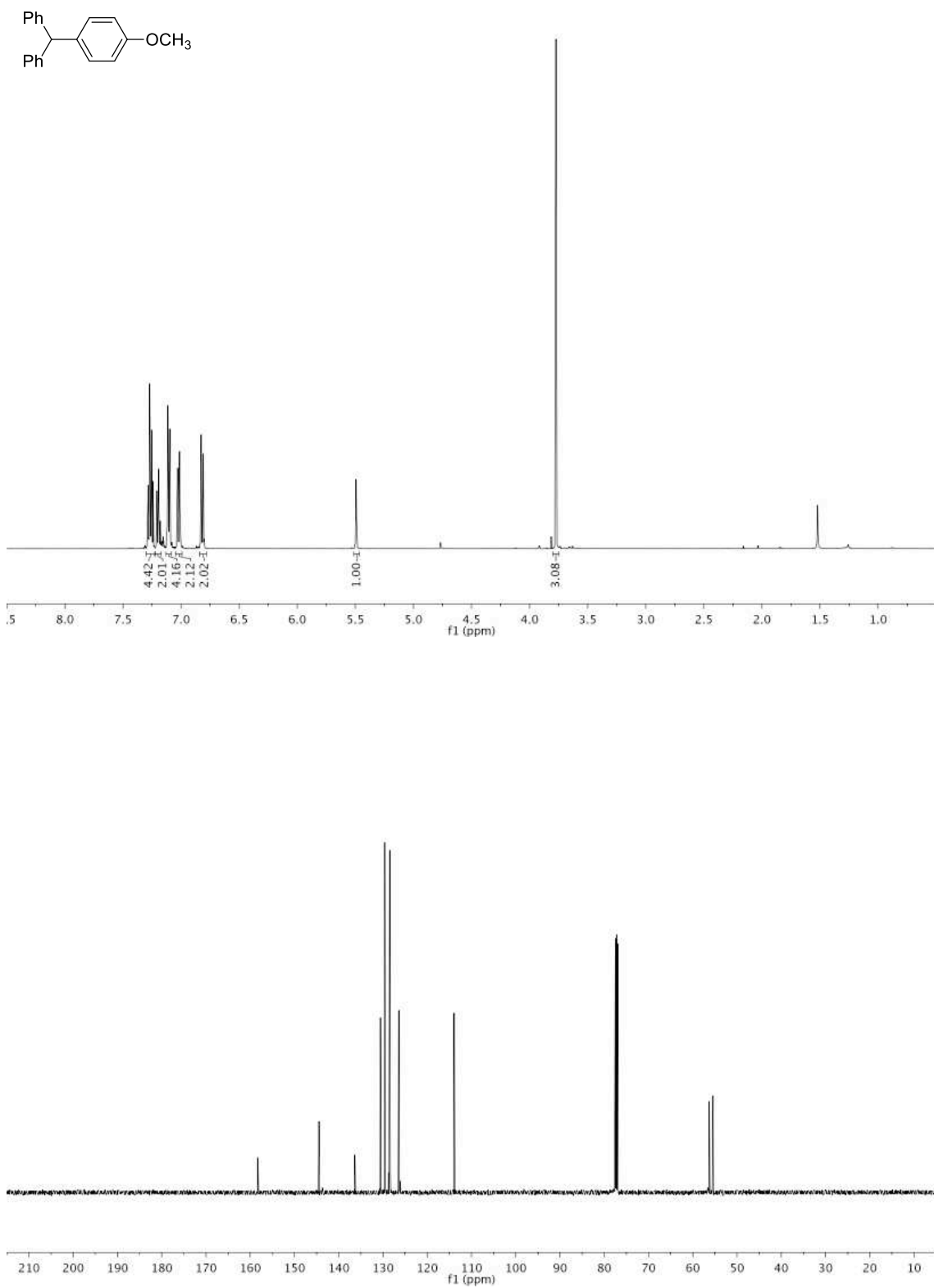


Figure A3.16 500 MHz ^1H and 125 MHz $^{13}\text{C}\{^1\text{H}\}$ NMR of **3.3ah** in CDCl_3

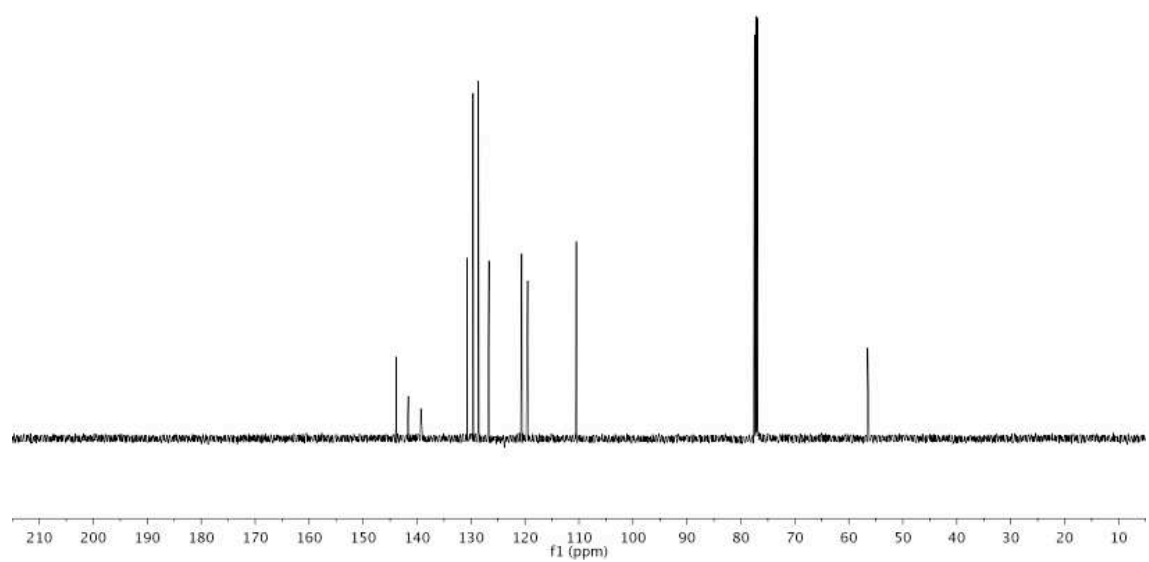
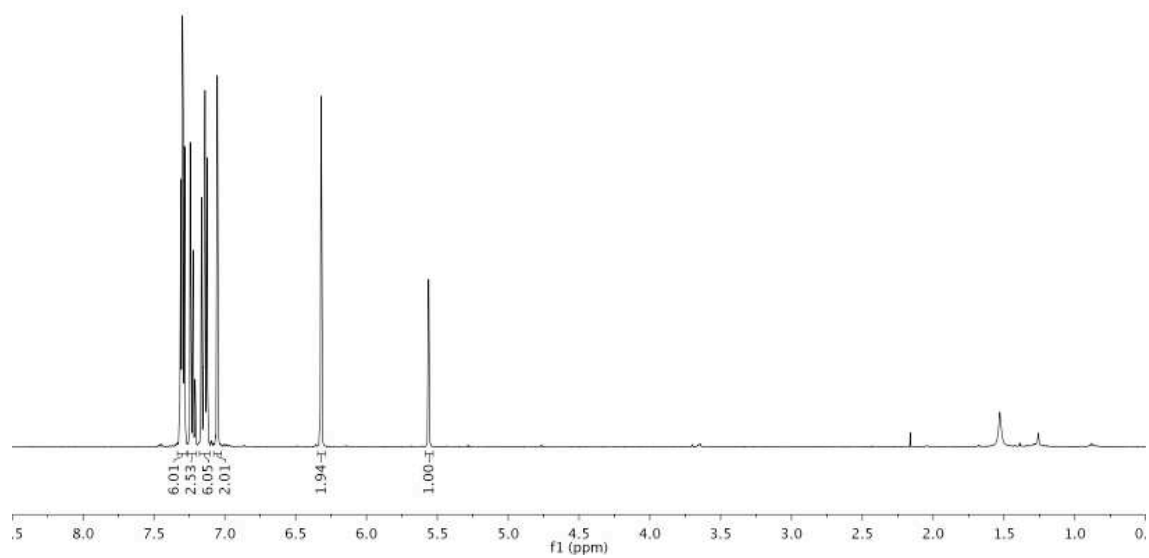
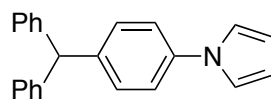


Figure A3.17 500 MHz ^1H and 125 MHz $^{13}\text{C}\{^1\text{H}\}$ NMR of **3.3ai** in CDCl_3

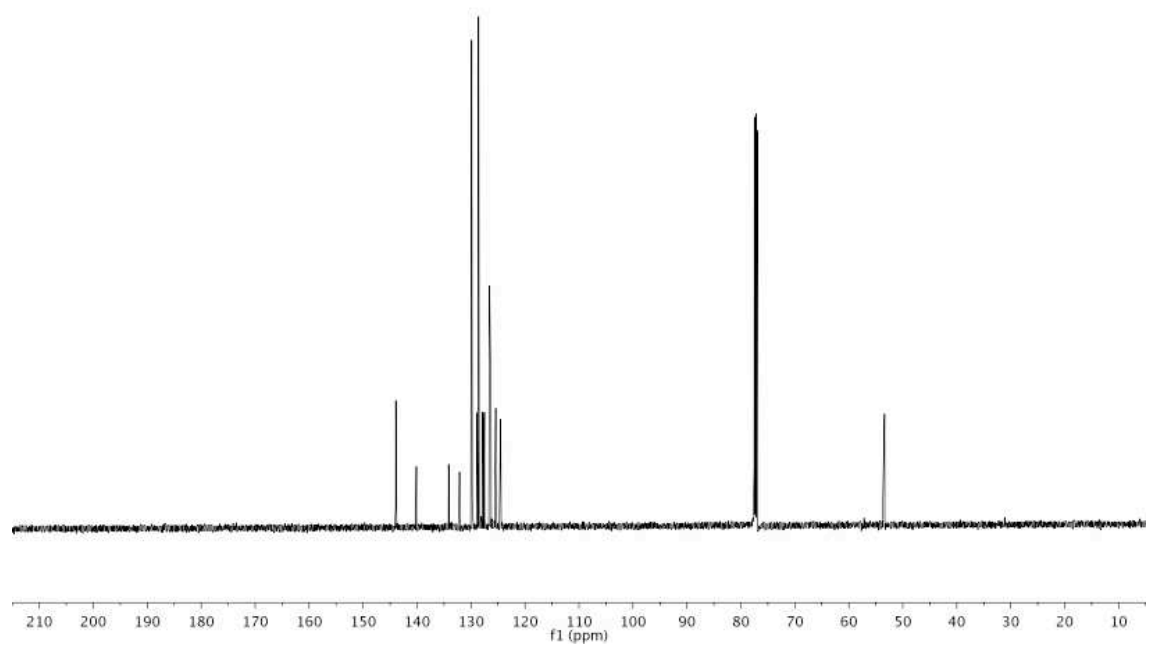
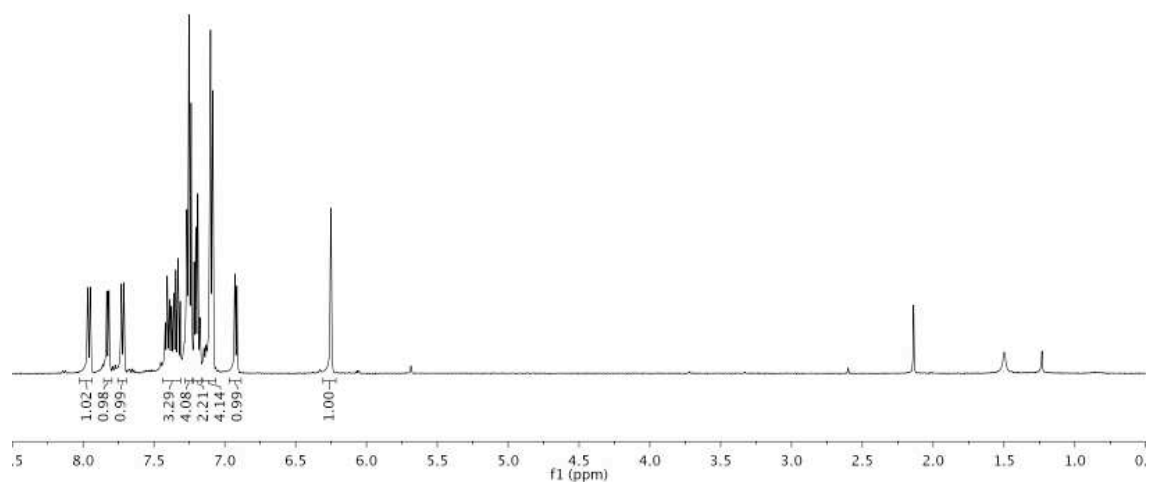
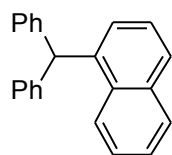


Figure A3.18 500 MHz ^1H and 125 MHz $^{13}\text{C}\{^1\text{H}\}$ NMR of **3.3aj** in CDCl_3

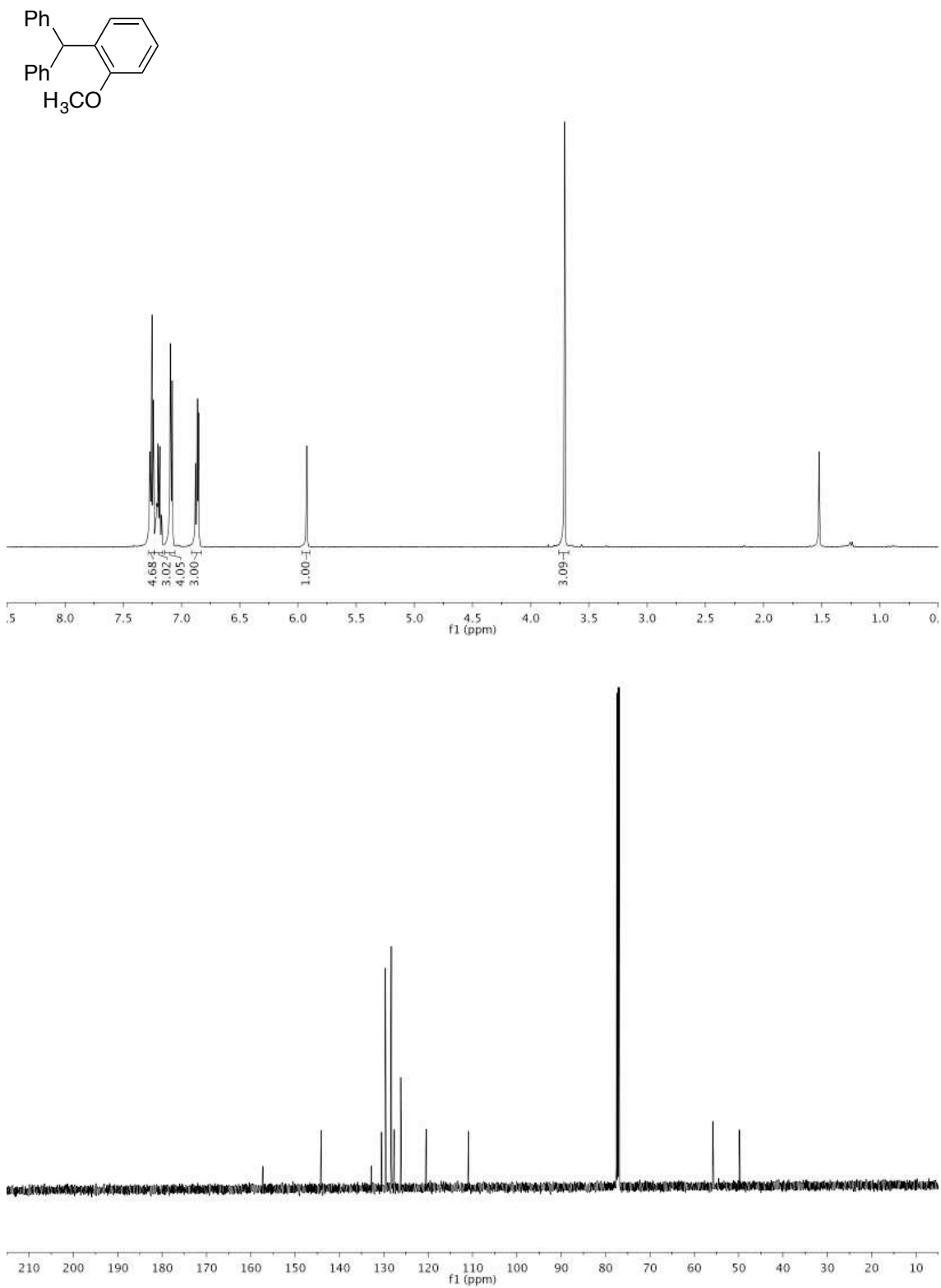


Figure A3.19 500 MHz ^1H and 125 MHz $^{13}\text{C}\{^1\text{H}\}$ NMR of **3.3ak** in CDCl_3

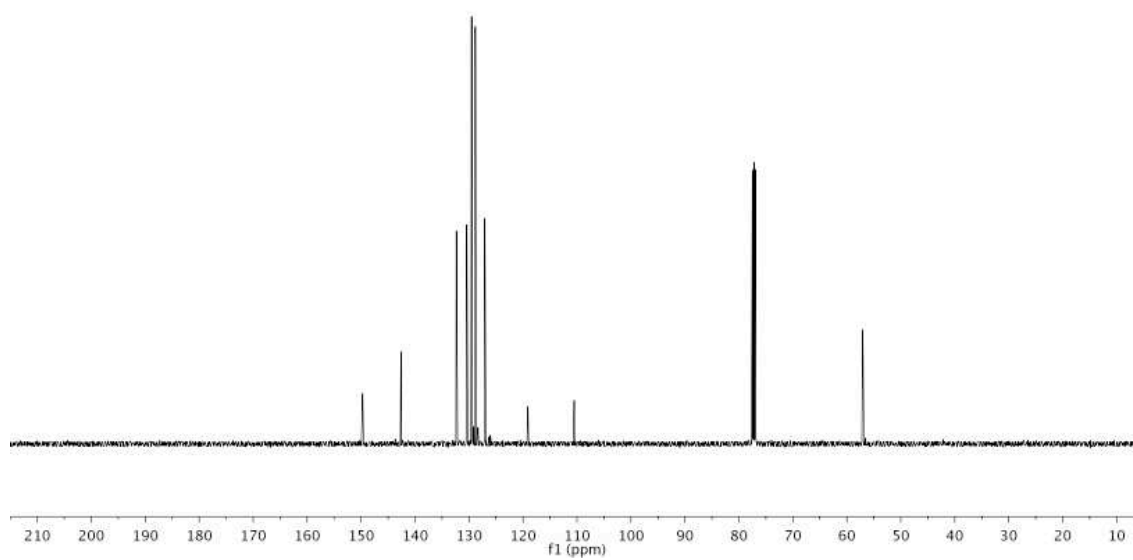
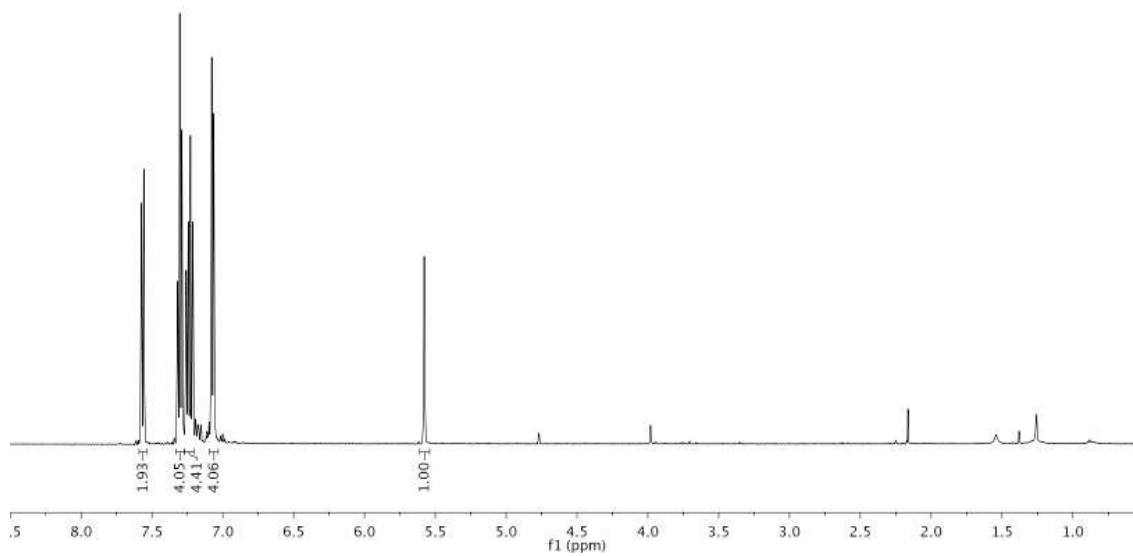
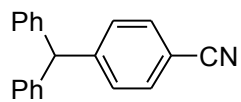


Figure A3.20 500 MHz ^1H and 125 MHz $^{13}\text{C}\{^1\text{H}\}$ NMR of **3.3al** in CDCl_3

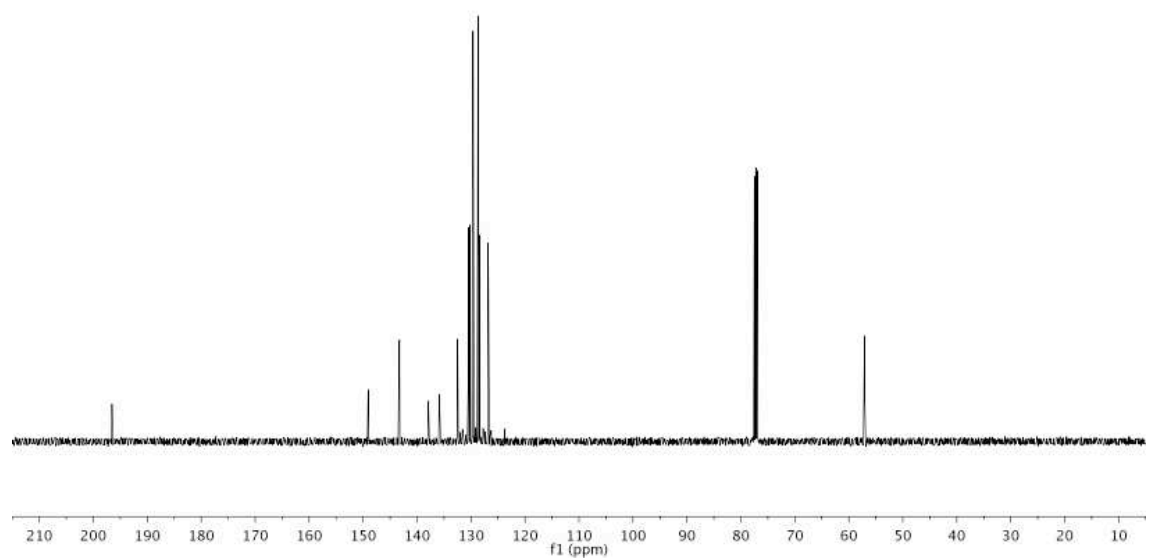
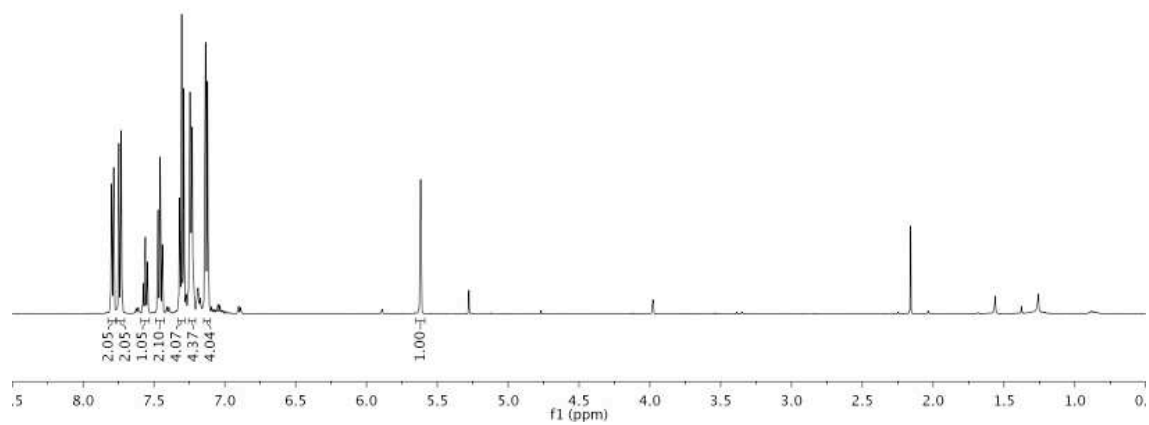
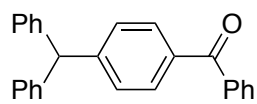


Figure A3.21 500 MHz ¹H and 125 MHz ¹³C{¹H} NMR of 3.3am in CDCl₃

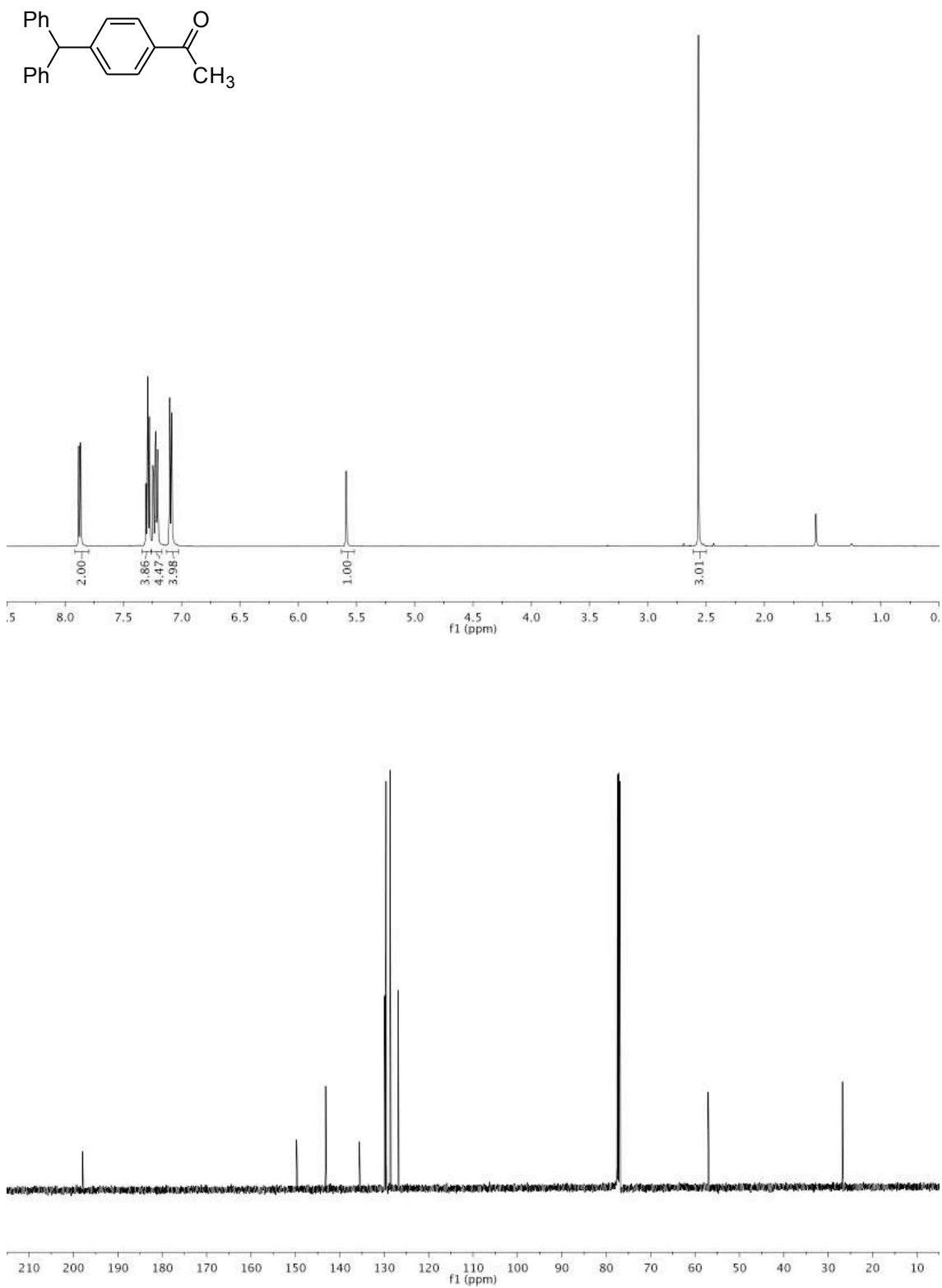


Figure A3.22 500 MHz ^1H and 125 MHz $^{13}\text{C}\{^1\text{H}\}$ NMR of **3.3an** in CDCl_3

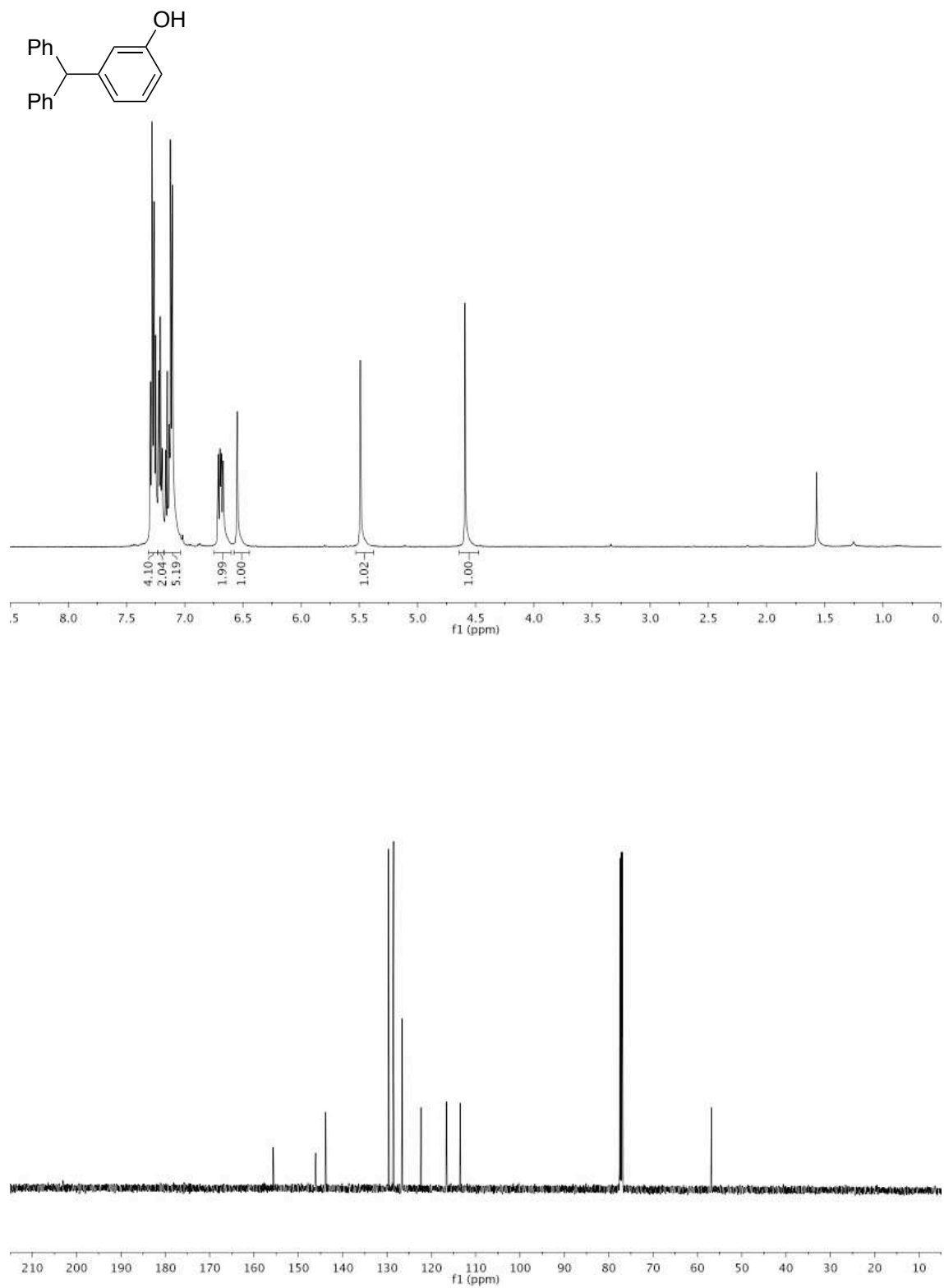


Figure A3.23 500 MHz ^1H and 125 MHz $^{13}\text{C}\{^1\text{H}\}$ NMR of **3.3ao** in CDCl_3

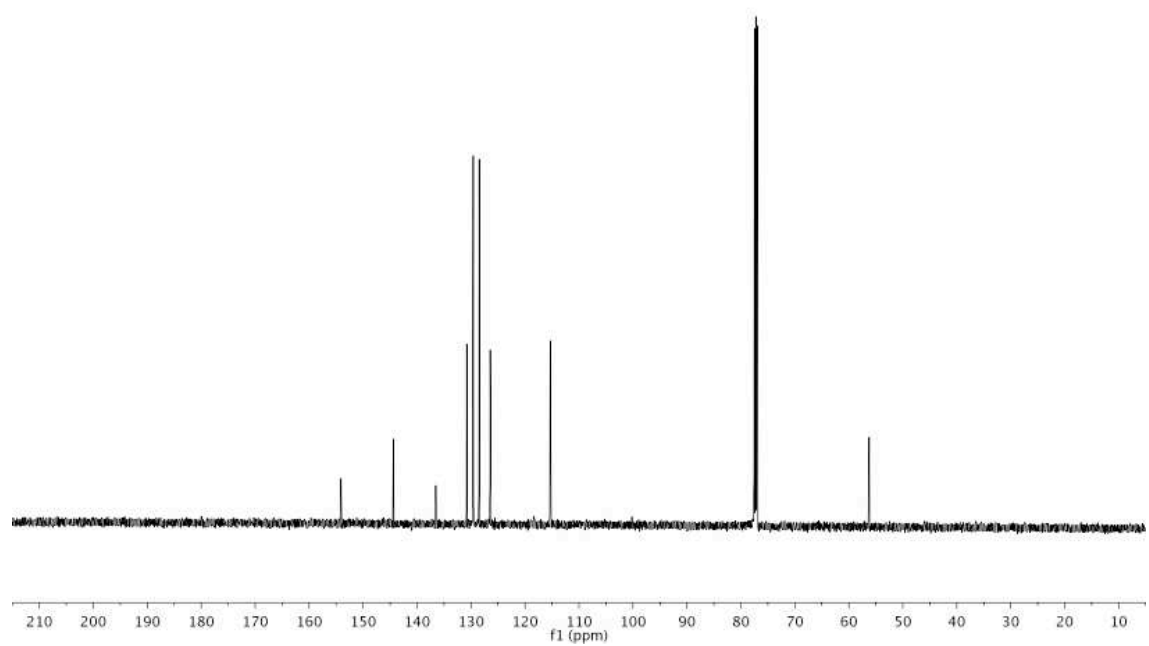
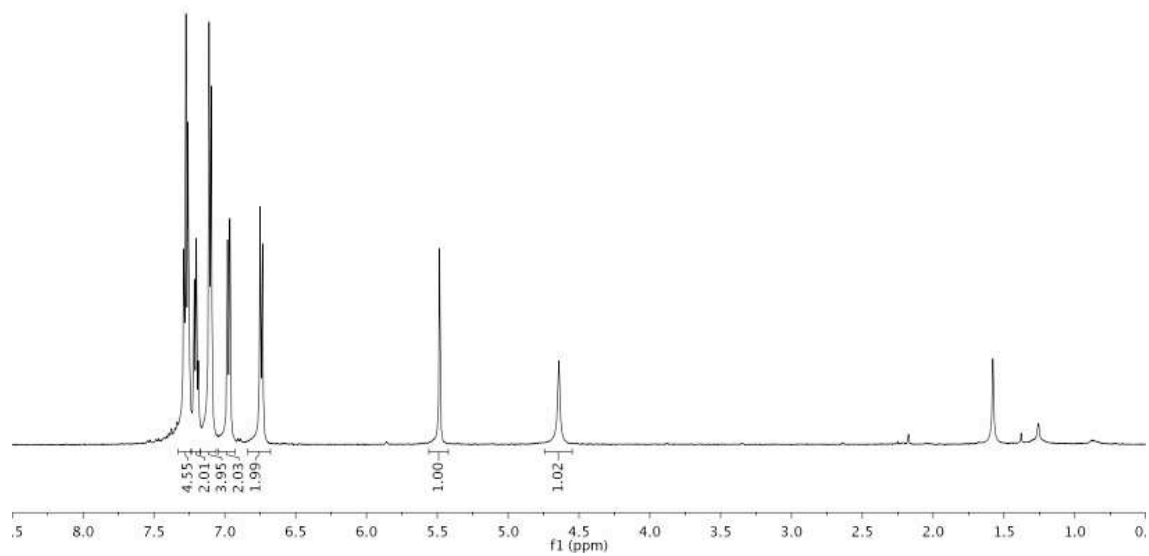
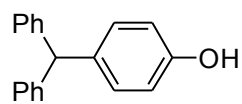


Figure A3.24 500 MHz ^1H and 125 MHz $^{13}\text{C}\{^1\text{H}\}$ NMR of **3.3ap** in CDCl_3

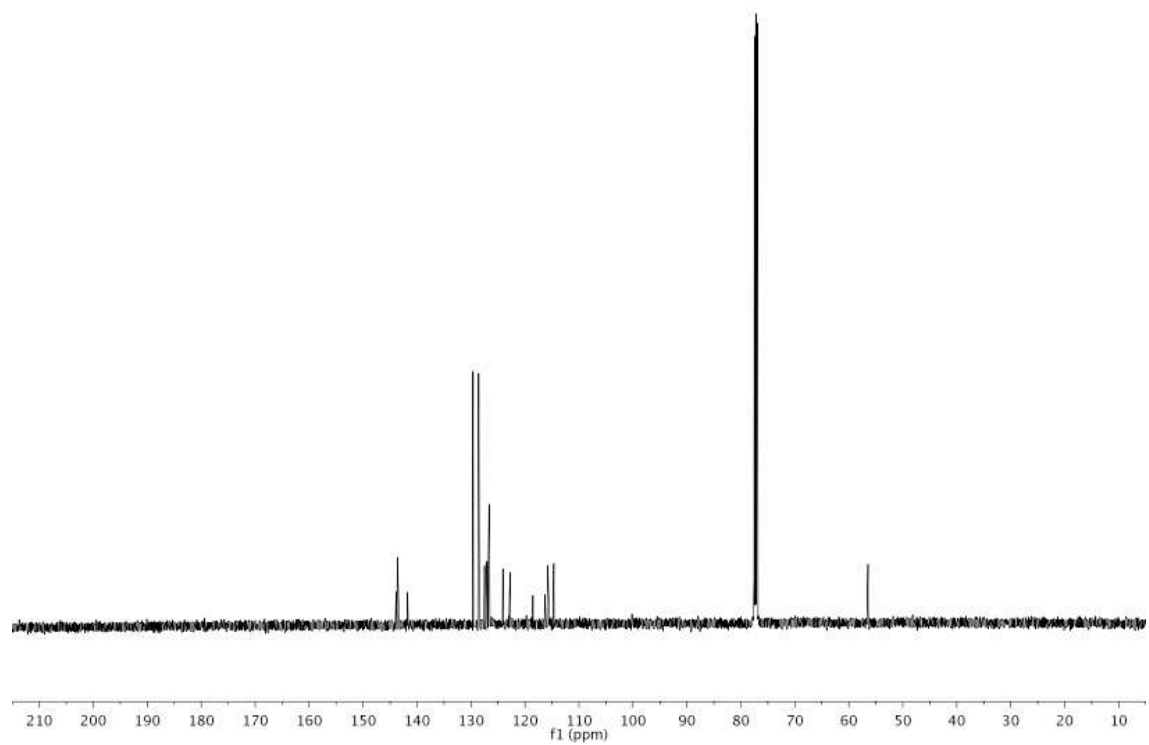
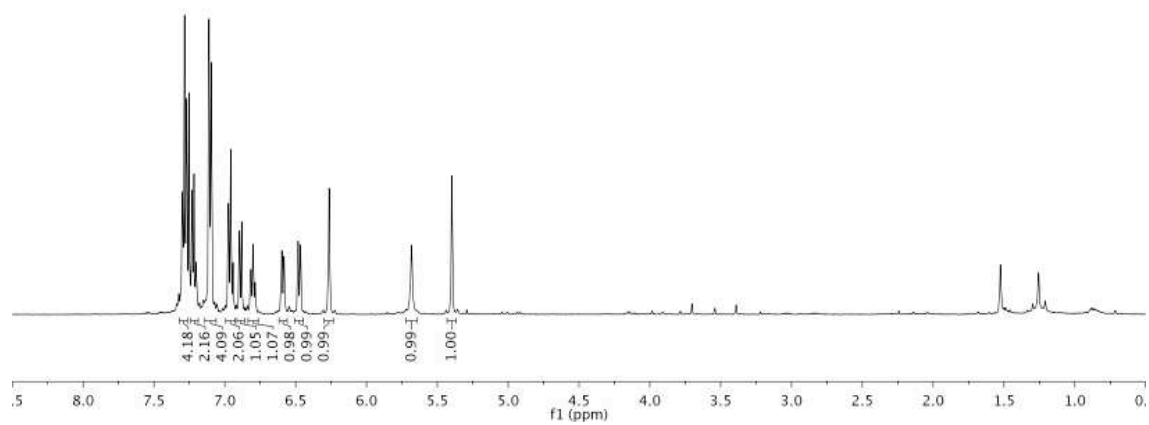
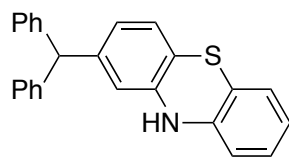


Figure A3.25 500 MHz ^1H and 125 MHz $^{13}\text{C}\{^1\text{H}\}$ NMR of 3.3aq in CDCl_3

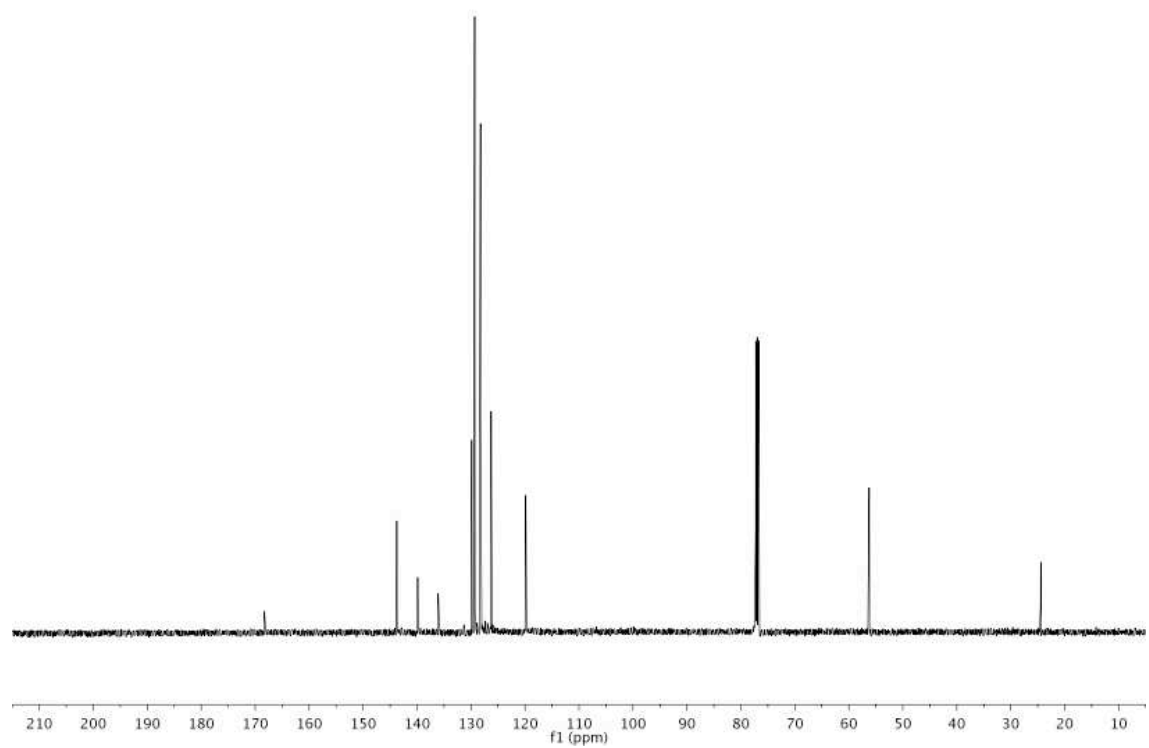
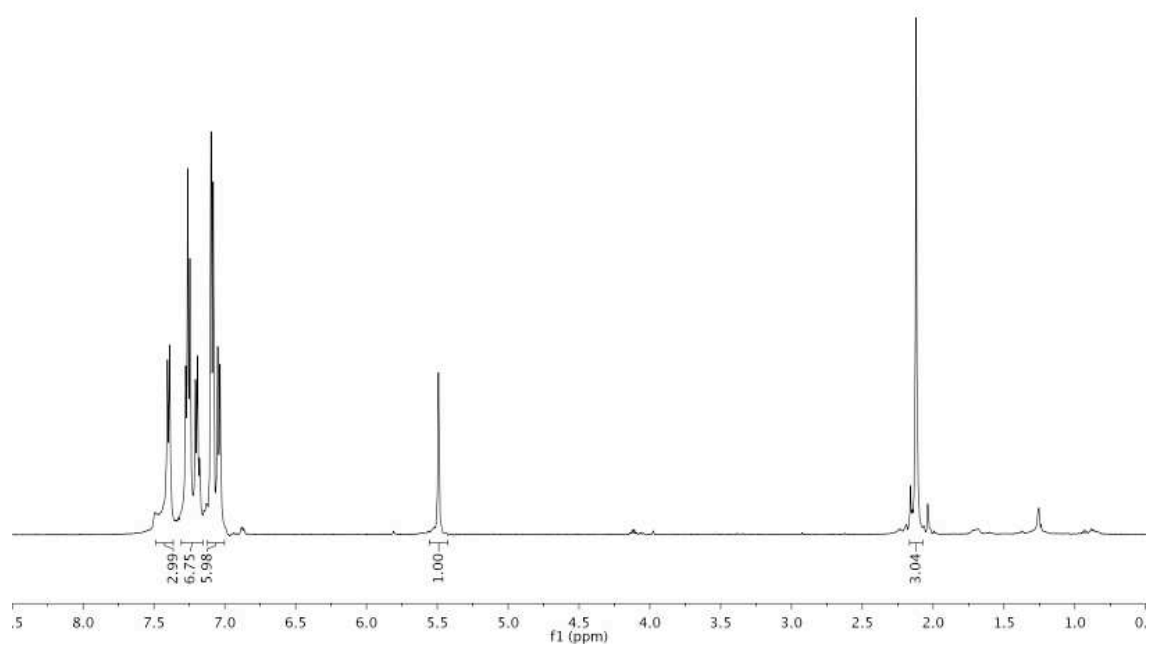
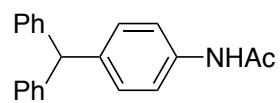


Figure A3.26 500 MHz ¹H and 125 MHz ¹³C{¹H} NMR of **3.3ar** in CDCl₃

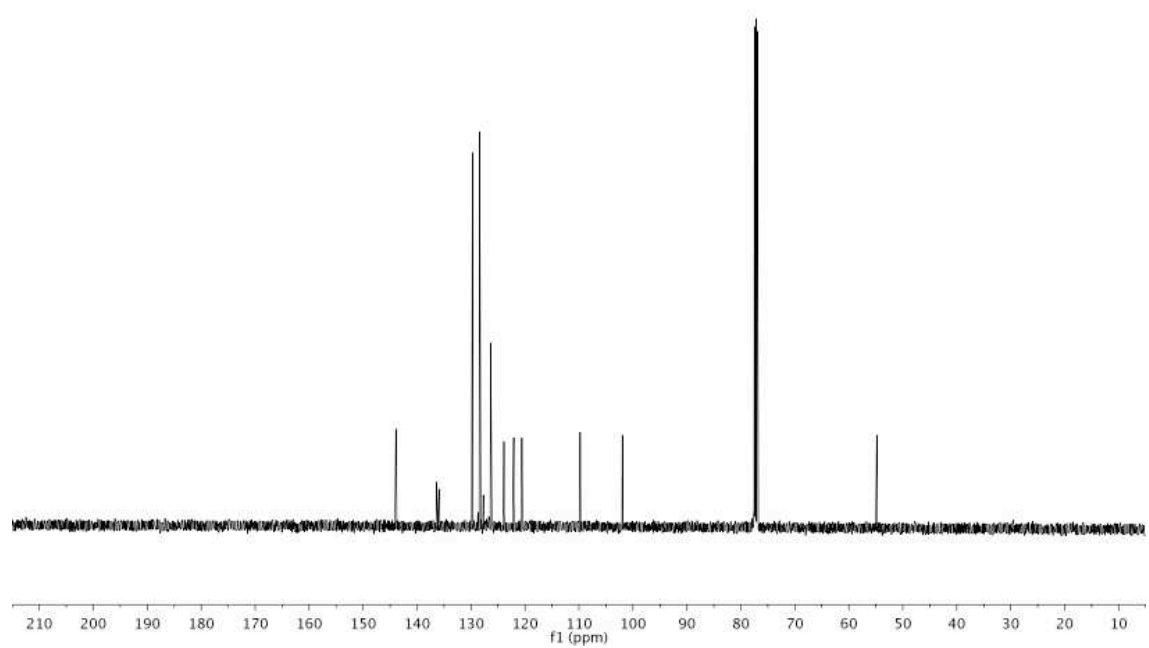
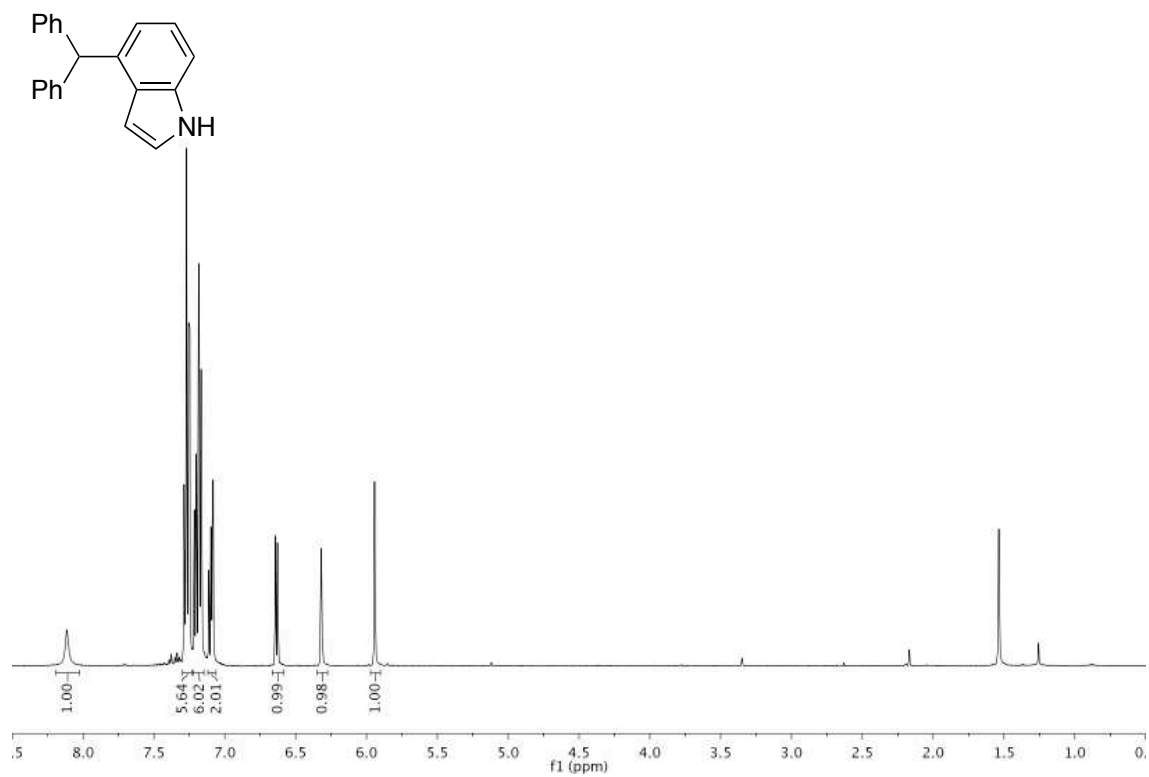


Figure A3.27 500 MHz ^1H and 125 MHz $^{13}\text{C}\{^1\text{H}\}$ NMR of **3.3as** in CDCl_3

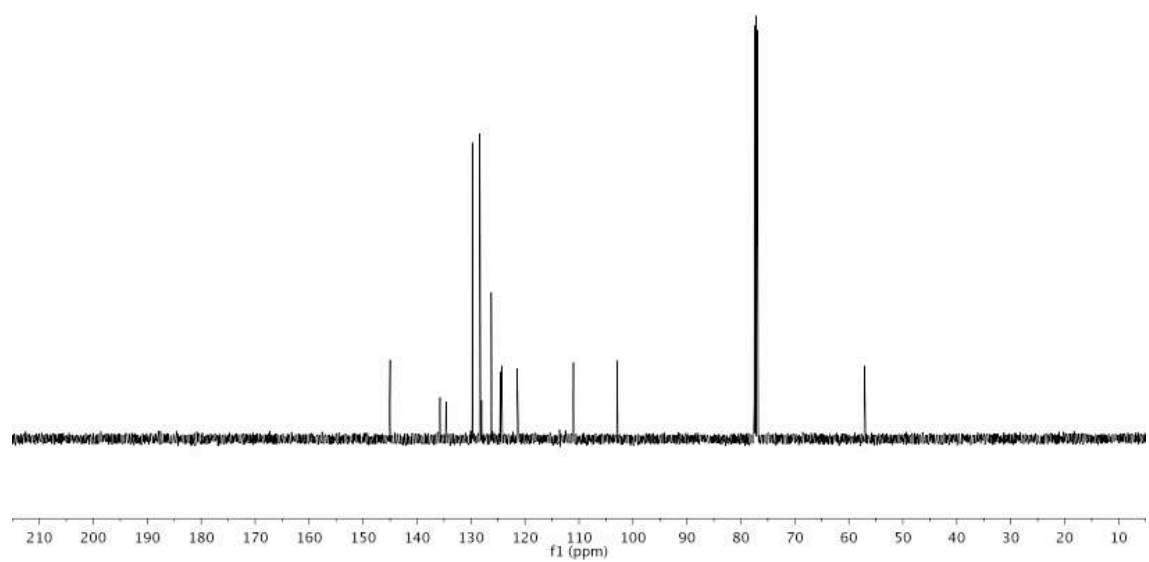
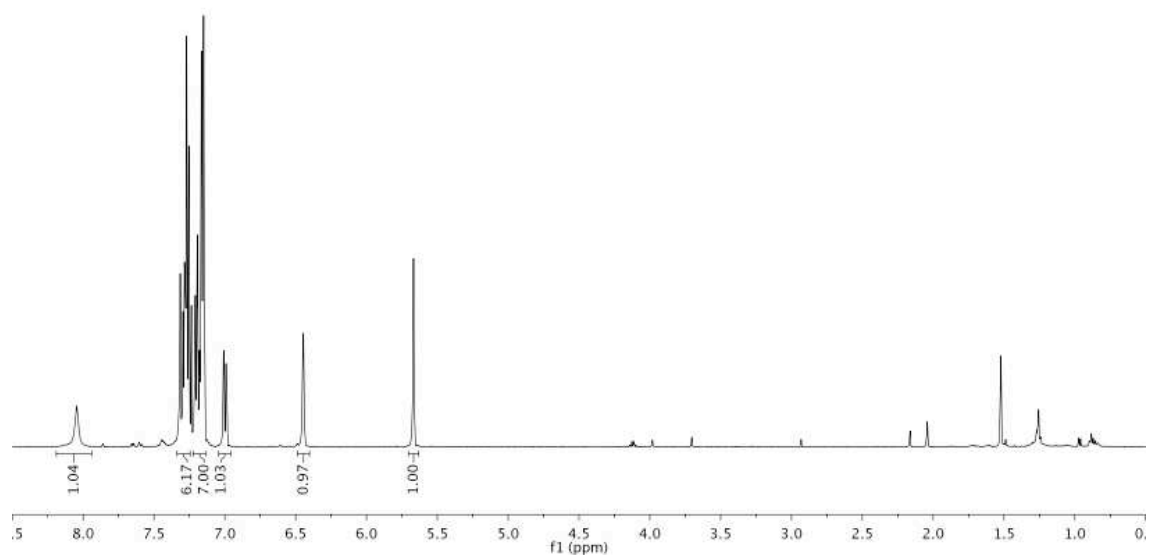
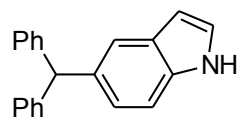


Figure A3.28 500 MHz ^1H and 125 MHz $^{13}\text{C}\{^1\text{H}\}$ NMR of **3.3at** in CDCl_3

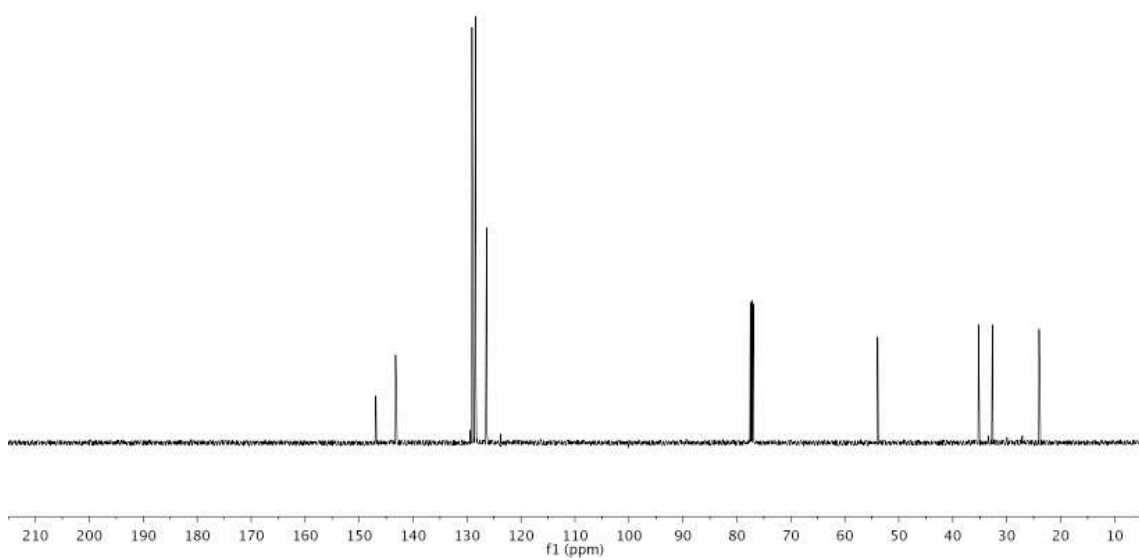
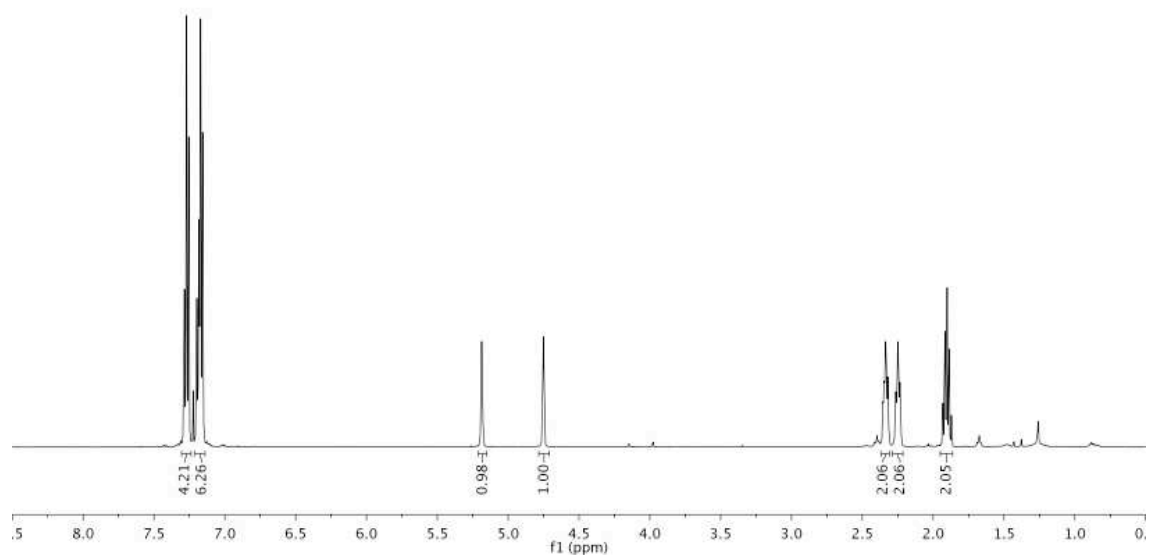
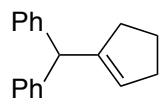


Figure A3.29 500 MHz ^1H and 125 MHz $^{13}\text{C}\{^1\text{H}\}$ NMR of **3.3au** in CDCl_3

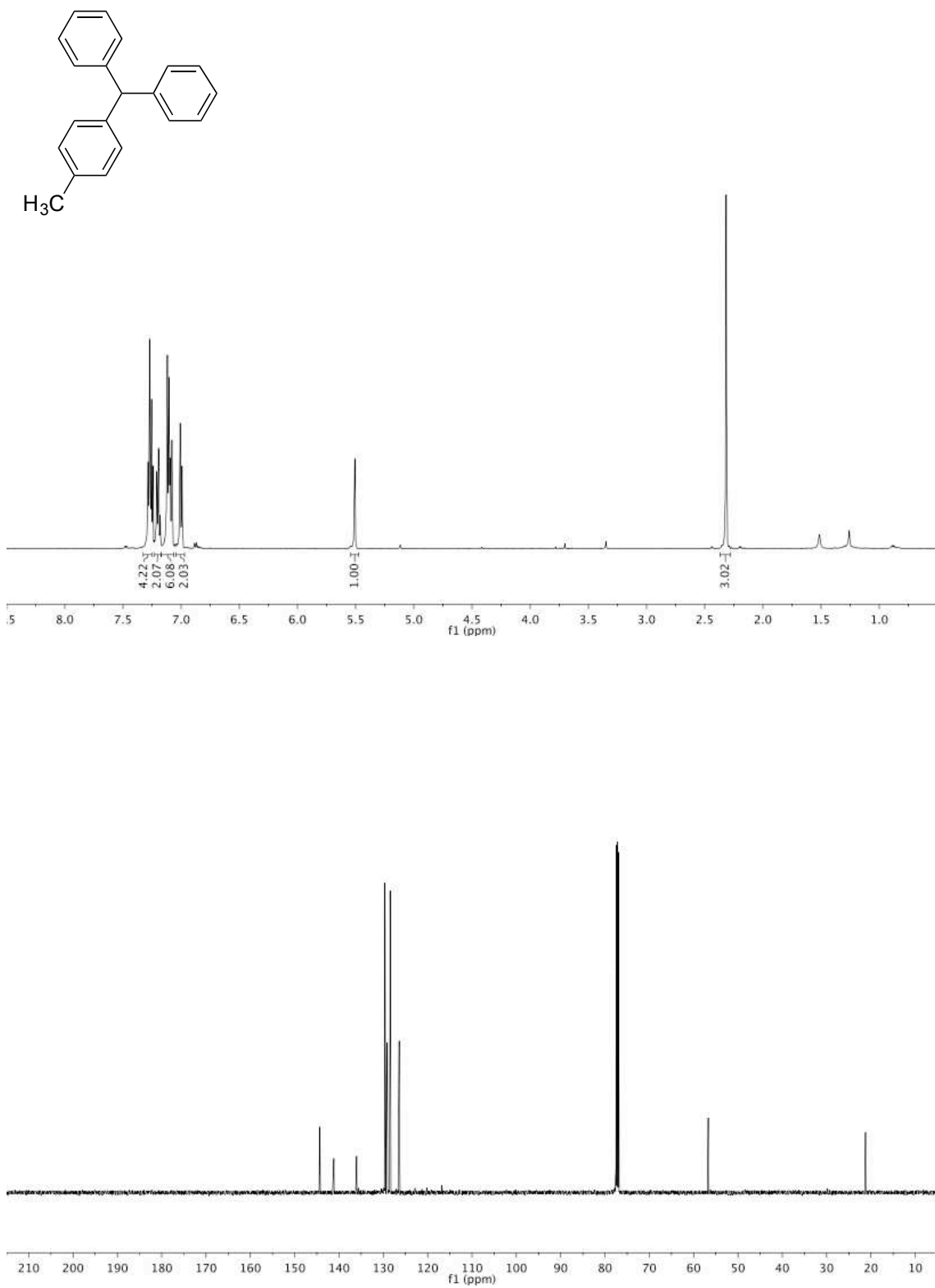


Figure A3.30 500 MHz ^1H and 125 MHz $^{13}\text{C}\{^1\text{H}\}$ NMR of **3.3bb** in CDCl_3

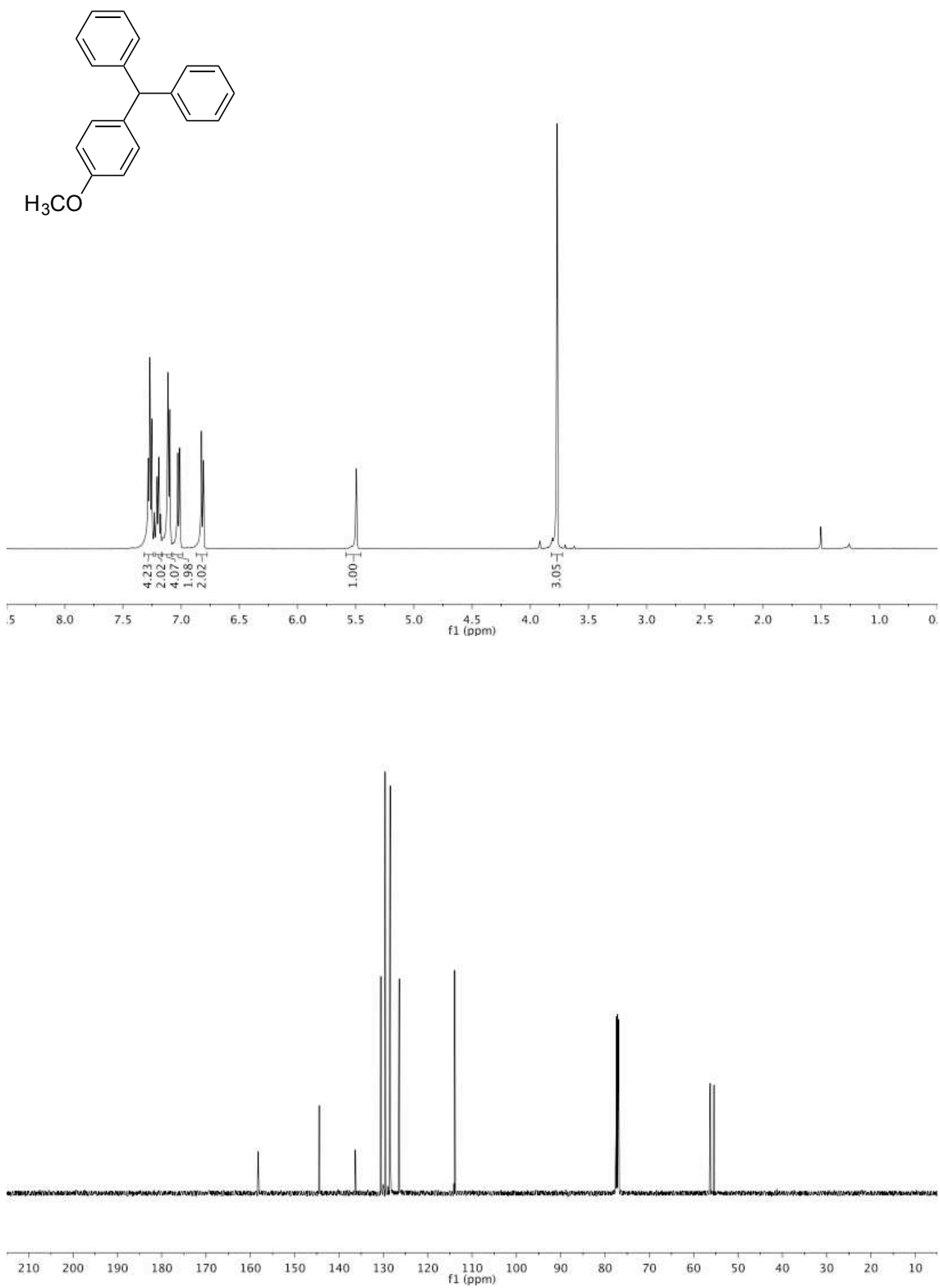


Figure A3.31 500 MHz ^1H and 125 MHz $^{13}\text{C}\{^1\text{H}\}$ NMR of **3.3cb** in CDCl_3

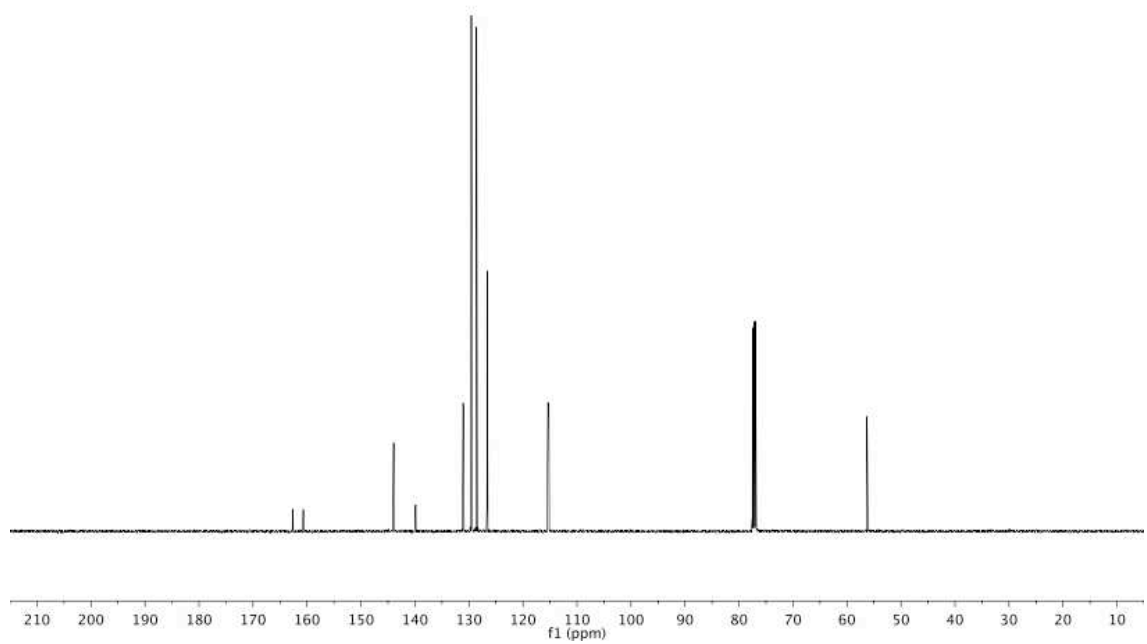
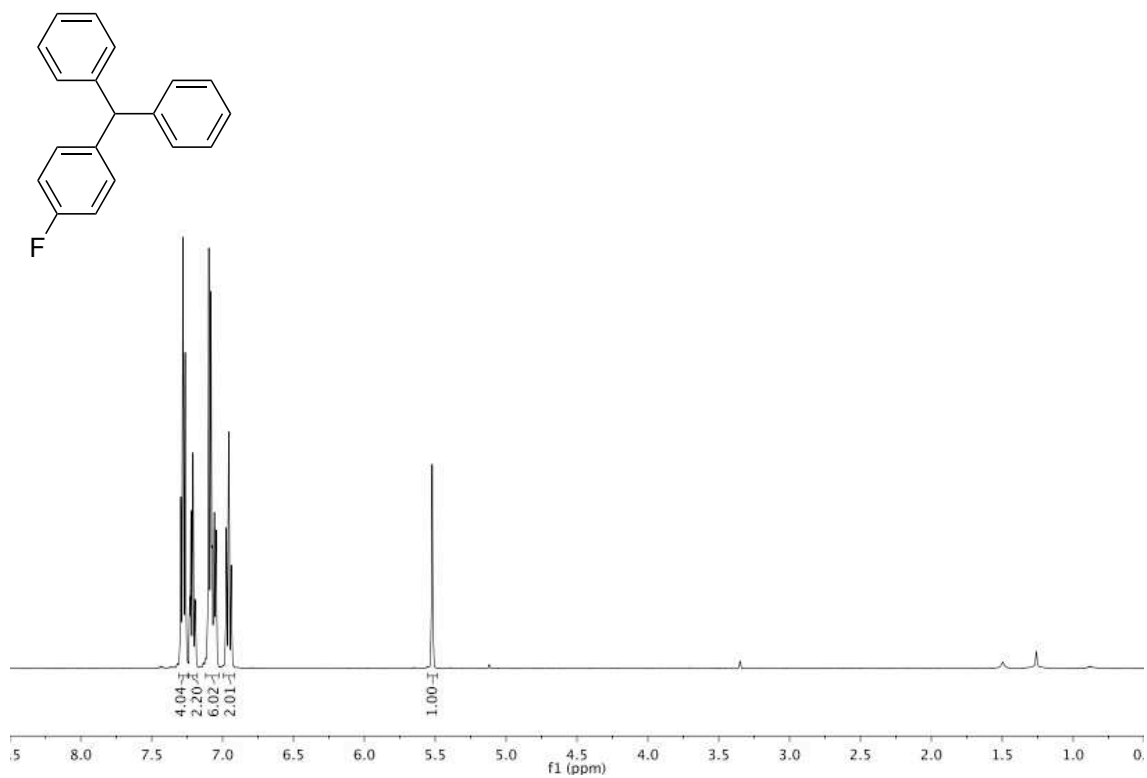


Figure A3.32 500 MHz ^1H and 125 MHz $^{13}\text{C}\{^1\text{H}\}$ NMR of **3.3db** in CDCl_3

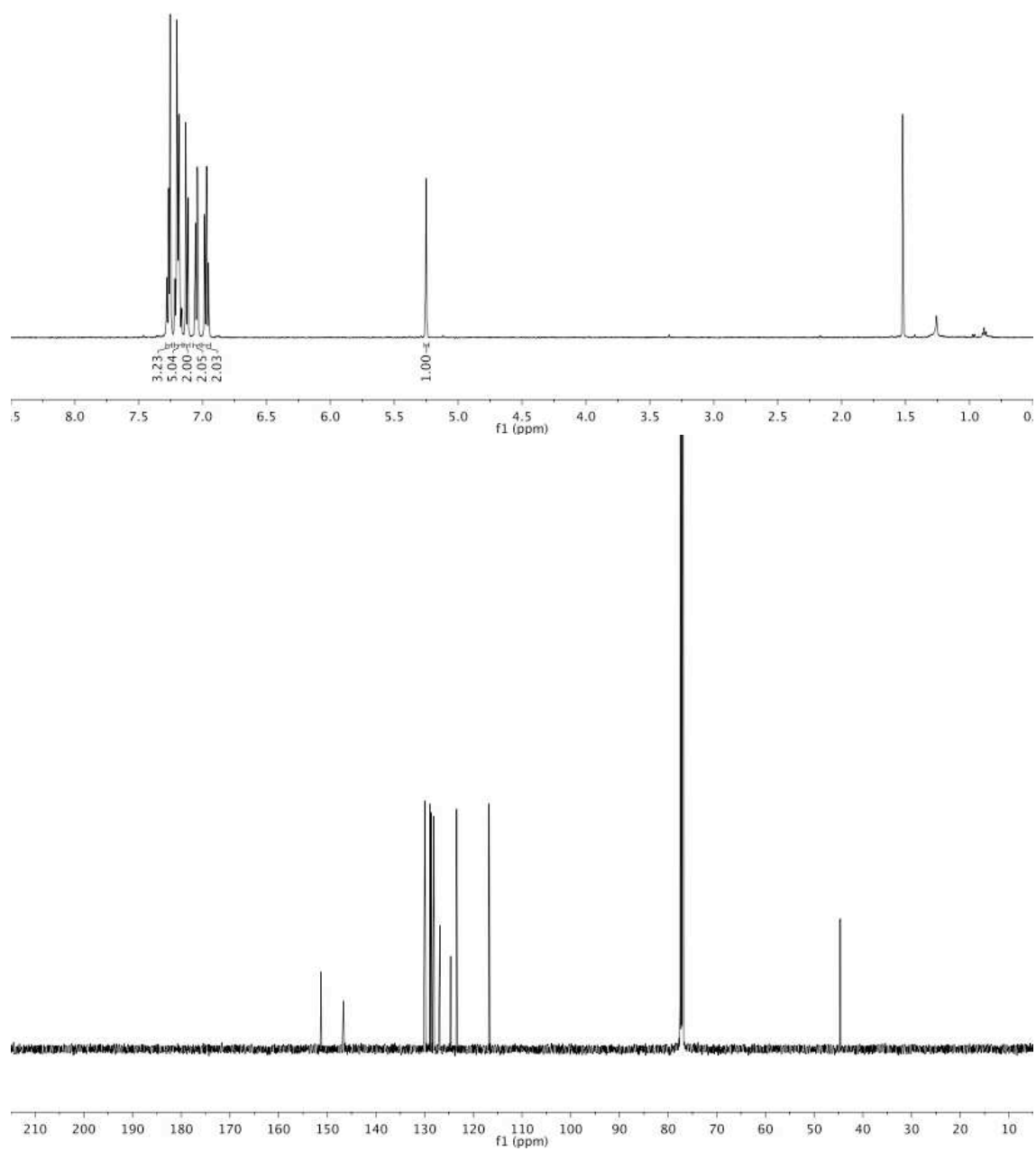
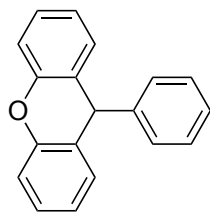


Figure A3.33 500 MHz ¹H and 125 MHz ¹³C{¹H} NMR of **3.3eb** in CDCl₃

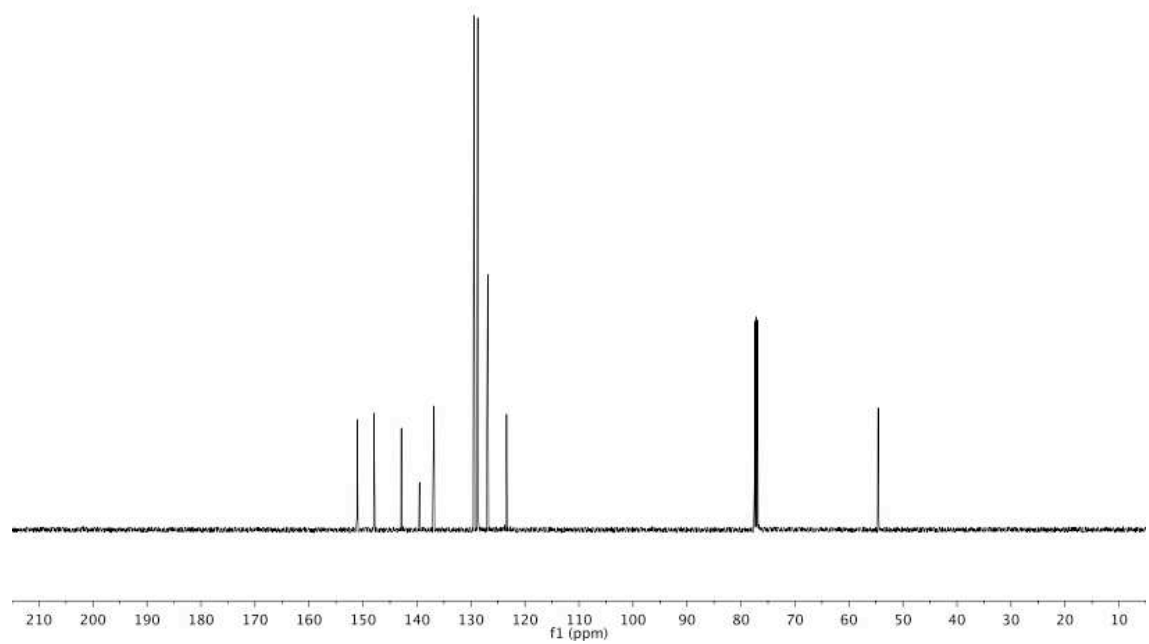
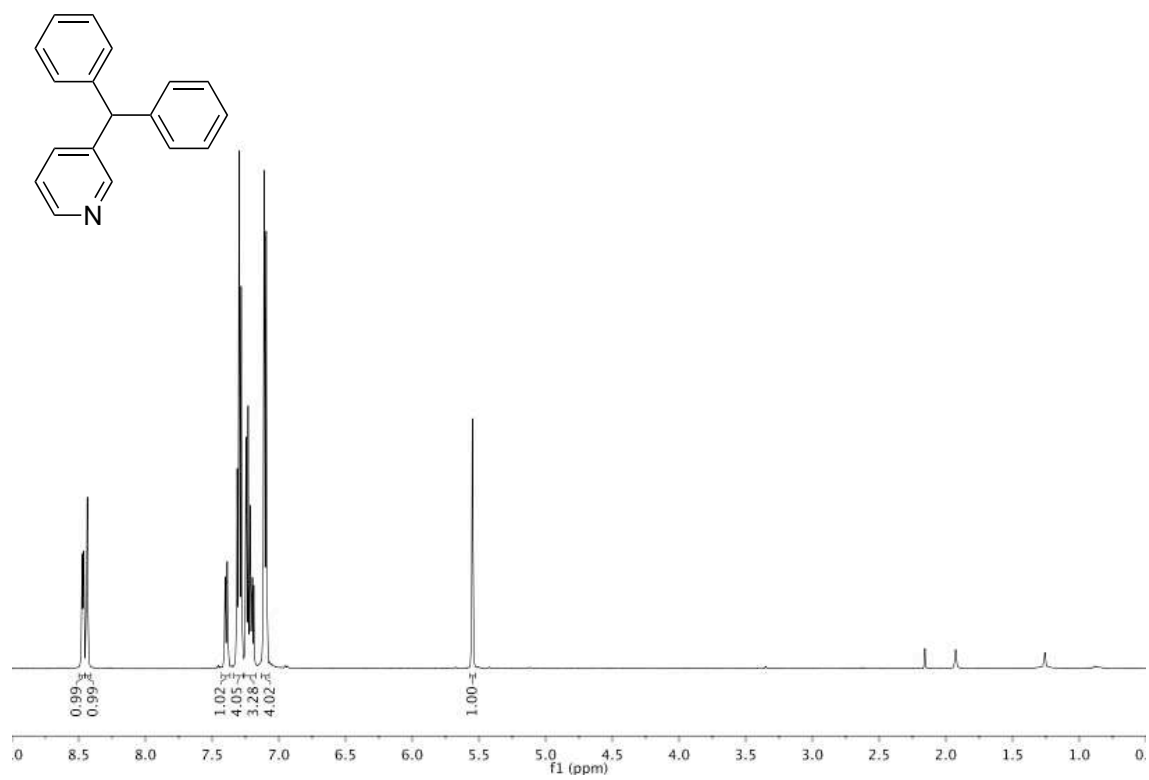


Figure A3.34 500 MHz ^1H and 125 MHz $^{13}\text{C}\{^1\text{H}\}$ NMR of **3.3fb** in CDCl_3

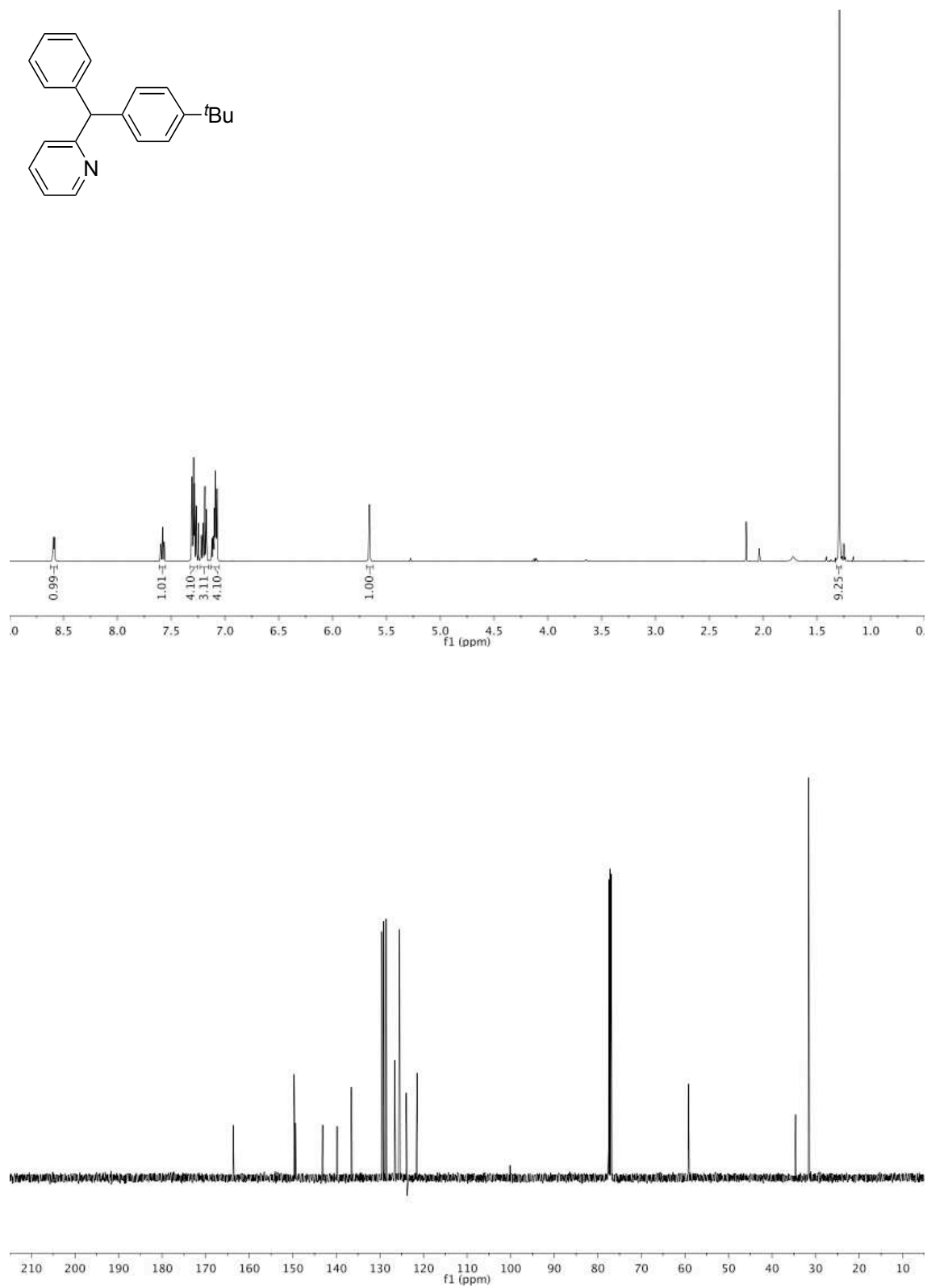


Figure A3.35 500 MHz ^1H and 125 MHz $^{13}\text{C}\{^1\text{H}\}$ NMR of 3.3ga in CDCl_3

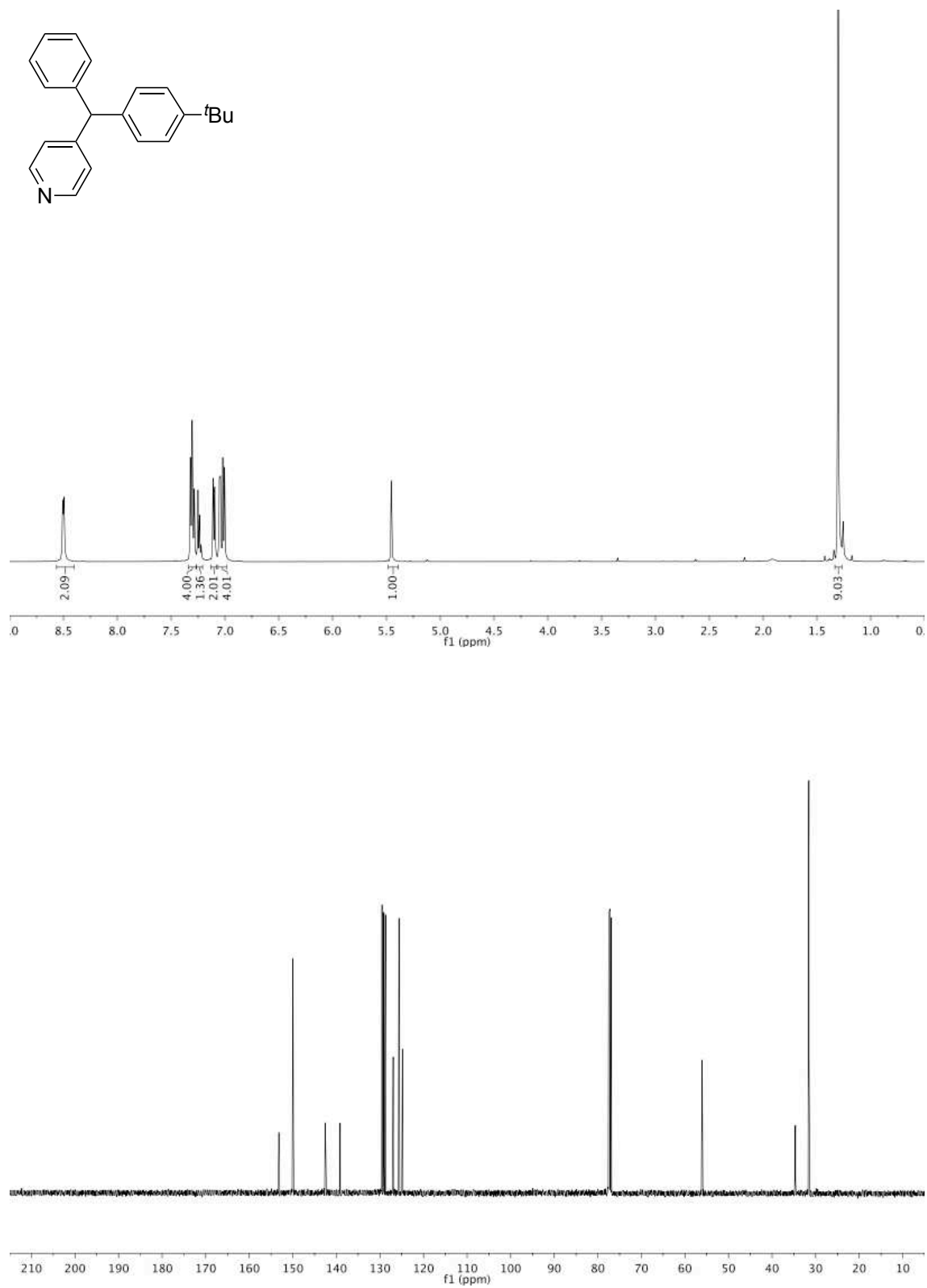


Figure A3.36 500 MHz ^1H and 125 MHz $^{13}\text{C}\{^1\text{H}\}$ NMR of **3.3ha** in CDCl_3

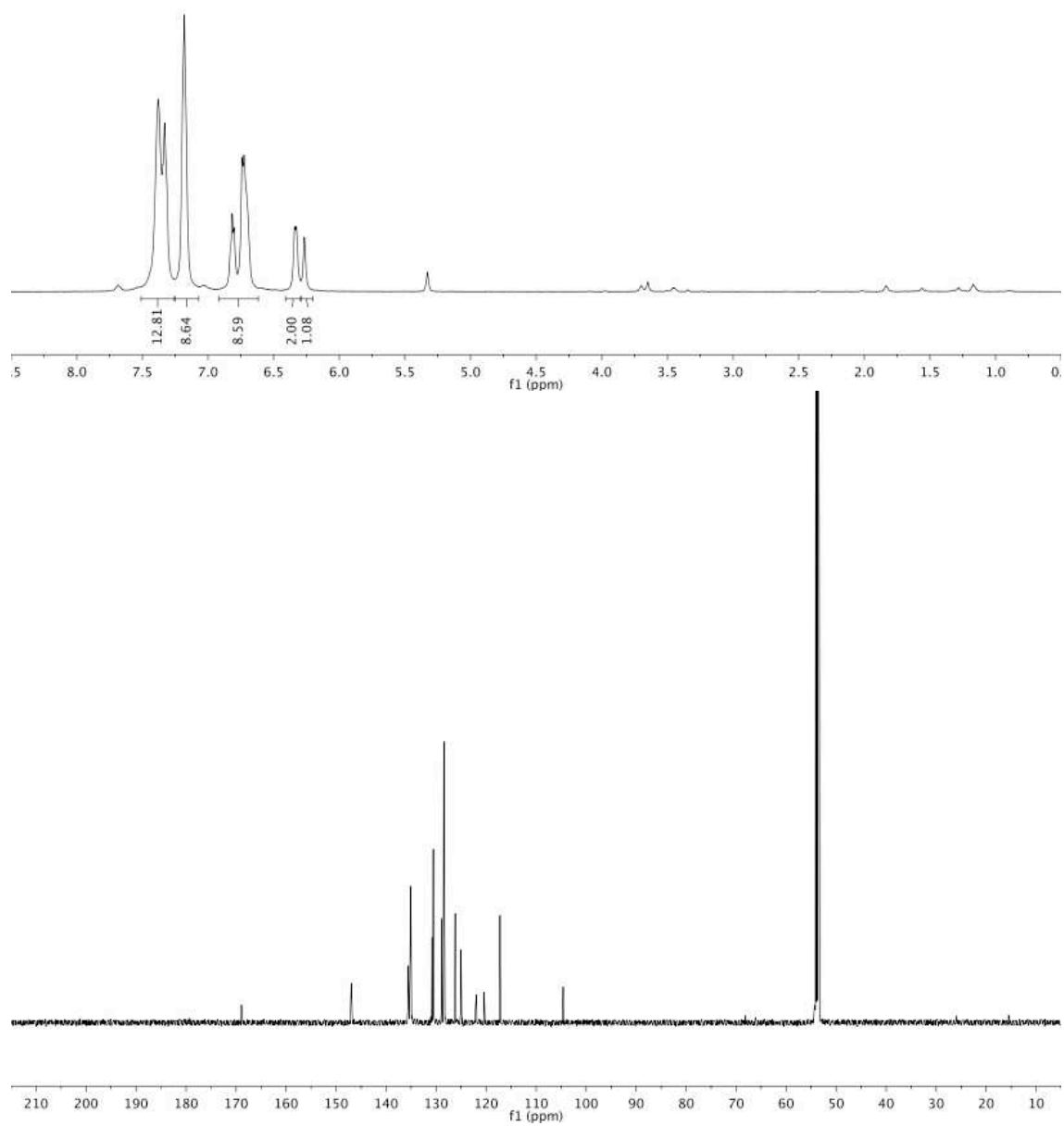


Figure A3.37 500 MHz ¹H and 125 MHz ¹³C{¹H} NMR of **3.5** in CD₂Cl₂

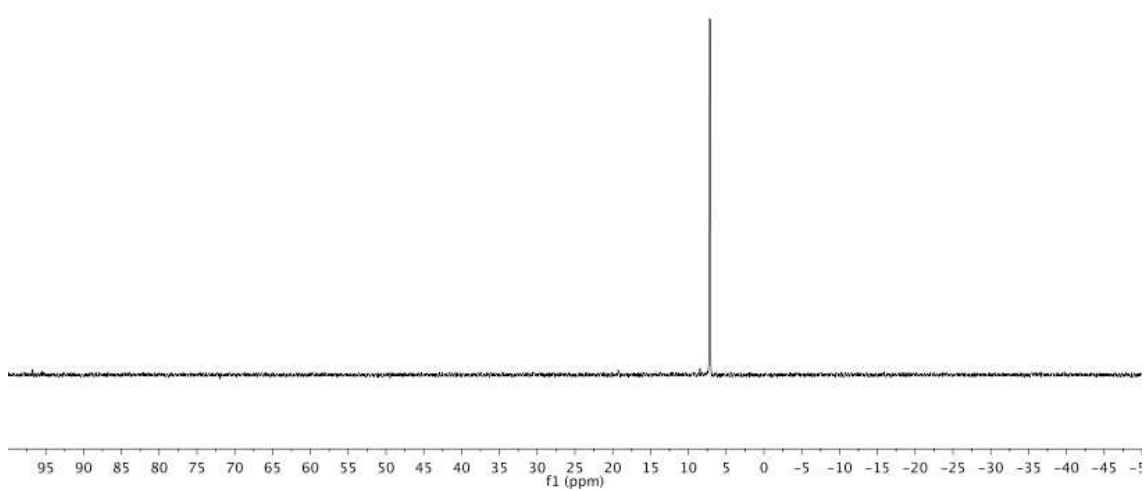


Figure A3.38 145.8 MHz $^{31}\text{P}\{^1\text{H}\}$ NMR of **3.5** in CD_2Cl_2

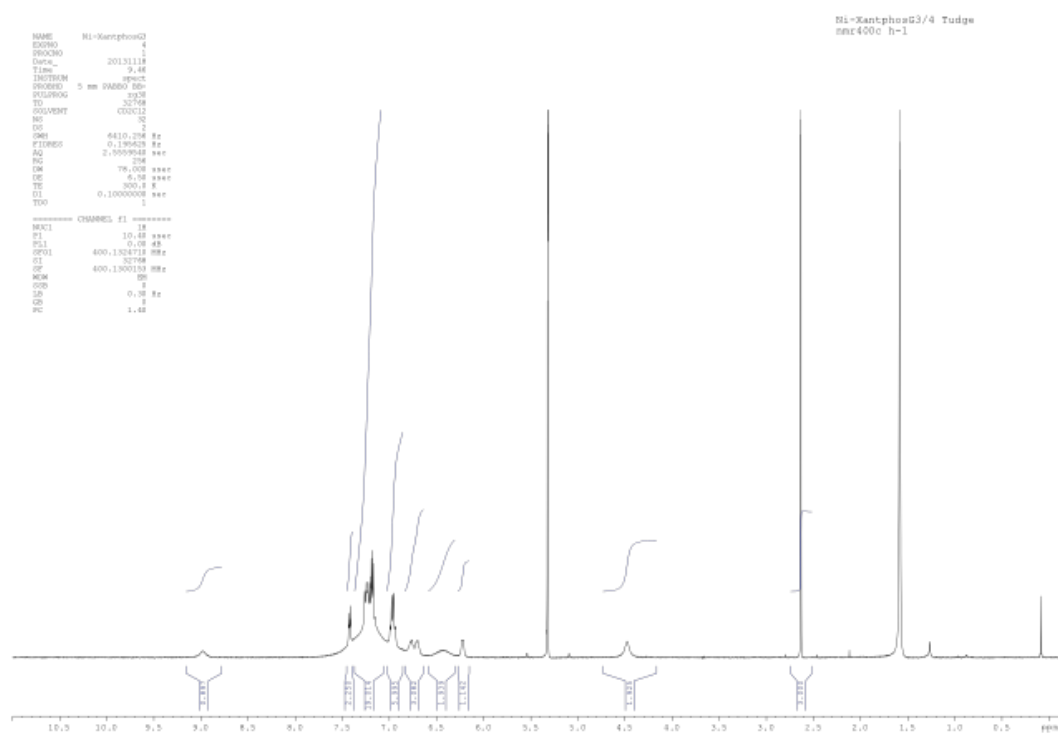


Figure A3.39 400 MHz ^1H NMR of **3.4** in CD_2Cl_2

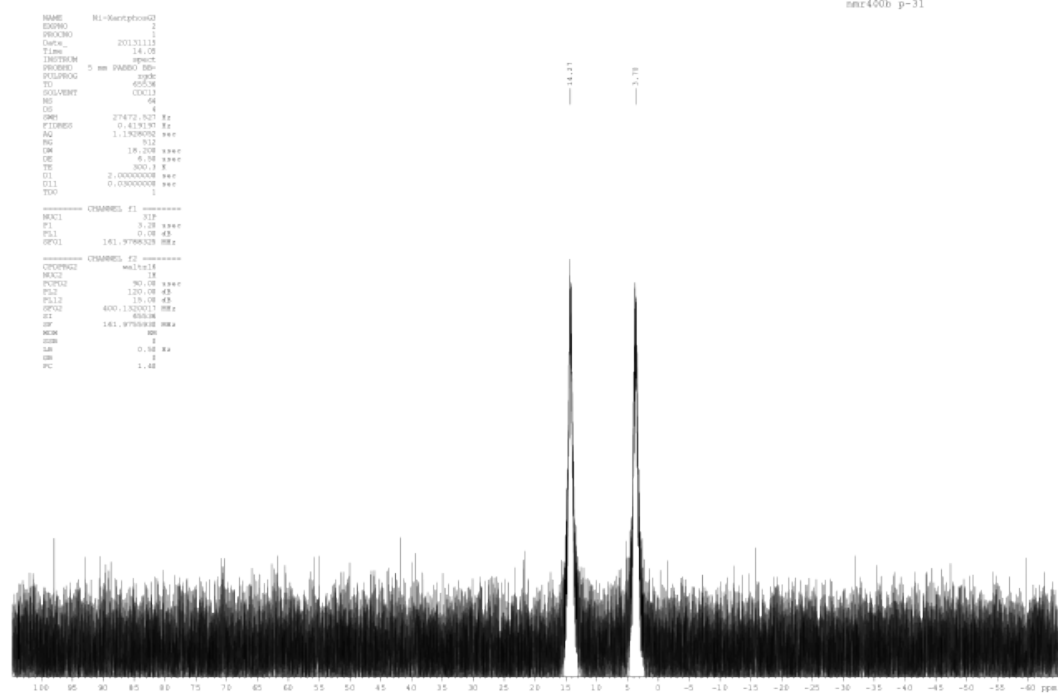


Figure A3.40 162.0 MHz $^{31}\text{P}\{^1\text{H}\}$ NMR of **3.4** in CDCl_3

Appendix A4. NMR Spectra Relevant to Chapter 4

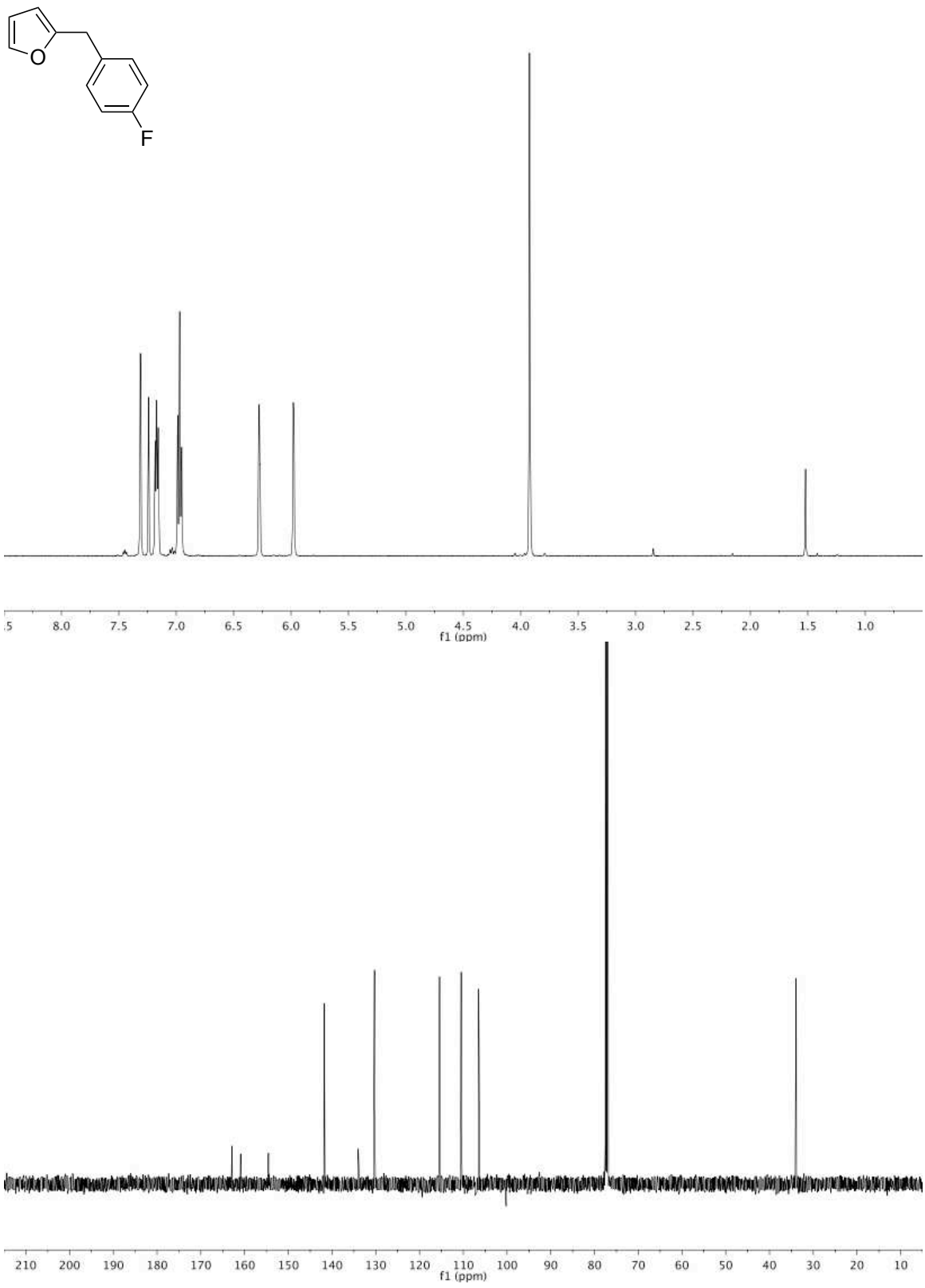


Figure A4.1 500 MHz ^1H and 125 MHz $^{13}\text{C}\{^1\text{H}\}$ NMR of **4.1b** in CDCl_3

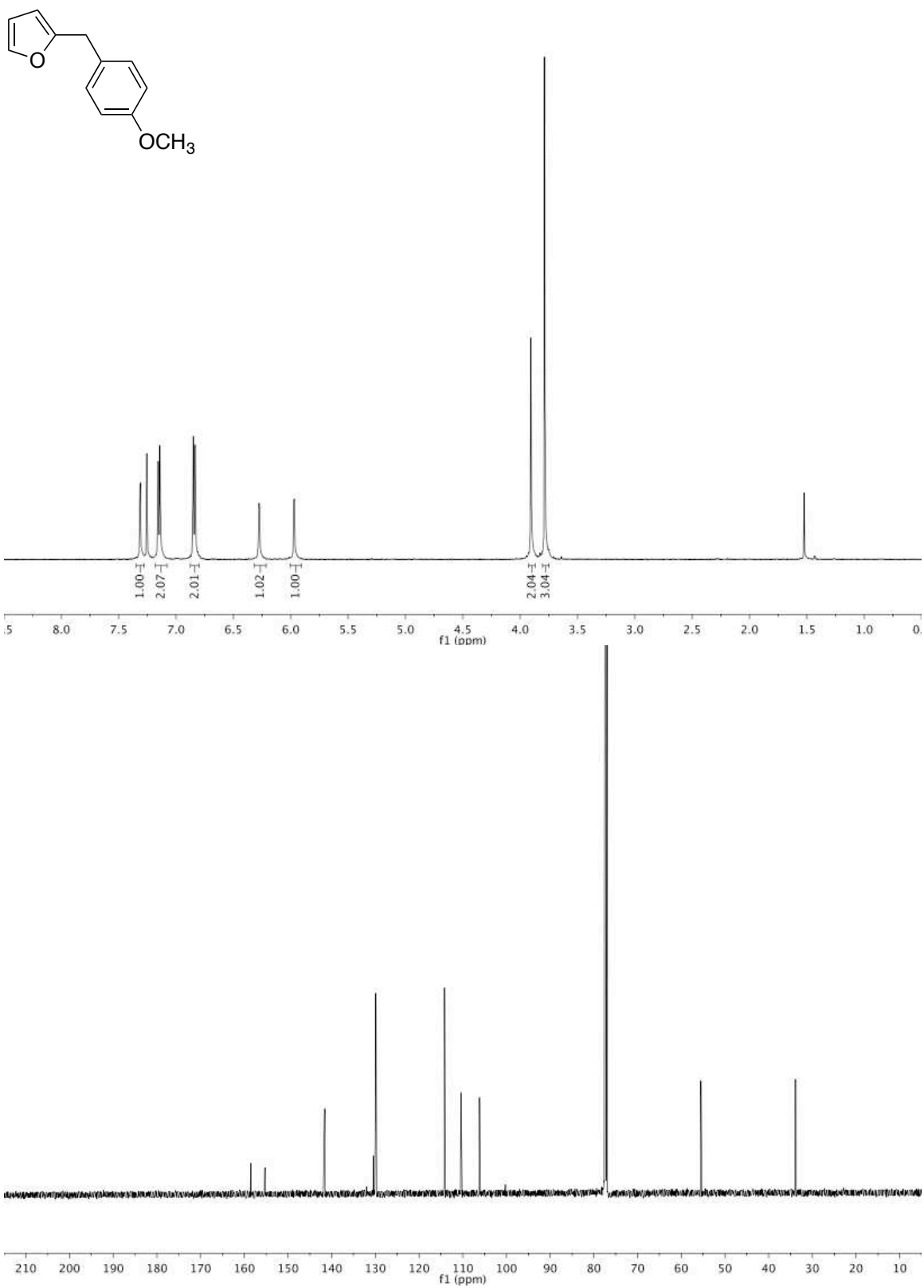


Figure A4.2 500 MHz ^1H and 125 MHz $^{13}\text{C}\{^1\text{H}\}$ NMR of 4.1c in CDCl_3

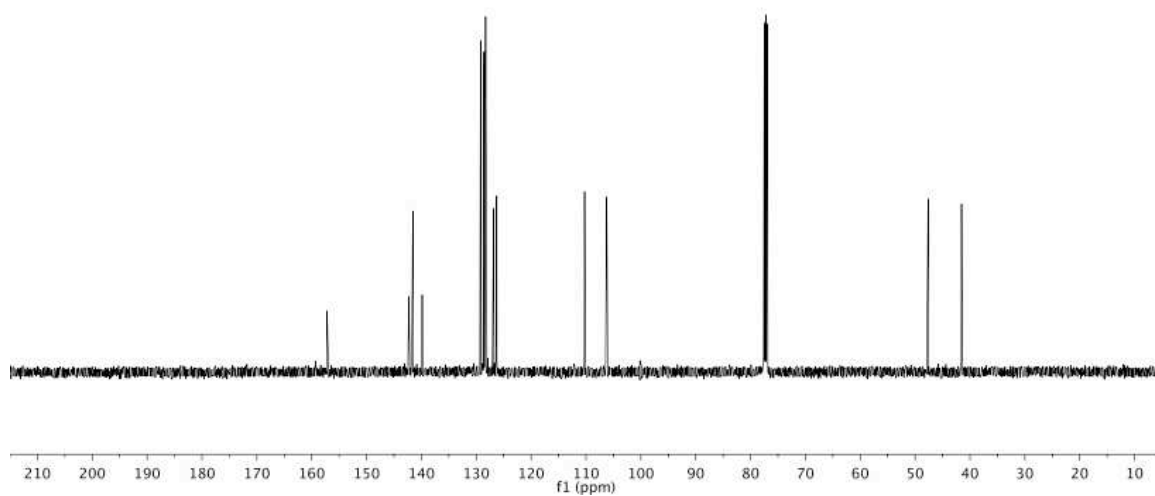
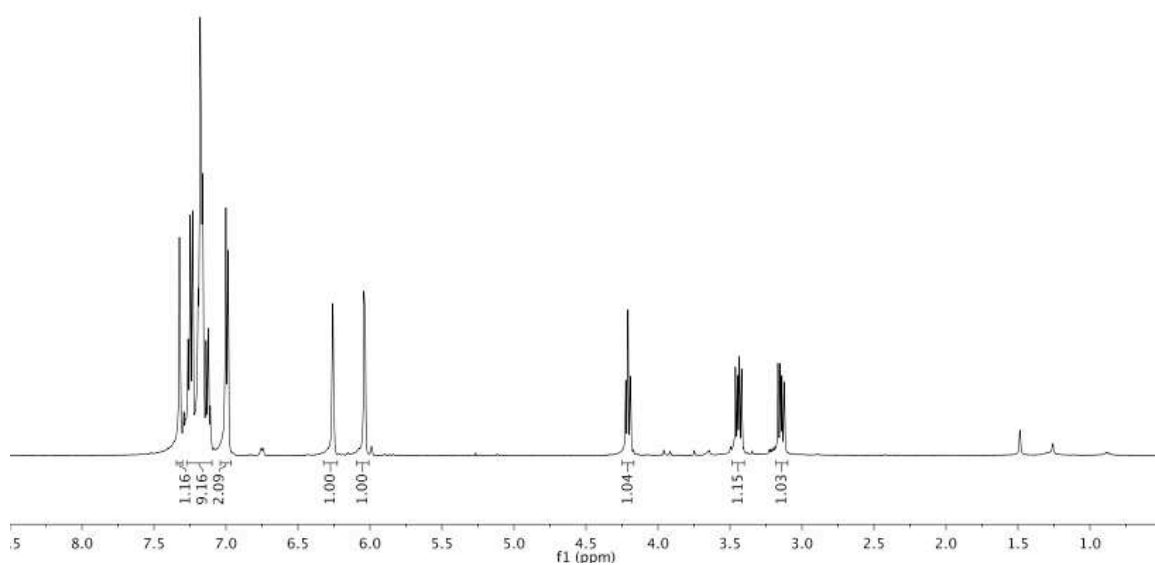
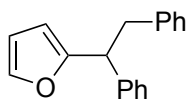


Figure A4.3 500 MHz ^1H and 125 MHz $^{13}\text{C}\{^1\text{H}\}$ NMR of **4.6** in CDCl_3

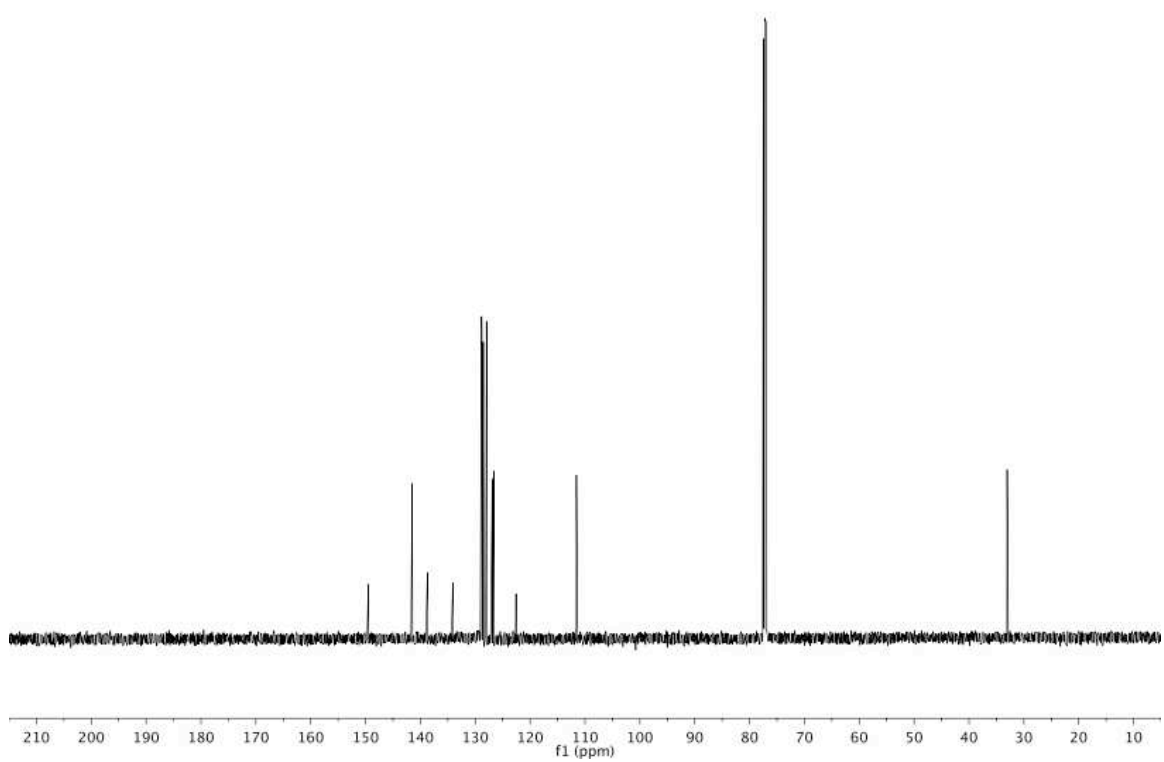
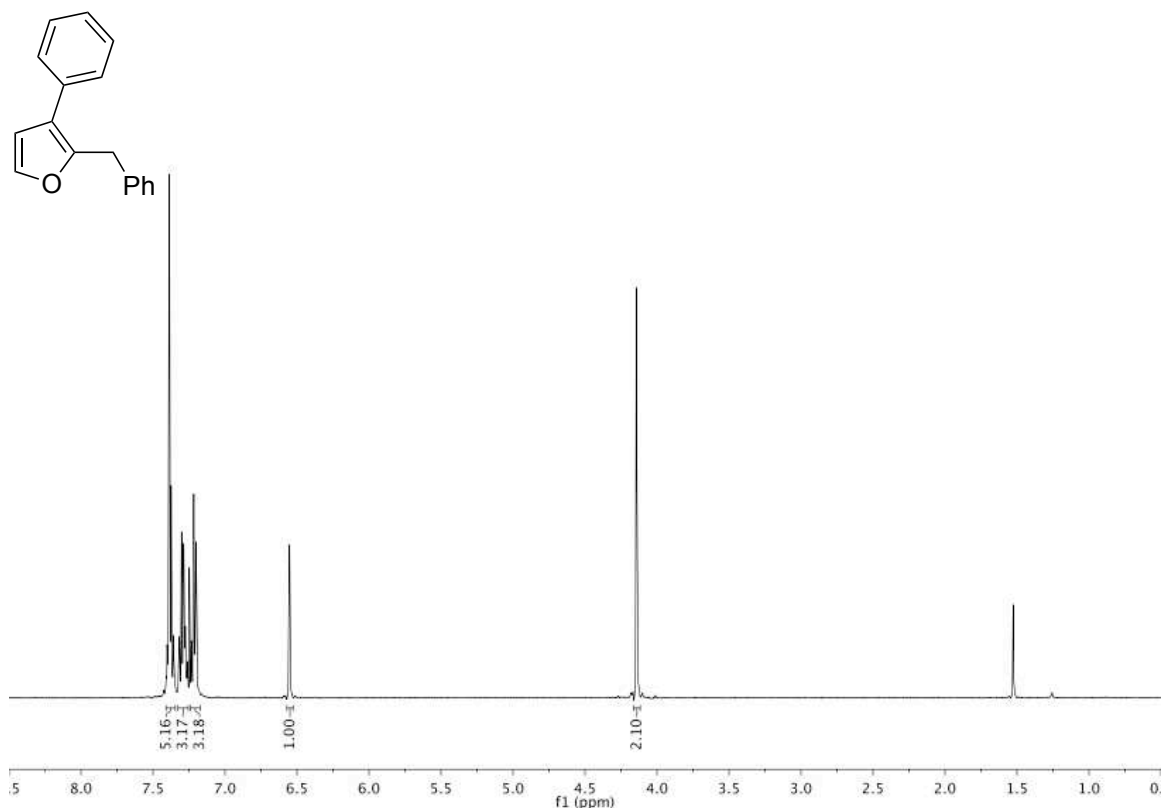


Figure A4.4 500 MHz ^1H and 125 MHz $^{13}\text{C}\{^1\text{H}\}$ NMR of 4.3aa in CDCl_3

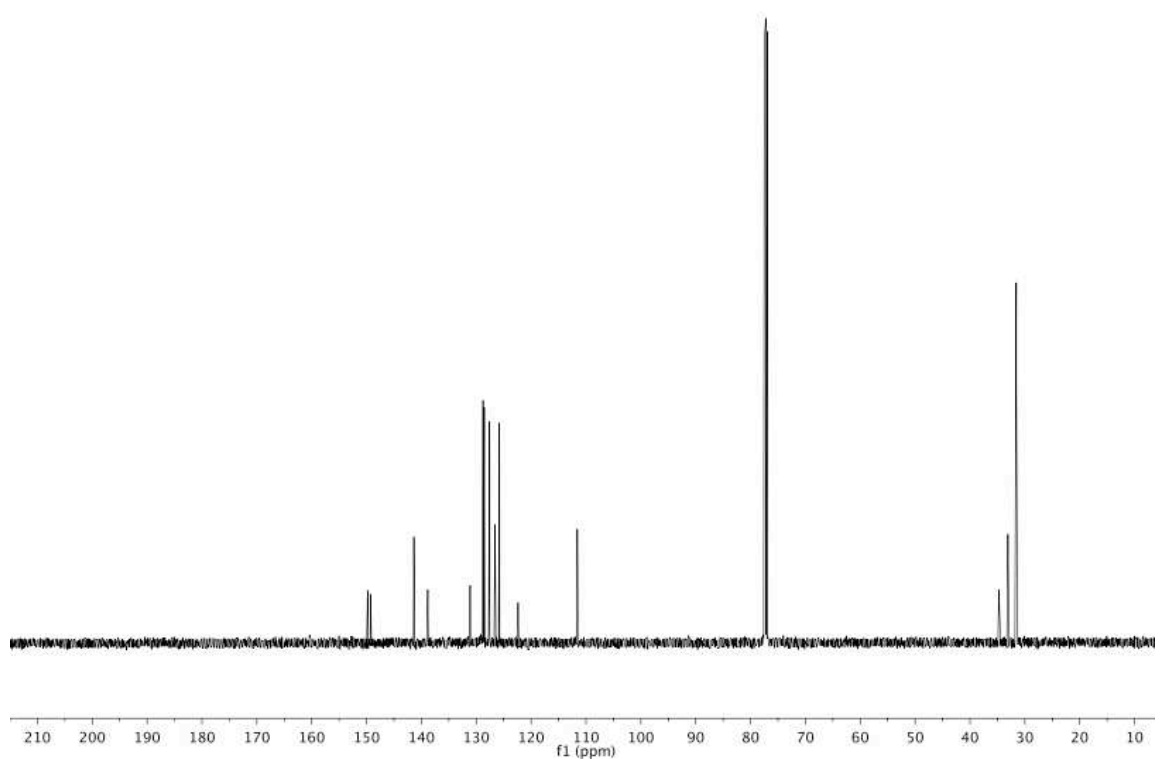
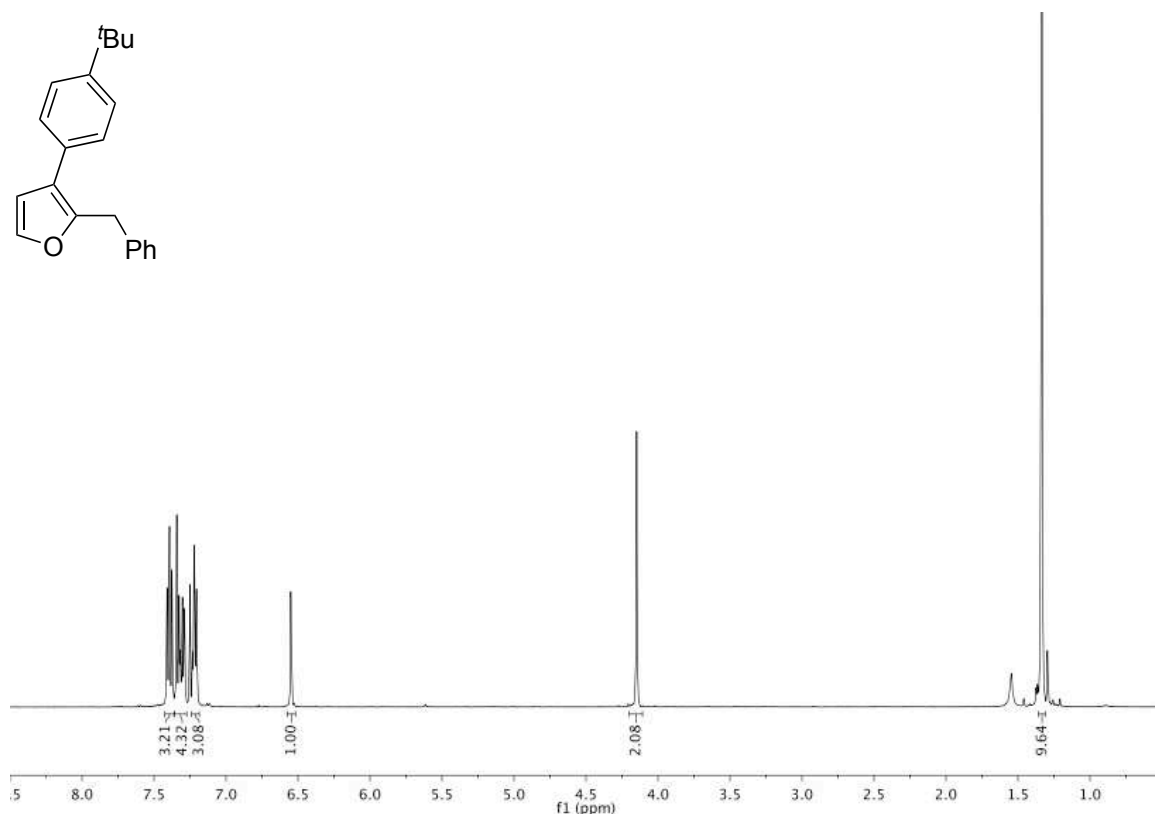
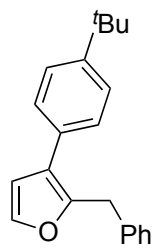


Figure A4.5 500 MHz ^1H and 125 MHz $^{13}\text{C}\{^1\text{H}\}$ NMR of **4.3ab** in CDCl_3

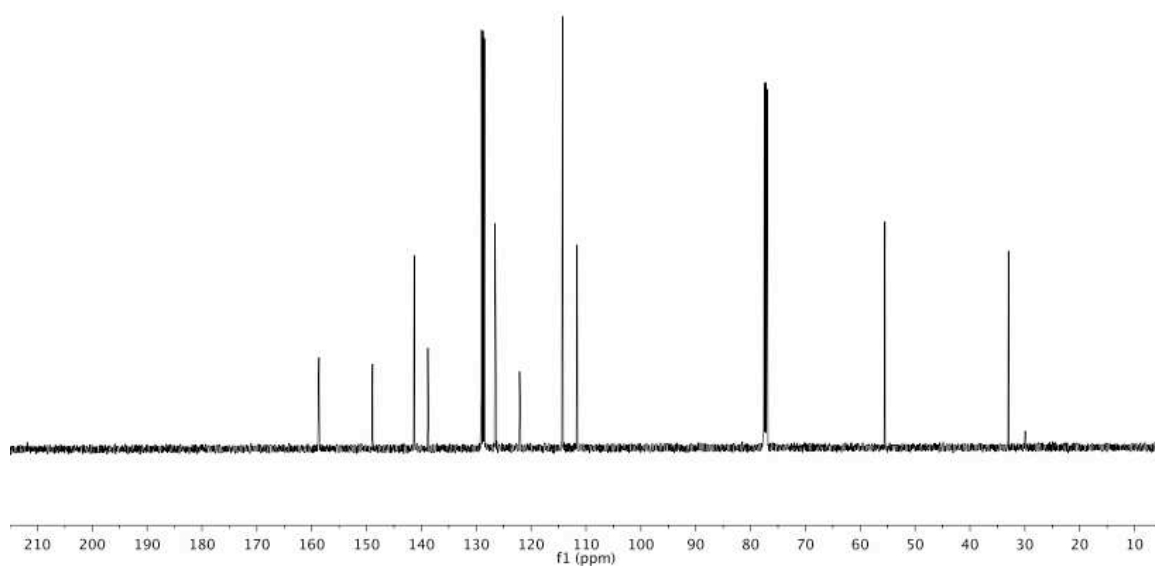
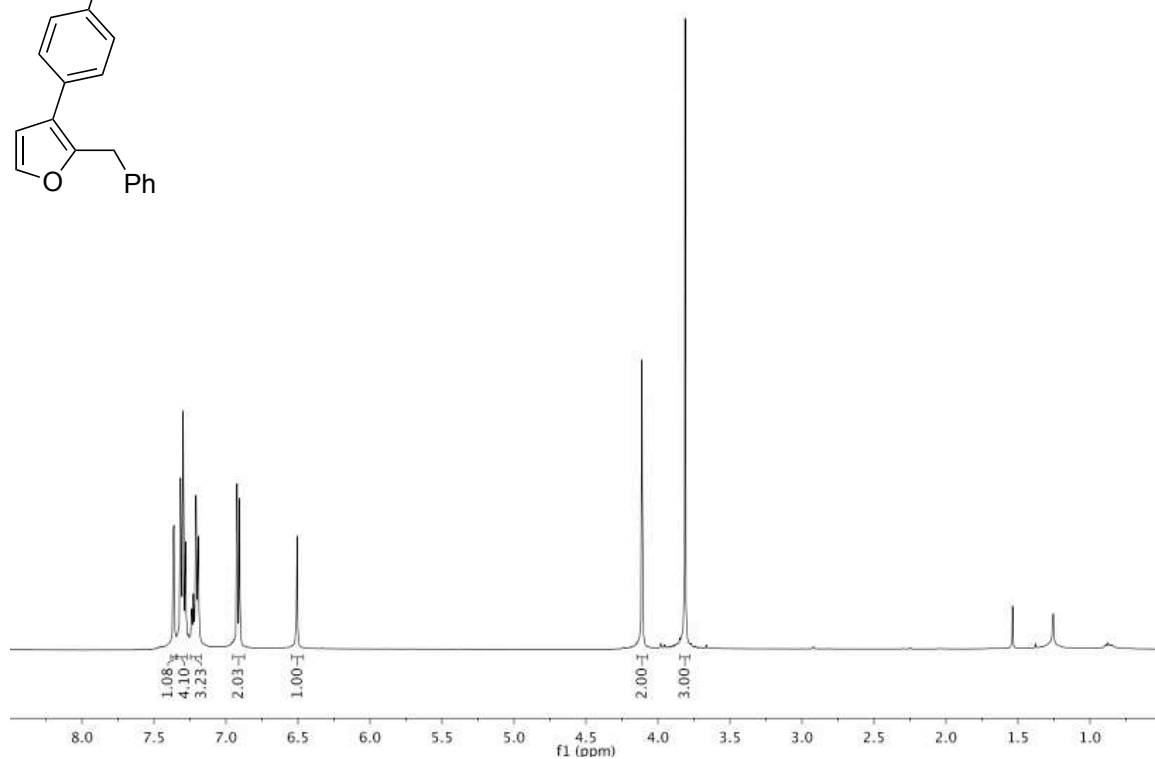
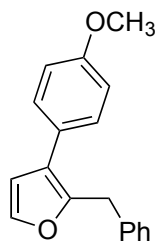


Figure A4.6 500 MHz ¹H and 125 MHz ¹³C{¹H} NMR of 4.3ac in CDCl₃

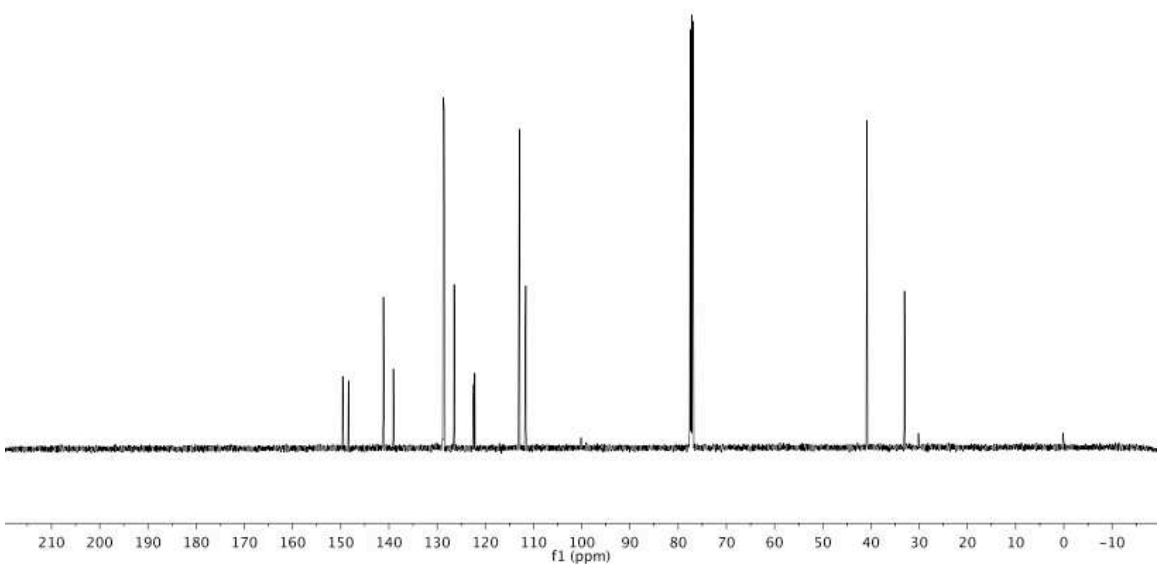
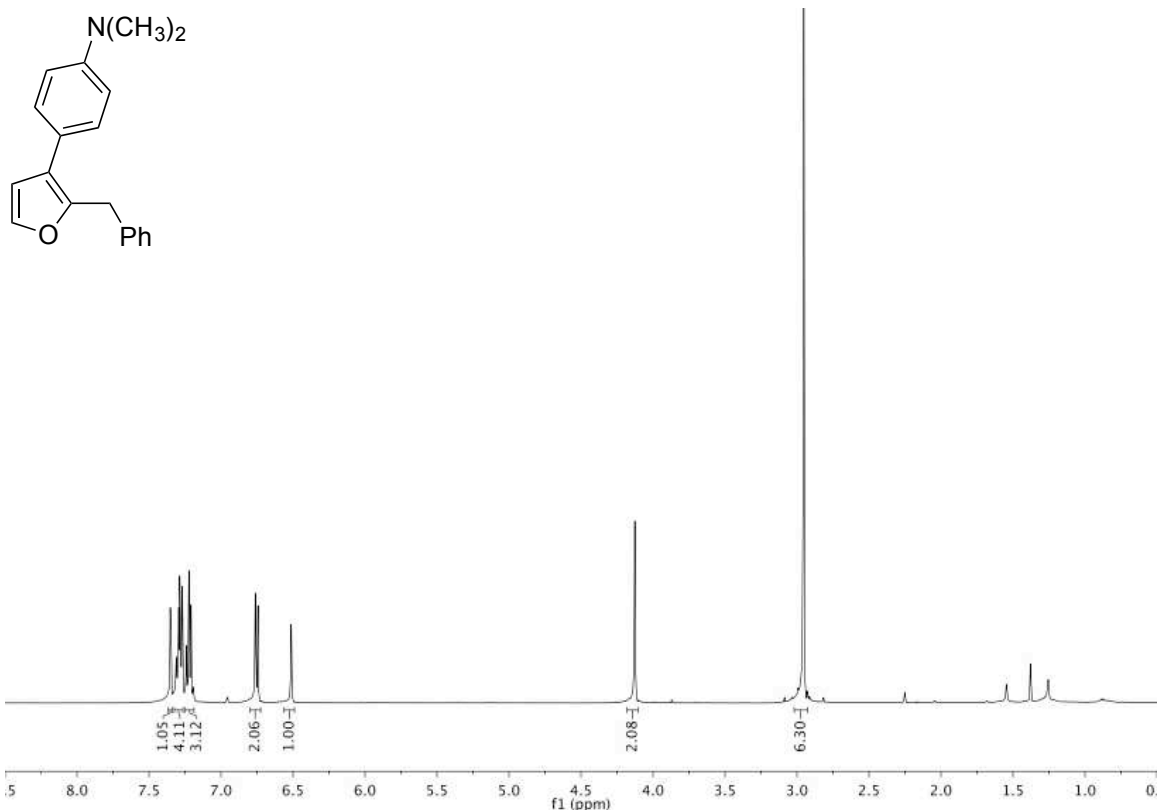


Figure A4.7 500 MHz ¹H and 125 MHz ¹³C{¹H} NMR of 4.3ad in CDCl₃

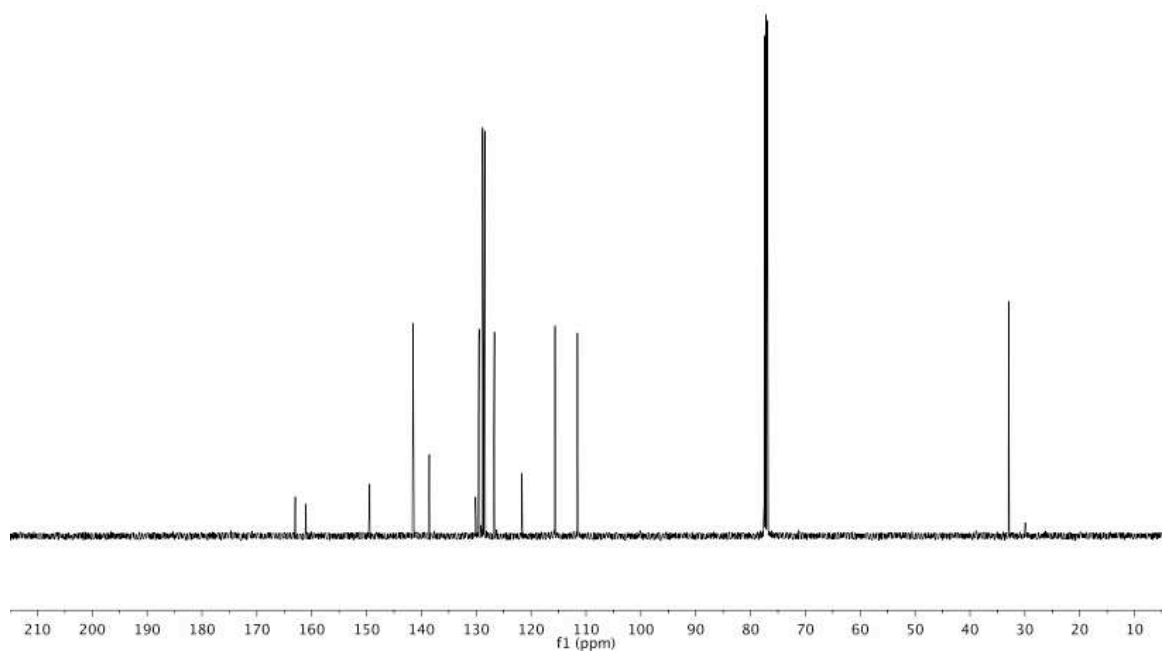
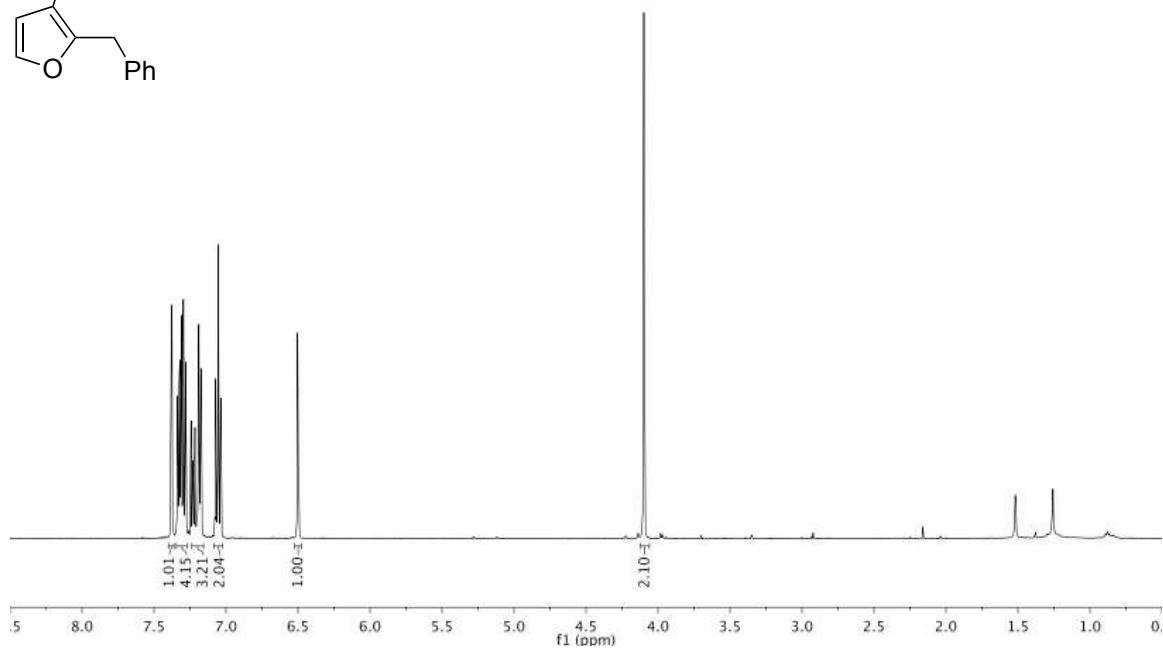
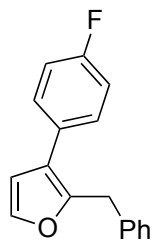


Figure A4.8 500 MHz ^1H and 125 MHz $^{13}\text{C}\{^1\text{H}\}$ NMR of **4.3ae** in CDCl_3

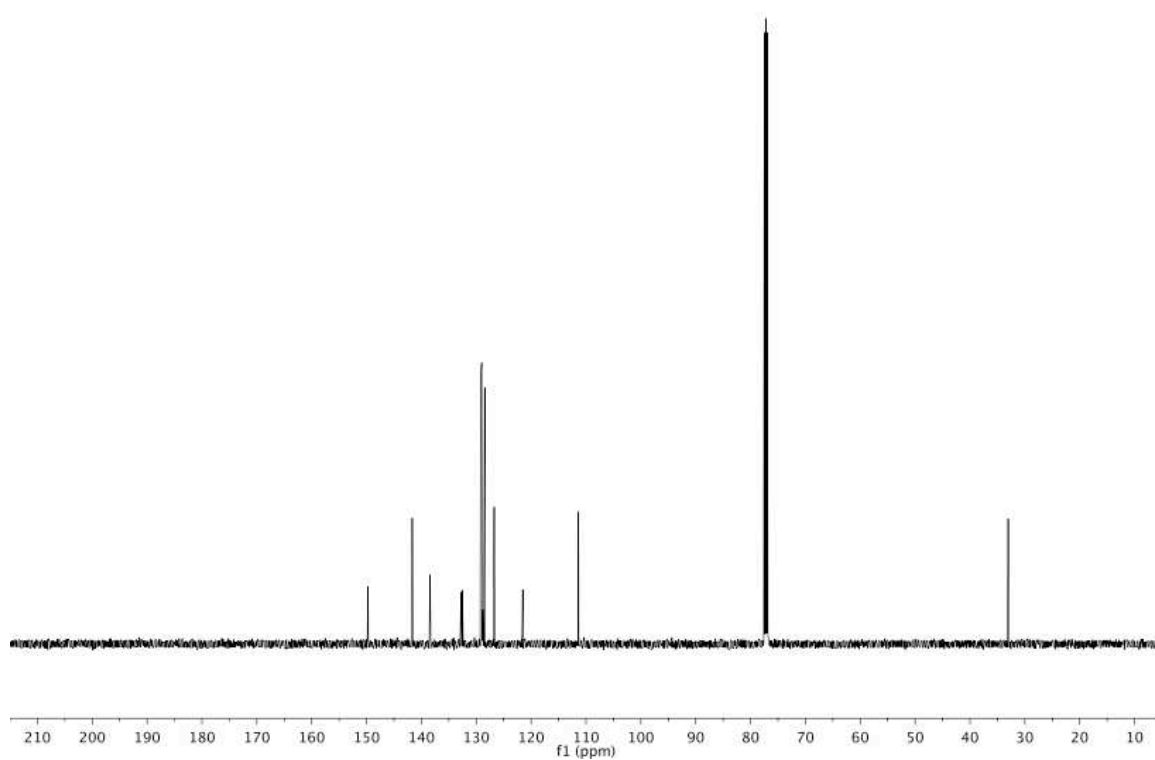
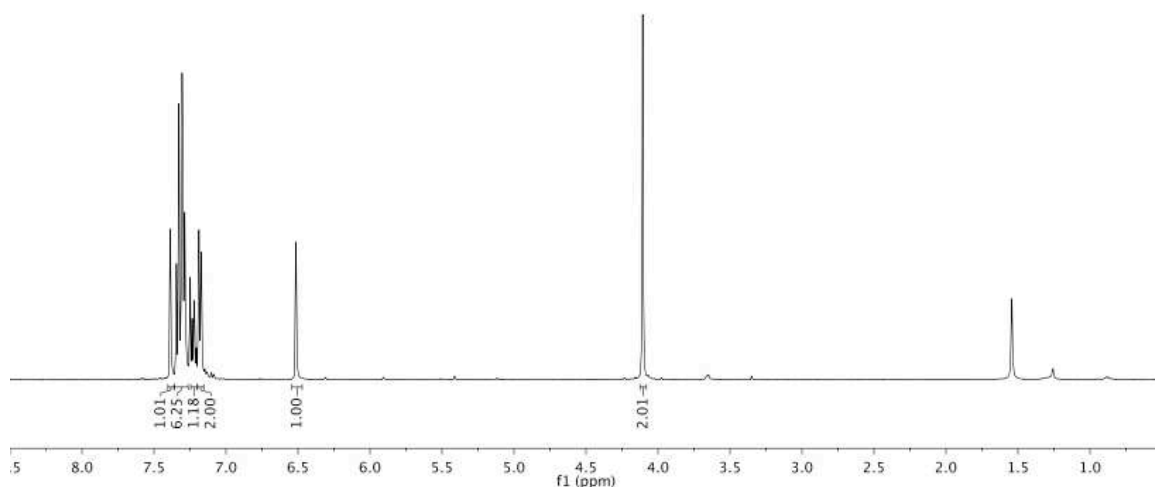
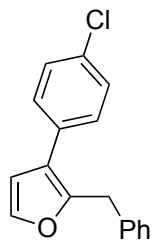


Figure A4.9 500 MHz ^1H and 125 MHz $^{13}\text{C}\{^1\text{H}\}$ NMR of **4.3af** in CDCl_3

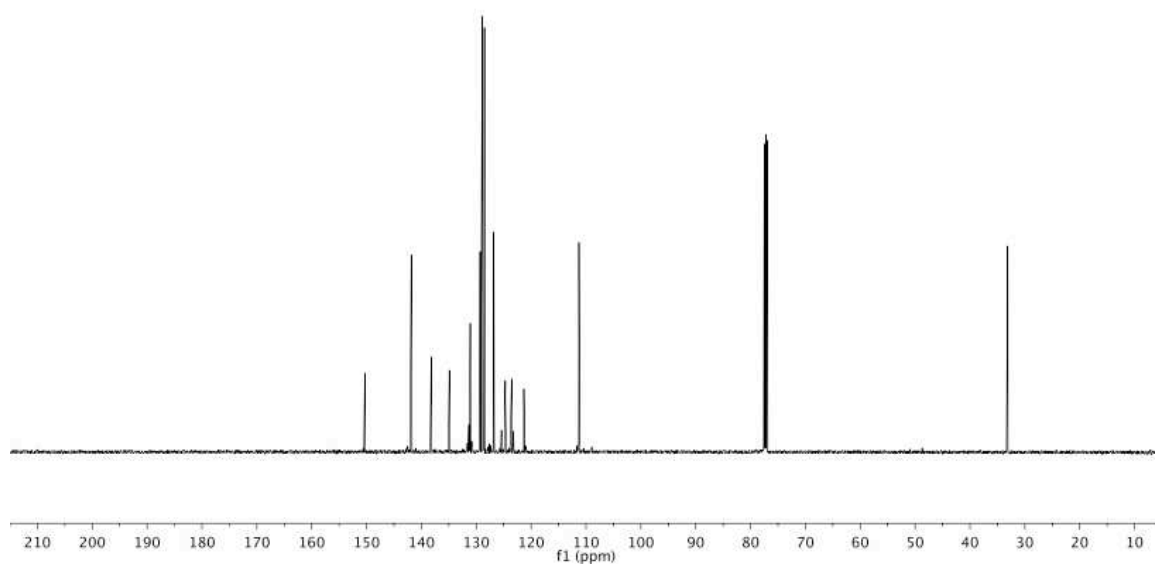
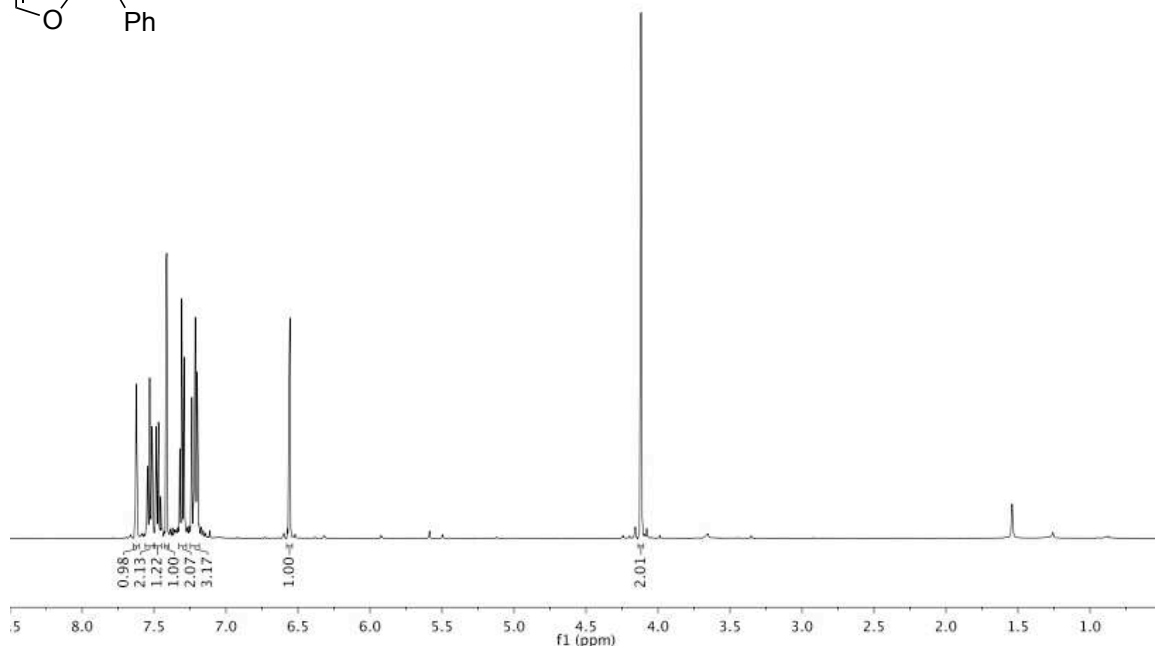
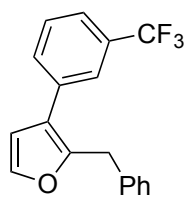


Figure A4.10 500 MHz ¹H and 125 MHz ¹³C{¹H} NMR of **4.3ag** in CDCl₃

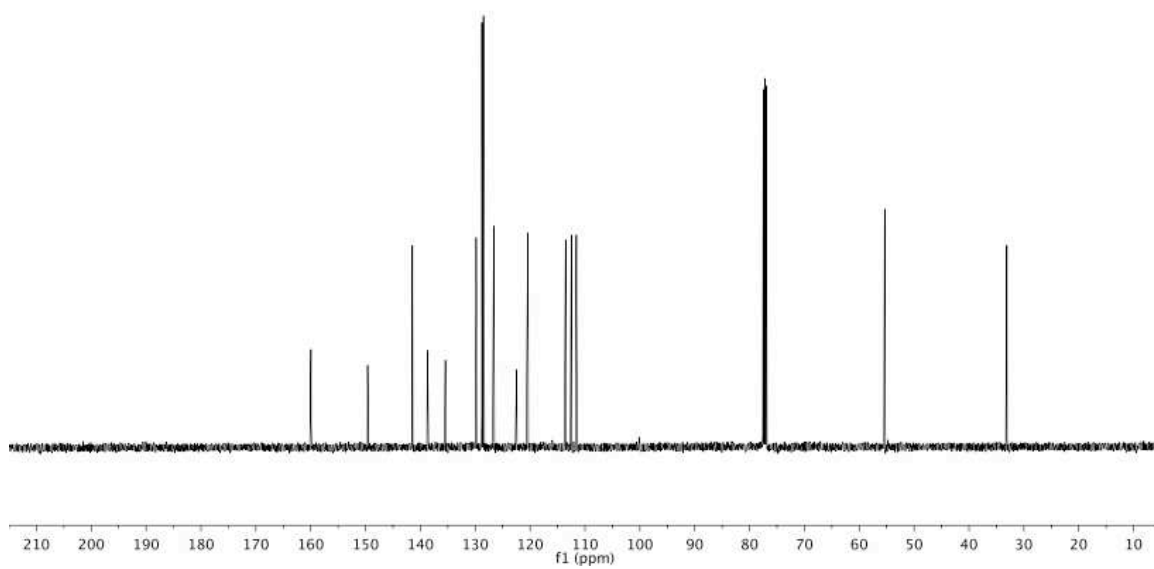
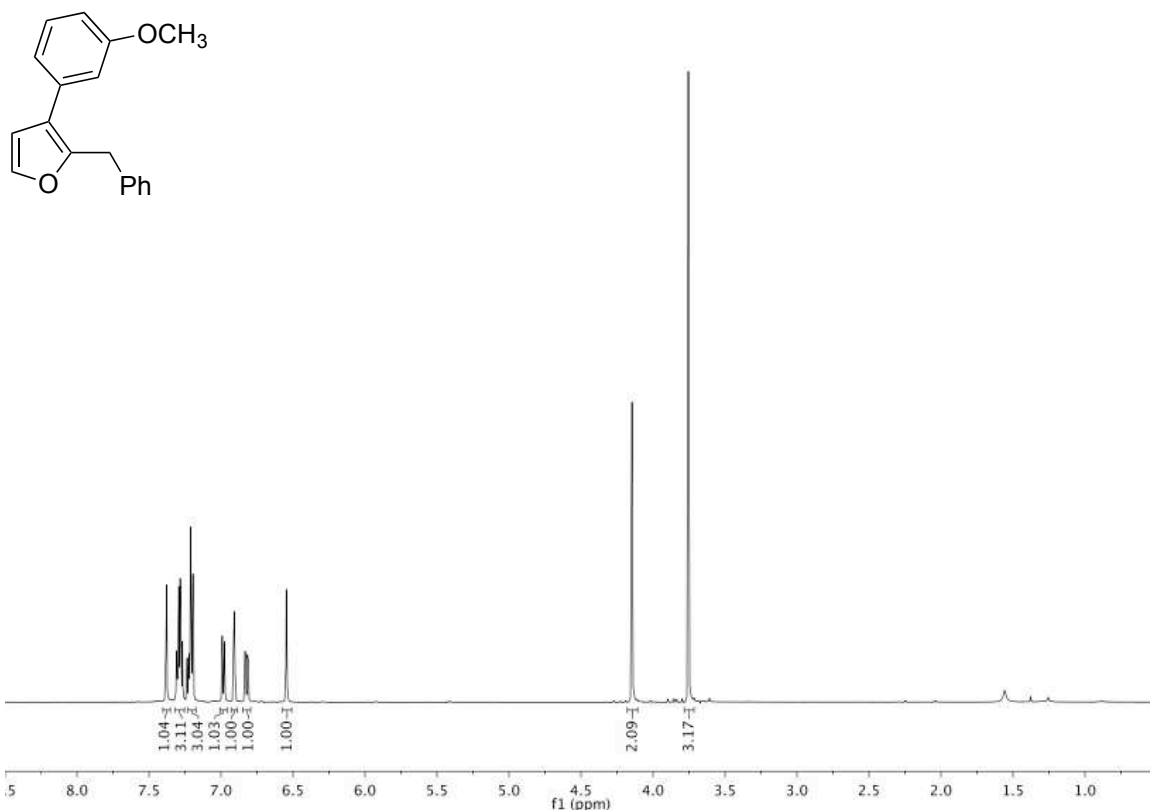


Figure A4.11 500 MHz ¹H and 125 MHz ¹³C{¹H} NMR of **4.3ah** in CDCl₃

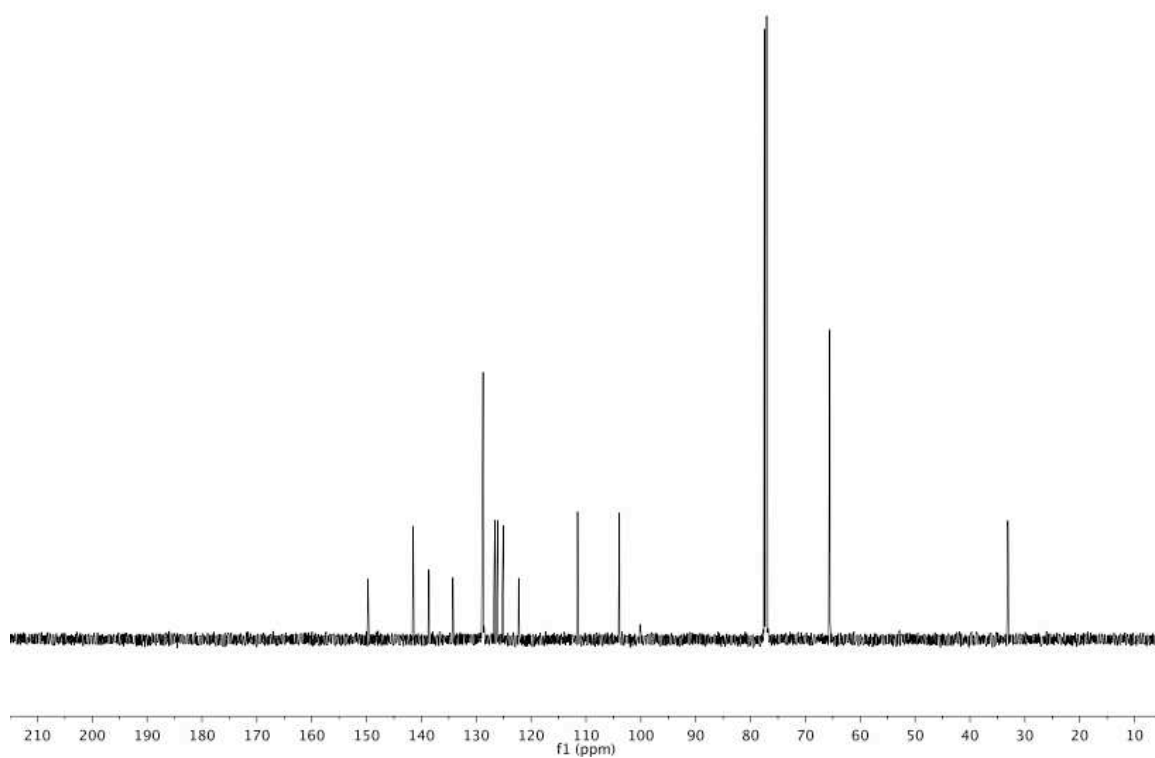
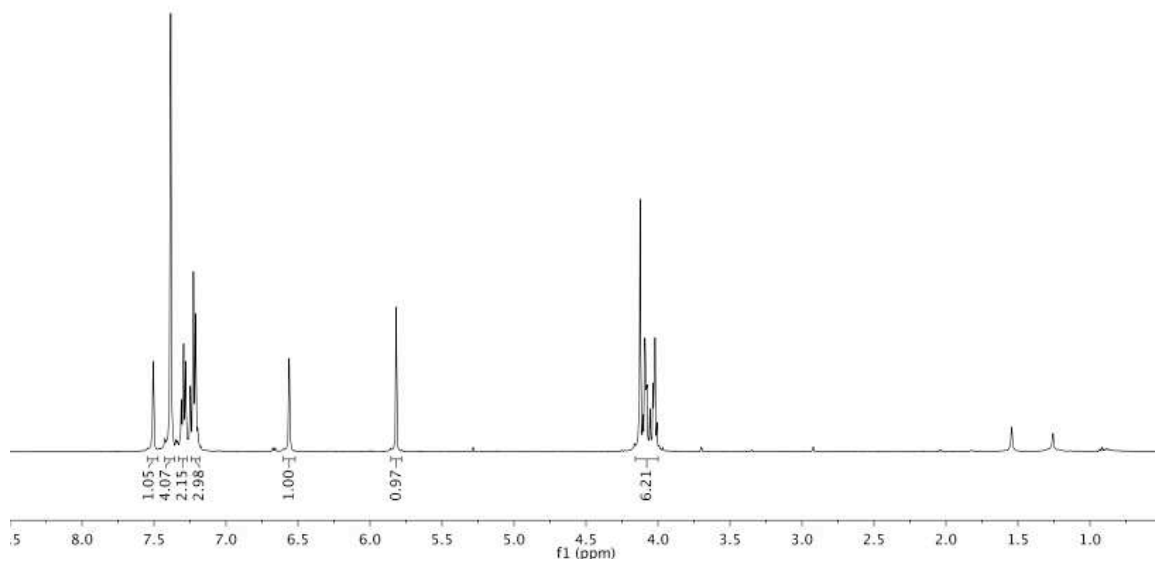
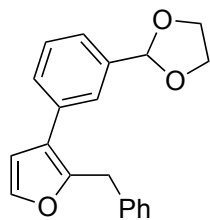


Figure A4.12 500 MHz ^1H and 125 MHz $^{13}\text{C}\{^1\text{H}\}$ NMR of **4.3ai** in CDCl_3

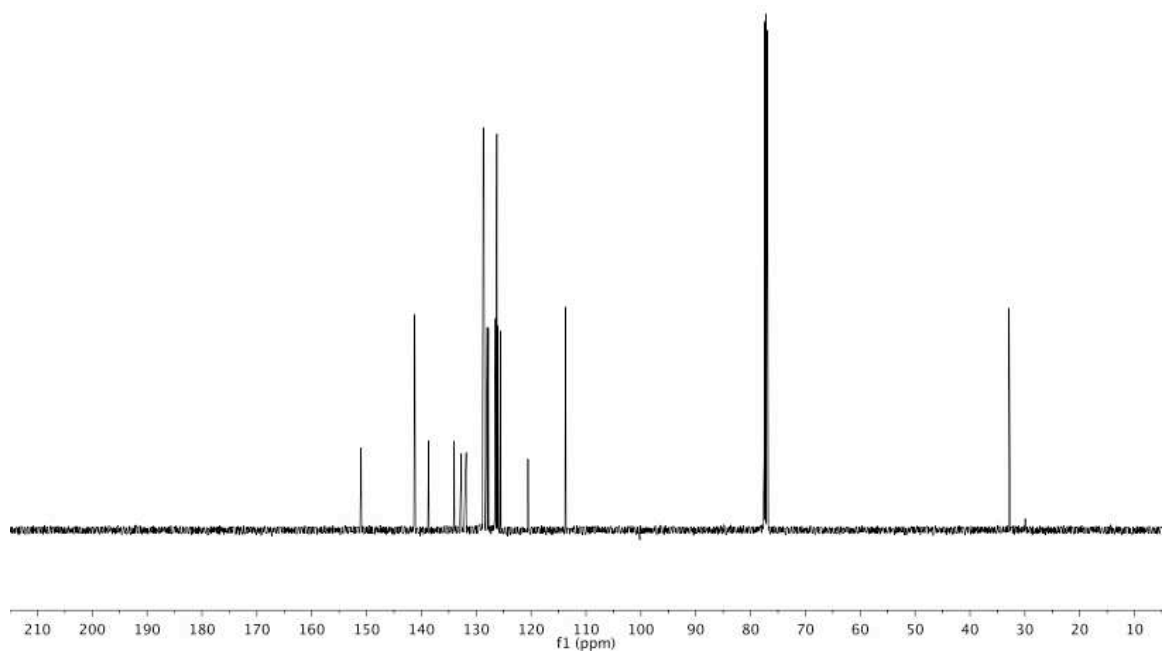
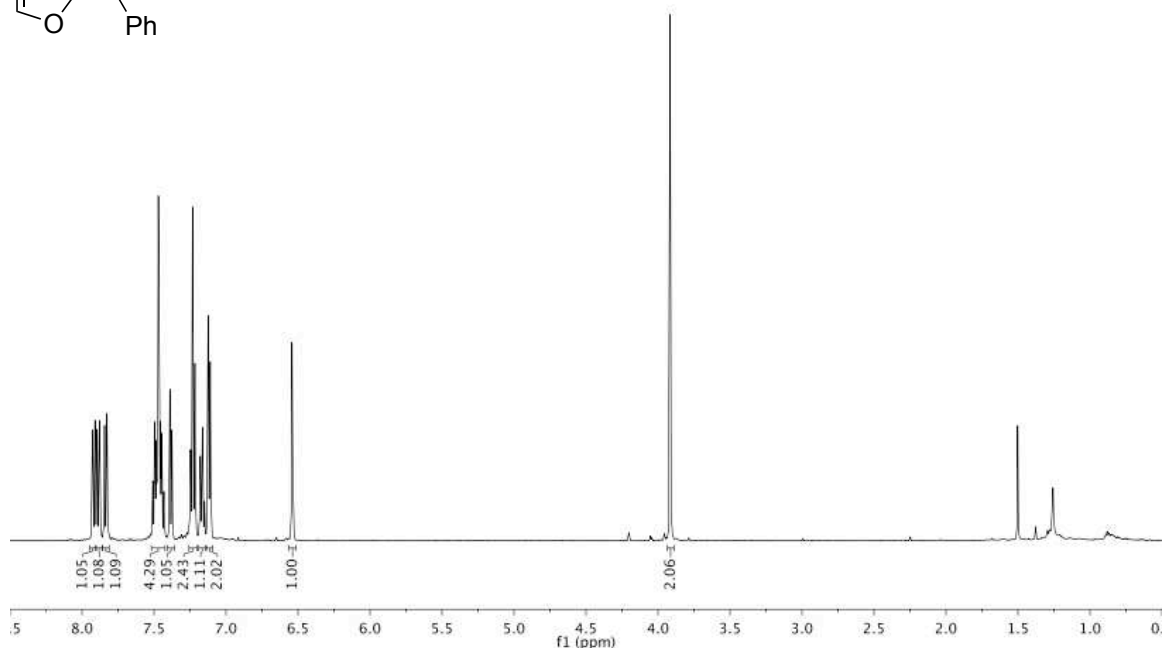
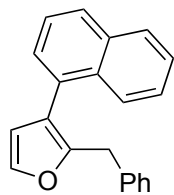


Figure A4.13 500 MHz ¹H and 125 MHz ¹³C{¹H} NMR of 4.3aj in CDCl₃

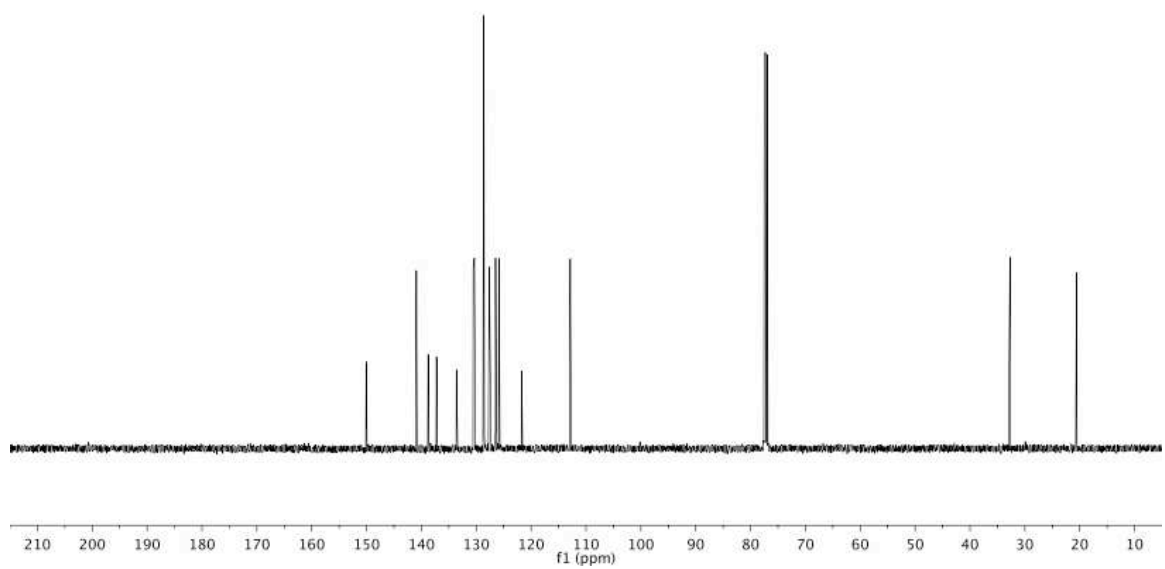
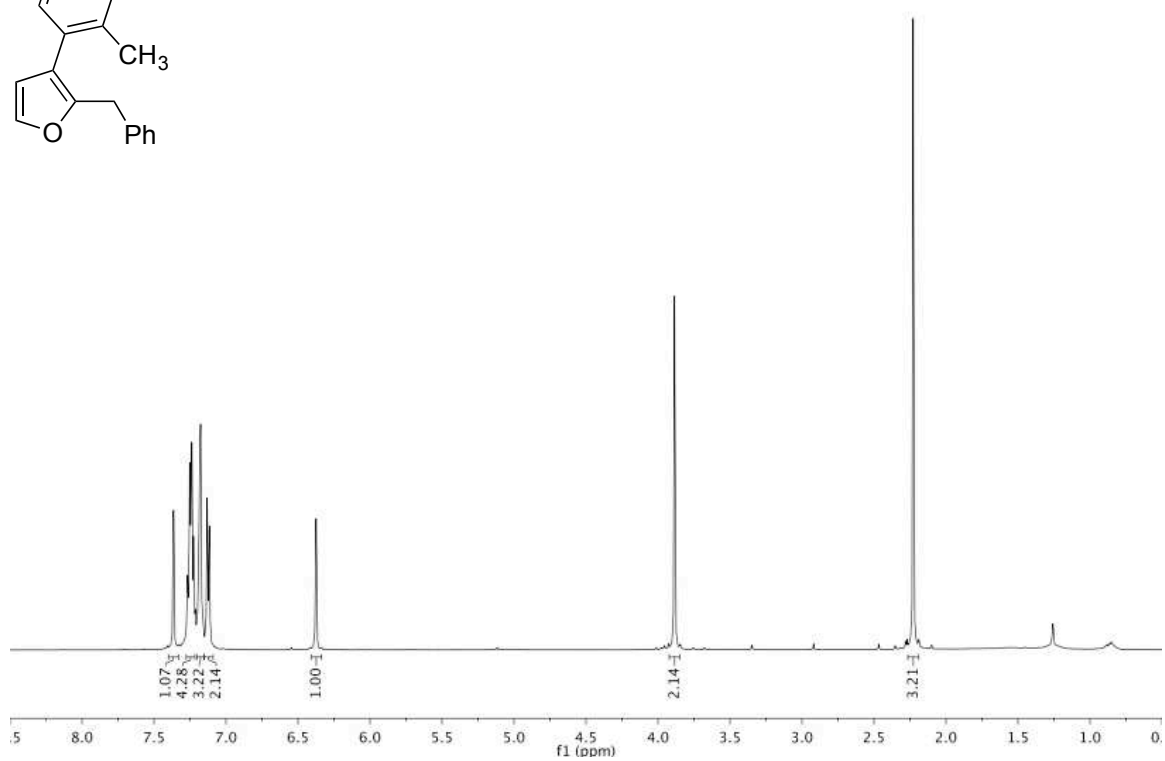
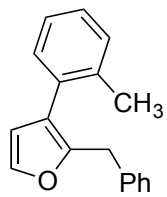


Figure A4.14 500 MHz ¹H and 125 MHz ¹³C{¹H} NMR of **4.3ak** in CDCl₃

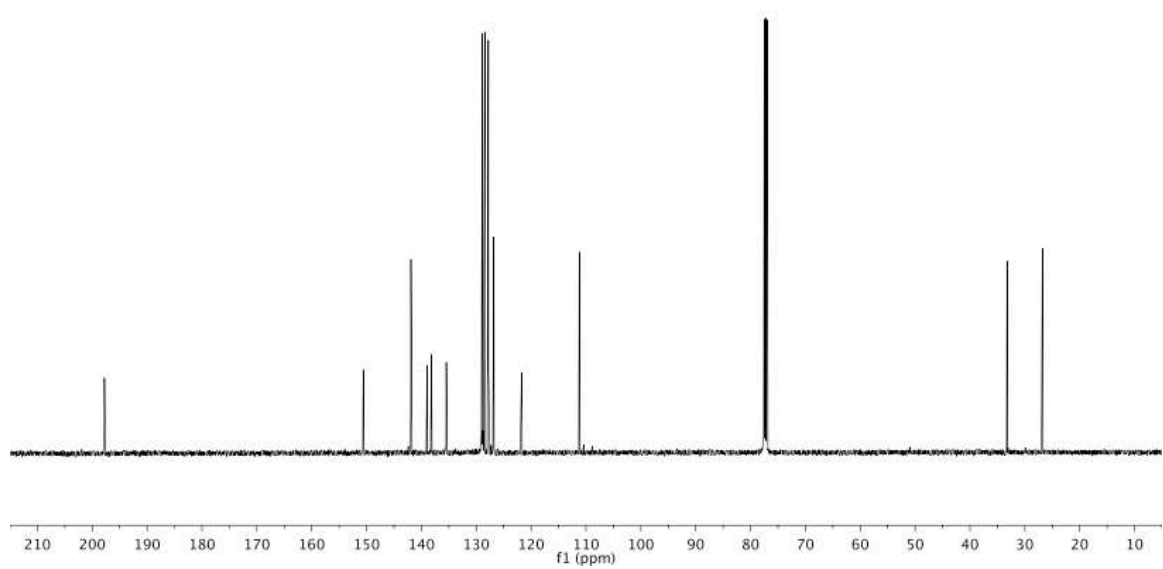
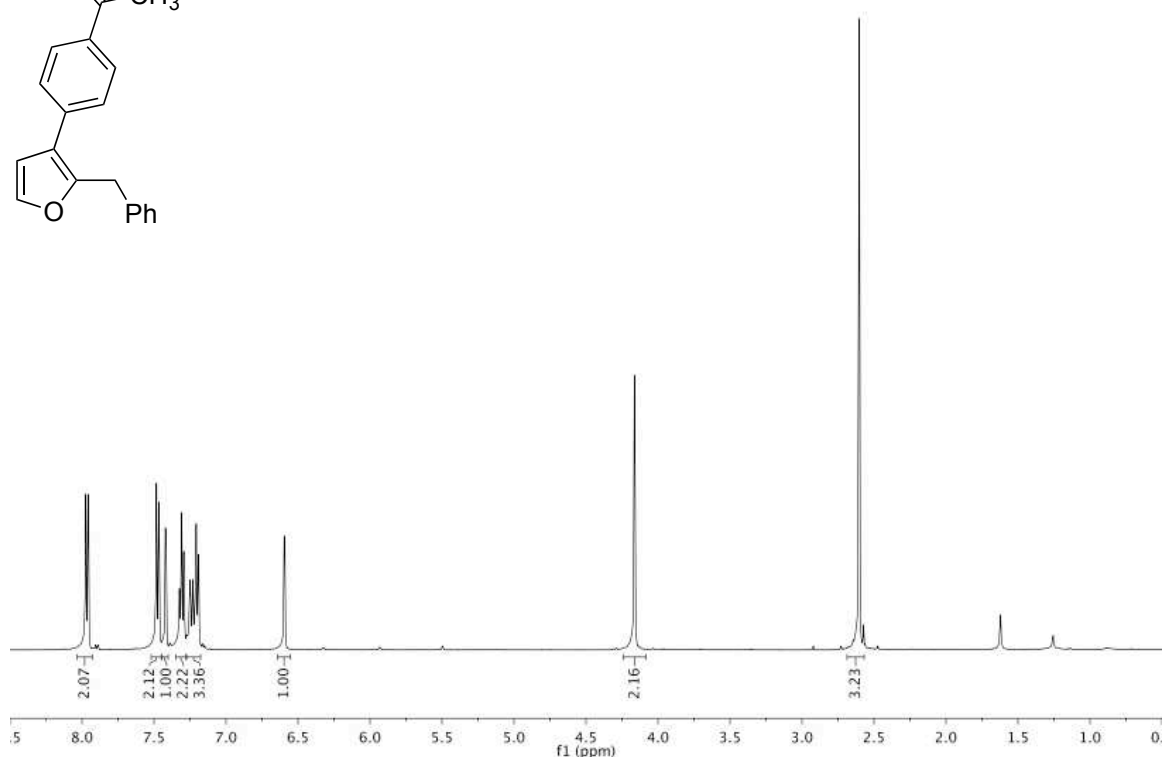
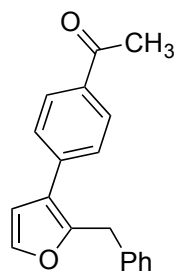


Figure A4.15 500 MHz ^1H and 125 MHz $^{13}\text{C}\{^1\text{H}\}$ NMR of **4.3aI** in CDCl_3

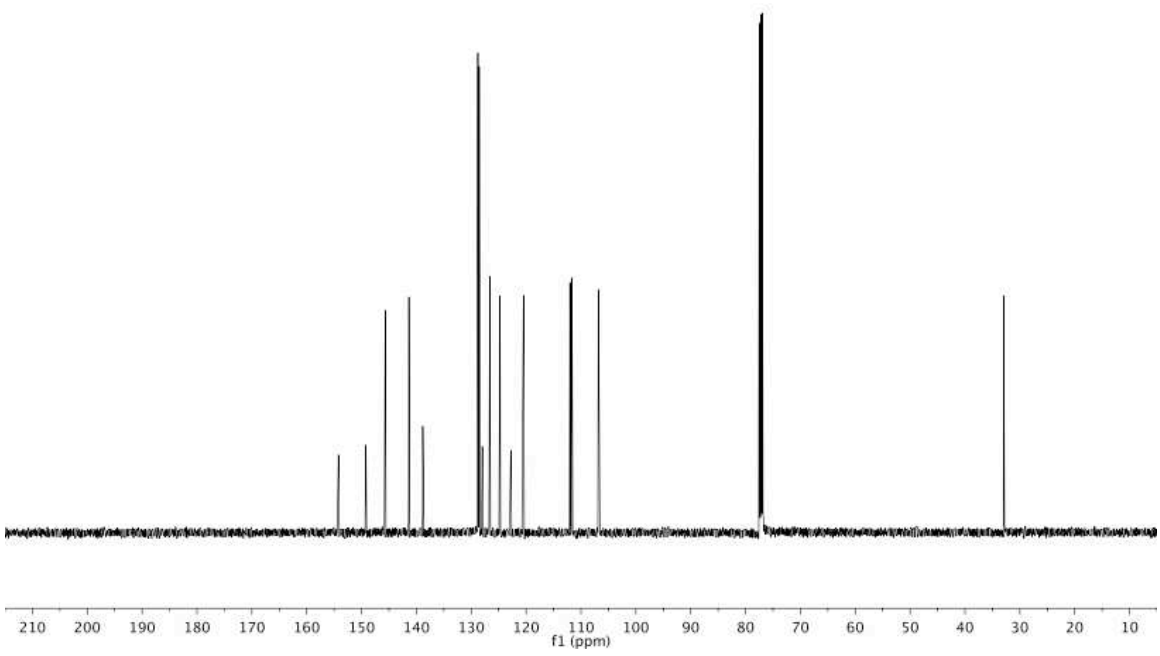
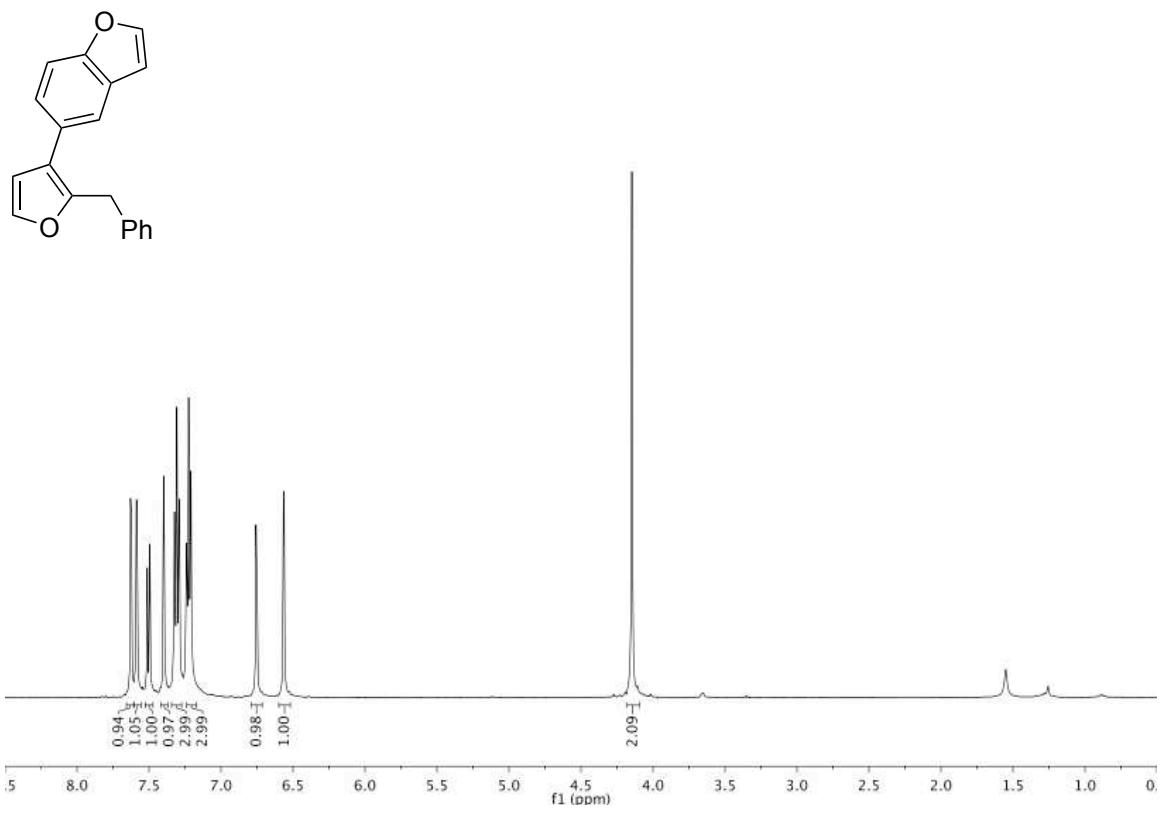


Figure A4.16 500 MHz ^1H and 125 MHz $^{13}\text{C}\{^1\text{H}\}$ NMR of 4.3am in CDCl_3

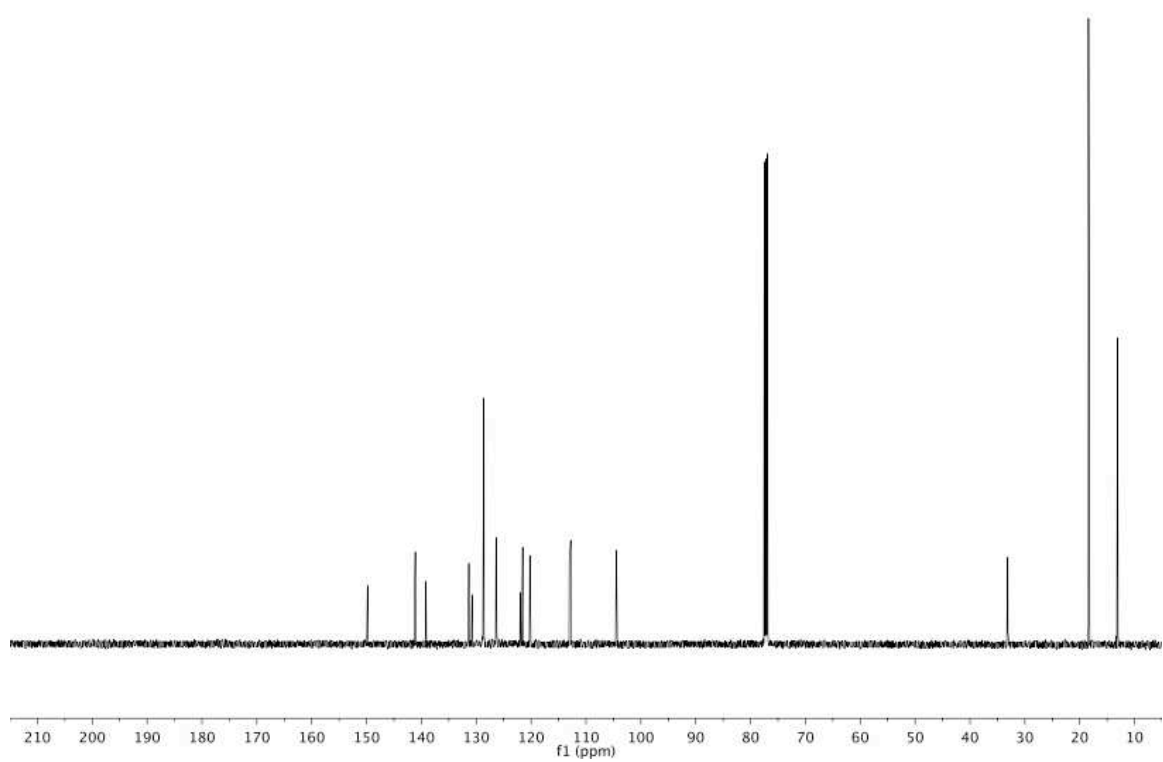
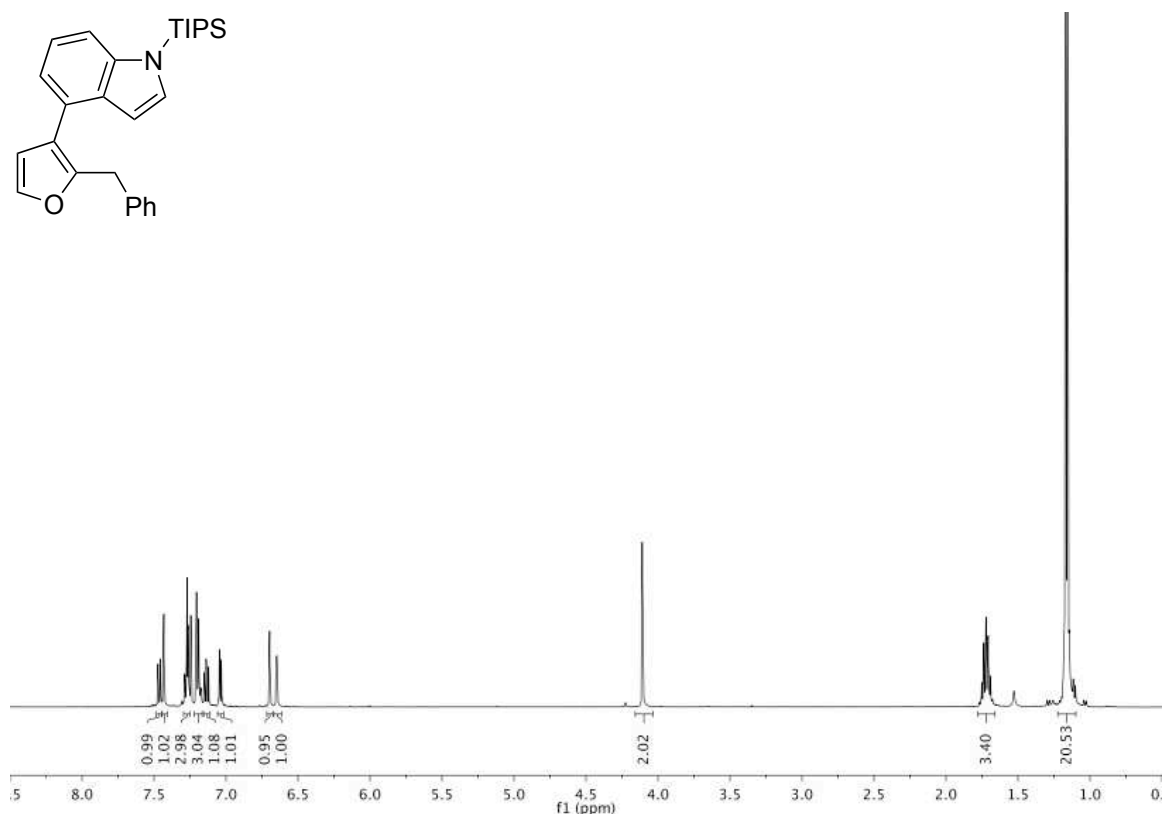
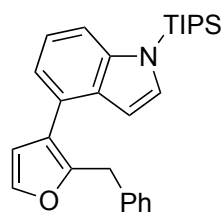


Figure A4.17 500 MHz ^1H and 125 MHz $^{13}\text{C}\{^1\text{H}\}$ NMR of 4.3an in CDCl_3

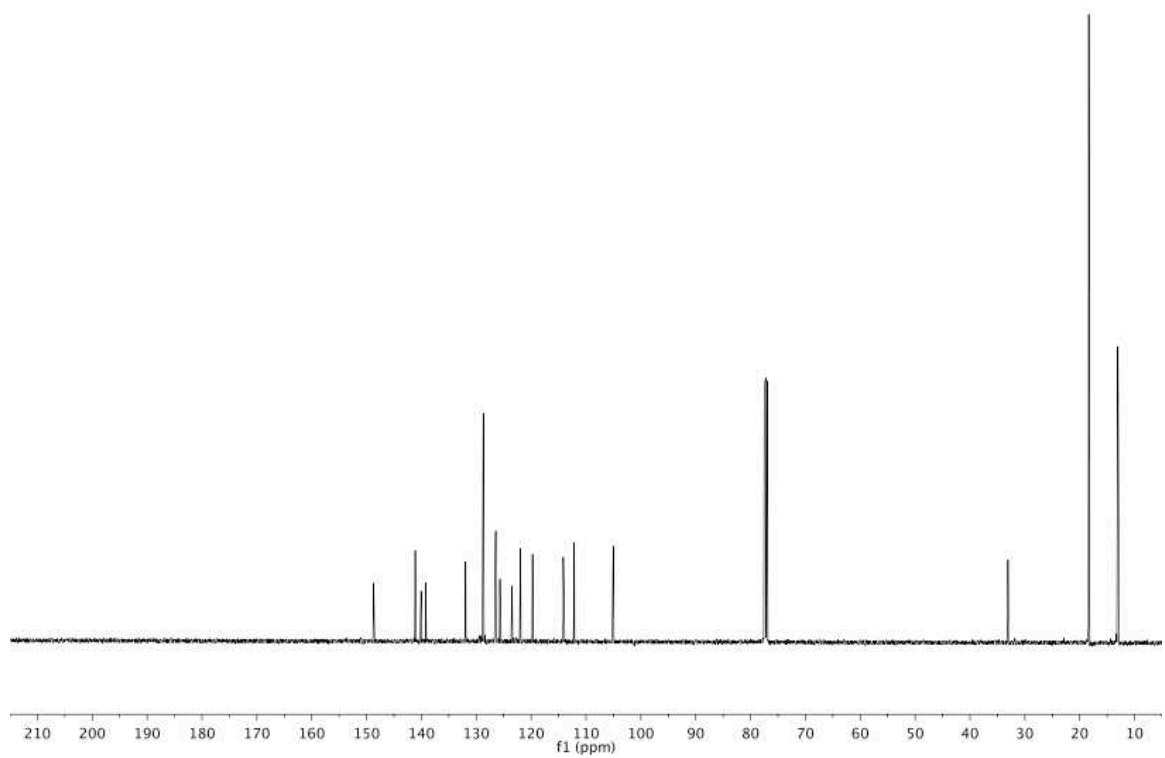
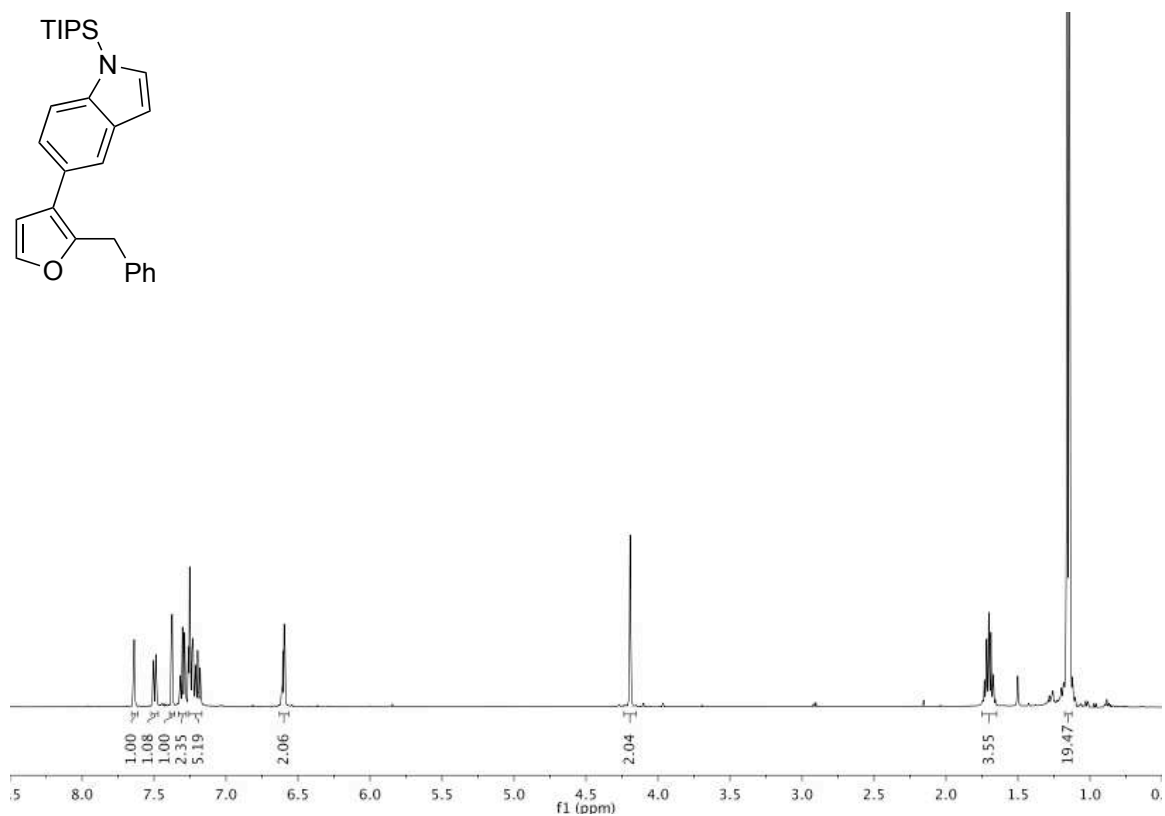
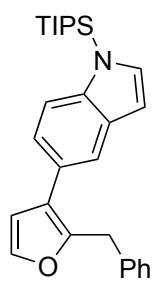


Figure A4.18 500 MHz ¹H and 125 MHz ¹³C{¹H} NMR of **4.3ao** in CDCl₃

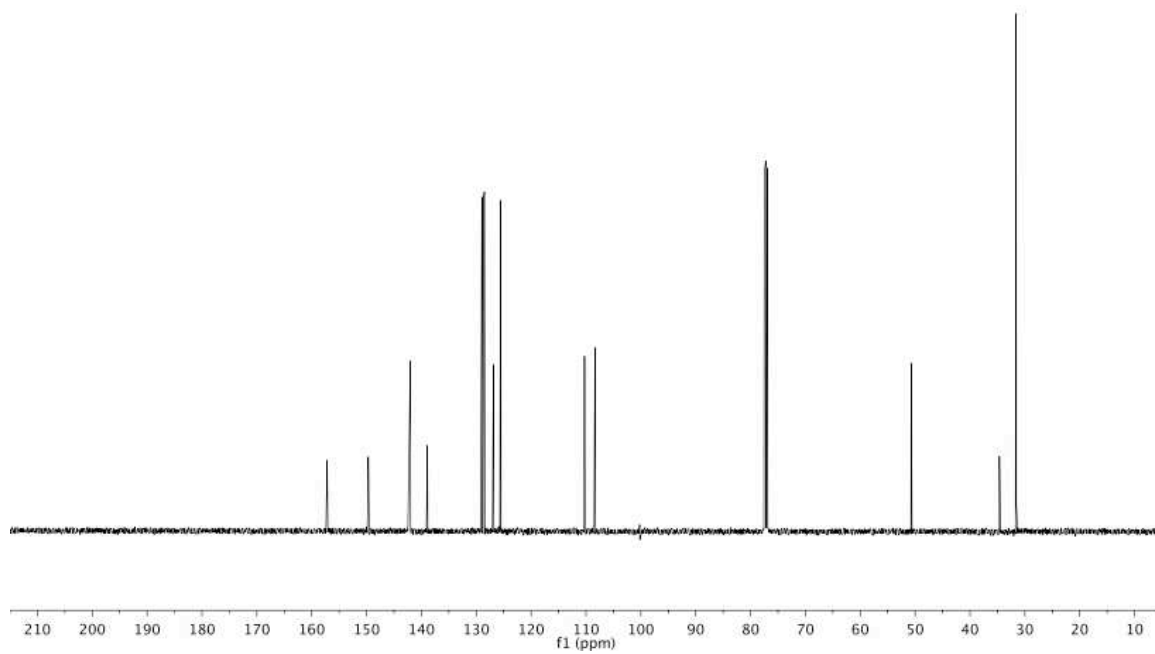
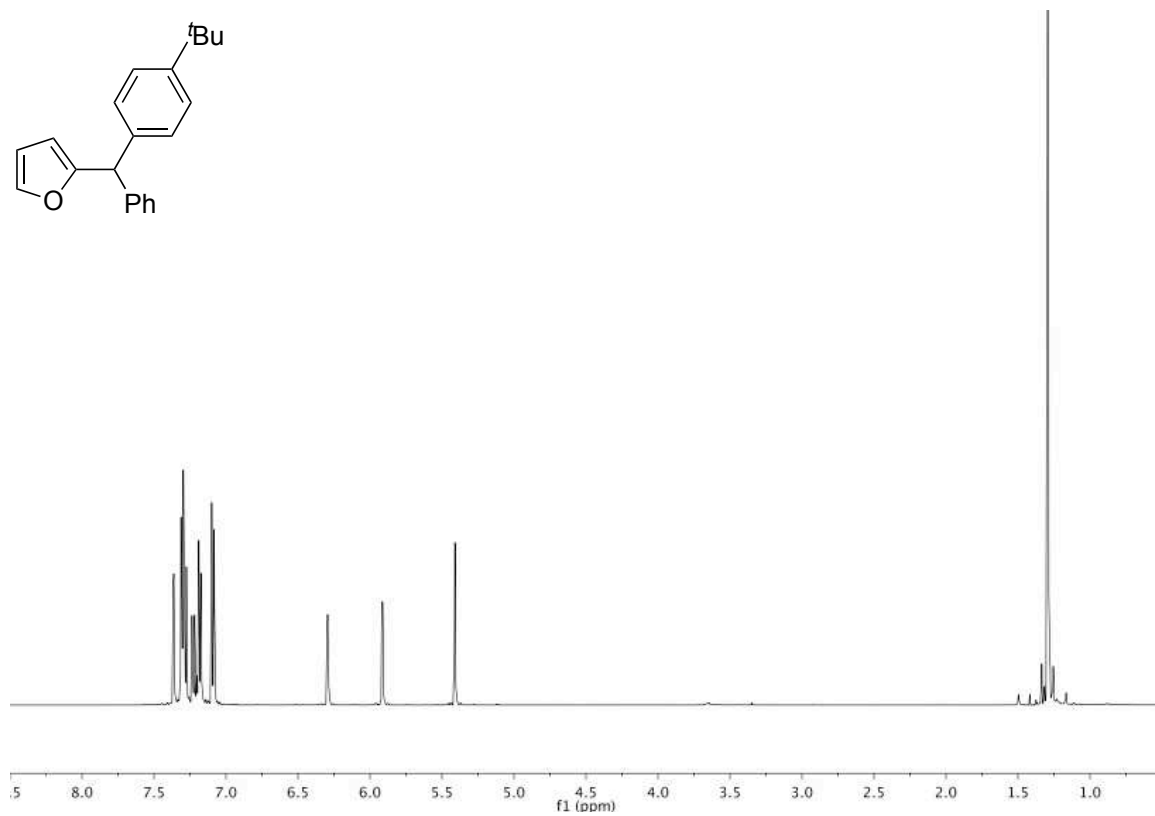
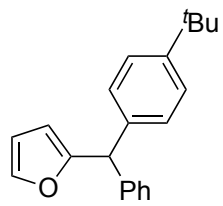


Figure A4.19 500 MHz ^1H and 125 MHz $^{13}\text{C}\{^1\text{H}\}$ NMR of **4.5ab** in CDCl_3

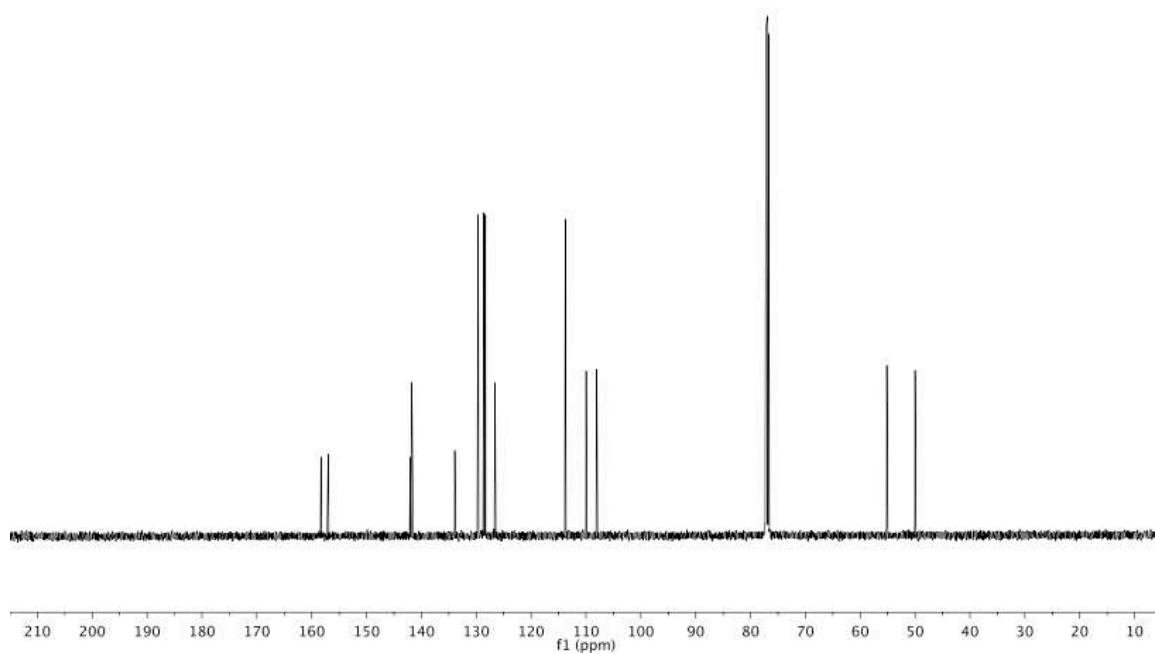
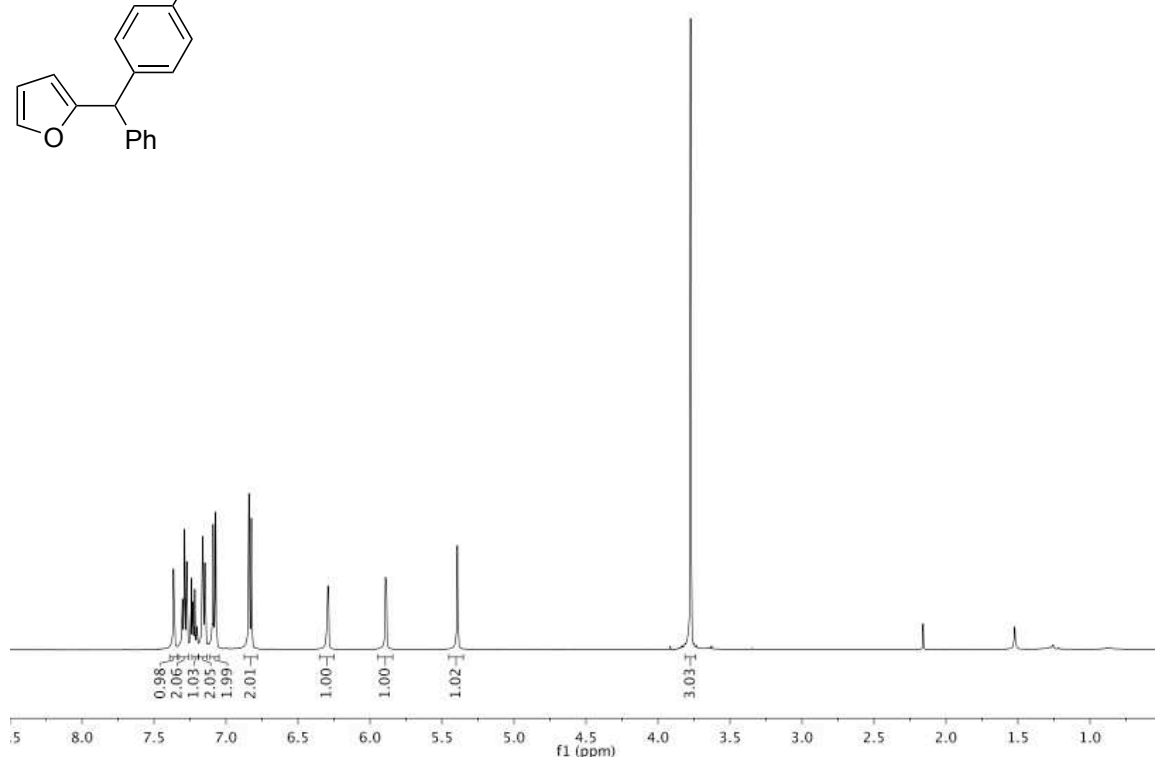
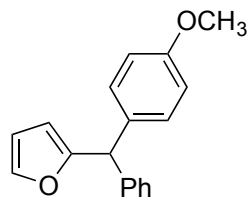


Figure A4.20 500 MHz ^1H and 125 MHz $^{13}\text{C}\{^1\text{H}\}$ NMR of 4.5ac in CDCl_3

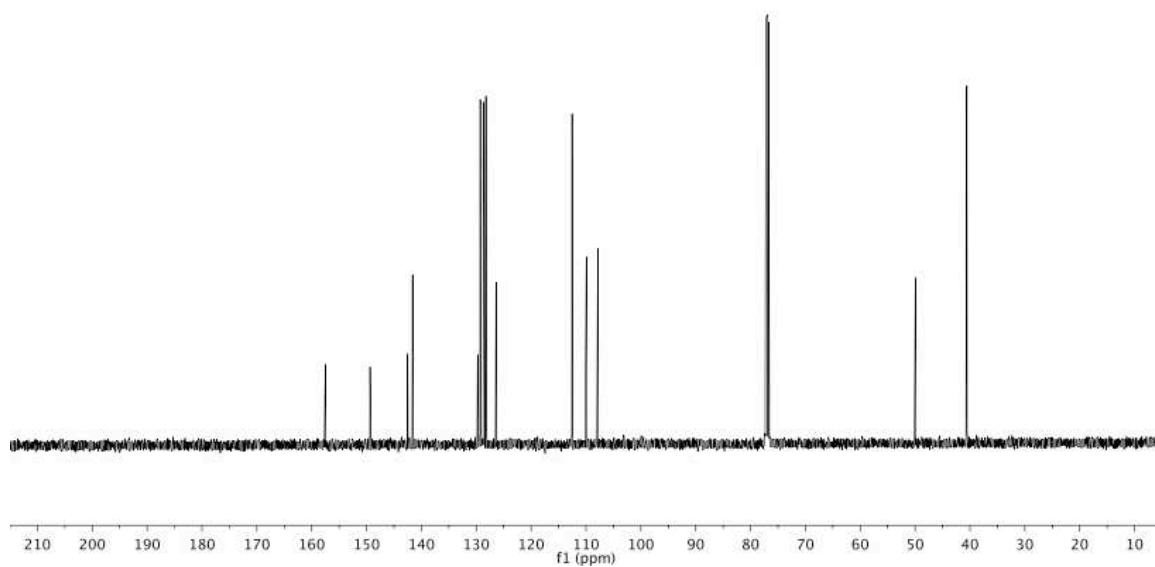
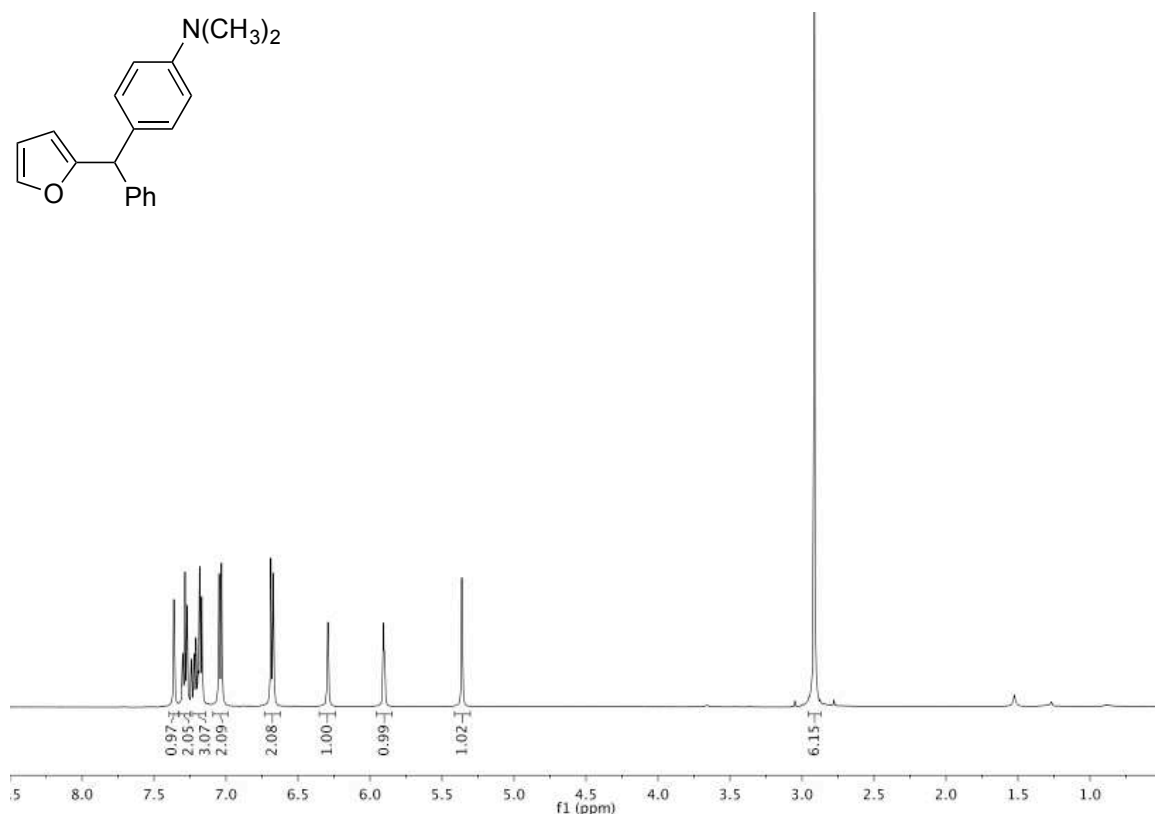
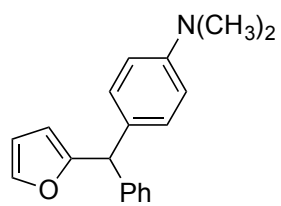


Figure A4.21 500 MHz ^1H and 125 MHz $^{13}\text{C}\{^1\text{H}\}$ NMR of **4.5ad** in CDCl_3

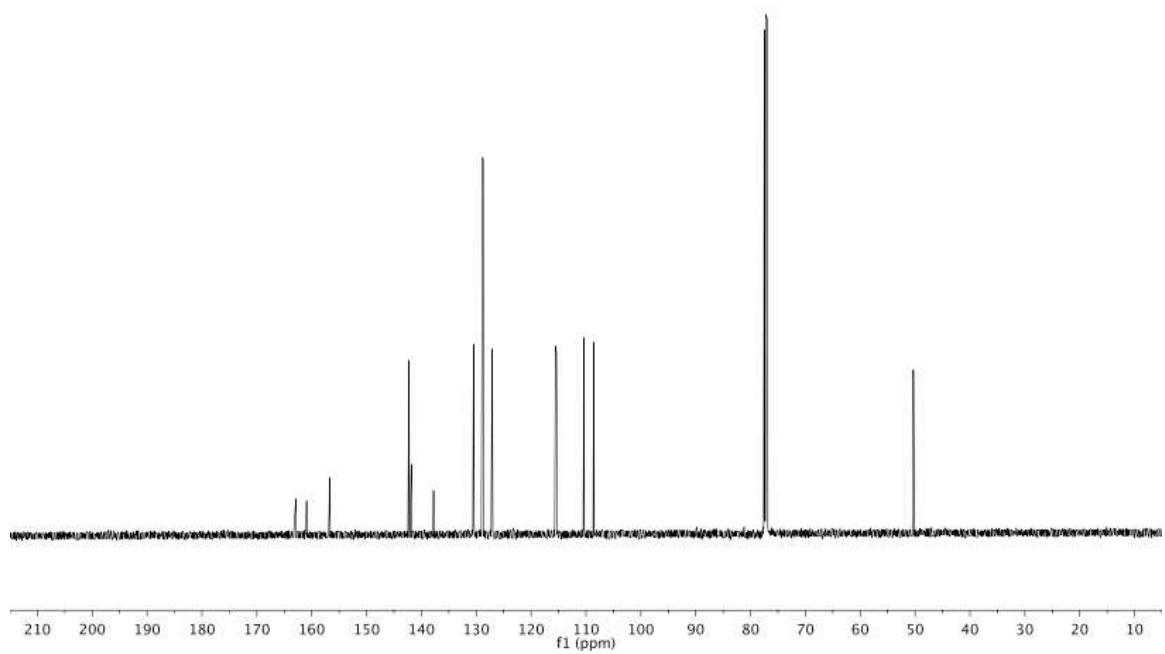
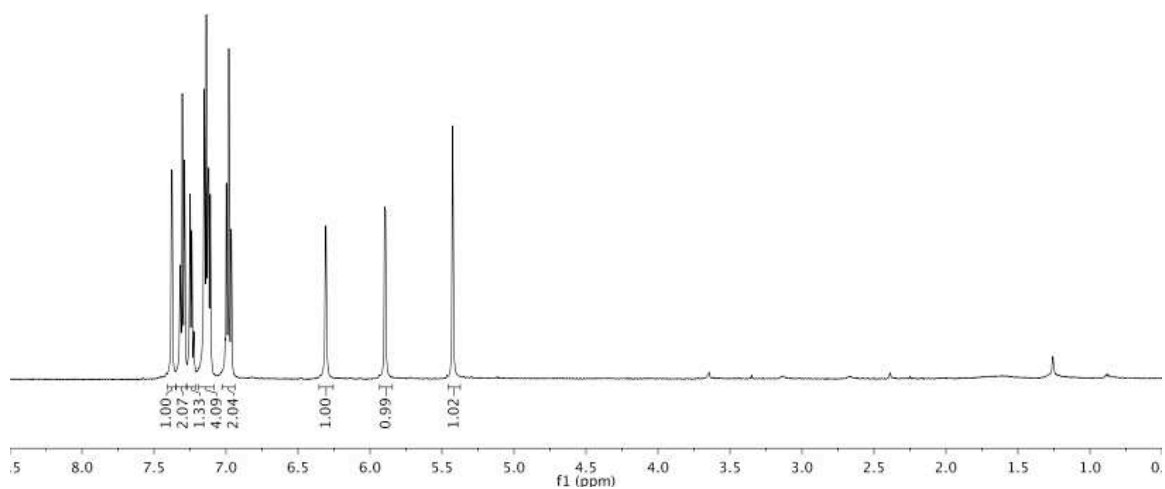
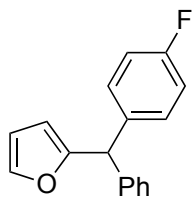


Figure A4.22 500 MHz ^1H and 125 MHz $^{13}\text{C}\{^1\text{H}\}$ NMR of **4.5ae** in CDCl_3

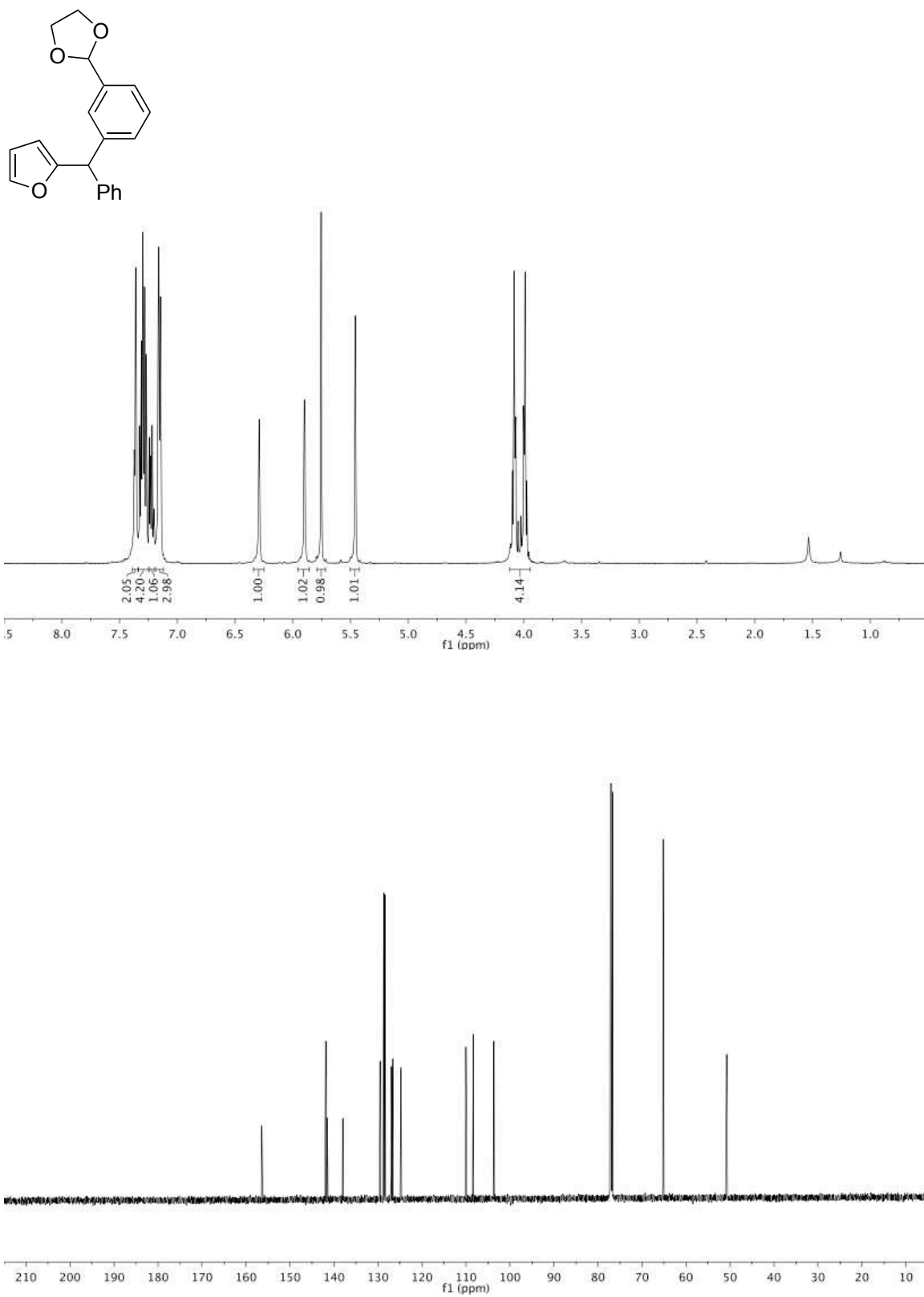


Figure A4.23 500 MHz ^1H and 125 MHz $^{13}\text{C}\{^1\text{H}\}$ NMR of **4.5ai** in CDCl_3

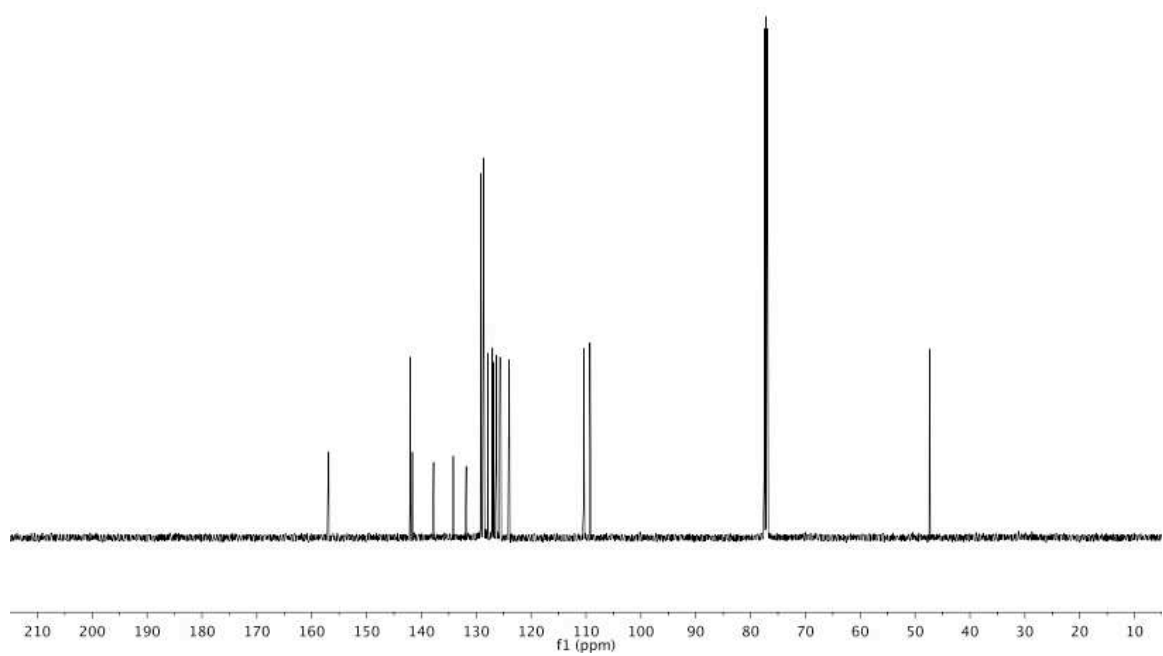
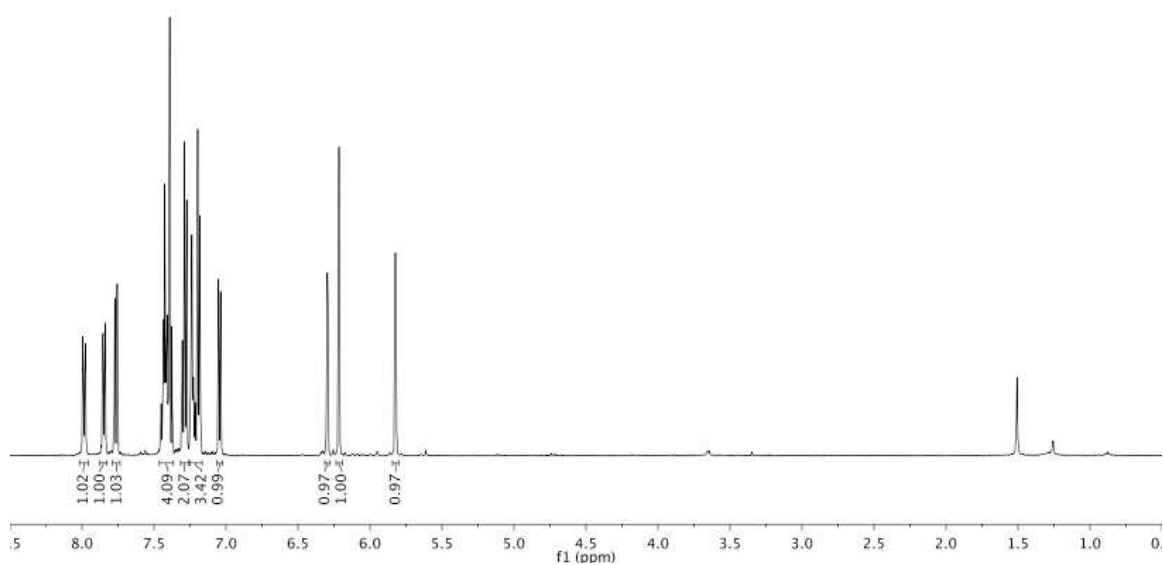
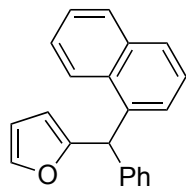


Figure A4.24 500 MHz ^1H and 125 MHz $^{13}\text{C}\{^1\text{H}\}$ NMR of **4.5aj** in CDCl_3

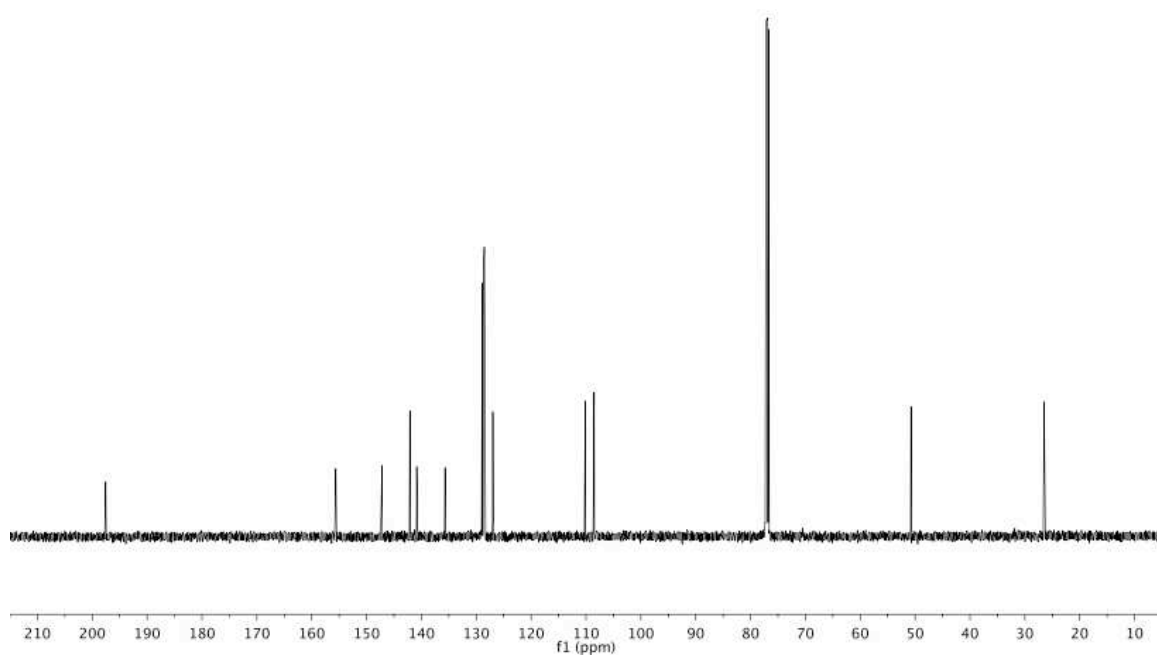
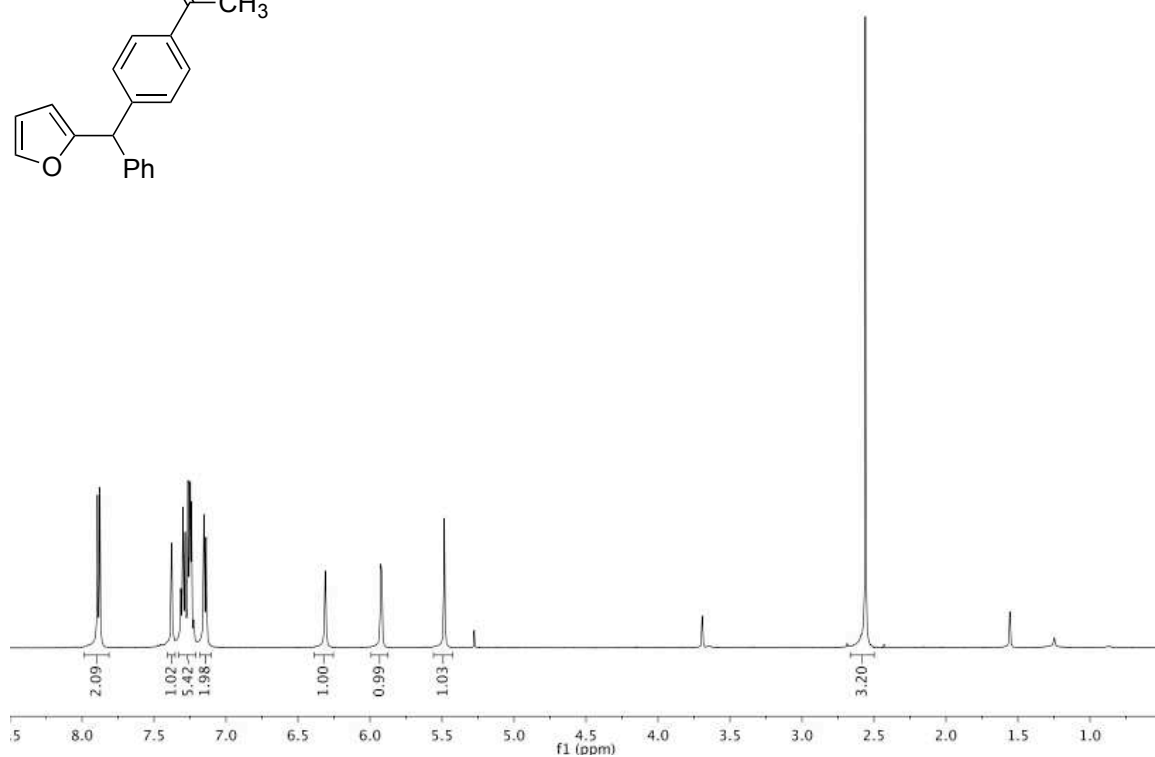
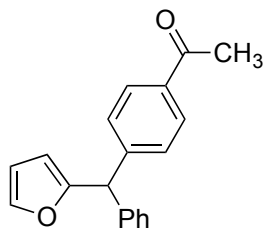


Figure A4.25 500 MHz ¹H and 125 MHz ¹³C{¹H} NMR of **4.5aI** in CDCl₃

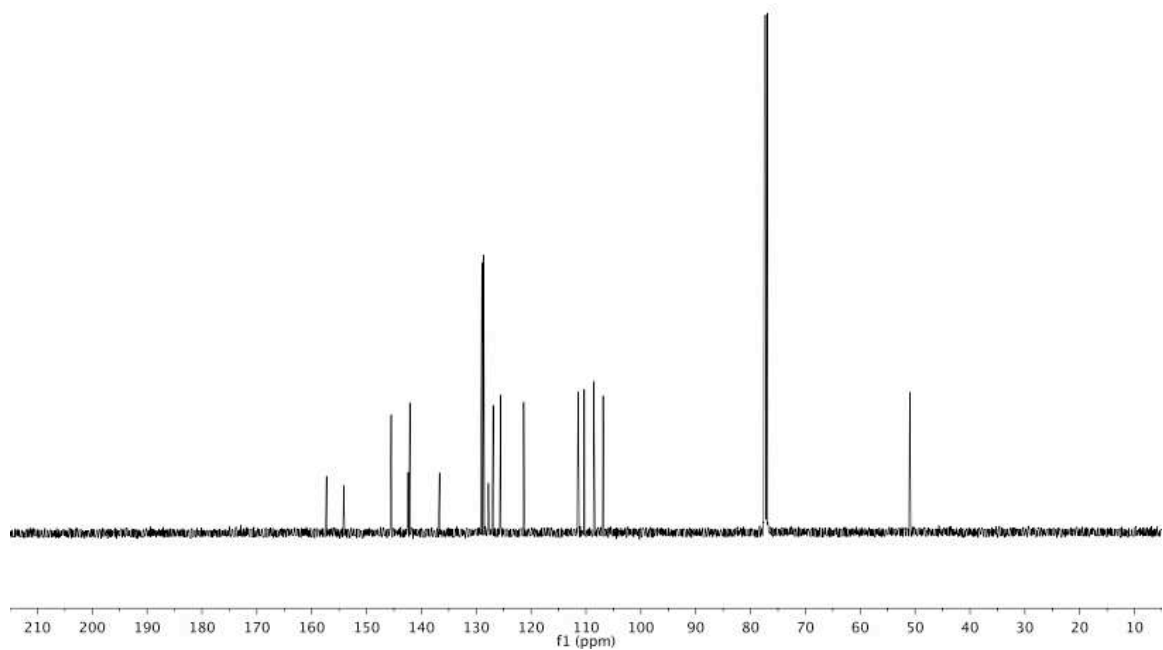
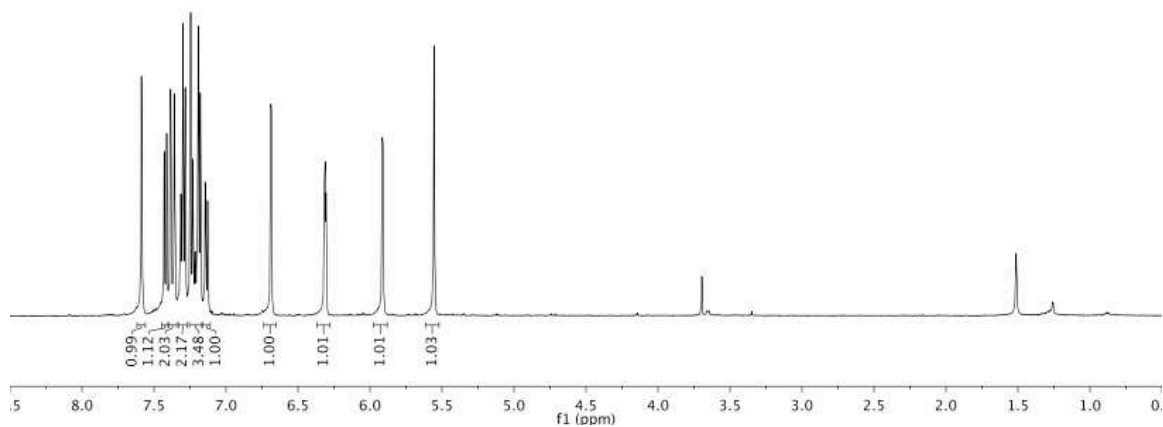
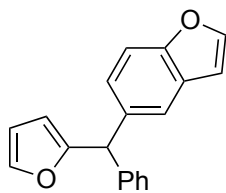


Figure A4.26 500 MHz ^1H and 125 MHz $^{13}\text{C}\{^1\text{H}\}$ NMR of 4.5am in CDCl_3

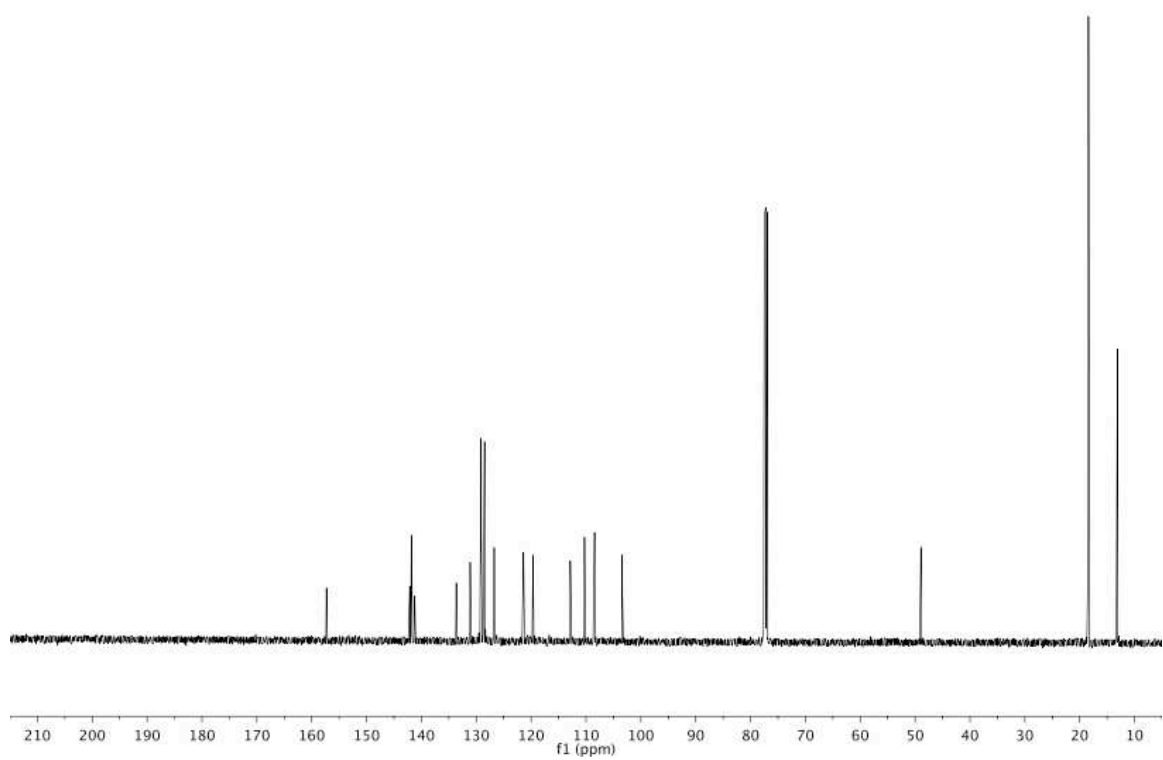
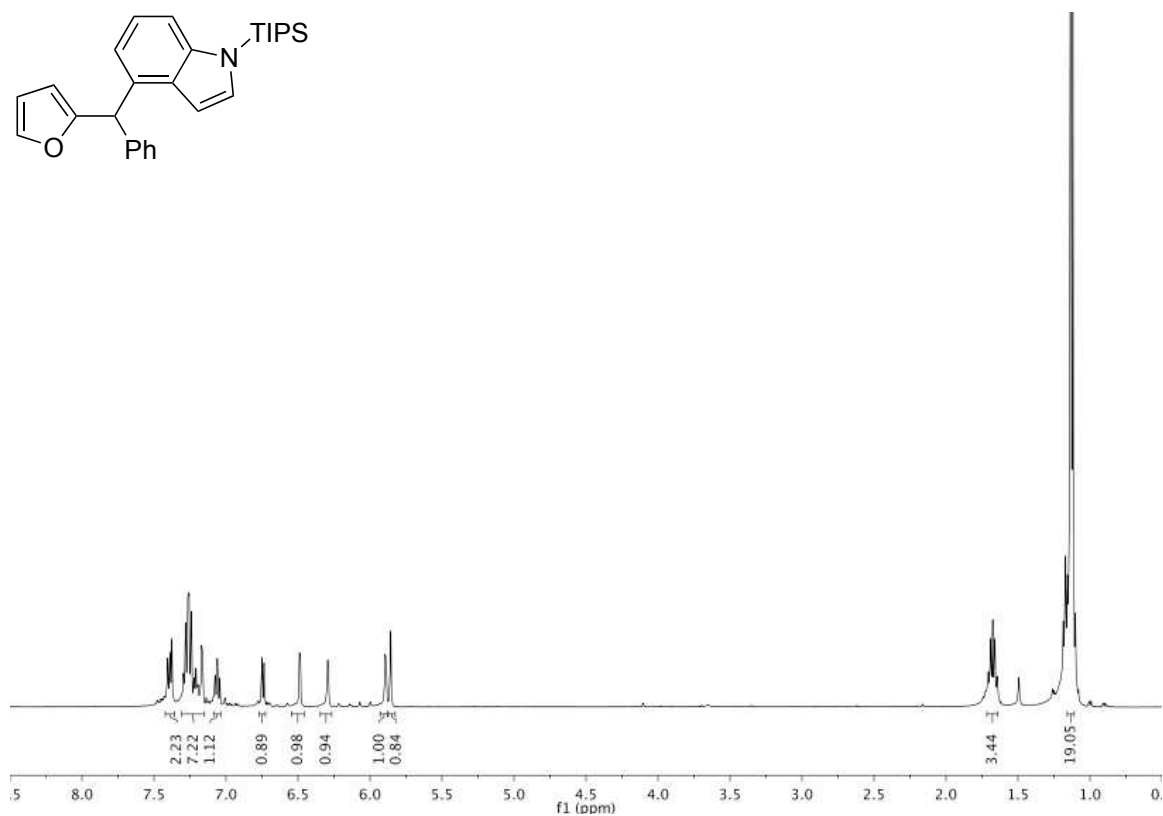
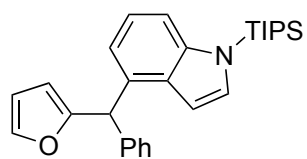


Figure A4.27 500 MHz ^1H and 125 MHz $^{13}\text{C}\{^1\text{H}\}$ NMR of **4.5an** in CDCl_3

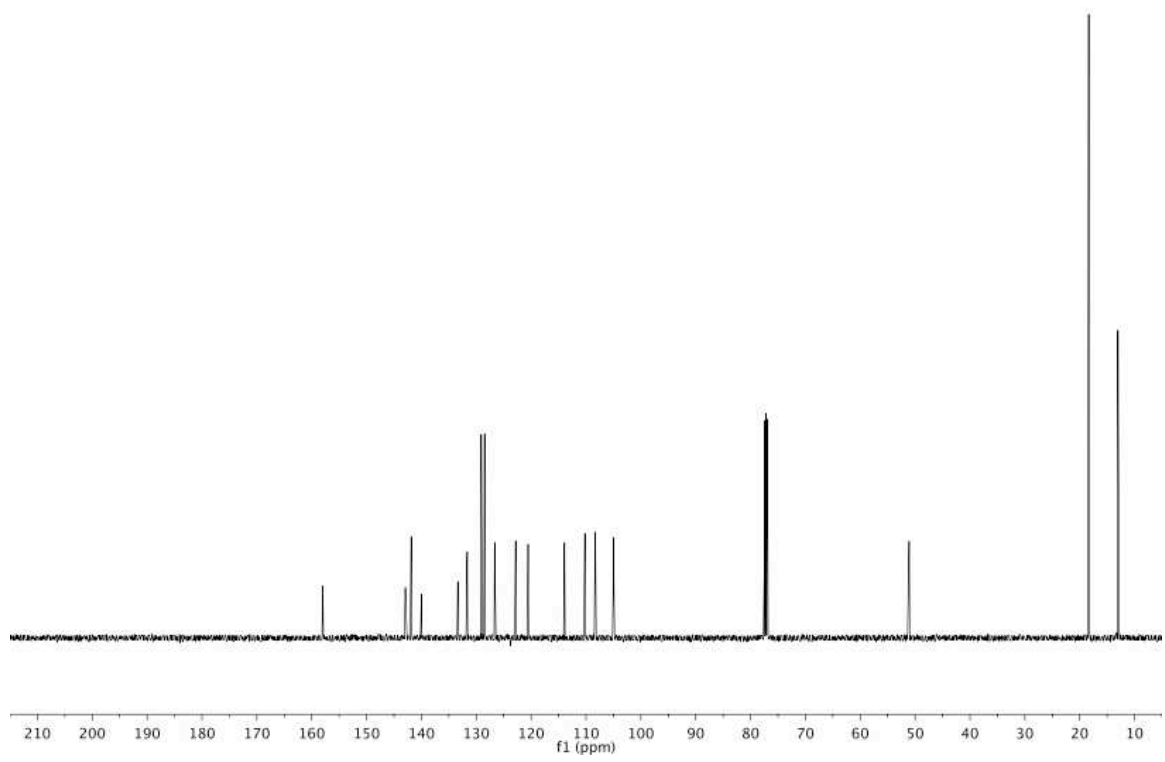
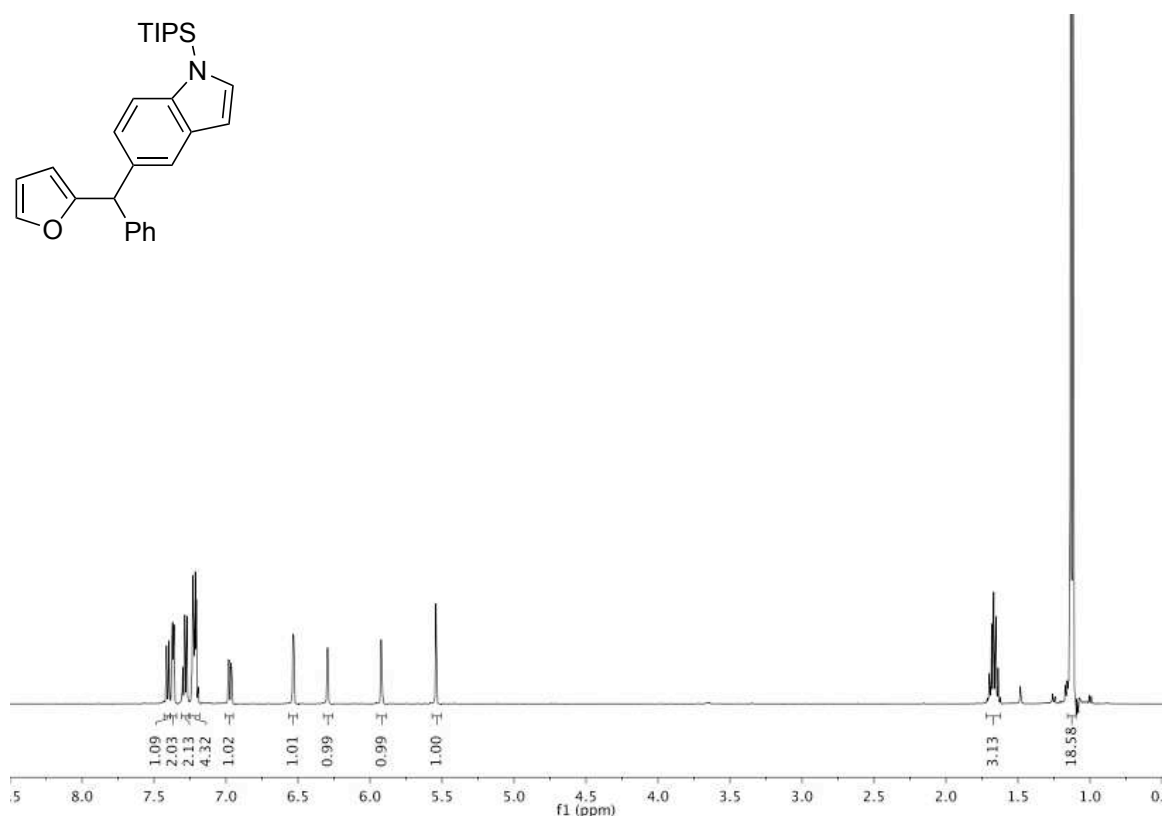
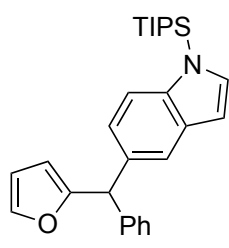


Figure A4.28 500 MHz ^1H and 125 MHz $^{13}\text{C}\{^1\text{H}\}$ NMR of **4.5ao** in CDCl_3

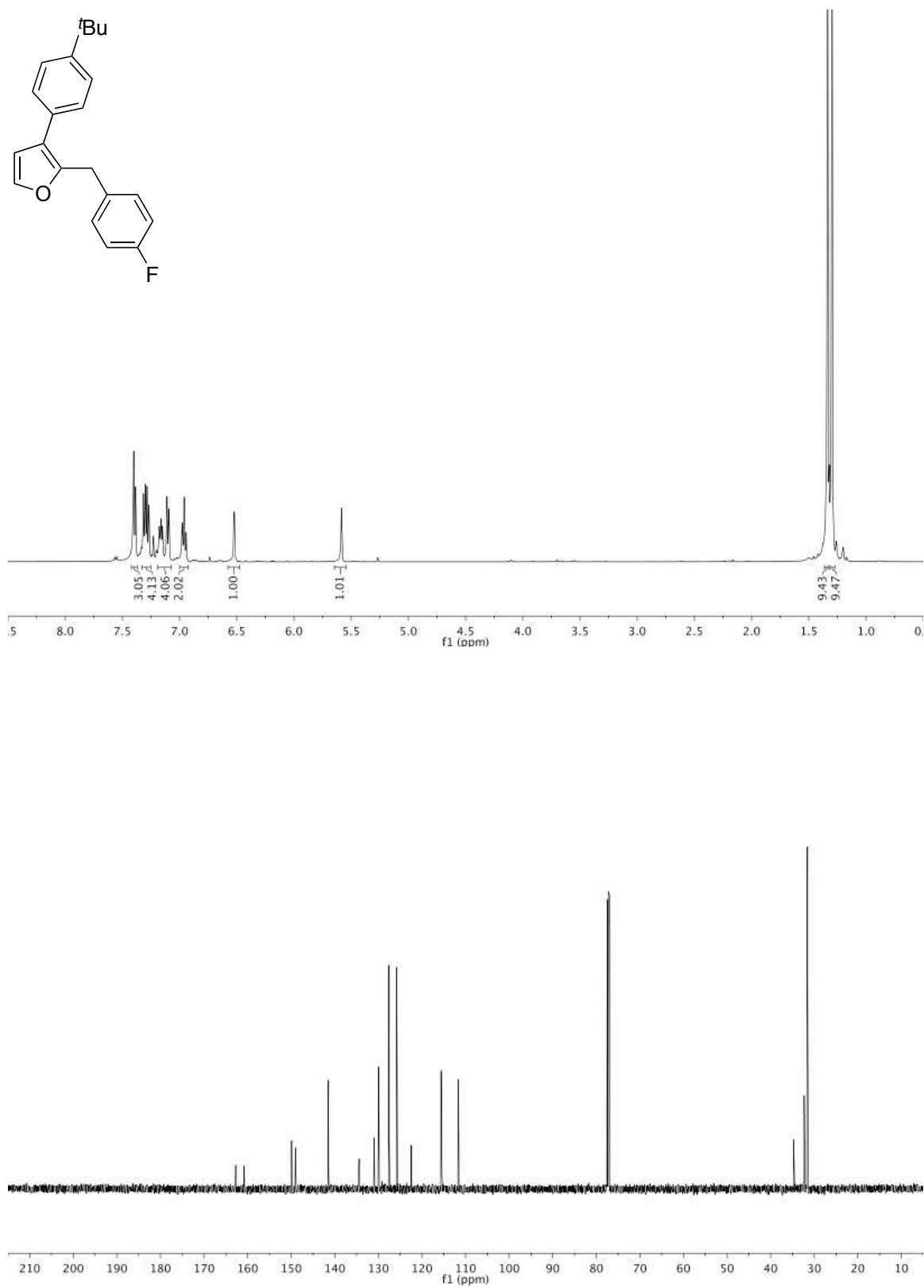


Figure A4.29 500 MHz ^1H and 125 MHz $^{13}\text{C}\{^1\text{H}\}$ NMR of **4.3bb** in CDCl_3

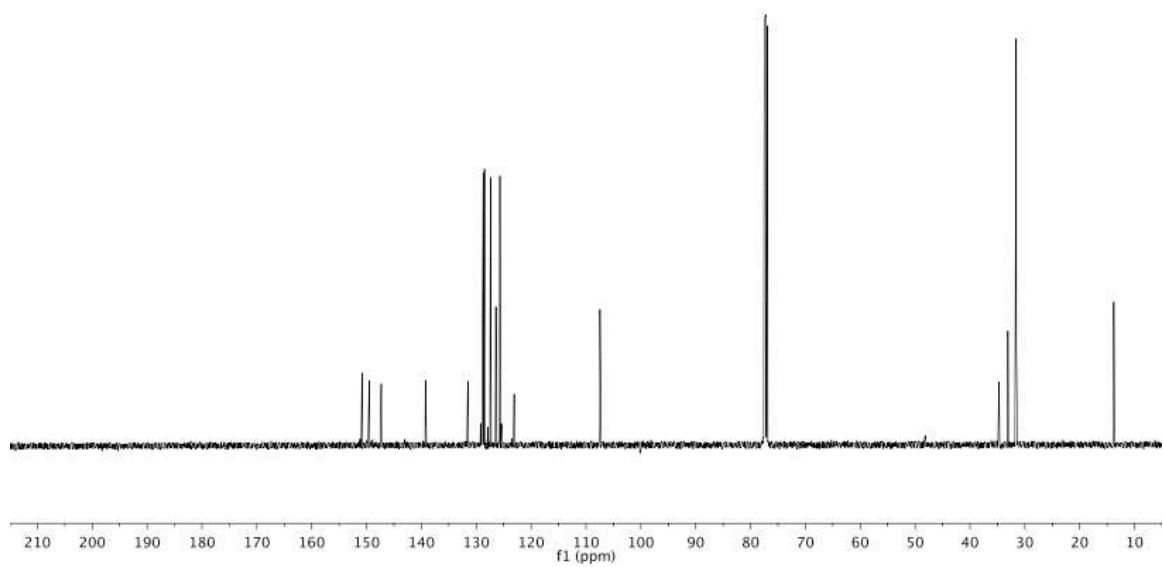
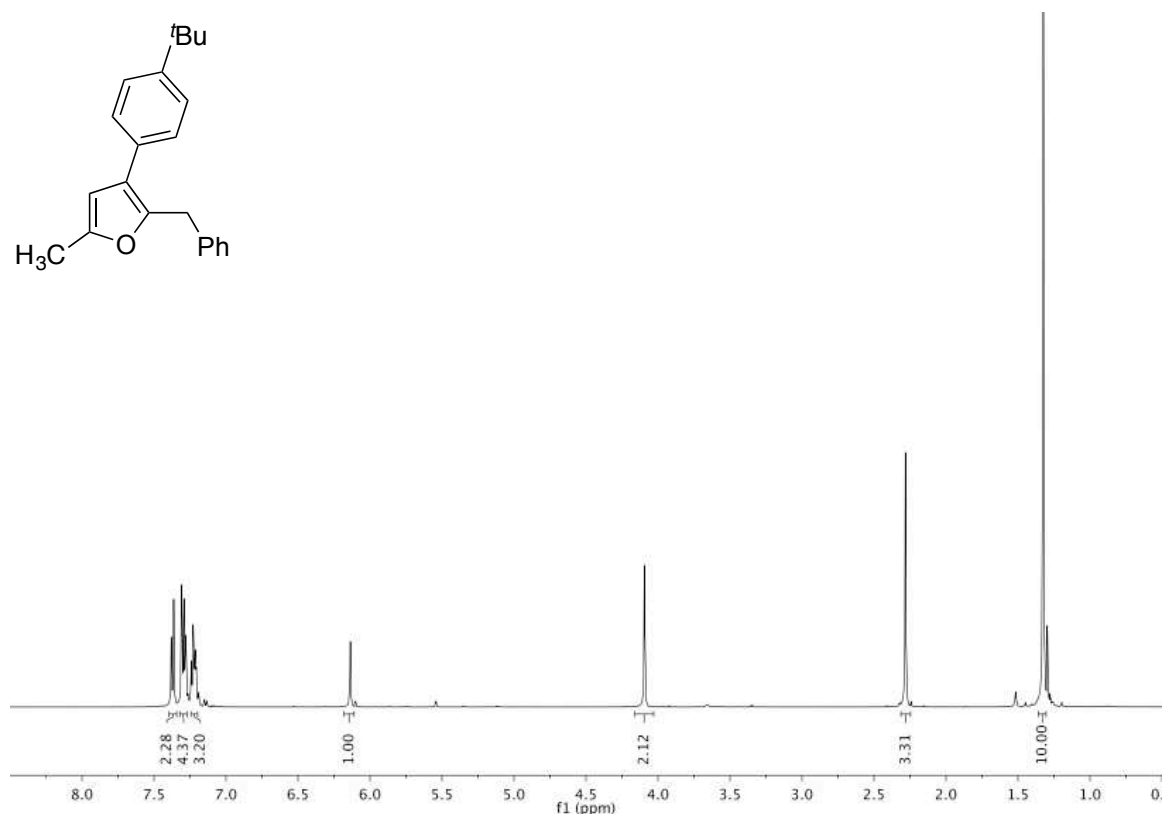
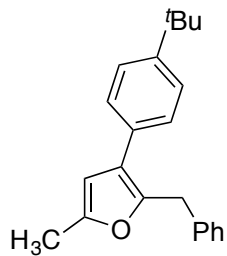


Figure A4.30 500 MHz ^1H and 125 MHz $^{13}\text{C}\{^1\text{H}\}$ NMR of **4.3db** in CDCl_3

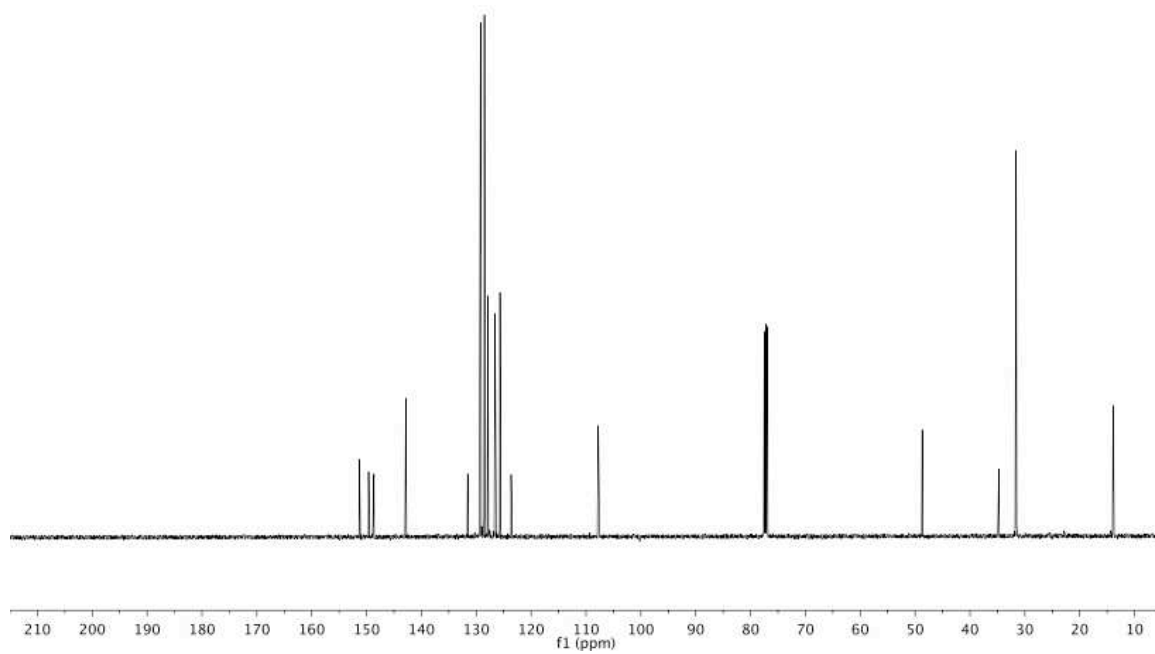
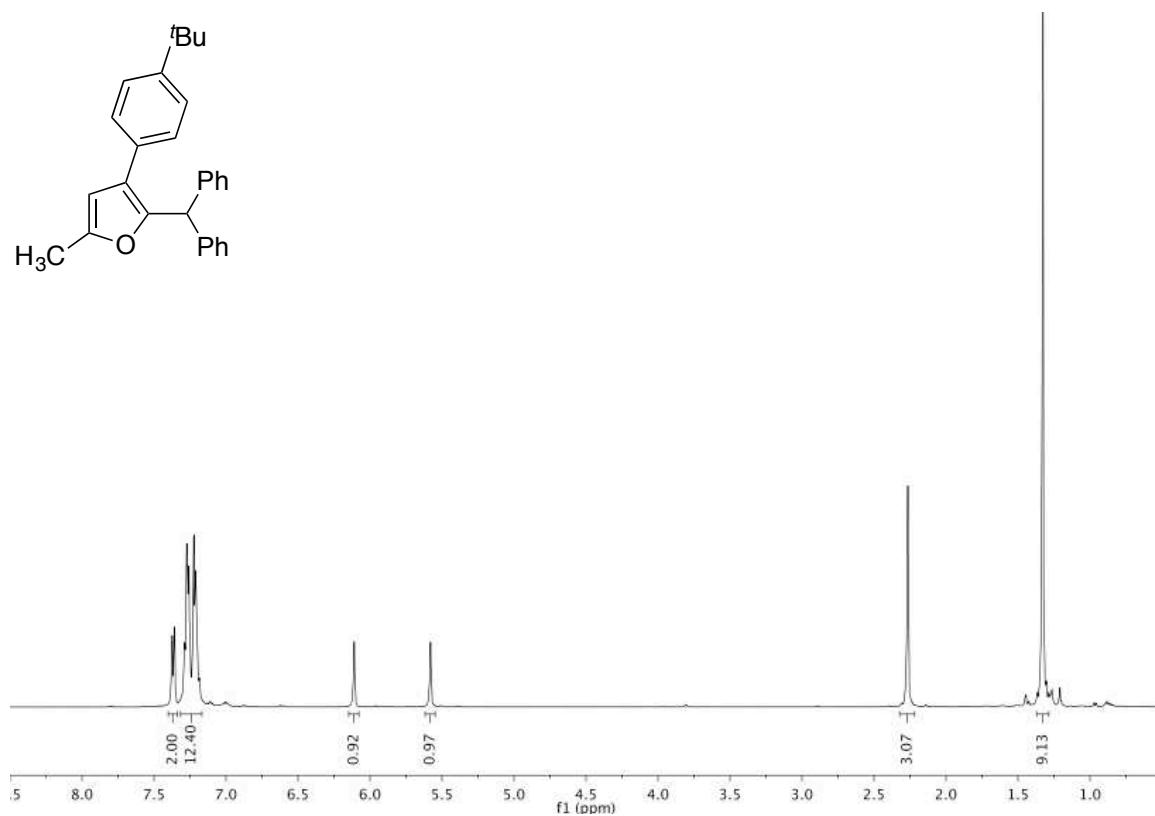
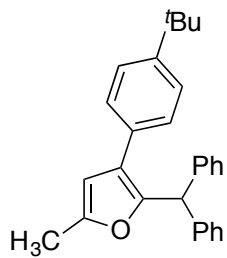


Figure A4.31 500 MHz ¹H and 125 MHz ¹³C{¹H} NMR of **4.3eb** in CDCl₃

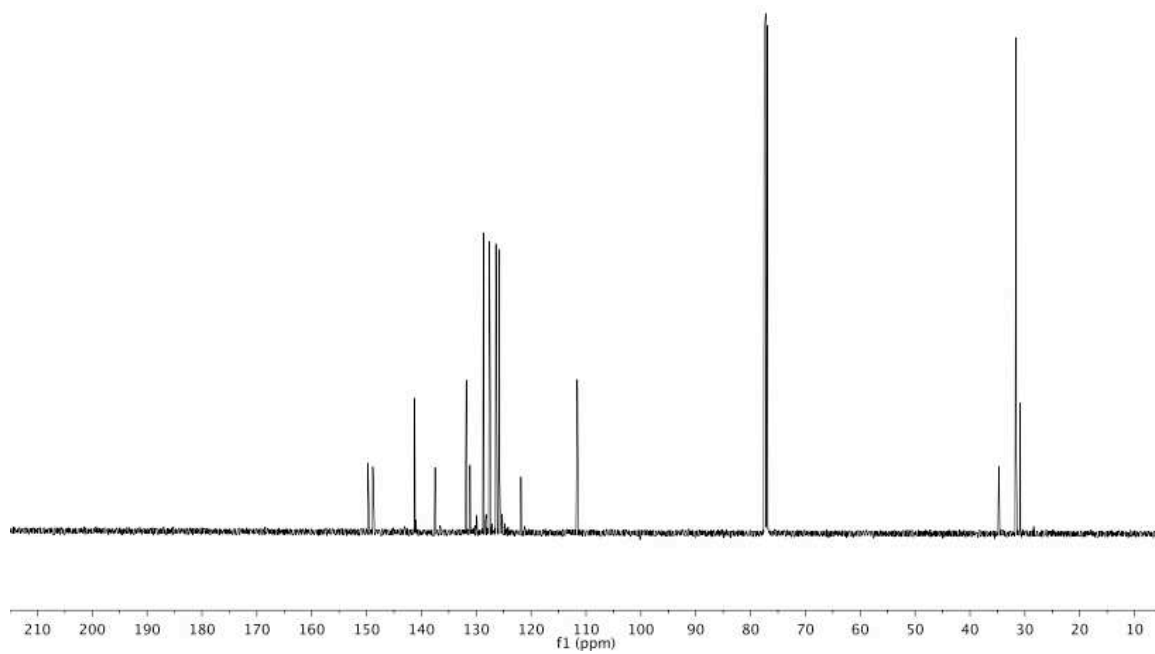
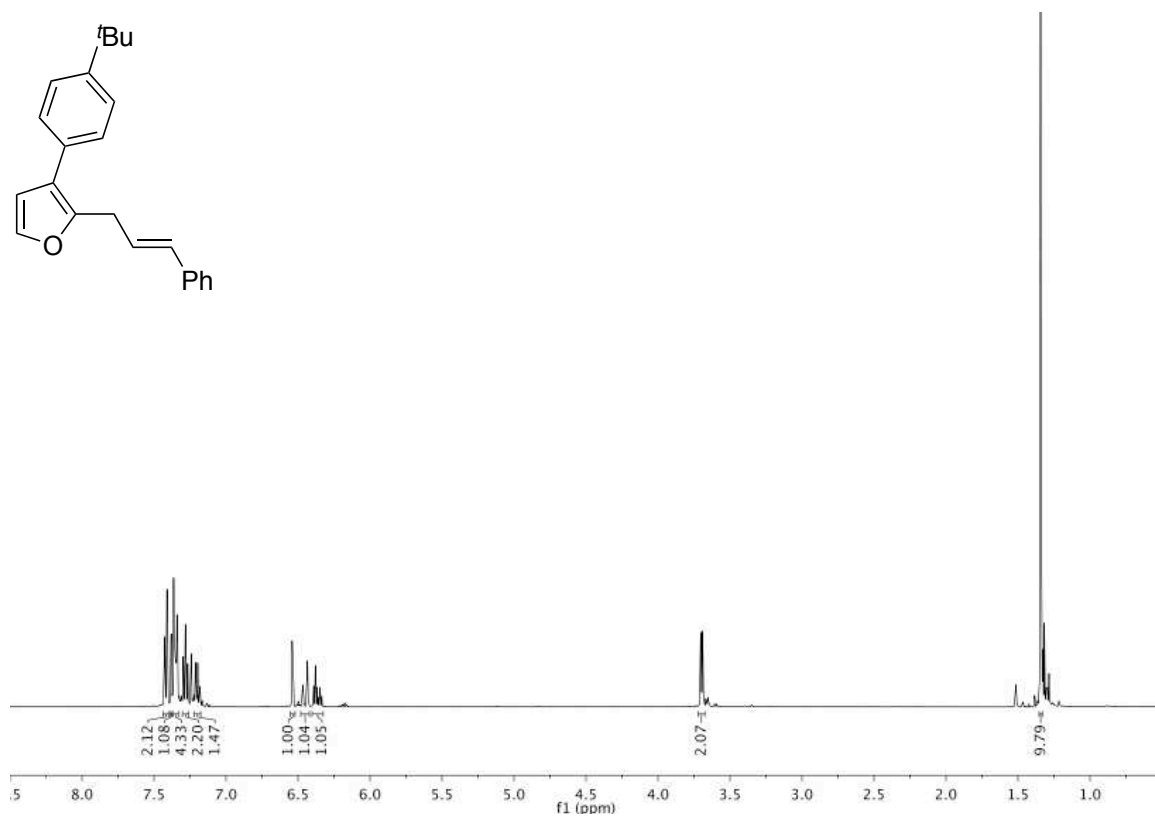
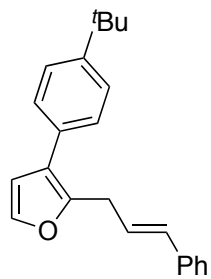


Figure A4.32 500 MHz ^1H and 125 MHz $^{13}\text{C}\{^1\text{H}\}$ NMR of **4.3fb** in CDCl_3

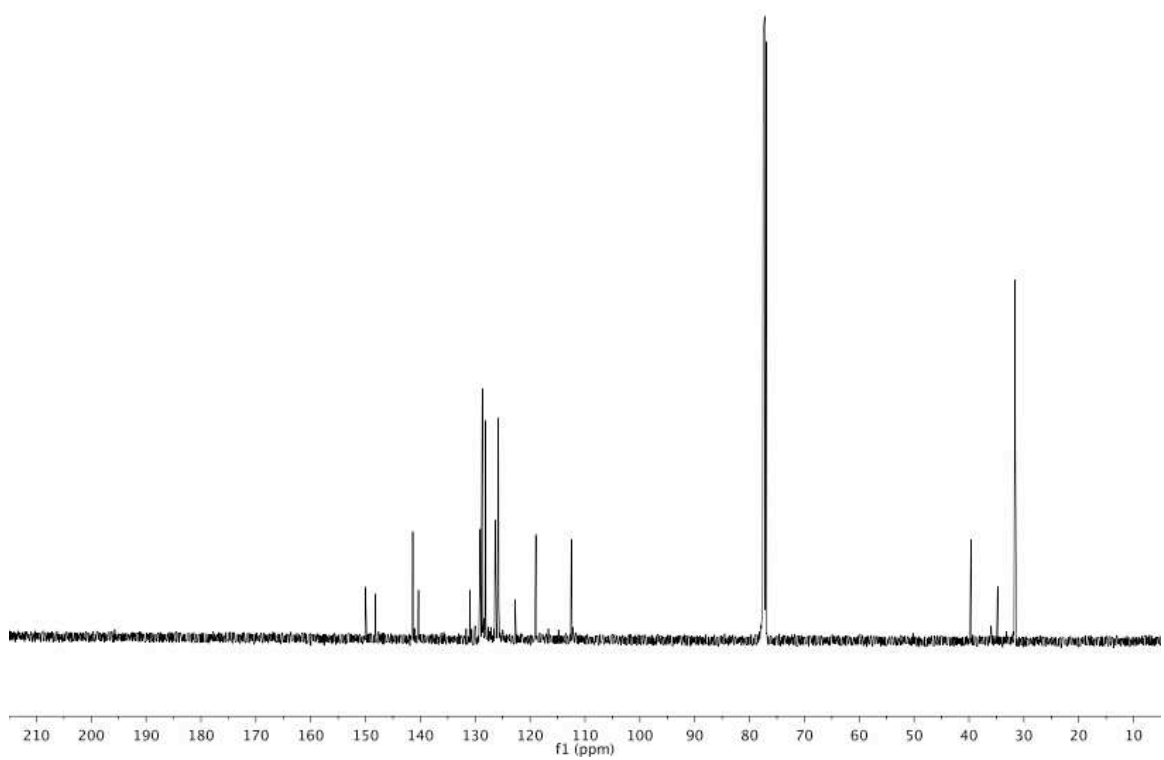
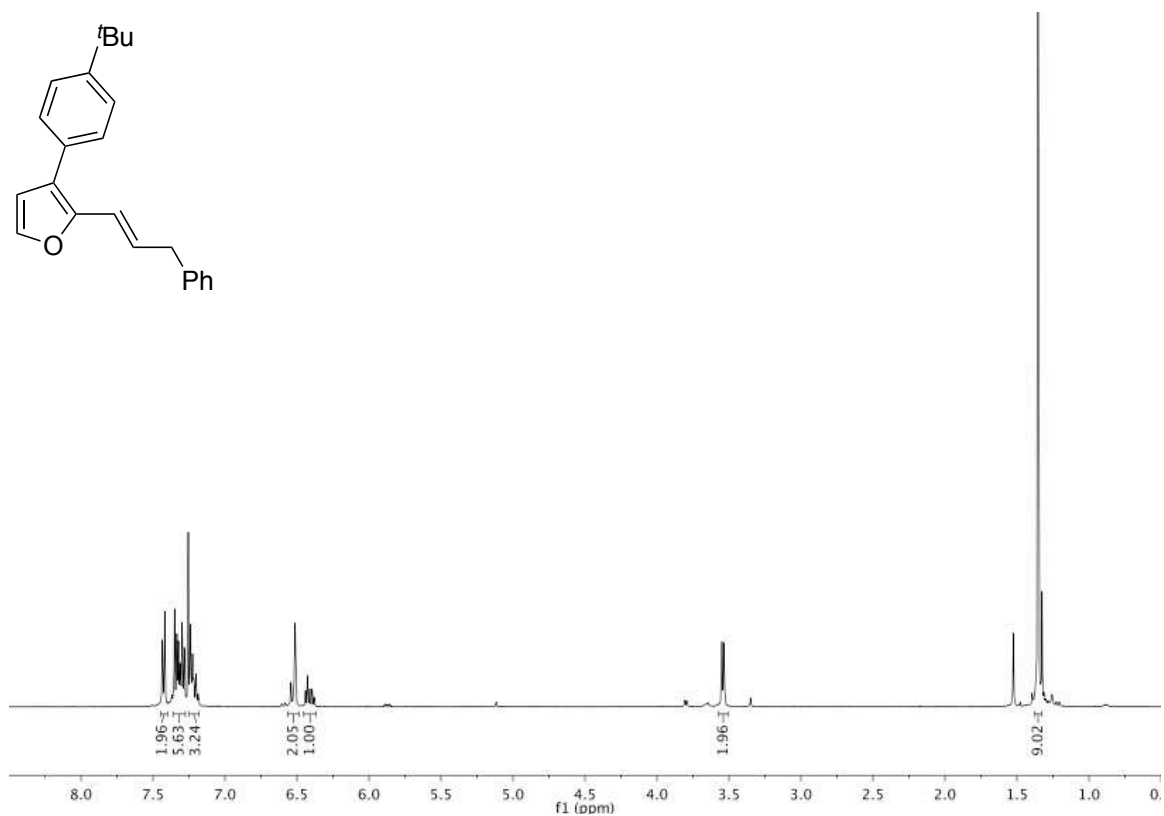
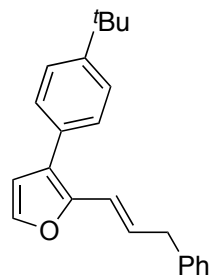


Figure A4.33 500 MHz ^1H and 125 MHz $^{13}\text{C}\{^1\text{H}\}$ NMR of **4.3'fb** in CDCl_3

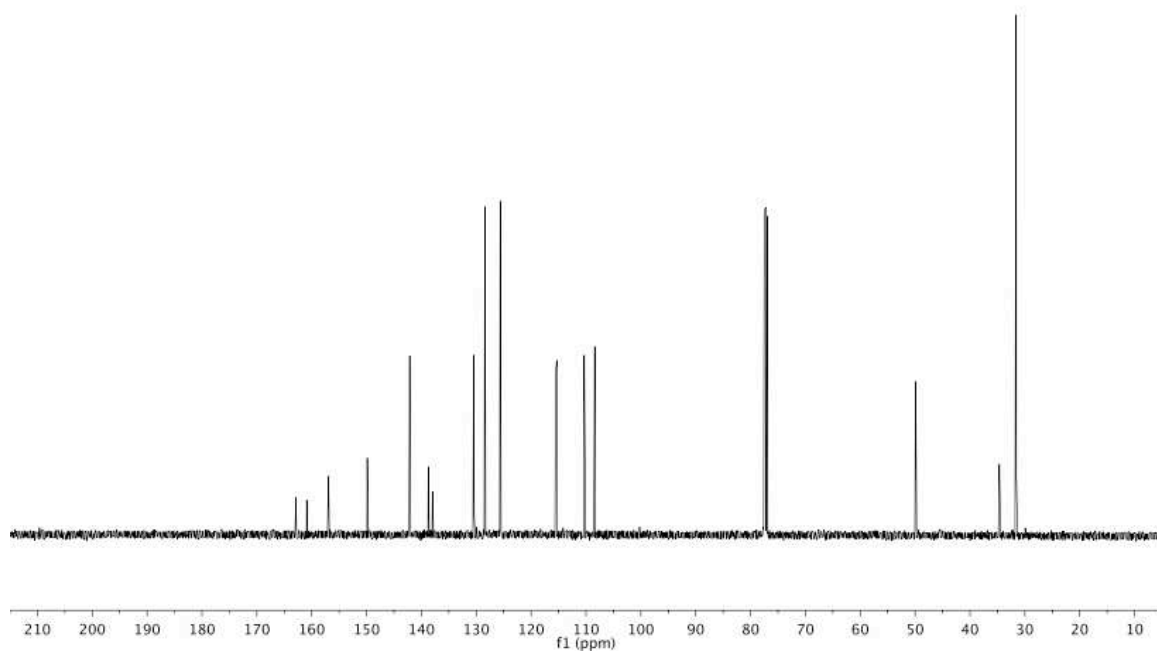
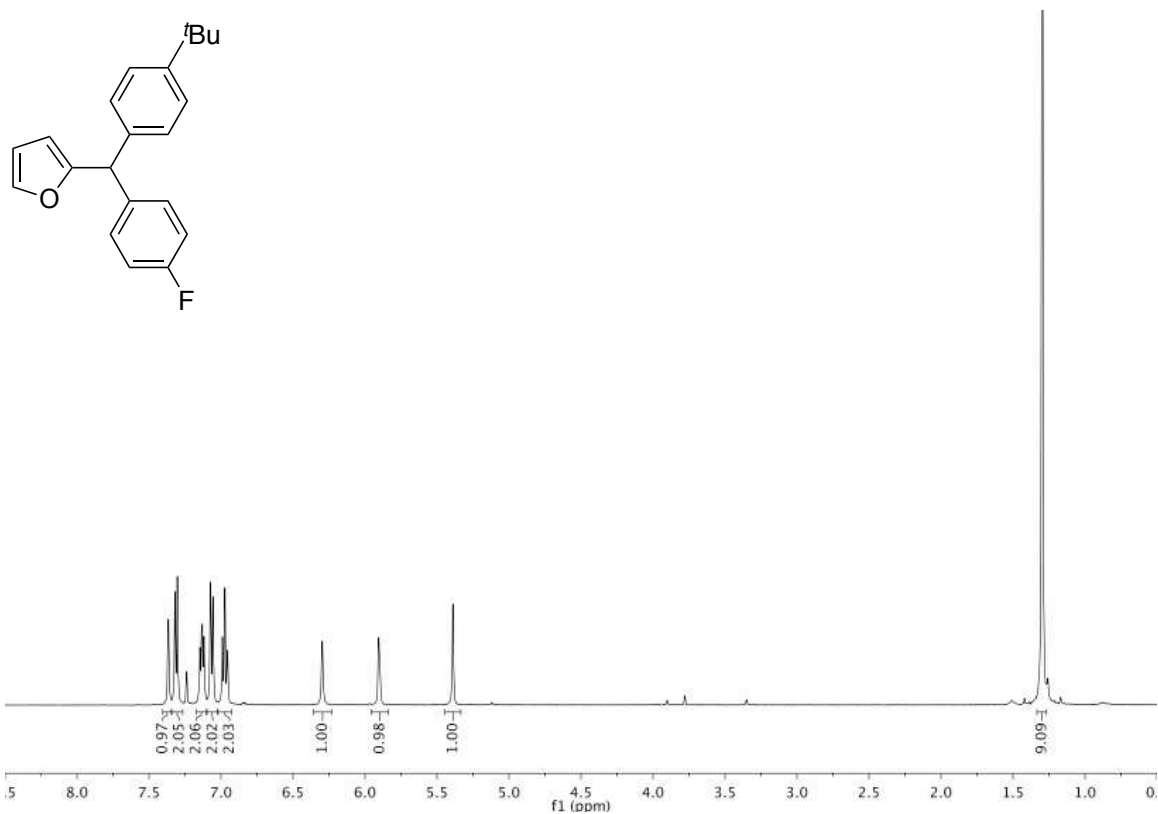


Figure A4.34 500 MHz ^1H and 125 MHz $^{13}\text{C}\{^1\text{H}\}$ NMR of **4.5bb** in CDCl_3

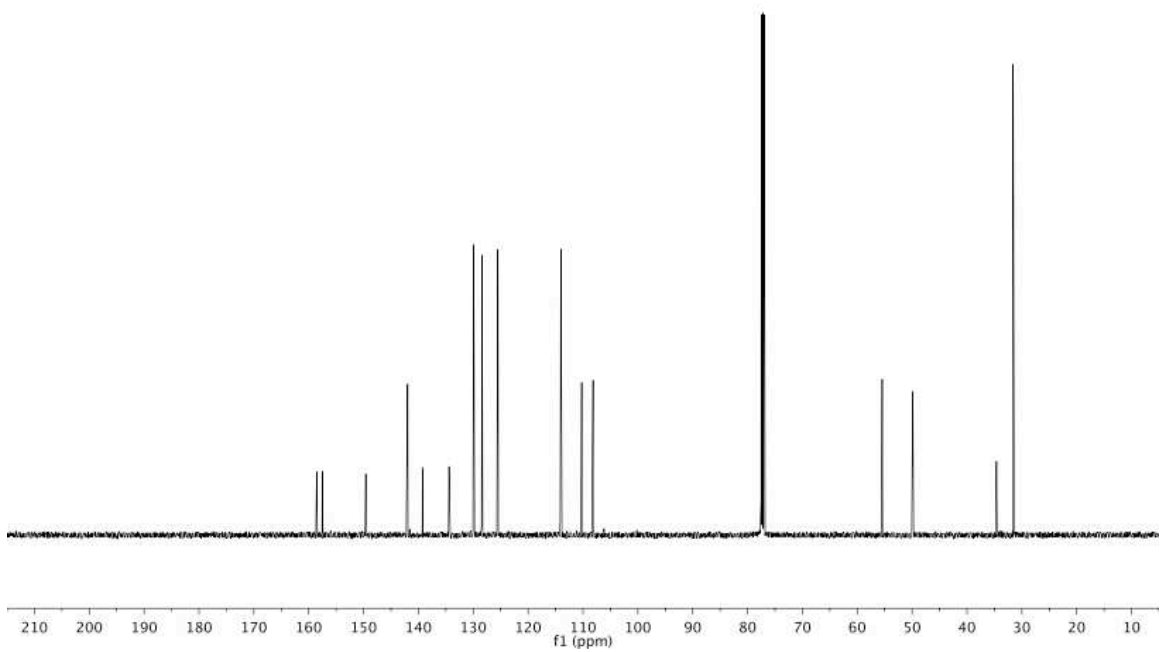
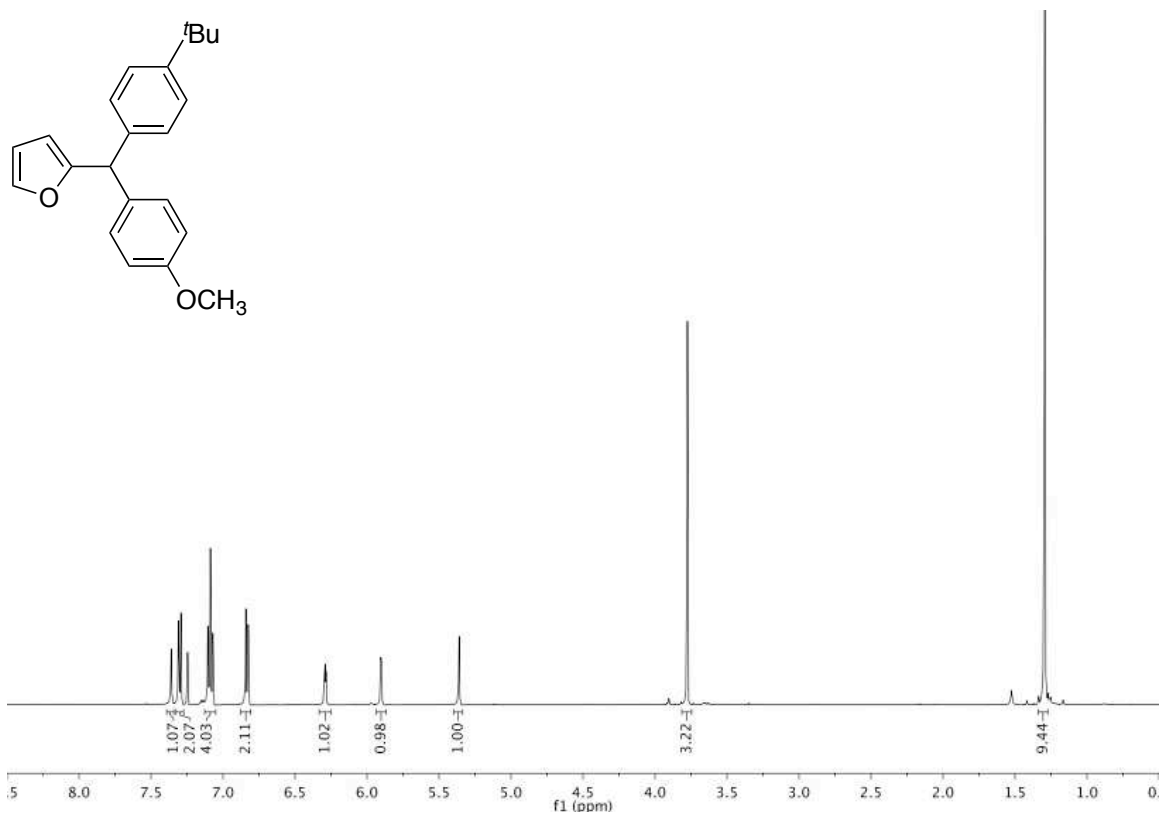


Figure A4.35 500 MHz ^1H and 125 MHz $^{13}\text{C}\{^1\text{H}\}$ NMR of **4.5cb** in CDCl₃

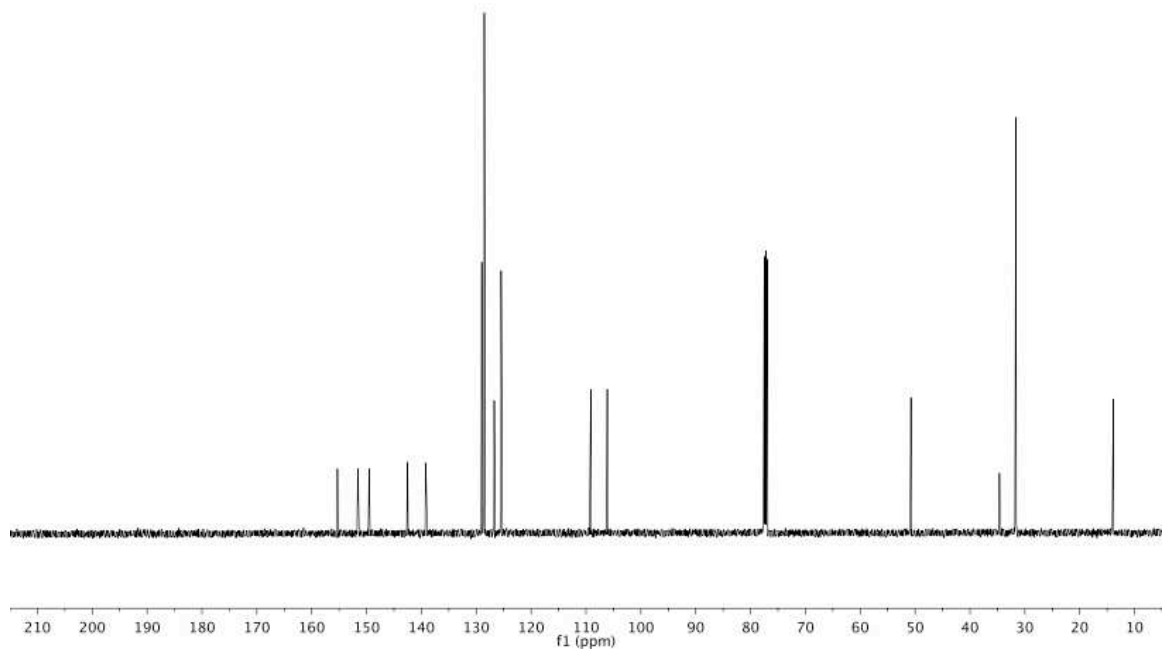
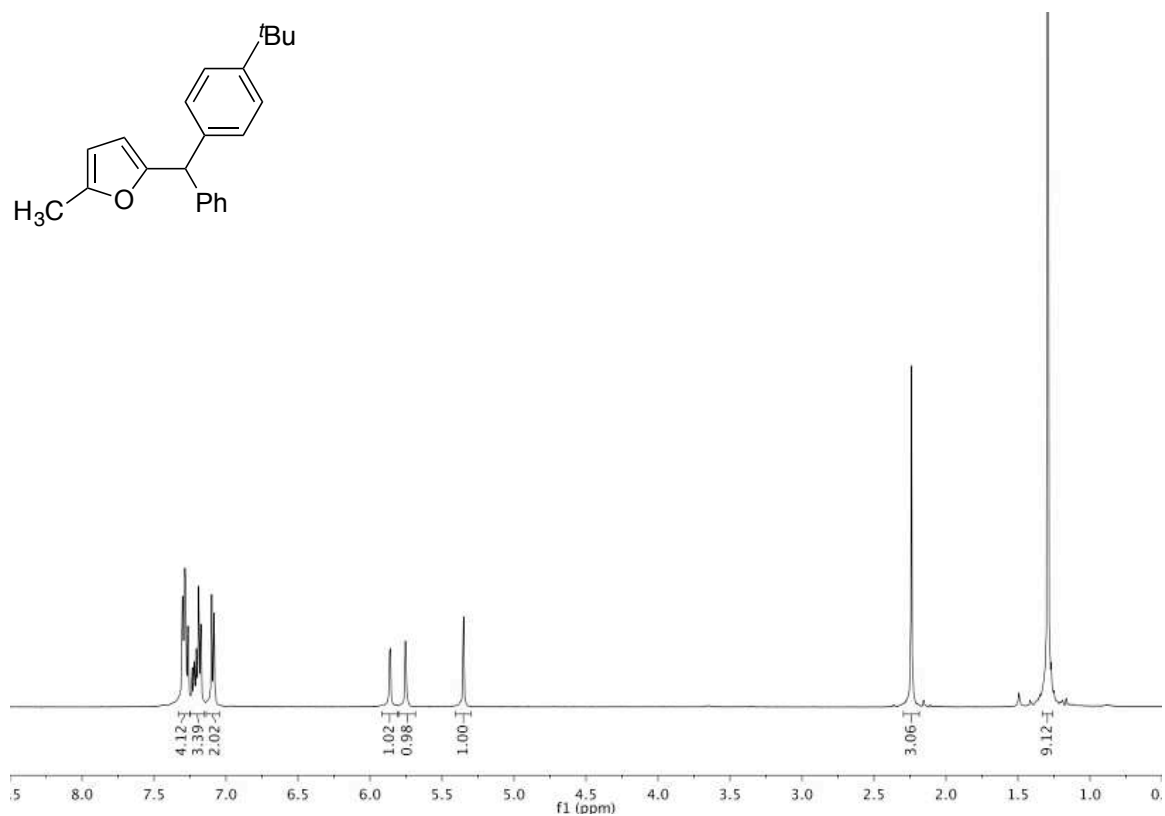
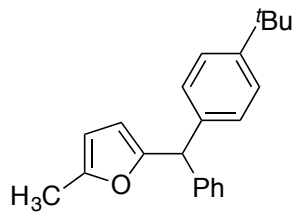


Figure A4.36 500 MHz ¹H and 125 MHz ¹³C{¹H} NMR of **4.5db** in CDCl₃

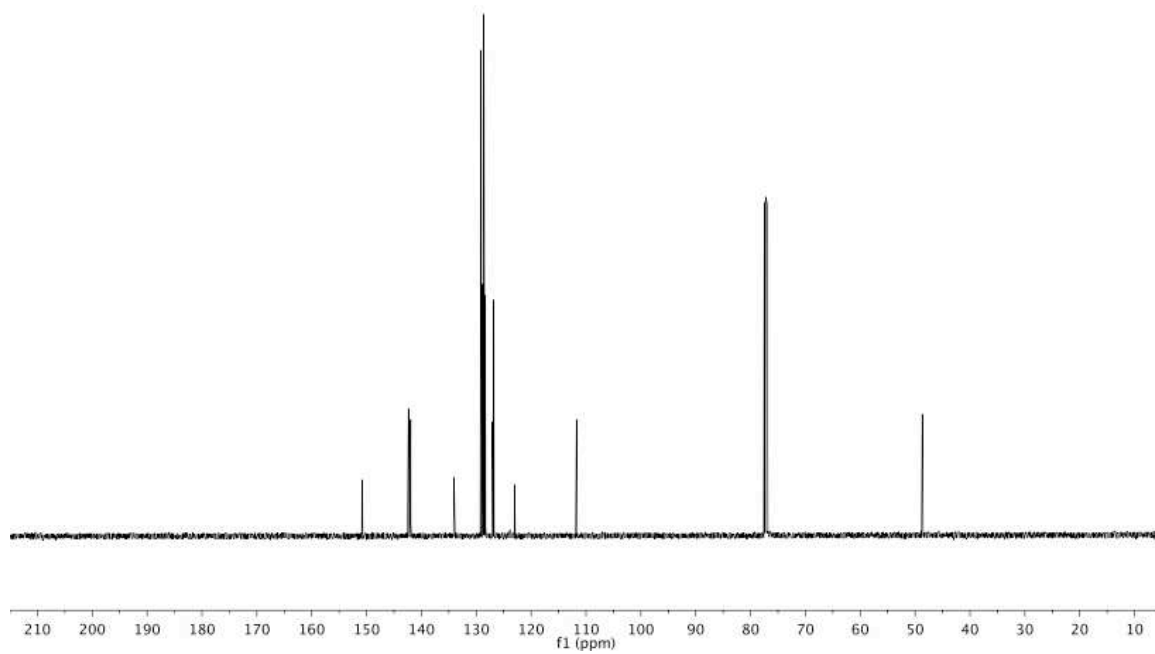
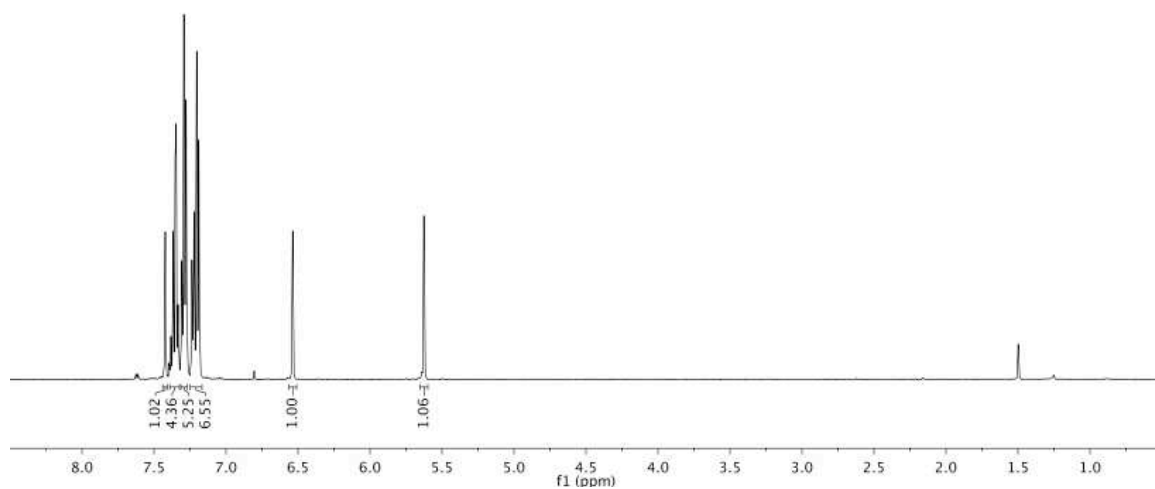
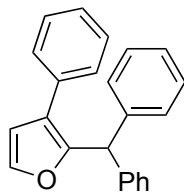


Figure A4.37 500 MHz ^1H and 125 MHz $^{13}\text{C}\{^1\text{H}\}$ NMR of 4.4aa in CDCl_3

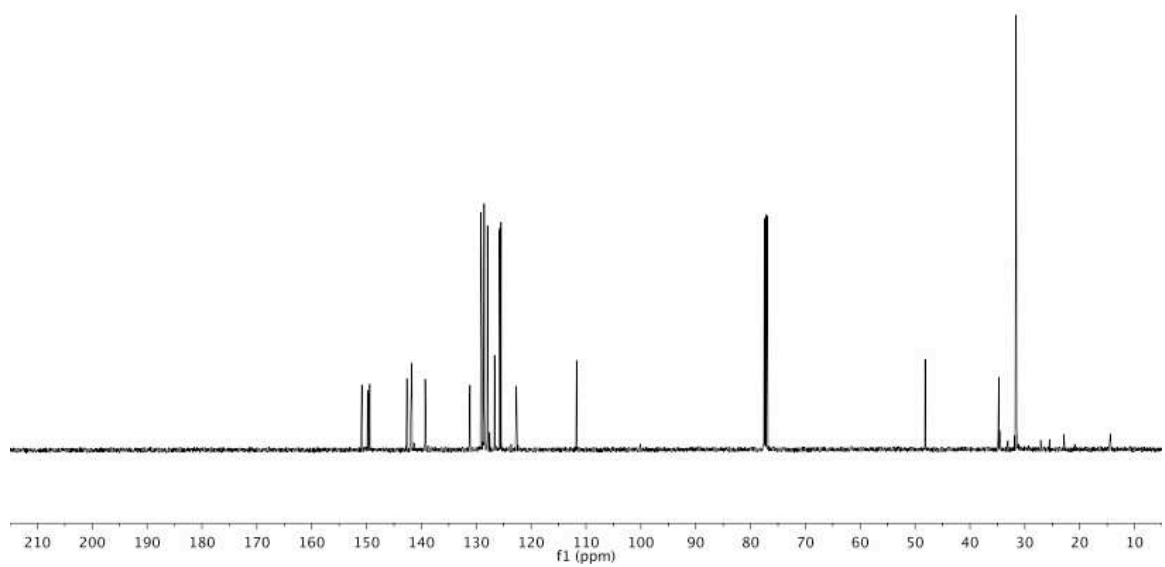
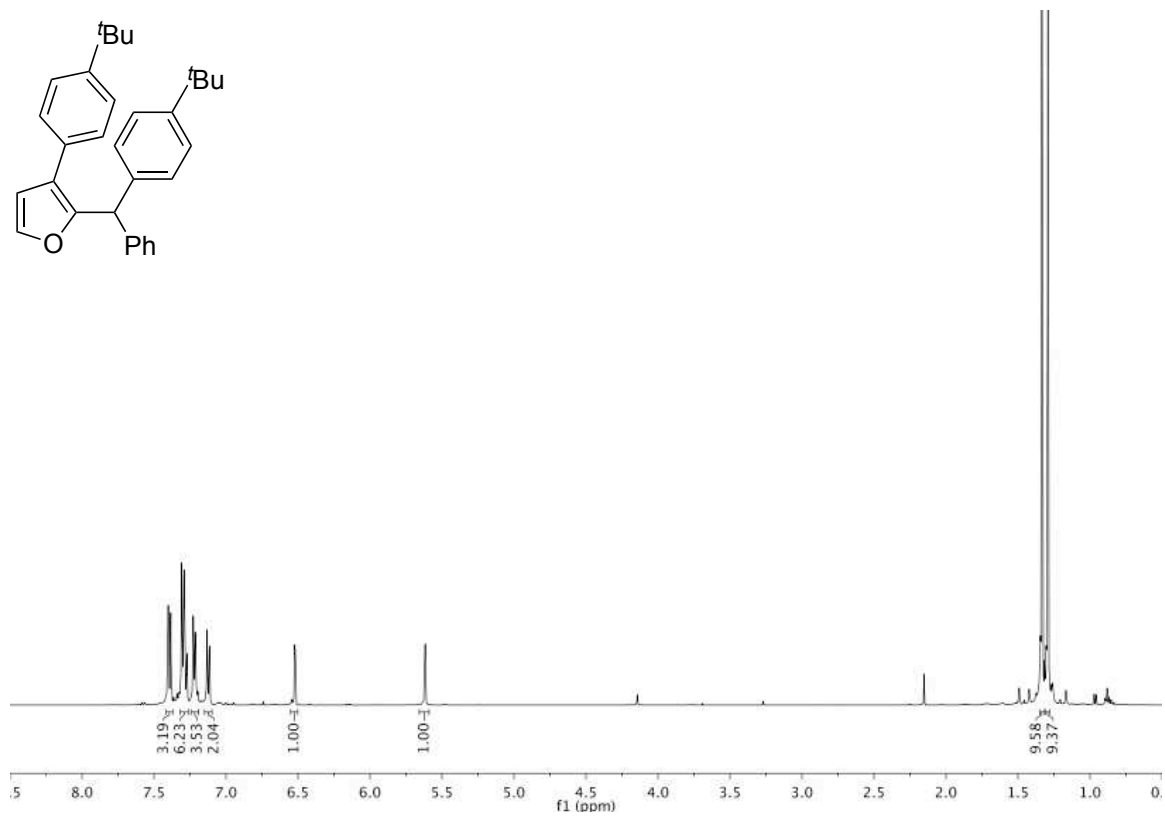
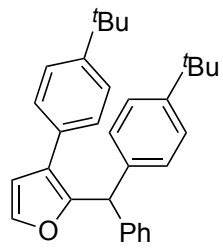


Figure A4.38 500 MHz ^1H and 125 MHz $^{13}\text{C}\{^1\text{H}\}$ NMR of 4.4ab in CDCl_3

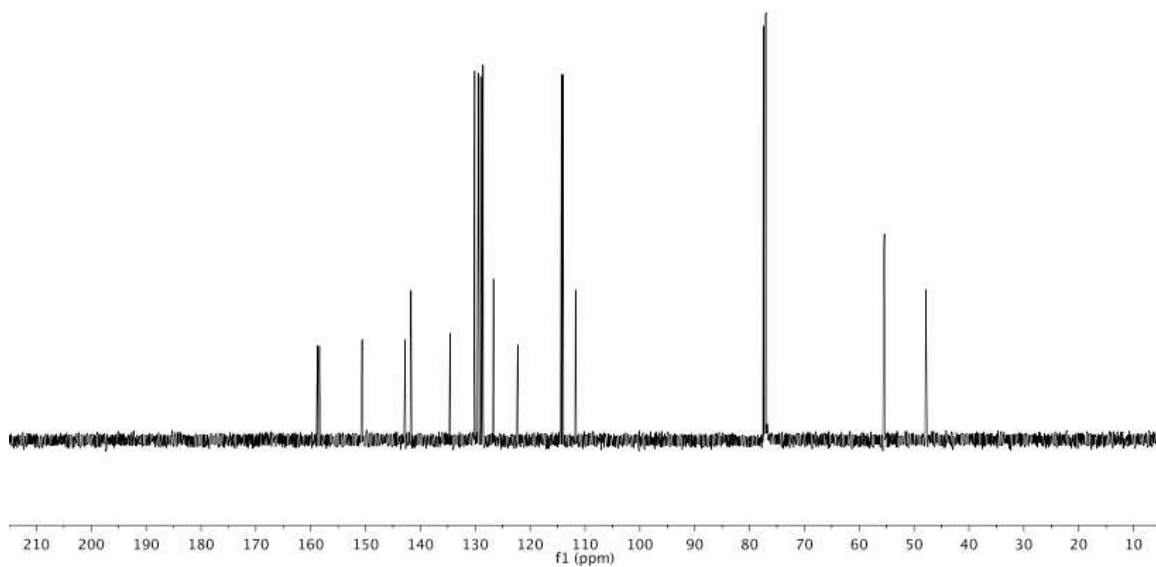
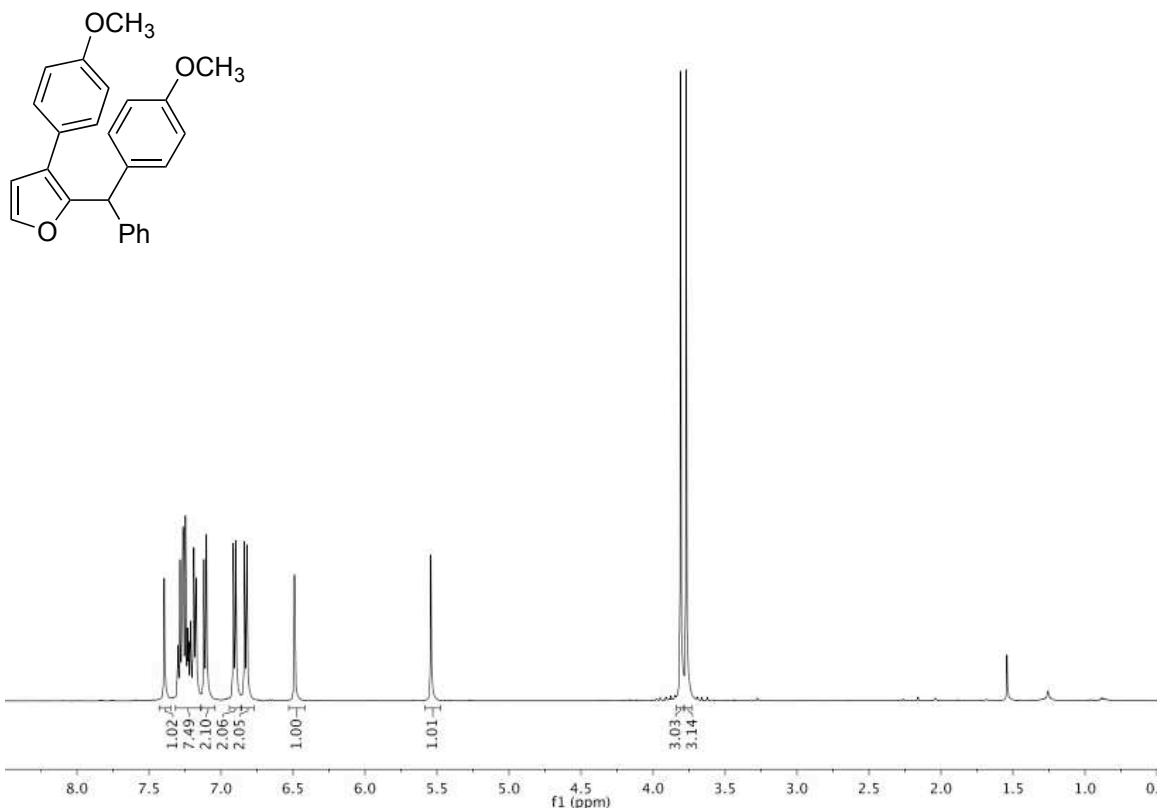


Figure A4.39 500 MHz ¹H and 125 MHz ¹³C{¹H} NMR of **4.4ac** in CDCl₃

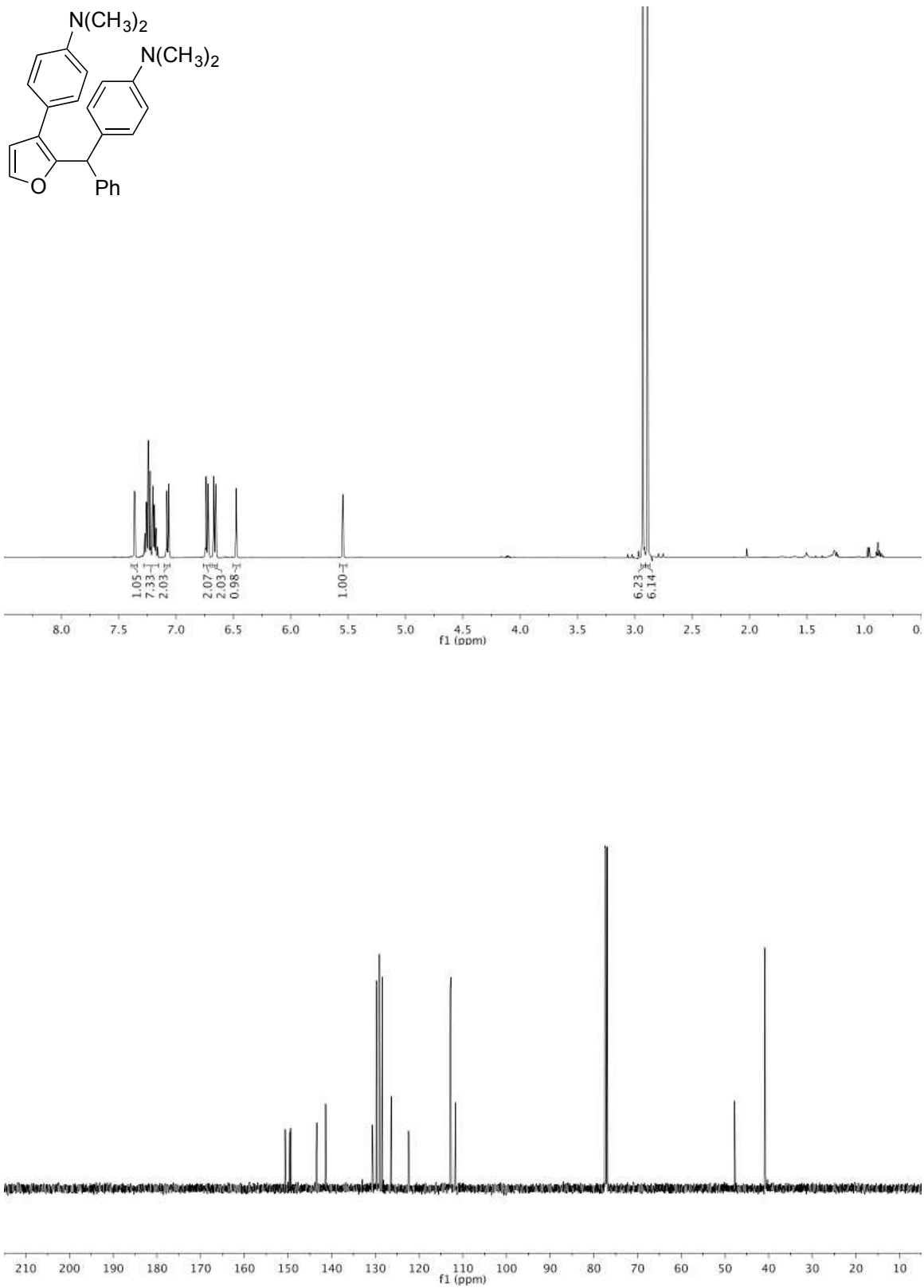


Figure A4.40 500 MHz ^1H and 125 MHz $^{13}\text{C}\{^1\text{H}\}$ NMR of **4.4ad** in CDCl_3

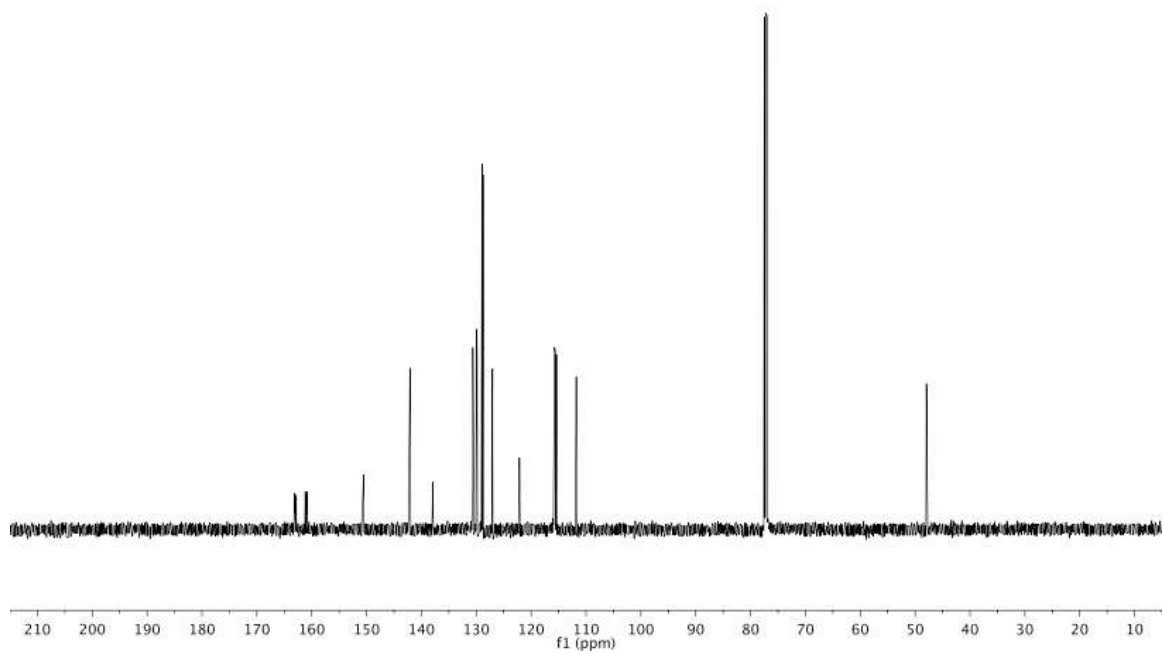
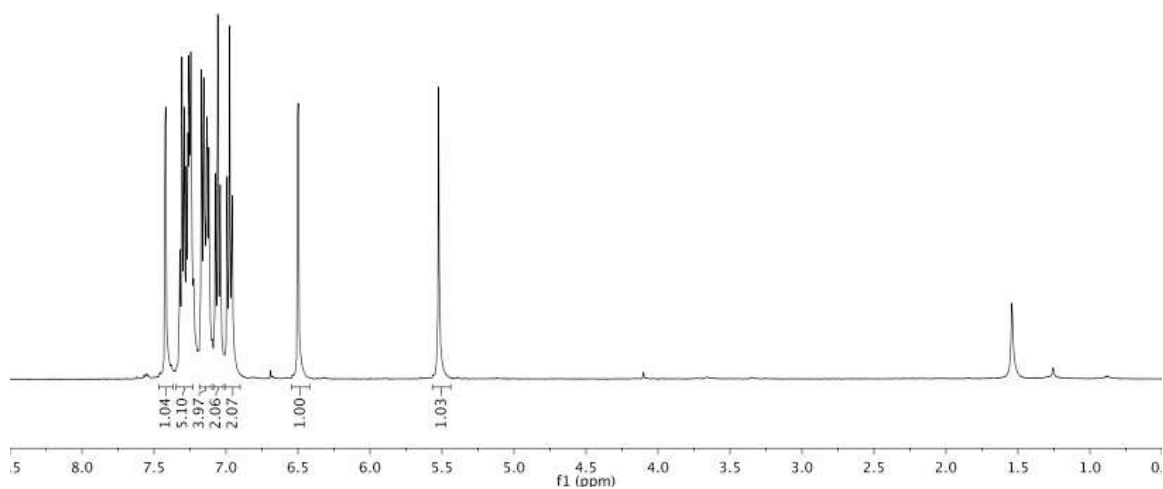
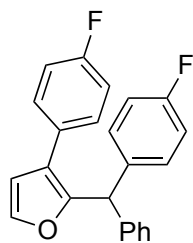


Figure A4.41 500 MHz ^1H and 125 MHz $^{13}\text{C}\{^1\text{H}\}$ NMR of **4.4ae** in CDCl_3

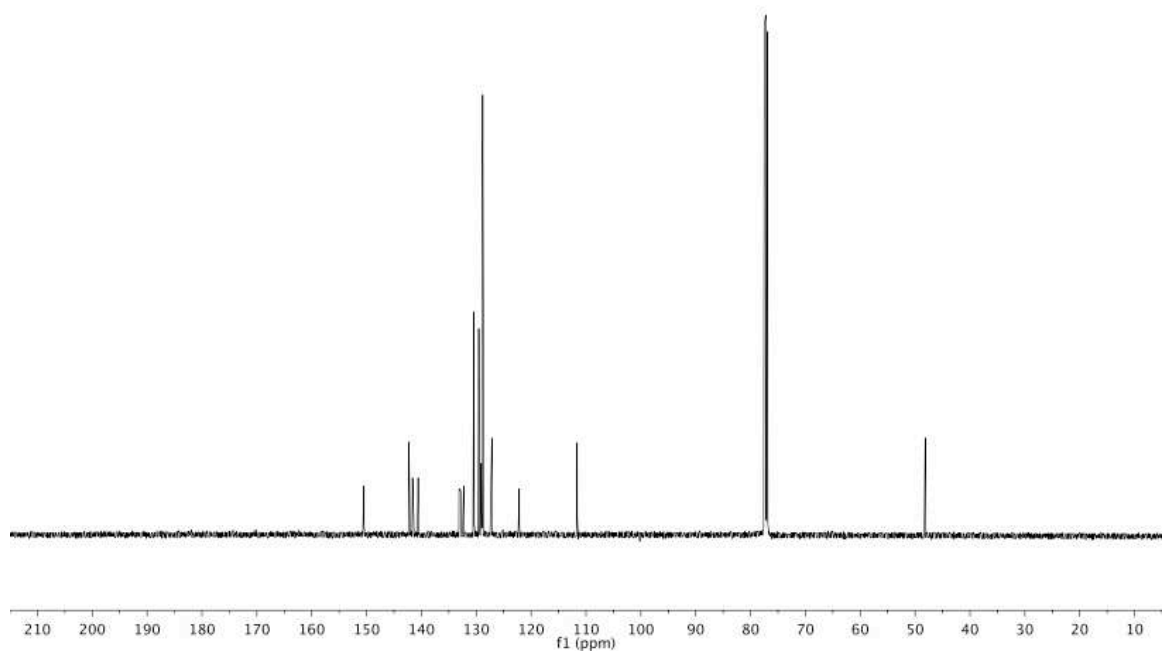
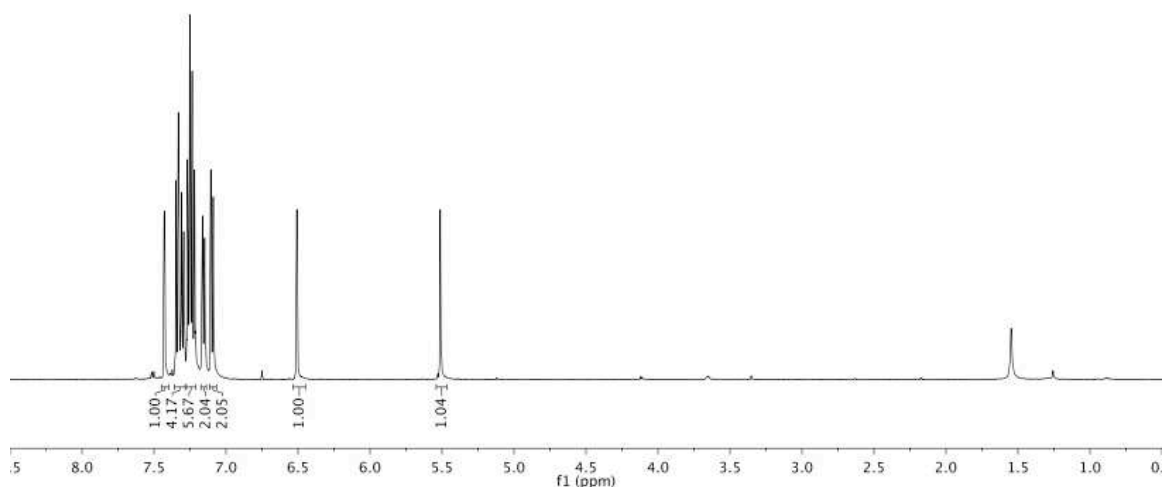
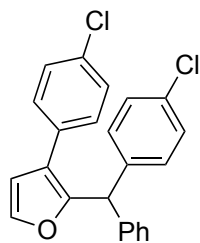


Figure A4.42 500 MHz ^1H and 125 MHz $^{13}\text{C}\{^1\text{H}\}$ NMR of **4.4af** in CDCl_3

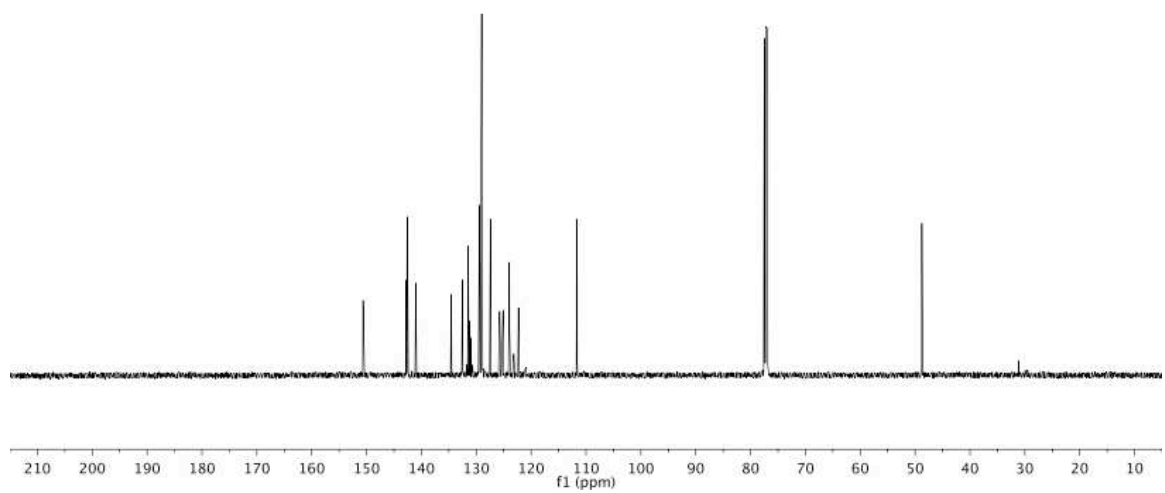
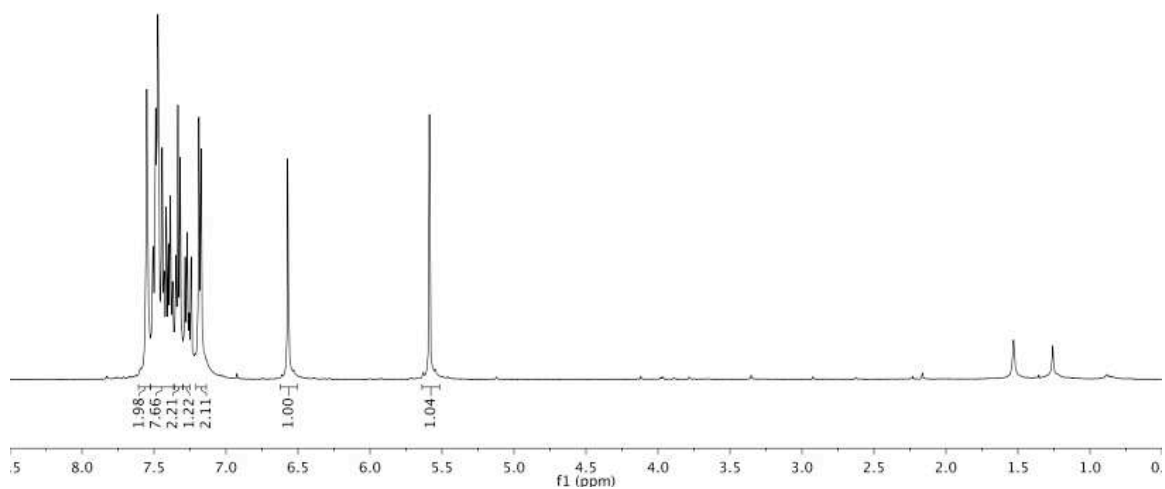
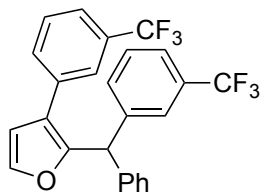


Figure A4.43 500 MHz ¹H and 125 MHz ¹³C{¹H} NMR of 4.4ag in CDCl₃

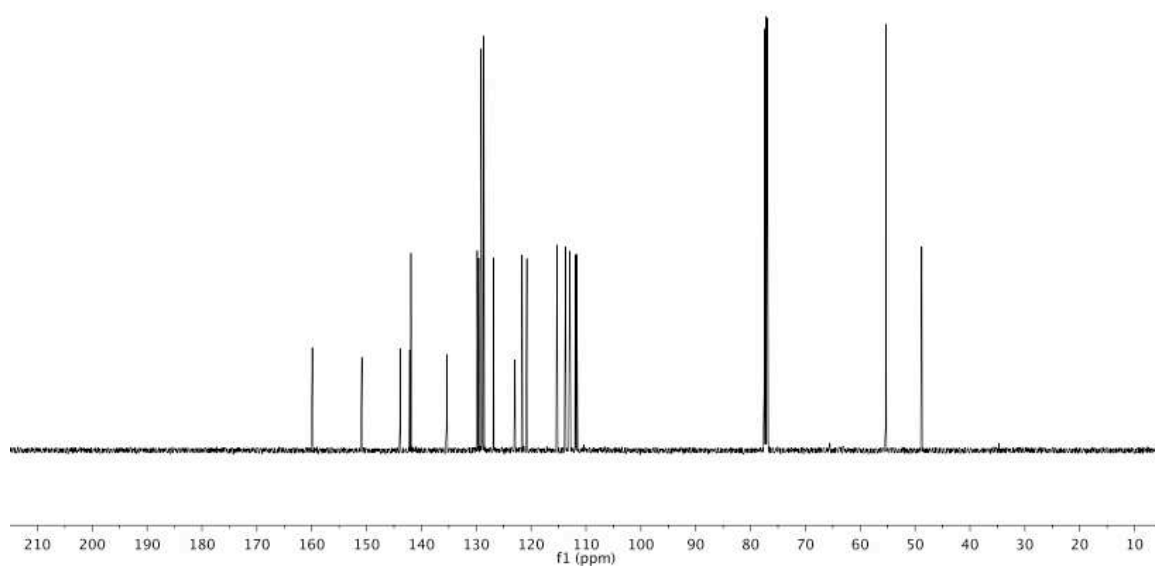
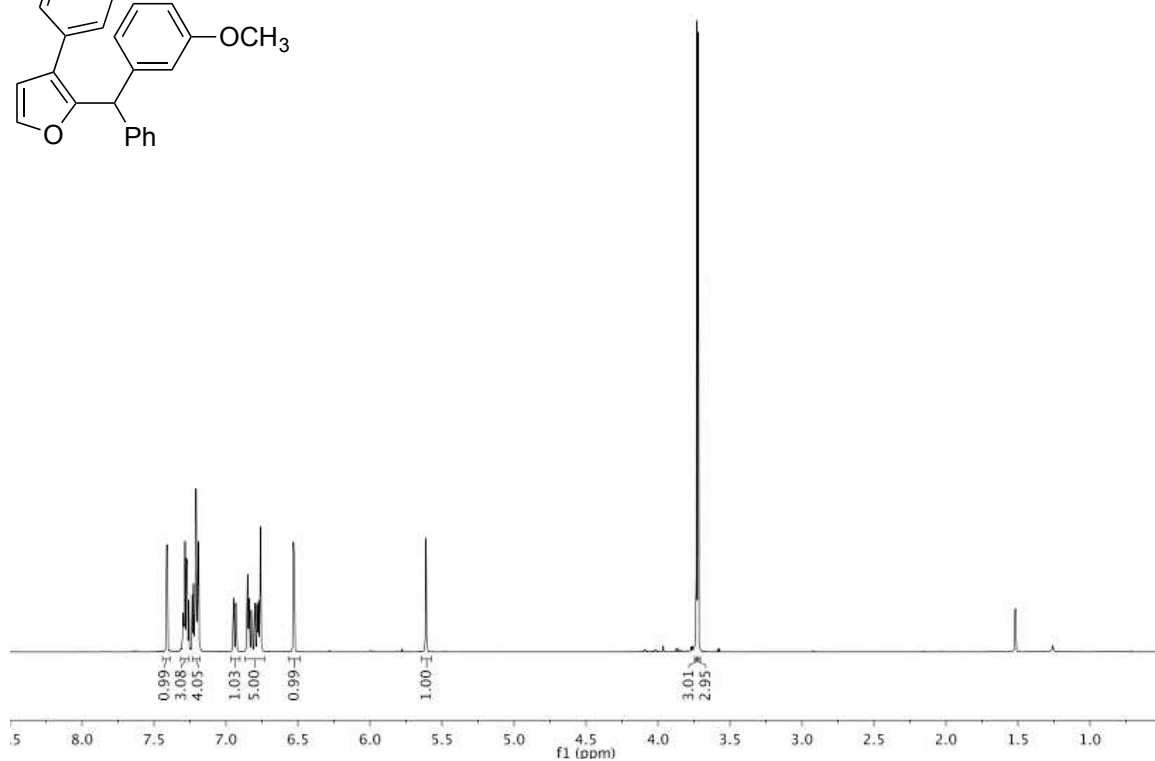
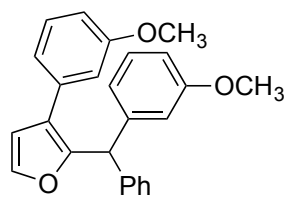


Figure A4.44 500 MHz ^1H and 125 MHz $^{13}\text{C}\{^1\text{H}\}$ NMR of **4.4ah** in CDCl_3

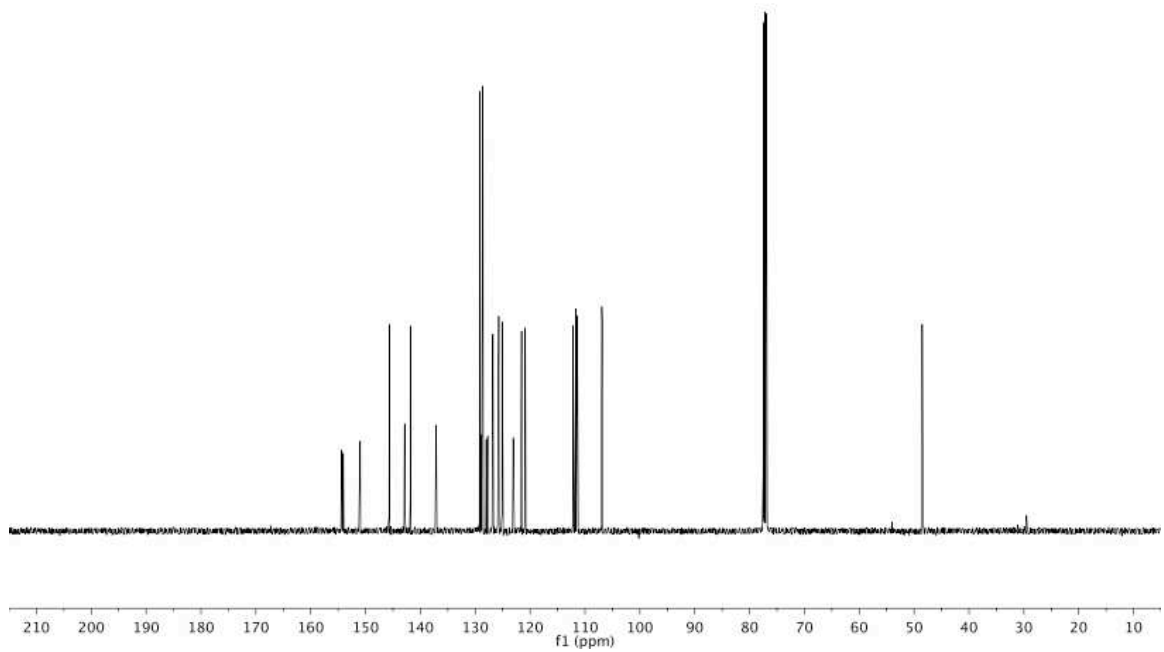
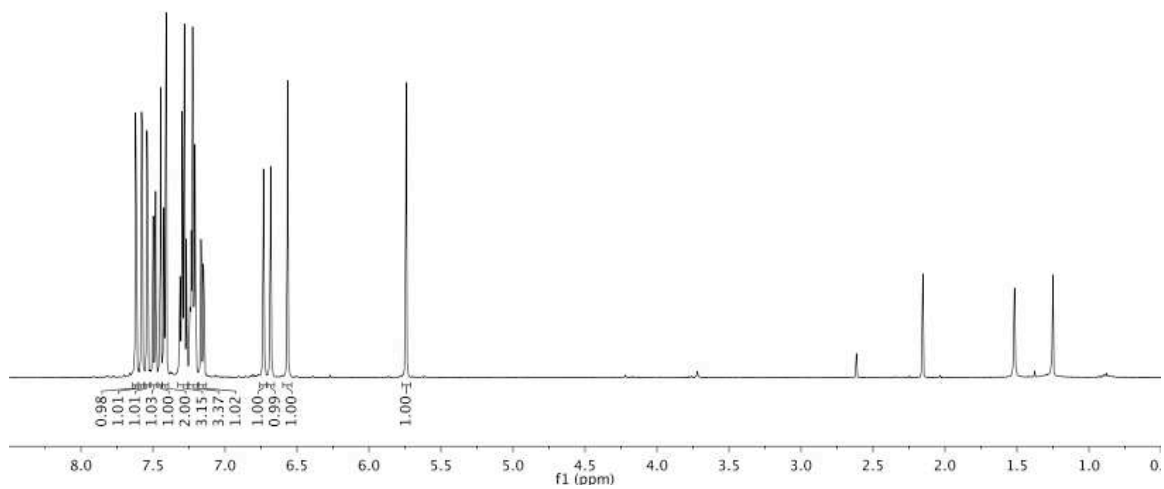
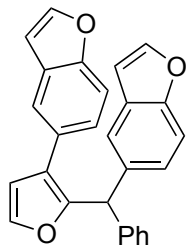


Figure A4.45 500 MHz ^1H and 125 MHz $^{13}\text{C}\{^1\text{H}\}$ NMR of **4.4am** in CDCl_3

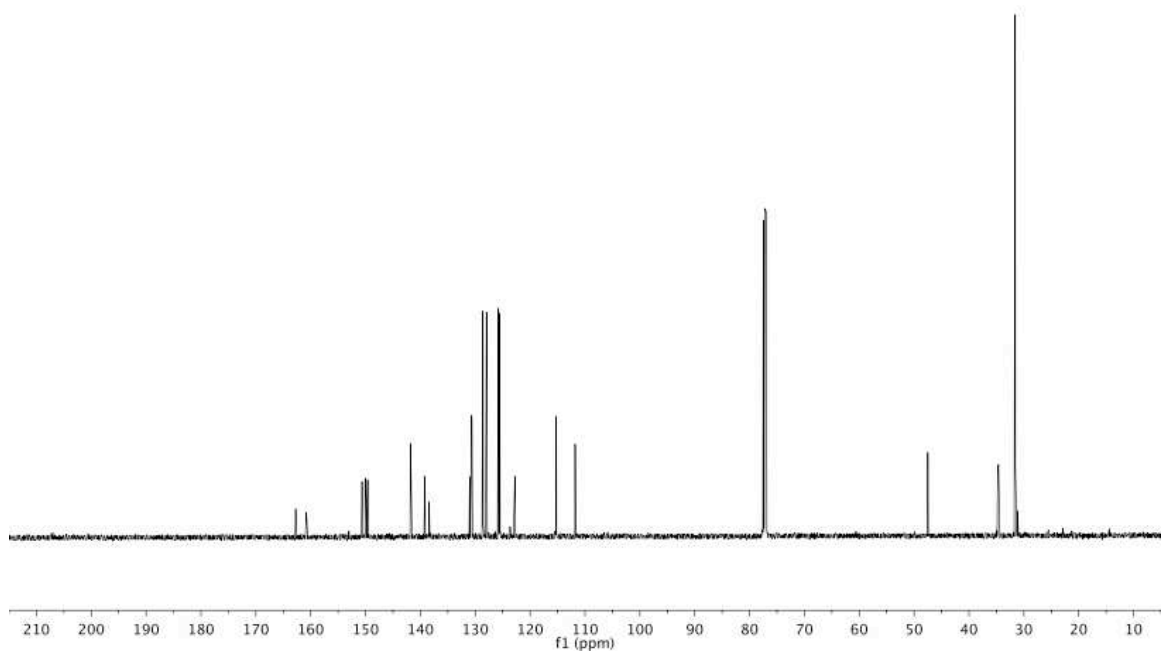
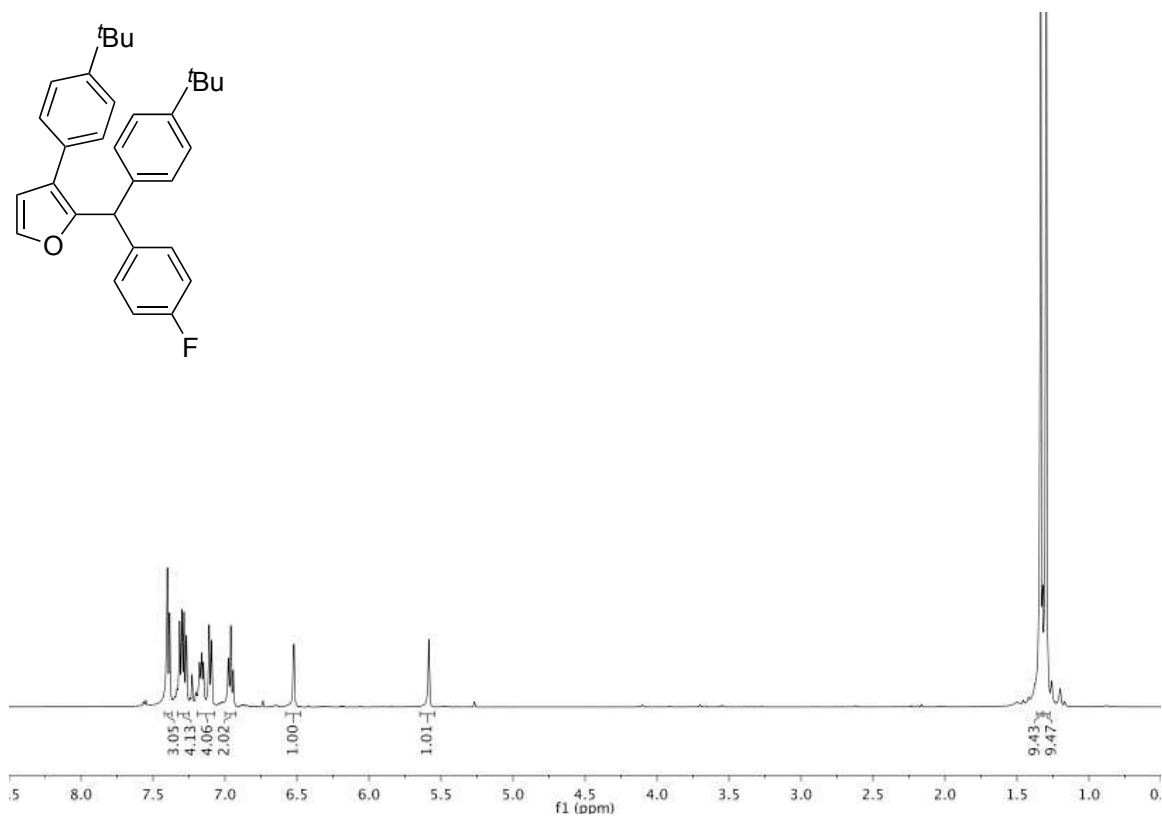


Figure A4.46 500 MHz ^1H and 125 MHz $^{13}\text{C}\{^1\text{H}\}$ NMR of **4.4bb** in CDCl_3

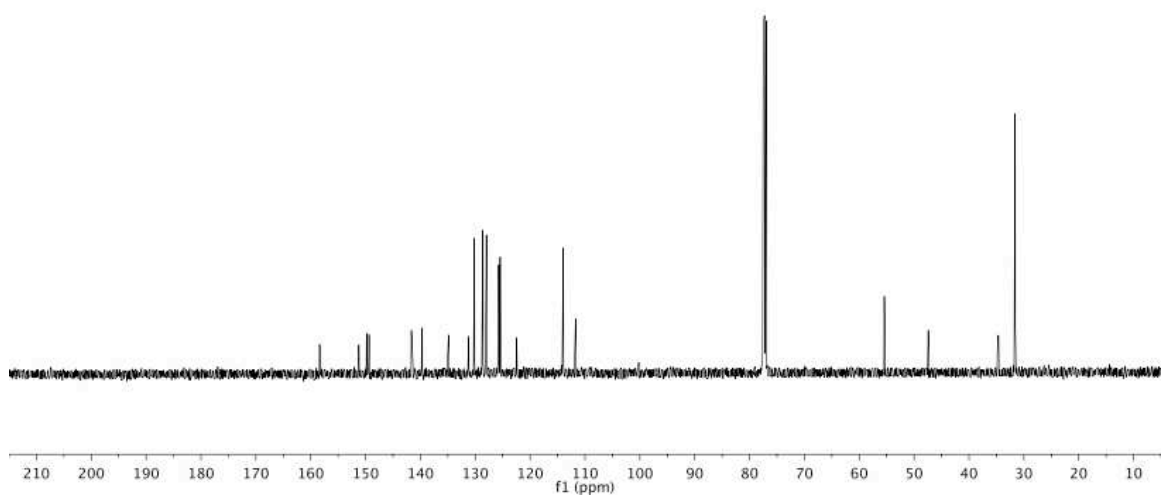
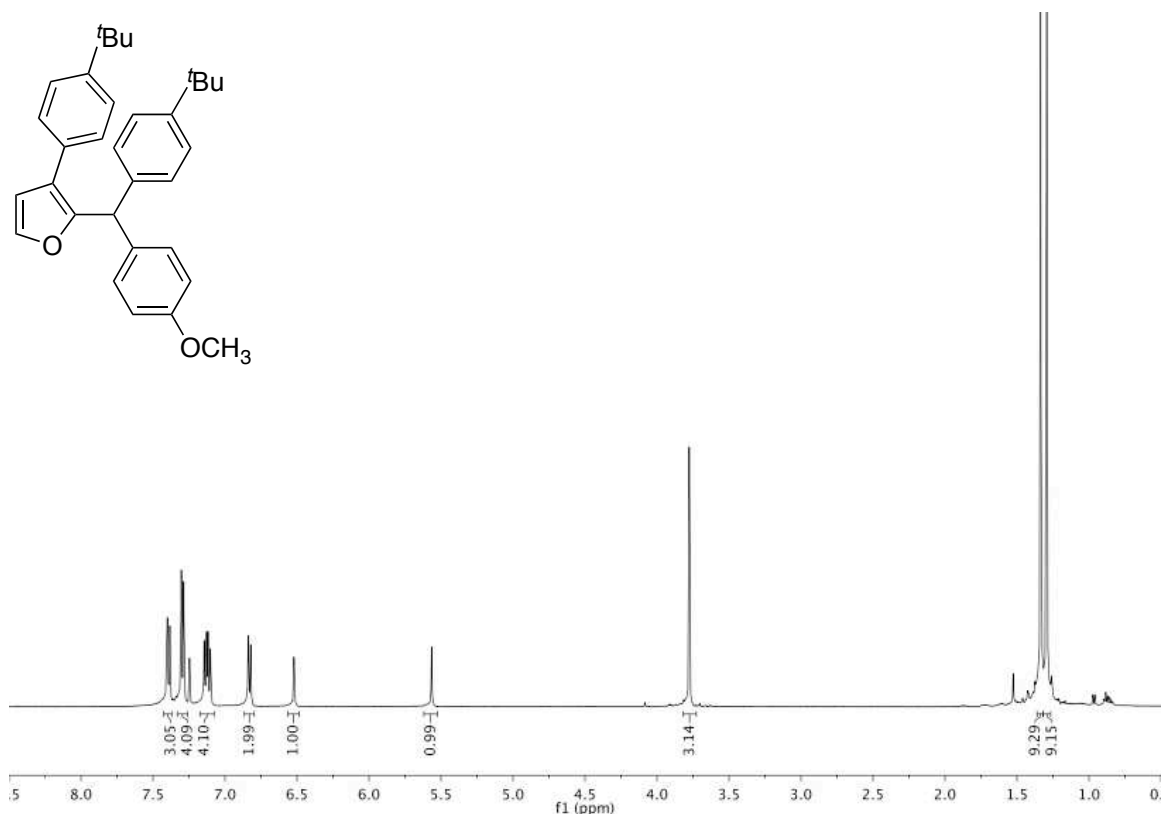


Figure A4.47 500 MHz ^1H and 125 MHz $^{13}\text{C}\{^1\text{H}\}$ NMR of 4.4cb in CDCl_3

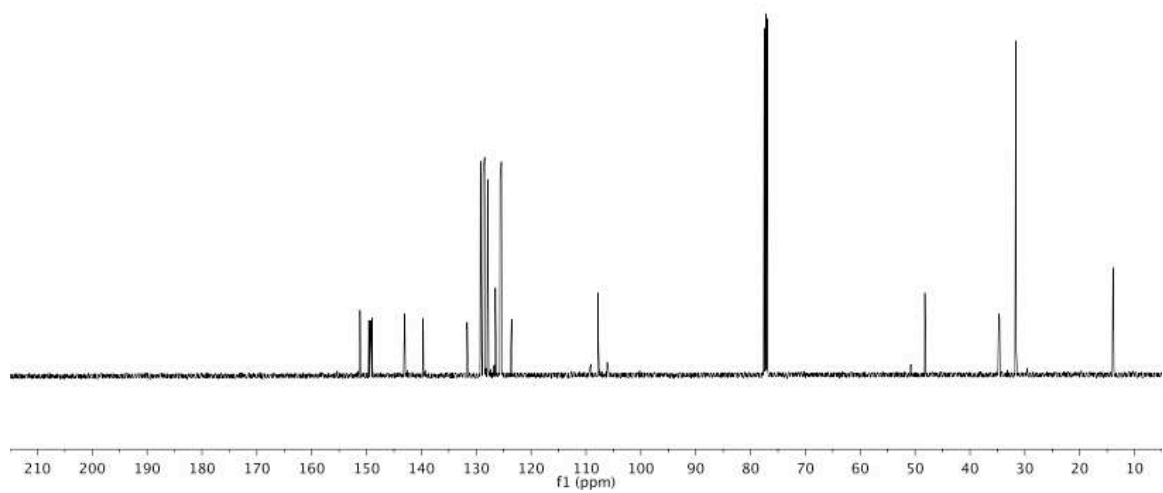
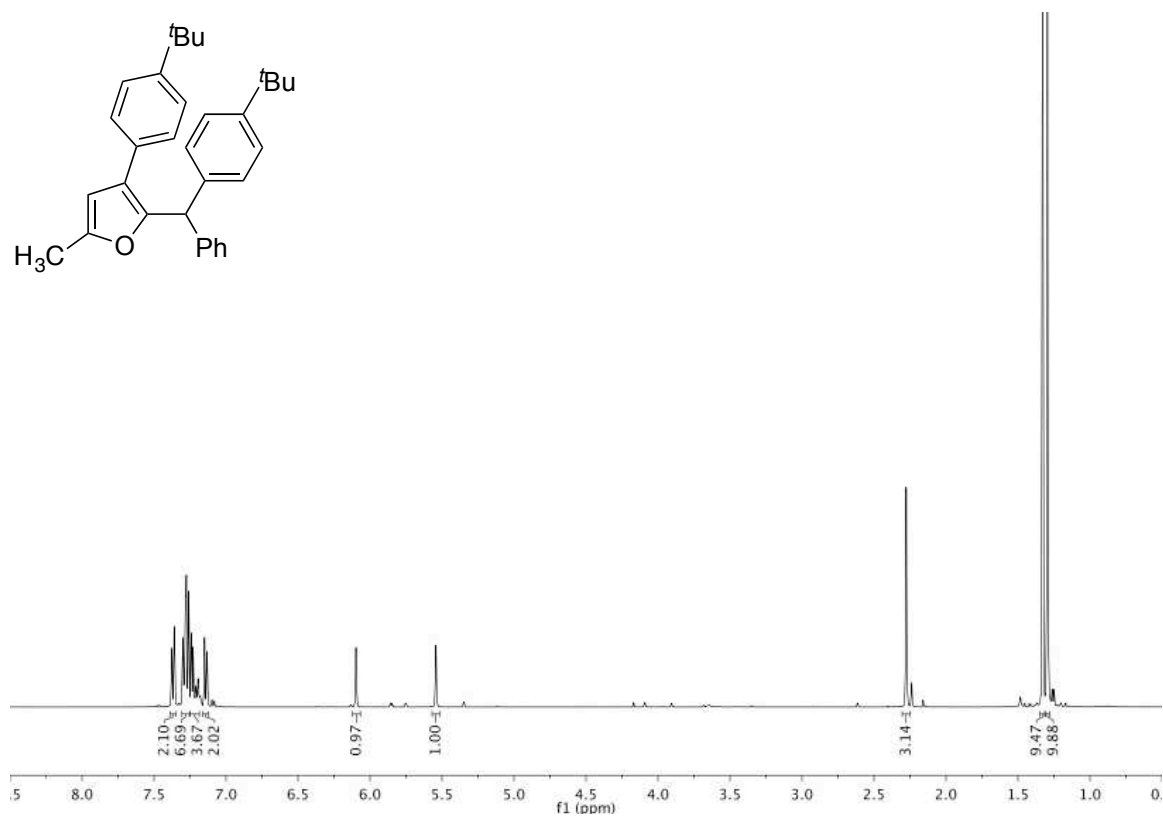
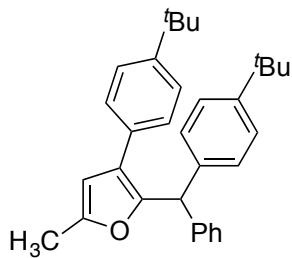
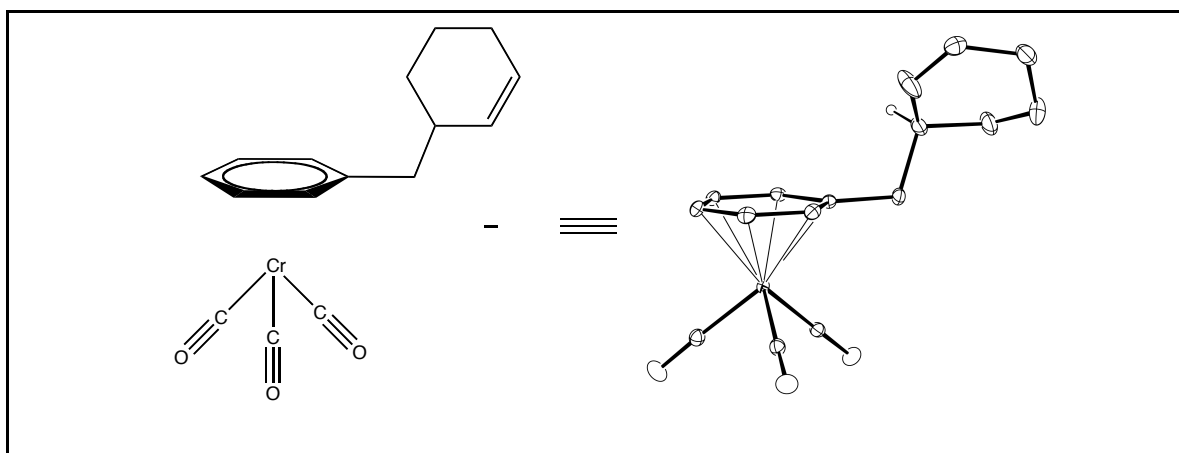


Figure A4.48 500 MHz ^1H and 125 MHz $^{13}\text{C}\{^1\text{H}\}$ NMR of **4.4db** in CDCl_3

Appendix B. X-ray Structure Reports

X-ray Structure Determination of Compound 6171



Compound 6171, $C_{16}H_{16}O_3Cr$, crystallizes in the monoclinic space group $P2_1/n$ (systematic absences $0k0$: $k=\text{odd}$ and $h0l$: $h+l=\text{odd}$) with $a=5.9990(5)\text{\AA}$, $b=11.8071(9)\text{\AA}$, $c=19.7318(15)\text{\AA}$, $\beta=92.184(4)^\circ$, $V=1396.60(19)\text{\AA}^3$, $Z=4$, and $d_{\text{calc}}=1.466\text{ g/cm}^3$. X-ray intensity data were collected on a Bruker APEXII CCD area detector employing graphite-monochromated Mo-K α radiation ($\lambda=0.71073\text{ \AA}$) at a temperature of $100(1)\text{K}$. Preliminary indexing was performed from a series of thirty-six 0.5° rotation frames with exposures of 3seconds. A total of 2306 frames were collected with a crystal to detector distance of 37.600 mm, rotation widths of 0.5° and exposures of 30 seconds:

scan type	2 θ	w	f	c	frames
f	24.50	7.41	-347.34	28.88	723
f	-15.50	258.48	-138.21	19.46	309
f	-23.00	315.83	-345.17	28.88	734
f	-23.00	123.37	-65.26	-94.51	540

Rotation frames were integrated using SAINTⁱ, producing a listing of unaveraged F^2 and $s(F^2)$ values which were then passed to the SHELXTLⁱⁱ program package for further processing and structure solution. A total of 26318 reflections were measured over the ranges $2.01 \leq \theta \leq 27.50^\circ$, $-7 \leq h \leq 7$, $-15 \leq k \leq 15$, $-25 \leq l \leq 25$ yielding 3209 unique reflections ($R_{\text{int}} = 0.0267$). The intensity data were corrected for Lorentz and polarization effects and for absorption using SADABSⁱⁱⁱ (minimum and maximum transmission 0.6477, 0.7456).

The structure was solved by direct methods (SHELXS-97^{iv}). Refinement was by full-matrix least squares based on F^2 using SHELXL-97.^v All reflections were used during refinement. The weighting scheme used was $w=1/[s^2(F_o^2) + (0.0307P)^2 + 3.7282P]$ where $P = (F_o^2 + 2F_c^2)/3$. Non-hydrogen atoms were refined anisotropically and hydrogen atoms were refined using a riding model. Refinement converged to $R1=0.0434$ and $wR2=0.1014$ for 3011 observed reflections for which $F > 4s(F)$ and $R1=0.0462$ and $wR2=0.1034$ and $GOF = 1.062$ for all 3209

unique, non-zero reflections and 182 variables.^{vi} The maximum D/s in the final cycle of least squares was 0.005 and the two most prominent peaks in the final difference Fourier were +1.494 and -1.252 e/Å³.

Table 1. lists cell information, data collection parameters, and refinement data. Final positional and equivalent isotropic thermal parameters are given in Tables 2. and 3. Anisotropic thermal parameters are in Table 4. Tables 5. and 6. list bond distances and bond angles. Figure 1. is an ORTEP^{vii} representation of the molecule with 30% probability thermal ellipsoids displayed.

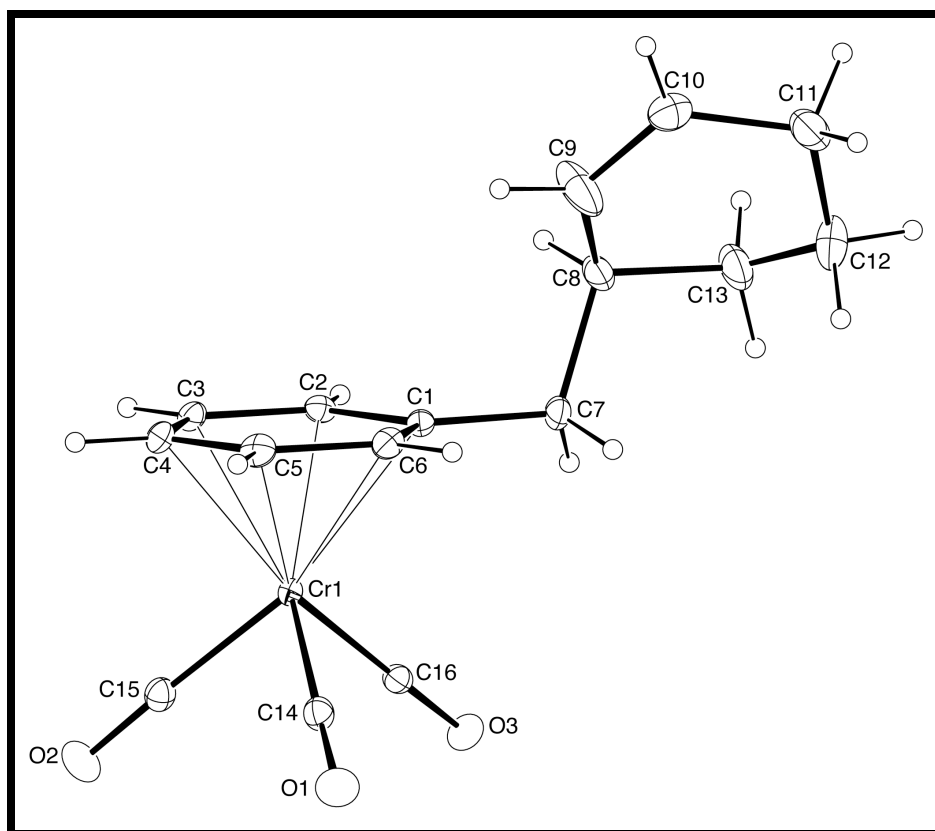


Figure 1. ORTEP drawing of the title compound with 30% probability thermal ellipsoids.

Table 1. Summary of Structure Determination of Compound 6171

Empirical formula	C ₁₆ H ₁₆ O ₃ Cr
Formula weight	308.29
Temperature	100(1) K
Wavelength	0.71073 Å
Crystal system	monoclinic
Space group	P2 ₁ /n
Cell constants:	
a	5.9990(5) Å

b	11.8071(9) Å
c	19.7318(15) Å
b	92.184(4)°
Volume	1396.60(19) Å ³
Z	4
Density (calculated)	1.466 Mg/m ³
Absorption coefficient	0.822 mm ⁻¹
F(000)	640
Crystal size	0.48 x 0.32 x 0.01 mm ³
Theta range for data collection	2.01 to 27.50°
Index ranges	-7 ≤ h ≤ 7, -15 ≤ k ≤ 15, -25 ≤ l ≤ 25
Reflections collected	26318
Independent reflections	3209 [R(int) = 0.0267]
Completeness to theta = 27.50°	100.0 %
Absorption correction	Semi-empirical from equivalents
Max. and min. transmission	0.7456 and 0.6477
Refinement method	Full-matrix least-squares on F ²
Data / restraints / parameters	3209 / 0 / 182
Goodness-of-fit on F ²	1.062
Final R indices [I > 2σ(I)]	R1 = 0.0434, wR2 = 0.1014
R indices (all data)	R1 = 0.0462, wR2 = 0.1034
Largest diff. peak and hole	1.494 and -1.252 e.Å ⁻³

Table 2. Refined Positional Parameters for Compound 6171

Atom	x	y	z	U _{eq} , Å ²
Cr1	0.60710(6)	0.51960(3)	0.745683(17)	0.01304(11)
C1	0.6618(4)	0.44322(19)	0.64398(11)	0.0158(4)
C2	0.4947(4)	0.5283(2)	0.63725(11)	0.0166(4)
C3	0.5341(4)	0.6386(2)	0.66084(12)	0.0197(5)
C4	0.7433(4)	0.6673(2)	0.69169(12)	0.0215(5)
C5	0.9092(4)	0.5847(2)	0.69831(12)	0.0214(5)
C6	0.8692(4)	0.4728(2)	0.67450(12)	0.0189(5)
C7	0.6159(4)	0.3256(2)	0.61734(13)	0.0212(5)
C8	0.6258(6)	0.3195(2)	0.53925(15)	0.0373(7)
C9	0.8418(9)	0.3588(3)	0.5137(2)	0.0778(18)

C10	0.9669(5)	0.2997(3)	0.47112(15)	0.0336(6)
C11	0.9327(5)	0.1743(3)	0.45956(15)	0.0364(7)
C12	0.7512(6)	0.1274(3)	0.50240(19)	0.0411(7)
C13	0.5679(6)	0.2003(3)	0.51388(18)	0.0456(9)
C14	0.7879(4)	0.4750(2)	0.81929(12)	0.0209(5)
C15	0.4473(4)	0.6068(2)	0.80447(12)	0.0200(5)
C16	0.4124(4)	0.4039(2)	0.76258(11)	0.0175(4)
O1	0.9021(3)	0.44702(18)	0.86420(10)	0.0317(4)
O2	0.3470(3)	0.65866(18)	0.84244(10)	0.0323(5)
O3	0.2886(3)	0.33127(16)	0.77239(9)	0.0258(4)

$U_{eq} = \frac{1}{3}[U_{11}(aa^*)^2 + U_{22}(bb^*)^2 + U_{33}(cc^*)^2 + 2U_{12}aa^*bb^*\cos g + 2U_{13}aa^*cc^*\cos b + 2U_{23}bb^*cc^*\cos a]$

Table 3. Positional Parameters for Hydrogens in Compound 6171

Atom	x	y	z	$U_{iso}, \text{\AA}^2$
H2	0.3569	0.5104	0.6168	0.022
H3	0.4226	0.6931	0.6562	0.026
H4	0.7700	0.7405	0.7074	0.029
H5	1.0470	0.6032	0.7185	0.028
H6	0.9812	0.4186	0.6791	0.025
H7a	0.4693	0.3016	0.6308	0.028
H7b	0.7248	0.2736	0.6375	0.028
H8	0.5104	0.3706	0.5205	0.050
H9	0.8944	0.4291	0.5283	0.104
H10	1.0776	0.3371	0.4481	0.045
H11a	0.8937	0.1611	0.4121	0.048
H11b	1.0711	0.1347	0.4704	0.048
H12a	0.6940	0.0589	0.4809	0.055
H12b	0.8179	0.1060	0.5461	0.055
H13a	0.4744	0.1645	0.5467	0.061
H13b	0.4800	0.2072	0.4718	0.061

Table 4. Refined Thermal Parameters (U's) for Compound 6171

Atom	U_{11}	U_{22}	U_{33}	U_{23}	U_{13}	U_{12}
Cr1	0.01308(18)	0.01133(18)	0.01471(18)	0.00061(13)	0.00030(12)	0.00041(13)
C1	0.0172(10)	0.0145(10)	0.0159(10)	0.0004(8)	0.0044(8)	-0.0008(8)
C2	0.0162(10)	0.0198(11)	0.0139(10)	0.0006(8)	0.0004(8)	0.0013(9)

C3	0.0250(12)	0.0155(11)	0.0188(11)	0.0046(9)	0.0033(9)	0.0066(9)
C4	0.0291(12)	0.0135(10)	0.0222(11)	0.0014(9)	0.0047(10)	-0.0049(9)
C5	0.0169(11)	0.0239(12)	0.0236(12)	0.0014(9)	0.0022(9)	-0.0063(9)
C6	0.0148(10)	0.0195(11)	0.0225(11)	0.0034(9)	0.0043(8)	0.0022(9)
C7	0.0260(12)	0.0130(10)	0.0249(12)	-0.0014(9)	0.0071(9)	-0.0026(9)
C8	0.063(2)	0.0214(13)	0.0291(14)	-0.0095(11)	0.0228(14)	-0.0133(13)
C9	0.113(4)	0.050(2)	0.076(3)	-0.040(2)	0.074(3)	-0.052(2)
C10	0.0351(15)	0.0357(15)	0.0299(14)	0.0069(12)	0.0008(11)	0.0017(12)
C11	0.0446(17)	0.0379(16)	0.0266(14)	-0.0077(12)	0.0001(12)	0.0097(13)
C12	0.0455(18)	0.0202(13)	0.057(2)	-0.0051(13)	0.0023(15)	0.0044(12)
C13	0.067(2)	0.0260(15)	0.0458(18)	-0.0161(14)	0.0276(17)	-0.0160(15)
C14	0.0216(11)	0.0185(11)	0.0227(12)	-0.0011(9)	0.0030(9)	0.0015(9)
C15	0.0206(11)	0.0181(11)	0.0210(11)	0.0008(9)	-0.0026(9)	0.0013(9)
C16	0.0185(10)	0.0182(11)	0.0157(10)	-0.0002(8)	0.0009(8)	0.0023(9)
O1	0.0329(10)	0.0372(11)	0.0244(9)	0.0036(8)	-0.0084(8)	0.0070(9)
O2	0.0345(11)	0.0349(11)	0.0276(10)	-0.0074(8)	0.0037(8)	0.0128(9)
O3	0.0265(9)	0.0216(9)	0.0297(9)	0.0038(7)	0.0042(7)	-0.0072(7)

The form of the anisotropic displacement parameter is:

$$\exp[-2p^2(a^2U_{11}h^2+b^2U_{22}k^2+c^2U_{33}l^2+2b*c*U_{23}kl+2a*c*U_{13}hl+2a*b*U_{12}hk)]$$

Table 5. Bond Distances in Compound 6171, Å

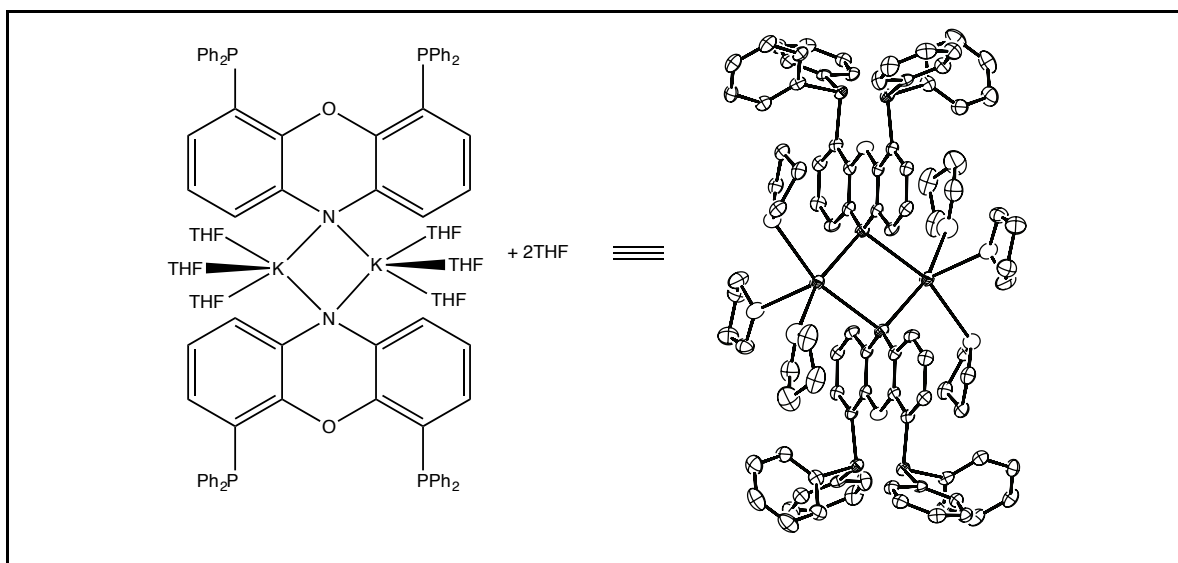
Cr1-C16	1.836(2)	Cr1-C15	1.847(2)	Cr1-C14	1.855(3)
Cr1-C5	2.209(2)	Cr1-C4	2.216(2)	Cr1-C3	2.217(2)
Cr1-C6	2.218(2)	Cr1-C2	2.221(2)	Cr1-C1	2.236(2)
C1-C6	1.405(3)	C1-C2	1.422(3)	C1-C7	1.507(3)
C2-C3	1.400(3)	C3-C4	1.415(4)	C4-C5	1.396(4)
C5-C6	1.420(3)	C7-C8	1.546(4)	C8-C9	1.482(5)
C8-C13	1.529(4)	C9-C10	1.343(5)	C10-C11	1.511(4)
C11-C12	1.509(5)	C12-C13	1.422(5)	C14-O1	1.148(3)
C15-O2	1.154(3)	C16-O3	1.155(3)		

Table 6. Bond Angles in Compound 6171, °

C16-Cr1-C15	87.24(11)	C16-Cr1-C14	90.21(11)	C15-Cr1-C14	88.19(10)
C16-Cr1-C5	150.89(10)	C15-Cr1-C5	121.71(10)	C14-Cr1-C5	88.03(10)
C16-Cr1-C4	157.16(10)	C15-Cr1-C4	94.18(10)	C14-Cr1-C4	112.61(10)
C5-Cr1-C4	36.78(9)	C16-Cr1-C3	120.01(10)	C15-Cr1-C3	91.64(10)

C14-Cr1-C3	149.75(10)	C5-Cr1-C3	66.50(9)	C4-Cr1-C3	37.22(9)
C16-Cr1-C6	113.62(10)	C15-Cr1-C6	159.13(10)	C14-Cr1-C6	91.02(10)
C5-Cr1-C6	37.42(9)	C4-Cr1-C6	66.95(9)	C3-Cr1-C6	78.70(9)
C16-Cr1-C2	92.15(9)	C15-Cr1-C2	115.70(9)	C14-Cr1-C2	156.08(10)
C5-Cr1-C2	78.46(9)	C4-Cr1-C2	66.69(9)	C3-Cr1-C2	36.79(9)
C6-Cr1-C2	66.29(9)	C16-Cr1-C1	88.79(9)	C15-Cr1-C1	152.41(10)
C14-Cr1-C1	119.14(10)	C5-Cr1-C1	67.03(9)	C4-Cr1-C1	79.43(9)
C3-Cr1-C1	67.00(8)	C6-Cr1-C1	36.79(8)	C2-Cr1-C1	37.20(8)
C6-C1-C2	118.3(2)	C6-C1-C7	121.7(2)	C2-C1-C7	120.0(2)
C6-C1-Cr1	70.91(13)	C2-C1-Cr1	70.85(13)	C7-C1-Cr1	130.84(16)
C3-C2-C1	121.1(2)	C3-C2-Cr1	71.43(13)	C1-C2-Cr1	71.95(13)
C2-C3-C4	120.1(2)	C2-C3-Cr1	71.78(13)	C4-C3-Cr1	71.36(13)
C5-C4-C3	119.4(2)	C5-C4-Cr1	71.33(14)	C3-C4-Cr1	71.42(13)
C4-C5-C6	120.5(2)	C4-C5-Cr1	71.89(14)	C6-C5-Cr1	71.64(13)
C1-C6-C5	120.6(2)	C1-C6-Cr1	72.30(13)	C5-C6-Cr1	70.94(13)
C1-C7-C8	112.2(2)	C9-C8-C13	111.6(3)	C9-C8-C7	113.0(3)
C13-C8-C7	110.6(2)	C10-C9-C8	124.5(3)	C9-C10-C11	121.8(3)
C12-C11-	111.8(2)	C13-C12-	116.5(3)	C12-C13-C8	116.2(3)
C10		C11			
O1-C14-Cr1	179.0(2)	O2-C15-Cr1	178.0(2)	O3-C16-Cr1	179.1(2)

X-ray Structure Determination of Compound 6188



Compound 6188, $C_{52}H_{58}NP_2O_5K$, crystallizes in the triclinic space group $P\bar{1}$ with $a=10.8873(6)\text{\AA}$, $b=14.8827(9)\text{\AA}$, $c=15.9049(9)\text{\AA}$, $\alpha=74.193(3)^\circ$, $\beta=72.570(3)^\circ$, $\gamma=74.146(2)^\circ$, $V=2313.7(2)\text{\AA}^3$, $Z=2$, and $d_{\text{calc}}=1.260\text{ g/cm}^3$. X-ray intensity data were collected on a Bruker APEXII CCD area detector employing graphite-monochromated Mo-K α radiation ($\lambda=0.71073\text{ \AA}$) at a temperature of 100(1)K. Preliminary indexing was performed from a series of thirty-six 0.5° rotation frames with exposures of 10 seconds. A total of 2856 frames were collected with a crystal to detector distance of 37.4 mm, rotation widths of 0.5° and exposures of 20 seconds:

scan type	2 θ	w	f	c	frames
f	9.50	319.15	11.63	27.01	739
f	-10.50	336.23	107.70	73.66	173
w	-15.50	242.98	18.69	41.79	212
f	-23.00	328.34	44.17	79.39	509
f	-10.50	300.13	81.17	39.97	484
f	-13.00	335.42	31.84	64.29	739

Rotation frames were integrated using SAINTⁱ, producing a listing of unaveraged F^2 and $s(F^2)$ values which were then passed to the SHELXTLⁱⁱ program package for further processing and structure solution. A total of 55008 reflections were measured over the ranges $1.78 \leq \theta \leq 25.45^\circ$, $-13 \leq h \leq 13$, $-17 \leq k \leq 17$, $-19 \leq l \leq 19$ yielding 8300 unique reflections ($R_{\text{int}} = 0.0498$). The intensity data were corrected for Lorentz and polarization effects and for absorption using SADABSⁱⁱⁱ (minimum and maximum transmission 0.6170, 0.7452).

The structure was solved by direct methods (SHELXS-97^{iv}). The compound forms a dimer that lies on a crystallographic center of symmetry (at $\frac{1}{2}, \frac{1}{2}, \frac{1}{2}$). Refinement was by full-

matrix least squares based on F^2 using SHELXL-97.^v All reflections were used during refinement. The weighting scheme used was $w=1/[s^2(F_o^2) + (0.0784P)^2 + 4.1542P]$ where $P = (F_o^2 + 2F_c^2)/3$. Non-hydrogen atoms were refined anisotropically and hydrogen atoms were refined using a riding model. Refinement converged to $R1=0.0578$ and $wR2=0.1423$ for 5950 observed reflections for which $F > 4s(F)$ and $R1=0.0906$ and $wR2=0.1718$ and $GOF = 1.045$ for all 8300 unique, non-zero reflections and 551 variables.^{vi} The maximum D/s in the final cycle of least squares was 0.000 and the two most prominent peaks in the final difference Fourier were +0.651 and -0.474 e/Å³.

Table 1. lists cell information, data collection parameters, and refinement data. Final positional and equivalent isotropic thermal parameters are given in Tables 2. and 3. Anisotropic thermal parameters are in Table 4. Tables 5. and 6. list bond distances and bond angles. Figure 1. is an ORTEP^{vii} representation of the molecule with 50% probability thermal ellipsoids displayed.

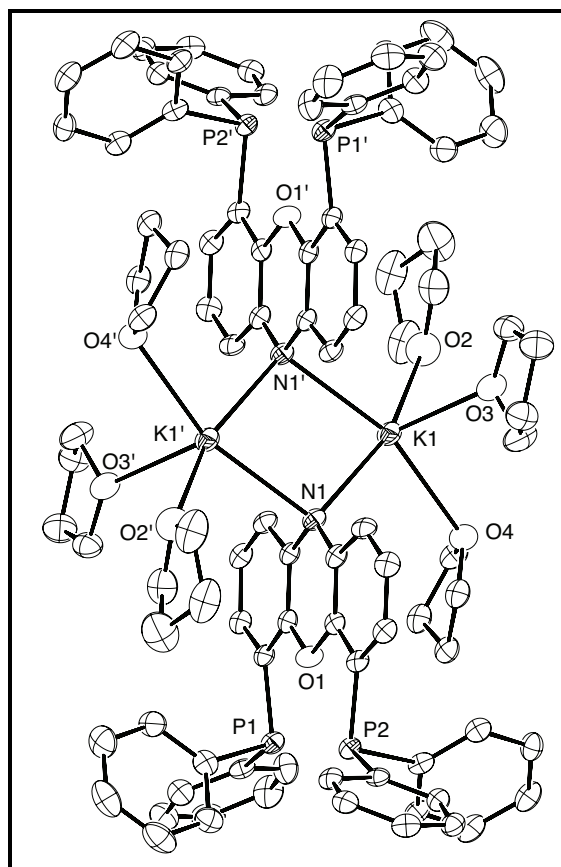


Figure 1. ORTEP drawing of the title compound with 50% probability thermal ellipsoids.

Table 1. Summary of Structure Determination of Compound 6188

Empirical formula

$C_{52}H_{58}NP_2O_5K$

452

Formula weight	878.03
Temperature	100(1) K
Wavelength	0.71073 Å
Crystal system	triclinic
Space group	$P\bar{1}$
Cell constants:	
a	10.8873(6) Å
b	14.8827(9) Å
c	15.9049(9) Å
α	74.193(3)°
β	72.570(3)°
γ	74.146(2)°
Volume	2313.7(2) Å ³
Z	2
Density (calculated)	1.260 Mg/m ³
Absorption coefficient	0.232 mm ⁻¹
F(000)	932
Crystal size	0.42 x 0.15 x 0.04 mm ³
Theta range for data collection	1.78 to 25.45°
Index ranges	-13 ≤ h ≤ 13, -17 ≤ k ≤ 17, -19 ≤ l ≤ 19
Reflections collected	55008
Independent reflections	8300 [R(int) = 0.0498]
Completeness to theta = 25.45°	96.9 %
Absorption correction	Semi-empirical from equivalents
Max. and min. transmission	0.7452 and 0.6170
Refinement method	Full-matrix least-squares on F ²
Data / restraints / parameters	8300 / 0 / 551
Goodness-of-fit on F ²	1.045
Final R indices [I > 2σ(I)]	R1 = 0.0578, wR2 = 0.1423
R indices (all data)	R1 = 0.0906, wR2 = 0.1718
Largest diff. peak and hole	0.651 and -0.474 e.Å ⁻³

Table 2. Refined Positional Parameters for Compound 6188

Atom	x	y	z	U _{eq} , Å ²
------	---	---	---	----------------------------------

K1	0.57532(7)	0.58115(5)	0.55707(5)	0.02716(19)
P1	0.57845(8)	0.13422(6)	0.83614(6)	0.0223(2)
P2	0.17860(8)	0.26785(6)	0.92511(5)	0.0205(2)
O1	0.3921(2)	0.29231(15)	0.77391(14)	0.0241(5)
O2	0.7728(3)	0.6740(2)	0.4688(2)	0.0455(7)
O3	0.4366(2)	0.75355(18)	0.58531(16)	0.0357(6)
O4	0.6025(2)	0.53880(16)	0.73068(16)	0.0313(6)
N1	0.4180(3)	0.44002(18)	0.61443(17)	0.0219(6)
C1	0.6113(3)	0.2143(2)	0.7254(2)	0.0210(7)
C2	0.7312(3)	0.2077(2)	0.6609(2)	0.0216(7)
C3	0.7459(3)	0.2771(2)	0.5825(2)	0.0233(7)
C4	0.6421(3)	0.3532(2)	0.5674(2)	0.0234(7)
C5	0.5198(3)	0.3633(2)	0.6300(2)	0.0209(7)
C6	0.5088(3)	0.2904(2)	0.7088(2)	0.0196(6)
C7	0.1749(3)	0.3693(2)	0.8287(2)	0.0198(6)
C8	0.0665(3)	0.4459(2)	0.8198(2)	0.0235(7)
C9	0.0788(3)	0.5174(2)	0.7428(2)	0.0255(7)
C10	0.1931(3)	0.5154(2)	0.6758(2)	0.0247(7)
C11	0.3038(3)	0.4406(2)	0.6812(2)	0.0212(7)
C12	0.2878(3)	0.3697(2)	0.7601(2)	0.0198(6)
C13	0.7375(3)	0.0512(2)	0.8340(2)	0.0226(7)
C14	0.8316(3)	0.0796(3)	0.8588(3)	0.0332(8)
C15	0.9513(4)	0.0187(3)	0.8657(3)	0.0383(9)
C16	0.9784(3)	-0.0717(3)	0.8498(2)	0.0339(8)
C17	0.8871(4)	-0.1006(3)	0.8241(3)	0.0337(8)
C18	0.7680(3)	-0.0397(2)	0.8159(2)	0.0279(7)
C19	0.4802(3)	0.0620(2)	0.8179(2)	0.0248(7)
C20	0.4832(4)	0.0510(2)	0.7340(2)	0.0316(8)
C21	0.4067(4)	-0.0050(3)	0.7242(3)	0.0397(9)
C22	0.3263(4)	-0.0494(3)	0.7991(3)	0.0419(10)
C23	0.3207(4)	-0.0383(3)	0.8831(3)	0.0441(10)
C24	0.3970(3)	0.0174(2)	0.8931(3)	0.0319(8)
C25	0.2611(3)	0.3088(2)	0.9887(2)	0.0220(7)
C26	0.2430(3)	0.4035(2)	0.9919(2)	0.0252(7)
C27	0.3010(3)	0.4296(2)	1.0458(2)	0.0283(8)
C28	0.3780(3)	0.3602(3)	1.0969(2)	0.0313(8)

C29	0.4024(3)	0.2658(3)	1.0917(2)	0.0309(8)
C30	0.3436(3)	0.2395(2)	1.0373(2)	0.0255(7)
C31	0.0073(3)	0.2913(2)	0.9903(2)	0.0207(7)
C32	-0.0397(3)	0.3339(2)	1.0640(2)	0.0223(7)
C33	-0.1695(3)	0.3427(2)	1.1122(2)	0.0261(7)
C34	-0.2566(3)	0.3092(2)	1.0855(2)	0.0269(7)
C35	-0.2125(3)	0.2675(2)	1.0113(2)	0.0256(7)
C36	-0.0828(3)	0.2579(2)	0.9647(2)	0.0237(7)
C37	0.9117(4)	0.6411(4)	0.4378(3)	0.0556(12)
C38	0.9520(4)	0.6964(4)	0.3441(3)	0.0544(12)
C39	0.8526(5)	0.7897(4)	0.3463(4)	0.0643(14)
C40	0.7303(4)	0.7580(3)	0.4063(3)	0.0454(10)
C41	0.3842(4)	0.8421(3)	0.5320(3)	0.0357(9)
C42	0.2422(4)	0.8739(3)	0.5815(3)	0.0423(9)
C43	0.2142(4)	0.7881(3)	0.6557(3)	0.0414(9)
C44	0.3496(4)	0.7414(3)	0.6710(3)	0.0442(10)
C45	0.5103(3)	0.4873(2)	0.7989(2)	0.0288(8)
C46	0.5903(3)	0.4039(2)	0.8517(2)	0.0280(7)
C47	0.7231(3)	0.3891(2)	0.7861(2)	0.0297(8)
C48	0.7340(3)	0.4891(3)	0.7364(2)	0.0298(8)
O5	0.0655(3)	0.2209(2)	0.4173(3)	0.0681(10)
C49	0.1045(5)	0.1207(3)	0.4333(3)	0.0558(12)
C50	0.2504(4)	0.0999(3)	0.4238(3)	0.0499(11)
C51	0.2957(4)	0.1864(3)	0.3563(3)	0.0452(10)
C52	0.1684(5)	0.2578(3)	0.3485(3)	0.0546(12)

$U_{eq} = \frac{1}{3}[U_{11}(aa^*)^2 + U_{22}(bb^*)^2 + U_{33}(cc^*)^2 + 2U_{12}aa^*bb^*\cos g + 2U_{13}aa^*cc^*\cos b + 2U_{23}bb^*cc^*\cos a]$

Table 3. Positional Parameters for Hydrogens in Compound 6188

Atom	x	y	z	$U_{iso}, \text{\AA}^2$
H2	0.8010	0.1569	0.6706	0.029
H3	0.8258	0.2728	0.5396	0.031
H4	0.6542	0.3989	0.5142	0.031
H8	-0.0114	0.4483	0.8646	0.031
H9	0.0077	0.5681	0.7363	0.034
H10	0.1973	0.5650	0.6254	0.033
H14	0.8135	0.1402	0.8709	0.044

H15	1.0135	0.0391	0.8812	0.051
H16	1.0578	-0.1132	0.8562	0.045
H17	0.9058	-0.1615	0.8123	0.045
H18	0.7077	-0.0597	0.7980	0.037
H20	0.5371	0.0814	0.6831	0.042
H21	0.4101	-0.0123	0.6672	0.053
H22	0.2754	-0.0871	0.7928	0.056
H23	0.2656	-0.0681	0.9335	0.059
H24	0.3926	0.0248	0.9502	0.042
H26	0.1913	0.4504	0.9575	0.034
H27	0.2880	0.4935	1.0476	0.038
H28	0.4137	0.3773	1.1351	0.042
H29	0.4577	0.2197	1.1240	0.041
H30	0.3597	0.1758	1.0336	0.034
H32	0.0175	0.3573	1.0817	0.030
H33	-0.1987	0.3708	1.1622	0.035
H34	-0.3442	0.3149	1.1176	0.036
H35	-0.2707	0.2460	0.9928	0.034
H36	-0.0538	0.2288	0.9153	0.031
H37a	0.9320	0.5733	0.4383	0.074
H37b	0.9581	0.6517	0.4765	0.074
H38a	0.9459	0.6649	0.3001	0.072
H38b	1.0411	0.7060	0.3309	0.072
H39a	0.8787	0.8321	0.3714	0.086
H39b	0.8406	0.8218	0.2865	0.086
H40a	0.6742	0.8074	0.4380	0.060
H40b	0.6814	0.7439	0.3712	0.060
H41a	0.3882	0.8335	0.4729	0.047
H41b	0.4344	0.8896	0.5247	0.047
H42a	0.2320	0.9290	0.6063	0.056
H42b	0.1838	0.8898	0.5416	0.056
H43a	0.1535	0.8072	0.7095	0.055
H43b	0.1787	0.7461	0.6364	0.055
H44a	0.3704	0.7717	0.7104	0.059
H44b	0.3547	0.6741	0.6982	0.059
H45a	0.4596	0.4647	0.7711	0.038

H45b	0.4500	0.5284	0.8383	0.038
H46a	0.5964	0.4192	0.9056	0.037
H46b	0.5526	0.3477	0.8685	0.037
H47a	0.7929	0.3597	0.8174	0.040
H47b	0.7261	0.3499	0.7456	0.040
H48a	0.7684	0.5192	0.7689	0.040
H48b	0.7919	0.4890	0.6767	0.040
H49a	0.0845	0.0958	0.3897	0.074
H49b	0.0598	0.0924	0.4933	0.074
H50a	0.2930	0.0418	0.4013	0.066
H50b	0.2698	0.0931	0.4812	0.066
H51a	0.3509	0.2113	0.3784	0.060
H51b	0.3443	0.1701	0.2986	0.060
H52a	0.1729	0.3191	0.3563	0.073
H52b	0.1527	0.2662	0.2897	0.073

Table 4. Refined Thermal Parameters (U's) for Compound 6188

Atom	U ₁₁	U ₂₂	U ₃₃	U ₂₃	U ₁₃	U ₁₂
K1	0.0310(4)	0.0313(4)	0.0233(4)	-0.0039(3)	-0.0132(3)	-0.0075(3)
P1	0.0205(4)	0.0265(4)	0.0205(4)	-0.0038(3)	-0.0097(3)	-0.0021(3)
P2	0.0185(4)	0.0248(4)	0.0204(4)	-0.0042(3)	-0.0092(3)	-0.0037(3)
O1	0.0171(11)	0.0294(12)	0.0216(11)	-0.0002(9)	-0.0075(10)	0.0001(9)
O2	0.0305(15)	0.0593(18)	0.0502(17)	-0.0099(14)	-0.0104(14)	-0.0160(13)
O3	0.0330(14)	0.0420(15)	0.0288(13)	-0.0061(11)	-0.0106(12)	-0.0004(11)
O4	0.0293(13)	0.0353(13)	0.0321(13)	-0.0027(10)	-0.0171(11)	-0.0051(10)
N1	0.0205(14)	0.0266(14)	0.0197(13)	-0.0034(11)	-0.0094(12)	-0.0028(11)
C1	0.0248(17)	0.0246(16)	0.0193(16)	-0.0038(12)	-0.0115(14)	-0.0081(13)
C2	0.0182(16)	0.0255(16)	0.0233(16)	-0.0064(13)	-0.0097(14)	-0.0016(13)
C3	0.0170(16)	0.0343(18)	0.0217(16)	-0.0090(14)	-0.0049(14)	-0.0068(13)
C4	0.0224(17)	0.0319(18)	0.0190(16)	-0.0039(13)	-0.0084(14)	-0.0083(14)
C5	0.0233(17)	0.0259(16)	0.0196(16)	-0.0054(13)	-0.0124(14)	-0.0063(13)
C6	0.0174(16)	0.0251(16)	0.0208(16)	-0.0077(12)	-0.0081(13)	-0.0049(12)
C7	0.0171(16)	0.0264(16)	0.0209(16)	-0.0032(12)	-0.0121(13)	-0.0059(12)
C8	0.0173(16)	0.0317(18)	0.0244(17)	-0.0067(14)	-0.0083(14)	-0.0051(13)
C9	0.0188(17)	0.0288(17)	0.0299(18)	-0.0058(14)	-0.0135(15)	0.0016(13)
C10	0.0260(18)	0.0276(17)	0.0214(16)	0.0002(13)	-0.0127(15)	-0.0047(14)

C11	0.0185(16)	0.0288(17)	0.0212(16)	-0.0070(13)	-0.0106(14)	-0.0049(13)
C12	0.0200(16)	0.0226(16)	0.0225(16)	-0.0050(12)	-0.0142(14)	-0.0034(12)
C13	0.0199(16)	0.0295(17)	0.0172(15)	0.0000(13)	-0.0072(14)	-0.0050(13)
C14	0.0296(19)	0.0350(19)	0.042(2)	-0.0136(16)	-0.0175(17)	-0.0036(15)
C15	0.029(2)	0.048(2)	0.046(2)	-0.0122(18)	-0.0234(19)	-0.0030(17)
C16	0.0203(18)	0.039(2)	0.037(2)	0.0017(16)	-0.0143(16)	0.0014(15)
C17	0.0294(19)	0.0298(19)	0.040(2)	-0.0046(15)	-0.0122(17)	-0.0026(15)
C18	0.0234(18)	0.0297(18)	0.0332(19)	-0.0048(14)	-0.0140(16)	-0.0034(14)
C19	0.0172(16)	0.0238(16)	0.0327(19)	-0.0057(14)	-0.0103(15)	0.0012(13)
C20	0.033(2)	0.0339(19)	0.0315(19)	-0.0024(15)	-0.0121(17)	-0.0120(15)
C21	0.039(2)	0.043(2)	0.049(2)	-0.0114(18)	-0.019(2)	-0.0158(18)
C22	0.025(2)	0.033(2)	0.073(3)	-0.016(2)	-0.014(2)	-0.0081(16)
C23	0.032(2)	0.032(2)	0.058(3)	-0.0059(18)	0.005(2)	-0.0117(17)
C24	0.0297(19)	0.0286(18)	0.034(2)	-0.0036(15)	-0.0067(16)	-0.0051(15)
C25	0.0146(15)	0.0331(18)	0.0189(16)	-0.0017(13)	-0.0053(13)	-0.0083(13)
C26	0.0196(17)	0.0326(18)	0.0248(17)	-0.0044(14)	-0.0094(14)	-0.0045(14)
C27	0.0259(18)	0.0345(19)	0.0308(19)	-0.0125(15)	-0.0082(16)	-0.0092(15)
C28	0.0230(18)	0.049(2)	0.0285(19)	-0.0132(16)	-0.0134(16)	-0.0055(15)
C29	0.0231(18)	0.045(2)	0.0267(18)	-0.0084(15)	-0.0157(16)	0.0008(15)
C30	0.0228(17)	0.0334(18)	0.0207(16)	-0.0052(14)	-0.0083(14)	-0.0035(14)
C31	0.0208(16)	0.0238(16)	0.0178(15)	0.0018(12)	-0.0086(13)	-0.0069(13)
C32	0.0210(16)	0.0249(16)	0.0244(17)	-0.0040(13)	-0.0114(14)	-0.0047(13)
C33	0.0274(18)	0.0273(17)	0.0229(17)	-0.0050(13)	-0.0083(15)	-0.0024(14)
C34	0.0176(16)	0.0319(18)	0.0281(18)	-0.0003(14)	-0.0076(14)	-0.0041(13)
C35	0.0239(17)	0.0271(17)	0.0288(18)	0.0002(14)	-0.0146(15)	-0.0073(13)
C36	0.0242(17)	0.0289(17)	0.0211(16)	-0.0019(13)	-0.0125(14)	-0.0064(13)
C37	0.034(2)	0.081(3)	0.064(3)	-0.034(3)	-0.018(2)	-0.006(2)
C38	0.028(2)	0.085(3)	0.062(3)	-0.039(3)	-0.006(2)	-0.011(2)
C39	0.048(3)	0.062(3)	0.075(3)	-0.022(3)	0.010(3)	-0.019(2)
C40	0.035(2)	0.053(3)	0.055(3)	-0.019(2)	-0.010(2)	-0.0108(19)
C41	0.038(2)	0.036(2)	0.035(2)	0.0005(16)	-0.0170(18)	-0.0104(16)
C42	0.037(2)	0.042(2)	0.045(2)	-0.0019(18)	-0.0169(19)	-0.0023(17)
C43	0.036(2)	0.041(2)	0.042(2)	-0.0060(18)	-0.0045(19)	-0.0060(17)
C44	0.044(2)	0.049(2)	0.029(2)	-0.0052(17)	-0.0086(19)	0.0041(19)
C45	0.0238(18)	0.0374(19)	0.0318(19)	-0.0113(15)	-0.0145(16)	-0.0041(15)
C46	0.0270(18)	0.0346(19)	0.0283(18)	-0.0079(15)	-0.0127(15)	-0.0082(15)

C47	0.0260(18)	0.038(2)	0.0319(19)	-0.0116(15)	-0.0163(16)	-0.0031(15)
C48	0.0220(18)	0.044(2)	0.0257(18)	-0.0073(15)	-0.0082(15)	-0.0072(15)
O5	0.0427(19)	0.062(2)	0.102(3)	-0.023(2)	-0.024(2)	-0.0007(16)
C49	0.052(3)	0.063(3)	0.060(3)	-0.019(2)	-0.013(2)	-0.019(2)
C50	0.044(2)	0.054(3)	0.048(3)	-0.007(2)	-0.016(2)	-0.003(2)
C51	0.041(2)	0.052(2)	0.042(2)	-0.0048(19)	-0.015(2)	-0.0088(19)
C52	0.063(3)	0.048(3)	0.053(3)	-0.007(2)	-0.027(3)	-0.001(2)

The form of the anisotropic displacement parameter is:

$$\exp[-2p^2(a^2U_{11}h^2+b^2U_{22}k^2+c^2U_{33}l^2+2b*c*U_{23}kl+2a*c*U_{13}hl+2a*b*U_{12}hk)]$$

Table 5. Bond Distances in Compound 6188, Å

K1-O3	2.678(3)	K1-O2	2.694(3)	K1-O4	2.747(2)
K1-N1#1	2.808(3)	K1-N1	2.857(3)	P1-C13	1.829(3)
P1-C1	1.834(3)	P1-C19	1.835(3)	P2-C31	1.832(3)
P2-C7	1.837(3)	P2-C25	1.838(3)	O1-C6	1.377(4)
O1-C12	1.401(4)	O2-C40	1.430(5)	O2-C37	1.432(5)
O3-C44	1.405(5)	O3-C41	1.432(4)	O4-C48	1.438(4)
O4-C45	1.445(4)	N1-C11	1.372(4)	N1-C5	1.384(4)
N1-K1#1	2.808(3)	C1-C6	1.386(4)	C1-C2	1.396(5)
C2-C3	1.384(5)	C3-C4	1.390(4)	C4-C5	1.401(5)
C4-K1#1	3.312(3)	C5-C6	1.414(4)	C5-K1#1	3.263(3)
C7-C12	1.377(5)	C7-C8	1.410(4)	C8-C9	1.385(5)
C9-C10	1.374(5)	C10-C11	1.406(4)	C11-C12	1.403(4)
C13-C18	1.391(5)	C13-C14	1.397(5)	C14-C15	1.385(5)
C15-C16	1.372(5)	C16-C17	1.384(5)	C17-C18	1.384(5)
C19-C20	1.379(5)	C19-C24	1.392(5)	C20-C21	1.393(5)
C21-C22	1.372(6)	C22-C23	1.372(6)	C23-C24	1.389(5)
C25-C26	1.383(5)	C25-C30	1.394(4)	C26-C27	1.387(4)
C27-C28	1.381(5)	C28-C29	1.378(5)	C29-C30	1.401(5)
C31-C32	1.382(4)	C31-C36	1.411(4)	C32-C33	1.381(5)
C33-C34	1.394(5)	C34-C35	1.380(5)	C35-C36	1.372(5)
C37-C38	1.493(7)	C38-C39	1.511(7)	C39-C40	1.497(6)
C41-C42	1.519(5)	C42-C43	1.514(5)	C43-C44	1.510(5)
C45-C46	1.511(5)	C46-C47	1.508(5)	C47-C48	1.500(5)
O5-C49	1.407(6)	O5-C52	1.424(6)	C49-C50	1.502(6)
C50-C51	1.526(6)	C51-C52	1.514(6)		

Symmetry transformations used to generate equivalent atoms:

#1 -x+1,-y+1,-z+1

Table 6. Bond Angles in Compound 6188, °

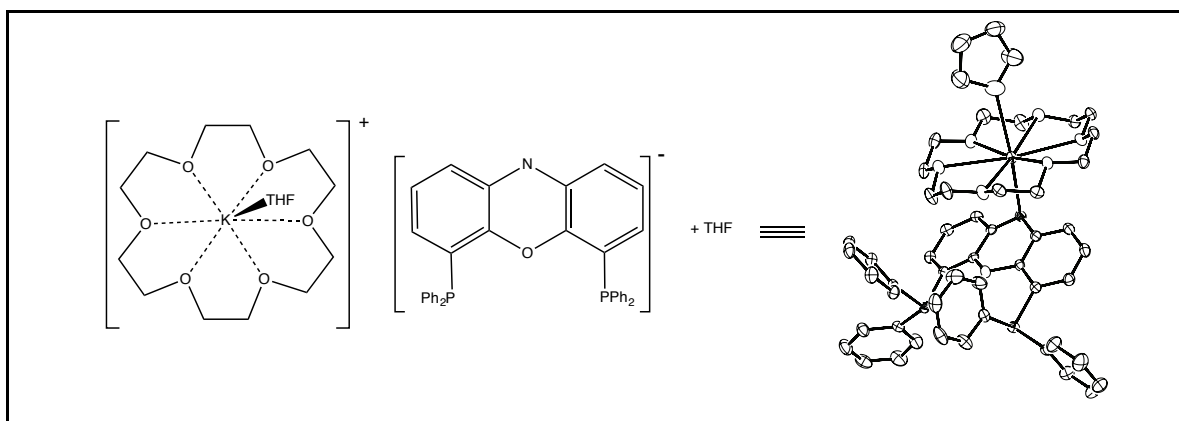
O3-K1-O2	84.31(9)	O3-K1-O4	87.77(7)	O2-K1-O4	101.20(8)
O3-K1-N1#1	110.75(8)	O2-K1-N1#1	84.68(8)	O4-K1-N1#1	161.15(8)
O3-K1-N1	113.00(8)	O2-K1-N1	161.26(9)	O4-K1-N1	87.16(7)
N1#1-K1-N1	82.43(8)	C13-P1-C1	101.80(15)	C13-P1-C19	101.97(14)
C1-P1-C19	101.17(14)	C31-P2-C7	100.88(14)	C31-P2-C25	101.25(14)
C7-P2-C25	99.67(14)	C6-O1-C12	117.6(2)	C40-O2-C37	108.8(3)
C40-O2-K1	111.2(2)	C37-O2-K1	132.4(3)	C44-O3-C41	108.2(3)
C44-O3-K1	108.2(2)	C41-O3-K1	136.8(2)	C48-O4-C45	108.7(2)
C48-O4-K1	111.63(19)	C45-O4-K1	116.89(17)	C11-N1-C5	115.1(3)
C11-N1-K1#1	120.26(18)	C5-N1-K1#1	96.31(17)	C11-N1-K1	125.92(19)
C5-N1-K1	95.46(18)	K1#1-N1-K1	97.57(8)	C6-C1-C2	118.9(3)
C6-C1-P1	115.5(2)	C2-C1-P1	125.5(2)	C3-C2-C1	119.7(3)
C2-C3-C4	120.5(3)	C3-C4-C5	122.0(3)	C3-C4-K1#1	137.3(2)
C5-C4-K1#1	75.76(17)	N1-C5-C4	121.3(3)	N1-C5-C6	123.1(3)
C4-C5-C6	115.6(3)	N1-C5-K1#1	58.77(15)	C4-C5-K1#1	79.65(17)
C6-C5-K1#1	136.4(2)	O1-C6-C1	116.4(3)	O1-C6-C5	120.4(3)
C1-C6-C5	123.3(3)	C12-C7-C8	118.0(3)	C12-C7-P2	116.7(2)
C8-C7-P2	125.3(2)	C9-C8-C7	118.6(3)	C10-C9-C8	121.7(3)
C9-C10-C11	122.0(3)	N1-C11-C12	123.9(3)	N1-C11-C10	121.5(3)
C12-C11- C10	114.6(3)	C7-C12-O1	115.1(3)	C7-C12-C11	125.1(3)
O1-C12-C11	119.9(3)	C18-C13- C14	118.1(3)	C18-C13-P1	125.0(2)
C14-C13-P1	116.8(2)	C15-C14- C13	120.9(3)	C16-C15- C14	120.3(3)
C15-C16- C17	119.6(3)	C18-C17- C16	120.4(3)	C17-C18- C13	120.7(3)
C20-C19- C24	118.6(3)	C20-C19-P1	123.5(3)	C24-C19-P1	117.9(3)
C19-C20- C21	121.0(4)	C22-C21- C20	119.6(4)	C23-C22- C21	120.2(3)
C22-C23- C24	120.3(4)	C23-C24- C25	120.2(4)	C26-C25- C24	119.1(3)

C24		C19		C30	
C26-C25-P2	123.4(2)	C30-C25-P2	117.5(2)	C25-C26-	120.8(3)
				C27	
C28-C27-	119.7(3)	C29-C28-	120.5(3)	C28-C29-	119.7(3)
C26		C27		C30	
C25-C30-	120.0(3)	C32-C31-	117.6(3)	C32-C31-P2	126.2(2)
C29		C36			
C36-C31-P2	116.1(2)	C33-C32-	121.7(3)	C32-C33-	119.6(3)
		C31		C34	
C35-C34-	119.8(3)	C36-C35-	120.1(3)	C35-C36-	121.2(3)
C33		C34		C31	
O2-C37-C38	107.0(4)	C37-C38-	102.1(4)	C40-C39-	102.4(4)
		C39		C38	
O2-C40-C39	106.3(4)	O3-C41-C42	107.1(3)	C43-C42-	104.0(3)
				C41	
C44-C43-	101.6(3)	O3-C44-C43	105.5(3)	O4-C45-C46	106.9(3)
C42					
C47-C46-	102.9(3)	C48-C47-	102.6(3)	O4-C48-C47	105.8(3)
C45		C46			
C49-O5-C52	107.0(3)	O5-C49-C50	105.3(4)	C49-C50-	104.4(4)
				C51	
C52-C51-	103.7(4)	O5-C52-C51	107.3(4)		
C50					

Symmetry transformations used to generate equivalent atoms:

#1 -x+1,-y+1,-z+1

X-ray Structure Determination of Compound 6189



Compound 6189, $C_{56}H_{66}NP_2O_9K$, crystallizes in the monoclinic space group $P2_1/n$ (systematic absences $0k0: k=\text{odd}$ and $h0l: h+l=\text{odd}$) with $a=10.8453(7)\text{\AA}$, $b=18.1426(13)\text{\AA}$, $c=26.2160(17)\text{\AA}$, $\beta=93.676(4)^\circ$, $V=5147.7(6)\text{\AA}^3$, $Z=4$, and $d_{\text{calc}}=1.288\text{ g/cm}^3$. X-ray intensity data were collected on a Bruker APEXII CCD area detector employing graphite-monochromated Mo-K α radiation ($\lambda=0.71073\text{ \AA}$) at a temperature of $100(1)\text{K}$. Preliminary indexing was performed from a series of thirty-six 0.5° rotation frames with exposures of 10 seconds. A total of 2814 frames were collected with a crystal to detector distance of 37.5 mm, rotation widths of 0.5° and exposures of 15 seconds:

scan type	2 θ	w	f	c	frames
f	-23.00	315.83	12.48	28.88	739
f	-13.00	335.42	230.34	64.29	341
f	-25.50	327.22	135.03	78.00	347
f	22.00	321.06	18.69	41.79	739
w	17.00	327.86	318.36	83.36	68
w	9.50	122.45	150.48	-95.28	72
f	22.00	14.84	188.65	97.50	508

Rotation frames were integrated using SAINTⁱ, producing a listing of unaveraged F^2 and $s(F^2)$ values which were then passed to the SHELXTLⁱⁱ program package for further processing and structure solution. A total of 131835 reflections were measured over the ranges $1.56 \leq \theta \leq 27.53^\circ$, $-14 \leq h \leq 14$, $-23 \leq k \leq 23$, $-34 \leq l \leq 33$ yielding 11849 unique reflections ($R_{\text{int}} = 0.0230$). The intensity data were corrected for Lorentz and polarization effects and for absorption using SADABSⁱⁱⁱ (minimum and maximum transmission 0.6876, 0.7456).

The structure was solved by direct methods (SHELXS-97^{iv}). Refinement was by full-matrix least squares based on F^2 using SHELXL-97.^v All reflections were used during refinement. The weighting scheme used was $w=1/[s^2(F_o^2) + (0.0660P)^2 + 8.1221P]$ where $P = (F_o^2 +$

$2F_c^2/3$. Non-hydrogen atoms were refined anisotropically and hydrogen atoms were refined using a riding model. Refinement converged to $R1=0.0535$ and $wR2=0.1391$ for 10556 observed reflections for which $F > 4\sigma(F)$ and $R1=0.0602$ and $wR2=0.1456$ and $GOF = 1.028$ for all 11849 unique, non-zero reflections and 632 variables.^{vi} The maximum D/s in the final cycle of least squares was 0.002 and the two most prominent peaks in the final difference Fourier were +1.585 and -0.990 $e/\text{\AA}^3$.

Table 1. lists cell information, data collection parameters, and refinement data. Final positional and equivalent isotropic thermal parameters are given in Tables 2. and 3. Anisotropic thermal parameters are in Table 4. Tables 5. and 6. list bond distances and bond angles. Figure 1. is an ORTEP^{vii} representation of the molecule with 50% probability thermal ellipsoids displayed.

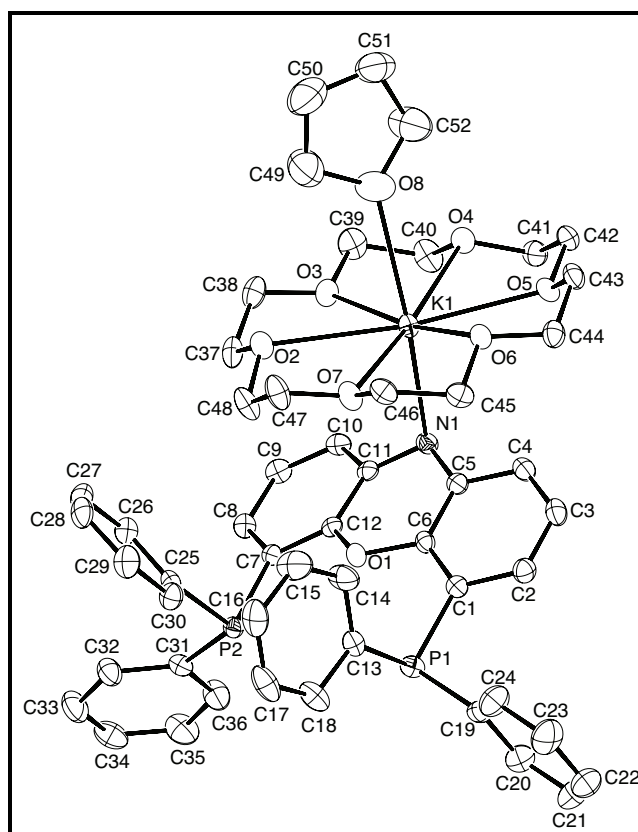


Figure 1. ORTEP drawing of the title compound with 50% probability thermal ellipsoids.

Table 1. Summary of Structure Determination of Compound 6189

Empirical formula	$C_{56}H_{66}NP_2O_9K$
Formula weight	998.14
Temperature	100(1) K
Wavelength	0.71073 \AA
	463

Crystal system	monoclinic
Space group	P2 ₁ /n
Cell constants:	
a	10.8453(7) Å
b	18.1426(13) Å
c	26.2160(17) Å
β	93.676(4)°
Volume	5147.7(6) Å ³
Z	4
Density (calculated)	1.288 Mg/m ³
Absorption coefficient	0.223 mm ⁻¹
F(000)	2120
Crystal size	0.48 x 0.18 x 0.10 mm ³
Theta range for data collection	1.56 to 27.53°
Index ranges	-14 ≤ h ≤ 14, -23 ≤ k ≤ 23, -34 ≤ l ≤ 33
Reflections collected	131835
Independent reflections	11849 [R(int) = 0.0230]
Completeness to theta = 27.53°	99.8 %
Absorption correction	Semi-empirical from equivalents
Max. and min. transmission	0.7456 and 0.6876
Refinement method	Full-matrix least-squares on F ²
Data / restraints / parameters	11849 / 70 / 632
Goodness-of-fit on F ²	1.028
Final R indices [I > 2σ(I)]	R1 = 0.0535, wR2 = 0.1391
R indices (all data)	R1 = 0.0602, wR2 = 0.1456
Largest diff. peak and hole	1.585 and -0.990 e.Å ⁻³

Table 2. Refined Positional Parameters for Compound 6189

Atom	x	y	z	U _{eq} , Å ²
C1	0.50372(18)	0.50834(11)	0.30940(8)	0.0183(4)
C2	0.5601(2)	0.55069(12)	0.34935(8)	0.0230(4)
C3	0.6558(2)	0.59803(12)	0.33949(8)	0.0246(4)
C4	0.70042(19)	0.60346(12)	0.29097(8)	0.0216(4)
C5	0.64887(18)	0.56141(11)	0.24995(8)	0.0182(4)
C6	0.54713(18)	0.51643(11)	0.26102(8)	0.0170(4)

C7	0.50077(17)	0.41258(11)	0.14468(8)	0.0169(4)
C8	0.56166(19)	0.39993(12)	0.09945(8)	0.0203(4)
C9	0.66564(19)	0.44117(12)	0.09003(8)	0.0218(4)
C10	0.70986(18)	0.49494(12)	0.12419(8)	0.0198(4)
C11	0.65223(17)	0.51045(11)	0.16956(8)	0.0172(4)
C12	0.54669(17)	0.46675(11)	0.17795(7)	0.0156(4)
C13	0.24051(19)	0.48007(12)	0.29891(8)	0.0215(4)
C14	0.2268(2)	0.54949(15)	0.27818(11)	0.0343(6)
C15	0.1099(2)	0.57529(17)	0.26223(12)	0.0430(7)
C16	0.0059(2)	0.53238(17)	0.26643(10)	0.0362(6)
C17	0.0192(2)	0.46347(16)	0.28751(11)	0.0376(6)
C18	0.1352(2)	0.43715(14)	0.30358(10)	0.0322(5)
C19	0.3829(2)	0.43800(12)	0.38816(8)	0.0244(4)
C20	0.4546(2)	0.38677(15)	0.41581(10)	0.0338(5)
C21	0.4567(3)	0.38530(18)	0.46900(11)	0.0454(7)
C22	0.3868(3)	0.43448(18)	0.49458(10)	0.0434(7)
C23	0.3154(3)	0.48563(18)	0.46777(10)	0.0425(7)
C24	0.3131(2)	0.48781(16)	0.41478(9)	0.0343(5)
C25	0.24097(18)	0.41677(11)	0.12792(8)	0.0182(4)
C26	0.2449(2)	0.43851(12)	0.07697(8)	0.0233(4)
C27	0.1511(2)	0.48127(13)	0.05387(9)	0.0268(5)
C28	0.0532(2)	0.50423(13)	0.08182(9)	0.0284(5)
C29	0.0496(2)	0.48442(14)	0.13258(9)	0.0300(5)
C30	0.1430(2)	0.44063(13)	0.15557(9)	0.0243(4)
C31	0.37500(19)	0.27906(11)	0.12330(8)	0.0206(4)
C32	0.2879(2)	0.25630(13)	0.08529(10)	0.0291(5)
C33	0.3011(3)	0.18895(14)	0.06079(11)	0.0377(6)
C34	0.4004(3)	0.14367(13)	0.07377(11)	0.0357(6)
C35	0.4875(2)	0.16517(14)	0.11183(12)	0.0371(6)
C36	0.4742(2)	0.23205(14)	0.13645(10)	0.0316(5)
N1	0.69699(16)	0.56408(10)	0.20274(7)	0.0192(3)
O1	0.48188(13)	0.47981(8)	0.22117(5)	0.0185(3)
P1	0.38819(5)	0.43668(3)	0.31841(2)	0.02033(12)
P2	0.36279(5)	0.36234(3)	0.162311(19)	0.01701(12)
K1	0.61374(4)	0.71209(2)	0.179582(16)	0.01963(11)
O2	0.42900(14)	0.66138(9)	0.10400(6)	0.0246(3)

O3	0.67980(15)	0.66302(9)	0.08592(6)	0.0249(3)
O4	0.85229(14)	0.74673(9)	0.14767(6)	0.0233(3)
O5	0.78217(14)	0.78178(8)	0.24906(6)	0.0233(3)
O6	0.52620(14)	0.78683(9)	0.26535(6)	0.0230(3)
O7	0.36875(14)	0.69367(9)	0.20640(6)	0.0261(3)
O8	0.5961(2)	0.84626(12)	0.12267(10)	0.0543(6)
C37	0.4796(2)	0.61255(13)	0.06829(9)	0.0266(5)
C38	0.5880(2)	0.64872(14)	0.04611(9)	0.0294(5)
C39	0.7927(2)	0.68864(15)	0.06852(9)	0.0328(5)
C40	0.8868(2)	0.69135(15)	0.11303(10)	0.0320(5)
C41	0.9351(2)	0.75019(13)	0.19196(9)	0.0259(5)
C42	0.8908(2)	0.80813(13)	0.22730(9)	0.0254(4)
C43	0.7301(2)	0.83583(12)	0.28078(9)	0.0246(4)
C44	0.6197(2)	0.80370(13)	0.30429(8)	0.0248(4)
C45	0.4251(2)	0.74957(13)	0.28602(9)	0.0256(5)
C46	0.3242(2)	0.74026(13)	0.24483(9)	0.0257(5)
C47	0.2799(2)	0.68187(16)	0.16521(10)	0.0339(6)
C48	0.3309(2)	0.62714(15)	0.12907(10)	0.0341(6)
C49	0.5058(4)	0.8536(2)	0.08107(17)	0.0640(10)
C50	0.5079(4)	0.9313(2)	0.06488(17)	0.0710(11)
C51	0.6212(3)	0.9650(2)	0.08853(13)	0.0542(8)
C52	0.6880(3)	0.9015(2)	0.11541(18)	0.0646(10)
O9	0.6923(3)	0.7525(2)	0.44208(13)	0.0958(10)
C53	0.5791(6)	0.8023(5)	0.4418(3)	0.0727(17)
C53'	0.5601(7)	0.7598(6)	0.4386(3)	0.0700(18)
C54	0.5419(4)	0.8002(3)	0.49110(15)	0.0784(12)
C55	0.6587(5)	0.8145(3)	0.5184(2)	0.0967(15)
C56	0.7456(4)	0.7671(3)	0.49442(17)	0.0749(11)

$U_{eq} = \frac{1}{3}[U_{11}(aa^*)^2 + U_{22}(bb^*)^2 + U_{33}(cc^*)^2 + 2U_{12}aa^*bb^*\cos g + 2U_{13}aa^*cc^*\cos b + 2U_{23}bb^*cc^*\cos a]$

Table 3. Positional Parameters for Hydrogens in Compound 6189

Atom	x	y	z	$U_{iso}, \text{\AA}^2$
H2	0.5333	0.5469	0.3822	0.031
H3	0.6911	0.6269	0.3659	0.033
H4	0.7654	0.6354	0.2856	0.029
H8	0.5324	0.3643	0.0762	0.027

H9	0.7063	0.4327	0.0604	0.029
H10	0.7798	0.5215	0.1168	0.026
H14	0.2957	0.5792	0.2748	0.046
H15	0.1016	0.6224	0.2485	0.057
H16	-0.0717	0.5499	0.2552	0.048
H17	-0.0501	0.4342	0.2910	0.050
H18	0.1429	0.3902	0.3177	0.043
H20	0.5018	0.3531	0.3987	0.045
H21	0.5056	0.3509	0.4872	0.060
H22	0.3879	0.4331	0.5301	0.058
H23	0.2683	0.5190	0.4852	0.057
H24	0.2647	0.5227	0.3969	0.046
H26	0.3110	0.4242	0.0583	0.031
H27	0.1536	0.4946	0.0197	0.036
H28	-0.0098	0.5328	0.0663	0.038
H29	-0.0151	0.5003	0.1514	0.040
H30	0.1400	0.4272	0.1897	0.032
H32	0.2205	0.2863	0.0762	0.039
H33	0.2423	0.1743	0.0354	0.050
H34	0.4088	0.0989	0.0571	0.048
H35	0.5546	0.1349	0.1208	0.049
H36	0.5324	0.2459	0.1623	0.042
H37A	0.4175	0.6007	0.0413	0.035
H37B	0.5055	0.5671	0.0853	0.035
H38a	0.6213	0.6167	0.0207	0.039
H38b	0.5624	0.6945	0.0295	0.039
H39a	0.7816	0.7374	0.0537	0.044
H39b	0.8206	0.6558	0.0424	0.044
H40a	0.8912	0.6439	0.1301	0.043
H40b	0.9677	0.7024	0.1011	0.043
H41a	1.0175	0.7623	0.1823	0.034
H41b	0.9384	0.7027	0.2090	0.034
H42a	0.9544	0.8184	0.2541	0.034
H42b	0.8728	0.8534	0.2085	0.034
H43a	0.7057	0.8788	0.2606	0.033
H43b	0.7910	0.8511	0.3074	0.033

H44a	0.6434	0.7592	0.3230	0.033
H44b	0.5879	0.8387	0.3282	0.033
H45a	0.3950	0.7779	0.3140	0.034
H45b	0.4516	0.7017	0.2991	0.034
H46a	0.2521	0.7183	0.2588	0.034
H46b	0.3008	0.7878	0.2303	0.034
H47a	0.2616	0.7280	0.1476	0.045
H47b	0.2040	0.6631	0.1780	0.045
H48a	0.3616	0.5841	0.1478	0.045
H48b	0.2665	0.6115	0.1040	0.045
H49a	0.4247	0.8405	0.0917	0.085
H49b	0.5255	0.8215	0.0531	0.085
H50a	0.4356	0.9568	0.0759	0.094
H50b	0.5076	0.9344	0.0279	0.094
H51a	0.6016	1.0030	0.1127	0.072
H51b	0.6708	0.9863	0.0628	0.072
H52a	0.7518	0.8824	0.0947	0.086
H52b	0.7261	0.9174	0.1481	0.086
H53a	0.6001	0.8522	0.4323	0.097
H53b	0.5142	0.7842	0.4178	0.097
H53a'	0.5192	0.7122	0.4369	0.093
H53b'	0.5311	0.7896	0.4096	0.093
H54a	0.5089	0.7523	0.4996	0.104
H54b	0.4815	0.8381	0.4971	0.104
H54a'	0.4987	0.8464	0.4845	0.104
H54b'	0.4915	0.7697	0.5120	0.104
H55a	0.6553	0.8025	0.5544	0.129
H55b	0.6818	0.8659	0.5153	0.129
H56a	0.7567	0.7214	0.5133	0.100
H56b	0.8251	0.7912	0.4933	0.100

Table 4. Refined Thermal Parameters (U's) for Compound 6189

Atom	U ₁₁	U ₂₂	U ₃₃	U ₂₃	U ₁₃	U ₁₂
C1	0.0165(9)	0.0180(9)	0.0203(9)	-0.0006(7)	0.0014(7)	0.0014(7)
C2	0.0257(11)	0.0235(10)	0.0197(10)	-0.0022(8)	0.0014(8)	0.0002(8)
C3	0.0248(10)	0.0238(11)	0.0247(10)	-0.0059(8)	-0.0035(8)	-0.0011(8)

C4	0.0184(9)	0.0185(10)	0.0275(11)	-0.0014(8)	-0.0012(8)	-0.0010(8)
C5	0.0151(9)	0.0166(9)	0.0225(10)	0.0016(7)	-0.0015(7)	0.0022(7)
C6	0.0145(9)	0.0160(9)	0.0200(9)	-0.0014(7)	-0.0016(7)	0.0011(7)
C7	0.0133(8)	0.0168(9)	0.0205(9)	0.0016(7)	-0.0004(7)	0.0016(7)
C8	0.0195(9)	0.0208(10)	0.0205(9)	-0.0025(8)	0.0005(7)	0.0024(8)
C9	0.0184(9)	0.0245(10)	0.0233(10)	0.0011(8)	0.0062(8)	0.0041(8)
C10	0.0139(9)	0.0205(10)	0.0253(10)	0.0038(8)	0.0044(7)	0.0023(7)
C11	0.0134(8)	0.0176(9)	0.0203(9)	0.0048(7)	-0.0009(7)	0.0028(7)
C12	0.0131(8)	0.0169(9)	0.0169(9)	0.0028(7)	0.0009(7)	0.0034(7)
C13	0.0185(9)	0.0252(10)	0.0212(10)	-0.0055(8)	0.0035(7)	-0.0021(8)
C14	0.0181(11)	0.0323(13)	0.0522(16)	0.0109(11)	-0.0001(10)	-0.0027(9)
C15	0.0237(12)	0.0436(16)	0.0614(18)	0.0182(14)	0.0004(12)	0.0041(11)
C16	0.0162(10)	0.0565(17)	0.0360(13)	-0.0083(12)	0.0016(9)	0.0021(11)
C17	0.0207(11)	0.0451(15)	0.0478(15)	-0.0178(12)	0.0078(10)	-0.0101(10)
C18	0.0260(11)	0.0291(12)	0.0424(14)	-0.0091(10)	0.0085(10)	-0.0069(9)
C19	0.0270(11)	0.0235(11)	0.0231(10)	0.0026(8)	0.0051(8)	-0.0042(8)
C20	0.0367(13)	0.0304(12)	0.0338(13)	0.0040(10)	-0.0007(10)	0.0008(10)
C21	0.0551(18)	0.0451(16)	0.0345(14)	0.0132(12)	-0.0085(12)	0.0015(14)
C22	0.0547(17)	0.0521(17)	0.0234(12)	0.0073(11)	0.0027(11)	-0.0123(14)
C23	0.0474(16)	0.0562(18)	0.0249(12)	-0.0036(12)	0.0097(11)	0.0011(14)
C24	0.0379(13)	0.0405(14)	0.0250(12)	0.0009(10)	0.0053(10)	0.0069(11)
C25	0.0150(9)	0.0160(9)	0.0233(10)	-0.0029(7)	-0.0020(7)	-0.0008(7)
C26	0.0222(10)	0.0251(11)	0.0224(10)	-0.0029(8)	0.0000(8)	0.0028(8)
C27	0.0303(11)	0.0268(11)	0.0226(10)	-0.0003(9)	-0.0055(9)	0.0033(9)
C28	0.0221(10)	0.0279(11)	0.0338(12)	-0.0043(9)	-0.0101(9)	0.0067(9)
C29	0.0193(10)	0.0371(13)	0.0335(12)	-0.0049(10)	0.0003(9)	0.0073(9)
C30	0.0188(10)	0.0300(11)	0.0240(10)	-0.0006(9)	0.0006(8)	0.0021(8)
C31	0.0198(10)	0.0171(9)	0.0252(10)	-0.0003(8)	0.0027(8)	-0.0017(8)
C32	0.0268(11)	0.0217(11)	0.0376(13)	-0.0033(9)	-0.0064(9)	0.0007(9)
C33	0.0423(15)	0.0251(12)	0.0442(15)	-0.0099(11)	-0.0088(12)	-0.0035(11)
C34	0.0399(14)	0.0191(11)	0.0489(15)	-0.0070(10)	0.0084(12)	-0.0015(10)
C35	0.0308(13)	0.0235(12)	0.0568(17)	-0.0029(11)	0.0013(11)	0.0073(10)
C36	0.0262(11)	0.0247(11)	0.0428(14)	-0.0047(10)	-0.0055(10)	0.0042(9)
N1	0.0165(8)	0.0190(8)	0.0221(8)	0.0009(7)	0.0008(6)	-0.0021(6)
O1	0.0141(6)	0.0231(7)	0.0183(7)	-0.0029(6)	0.0014(5)	-0.0024(5)
P1	0.0217(3)	0.0182(3)	0.0216(3)	-0.00093(19)	0.0050(2)	-0.0007(2)

P2	0.0142(2)	0.0174(2)	0.0193(2)	0.00054(18)	-0.00021(18)	0.00015(18)
K1	0.0172(2)	0.0210(2)	0.0205(2)	-0.00228(16)	-0.00049(15)	-0.00100(16)
O2	0.0232(7)	0.0230(8)	0.0273(8)	-0.0065(6)	-0.0004(6)	0.0007(6)
O3	0.0246(8)	0.0288(8)	0.0211(7)	-0.0028(6)	-0.0001(6)	0.0014(6)
O4	0.0192(7)	0.0228(8)	0.0278(8)	-0.0022(6)	0.0004(6)	0.0025(6)
O5	0.0215(7)	0.0209(7)	0.0275(8)	-0.0026(6)	0.0004(6)	-0.0052(6)
O6	0.0205(7)	0.0247(8)	0.0236(7)	-0.0018(6)	-0.0004(6)	-0.0037(6)
O7	0.0184(7)	0.0290(8)	0.0307(8)	-0.0071(7)	0.0016(6)	-0.0016(6)
O8	0.0486(12)	0.0312(10)	0.0816(17)	0.0171(11)	-0.0065(11)	0.0071(9)
C37	0.0265(11)	0.0272(11)	0.0248(11)	-0.0083(9)	-0.0079(8)	0.0070(9)
C38	0.0321(12)	0.0361(13)	0.0196(10)	-0.0056(9)	-0.0025(9)	0.0080(10)
C39	0.0316(12)	0.0396(14)	0.0281(12)	-0.0069(10)	0.0090(10)	-0.0005(10)
C40	0.0221(11)	0.0327(13)	0.0417(13)	-0.0106(11)	0.0054(10)	0.0033(9)
C41	0.0157(9)	0.0269(11)	0.0346(12)	0.0043(9)	-0.0022(8)	0.0006(8)
C42	0.0196(10)	0.0269(11)	0.0292(11)	0.0016(9)	-0.0035(8)	-0.0069(8)
C43	0.0246(10)	0.0181(10)	0.0302(11)	-0.0046(8)	-0.0065(9)	-0.0010(8)
C44	0.0270(11)	0.0239(11)	0.0229(10)	-0.0053(8)	-0.0025(8)	0.0019(9)
C45	0.0244(11)	0.0260(11)	0.0272(11)	-0.0010(9)	0.0079(9)	-0.0010(9)
C46	0.0198(10)	0.0249(11)	0.0331(12)	-0.0029(9)	0.0065(9)	-0.0013(8)
C47	0.0181(10)	0.0431(14)	0.0404(14)	-0.0125(11)	0.0007(9)	-0.0053(10)
C48	0.0257(11)	0.0357(13)	0.0406(14)	-0.0129(11)	0.0003(10)	-0.0103(10)
C49	0.065(2)	0.0466(19)	0.078(3)	0.0011(18)	-0.0152(19)	-0.0056(17)
C50	0.071(3)	0.075(3)	0.065(2)	0.026(2)	-0.0117(19)	0.002(2)
C51	0.066(2)	0.0480(18)	0.0495(18)	0.0120(15)	0.0097(16)	-0.0041(16)
C52	0.0389(17)	0.050(2)	0.104(3)	0.021(2)	-0.0032(18)	0.0012(15)
O9	0.0886(19)	0.116(3)	0.086(2)	-0.0426(19)	0.0278(16)	-0.0265(19)
C53	0.048(3)	0.099(4)	0.071(3)	0.038(4)	0.003(2)	-0.028(3)
C53'	0.066(3)	0.104(5)	0.041(3)	0.027(3)	0.012(3)	-0.014(4)
C54	0.084(2)	0.082(3)	0.073(2)	0.023(2)	0.0355(18)	0.054(2)
C55	0.102(3)	0.112(4)	0.078(3)	-0.050(3)	0.023(2)	-0.012(3)
C56	0.059(2)	0.082(3)	0.082(3)	0.002(2)	-0.0111(18)	-0.0285(19)

The form of the anisotropic displacement parameter is:

$$\exp[-2p^2(a^*2U_{11}h^2+b^*2U_{22}k^2+c^*2U_{33}l^2+2b^*c^*U_{23}kl+2a^*c^*U_{13}hl+2a^*b^*U_{12}hk)]$$

Table 5. Bond Distances in Compound 6189, Å

C1-C6	1.389(3)	C1-C2	1.407(3)	C1-P1	1.831(2)
-------	----------	-------	----------	-------	----------

C2-C3	1.384(3)	C3-C4	1.393(3)	C4-C5	1.405(3)
C5-N1	1.374(3)	C5-C6	1.417(3)	C5-K1	3.306(2)
C6-O1	1.392(2)	C7-C12	1.385(3)	C7-C8	1.413(3)
C7-P2	1.836(2)	C8-C9	1.389(3)	C9-C10	1.389(3)
C10-C11	1.407(3)	C11-N1	1.373(3)	C11-C12	1.421(3)
C12-O1	1.392(2)	C13-C14	1.376(3)	C13-C18	1.394(3)
C13-P1	1.828(2)	C14-C15	1.390(3)	C15-C16	1.381(4)
C16-C17	1.371(4)	C17-C18	1.385(4)	C19-C20	1.386(3)
C19-C24	1.395(3)	C19-P1	1.833(2)	C20-C21	1.393(4)
C21-C22	1.373(5)	C22-C23	1.373(4)	C23-C24	1.388(3)
C25-C30	1.393(3)	C25-C26	1.396(3)	C25-P2	1.839(2)
C26-C27	1.387(3)	C27-C28	1.392(3)	C28-C29	1.381(4)
C29-C30	1.394(3)	C31-C32	1.391(3)	C31-C36	1.399(3)
C31-P2	1.834(2)	C32-C33	1.392(3)	C33-C34	1.380(4)
C34-C35	1.386(4)	C35-C36	1.386(3)	N1-K1	2.8852(18)
K1-O3	2.7497(16)	K1-O5	2.7976(16)	K1-O7	2.8115(16)
K1-O4	2.8401(16)	K1-O6	2.8406(16)	K1-O8	2.855(2)
K1-O2	2.8772(16)	O2-C37	1.424(3)	O2-C48	1.428(3)
O3-C39	1.413(3)	O3-C38	1.419(3)	O4-C40	1.421(3)
O4-C41	1.423(3)	O5-C42	1.425(3)	O5-C43	1.426(3)
O6-C45	1.425(3)	O6-C44	1.425(3)	O7-C47	1.417(3)
O7-C46	1.423(3)	O8-C49	1.425(4)	O8-C52	1.435(4)
C37-C38	1.496(4)	C39-C40	1.501(4)	C41-C42	1.500(3)
C43-C44	1.500(3)	C45-C46	1.497(3)	C47-C48	1.502(3)
C49-C50	1.472(5)	C50-C51	1.474(5)	C51-C52	1.510(5)
O9-C53'	1.437(8)	O9-C56	1.478(5)	O9-C53	1.524(7)
C53-C54	1.380(7)	C53'-C54	1.582(8)	C54-C55	1.439(6)
C55-C56	1.449(6)				

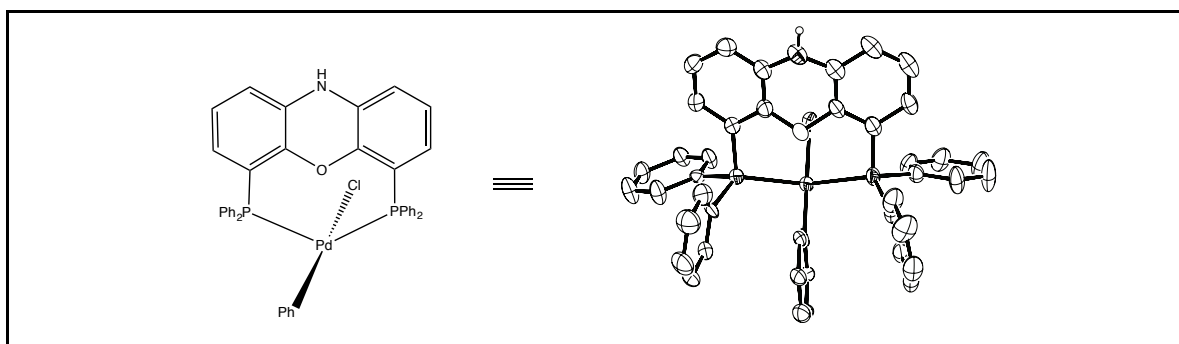
Table 6. Bond Angles in Compound 6189, °

C6-C1-C2	117.74(19)	C6-C1-P1	117.89(15)	C2-C1-P1	124.06(16)
C3-C2-C1	119.7(2)	C2-C3-C4	121.5(2)	C3-C4-C5	121.1(2)
N1-C5-C4	120.97(19)	N1-C5-C6	123.39(18)	C4-C5-C6	115.63(19)
N1-C5-K1	60.35(10)	C4-C5-K1	90.23(13)	C6-C5-K1	121.80(13)
C1-C6-O1	116.68(17)	C1-C6-C5	124.19(18)	O1-C6-C5	119.07(17)
C12-C7-C8	118.37(18)	C12-C7-P2	117.37(15)	C8-C7-P2	124.26(16)

C9-C8-C7	119.37(19)	C10-C9-C8	120.97(19)	C9-C10-C11	122.14(19)
N1-C11-C10	121.28(18)	N1-C11-C12	123.57(18)	C10-C11- C12	115.15(18)
C7-C12-O1	116.96(17)	C7-C12-C11	124.00(18)	O1-C12-C11	119.01(17)
C14-C13- C18	118.5(2)	C14-C13-P1	125.12(17)	C18-C13-P1	116.30(18)
C13-C14- C15	120.0(2)	C16-C15- C14	121.3(3)	C17-C16- C15	118.8(2)
C16-C17- C18	120.5(2)	C17-C18- C13	120.9(2)	C20-C19- C24	118.5(2)
C20-C19-P1	117.42(18)	C24-C19-P1	124.08(18)	C19-C20- C21	120.6(3)
C22-C21- C20	120.1(3)	C21-C22- C23	120.0(3)	C22-C23- C24	120.3(3)
C23-C24- C19	120.5(3)	C30-C25- C26	118.76(19)	C30-C25-P2	117.36(16)
C26-C25-P2	123.78(16)	C27-C26- C25	120.6(2)	C26-C27- C28	120.0(2)
C29-C28- C27	119.9(2)	C28-C29- C30	120.1(2)	C25-C30- C29	120.6(2)
C32-C31- C36	118.1(2)	C32-C31-P2	125.04(17)	C36-C31-P2	116.54(17)
C33-C32- C31	120.4(2)	C34-C33- C32	120.7(2)	C33-C34- C35	119.7(2)
C34-C35- C36	119.7(2)	C35-C36- C31	121.4(2)	C11-N1-C5	113.97(17)
C11-N1-K1	115.67(12)	C5-N1-K1	95.20(12)	C6-O1-C12	115.68(15)
C13-P1-C1	104.63(10)	C13-P1-C19	100.99(10)	C1-P1-C19	100.65(10)
C31-P2-C7	100.33(9)	C31-P2-C25	104.14(9)	C7-P2-C25	100.46(9)
O3-K1-O5	122.08(5)	O3-K1-O7	119.29(5)	O5-K1-O7	118.62(5)
O3-K1-O4	60.93(5)	O5-K1-O4	61.49(5)	O7-K1-O4	173.36(5)
O3-K1-O6	168.77(5)	O5-K1-O6	60.42(4)	O7-K1-O6	59.31(5)
O4-K1-O6	118.99(5)	O3-K1-O8	79.74(7)	O5-K1-O8	88.51(6)
O7-K1-O8	101.51(6)	O4-K1-O8	71.88(6)	O6-K1-O8	89.55(6)
O3-K1-O2	59.42(5)	O5-K1-O2	171.78(5)	O7-K1-O2	60.44(5)
O4-K1-O2	118.37(5)	O6-K1-O2	116.39(5)	O8-K1-O2	83.83(6)

O3-K1-N1	77.91(5)	O5-K1-N1	95.80(5)	O7-K1-N1	97.16(5)
O4-K1-N1	89.38(5)	O6-K1-N1	113.18(5)	O8-K1-N1	155.93(7)
O2-K1-N1	92.41(5)	O3-K1-C5	101.72(5)	O5-K1-C5	87.90(5)
O7-K1-C5	80.74(5)	O4-K1-C5	105.83(5)	O6-K1-C5	89.17(5)
O8-K1-C5	176.36(6)	O2-K1-C5	99.79(5)	N1-K1-C5	24.45(5)
C37-O2-C48	111.22(18)	C37-O2-K1	111.76(12)	C48-O2-K1	109.18(13)
C39-O3-C38	113.85(18)	C39-O3-K1	117.56(13)	C38-O3-K1	120.35(13)
C40-O4-C41	111.99(17)	C40-O4-K1	108.33(13)	C41-O4-K1	107.97(12)
C42-O5-C43	111.82(17)	C42-O5-K1	114.41(12)	C43-O5-K1	115.09(12)
C45-O6-C44	111.03(17)	C45-O6-K1	112.28(12)	C44-O6-K1	114.28(12)
C47-O7-C46	112.58(17)	C47-O7-K1	115.78(13)	C46-O7-K1	118.41(12)
C49-O8-C52	106.4(3)	C49-O8-K1	119.94(19)	C52-O8-K1	129.90(19)
O2-C37-C38	109.17(19)	O3-C38-C37	109.02(18)	O3-C39-C40	108.7(2)
O4-C40-C39	109.03(19)	O4-C41-C42	108.95(17)	O5-C42-C41	108.53(18)
O5-C43-C44	109.21(17)	O6-C44-C43	109.83(18)	O6-C45-C46	108.91(18)
O7-C46-C45	108.17(18)	O7-C47-C48	108.7(2)	O2-C48-C47	108.6(2)
O8-C49-C50	106.7(3)	C49-C50-	107.7(3)	C50-C51-	104.0(3)
		C51		C52	
O8-C52-C51	106.1(3)	C53'-O9-C56	111.8(4)	C53'-O9-C53	31.2(4)
C56-O9-C53	99.5(4)	C54-C53-O9	105.2(5)	O9-C53'-C54	99.7(5)
C53-C54-	99.2(5)	C53-C54-	30.4(4)	C55-C54-	111.2(4)
C55		C53'		C53'	
C54-C55-	104.6(3)	C55-C56-O9	106.5(4)		
C56					

X-ray Structure Determination of Compound 6190



Compound 6190, $C_{42}H_{32}P_2NPClPd$, crystallizes in the monoclinic space group $C2/c$ (systematic absences hkl : $h+k=\text{odd}$ and $h0l$: $l=\text{odd}$) with $a=39.5647(19)\text{\AA}$, $b=12.2212(6)\text{\AA}$, $c=24.1733(13)\text{\AA}$, $\beta=124.594(2)^\circ$, $V=9621.9(8)\text{\AA}^3$, $Z=8$, and $d_{\text{calc}}=1.064\text{ g/cm}^3$. X-ray intensity data were collected on a Bruker APEXII CCD area detector employing graphite-monochromated Mo-K α radiation ($\lambda=0.71073\text{ \AA}$) at a temperature of $100(1)\text{K}$. Preliminary indexing was performed from a series of thirty-six 0.5° rotation frames with exposures of 10 seconds. A total of 2508 frames were collected with a crystal to detector distance of 37.5 mm, rotation widths of 0.5° and exposures of 30 seconds:

scan type	2 θ	w	f	c	frames
f	24.50	7.41	12.48	28.88	739
f	-23.00	334.21	38.95	73.55	427
w	7.00	356.72	261.23	-20.60	153
f	-23.00	315.83	87.08	28.88	589
f	-13.00	335.42	98.29	64.29	600

Rotation frames were integrated using SAINTⁱ, producing a listing of unaveraged F^2 and $s(F^2)$ values which were then passed to the SHELXTLⁱⁱ program package for further processing and structure solution. A total of 112434 reflections were measured over the ranges $1.69 \leq \theta \leq 27.59^\circ$, $-51 \leq h \leq 51$, $-15 \leq k \leq 15$, $-31 \leq l \leq 31$ yielding 11102 unique reflections ($R_{\text{int}} = 0.0703$). The intensity data were corrected for Lorentz and polarization effects and for absorption using SADABSⁱⁱⁱ (minimum and maximum transmission 0.6809, 0.7456).

The structure was solved by direct methods (SHELXS-97^{iv}). There was a region of disordered solvent for which a reliable disorder model could not be devised; the X-ray data were corrected for the presence of disordered solvent using SQUEEZE^{viii}. Refinement was by full-matrix least squares based on F^2 using SHELXL-97.^v All reflections were used during refinement. The weighting scheme used was $w=1/[s^2(F_o^2) + (0.0651P)^2 + 15.6436P]$ where $P = (F_o^2 + 2F_c^2)/3$. Non-hydrogen atoms were refined anisotropically and hydrogen atoms were refined using a riding model. Refinement converged to $R1=0.0507$ and $wR2=0.1313$ for 8039 observed

reflections for which $F > 4s(F)$ and $R1=0.0727$ and $wR2=0.1383$ and $GOF = 1.073$ for all 11102 unique, non-zero reflections and 528 variables.^{vi} The maximum D/s in the final cycle of least squares was 0.002 and the two most prominent peaks in the final difference Fourier were +1.295 and -1.147 e/Å³.

Table 1. lists cell information, data collection parameters, and refinement data. Final positional and equivalent isotropic thermal parameters are given in Tables 2. and 3. Anisotropic thermal parameters are in Table 4. Tables 5. and 6. list bond distances and bond angles. Figure 1. is an ORTEP^{vii} representation of the molecule with 50% probability thermal ellipsoids displayed.

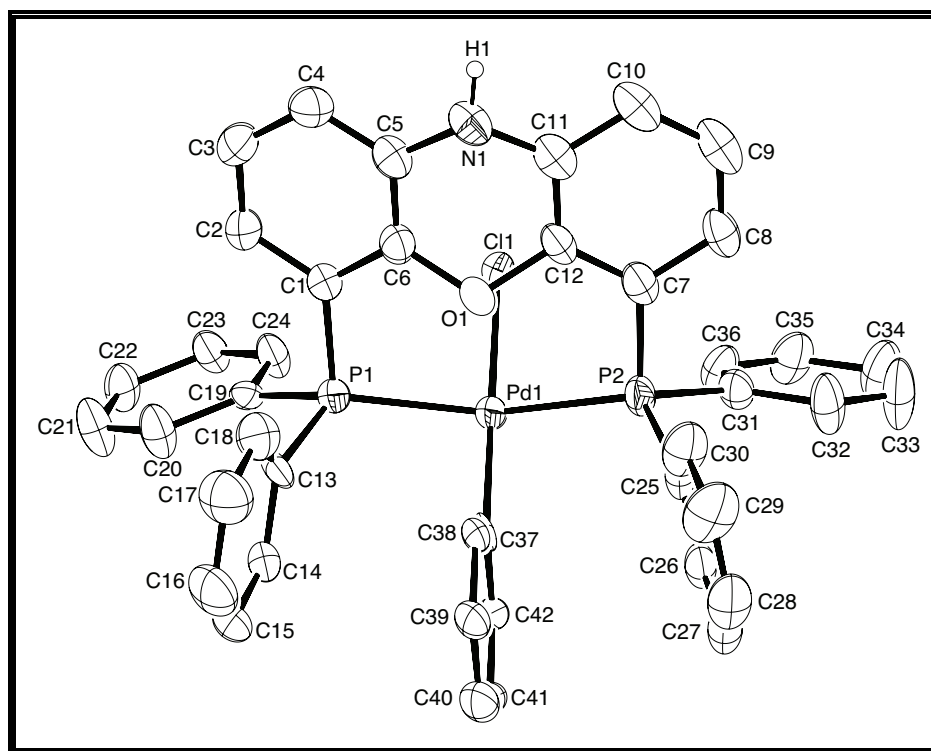


Figure 1. ORTEP drawing of the title compound with 50% probability thermal ellipsoids.

Table 1. Summary of Structure Determination of Compound 6190

Empirical formula	C ₄₂ H ₃₂ P ₂ NPCIPd
Formula weight	770.48
Temperature	100(1) K
Wavelength	0.71073 Å
Crystal system	monoclinic
Space group	C2/c
Cell constants:	
a	39.5647(19) Å

b	12.2212(6) Å
c	24.1733(13) Å
b	124.594(2)°
Volume	9621.9(8) Å ³
Z	8
Density (calculated)	1.064 Mg/m ³
Absorption coefficient	0.533 mm ⁻¹
F(000)	3136
Crystal size	0.14 x 0.04 x 0.02 mm ³
Theta range for data collection	1.69 to 27.59°
Index ranges	-51 ≤ h ≤ 51, -15 ≤ k ≤ 15, -31 ≤ l ≤ 31
Reflections collected	112434
Independent reflections	11102 [R(int) = 0.0703]
Completeness to theta = 27.59°	99.6 %
Absorption correction	Semi-empirical from equivalents
Max. and min. transmission	0.7456 and 0.6809
Refinement method	Full-matrix least-squares on F ²
Data / restraints / parameters	11102 / 570 / 528
Goodness-of-fit on F ²	1.073
Final R indices [I > 2σ(I)]	R1 = 0.0507, wR2 = 0.1313
R indices (all data)	R1 = 0.0727, wR2 = 0.1383
Largest diff. peak and hole	1.295 and -1.147 e.Å ⁻³

Table 2. Refined Positional Parameters for Compound 6190

Atom	x	y	z	U _{eq} , Å ²
Pd1	0.140590(7)	0.52801(2)	0.221579(12)	0.03595(9)
Cl1	0.18408(2)	0.51214(6)	0.18046(4)	0.03080(17)
P1	0.09932(2)	0.65709(8)	0.14040(4)	0.0385(2)
P2	0.19428(3)	0.48967(8)	0.33071(4)	0.0336(2)
N1	0.23728(9)	0.8655(3)	0.28928(15)	0.0402(7)
O1	0.18074(6)	0.71859(19)	0.27068(10)	0.0344(5)
C1	0.13544(10)	0.7638(3)	0.15324(16)	0.0357(7)
C2	0.12728(10)	0.8330(3)	0.10073(17)	0.0431(8)
C3	0.15459(11)	0.9123(3)	0.11091(19)	0.0485(9)
C4	0.19126(11)	0.9261(3)	0.17265(19)	0.0450(9)

C5	0.20030(10)	0.8583(3)	0.22535(17)	0.0378(8)
C6	0.17228(10)	0.7800(3)	0.21547(16)	0.0354(7)
C7	0.23298(10)	0.5937(3)	0.35086(15)	0.0357(7)
C8	0.27474(10)	0.5782(3)	0.40178(16)	0.0391(8)
C9	0.30361(11)	0.6555(3)	0.41408(18)	0.0462(9)
C10	0.29252(10)	0.7505(3)	0.37651(17)	0.0427(9)
C11	0.25100(10)	0.7706(3)	0.32717(16)	0.0370(8)
C12	0.22247(9)	0.6931(3)	0.31645(15)	0.0334(7)
C13	0.0634(2)	0.7436(6)	0.1525(4)	0.039(2)
C14	0.0287(2)	0.6898(5)	0.1402(3)	0.042(2)
C15	0.00298(18)	0.7418(6)	0.1540(3)	0.051(2)
C16	0.0119(2)	0.8475(6)	0.1801(4)	0.060(3)
C17	0.0466(2)	0.9013(4)	0.1923(4)	0.065(3)
C18	0.0724(2)	0.8494(6)	0.1785(5)	0.051(2)
C13'	0.0621(3)	0.7151(8)	0.1456(5)	0.041(3)
C14'	0.0229(3)	0.6705(7)	0.1135(4)	0.043(2)
C15'	-0.0055(2)	0.7158(8)	0.1237(4)	0.052(3)
C16'	0.0054(3)	0.8057(8)	0.1661(5)	0.068(4)
C17'	0.0447(3)	0.8503(7)	0.1982(5)	0.069(3)
C18'	0.0730(2)	0.8050(7)	0.1879(5)	0.054(3)
C19	0.06862(19)	0.6377(5)	0.0532(2)	0.0259(17)
C20	0.03059(19)	0.6861(5)	0.0078(3)	0.045(2)
C21	0.00920(15)	0.6621(5)	-0.0605(3)	0.050(2)
C22	0.02583(16)	0.5896(5)	-0.0834(2)	0.037(2)
C23	0.06387(16)	0.5411(4)	-0.0380(3)	0.0352(16)
C24	0.08527(15)	0.5652(5)	0.0303(3)	0.0355(19)
C19'	0.0736(2)	0.6080(6)	0.0489(3)	0.029(2)
C20'	0.0414(2)	0.6709(5)	-0.0019(3)	0.037(2)
C21'	0.02160(18)	0.6395(6)	-0.0688(3)	0.044(3)
C22'	0.0340(2)	0.5452(7)	-0.0850(3)	0.050(3)
C23'	0.0661(2)	0.4823(6)	-0.0343(4)	0.060(3)
C24'	0.0859(2)	0.5137(6)	0.0327(3)	0.040(3)
C25	0.18553(11)	0.5072(3)	0.39660(16)	0.0390(8)
C26	0.16169(10)	0.4304(3)	0.40208(16)	0.0400(8)
C27	0.15226(12)	0.4455(4)	0.44880(18)	0.0483(10)
C28	0.16708(13)	0.5367(4)	0.4900(2)	0.0552(11)

C29	0.19096(16)	0.6110(4)	0.4853(2)	0.0674(13)
C30	0.19989(13)	0.5971(3)	0.43794(19)	0.0522(10)
C31	0.22164(10)	0.3608(3)	0.35122(16)	0.0354(7)
C32	0.24635(12)	0.3219(4)	0.41728(17)	0.0562(12)
C33	0.26815(14)	0.2267(4)	0.43122(19)	0.0678(14)
C34	0.26556(14)	0.1680(4)	0.3801(2)	0.0601(12)
C35	0.24085(13)	0.2042(3)	0.31500(19)	0.0483(9)
C36	0.21894(11)	0.2996(3)	0.30077(17)	0.0406(8)
C37	0.10487(9)	0.5441(3)	0.25762(16)	0.0283(11)
C38	0.10547(9)	0.6340(2)	0.29355(17)	0.0301(11)
C39	0.07965(11)	0.6367(3)	0.31546(18)	0.0397(13)
C40	0.05320(11)	0.5496(3)	0.3014(2)	0.0481(16)
C41	0.05258(11)	0.4597(3)	0.2655(2)	0.0418(16)
C42	0.07841(11)	0.4570(3)	0.24356(17)	0.0322(12)
C37'	0.09926(16)	0.4753(4)	0.2393(3)	0.0365(17)
C38'	0.08551(19)	0.5449(4)	0.2682(3)	0.0434(19)
C39'	0.0604(2)	0.5047(5)	0.2869(3)	0.046(2)
C40'	0.04913(18)	0.3948(6)	0.2768(3)	0.054(2)
C41'	0.06289(18)	0.3252(4)	0.2479(3)	0.051(2)
C42'	0.08795(18)	0.3655(4)	0.2292(3)	0.0374(18)

$U_{eq} = \frac{1}{3}[U_{11}(aa^*)^2 + U_{22}(bb^*)^2 + U_{33}(cc^*)^2 + 2U_{12}aa^*bb^*\cos g + 2U_{13}aa^*cc^*\cos b + 2U_{23}bb^*cc^*\cos a]$

Table 3. Positional Parameters for Hydrogens in Compound 6190

Atom	x	y	z	$U_{iso}, \text{\AA}^2$
H2	0.1030	0.8247	0.0584	0.057
H3	0.1483	0.9580	0.0755	0.064
H4	0.2097	0.9802	0.1788	0.060
H8	0.2830	0.5148	0.4276	0.052
H9	0.3311	0.6435	0.4483	0.061
H10	0.3124	0.8004	0.3840	0.057
H14	0.0228	0.6192	0.1228	0.056
H15	-0.0202	0.7059	0.1458	0.068
H16	-0.0053	0.8823	0.1893	0.080
H17	0.0526	0.9719	0.2097	0.086
H18	0.0955	0.8853	0.1867	0.067
H14'	0.0156	0.6105	0.0852	0.058

H15'	-0.0317	0.6860	0.1023	0.069
H16'	-0.0135	0.8360	0.1729	0.091
H17'	0.0520	0.9104	0.2264	0.091
H18'	0.0992	0.8348	0.2093	0.072
H20	0.0195	0.7346	0.0231	0.060
H21	-0.0162	0.6944	-0.0908	0.067
H22	0.0116	0.5735	-0.1290	0.050
H23	0.0750	0.4927	-0.0533	0.047
H24	0.1106	0.5329	0.0605	0.047
H20'	0.0331	0.7339	0.0089	0.049
H21'	0.0001	0.6815	-0.1027	0.059
H22'	0.0208	0.5242	-0.1297	0.066
H23'	0.0744	0.4194	-0.0451	0.079
H24'	0.1074	0.4717	0.0665	0.053
H26	0.1521	0.3690	0.3745	0.053
H27	0.1361	0.3947	0.4524	0.064
H28	0.1607	0.5472	0.5212	0.073
H29	0.2013	0.6713	0.5139	0.090
H30	0.2157	0.6490	0.4342	0.069
H32	0.2480	0.3607	0.4518	0.075
H33	0.2847	0.2015	0.4753	0.090
H34	0.2806	0.1038	0.3899	0.080
H35	0.2389	0.1643	0.2806	0.064
H36	0.2020	0.3234	0.2565	0.054
H38	0.1231	0.6922	0.3029	0.040
H39	0.0801	0.6968	0.3395	0.053
H40	0.0360	0.5515	0.3160	0.064
H41	0.0349	0.4015	0.2561	0.056
H42	0.0780	0.3969	0.2195	0.043
H38'	0.0931	0.6183	0.2750	0.058
H39'	0.0513	0.5512	0.3062	0.061
H40'	0.0324	0.3679	0.2893	0.071
H41'	0.0553	0.2518	0.2411	0.068
H42'	0.0971	0.3190	0.2099	0.050
H1	0.2567(13)	0.903(4)	0.297(2)	0.052(13)

Table 4. Refined Thermal Parameters (U's) for Compound 6190

Atom	U ₁₁	U ₂₂	U ₃₃	U ₂₃	U ₁₃	U ₁₂
Pd1	0.02243(13)	0.05583(18)	0.02659(14)	0.01548(11)	0.01212(10)	0.00317(11)
Cl1	0.0268(4)	0.0388(4)	0.0250(3)	0.0079(3)	0.0137(3)	0.0009(3)
P1	0.0231(4)	0.0568(6)	0.0292(4)	0.0158(4)	0.0110(4)	-0.0001(4)
P2	0.0288(4)	0.0494(5)	0.0231(4)	0.0103(3)	0.0150(3)	0.0125(4)
N1	0.0315(15)	0.0379(17)	0.0451(17)	-0.0067(14)	0.0181(14)	0.0012(13)
O1	0.0227(10)	0.0483(14)	0.0284(11)	0.0037(10)	0.0124(9)	0.0053(10)
C1	0.0278(16)	0.0415(19)	0.0361(17)	0.0099(14)	0.0171(14)	0.0044(14)
C2	0.0327(18)	0.051(2)	0.0353(18)	0.0118(16)	0.0129(15)	-0.0009(16)
C3	0.046(2)	0.045(2)	0.047(2)	0.0131(17)	0.0220(18)	-0.0040(17)
C4	0.0397(19)	0.042(2)	0.052(2)	0.0026(17)	0.0253(18)	-0.0035(16)
C5	0.0314(17)	0.0379(19)	0.0395(18)	-0.0014(15)	0.0174(15)	0.0045(14)
C6	0.0320(17)	0.0407(19)	0.0341(17)	0.0070(14)	0.0191(15)	0.0080(14)
C7	0.0292(16)	0.053(2)	0.0246(15)	-0.0002(14)	0.0149(13)	0.0087(15)
C8	0.0314(17)	0.051(2)	0.0261(16)	-0.0036(15)	0.0112(14)	0.0099(16)
C9	0.0308(17)	0.055(2)	0.0372(19)	-0.0189(17)	0.0101(15)	0.0090(17)
C10	0.0300(17)	0.050(2)	0.0384(19)	-0.0204(17)	0.0137(15)	0.0001(16)
C11	0.0335(17)	0.044(2)	0.0316(17)	-0.0124(15)	0.0174(15)	0.0031(15)
C12	0.0230(15)	0.051(2)	0.0236(15)	-0.0020(14)	0.0116(13)	0.0071(14)
C13	0.015(3)	0.059(6)	0.036(5)	0.010(4)	0.010(3)	0.010(3)
C14	0.028(4)	0.056(5)	0.039(5)	0.020(4)	0.017(4)	0.011(3)
C15	0.029(4)	0.069(7)	0.061(6)	0.025(5)	0.029(4)	0.018(4)
C16	0.043(5)	0.070(7)	0.069(6)	0.006(5)	0.034(4)	0.018(5)
C17	0.061(5)	0.057(6)	0.078(6)	0.001(5)	0.042(5)	0.009(4)
C18	0.048(4)	0.047(5)	0.058(5)	0.010(4)	0.030(4)	0.010(4)
C13'	0.035(5)	0.044(6)	0.042(6)	0.024(4)	0.020(5)	0.011(4)
C14'	0.033(5)	0.054(6)	0.036(6)	0.014(4)	0.015(5)	0.007(4)
C15'	0.035(5)	0.064(6)	0.049(7)	0.008(5)	0.019(5)	0.008(4)
C16'	0.040(5)	0.055(8)	0.106(9)	-0.003(6)	0.040(6)	0.008(5)
C17'	0.063(6)	0.066(8)	0.084(8)	-0.022(6)	0.046(6)	-0.013(6)
C18'	0.027(4)	0.067(9)	0.062(7)	0.002(6)	0.021(4)	-0.001(5)
C19	0.023(3)	0.028(4)	0.033(3)	0.005(3)	0.021(3)	0.004(3)
C20	0.038(4)	0.058(5)	0.031(3)	0.002(3)	0.015(3)	0.021(4)
C21	0.036(4)	0.059(5)	0.036(4)	-0.003(3)	0.009(3)	0.019(4)
C22	0.038(4)	0.046(5)	0.020(3)	-0.001(3)	0.012(3)	0.007(3)
C23	0.026(3)	0.050(5)	0.026(3)	-0.001(3)	0.013(3)	0.007(3)

C24	0.026(3)	0.048(5)	0.026(3)	0.002(3)	0.011(3)	0.012(3)
C19'	0.016(4)	0.048(6)	0.015(3)	0.008(3)	0.005(3)	-0.003(4)
C20'	0.027(4)	0.037(5)	0.038(4)	0.012(3)	0.013(4)	0.000(3)
C21'	0.024(5)	0.072(8)	0.021(4)	0.019(5)	0.003(3)	0.002(5)
C22'	0.030(5)	0.091(9)	0.028(4)	0.001(5)	0.016(4)	-0.004(5)
C23'	0.040(5)	0.107(9)	0.027(4)	-0.004(5)	0.017(4)	0.021(6)
C24'	0.027(4)	0.065(7)	0.029(4)	0.001(4)	0.017(3)	0.009(4)
C25	0.0392(18)	0.054(2)	0.0260(16)	0.0139(15)	0.0198(15)	0.0241(16)
C26	0.0350(17)	0.057(2)	0.0308(17)	0.0159(16)	0.0204(15)	0.0212(16)
C27	0.047(2)	0.068(3)	0.0383(19)	0.0225(18)	0.0292(18)	0.0279(19)
C28	0.065(3)	0.074(3)	0.044(2)	0.014(2)	0.042(2)	0.030(2)
C29	0.097(4)	0.069(3)	0.061(3)	0.004(2)	0.060(3)	0.018(3)
C30	0.069(3)	0.056(2)	0.045(2)	0.0081(18)	0.040(2)	0.018(2)
C31	0.0317(16)	0.048(2)	0.0317(16)	0.0082(14)	0.0212(14)	0.0127(15)
C32	0.057(2)	0.088(3)	0.0270(17)	0.0171(18)	0.0262(18)	0.041(2)
C33	0.080(3)	0.092(3)	0.0333(19)	0.028(2)	0.033(2)	0.058(3)
C34	0.081(3)	0.067(3)	0.050(2)	0.024(2)	0.047(2)	0.039(2)
C35	0.068(3)	0.051(2)	0.043(2)	0.0105(17)	0.041(2)	0.0193(19)
C36	0.052(2)	0.044(2)	0.0301(17)	0.0092(14)	0.0254(16)	0.0053(16)
C37	0.012(2)	0.036(3)	0.024(3)	0.011(2)	0.003(2)	0.012(2)
C38	0.019(2)	0.038(3)	0.033(3)	0.014(2)	0.015(2)	0.012(2)
C39	0.029(3)	0.054(3)	0.042(3)	0.015(3)	0.023(3)	0.015(2)
C40	0.032(3)	0.078(5)	0.038(3)	0.017(3)	0.022(3)	0.011(3)
C41	0.024(3)	0.060(4)	0.030(4)	0.017(3)	0.008(3)	-0.008(3)
C42	0.022(2)	0.043(3)	0.027(3)	0.010(2)	0.010(2)	-0.002(2)
C37'	0.035(5)	0.041(4)	0.023(4)	0.013(4)	0.010(3)	0.016(4)
C38'	0.036(4)	0.053(5)	0.035(4)	0.011(4)	0.017(4)	0.018(4)
C39'	0.029(5)	0.069(6)	0.035(6)	0.021(5)	0.016(4)	0.013(5)
C40'	0.026(4)	0.089(7)	0.049(5)	0.020(5)	0.023(4)	0.001(5)
C41'	0.052(5)	0.062(6)	0.035(5)	0.017(4)	0.022(4)	-0.003(5)
C42'	0.036(4)	0.045(4)	0.031(4)	0.004(3)	0.020(4)	-0.008(4)

The form of the anisotropic displacement parameter is:

$$\exp[-2p^2(a^*2U_{11}h^2+b^*2U_{22}k^2+c^*2U_{33}l^2+2b^*c^*U_{23}kl+2a^*c^*U_{13}hl+2a^*b^*U_{12}hk)]$$

Table 5. Bond Distances in Compound 6190, Å

Pd1-C37'	2.017(4)	Pd1-C37	2.048(2)	Pd1-P2	2.3083(8)
----------	----------	---------	----------	--------	-----------

Pd1-P1	2.3168(9)	Pd1-CI1	2.4348(8)	P1-C13'	1.702(8)
P1-C19	1.752(4)	P1-C1	1.826(3)	P1-C13	1.921(6)
P1-C19'	1.932(5)	P2-C31	1.813(3)	P2-C25	1.824(3)
P2-C7	1.831(4)	N1-C11	1.383(5)	N1-C5	1.403(4)
N1-H1	0.82(4)	O1-C6	1.396(4)	O1-C12	1.404(3)
C1-C6	1.392(5)	C1-C2	1.402(5)	C2-C3	1.366(5)
C2-H2	0.9300	C3-C4	1.379(5)	C3-H3	0.9300
C4-C5	1.386(5)	C4-H4	0.9300	C5-C6	1.379(5)
C7-C12	1.396(5)	C7-C8	1.404(4)	C8-C9	1.378(5)
C8-H8	0.9300	C9-C10	1.383(6)	C9-H9	0.9300
C10-C11	1.399(5)	C10-H10	0.9300	C11-C12	1.381(5)
C13-C18	1.3924	C13-C14	1.3937	C14-C15	1.3931
C14-H14	0.9300	C15-C16	1.3923	C15-H15	0.9300
C16-C17	1.3937	C16-H16	0.9300	C17-C18	1.3928
C17-H17	0.9300	C18-H18	0.9300	C13'-C18'	1.3924
C13'-C14'	1.3940	C14'-C15'	1.3932	C14'-H14'	0.9300
C15'-C16'	1.3925	C15'-H15'	0.9300	C16'-C17'	1.3943
C16'-H16'	0.9300	C17'-C18'	1.3933	C17'-H17'	0.9300
C18'-H18'	0.9300	C19-C24	1.3924	C19-C20	1.3941
C20-C21	1.3936	C20-H20	0.9300	C21-C22	1.3922
C21-H21	0.9300	C22-C23	1.3943	C22-H22	0.9300
C23-C24	1.3934	C23-H23	0.9300	C24-H24	0.9300
C19'-C24'	1.3923	C19'-C20'	1.3938	C20'-C21'	1.3933
C20'-H20'	0.9300	C21'-C22'	1.3921	C21'-H21'	0.9300
C22'-C23'	1.3937	C22'-H22'	0.9300	C23'-C24'	1.3933
C23'-H23'	0.9300	C24'-H24'	0.9300	C25-C30	1.373(6)
C25-C26	1.389(5)	C26-C27	1.388(5)	C26-H26	0.9300
C27-C28	1.384(6)	C27-H27	0.9300	C28-C29	1.362(6)
C28-H28	0.9300	C29-C30	1.387(5)	C29-H29	0.9300
C30-H30	0.9300	C31-C36	1.382(5)	C31-C32	1.400(5)
C32-C33	1.372(5)	C32-H32	0.9300	C33-C34	1.380(6)
C33-H33	0.9300	C34-C35	1.372(5)	C34-H34	0.9300
C35-C36	1.375(5)	C35-H35	0.9300	C36-H36	0.9300
C37-C38	1.3922	C37-C42	1.3929	C38-C39	1.3928
C38-H38	0.9300	C39-C40	1.3931	C39-H39	0.9300
C40-C41	1.3922	C40-H40	0.9300	C41-C42	1.3930

C41-H41	0.9300	C42-H42	0.9300	C37'-C38'	1.3920
C37'-C42'	1.3923	C38'-C39'	1.3932	C38'-H38'	0.9300
C39'-C40'	1.3926	C39'-H39'	0.9300	C40'-C41'	1.3925
C40'-H40'	0.9300	C41'-C42'	1.3930	C41'-H41'	0.9300
C42'-H42'	0.9300				

Table 6. Bond Angles in Compound 6190, °

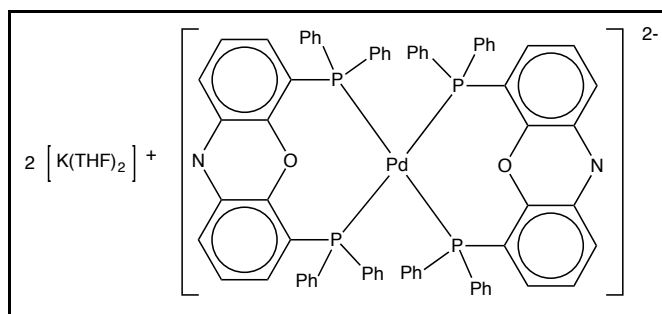
C37'-Pd1-	26.04(18)	C37'-Pd1-P2	91.34(16)	C37'-Pd1-P2	86.73(9)
C37					
C37'-Pd1-P1	97.52(16)	C37'-Pd1-P1	88.30(10)	P2-Pd1-P1	148.76(4)
C37'-Pd1-Cl1	155.16(17)	C37'-Pd1-Cl1	178.70(10)	P2-Pd1-Cl1	92.59(3)
P1-Pd1-Cl1	91.72(3)	C13'-P1-C19	96.2(4)	C13'-P1-C1	108.4(4)
C19-P1-C1	104.0(3)	C13'-P1-C13	9.7(5)	C19-P1-C13	101.0(3)
C1-P1-C13	98.9(3)	C13'-P1-C19'	107.3(4)	C19-P1-C19'	12.9(3)
C1-P1-C19'	105.7(3)	C13-P1-C19'	112.9(3)	C13'-P1-Pd1	116.4(3)
C19-P1-Pd1	126.9(2)	C1-P1-Pd1	103.60(10)	C13-P1-Pd1	118.2(2)
C19'-P1-Pd1	114.7(2)	C31-P2-C25	104.05(15)	C31-P2-C7	104.55(15)
C25-P2-C7	103.35(16)	C31-P2-Pd1	120.53(11)	C25-P2-Pd1	117.79(11)
C7-P2-Pd1	104.54(10)	C11-N1-C5	116.7(3)	C11-N1-H1	111(3)
C5-N1-H1	122(3)	C6-O1-C12	114.1(2)	C6-C1-C2	117.0(3)
C6-C1-P1	121.6(2)	C2-C1-P1	121.4(3)	C3-C2-C1	120.9(3)
C3-C2-H2	119.6	C1-C2-H2	119.6	C2-C3-C4	121.3(3)
C2-C3-H3	119.3	C4-C3-H3	119.3	C3-C4-C5	119.0(3)
C3-C4-H4	120.5	C5-C4-H4	120.5	C6-C5-C4	119.6(3)
C6-C5-N1	117.9(3)	C4-C5-N1	122.6(3)	C5-C6-C1	122.1(3)
C5-C6-O1	118.3(3)	C1-C6-O1	119.5(3)	C12-C7-C8	116.4(3)
C12-C7-P2	121.7(2)	C8-C7-P2	121.9(3)	C9-C8-C7	121.0(3)
C9-C8-H8	119.5	C7-C8-H8	119.5	C8-C9-C10	121.2(3)
C8-C9-H9	119.4	C10-C9-H9	119.4	C9-C10-C11	119.3(4)
C9-C10-H10	120.4	C11-C10-	120.4	C12-C11-N1	118.6(3)
		H10			
C12-C11-	118.6(3)	N1-C11-C10	122.8(3)	C11-C12-C7	123.4(3)
C10					
C11-C12-O1	117.8(3)	C7-C12-O1	118.8(3)	C18-C13-	120.0
				C14	
C18-C13-P1	124.1(4)	C14-C13-P1	115.6(4)	C15-C14-	120.0

C15-C14- H14	120.0	C13-C14- H14	120.0	C13 C16-C15- C14	120.0
C16-C15- H15	120.0	C14-C15- H15	120.0	C15-C16- C17	120.0
C15-C16- H16	120.0	C17-C16- H16	120.0	C18-C17- C16	120.1
C18-C17- H17	120.0	C16-C17- H17	120.0	C13-C18- C17	120.0
C13-C18- H18	120.0	C17-C18- H18	120.0	C18'-C13'- C14'	120.0
C18'-C13'-P1	117.6(6)	C14'-C13'-P1	122.2(6)	C15'-C14'- C13'	120.0
C15'-C14'- H14'	120.0	C13'-C14'- H14'	120.0	C16'-C15'- C14'	119.9
C16'-C15'- H15'	120.0	C14'-C15'- H15'	120.0	C15'-C16'- C17'	120.0
C15'-C16'- H16'	120.0	C17'-C16'- H16'	120.0	C18'-C17'- C16'	120.1
C18'-C17'- H17'	120.0	C16'-C17'- H17'	120.0	C13'-C18'- C17'	119.9
C13'-C18'- H18'	120.0	C17'-C18'- H18'	120.0	C24-C19- C20	120.0
C24-C19-P1	113.8(3)	C20-C19-P1	126.2(3)	C21-C20- C19	120.1
C21-C20- H20	120.0	C19-C20- H20	120.0	C22-C21- C20	119.9
C22-C21- H21	120.0	C20-C21- H21	120.0	C21-C22- C23	120.0
C21-C22- H22	120.0	C23-C22- H22	120.0	C24-C23- C22	120.1
C24-C23- H23	120.0	C22-C23- H23	120.0	C19-C24- C23	119.9
C19-C24- H24	120.0	C23-C24- H24	120.0	C24'-C19'- C20'	120.0
C24'-C19'-P1	122.5(3)	C20'-C19'-P1	117.5(3)	C21'-C20'-	120.1

C21'-C20'- H20'	120.0	C19'-C20'- H20'	120.0	C19'	
C22'-C21'- H21'	120.0	C20'-C21'- H21'	120.0	C22'-C21'- C20'	119.9
C21'-C22'- H22'	120.0	C23'-C22'- H22'	120.0	C21'-C22'- C23'	120.0
C24'-C23'- H23'	120.0	C22'-C23'- H23'	120.0	C24'-C23'- C22'	120.1
C19'-C24'- H24'	120.0	C23'-C24'- H24'	120.0	C19'-C24'- C23'	119.9
C30-C25-P2	121.6(3)	C26-C25-P2	118.7(3)	C30-C25- C26	119.6(3)
C27-C26- H26	120.0	C25-C26- H26	120.0	C27-C26- C25	119.9(4)
C28-C27- H27	120.2	C26-C27- H27	120.2	C28-C27- C26	119.5(4)
C29-C28- H28	119.7	C27-C28- H28	119.7	C29-C28- C27	120.5(4)
C28-C29- H29	120.0	C30-C29- H29	120.0	C28-C29- C30	120.1(4)
C25-C30- H30	119.8	C29-C30- H30	119.8	C25-C30- C29	120.3(4)
C36-C31-P2	119.6(2)	C32-C31-P2	121.9(3)	C36-C31- C32	118.5(3)
C33-C32- H32	119.9	C31-C32- H32	119.9	C33-C32- C31	120.2(3)
C32-C33- H33	119.9	C34-C33- H33	119.9	C32-C33- C34	120.3(3)
C35-C34- H34	119.9	C33-C34- H34	119.9	C35-C34- C33	120.1(4)
C34-C35- H35	120.1	C36-C35- H35	120.1	C34-C35- C36	119.9(3)
C35-C36- H36	119.5	C31-C36- H36	119.5	C35-C36- C31	121.1(3)
C38-C37-	124.72(18)	C42-C37-	115.28(18)	C38-C37- C42	120.0
				C37-C38-	120.0

Pd1		Pd1		C39	
C37-C38-	120.0	C39-C38-	120.0	C38-C39-	120.0
H38		H38		C40	
C38-C39-	120.0	C40-C39-	120.0	C41-C40-	120.0
H39		H39		C39	
C41-C40-	120.0	C39-C40-	120.0	C40-C41-	120.0
H40		H40		C42	
C40-C41-	120.0	C42-C41-	120.0	C37-C42-	120.0
H41		H41		C41	
C37-C42-	120.0	C41-C42-	120.0	C38'-C37'-	120.0
H42		H42		C42'	
C38'-C37'-	120.4(3)	C42'-C37'-	119.2(3)	C37'-C38'-	120.0
Pd1		Pd1		C39'	
C37'-C38'-	120.0	C39'-C38'-	120.0	C40'-C39'-	120.0
H38'		H38'		C38'	
C40'-C39'-	120.0	C38'-C39'-	120.0	C41'-C40'-	120.0
H39'		H39'		C39'	
C41'-C40'-	120.0	C39'-C40'-	120.0	C40'-C41'-	120.0
H40'		H40'		C42'	
C40'-C41'-	120.0	C42'-C41'-	120.0	C37'-C42'-	120.0
H41'		H41'		C41'	
C37'-C42'-	120.0	C41'-C42'-	120.0		
H42'		H42'			

X-ray Structure Determination of Compound 6199



Compound 6199, $C_{88}H_{84}P_4N_2O_6K_2Pd$, crystallizes in the monoclinic space group $C2/c$ (systematic absences $hkl: h+k=\text{odd}, h0l: l=\text{odd}$) with $a=31.977(4)\text{\AA}$, $b=14.9581(17)\text{\AA}$, $c=23.583(3)\text{\AA}$, $\beta=129.495(4)^\circ$, $V=8704.6(18)\text{\AA}^3$, $Z=4$, and $d_{\text{calc}}=1.201\text{ g/cm}^3$. X-ray intensity data were collected on a Bruker APEXII CCD area detector employing graphite-monochromated Mo-K α radiation ($\lambda=0.71073\text{ \AA}$) at a temperature of $100(1)\text{K}$. Preliminary indexing was performed from a series of thirty-six 0.5° rotation frames with exposures of 10 seconds. A total of 2170 frames were collected with a crystal to detector distance of 37.4 mm, rotation widths of 0.5° and exposures of 30 seconds:

scan type	2 θ	w	f	c	frames
f	-23.00	315.83	12.48	28.88	739
w	-23.00	333.49	158.99	-70.01	69
f	-23.00	334.21	50.51	73.66	623
f	24.50	7.41	12.48	28.88	739

Rotation frames were integrated using SAINTⁱ, producing a listing of unaveraged F^2 and $s(F^2)$ values which were then passed to the SHELXTLⁱⁱ program package for further processing and structure solution. A total of 97854 reflections were measured over the ranges $1.59 \leq \theta \leq 27.63^\circ$, $-41 \leq h \leq 32$, $0 \leq k \leq 19$, $0 \leq l \leq 30$ yielding 10071 unique reflections ($R_{\text{int}} = 0.1181$). The intensity data were corrected for Lorentz and polarization effects and for absorption using SADABSⁱⁱⁱ (minimum and maximum transmission 0.5714, 0.7456).

The structure was solved by direct methods (SHELXS-97^{iv}). The palladium atom lies on a crystallographic 2-fold axis (at $\frac{1}{2}, y, \frac{1}{4}$). The potassium ion is bonded to two THF molecules and to the N atoms of two different bidentate diphosphine ligands, creating an infinite chain as shown in Figure 1. Refinement was by full-matrix least squares based on F^2 using SHELXL-97.^v All reflections were used during refinement. The weighting scheme used was $w=1/[s^2(F_o^2) + (0.2000P)^2 + 0.0000P]$ where $P = (F_o^2 + 2F_c^2)/3$. Non-hydrogen atoms were refined anisotropically and hydrogen atoms were refined using a riding model. Refinement converged to $R1=0.1370$ and $wR2=0.3553$ for 5116 observed reflections for which $F > 4s(F)$ and $R1=0.2019$

and $wR2=0.3971$ and $GOF = 1.297$ for all 10071 unique, non-zero reflections and 475 variables.^{vi} The maximum D/s in the final cycle of least squares was 0.000 and the two most prominent peaks in the final difference Fourier were $+4.268$ and $-1.353 \text{ e}/\text{\AA}^3$.

Table 1. lists cell information, data collection parameters, and refinement data. Final positional and equivalent isotropic thermal parameters are given in Tables 2. and 3. Anisotropic thermal parameters are in Table 4. Tables 5. and 6. list bond distances and bond angles. Figure 1. is an ORTEP^{vii} representation of the molecule with 30% probability thermal ellipsoids displayed.

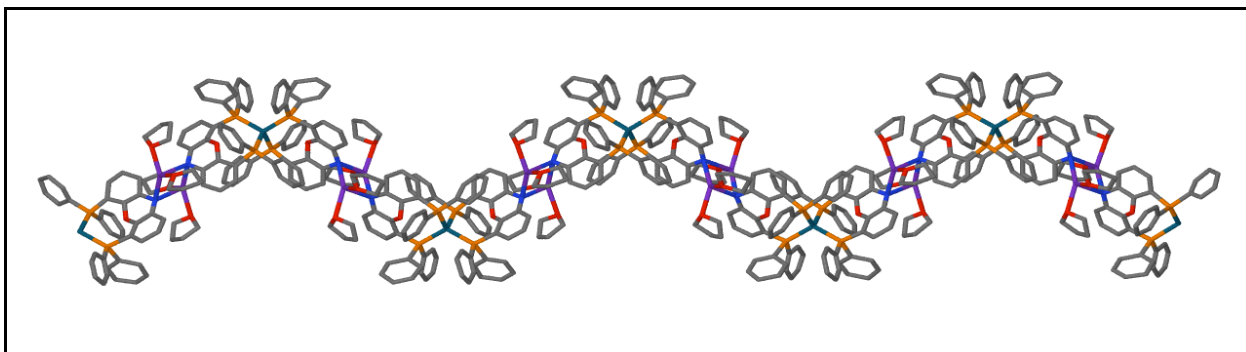


Figure 1. Infinite chain of $K(THF)_2+Pd$ complex - view is perpendicular to crystallographic 2-fold axis.

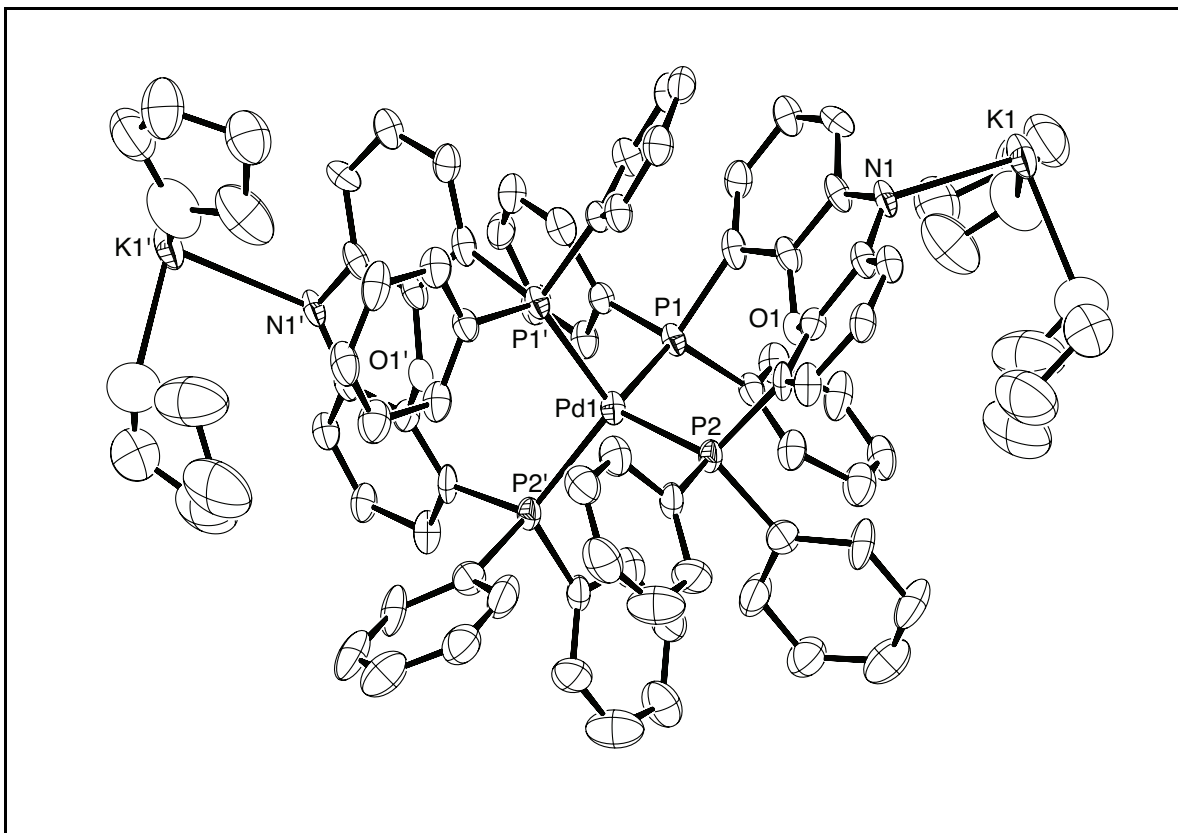


Figure 1. ORTEP drawing of the palladium anionic complex with 30% probability thermal

ellipsoids (the crystallographic 2-fold axis is vertical).

Table 1. Summary of Structure Determination of Compound 6199

Empirical formula	C ₈₈ H ₈₄ P ₄ N ₂ O ₆ K ₂ Pd
Formula weight	1574.05
Temperature	100(1) K
Wavelength	0.71073 Å
Crystal system	monoclinic
Space group	C2/c
Cell constants:	
a	31.977(4) Å
b	14.9581(17) Å
c	23.583(3) Å
β	129.495(4)°
Volume	8704.6(18) Å ³
Z	4
Density (calculated)	1.201 Mg/m ³
Absorption coefficient	0.432 mm ⁻¹
F(000)	3272
Crystal size	0.48 x 0.32 x 0.06 mm ³
Theta range for data collection	1.59 to 27.63°
Index ranges	-41 ≤ h ≤ 32, 0 ≤ k ≤ 19, 0 ≤ l ≤ 30
Reflections collected	97854
Independent reflections	10071 [R(int) = 0.1181]
Completeness to theta = 27.63°	99.3 %
Absorption correction	Semi-empirical from equivalents
Max. and min. transmission	0.7456 and 0.5714
Refinement method	Full-matrix least-squares on F ²
Data / restraints / parameters	10071 / 127 / 475
Goodness-of-fit on F ²	1.297
Final R indices [I > 2σ(I)]	R1 = 0.1370, wR2 = 0.3553
R indices (all data)	R1 = 0.2019, wR2 = 0.3971
Largest diff. peak and hole	4.268 and -1.353 e.Å ⁻³

Table 2. Refined Positional Parameters for Compound 6199

Atom	x	y	z	U _{eq} , Å ²
Pd1	0.5000	0.47248(7)	0.2500	0.0417(3)
K1	0.78498(8)	0.7093(2)	0.45609(13)	0.0703(8)
P1	0.53078(8)	0.57232(16)	0.20388(11)	0.0389(5)
P2	0.57164(8)	0.38435(15)	0.35252(12)	0.0400(5)
O1	0.6271(2)	0.5373(4)	0.3506(3)	0.0386(13)
N1	0.7051(2)	0.6500(5)	0.4629(4)	0.0466(18)
C1	0.5810(3)	0.6570(7)	0.2660(4)	0.047(2)
C2	0.5838(4)	0.7442(7)	0.2475(5)	0.051(2)
C3	0.6250(4)	0.8004(8)	0.3011(5)	0.057(3)
C4	0.6656(4)	0.7703(6)	0.3726(5)	0.051(2)
C5	0.6657(3)	0.6806(7)	0.3914(4)	0.045(2)
C6	0.6242(3)	0.6275(7)	0.3360(4)	0.043(2)
C7	0.6314(3)	0.4445(6)	0.4342(5)	0.046(2)
C8	0.6581(3)	0.4149(8)	0.5066(5)	0.054(2)
C9	0.7033(3)	0.4671(7)	0.5653(5)	0.052(2)
C10	0.7192(3)	0.5418(7)	0.5504(5)	0.051(2)
C11	0.6923(3)	0.5721(7)	0.4788(4)	0.046(2)
C12	0.6498(3)	0.5166(6)	0.4224(4)	0.0394(18)
C13	0.4774(3)	0.6455(6)	0.1249(4)	0.0395(18)
C14	0.4532(3)	0.6238(7)	0.0527(5)	0.050(2)
C15	0.4172(4)	0.6826(7)	-0.0035(5)	0.059(3)
C16	0.4031(4)	0.7597(7)	0.0120(5)	0.056(2)
C17	0.4236(4)	0.7768(7)	0.0830(5)	0.056(2)
C18	0.4598(3)	0.7209(7)	0.1381(5)	0.050(2)
C19	0.5683(3)	0.5307(6)	0.1734(4)	0.043(2)
C20	0.5753(4)	0.5790(8)	0.1298(5)	0.057(2)
C21	0.6086(4)	0.5497(9)	0.1172(5)	0.069(3)
C22	0.6358(4)	0.4694(9)	0.1473(6)	0.066(3)
C23	0.6290(4)	0.4208(9)	0.1911(6)	0.070(3)
C24	0.5938(4)	0.4521(7)	0.2033(5)	0.051(2)
C25	0.6071(4)	0.3008(6)	0.3378(5)	0.054(2)
C26	0.6613(4)	0.2782(9)	0.3886(7)	0.075(3)
C27	0.6847(5)	0.2181(10)	0.3727(7)	0.089(4)
C28	0.6565(6)	0.1748(10)	0.3095(8)	0.091(4)
C29	0.6012(5)	0.1940(9)	0.2578(7)	0.082(4)

C30	0.5771(5)	0.2571(9)	0.2728(7)	0.081(4)
C31	0.5549(3)	0.3132(6)	0.3995(5)	0.047(2)
C32	0.5650(5)	0.2226(7)	0.4115(7)	0.074(3)
C33	0.5482(8)	0.1753(10)	0.4432(9)	0.106(5)
C34	0.5236(5)	0.2154(10)	0.4665(7)	0.084(4)
C35	0.5134(5)	0.3054(8)	0.4538(6)	0.068(3)
C36	0.5280(4)	0.3533(8)	0.4204(6)	0.063(3)
O2	0.8123(7)	0.5451(8)	0.4555(11)	0.175(6)
C37	0.7675(9)	0.5066(12)	0.3863(9)	0.190(8)
C38	0.7598(9)	0.4147(11)	0.4033(10)	0.188(8)
C39	0.7802(9)	0.4222(13)	0.4809(10)	0.176(8)
C40	0.8251(7)	0.4902(13)	0.5148(9)	0.181(8)
O3	0.7581(4)	0.7061(8)	0.3273(4)	0.129(4)
C41	0.7059(6)	0.6778(10)	0.2603(7)	0.149(7)
C42	0.6902(5)	0.7452(10)	0.2027(5)	0.114(5)
C43	0.7427(6)	0.7838(14)	0.2290(8)	0.123(6)
C43'	0.7226(9)	0.8275(9)	0.2476(11)	0.122(11)
C44	0.7757(5)	0.7831(10)	0.3121(7)	0.129(5)
$U_{eq} = \frac{1}{3}[U_{11}(aa^*)^2 + U_{22}(bb^*)^2 + U_{33}(cc^*)^2 + 2U_{12}aa^*bb^*\cos g + 2U_{13}aa^*cc^*\cos b + 2U_{23}bb^*cc^*\cos a]$				

Table 3. Positional Parameters for Hydrogens in Compound 6199

Atom	x	y	z	$U_{iso}, \text{\AA}^2$
H2	0.5582	0.7645	0.1995	0.068
H3	0.6256	0.8594	0.2892	0.076
H4	0.6926	0.8093	0.4080	0.068
H8	0.6469	0.3637	0.5161	0.072
H9	0.7219	0.4496	0.6138	0.069
H10	0.7489	0.5737	0.5893	0.068
H14	0.4613	0.5697	0.0421	0.066
H15	0.4025	0.6698	-0.0516	0.078
H16	0.3799	0.8005	-0.0252	0.074
H17	0.4123	0.8274	0.0930	0.074
H18	0.4731	0.7332	0.1857	0.066
H20	0.5567	0.6325	0.1088	0.076
H21	0.6133	0.5833	0.0884	0.092
H22	0.6584	0.4482	0.1382	0.088

H23	0.6478	0.3675	0.2124	0.093
H24	0.5882	0.4191	0.2314	0.068
H26	0.6823	0.3046	0.4349	0.099
H27	0.7218	0.2074	0.4074	0.118
H28	0.6728	0.1331	0.2998	0.120
H29	0.5802	0.1644	0.2128	0.109
H30	0.5403	0.2692	0.2378	0.108
H32	0.5832	0.1938	0.3979	0.098
H33	0.5538	0.1138	0.4490	0.141
H34	0.5138	0.1831	0.4902	0.112
H35	0.4960	0.3341	0.4687	0.090
H36	0.5198	0.4139	0.4114	0.084
H37a	0.7756	0.5037	0.3530	0.253
H37b	0.7351	0.5421	0.3636	0.253
H38a	0.7807	0.3710	0.4001	0.249
H38b	0.7219	0.3976	0.3699	0.249
H39a	0.7938	0.3653	0.5062	0.234
H39b	0.7518	0.4428	0.4817	0.234
H40a	0.8270	0.5264	0.5505	0.241
H40b	0.8597	0.4607	0.5393	0.241
H41a	0.6791	0.6761	0.2674	0.199
H41b	0.7086	0.6186	0.2460	0.199
H42a	0.6714	0.7168	0.1552	0.151
H42b	0.6670	0.7910	0.1987	0.151
H42a'	0.6515	0.7572	0.1704	0.151
H42b'	0.7000	0.7249	0.1735	0.151
H43a	0.7381	0.8441	0.2106	0.164
H43b	0.7595	0.7471	0.2145	0.164
H43a'	0.7055	0.8598	0.2637	0.162
H43b'	0.7282	0.8675	0.2206	0.162
H44a	0.8141	0.7793	0.3370	0.172
H44b	0.7690	0.8369	0.3282	0.172
H44a'	0.7976	0.7664	0.2985	0.172
H44b'	0.7965	0.8226	0.3543	0.172

Table 4. Refined Thermal Parameters (U's) for Compound 6199

Atom	U ₁₁	U ₂₂	U ₃₃	U ₂₃	U ₁₃	U ₁₂
Pd1	0.0286(4)	0.0552(7)	0.0396(5)	0.000	0.0209(4)	0.000
K1	0.0428(11)	0.117(2)	0.0587(13)	-0.0325(13)	0.0360(11)	-0.0269(12)
P1	0.0267(9)	0.0539(14)	0.0302(10)	-0.0040(9)	0.0153(8)	-0.0078(9)
P2	0.0311(10)	0.0491(13)	0.0472(12)	0.0052(10)	0.0285(10)	0.0014(9)
O1	0.026(2)	0.055(4)	0.029(3)	-0.001(2)	0.014(2)	-0.003(2)
N1	0.023(3)	0.072(5)	0.037(4)	-0.010(3)	0.015(3)	-0.014(3)
C1	0.027(4)	0.083(7)	0.028(4)	-0.001(4)	0.016(3)	-0.005(4)
C2	0.041(5)	0.067(6)	0.056(5)	0.010(5)	0.035(4)	0.004(4)
C3	0.043(5)	0.079(7)	0.052(5)	0.000(5)	0.031(5)	-0.011(5)
C4	0.051(5)	0.052(5)	0.047(5)	-0.016(4)	0.029(4)	-0.022(4)
C5	0.033(4)	0.074(6)	0.031(4)	-0.005(4)	0.022(3)	-0.019(4)
C6	0.030(4)	0.069(6)	0.026(4)	-0.009(4)	0.015(3)	-0.012(4)
C7	0.019(3)	0.063(6)	0.048(5)	0.020(4)	0.018(3)	0.009(3)
C8	0.036(4)	0.086(7)	0.042(5)	0.014(5)	0.025(4)	0.008(4)
C9	0.030(4)	0.075(7)	0.036(4)	0.006(4)	0.015(4)	0.010(4)
C10	0.033(4)	0.070(7)	0.042(5)	-0.003(4)	0.021(4)	-0.003(4)
C11	0.031(4)	0.072(6)	0.032(4)	-0.009(4)	0.019(4)	-0.010(4)
C12	0.033(4)	0.053(5)	0.029(4)	-0.001(4)	0.019(3)	0.005(4)
C13	0.033(4)	0.046(5)	0.043(4)	0.000(4)	0.026(4)	-0.005(3)
C14	0.033(4)	0.071(6)	0.037(4)	0.000(4)	0.018(4)	-0.001(4)
C15	0.041(5)	0.076(7)	0.046(5)	0.008(5)	0.022(4)	0.009(5)
C16	0.037(4)	0.068(7)	0.053(5)	0.000(5)	0.024(4)	0.006(4)
C17	0.040(5)	0.074(7)	0.057(6)	0.004(5)	0.032(5)	0.004(5)
C18	0.042(4)	0.067(6)	0.038(4)	0.007(4)	0.024(4)	-0.007(4)
C19	0.032(4)	0.061(6)	0.035(4)	-0.010(4)	0.020(3)	-0.008(4)
C20	0.047(5)	0.083(7)	0.044(5)	-0.001(5)	0.030(4)	0.001(5)
C21	0.044(5)	0.122(10)	0.044(5)	0.008(6)	0.030(5)	0.020(6)
C22	0.042(5)	0.116(10)	0.052(5)	-0.027(6)	0.036(5)	-0.015(6)
C23	0.053(6)	0.102(9)	0.054(6)	-0.009(6)	0.033(5)	0.007(6)
C24	0.041(4)	0.084(7)	0.037(4)	-0.001(4)	0.028(4)	0.005(4)
C25	0.050(5)	0.046(5)	0.053(6)	0.015(4)	0.027(5)	0.007(4)
C26	0.048(5)	0.126(10)	0.076(7)	0.008(7)	0.052(6)	0.022(6)
C27	0.073(7)	0.125(11)	0.078(8)	0.006(8)	0.053(7)	0.045(8)
C28	0.113(11)	0.089(9)	0.087(9)	0.028(8)	0.072(9)	0.040(8)
C29	0.075(8)	0.086(9)	0.082(8)	-0.012(7)	0.048(7)	0.012(7)

C30	0.052(6)	0.096(9)	0.077(8)	-0.002(7)	0.033(6)	0.026(6)
C31	0.029(4)	0.057(6)	0.056(5)	0.010(4)	0.028(4)	0.004(4)
C32	0.085(8)	0.049(6)	0.104(9)	0.004(6)	0.068(8)	-0.008(6)
C33	0.162(15)	0.065(8)	0.114(12)	0.001(8)	0.098(12)	-0.011(9)
C34	0.076(8)	0.092(10)	0.088(9)	0.012(7)	0.054(7)	-0.019(7)
C35	0.066(6)	0.085(9)	0.071(7)	-0.022(6)	0.052(6)	-0.017(6)
C36	0.052(5)	0.081(8)	0.062(6)	-0.004(5)	0.038(5)	-0.006(5)
O2	0.187(12)	0.129(10)	0.324(19)	-0.051(10)	0.217(14)	-0.045(9)
C37	0.29(2)	0.132(14)	0.269(17)	-0.046(12)	0.238(16)	-0.054(14)
C38	0.238(19)	0.174(15)	0.241(18)	-0.033(13)	0.195(18)	-0.091(14)
C39	0.191(17)	0.149(15)	0.217(18)	-0.026(13)	0.143(17)	-0.057(13)
C40	0.127(14)	0.136(16)	0.267(17)	-0.023(12)	0.119(15)	-0.015(11)
O3	0.124(8)	0.192(11)	0.071(5)	-0.028(6)	0.061(5)	-0.041(7)
C41	0.133(12)	0.180(14)	0.093(9)	-0.010(9)	0.052(8)	-0.062(11)
C42	0.093(8)	0.149(13)	0.085(7)	-0.009(7)	0.050(6)	-0.013(8)
C43	0.099(11)	0.179(18)	0.126(11)	0.011(12)	0.088(11)	0.003(12)
C43'	0.072(14)	0.163(16)	0.14(2)	-0.016(11)	0.070(13)	-0.037(14)
C44	0.090(8)	0.150(13)	0.125(9)	-0.033(9)	0.058(7)	-0.035(8)

The form of the anisotropic displacement parameter is:

$$\exp[-2p^2(a^2U_{11}h^2+b^2U_{22}k^2+c^2U_{33}l^2+2b*c*U_{23}kl+2a*c*U_{13}hl+2a*b*U_{12}hk)]$$

Table 5. Bond Distances in Compound 6199, Å

Pd1-P1#1	2.397(2)	Pd1-P1	2.397(2)	Pd1-P2#1	2.405(2)
Pd1-P2	2.405(2)	K1-O3	2.577(9)	K1-O2	2.610(13)
K1-N1#2	2.722(8)	K1-N1	2.804(7)	K1-C16#3	3.145(9)
K1-C4#2	3.284(9)	K1-C5#2	3.305(9)	K1-C17#3	3.431(9)
K1-C40	3.47(2)	K1-C11#2	3.487(10)	K1-K1#2	4.083(4)
P1-C1	1.827(9)	P1-C19	1.854(9)	P1-C13	1.881(8)
P2-C31	1.844(9)	P2-C25	1.863(11)	P2-C7	1.868(9)
O1-C6	1.380(11)	O1-C12	1.389(9)	N1-C11	1.364(12)
N1-C5	1.393(11)	N1-K1#2	2.722(8)	C1-C6	1.388(11)
C1-C2	1.397(14)	C2-C3	1.387(13)	C3-C4	1.396(13)
C4-C5	1.411(13)	C4-K1#2	3.284(9)	C5-C6	1.375(11)
C5-K1#2	3.305(9)	C7-C12	1.339(12)	C7-C8	1.409(12)
C8-C9	1.438(13)	C9-C10	1.362(14)	C10-C11	1.397(12)
C11-C12	1.416(12)	C11-K1#2	3.487(10)	C13-C18	1.381(13)

C13-C14	1.389(12)	C14-C15	1.384(13)	C15-C16	1.370(14)
C16-C17	1.380(14)	C17-C18	1.347(13)	C19-C24	1.348(13)
C19-C20	1.388(13)	C20-C21	1.347(13)	C21-C22	1.385(16)
C22-C23	1.388(16)	C23-C24	1.409(14)	C25-C30	1.351(16)
C25-C26	1.381(13)	C26-C27	1.368(15)	C27-C28	1.321(19)
C28-C29	1.397(18)	C29-C30	1.399(16)	C31-C36	1.370(14)
C31-C32	1.380(14)	C32-C33	1.364(19)	C33-C34	1.35(2)
C34-C35	1.372(18)	C35-C36	1.351(15)	O2-C40	1.439(8)
O2-C37	1.440(9)	C37-C38	1.496(9)	C38-C39	1.505(9)
C39-C40	1.509(9)	O3-C44	1.424(8)	O3-C41	1.452(8)
C41-C42	1.500(8)	C42-C43	1.488(9)	C42-C43'	1.522(10)
C43-C44	1.526(9)	C43'-C44	1.533(10)		

Symmetry transformations used to generate equivalent atoms:

#1 -x+1,y,-z+1/2 #2 -x+3/2,-y+3/2,-z+1 #3 x+1/2,-y+3/2,z+1/2

Table 6. Bond Angles in Compound 6199, °

P1#1-Pd1-P1	102.91(12)	P1#1-Pd1-P2#1	113.22(7)	P1-Pd1-P2#1	106.78(7)
P1#1-Pd1-P2	106.78(7)	P1-Pd1-P2	113.22(7)	P2#1-Pd1-P2	113.54(12)
O3-K1-O2	80.7(5)	O3-K1-N1#2	130.1(3)	O2-K1-N1#2	147.3(5)
O3-K1-N1	115.4(3)	O2-K1-N1	91.3(3)	N1#2-K1-N1	84.7(2)
O3-K1-C16#3	84.8(3)	O2-K1-C16#3	79.8(3)	N1#2-K1- C16#3	91.1(2)
N1-K1-C16#3	156.6(3)	O3-K1-C4#2	171.8(3)	O2-K1-C4#2	101.1(5)
N1#2-K1-C4#2	46.8(2)	N1-K1-C4#2	72.7(2)	C16#3-K1- C4#2	87.7(3)
O3-K1-C5#2	149.6(3)	O2-K1-C5#2	123.0(5)	N1#2-K1-C5#2	24.4(2)
N1-K1-C5#2	85.2(2)	C16#3-K1- C5#2	81.7(2)	C4#2-K1-C5#2	24.7(2)
O3-K1-C17#3	107.9(3)	O2-K1-C17#3	79.1(4)	N1#2-K1- C17#3	80.3(2)
N1-K1-C17#3	133.4(2)	C16#3-K1- C17#3	23.7(2)	C4#2-K1- C17#3	65.0(2)
C5#2-K1- C17#3	64.1(2)	O3-K1-C40	102.4(4)	O2-K1-C40	22.1(4)
N1#2-K1-C40	127.0(3)	N1-K1-C40	78.3(4)	C16#3-K1-C40	86.1(4)
C4#2-K1-C40	80.2(3)	C5#2-K1-C40	103.7(3)	C17#3-K1-C40	76.4(3)

O3-K1-C11#2	110.9(3)	O2-K1-C11#2	155.2(4)	N1#2-K1- C11#2	21.1(2)
N1-K1-C11#2	102.4(2)	C16#3-K1- C11#2	79.5(2)	C4#2-K1- C11#2	64.4(2)
C5#2-K1- C11#2	39.8(2)	C17#3-K1- C11#2	76.5(2)	C40-K1-C11#2	142.1(3)
O3-K1-K1#2	136.3(3)	O2-K1-K1#2	125.2(3)	N1#2-K1-K1#2	43.15(15)
N1-K1-K1#2	41.60(16)	C16#3-K1-K1#2	130.0(2)	C4#2-K1-K1#2	48.60(18)
C5#2-K1-K1#2	48.35(14)	C17#3-K1-K1#2	111.09(19)	C40-K1-K1#2	105.2(4)
C11#2-K1- K1#2	61.65(15)	C1-P1-C19	95.1(4)	C1-P1-C13	99.9(4)
C19-P1-C13	102.4(4)	C1-P1-Pd1	118.2(3)	C19-P1-Pd1	121.4(3)
C13-P1-Pd1	115.8(2)	C31-P2-C25	99.7(4)	C31-P2-C7	99.0(4)
C25-P2-C7	99.8(4)	C31-P2-Pd1	117.8(3)	C25-P2-Pd1	118.9(3)
C7-P2-Pd1	117.9(3)	C6-O1-C12	115.0(6)	C11-N1-C5	114.5(6)
C11-N1-K1#2	112.9(5)	C5-N1-K1#2	102.0(6)	C11-N1-K1	136.9(6)
C5-N1-K1	88.9(5)	K1#2-N1-K1	95.3(2)	C6-C1-C2	117.1(8)
C6-C1-P1	115.9(7)	C2-C1-P1	126.5(6)	C3-C2-C1	119.6(9)
C2-C3-C4	121.4(9)	C3-C4-C5	120.0(8)	C3-C4-K1#2	143.8(7)
C5-C4-K1#2	78.5(5)	C6-C5-N1	122.9(8)	C6-C5-C4	116.3(8)
N1-C5-C4	120.8(7)	C6-C5-K1#2	145.6(6)	N1-C5-K1#2	53.7(4)
C4-C5-K1#2	76.8(5)	C5-C6-O1	117.1(7)	C5-C6-C1	125.1(9)
O1-C6-C1	117.7(7)	C12-C7-C8	119.7(8)	C12-C7-P2	118.1(6)
C8-C7-P2	122.2(7)	C7-C8-C9	117.3(9)	C10-C9-C8	120.6(8)
C9-C10-C11	122.3(8)	N1-C11-C10	123.2(8)	N1-C11-C12	121.3(7)
C10-C11-C12	115.5(9)	N1-C11-K1#2	46.0(4)	C10-C11-K1#2	88.7(6)
C12-C11-K1#2	140.4(6)	C7-C12-O1	118.4(7)	C7-C12-C11	124.3(8)
O1-C12-C11	117.3(7)	C18-C13-C14	118.6(8)	C18-C13-P1	119.7(6)
C14-C13-P1	121.6(7)	C15-C14-C13	120.0(9)	C16-C15-C14	119.6(10)
C15-C16-C17	119.9(10)	C18-C17-C16	120.6(10)	C17-C18-C13	120.9(9)
C24-C19-C20	120.8(9)	C24-C19-P1	114.6(7)	C20-C19-P1	124.3(7)
C21-C20-C19	121.2(11)	C20-C21-C22	119.7(11)	C21-C22-C23	119.5(10)
C22-C23-C24	120.1(11)	C19-C24-C23	118.7(10)	C30-C25-C26	117.3(10)
C30-C25-P2	117.3(7)	C26-C25-P2	125.3(8)	C27-C26-C25	121.8(12)
C28-C27-C26	122.1(12)	C27-C28-C29	117.5(13)	C28-C29-C30	120.8(12)
C25-C30-C29	120.4(10)	C36-C31-C32	118.3(10)	C36-C31-P2	116.8(8)

C32-C31-P2	124.8(8)	C33-C32-C31	120.1(13)	C34-C33-C32	121.7(14)
C33-C34-C35	117.7(12)	C36-C35-C34	121.7(11)	C35-C36-C31	120.4(11)
C40-O2-C37	109.6(5)	C40-O2-K1	114.9(12)	C37-O2-K1	106.7(12)
O2-C37-C38	106.2(6)	C37-C38-C39	103.9(7)	C38-C39-C40	103.0(7)
O2-C40-C39	106.5(6)	O2-C40-K1	43.0(9)	C39-C40-K1	116.1(12)
C44-O3-C41	109.1(5)	C44-O3-K1	113.1(8)	C41-O3-K1	125.3(8)
O3-C41-C42	106.3(5)	C43-C42-C41	104.2(6)	C43-C42-C43'	46.1(15)
C41-C42-C43'	103.0(7)	C42-C43-C44	102.0(6)	C42-C43'-C44	100.1(7)
O3-C44-C43	105.6(6)	O3-C44-C43'	103.6(7)	C43-C44-C43'	45.3(15)

Symmetry transformations used to generate equivalent atoms:

#1 -x+1,y,-z+1/2 #2 -x+3/2,-y+3/2,-z+1 #3 x+1/2,-y+3/2,z+1/2

ⁱBruker (2009) SAINT. Bruker AXS Inc., Madison, Wisconsin, USA.

ⁱⁱBruker (2009) SHELXTL. Bruker AXS Inc., Madison, Wisconsin, USA.

ⁱⁱⁱSheldrick, G.M. (2007) SADABS. University of Gottingen, Germany.

^{iv}Sheldrick, G.M. (2008) Acta Cryst. A64,112-122.

^vSheldrick, G.M. (2008) Acta Cryst. A64,112-122.

^{vi} $R1 = \frac{\sum ||F_o| - |F_c||}{\sum |F_o|}$

$wR2 = [\sum w(F_o^2 - F_c^2)^2 / \sum w(F_o^2)^2]^{1/2}$

$GOF = [\sum w(F_o^2 - F_c^2)^2 / (n - p)]^{1/2}$

where n = the number of reflections and p = the number of parameters refined.

^{vii}“ORTEP-II: A Fortran Thermal Ellipsoid Plot Program for Crystal Structure Illustrations”. C.K. Johnson (1976) ORNL-5138.

^{viii}v.d. Sluis, P. & A.L. Spek (1990). *Acta. Cryst.*, **A46**, 194.